Sedimentology and sequence stratigraphy of the Jurassic, Jabal Tuwaiq, Central Saudi Arabia

Abdullah Al-Mojel

THÈSE

Présentée à

L'Université Bordeaux Montaigne

Par **Abdullah AL-MOJEL**

Ecole doctorale Montaigne Humanité

Discipline : Science et Technologie

Spécialité : Sciences de la Terre

Sedimentology and Sequence Stratigraphy of the Jurassic, Jabal Tuwaiq, Central Saudi Arabia

Soutenue le 1/12/2017

Jury de thèse :

Frans van Buchem, Dr, Principal Advisor Geoscience Halliburton..... Rapporteur

Volker Vahrenkamp, Professor Kaust University (KSA)..... Rapporteur

Denis Vaslet, Dr, Consultant ..... Examinateur

Guillaume Dera, MCF, Université de Toulouse..... Examinateur

Cécile Robin, MCF-HDR, Université de Rennes..... Examinateur

Carine Grélaud, MCF, Bordeaux INP ..... Examinateur

Yves-Michel Le Nindre, Dr, Consultant ..... co-Directeur de thèse

Philippe Razin, Professeur, Bordeaux INP..... Directeur de thèse

Sedimentology and Sequence Stratigraphy of the Jurassic, Jabal Tuwaiq, Central Saudi Arabia

Abdullah ALMOJEL

Abstract

High-resolution sequence stratigraphic transects of the Jurassic Shaqra Group (Toarcian to Kimmeridgian) outcrops in Central Saudi Arabia provide a continuous stratigraphic record of a large (>1000 km) epeiric, continental to shallow marine, tropical mixed carbonate-siliciclastic platform system. They serve as westernmost reference for adjacent prolific reservoirs in giant oil fields and source-rock bearing intrashelf basins. Several hierarchical stratigraphic sequences (second to fourth order) have been recognized in outcrops sections (600 km long south of Riyadh) and correlated with gamma-ray logs of subsurface wells (550 km long crossing the Arabian Basin from Riyadh to Rimthan Arch).

The Jurassic platform evolved from very-flat continental-to-nearshore mixed carbonate-siliciclastic platform (Marrat-Dhruma; Toarcian to Middle Callovian) to differentiated ramp platform with deep intrashelf basins (Tuwaiq-Hanifa; Middle Callovian to Early Kimmeridgian) to a lowstand followed by flat aggraded platform (Jubaila Arab-D; Kimmeridgian). Tectonic related siliciclastic influx took place in arid condition during the Kimmeridgian (Jubaila Fm.). The Jurassic platform ends with the mixed carbonate-evaporite systems of the Arab Fm. A first second-order tectono-eustatic cycle (Marrat to Tuwaiq) is bounded at the base and top by regional unconformities. It has a stationary depocenter, and show long-term coastal onlap and marine transgression that reached its maximum extent during the upper Tuwaiq (Middle Callovian). The Hanifa Fm. consists of four 3rd-order sequences aggraded flat-toped platform (outcrops to Khurais) marked at the base by argillaceous limestone and top by

pure high-energy carbonates with localized reef buildups. These shallow marine carbonates grade downslope to starved lime-mudstone intrashelf basin during maximum marine transgressions (Khurais to southern Rimthan Arch). The Jubaila Arab-D is two 3rd-order sequences begin with low-stand deposits followed by long-term transgression. These formed flat horizontal successions with lateral thickness variations controlled by differential subsidence increased in the Arabian Basin. The transgression is marked by storm-influenced inner-platform with sandstone quartz, grainstones and restricted lime-mudstone. The Maximum marine transgression is placed in the Arab-D Reservoir (upper Jubaila) with reef buildups in the westernmost inner-platform. During highstand, the reef facies are gently prograding out into Rimthan Arch leaving behind restricted lagoon and sabkhah/salina anhydrite.

For the first time, this detailed outcropping study reveals depositional models that subdivided the Shaqra group into genetically related sequences that are not always obvious from core, wireline logs or seismic data. It provides significant understanding of the Jurassic history and tectono-stratigraphic events of the Arabian Platform.

Résumé étendu

Sédimentologie et stratigraphie séquentielle des séries jurassiques du Jabal Tuwaiq, Arabie Saoudite

Abdullah Al Mojel

Mots clefs : Jurassique, Plateforme arabe, Plateforme épicontinentale, Système mixte carbonaté – silicoclastique, stratigraphie séquentielle

Les séries jurassiques du Toarcien au Kimmeridgien affleurent de manière spectaculaire et continue sur plus de 1000km le long de l'escarpement Tuwayq situé dans la partie centrale de la plaque arabe en Arabie Saoudite. Elles sont principalement composées d'argile, de carbonates et plus accessoirement de grès et d'évaporites. Elles se sont accumulées sur un vaste domaine de plate-forme épicontinentale peu profonde formant la partie proximale de la marge passive néotéthysienne, en contexte de climat tropical. La série stratigraphique étudiée atteint plus de 1000 m d'épaisseur et couvre une période de temps de 30 millions d'années environ.

Notre analyse complète de cette série jurassique constitue la première étude visant à appliquer dans cette région une approche de stratigraphie séquentielle sur les analogues d'affleurement pour une meilleure compréhension des systèmes jurassiques en subsurface à l'échelle régionale, et en particulier des systèmes pétroliers d'Arabie Saoudite.

Les séries jurassiques qui affleurent en Arabie centrale n'ont fait l'objet que de peu d'études stratigraphiques. Les dernières d'entre elles s'appuient principalement sur une approche principalement lithostratigraphique et biostratigraphique (e.g., Bramkamp and Steineke, in Arkell, 1952 ; Powers et

al., 1966 ; Powers, 1968 ; Manivit et al., 1990). Le découpage en séquences de dépôt, la hiérarchie des cycles, les modalités d'empilement de ces cycles, l'évolution des systèmes de dépôt, les effets des déformations synsédimentaires n'ont jusqu'ici pas été abordés précisément dans les travaux antérieurs. Aussi, notre étude vise à intégrer les données biostratigraphiques existantes et de nouvelles analyses sédimentologiques réalisées sur de multiples coupes de terrain, ainsi que des diagraphies de forages, afin de reconstituer des modèles de dépôt factuels et fiables, et de proposer un schéma séquentiel de haute résolution.

Cette étude pourra servir de modèle de référence pour une meilleure compréhension des formations jurassiques qui renferment des systèmes pétroliers de grand intérêt économique sur la plate-forme arabe. Elle fournit en effet des enseignements importants que ce soit pour des finalités d'exploration, de distribution des réservoirs, d'interprétation sismique et de modélisation de réservoir. Par ailleurs, l'analyse stratigraphique et sédimentologique de l'ensemble de cette série jurassique apporte des connaissances supplémentaires sur l'évolution des paléo-environnements, de la paléogéographie et des déformations structurales de la plate-forme arabe sur la bordure de la Néotéthys.

Jurassique inférieur : Formation Marrat

Les séries d'âge toarcien offrent à l'affleurement un enregistrement continu de la transgression jurassique sur dépôts les continentaux du Trias. Ces séries sont formées d'associations de faciès allant de dépôts fluviatiles méandriformes à des dépôts marins peu profonds issus de systèmes silico-

clastiques influencés par les marées et/ou les vagues, et de systèmes carbonatés peu profonds de plateforme interne. Ils se sont accumulés sur un domaine de type « flat-topped platform ». L'épaississement des dépôts vers le nord démontre une subsidence différentielle de la plateforme à cette époque. Cette succession sédimentaire s'organise en deux séquences de dépôt de 3ème ordre reposant en onlap vers le sud-ouest sur les séries continentales du Trias. Le maximum de transgression est atteint au Toarcien moyen dans la zone à Bifrons, à l'instar du reste de la plateforme arabe et du domaine européen. La géométrie tabulaire des dépôts atteste un contexte géotectonique relativement stable où la subsidence différentielle est compensée par les apports silico-clastiques et la production carbonatée. Des systèmes sédimentaires éphémères de haute-énergie se mettent en place pendant les périodes de fort taux d'accommodation (« late TST » et « HST »). Des dépôts carbonatés à dominance boueuse se développent autour des périodes de maximum d'accommodation des deux séquences de dépôt. La phase régressive entre ces deux pics transgressifs est représentée par un intervalle d'argile rouge et de grès fluviatile de grande extension, correspondant au Middle Marrat Member. Cet épisode d'influx clastique important est interprété comme résultant d'un contexte climatique chaud et humide et non d'une chute du potentiel d'accommodation.

Jurassique moyen : formations Dhruma et Tuwaiq Mountain

Les affleurements offrent un transect continu de plusieurs centaines de kilomètres à travers la plateforme arabe. Ils sont formés d'associations de faciès variés allant de dépôts fluviatiles en tresses à des dépôts lagunaires

mixtes à dominance tidale ou de vagues. Ces dépôts de plate-forme s'épaississent clairement vers le nord indiquant une subsidence différentielle de la plateforme dans cette direction. Des apports fluviatiles importants interviennent à certaines périodes dans cet environnement à dominance boueuse. Les plateformes carbonatées sont également à dominance boueuse et évoluent de systèmes à dominance microbienne à des systèmes à organismes plus diversifiés (Fm. Dhruma, Bajocien inférieur à Bathonien inférieur) jusqu'à des systèmes carbonatés subrécifaux à stromatopores et coraux caractérisés par une faune très diversifiée (Tuwaiq Mt. Lst., Callovian moyen). La succession est formée de deux séquences de dépôt composites de 3ème ordre, DCS and TCS (~2.4 Myr), composées de plusieurs cycles de haute fréquence (4th-order, ~400 kyr) montrant une transgression progressive qui atteint un premier maximum au Bathonien inférieur (*zigzag* Zone), suivi d'un maximum transgressif dans la formation Tuwaiq Mountains au Callovian moyen (zone à *coronatum*). Les séquences de dépôts sont interprétées comme d'origine eustatique car corrélables avec les séquences téthysiennes. Une limite de séquence majeure entre les séquences DCS et TCS accompagnée d'un hiatus du Bathonien moyen est considérée comme résultant d'une chute eustatique importante couplée à une déformation tectonique de la plaque arabe. Le TST des séquences composites s'initient pendant des épisodes chauds et humides où un influx clastique important est responsable d'une chute de la production carbonatée. Les carbonates se développent alors pendant les phases de maximum d'accommodation des séquences composites en relation avec une chute des flux clastiques pendant ces épisodes. Le synchronisme entre cette transgression et les épisodes de

réchauffement tend à indiquer un contrôle climato-eustatique des séquences du Jurassique moyen d'Arabie centrale.

Jurassique supérieur : formations Hanifa et Jubaila-Arab D

Les environnements de dépôt des séries à l'affleurement s'étalent de systèmes littoraux semi-arides à des environnements de lagon et d'arrière-barrière carbonatés. La géométrie et la distribution des facies témoignent d'une subsidence différentielle synsédimentaire du domaine de plateforme étudié. La série du Jurassique supérieur est composée de plusieurs séquences composites de 3ème ordre limitées par des surfaces d'émersion de relative courte durée. La Formation Hanifa débute par des dépôts argilo-carbonatés proximaux à faune peu diversifiée évolutant vers des dépôts sub-récifaux à stromatopores et coraux (Oxfordien supérieur à Kimmeridgien inférieur). Ces dépôts de plateforme de haute-énergie s'accumulent sur la bordure d'un bassin intra-shelf reconnu en subsurface plus vers l'est. La Formation Hanifa comprend deux phases d'inondation majeures (MFS) représentées par des dépôts purement carbonatés d'âge oxfordien supérieur et kimméridgien inférieur. The bassin intrashelf adjacent est comblé durant la phase régressive de la Formation Hanifa. Les formations Jubaila-Arab-D reposent en concordance sur la surface d'émersion du sommet de la Formation Hanifa. Cette unité est composée de deux séquences composites dans un contexte globalement transgressif. Elle débute par un intervalle calcaréo-gréseux accumulé par l'action des vagues de tempête. Le maximum de trangression est localisé dans les faciès rétrogradants d'arrière-barrière du Membre Arab-D. Pendant la période haut-niveau marin (HST) suivante, des

faciès récifaux progradent vers le Rimthan Arch laissant en amont un domaine évaporitique de type sabkhah/salina à anhydrite. Ces séquences composites du Jurassique supérieur sont interprétées comme principalement contrôlées par des variations climato-eustatiques du niveau marin modulées par des déformations tectoniques locales de faible amplitude.

Conclusion

La plateforme arabe évolue durant le Jurassique depuis un système mixte carbonaté – silico-clastique très plat en domaine de transition continental marin (Fms. Marrat-Dhruma; Toarcien à Callovien moyen) vers une rampe carbonatée passant à un bassin intrashelf relativement profond (Fms. Tuwaiq-Hanifa; Callovien moyen à Kimmeridgien inférieur) puis un système de plate-forme aggradante (Fms. Jubaila Arab-D; Kimmeridgian). Un flux clastique d'origine tectonique se développe en contexte climatique aride au Kimmeridgien (Fms. Jubaila Fm.). Cette série de plate-forme jurassique se termine par les dépôts mixtes carbonatés et évaporitiques de la Formation Arab. Les cycles du Toarcien (Fm. Marrat) et du Jurassique moyen (Fms. Dhruma et Tuwaiq) sont limités par des surfaces d'émersion majeures d'extension régionale. Ils présentent un dépocentre stationnaire et décrivent un onlap côtier de grande ampleur avec un maximum transgressif au Callovien moyen (Upper Tuwaiq Mb.). Durant le Jurassique supérieur, les dépôts de rampe carbonatée de la Formation Hanifa passent progressivement vers l'ouest à des dépôts plus profonds de bassin intrashelf relativement riches en matière organique (Khurais - Rimthan Arch). La séquence Jubaila – Arab-D montre des variations d'épaisseur qui indiquent

une déformation de grande longueur d'onde de la plate-forme arabe à cette période. Les faciès récifaux du membre Arab D sont interprétés comme représentant le maximum d'inondation de ce cycle qui se termine par le développement de systèmes carbonatés – évaporitiques à la fin du Jurassique.

Acknowledgments

All praise to almighty ALLAH, the most Merciful and the most Benevolent, who gave me the chance, talent and time to achieve this work.

I would like to express my thanks to my committee members; I which to express my appreciation to my supervisors Prof. Philippe Razin, Dr. Yves-Michel Le Nindre and Dr. Guillaume Dera for their supervision, mentorship, professional guidance, and informative reviews of the thesis and manuscripts.

Special thanks go to the management of Saudi Aramco for the permission to use and publish the data. My sincere appreciations are due to my manager Dr. Aus Al-Tawil, Reservoir Characterization Manager, for his invaluable support and funding. Without his persistent backing, this study would never have seen the light.

I also thank Dr. Denis Vaslet, Prof. J. Fred Read and Prof. Charles Kerans for providing valuable suggestions and constructive comments. We also extend our thanks to Mahmoud Alnazghah, Dr. Raed Al-Dukhayyil, Dr. Khalaf Al-Tamimi, Jamil Hajhog, Abdullah Shamsi and Abdulaziz Al-Gaoud for field support. Thanks go to Dr. G.W. Hughes and Dr. J.P. Platel for helping identifying the first Jurassic rudist record in the Jubaila Limestone.

Lastly, I owe my deepest gratitude to my Father and my Mother for their encouragement and never-ending prayer during my life and this study. Most significantly, I would like to express my sincere gratefulness to my wife: Eman Al-Razooq, and my beautiful children; Norah, Saad, Al-Jawharah and Dalal for their emotional support during the length of this study.

Table of contents

Chapter 1: Introduction

MAX STEINEKE (1898-1952): *"He played a leading role in the oil exploration and geologic mapping in Saudi Arabia during a period when fieldwork, especially in remote areas, demanded diligence and resilience, and oil exploration was conducted by simple down-to-earth methods"* Sorkhabi, R. (2012).

1.1 Scope and aim of the study

The Jurassic outcrops (Toarcian to Kimmeridgian) are located in the central part of the Arabian Plate (Fig. 1.1 and 1.2), which corresponds to an intra-cratonic passive margin facing the Neo-Tethys to the south (Fig. 1.3). The Arabian Platform was an extensive (>1000 km) tropical shallow marine epeiric platform system. The Jurassic outcrop is the westernmost and landward stratigraphic record of the Jurassic stratigraphy and is mainly consisting of shales, carbonates and lesser sandstone and anhydrites. These outcrops are very well exposed and easily accessible along the Tuwayq Escarpment forming spectacular west facing continuous cuests along 1000 km N-S near Ar Riyadh (Fig. 1.2). The study interval reach up to 1000 m in thickness and the time duration is around 30 Myr including disconformity levels. The Middle East host near 60% of the world’s known oil reserve and around third of its remaining gas reserves (Sharland et al., 2001). In the Arabian Plate, the studied interval hosts the world's most prolific petroleum system, reservoirs, seals and richest source rock intervals (Powers, 1962; Powers et al., 1966; Powers, 1968; Murris, 1980).

This study of the entire Jurassic outcrop represents one of the first attempts to apply modern sequence stratigraphic data from outcrop analogs to improve our understanding of Jurassic system regionally and globally. To date, very few studies have addressed the Jurassic outcrop of the Central Arabia. The last comprehensive studies were using mainly lithostratigraphy and biostratigraphy approaches (e.g., Bramkamp and Steineke, in Arkell, 1952; Powers et al., 1966; Powers, 1968; Manivit et al., 1990). However, genetically related depositional sequences, cycle hierarchy, stacking patterns,

depositional environment evolution, and effects of syndepositional tectonic events were not documented in detail. Therefore, our approach is to integrate the previous biostratigraphic data with detailed sedimentological measured sections and subsurface gamma-ray logs, offering a factual and correct depositional models and robust high-resolution sequence stratigraphic frameworks. This integration can provides a comprehensive reference for the most economically important formations in the Arabian Platform. This rock-based and direct assessment study should provide guidelines for reservoir modeling, hydrocarbon exploration, better predict reservoir distribution and improve seismic interpretation. Moreover, this continuous record of the Jurassic can contribute to a broad understanding of controlling factors and reconstruction of the paleogeographic of the Arabian Platform as well as the Neo-Tethys Ocean.

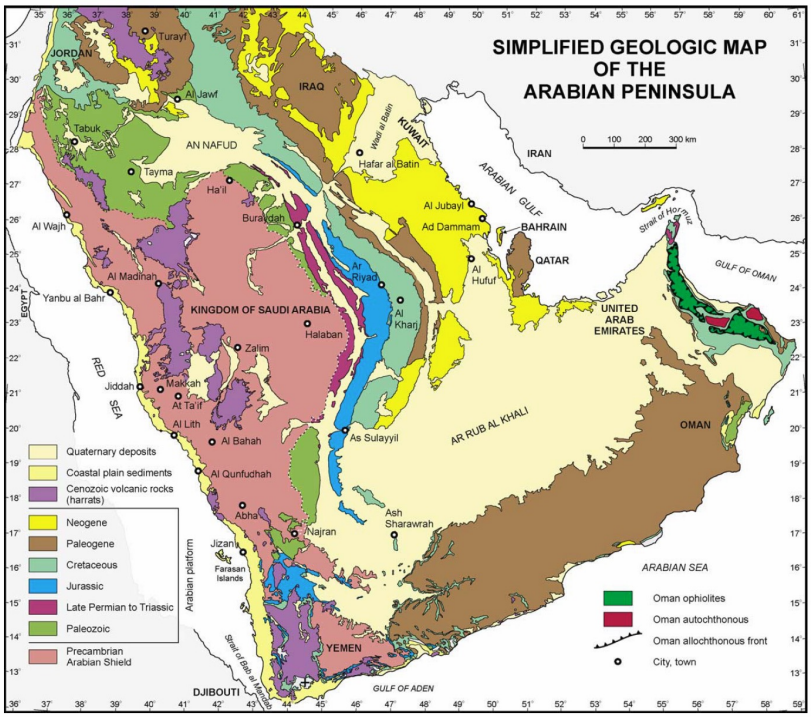

Figure 1.1: A simplified geological map of the Arabian Peninsula shows the extent of the Jurassic outcrop in central Saudi Arabia (Le Nindre et al., 2003).

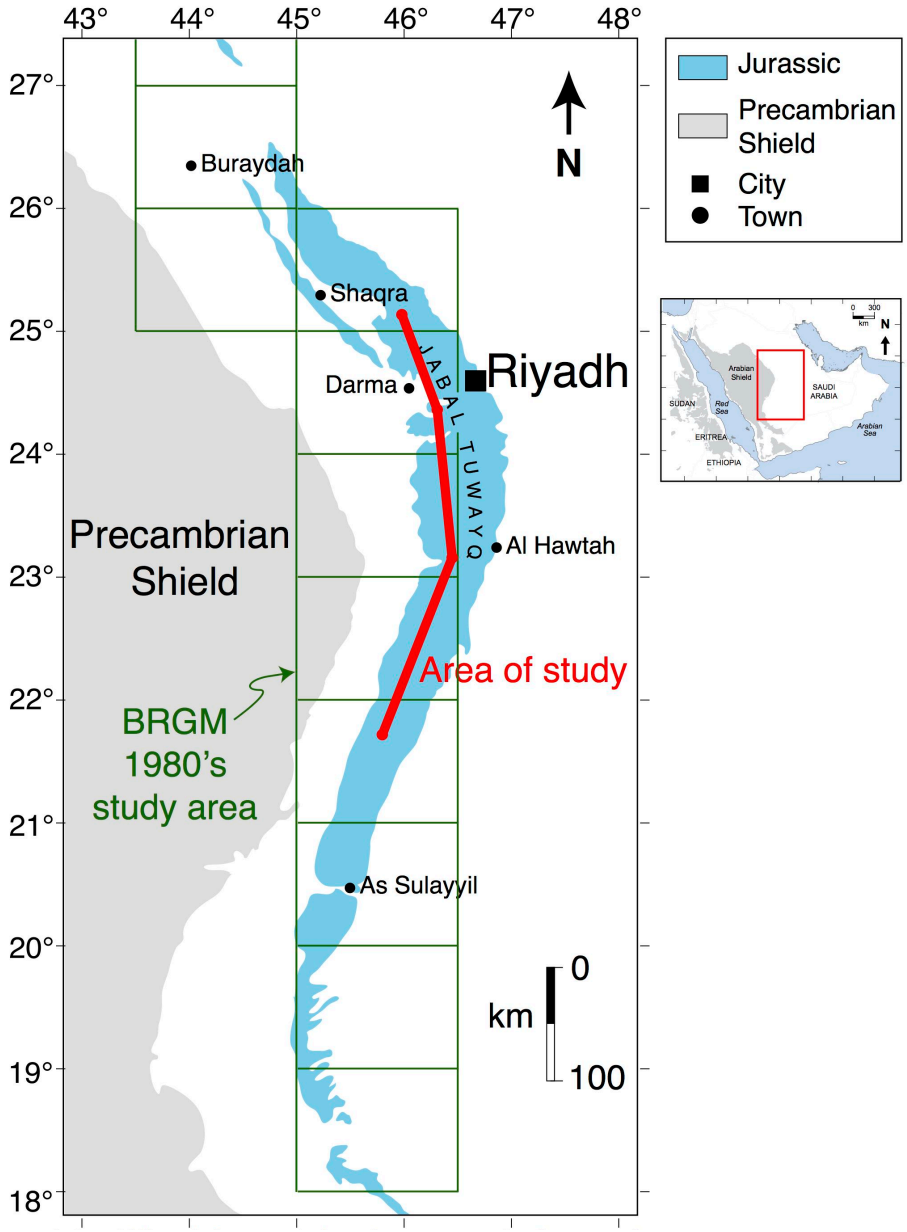

Figure 1.2: A close-up map showing the Jurassic outcrops and the area of study. Green squares are the latest mapping studies (modified after Fischer et al., 2001).

1.2 Tectonic and paleogeographic setting

The study area is located in the central part of the Arabian Plate, in an intra-cratonic passive margin. The Arabian Plate was tectonically stable since the beginning of the Late Permian up to the onset of convergence and obduction of the Neo-Tethys margin in the Late Cretaceous (i.e., Late Cenomanian – Turonian) (Glennie et al., 1995; Le Métour et al., 1990). The structure of the Arabian plate was partly controlled by pre-existing features of the Precambrian basement (Fig. 1.4 and 1.5).

The study area is very far from the shelf margin and close to the coastal zone and hinterland that is progressively onlapped by the Mesozoic sediments. This passive margin undergoes several 2nd-order tectonic events resulting in several Mesozoic unconformities and associated stratigraphic hiatuses (e.g., Late Triassic – Early Jurassic, Late Jurassic-Early Cretaceous). These two unconformities delimit the Jurassic stratigraphy (Fig. 1.6). The Late Triassic – Early Jurassic is one of the major unconformities lasting approximately 20 Myr that corresponds to the basal limit of the studied interval. The tectonic control of this unconformity is poorly understood. It could be related to the tectonic inversion of the Karoo rifting between Madagascar and East Africa that caused a long period of regional uplift and erosion (Delvaux, 2001; Baud et al., 2005). Within the Jurassic stratigraphy, there are several tectonic related unconformities such as Late Toarcian – Aalenian, that could relates to subsidence resistance and large-scale uplift (Le Nindre et al., 2003). The Middle-Late Jurassic transition was probably a time of tectonic instability and tilting. Incipient breaking of the Arabian-Indian plate boundary is marked by a volcanic interruption in eastern Oman (Ziegler, 2001). Eastern

Lebanon shows an extensive erosion and karstification at the end of the Middle Jurassic (Callovian). The intrashelf basins became more prominent, well developed and extended further to the south in the Rub' Al Khali (Ziegler, 2001). The intrashelf basins were partitioned by paleohigh or less subsiding zones inherited from the Hercynian orogeny of Paleozoic deformation. The Arabian Platform has continued to evolve from the slightly differentiated carbonate platform during late Middle Jurassic (Callovian) to a shelf with clear facies differentiation and clinoform geometries during early Late Jurassic (Oxfordian) associated with intrashelf basin (c.f. Figure 24, 25 of Murris, 1980).

The tectonic instability probably extended to the Late Oxfordian-Early Kimmeridgian time. Evidence of post-deposition broad erosion and exposure south of Iraq (southern Gotnia Basin) was attributed to basement faulting and uplift (Sadooni, 1997 in Ziegler, 2001). In Lebanon, volcanic-basalt magmatism and block faulting is documented (Walley, 2001 in Ziegler, 2001). In Yemen, active rifting initiated from Early Kimmeridgian and lasted up to the Tithonian is marked by a thick succession of open marine deposits (Brannan et al., 1999). In Oman, the Jurassic continental margin is characterized by extensive conglomerate gravity flow deposits by end of the Jurassic (Béchennec et al., 1990). The central part of the Arabian Plate shows an overall inward tilting of the basement blocks marked by eastward thinning of the Late Jurassic sequence towards the shelf margin as documented by regional east-west stratigraphic section (Murris, 1980) and by regional isopach maps (Abu-Ali and Littke, 2005). Consequently, the inner platform has been protected from the open-ocean circulation during Late Kimmeridgian

to the Tithonian resulting in a restricted depositional environment marked by carbonate-evaporite successions shown an upward increase in evaporite and decrease in faunal diversity (Hughes, 2004).

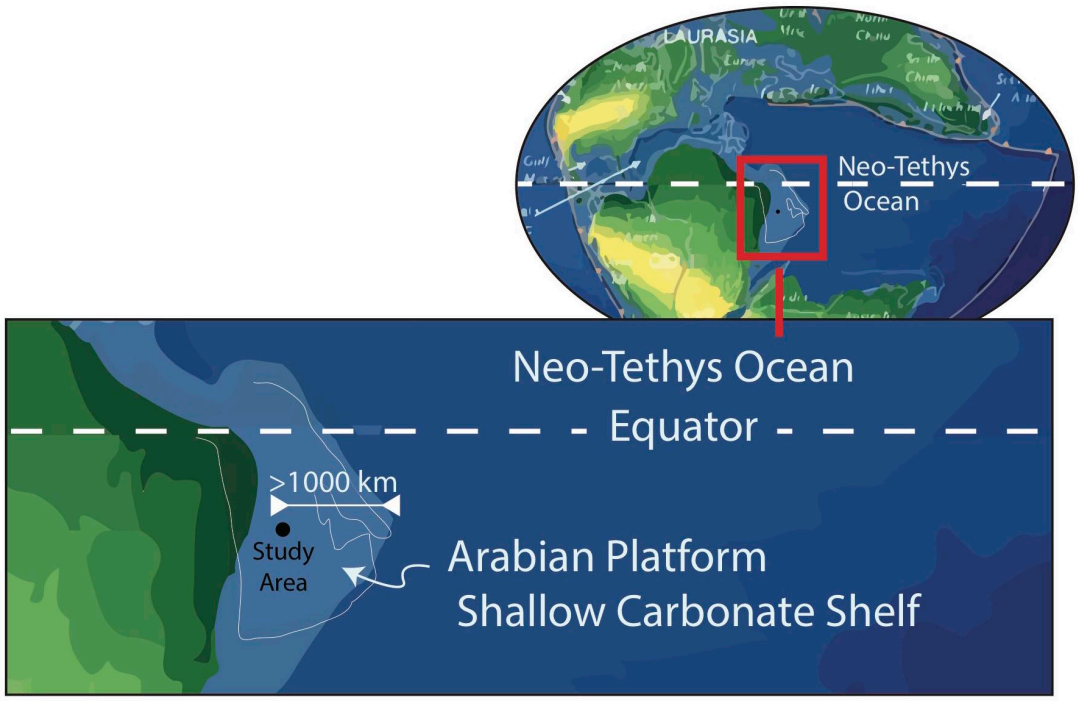

Figure 1.3: Palaeogeographic map of the Late Jurassic showing the study area located in the southern margin of the Neo-Tethys Ocean corresponding to a an extensive wide shallow-marine continental shelf close to western hinterland (modified after Scotese, 2003).

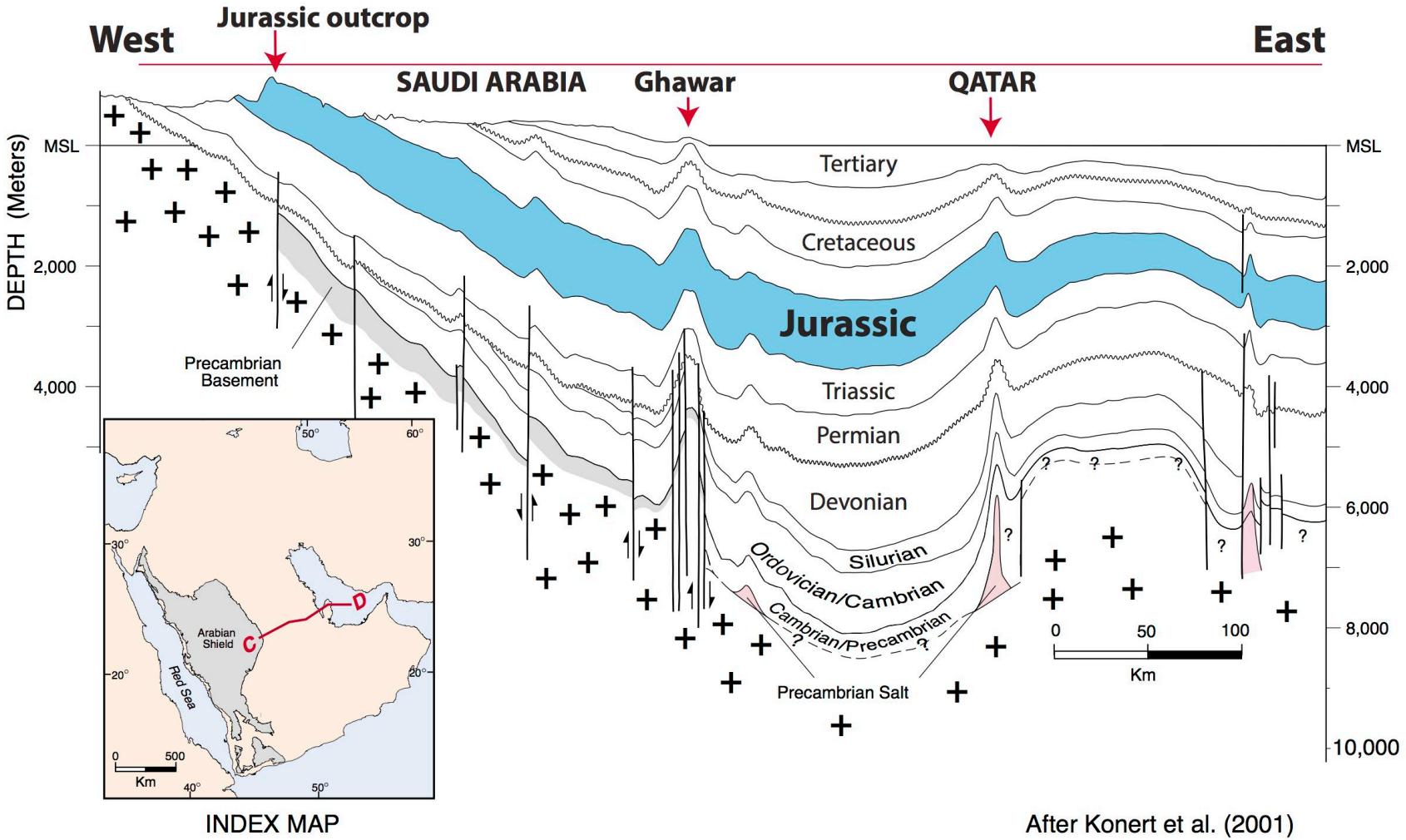

Figure 1.4: Cross section of the Arabian Plate showing Phanerozoic sediment (After Konert et al., 2001).

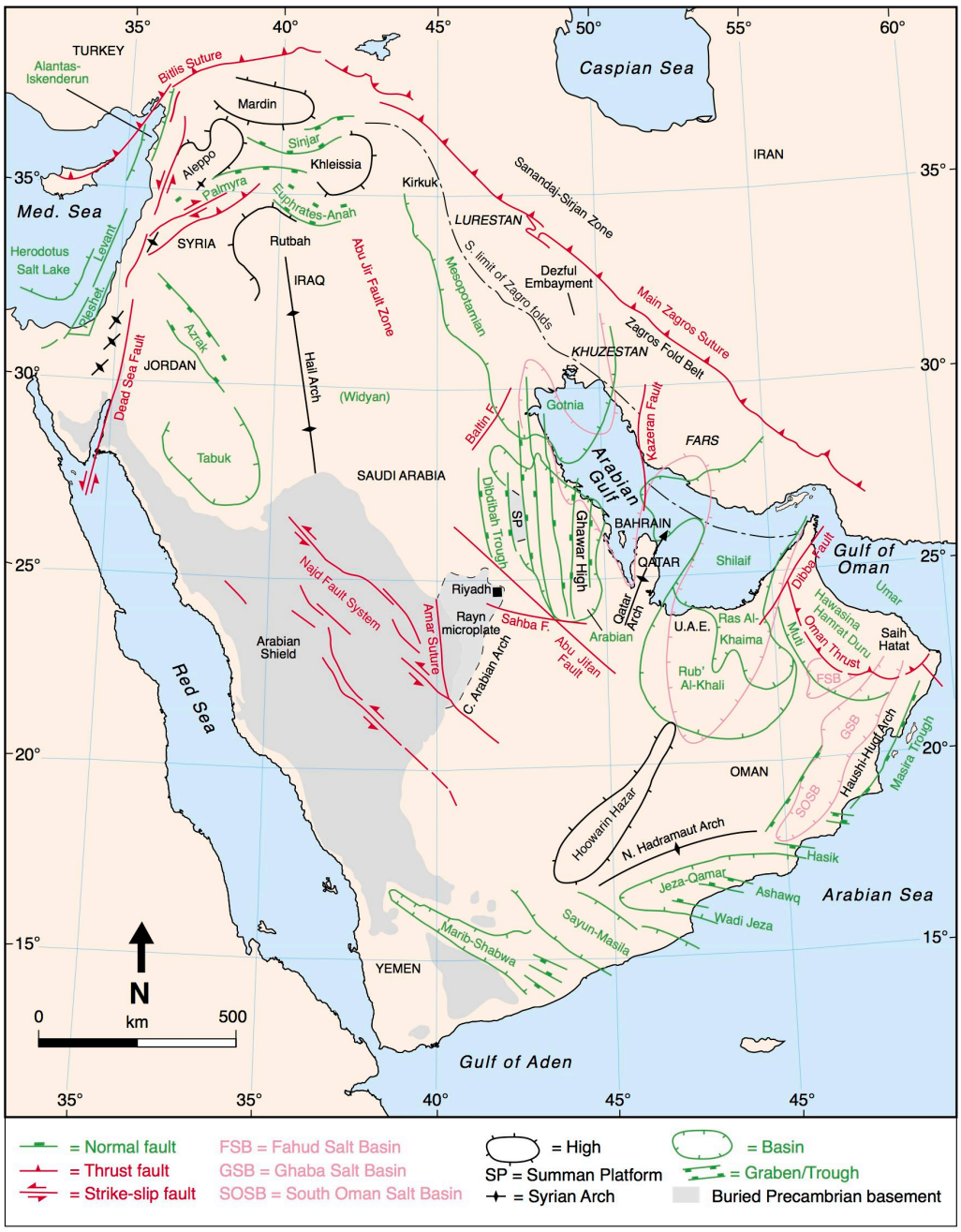

Figure 1.5: Main structure elements of the Arabian Plat (Fig. 2 in Ziegler, 2001).

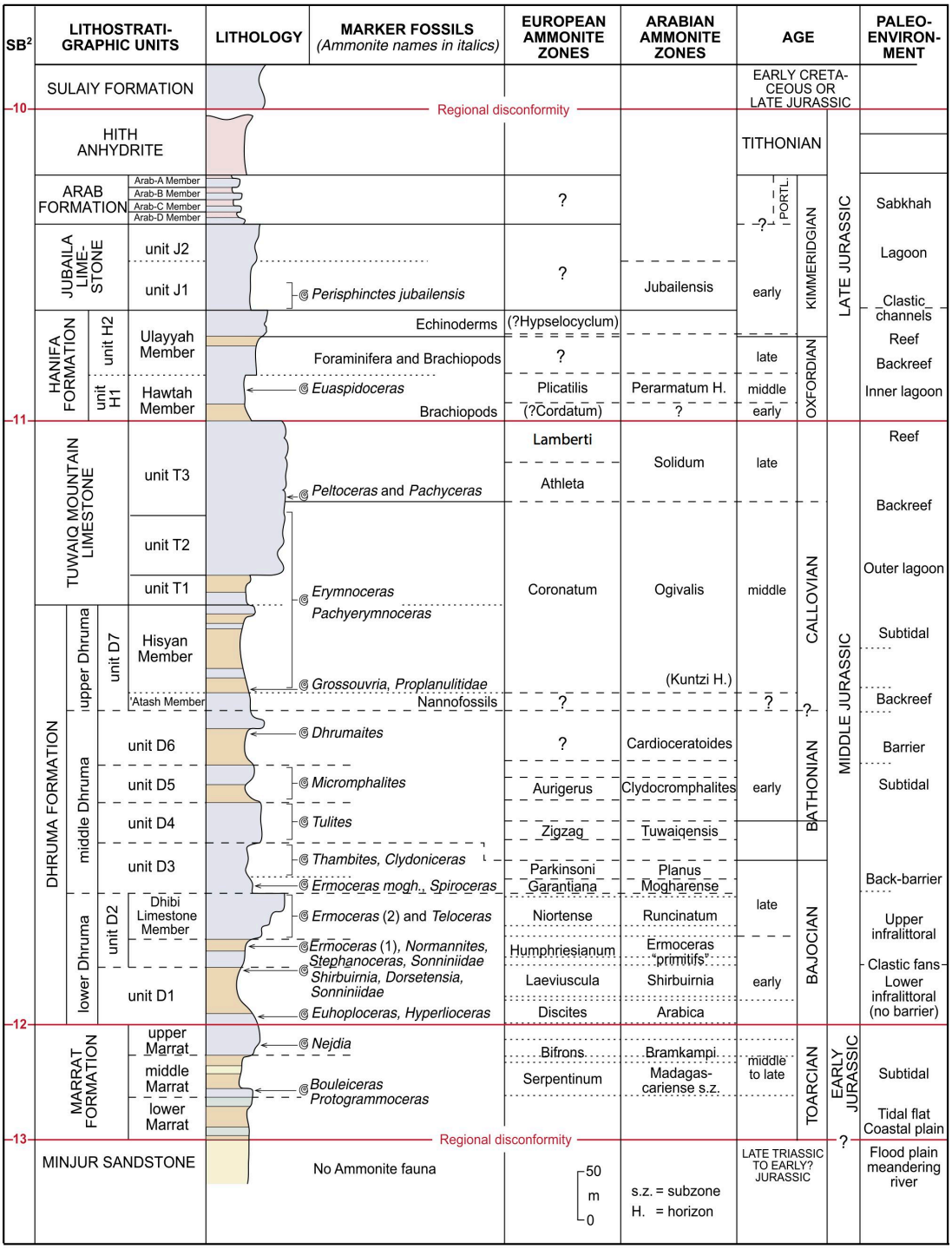

Figure 1.6: Lithostratigraphy and chronostratigraphy of the Jurassic succession in Saudi Arabia combined with second-order sequence boundaries (SB) of Al-Husseini and Matthews (2005) (compiled in Fischer et al., 2001; modified from Al-Husseini et al., 2006).

1.3 Stratigraphic setting

Seven Jurassic formations, mainly consisting of shales, carbonates and lesser anhydrites, form the Shaqra Group (Vaslet, 1987), which is very well exposed along the Jabal Tuwayq escarpments (Fig. 1.7). The shale is predominant in the Lower and Middle Jurassic interbedded with carbonate, which both grade to sandstone in the north and south ends of the outcrop (Fig. 1.8; Steineke et al., 1958; Powers, 1968; Le Nindre 1987; Manivit et al., 1990). The carbonate is progressively getting more dominant and thicker upward. Evaporites formed local and minor deposits during Early – Middle Jurassic transition and thick extensive deposits during Late Jurassic (Late Kimmeridgian-Tithonian time).

The group attains a maximum thickness of 1139 m in the central segment of the outcrop belt in Khashm Ad Dhibi (24° 30' N) and thins to about 300 m in the north and south ends of the outcrop (Fig. 1.7; Le Nindre et al., 2003). Its lower boundary is represented by Early Jurassic unconformity with a hiatus of approximately 20 Myr including (Hettangian to Pliensbachian), whereas its top is unconformably overlain by the Cretaceous Thamama Group, Sulaiy Formation of Berriasian age (Manivit et al., 1990; Powers, 1968). In the northern part of the outcrop belt, the top Shaqra Group (Upper Jurassic) has been eroded by the Early Cretaceous pre-Wasia unconformity (Fig. 1.7). In an ascending stratigraphic order, the Jurassic formations are the Marrat Formation (Lower Jurassic Toarcian), Dhruma Formation and Tuwaiq Mountain Limestone (Middle Jurassic Bajocian to Middle Callovian), Hanifa Formation, Jubaila Limestone, Arab Formation and the Hith Anhydrite (Upper Jurassic Oxfordian to Tithonian). All these formations were first recognized

and named by M. Steineke (1973) in unpublished report. Then, they have been formally defined in (Bramkamp and Steineke, in Arkell, 1952; Steineke et al., 1958, for the Arab Formation and Hith Anhydrite). The biostratigraphy of formations have been defined by the presence of ammonites and subordinate fauna (i.e., nautiles, echinoderms, brachiopods and foraminifera) (Fig 1.9; Manivit et al., 1990). The Shaqra Group in Saudi Arabia hosts twelve hydrocarbon reservoirs (Steineke et al., 1958; Powers et al., 1966; Hughes, 2009; Al-Husseini, 2009) and significant source rock intervals (Murris, 1980).

The Shaqra Group is partly equivalent to the Zuni supersequence of Sloss (1963) (Alsharhan and Nairn, 1997). The top-Marrat unconformity corresponds to a major sequence boundary between the supercycle sets UAB (upper Absaroka, below) and ZA (Zuni A, above) of Haq et al. (1987) (Le Nindre et al, 1990). The Shaqra group covers the 2nd order supercycles UAB-4, ZA-1 to 4, and base of ZB-1 (Fi.g 1.10; Le Nindre et al, 1990). Le Nindre et al. (1990) allocated five depositional sequences for the Jurassic outcrops. Sharland et al., (2001) divided the Jurassic successions into tectonostratigraphic mega-sequences (TMS) based on a review of plate tectonic and sediment accumulation events. They interpreted the Middle and Late Jurassic successions, from the Aalenian to Tithonian as single megasequence (TMS AP7; Fig. 1.11) bounded by tectonically controlled unconformities. Within this megasequence, several genetic stratigraphic sequences (GSS) were interpreted which are defined by nine maximum flooding intervals (J20-J100). Moreover, they interpreted two 2nd-order sequences (*sensu* Vail et al., 1977) separated by a disconformity within the Dhruma Formation and correspond to a major eustatic sea-level fall, evident

on the global sea-level curve. The Early Jurassic Marrat Formation was excluded from this megasequence (TMS AP7) and was assigned to the Mid-Permian to Early Jurassic megasequence (TMS AP6, Sharland et al., 2001). Based on orbital time calculation and regional chronological correlations, the Shaqra Group was divided into three 2nd-order depositional sequences (DS^2 13 to 11), each lasting about 14.58 Myr (Al-Husseini and Matthews, 2005). The boundaries of these sequences were assigned to the regional stratigraphic hiatuses. Higher order sequences (3rd-order DS^3) were interpreted for the Jurassic formations by Al-Husseini (2009). He assigned eleven 3rd-order sequences based on an updated regional chronostratigraphic framework and a review of the previous studies. These 3rd-order sequences will be explained (below) in each formation.

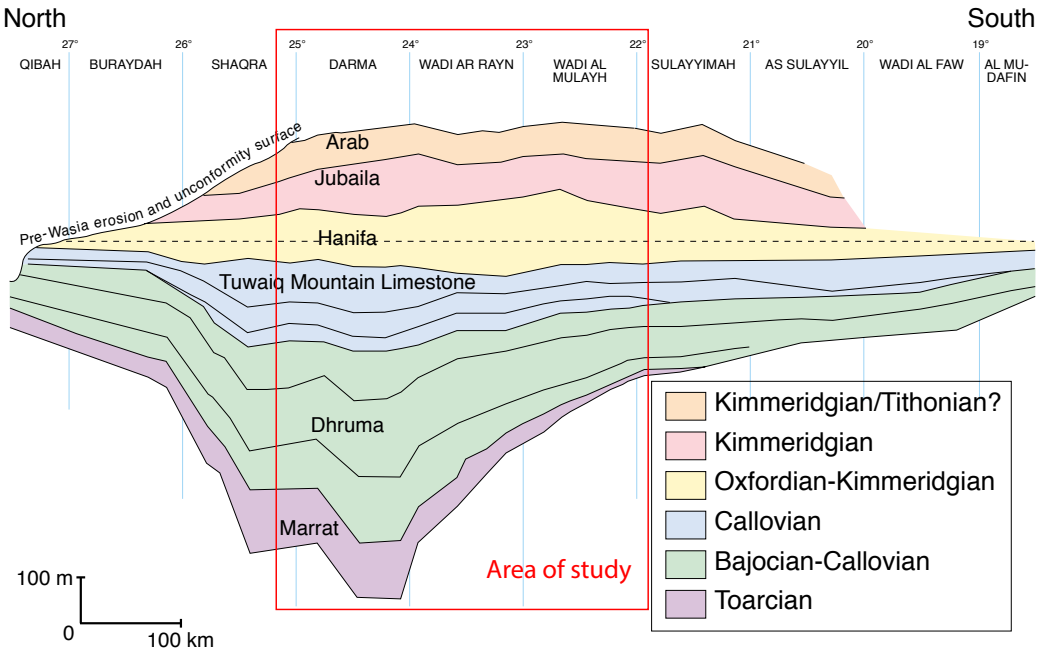

Figure 1.7: North-south cross section of the Jurassic formations along outcrops showing the area of the study (modified from Fischer et al., 2001)

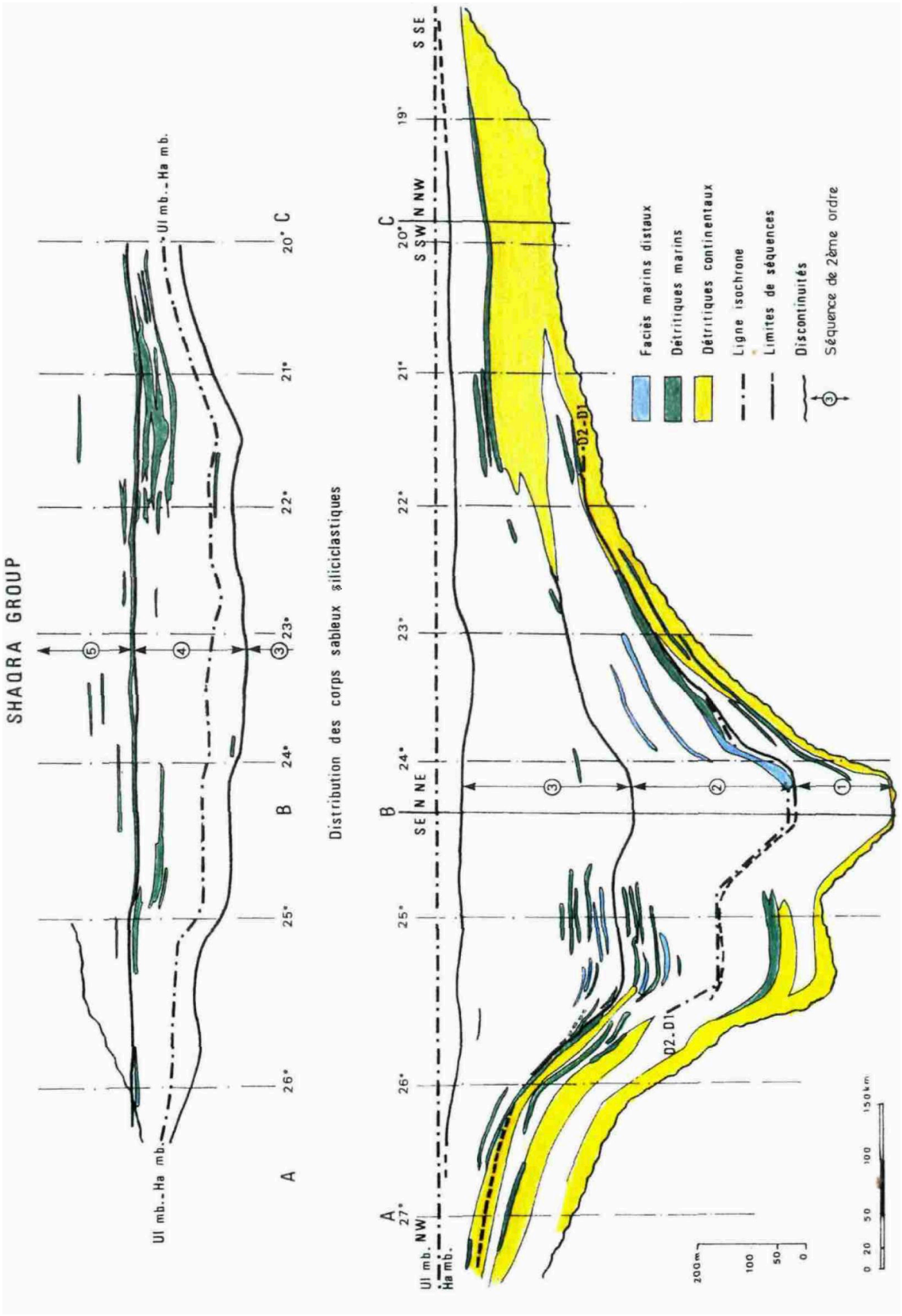

Figure 1.8: Distribution of siliciclastic sandstones in the Shaqra Group (Fig. 72 in Manivit et al., 1990).

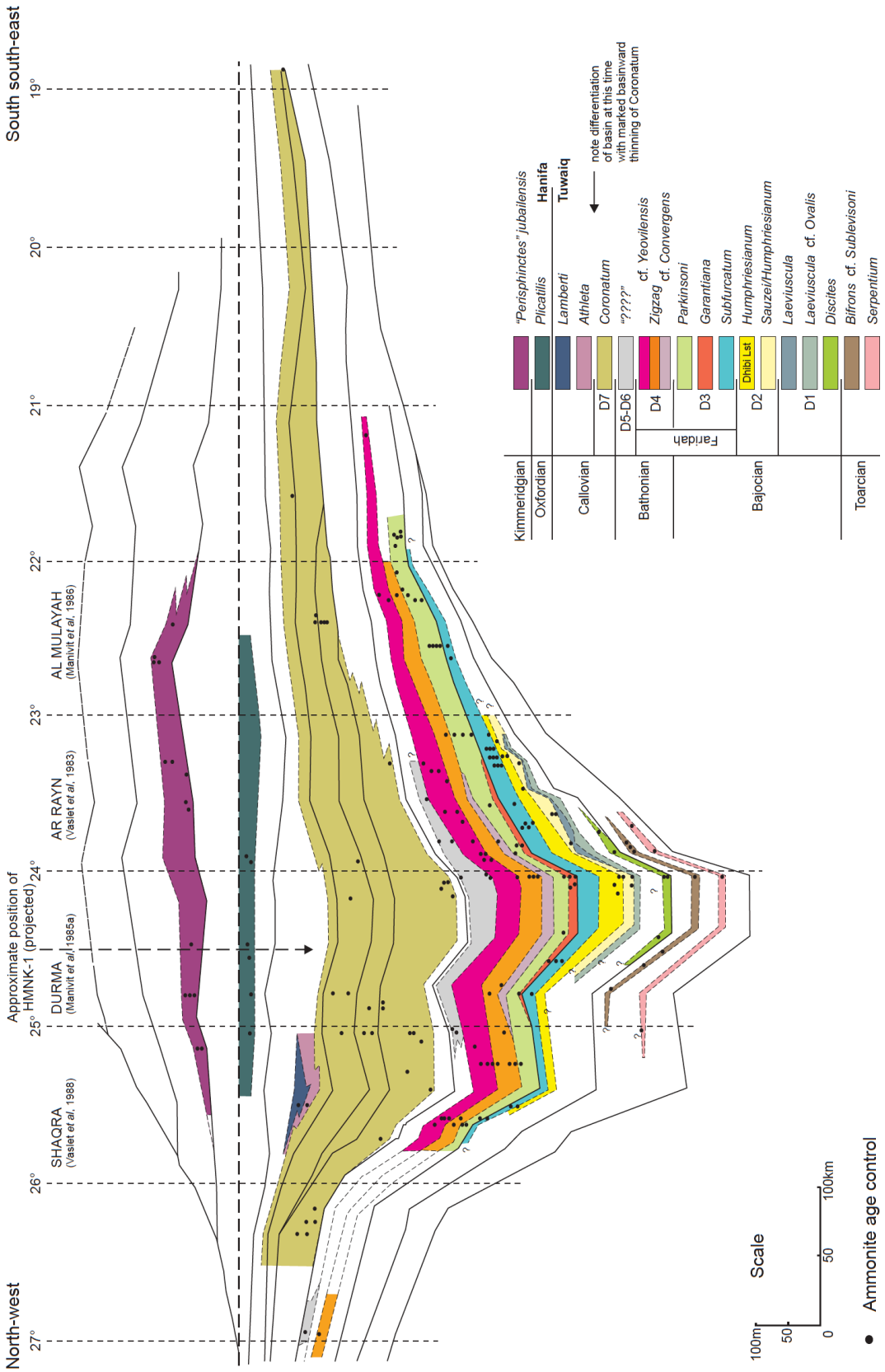

Figure 1.9: North-South cross-section of the Jurassic outcrop shows the biostratigraphic control and ammonite distribution (Modified from Manivit et al., 1990; Le Nindre et al., 1990)

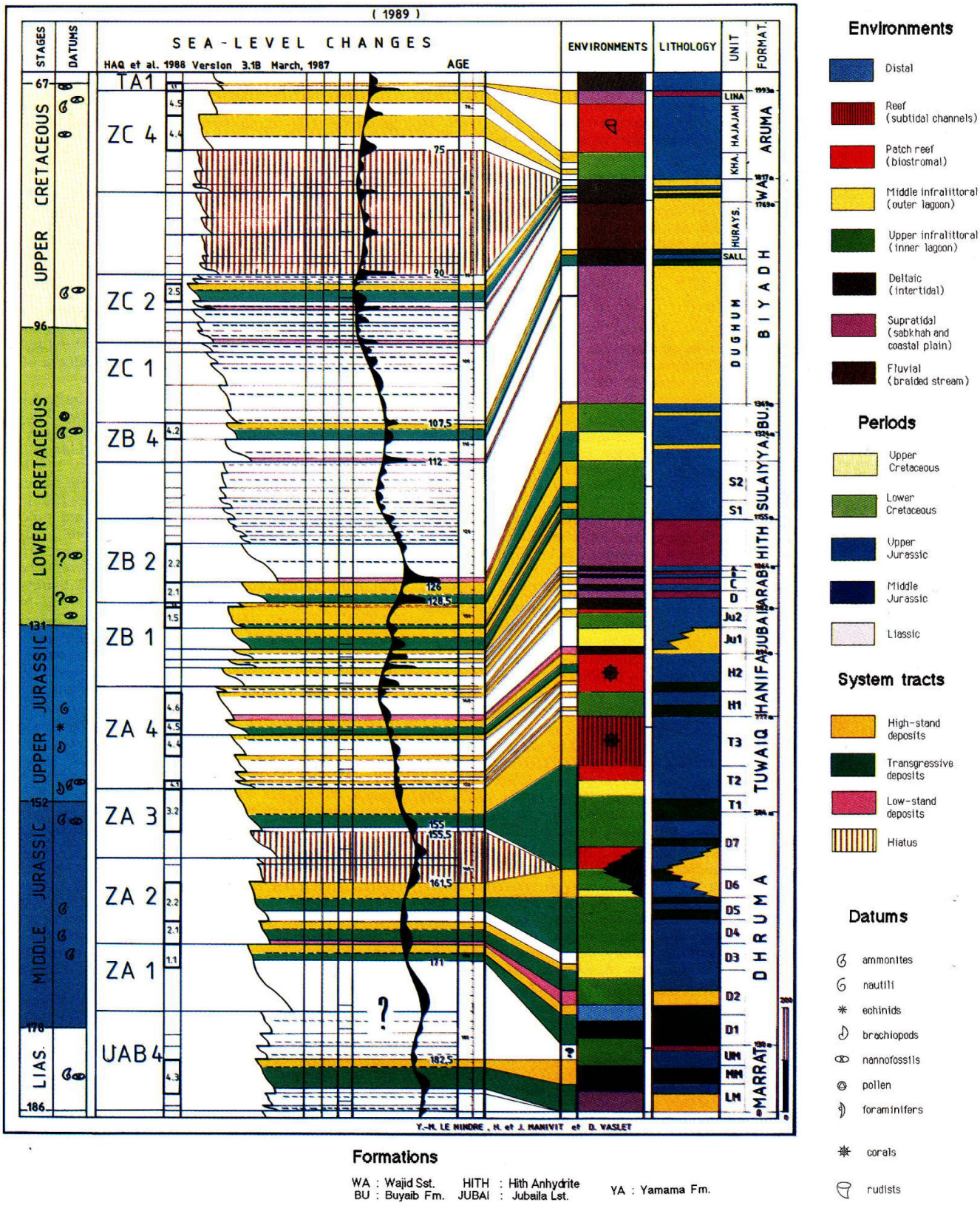

Figure 1.10: Sequence stratigraphy of the Jurassic and Cretaceous of Saudi Arabia (Fig. 3 in Le Nindre et al., 1990).

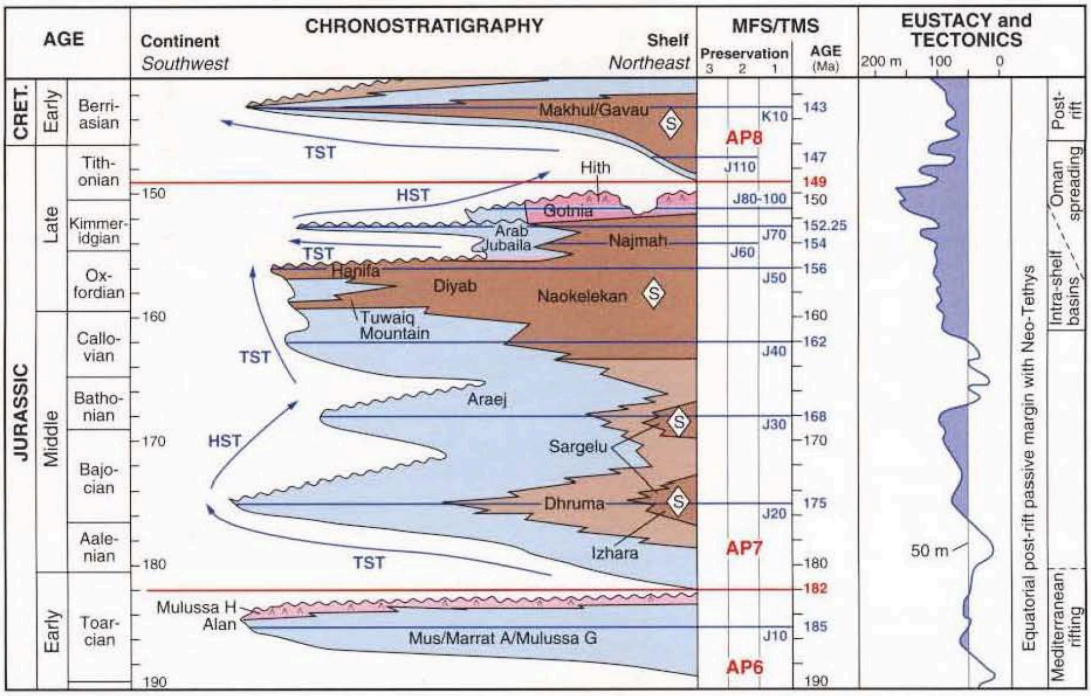

Figure 1.11: Chronostratigraphic history for the Jurassic AP7 megasequence of Sharland et al. (2001) supplemented with rescaled eustatic curve of Haq et al. (1988). The section goes from Saudi Arabia (SE) to Kuwait and southern Iraq (NE) (Fig. 3.25 in Sharland et al., 2001).

1.3.1 Marrat Formation

The Marrat Formation was first defined by Steineke (1937) in an unpublished report. The first formal definition was published by Bramkamp and Steineke (in Arkell, 1952). The lithostratigraphy of the Marrat Formation (Fig. 1.12) was updated by Powers et al. (1966), Powers (1968), in a type section located near the Marah town in Jabal Kumayt (25° 04' N). Then, Manivit et al. (1990) provided a new reference section in Khashm Ad Dhibi (24° 14' N). The Marrat Formation is bounded by two significant unconformities: the Early Jurassic hiatus at the base and the Late Toarcian – Aalenian at the top. Powers et al. (1966) divided the formation into three informal units corresponding to the lower, middle and upper Marrat Formation. Their boundaries were defined using morphologic and lithological criteria that

are clearly visible in the outcrop forming three cuestas. These boundaries have been slightly revised by Manivit et al. (1990) as following:

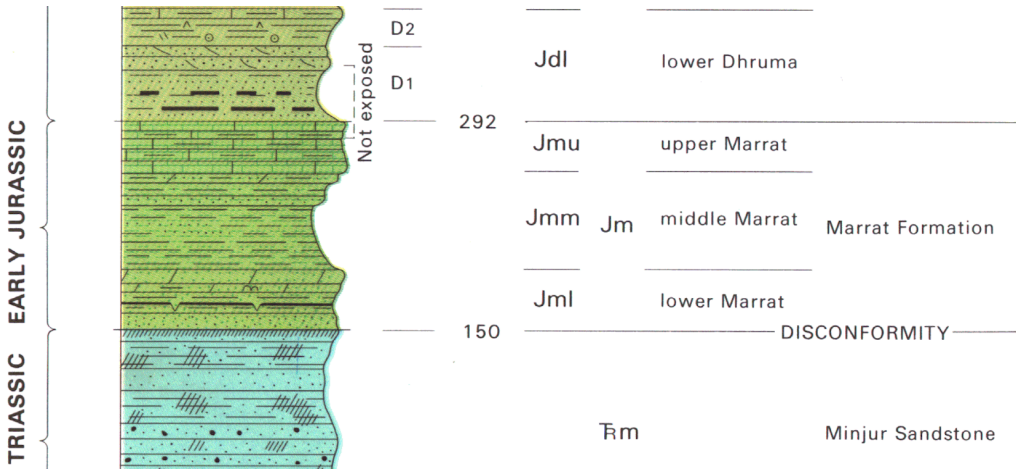

Figure 1.12: Lithostratigraphic column of the Marrat Formation (extracted from the Shaqra quadrangle map; Vaslet et al., 1988).

Lower Marrat Unit (47 m thick) is bounded at the base by the Early Jurassic unconformity marked by a black iron surface on the top of Late Triassic continental deposits (i.e., Minjur Sandstone). The lithology of the Lower Marrat unit is made up of barren shale, sandstone and thin dolomitic beds with poor fauna deposited in continental to intertidal-subtidal environments.

Middle Marrat Unit (40 m thick) is made up at the base by fossiliferous and bioturbated dolomitic limestone overlain by brick-red shale and siltstone that have no fossil record. The top of the unit is marked by calcareous shale with poor fauna. The depositional setting of this unit ranges from subtidal lagoon to intertidal setting. The base of the unit is dated by ammonites

(*Protogrammoceras, Bouleiceras*), which indicate the late-Early Toarcian Serpentinum Zone (Fig. 3).

Upper Marrat Unit (39 m thick) is a cliff-forming bioturbated lagoonal limestone dated by ammonites (*Nejdia*) indicating the Middle Toarcian Bifrons Zone. The limestone is overlain by gypsum that has been considered by Powers (1968) as the base of the Dhruma Formation.

1.3.1.1 Regional distribution of the Marrat Formation

The Marrat Formation shows lateral lithological and thickness changes along the southern part of the outcrop. The thickness of the Lower Marrat decreased rapidly up to 12 m in Wadi Birk (23° 12' N) and disappears in Al Ahmar (22° 30' N). The Lower Marrat lithology becomes mainly sandstone and shale at Khashm al Khalta (23° 35'N) and getting coarser associated with silicified wood in Wadi Birk (23° 12' N). The lower unconformity is well developed in Wadi Birk marked by black ferruginous crust on top of the Minjur Sandstone. The Lower Marrat thins and pinches out at Khashm Mawan (22° 50’N) and marked at the base by conglomeratic sandstone.

The Middle Marrat shows gradual decrease in thickness southward and reaches up to 29 m at Khashm al Hadafiyah (23° 05' N). The fossiliferous limestone, at the base of the unit, grades to bioclastic sandstone and ferruginous oolite with few fossils, echinoderms and gastropods, at Khashm al Khalta (23° 35’N) and Wadi Birk (23° 12' N). The brick-red shale is still well represented up to latitude (23° N), however, its upper third is replaced with coarse-grained sandstone with horizontal oblique stratications separated by ferrigenous-crust surfaces. Further to the south, the middle Marrat is changed

to channelized coarse and gravel sandstone with 13.5 m thick in Al Ahmar (22° 30' N) and 5 m thick at Khashm Munayyifiyah (22° 11' N).

The Upper Marrat is totally replaced by siliciclastics and thins up to 12 m at Khashm al Khalta (23° 35'N). The ammonite fauna (*Najdia*) is quickly disappeared south of latitude (23° 50'N). The siliciclastics consists of shale and cross-bedded sandstone with marine fauna. The sandstone is associated with small tidal channels. The sandstone is becoming coarser with large channels intercalated in paleosols with ferruginous-crusts and plant debris south of latitude (23° 50'N). The paleosols are well developed at Khashm Munayyifiyah (22° 11' N) and reaches to 9 m thick. At this locality, the paleosols are associated with ferruginous oolite which could be part of the overlying Dhruma Formation. South of Khashm Munayyifiyah (22° 11' N), the lithological definitions of Middle and Upper Marrat are undifferentiated.

1.3.1.2 Previous Marrat sequence stratigraphy

The Marrat Formation as a whole was considered as one transgressive – regressive cycle by Le Nindre et al. (1990) with an MFS at the base of the Middle Marrat (Serpentinum Zone) corresponding to UAB 4 of Haq et al. (1987) (Fig. 1.10). Al-Husseini (2009) subdivided the Marrat Formation into two 3rd-order sequences (Marrat Sequence B and A) based on a review and interpretation of a single section description of Powers et al. (1966), Powers (1968) and Manivit et al. (1990). These two Marrat sequences correspond to the so-called DS^3 13.5 and 13.6 of the Arabian Orbital Sequence (AROS; Al-Husseini and Matthews, 2008; Al-Husseini, 2009). The Marrat Sequence B includes Lower and Middle Marrat. The transgressive system tracts (TST) are

represented by the barren continental shale in the Lower Marrat. The maximum flooding interval (MFI) corresponds to fossiliferous and bioturbated limestone base of the Middle Marrat. The highstand coincides with brick-red shale and siltstone of the Middle Marrat. The Marrat sequence A includes the Upper Marrat where the TST and MFS are interpreted in the basal bioclastic limestone and the kaki shale with the ammonite fauna. The highstand corresponds to the upper gypsum unit in the upper part of the formation.

Based on regional correlations of the Jurassic system, Sharland et al. (2001) have placed a maximum flooding surface (MFS J10) in the Middle Toarcian upper Marrat Formation (Fig. 1.11). However, Kadar et al. (2015) have placed the MFS J10 in the lower part of the Middle Marrat, Early Toarcian (Serpentinum Zone), based on outcrop correlation of Saudi Arabia and subsurface of Kuwait.

1.3.1.3 Marrat Formation hydrocarbon reservoirs

In the subsurface, the Marrat Reservoir in the Eastern Province of Saudi Arabia is equivalent to the upper part of the formation (Ayres et al., 1982 in Al-Husseini, 2009 and Manivit et al., 1990).

1.3.2 Dhruma Formation

The Dhruma Formation was named after the Darmā city west of Ar Riyadh. Its type section was first described by Steineke and Bramkamp (in: Arkell, 1952) and is located near the Khashm Ad Dhibi between the coordinates 24° 12’ 04’’ N, 46° 07’ 05’’ E (Khashm Ad Dhibi) and 24°19’ N, 46°19’06’’ E (Khashm Madhrud or ‘Al Mazru’i’). Likewise, Steineke,

Bramkamp, and Sander (1958), divided the formation into three divisions: lower, middle and upper. These divisions were maintained by Powers et al. (1966) who subdivided the upper unit into two informal members (Atash Member and Hisyan Member) using lithological and faunal criteria. Powers (1968) raised the uppermost part of the lower Dhruma into an informal member called the Dhibi Limestone Member. Vaslet et al. (1983) divided the formation into seven units (Fig. 1.13). The units include: D1-D2 (lower Dhruma), D3-D6 (Middle Dhruma), and D7 (upper Dhruma). There is a critical stratigraphic hiatus and poorly dated interval between the middle and the upper Dhruma Formation. The lithostratigraphic and biostratigraphic definitions of the Dhruma Formation as described by Manivit et al. (1990) are:

D1 unit (57 m thick) is a mixed carbonate-siliciclastic dominated unit deposited in an inner platform environment. This unit overlies the Late Toarcian-Aalenian unconformity. The unit contains significant ammonite intervals indicating an Early Bajocian age (Discites and Laeviuscula Zone) (Fig. 1.6; Énay et al., 1986).

D2 unit (86 m thick) is dominated by green and yellow calcareous shale, lower 46 m. The upper part is equivalent to the Dhibi Limestone Member. Moreover, the member is characterized by a specific faunal association that has been recognized the subsurface of Saudi Arabia (Powers et al., 1966; Powers, 1968). The D2 unit is dated lower-Middle Bajocian (Humphriesianum Zone) (Énay et al., 1984) and Late Bajocian (Niortense Zone) (Fig. 1.6).

D3 unit (52.5 m thick) is made up of two lithological assemblages. The lower set is made of yellow bioclastic oolitic peloidal grainstone interbedded by fine limestone. The upper part of is made up of bioclastic peloidal

grainstone with some ooids limestones. The lower set is dated Late Bajocian (Garantiana and Parkinsoni Zone). The top D3 unit has Early Bathonian ammonite fauna (Zigzag Zone).

D4 unit (44 m thick) starts with coarse grainstones composed of intraclasts, bioclasts and oolites. These grainstones are occasionally interbedded with nodular fine-grained pelletal bioturbated limestone and capped by hardground. The D4 unit is dated Early Bathonian (Zigzag Zone; convergens Subzone) based on ammonite fauna (*Tulites tuwaiquensis* ARKELL) found in the middle of the unit (Manivit et al., 1990; Énay et al., 2009).

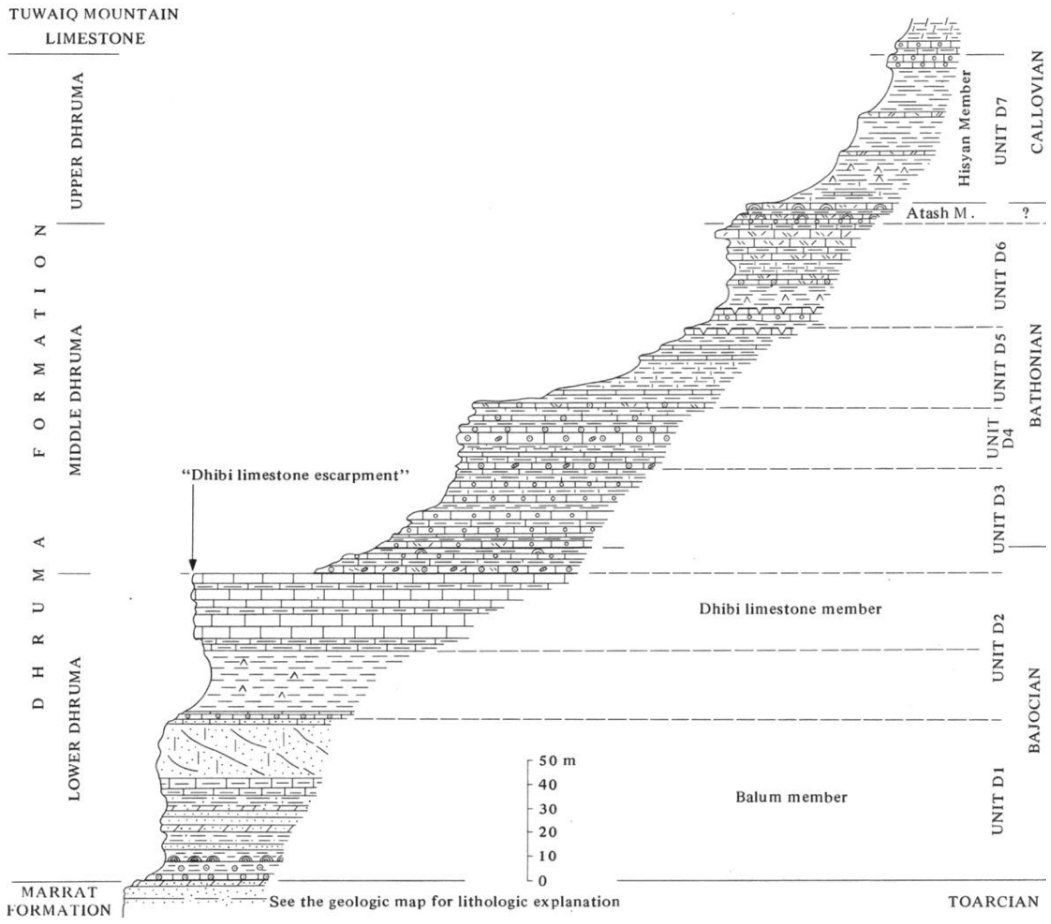

Figure 1.13: Generalized lithostratigraphy of the Dhruma Formation (extracted from the Wadi ar Rayn quadrangle map; Vaslet et al., 1983).

D5 unit (41 m thick) shows a progressive increase in shale content to the middle of the unit. The unit has been divided into three lithological assemblages. The lower part is brown bioclastic grainstone with ammonites. The middle part is platy laminated limestone and white or cream argillaceous limestone followed by green calcareous shale. The upper part is more carbonate-prone represented by fine white limestone and brown bioclastic oolitic grainstone. These carbonate successions are capped by cemented hardground and are interbedded with calcareous shale. The unit is dated early Bathonian (Zigzag Zone, Yeovilensis Subzone), which is equivalent to Aurigerus Zone (Recinctus Subzone) in the Submediterranean zonal scale *(*Manivit et al., 1990; Énay et al., 2009).

D6 unit (55.5 m thick) contains an alternation of shale and limestone. The lower and middle part of the unit made up of green shale and pelletal bioclastic limestone. The shale is capped by a brown cross-bedded peloidal grainstone forming a resistant benches. The age of D6 contains an endemic ammonite (*Dhrumaites*) which cannot be correlated with the European fauna associations. Moreover, a nautilus found in Wadi al Hisyan (24° 45'N) indicates an Early-Bathonian age (Tintant, 1987; in Fischer et al., 2001), whereas brachiopod faunas are suggest a Late-Bathonian age for the D6 unit (Alméras, 1987; in Fischer et al., 2001).

D7 unit (111 m thick) is made up of two members (Atash and Hisyan). ***The Atash Member*** (26 m thick) is a carbonate-dominated succession, at the base of D7 unit, of brown intraclastic reefal grainstone and highly fossiliferous bioturbated limestone. The member has been dated Callovian based on nautiloids (two species), echinoids, ostracods, foraminifers, and nannoflora.

The benthic foraminiferal assemblage containing *Trocholina* (*Trocholina elongata*), *Praekurnubia* and *Kurnubia* supports a Callovian age. According to Hélène Manivit (written comm. in Manivit et al., 1990) a more precise age is given by the nannoflora association, including *Watznaueria manivitae* and *Stephanolithion bigoti*, which indicates the Middle Callovian age. This age matches the *Stephanolithion bigoti* zone (Haq et al., 1988, in Le Nindre et al., 1990); however, from more recent work on nannoflora (Kadar et al., 2015), it seems that a larger range of ages would be possible e.g. zone NJT12, Late Bathonian – Late Callovian.

The Hisyan Member (85 m thick) is a shale-dominated succession which forms a recessive unit at the base of the Tuwaiq Mountain Limestone. The member is highly fossiliferous and contains a highly diverse fauna including a diversified ammonite fauna characterizing the late Middle Callovian, Coronatum Zone.

1.3.2.1 Regional distribution of the Dhruma Formation

The Dhruma Formation grades is mixed carbonate-siliciclastic inner platform that grades southward to deltaic and continental sandstone. Ferruginous oolite occurs at the transition between the mixed carbonate-siliciclastic and the deltaic sandstone, which has been mapped specifically by Le Nindre et al. (1984) (cf. Figure 48 in Manivit et al., 1990). The ferruginous oolite is associated with dolomite, sandstone and shale and composed of echinoderms, bivalve and plant debris. The depositional environment of the ferruginous oolite is transitional between marine and continental (Le Nindre et al., 1984).

The lower Dhruma (D1 and D2 units; Early Bajocian to Late Bajocian) kept their chronostratigraphic identity to the south up to Jabal Fahhamah (22° 02' N). At this locality, the D1 unit is made up of non-marine shale and sandstone. The D2 unit (Dhibi Limestone Member) becomes dolomitic and contains Late Bajocian ammonite. At Khashm Abu al Jiwar (21° 53' N), the D3 unit grades to dolomitic sandstone and shale with high-faunal diversity (e.g., ammonite, nautilus, echinoderms, coral, brachiopods, foraminifera *Lenticulina* sp., and ostracods). At this locality, the D4 and D5 units made up of cream-yellow limestone with reddish-brown dolomite beds. This limestone extends further to the south up to Khasha Mishlah (21° 07’ N) and dated Early-Bathonian (Zigzag Zone, Yeovilensis subzone) (Fig. 1.9; Manivit et al., 1990).

The D6 unit is poorly dated and is equivalent updip to coastal/continental siliciclastic sediments named "Wadi ad Dawasir delta" (Fig. 1.14; Le Nindre, 1987; Manivit et al., 1990) which lacks age-diagnostic fauna. Moreover, The lithology and biostratigraphy assemblages of the D6 unit are changing dramatically southward. For example, its endemic ammonite fauna (*Dhrumaites*) is not known south of Khashm Al Jufayr (23° 50' N). Further to the south, at Khashm Ushayrah (22° 37' N), the unit appears to have two distinct zones. The lower zone is shale dominated and the upper one is bioclastic grainstones interbedded with sandstone composed of crinoids and phosphatic debris. Near Al Haddar (22° 02' N), the upper grainstone is replaced with sandstone with plant debris. The Top of the D6 unit is marked by purplish-green pedogenic shale. South of Al Haddar (22° N), the D6 unit becomes continental sandstone sediments.

Based on this lithostratigraphic and biostratigraphic work of Le Nindre et al. (1987, 1990) and Manivit et al. (1990), there are two proposed chronostratigraphic and genetic correlation between the D6 unit and the "Wadi ad Dawasir delta" (Fig. 1.15, 1.16; Énay et al., 2009). The first interpretation is the original work of Le Nindre et al. (1987, 1990) and Manivit et al. (1990) (Fig. 1.15a). The second interpretation (Fig. 1.15b) was proposed by Énay et al. (2009) and was based on reevaluation of the biostratigraphic data (ammonite, nautilus, brachiopods and calcareous nannoplankton). Both interpretations placed the unconformity on top of the sandstone wedge "Wadi ad Dawasir delta". The first study correlated the unconformity to the top of D6 unit in the type section (Fig. 1.16). Énay et al. (2009) placed the unconformity between D5 and D6 in the type locality (Fig. 1.16). This is because, the D6 and D7 (Atash Member) are biostratigraphically related to each other, i.e., they contain same brachiopod fauna dated as Late Bathonian and Early Callovian.

The lateral biostratigraphic and lithostratigraphic changes of the upper Dhruma D7 unit is well controlled in the outcrop. The D7 unit is highly fossiliferous and its biostratigraphic characteristics extended further to south up to Fara'id al Ahmar (22° 27' N). At this locality, the Atash Member (10 m thick) still consists of isolated coral heads in argillaceous limestone facies. The Atash Member is no longer recognized south of Fara'id al Ahmar (22° 27' N). At Jabal Shimrakh (22° 10' N), the green shale of the Hisyan Member contains abundant microfauna dating Bathonian and Callovian age and starts to be interbedded with ferruginous oolite and sandstone at its base. Further to south, green shale of the Hisyan Member grades to sandstone. At Khashm

Abu al Jiwar (21° 53' N), the upper part of D7 unit is argillaceous limestone rich with fossils (e.g., nautilus, brachiopod and many bivalves). The lithology and biostratigraphy of the upper D7 unit is similar to the base of Tuwaiq Mountain Limestone which suggests a conformable stratigraphic contact. South of Khashm Abu al Jiwar (21° 53' N), the D7 unit is made up of continental sandstone, distributary channels and interdistributary bays (Fig. 1.14; Manivit et al., 1990).

1.3.2.2 Previous Dhruma sequence stratigraphy

The Lower Dhruma (D1 and D2 units) is considered as two T-R cycles separated by erosional surface known by pre-Dhibi unconformity (Powers 1968; Le Nindre et al., 1990; Hughes, 2009; Al-Husseini, 2009). The main maximum flooding surface (MFS) of the lower Dhruma was placed in the upper shaly interval of the D1 unit (Early Bajocian) (Manivit et al., 1990; Le Nindre et al., 1990; Sharland et al., 2001; Al-Husseini, 2009). However, others considered the Dhibi Limestone Member (Late Bajocian) as the main MFS of the Lower Dhruma Formation (Powers, 1968; Fischer et al., 2001).

The Middle Dhruma Formation was considered a 3rd-order depositional sequence (DS^3 12.4) by Al-Husseini (2009). The middle Dhruma Formation shows a transgression continuation overlying the Marrat Formation in the southern outcrop (Powers et al., 1966; Manivit et al., 1990). The main MFS of the Middle Dhruma Formation was placed in the D5 unit (Al-Husseini, 2009; Énay et al., 2009; Sharland et al., 2001). The regression of this sequence is marked by the a progradation of the deltaic sandstone wedge capped by the

Bathonian-Callovian disconformity (Al-Husseini, 2009; Énay et al., 2009; Le Nindre et al., 1990).

The Upper Dhruma Formation (Atash and Hisyan Members) and the overlaying Tuwaiq Mountain Limestone can be genetically related (Énay et al., 2009; Hughes, 2004, 2006; Le Nindre et al., 1990). However, other interpretation based on subsurface correlation suggested that an unconformity separating the Upper Dhruma Formation and the Tuwaiq Mountain Limestone (Powers, 1968).

1.3.2.3 Dhruma Formation hydrocarbon reservoirs

The Dhruma Formation contains three hydrocarbon reservoirs (Faridah, Sharar and Lower Fadhili). The Faridah and Sharar reservoirs are well developed in the NE area of Saudi Arabia. The Faridah reservoir consists of five zones (A-E). The equivalent of the Faridah reservoir in outcrop is the Dhibi Limestone Member and D4 unit. The Sharar reservoir is equivalent to D5 unit (Toland et al., 2013, unpublished Aramco report). The Lower Fadhili is an extensive broad hydrocarbon reservoir equivalent lithostratigraphically and biostratigraphically to the Atash Member (Powers et al., 1966; Al-Mojel, 2010). The Lower Fadhili Reservoir is economically significant interval appears in large oilfield in Saudi Arabia and in the Middle East (Powers et al., 1966; Al-Mojel, 2010).

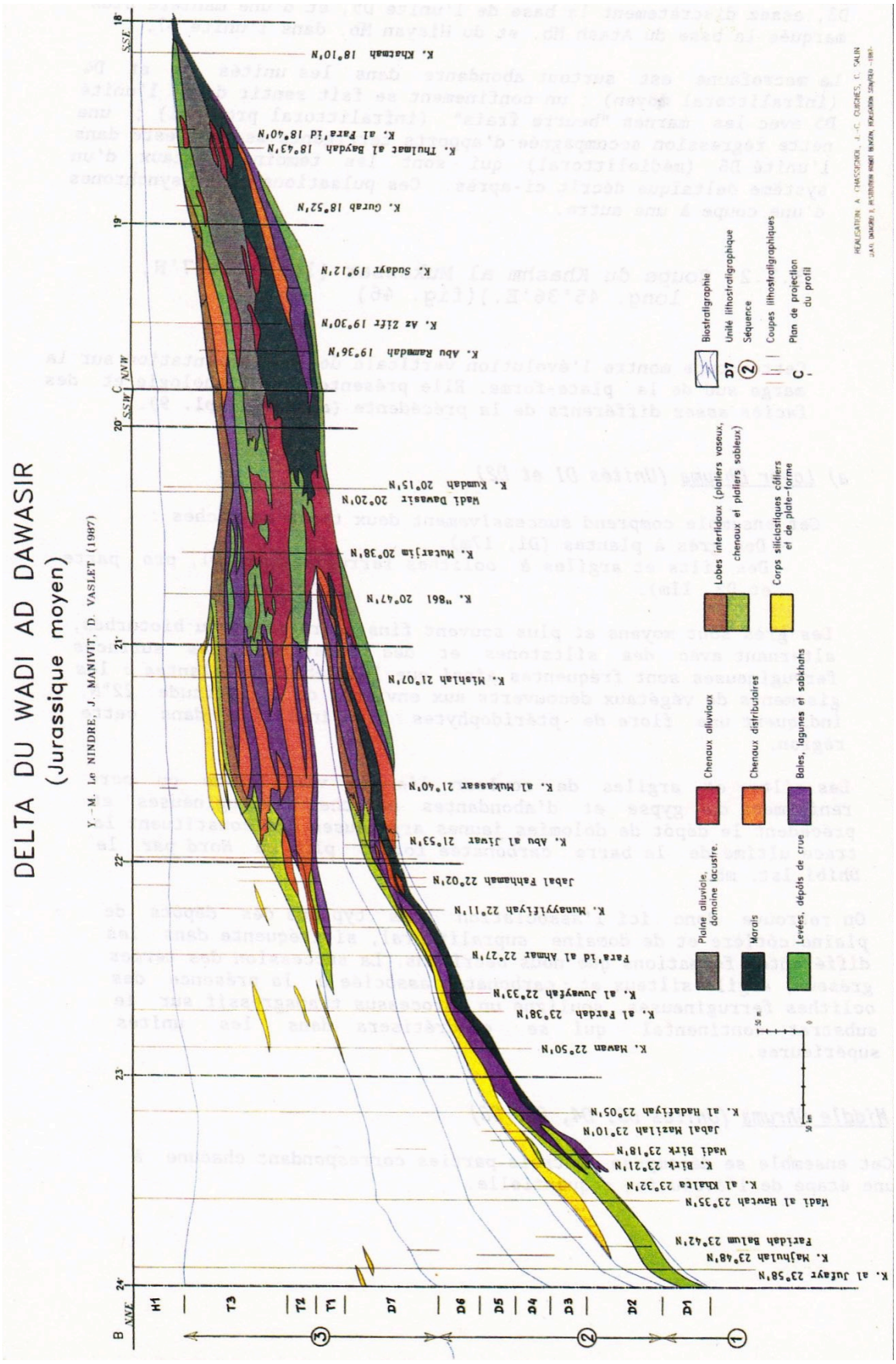

Figure 1.14: North-south cross-section of southern outcrop shows the depositional environments of Wadi ad Dawasir delta (Fig. 46 in Manivit et al., 1990).

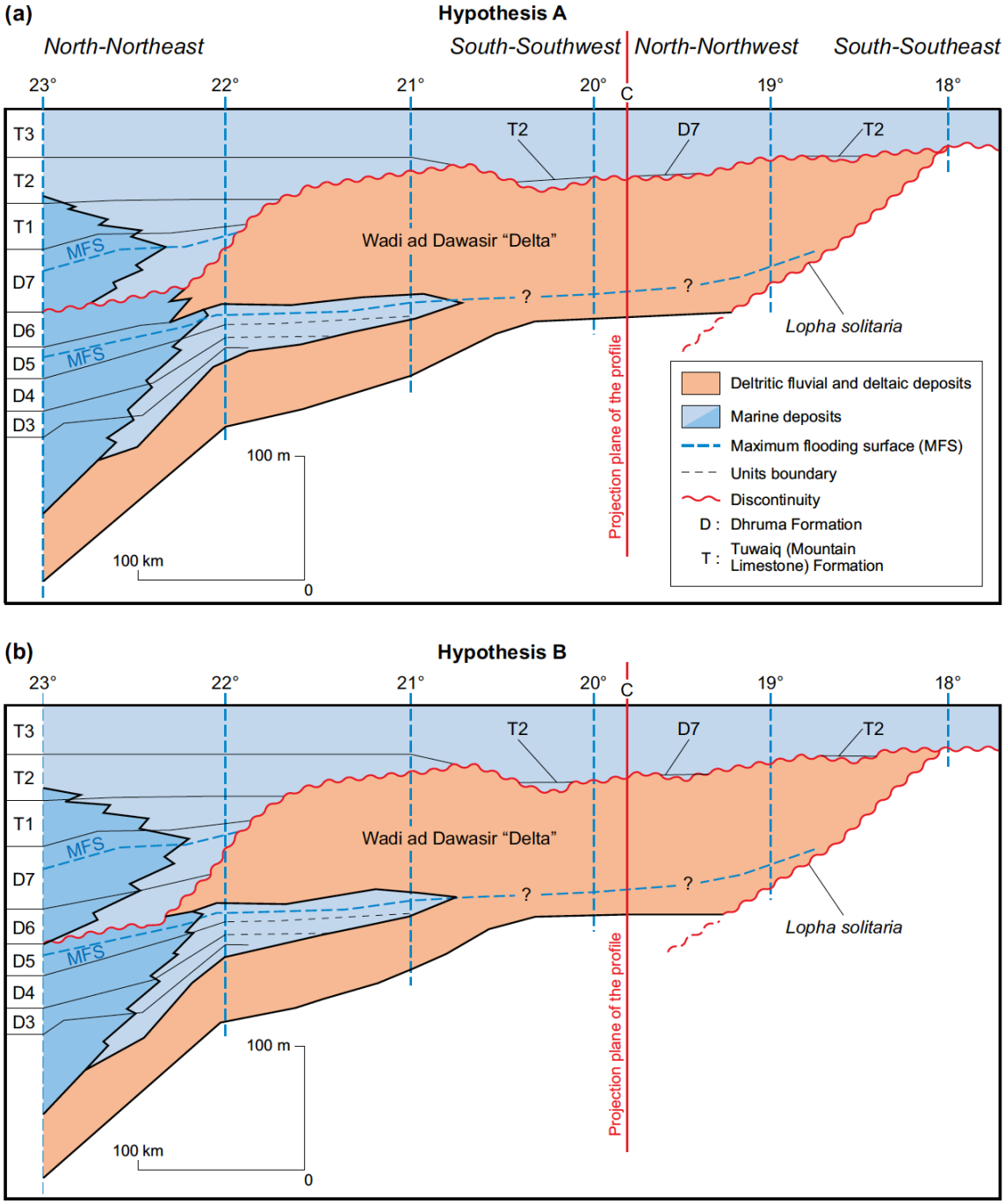

Figure 1.15: North-south cross-section of the southern outcrops shows two proposed chronostratigraphic and genetic correlation between the D6 unit and the "Wadi ad Dawasir delta" (Figure 9 of Énay et al., 2009).

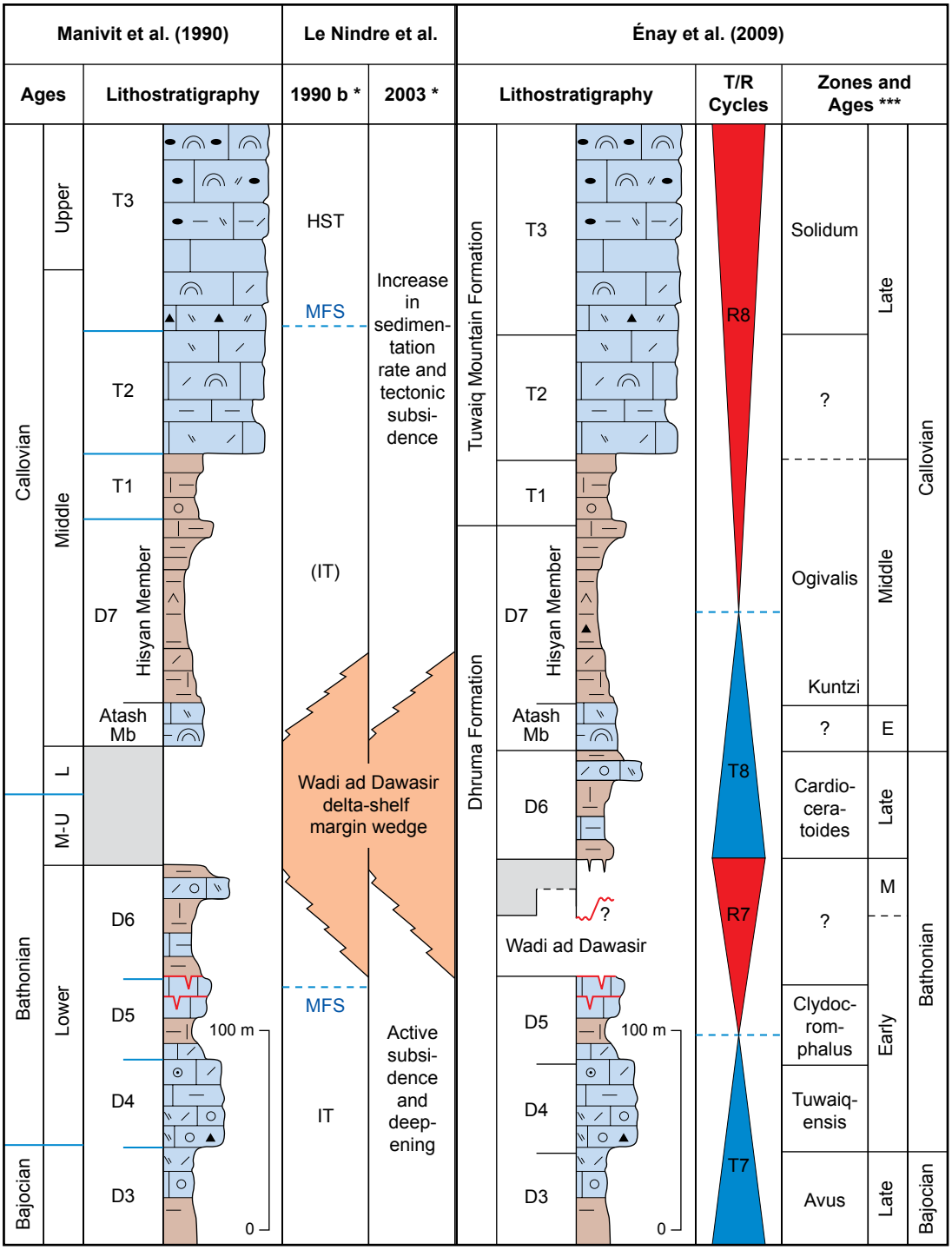

Figure 1.16: Khashm Ad Dhibi section with two proposed stratigraphic intervals that are equivalent to the "Wadi ad Dawasir delta" (modified after Énay et al., 2009).

1.3.3 Tuwaiq Mountain Limestone

The formation is named after the limestone escarpment called Jabal Tuwayq. The type section of the Tuwaiq Mountain Limestone is Haisiyan Pass (Wadi al Hisyan) (24° 55' N, 46° 10' E) with a thickness of 215 m. The formation was divided into three informal units (T1, T2 and T3; Fig. 1.17) by Vaslet et al. (1983) based on lithostratigraphic criteria. The reference section is in the road cut of the Riyadh-Mecca highway near Khashm Qaddiyah (24° 31' N). The formation is unconformably overlain by shale of the Hanifa Formation with silicified coral reef and oxidized-iron crust.

The lithostratigraphy and biostratigraphy of the these units as descried by Manivit et al. (1990) are as follow:

T1 unit (32 m thick) is a recessive-weathering unit at the toe of the escarpment. The unit consists of white limestone with slight calcareous shale interbedded with brown fossiliferous intraclastic grainstone beds. The sediments are rich with sandstone-quartz. The upper part of the unit has wavy nodular layering. The T1 and T2 units are Middle Callovian (Coronatum Zone) in age based on the ammonite fauna supplemented by echinoderms, brachiopods and foraminifera (Manivit et al., 1990).

T2 unit (56 m thick) is made up of massive bedded bioclastic white limestone (wackestone and packstone) interbedded with thin shale and intraclastic grainstone. The top of the massive beds are bioturbated and have isolated coral and stromatoporoid reef (with heads up to 40 cm diameter).

T3 unit (96 m thick) is a massive limestone characterized at the base by two beds of reworked bioclastic grainstone with a ravinement surface. The

unit is rich with domed reefs up to 10 m high and 15-30 m diameter. The upper part of the unit is characterized by branching coral debris. The lower T3 unit is dated Middle Callovian (Coronatum Zone) based on ammonite fauna (*Erymnoceras doliforme* and *Pachyerymnoceras* sp.) and nautilus fauna (*Paracenoceras* aff. *dilatatum*) in the southern outcrops. Whereas, in the northern outcrops, the upper T3 unit is dated Late Callovian (Athleta and Lamberti Zone) in Shaqra quadrangle (Fig. 1.9; Mu'ayshibah 25° 34’ N; El Asa’ad, 1989 in Manivit et al., 1990).

1.3.3.1 Regional Distribution of Tuwaiq Mountain Limestone

The Tuwaiq Mountain Limestone is the most prominent cliff forming and extensive traceable carbonate unit in the Jurassic outcrops. The formation overlays the "Wadi ad Dawasir delta" of the Dhruma Formation to the south at Huwaymil (17° 30' N; Fig. 1.14 and 1.15). The T1 and T2 units grade laterally to siliciclastic sediments to the south. The T1 unit becomes green shale with low-diversity fauna at Wadi al Haddar (22° 02' N). The T1 unit is no longer recognized at Khashm al Mukassar (21° 36' N). The lower carbonate of T2 unit has marine sandstone overlying pedogenic and conglomeratic sediments of the upper Dhruma Formation at Khashm al Mukassar (21° 36' N). At Khashm Kumdah (20° 18' N), the entire T2 unit is made up of siliciclastic with paleosol features and ferruginous oolite with plant debris. Further to the south at Khashm Ghurab (18° 52' N), the top of the T2 unit shows a white nodular limestone bed (1 m thick) contains the most southern biostratigraphic control of the Tuwaiq Mountain Limestone with the ammonite (*Erymnoceras*).

The T3 unit thins gradually to the south and maintained its lithological characteristics. At Khashm Abu al Jiwar (21° 53' N), the top of the unit still is rich with coral heads that reach up to 30 cm diameter. At Khashm al Mukassar (21° 36' N), the base of T3 unit yields the most southerly biostratigraphic control, which is Middle Callovian (Coronatum Zone) ammonite (*Erymnoceras doliforme*). Further southward, the base of T3 unit has sandstone layers, whereas, the upper part is still highly bioturbated nodular limestone with heads of coral.

1.3.3.2 Previous Tuwaiq sequence stratigraphy

Al-Husseini (2009) considered the Tuwaiq Formation as a single 3rd-order sequence (DS^3 12.6; Fig.). The Hisyan shale underneath the Tuwaiq Mountain Limestone considered as the main MFS of the Tuwaiq depositional sequence (Sharland et al., 2001; Énay et al., 2009). However, others considered the upper Tuwaiq Mountain Limestone (between T2 and T3 units) as the main MFS of the Tuwaiq deposits (Le Nindre et al., 1990; Manivit et al., 1990; R. B. Davies in Kadar et al., 2015).

1.3.3.3 Tuwaiq Mountain Limestone hydrocarbon reservoirs

The Tuwaiq Mountain Limestone hosts two hydrocarbon reservoirs in eastern Saudi Arabia, Upper Fadhili Reservoir (T1 unit) and Hadriya Reservoir (T3 unit) (Ayres et al., 1982; Powers, 1968). Moreover, the formation represents the most significant and extensive Jurassic source rock in the subsurface of central Arabia (Pollastro, 2003).

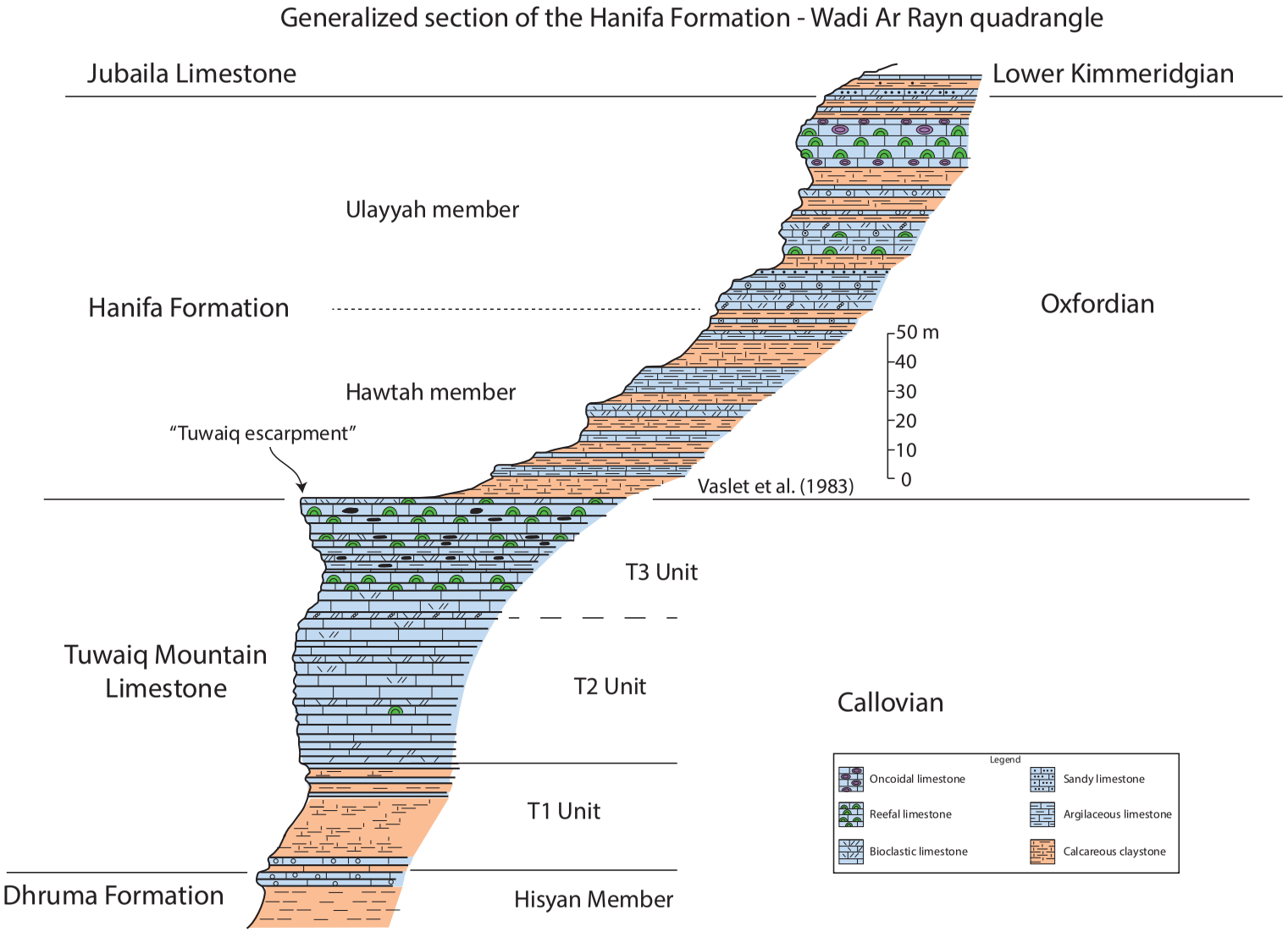

Figure 1.17: Generalized lithostratigraphy of the Tuwaiq Mountain Limestone and Hanifa Formation (extracted from the Wadi ar Rayn quadrangle map; Vaslet et al., 1983).

1.3.4 Hanifa Formation

The basal boundary of the Hanifa Formation shows a sharp lithological contrast between the cliff forming Tuwaiq Mountain Limestone and the base Hanifa shale. The basal boundary corresponds to a stratigraphic hiatus covering the lower part of the Oxfordian (Mariae Zone) (Le Nindre, personal communication, 2014; and in Kadar et al., 2015). Moreover, this boundary is known in subsurface to be marked by an erosional surface responsible for the truncation of the last Tuwaiq Mountain sequence in the Rub' al-Khali and northern of the Ghawar field ("pre-Hanifa unconformity" of Powers, 1968). The top boundary of the Hanifa formation is marked by a stained reddened surface but is considered as a conformable surface (Powers, 1968; Manivit et al., 1990). The Hanifa formation is classically divided into two formal members, the Hawtah (H1) and the Ulayyah (H2) members (Vaslet et al., 1983; Fig. 1.17). At the outcrop, the Hawtah Member is always represented by pale yellow calcareous shales at the base. The calcareous shales are interbedded with carbonate beds forming small cuestas on top of the Tuwaiq Mountain Limestone cliff. The lower part of the Member is attributed to the Early Oxfordian (? Cordatum Zone) based on brachiopod fauna (*Ornithella* gr. *hudlestoni* DAV.) and on nautilus (*Paracenoceras* sp. aff. *arduennense*; Ar Rawdah section) (Manivit et al., 1990). The only confirmed ammonite zone in the Hanifa Formation is Middle Oxfordian (Plicatilis Zone) based on ammonite fauna (*Euaspidoceras catenaperarmatum* and *Perisphinctidae*?), nautilus (*Paracenoceras* aff. *hexagonum*) and nannoflora (*Vekshinella stradneri*) found in the upper part of the Hawtah Member (Manivit et al., 1990).

Ulayyah Member is characterized by a brown intraclastic grainstone unit at the base and cliff forming reef dominated beds at the top. This member is defined by the first appearance of the foraminifer *Alveosepta Jaccardi.* No ammonite fauna have been found in the Ulayyah Member. However, the member is dated Late Oxfordian based on foraminifera (*Alveosepta Jaccardi*) and brachiopods (*Terebratula bisuffarcinata*) found at the lower half of the member (Manivit et al., 1990). The upper half is dated Early Kimmeridgian based on echinoids (*Monodiadema kselensis* and *Pseudocidaris thurmanni*) and *Alveosepta Jaccar* (Manivit et al., 1990).

1.3.4.1 Regional distribution of the Hanifa Formation

The maximum thickness of the Hanifa formation is 160 m in As Sitarah (22° 36’ N). The formation thins gradually to the north and south of As Sitarah area. Moreover, the formation maintained its lithological characteristics to the most southern outcrop Huwaymil (17° 30' N) and it is never changed laterally to sandstone.

The Hawtah Member is always characterized at the base by pale yellow calcareous shale (D. Vaslet, 2013, personal communication). The Hawtah Member shows little lateral lithological changes to the south. Hardgrounds and desiccation surfaces with quartz grains are noticed in Wasit (22° 24' N) and Wadi al Misyab (21° 50' N). Further to south, the succession shows isolated reef heads and beds of dolomite at Khashm Kumdah (20° 18' N). The biostratigraphy of the Hawtah Member is well controlled in the southern outcrops. At Khashm al Hadafiyah (23° 05' N), the Middle Oxfordian age is

controlled by nannoflora (*Vekshinella stradneri*) found in the upper half of the member.

The top of the Ulayyah Member is rich with reef limestone at As Sitarah (22° 36’ N). At Wadi al Haddar (22° 02' N), the top of the Ulayyah Member is rich with bioclastic grainstone with hardground surfaces and some dolomitization. The biostratigraphy of the Ullayyah Member is controlled by Oxfordian brachiopod (*Terebratula bisuffarcinata*) found at the base of the member in Al Hariq (23 ° 30' N). Moreover, at As Sitarah (22° 36’ N), the upper part of the Ulayyah Member is dated Late Kimmeridgian based on echinoderm (*Pseudocidaris thurmanni*).

1.3.4.2 Previous Hanifa sequence stratigraphy

Le Nindre et al (1990) allocated the main MFS of the Hanifa Formation in the Hawtah Member (H1) in the lithological assemblage [4] of Manivit et al. (1990). This is consistent with the 2nd order Middle Oxfordian MFS (J50 of Sharland et al., 2001). Le Nindre et al (1990) interpreted the reefs at the top of the Hanifa Formation as highstand system tracts (HST), whereas Fischer et al. (2001) interpreted the new appearance of the benthic foraminifera (*Alveosepta jaccardi*) and the bioherm reefs at the top if the formation as a new transgression event. Mattner and Al-Husseini (2002) divided the Hanifa Formation into two 3rd-order shallowing upward sequences (Hawtah sequence DS^3 11.1, Ulayyah sequence DS^3 11.2) based on a single lithological description of Manivit et al. (1990) and Vaslet et al. (1991). Simmons et al. (2007) revised the MFS J50 and placed it in the Early Oxfordian (Cordatum

Zone) and placed MFS J60 in the Late Oxfordian instead of Early Kimmeridgian (Al-Husseini, 2009).

Hughes et al. (2008) interpreted two T-R sequences for the Hanifa Formation along the road cut of Riyadh-Mecca highway (Fig. 1.18; near Khashm Qaddiyah 24° 31' N). This was based on microbiofacies and lithology studies. They considered each member as T-R sequence and placed their MFS in argillaceous limestone at the base of the members. In addition, they interpreted the upper part of the formation as late highstand system tracts (HST).

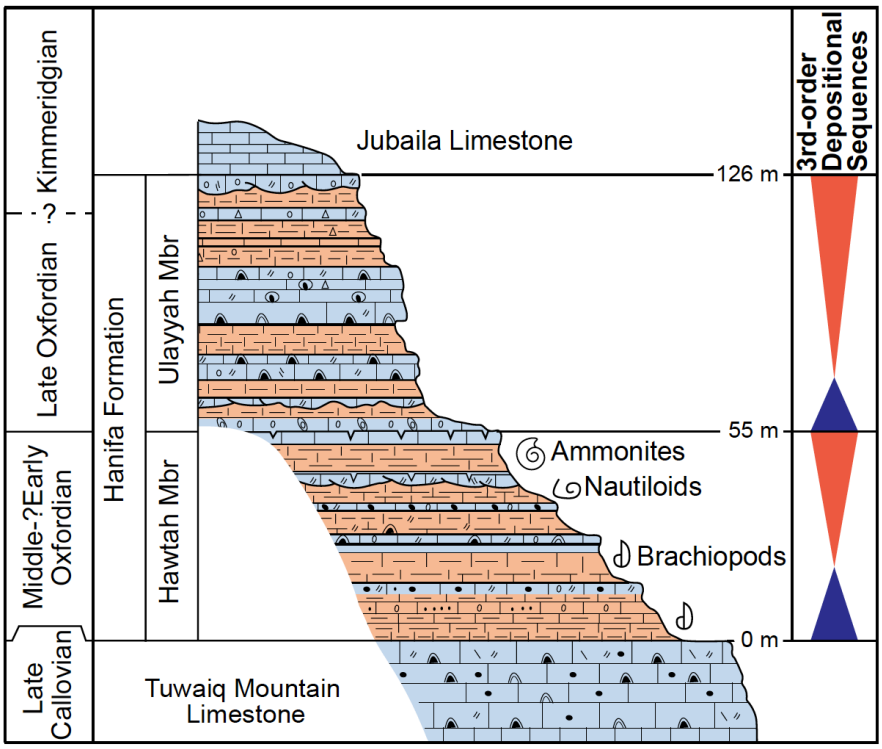

Figure 1.18: Lithostratigraphy and chronostratigraphy of the Hanifa Formation in Wadi Dirab (west of Riyadh) with sequence stratigraphy interpretation of Hughes et al (2008). (after Vaslet et al., 1991; Mattner and Al-Husseini, 2002; Al-Husseini et al., 2006; Hughes et al., 2008).

1.3.4.3 Hanifa Formation hydrocarbon reservoirs

The Ulayyah Member is equivalent to the Hanifa Reservoir in the subsurface of Saudi Arabia based on micropaleontological examination and correlation (Hughes, 2004). In addition, the upper part of the Hanifa Formation contains an important source rock interval with carbonate organic-rich deposits accumulated in dysoxic intrashelf basins (e.g., Central Arabia and South Arabian Gulf basin) (Ayres et al., 1982; Pollastro, 2003).

1.3.5 Jubaila Limestone

The Jubaila Limestone conformably overlies the Hanifa Formation (Manivit et al., 1990; Powers, 1968). This formation is classically divided into two informal units J1 and J2 (Fig. 1.19; Manivit et al., 1985b). The J1 unit is a homogenous limestone unit made up of white cream limestone interbedded with brown bioclastic and intraclastic grainstone beds. This lower unit is dated Early Kimmeridgian based on nautiless (*Paracenoceras* gr*. hexagonum, Paracenoceras* aff*. wepferi*) and endemic ammonites (*Perisphinctes* aff*. Jubailensis*) (Manivit et al., 1990). The nautiles and ammonites appear only in the middle part of the J1 unit, 25 m above the basal boundary. The J2 unit starts with reworked bioclastic cross-bedded grainstone followed by highly-bioturbated cream-color mudstone interbedded with intraclastic grainstone. The top of the unit is marked by a cliff-forming carbonate unit made up of highly bioturbated, partially dolomitized limestone including stromatoporoid buildups. The Jubaila Formation is conformably overlain by the Arab Formation (Arab-D Member; Manivit et al., 1990). Contrarily to the Hanifa

Formation, the Jubaila Limestone lacks of source rock or intrashelf basin in the nearby subsurface.

1.3.5.1 Regional distribution of the Jubaila Limestone

The significant lateral lithological changes of the Jubaila Limestone occur in J1 unit which grades totally to sandstone south of Wadi al Haddar (22° 00' N). The sandstone bodies are medium- to coarse-grained poorly sorted with local conglomerate grains (Manivit et al., 1990). The sandstone bodies are cemented by carbonate and contains bioclasts which suggest submarine depositional environment. In Wadi al Majami (21 ° 04' N), the J2 unit begins with reworking-bioclastic trough cross-bedded conglomeratic sandstone (5 m thick). The sandstone grades upward to thinly bedded bioclastic calcareous mudstones interbedded with intraclastic grainstone beds. The uppermost of J2 unit is marked by very thinly laminated mudstone (? algal control beds). Further to the south, the thickness of the Jubaila Limestone decreased and the sandstone at the base of each unit grades to dolomitic limestone in Al Hasi (20° 18' N). The top Jubaila Limestone is marked by ferruginous surface on dolomitized grainstone beds (Manivit et al., 1990).

1.3.6 Arab Formation, Arab-D Member

The Arab Formation is divided into four members A-D (in descending order) (Steineke et al., 1958; Fig. 1.4). The base contact of the Arab Formation has two different lithostratigraphic definitions, considering outcrop and subsurface. The subsurface Arab-D Member/reservoir (46 m thick in Dammam Well number 7) is bounded at the base by dense mudstone and

above by anhydrite (Steineke et al., 1958). At outcrop, the Arab-D Member (~20 m thick; Manivit et al., 1990) is resting on poorly developed reef facies that are included in the Arab-D reservoir in subsurface (Powers et al., 1966; Powers, 1968;). The Arab-D Member begins with bioclastic grainstone and bioturbated limestone containing fine quartz sandstone. The upper part is marked by a brown dolomitic bed capped by stromatolite boundstone. The Arab-D Member ends with collapse breccia interval below the Arab-C Member (Fig. 1.19). The breccia is due to the dissolution of anhydrite between the Arab-D and Arab-C Member, which have been lately defined as Arab-D Anhydrite (*sensu* Mitchell et al., 1988). The Arab Formation lacks ammonite and is dated Kimmeridgian to Tithonian based on microfaunal association including benthic foraminifera (Manivit et al., 1990; Hughes, 2009).

1.3.6.1 Previous Jubaila-Arab-D sequence stratigraphy

The sequence stratigraphy of the Jubaila Limestone and Arab-D reservoir has been subjected to many-detailed studied in outcrop and subsurface (Powers, 1962; Mitchell et al., 1988; Le Nindre et al., 1990; Meyer and Price, 1993; Handford et al., 2002; Lindsey et al., 2006; Al-Awwad and Collins, 2013a, 2013b; Al-Awwad and Pomar, 2015). Le Nindre et al. (1990) interpreted low stand deposits for the base Jubaila sandstone and two high stand cycles for upper Jubaila and Arab-D Member including the overlaying anhydrite. Meyer et al. (1996) measured two sections in Wadi Nisah (24° 15' N) covered the upper third of the Jubaila Limestone and Arab-D member, which considered a single shallowing-up sequence. Some of these previous studies divided the Jubaila-Arab-D into two depositional sequences (Powers,

1962; Mitchell et al, 1988; Meyer and Price 1993; Handford et al., 2002; Lindsay et al., 2006; Al-Awwad and Collins, 2013b). The lower sequence includes Jubaila Limestone (J1 unit) and base Arab-D reservoir. The upper sequence contains the Arab-D reservoirs (including J2 unit and Arab-D Member).

The sedimentological description in most of these previous studies are limited to the so-called “Arab-D reservoir”, which corresponds to upper part of the Jubaila Limestone and Arab-D Member. Moreover, what is lacking in the previous studies is a complete regional sequence stratigraphic cross-section documenting lateral facies changes of the lime mudstones of the Jubaila Limestone and base Arab-D Reservoir. These lateral facies changes are less evident in the subsurface and specifically across the Ghawar field, 300 km west of Riyadh (Mitchell et al., 1988).

1.3.6.2 Arab-D hydrocarbon reservoirs

The Arab-D reservoir represents one of the most significant oil-bearing intervals in the world. It is considered the primary producing reservoir in the Ghawar Field, the largest oil-field in the world. The Arab-D reservoir contains highly porous and permeable strata which make high flow units called "Super-K" (Meyer et al., 2000). The Arab-D reservoir is capped by an efficient anhydrite cap rock.

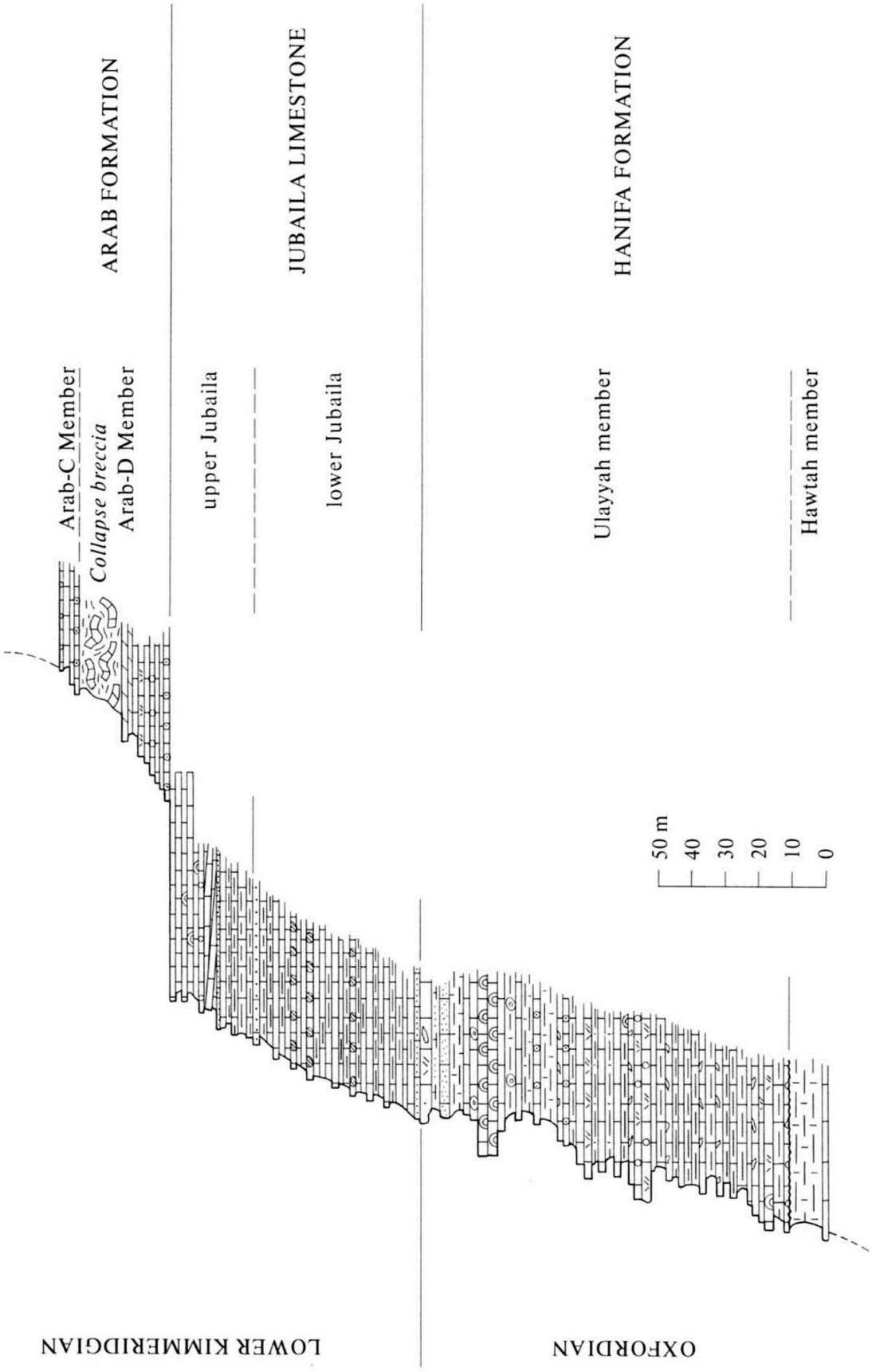

Figure 1.19: Generalized lithostratigraphy of the Hanifa Formation, Jubaila Limestone and Arab Formation (extracted from the Wadi al Mulayh quadrangle map; Manivit et al., 1985a).

1.4 Material and Methods

This sequence stratigraphic study is based on 45 detailed sedimentological log sections representing a cumulative length of 4800 m. Approximately 250 petrographic thin sections were acquired from the outcrop sections. Four shallow cores are descried (DHIBI-1, HMK-1, MRZU-2, MQBL-1 and WDLB-1) totaling of 800 m with gamma-ray logs. The shallow cores are located in Khashm Ad Dhibi (24° 14' N). The sedimentological data were plotted at scale of 1:200 for the outcrop sections and 1:120 for the logged core. The sedimentological data include: mineralogy, color, sedimentary structures, extended Dunham texture (Dunham, 1962; Embry and Klovan 1971), grain types, grain size, and fossil types and bioturbation. The vertical and lateral stacking patterns were analyzed in order to interpret different scale of depositional sequences and sequence boundaries. The sequence stratigraphic terminology in this study is adapted from Mitchum and Van Wagoner (1991).

High-resolution stratigraphic correlations have been defined using field physical correlation and sequence stratigraphic concepts. These outcrop and sedimentological-based sequences have been extended to the main hydrocarbon fields in the subsurface using gamma-ray log correlation.

The sequence stratigraphic cross-sections are complemented with biostratigraphic data of Manivit et al. (1990). The shallow cores are supplemented with semi-quantitative micropaleontological analysis of Hughes (2009; 2013, 2014; unpublished Aramco reports).

1.5 Structure and content of the manuscript

This PhD thesis is divided into four chapters, apart from a general introduction. Each chapter is designed as a research paper except for the last conclusion chapter. Each chapter contains its own list of cited references and appendices at the end of the chapter.

Chapter 1: Introduction (This Chapter)

This introductive chapter explains the general scope and aim of the study, presenting the study area, provides bibliographic synthesis of the geological context and presenting the overall structure of the thesis.

Chapter 2: Early Jurassic (Marrat Formation)

This chapter studies the stratigraphic record of the Early Jurassic (late-Early to Middle Toarcian) initial transgression of epeiric tropical Arabian Platform. It explores the dynamic of the epeiric platform and its impact to the sediments and stratigraphy. The study provides new depositional model and sequence stratigraphic framework for the Toarcian time. Moreover, the sedimentology of this work details the evolution of the Toarcian paleoclimatic changes and consequences in a paleoequatorial domain. This chapter includes a submitted paper in Marine and Petroleum Geology in August 2017.

Chapter 3: Middle Jurassic (Dhruma Formation and Tuwaiq Mountain Limestone)

This chapter deals with the stratigraphic record of the Middle Jurassic (Bajocian to Middle Callovian). It shows further continuation of the marine transgression after the Aalenian hiatus. It explores the evolution of the epeiric platform from very-flat profile to differentiated ramp platform with deep intrashelf basins in subsurface. In addition, the chapter provides a synthetic chronostratigraphic history of the Middle Jurassic with Tethyan domain sequence stratigraphy correlation. Moreover, the chapter evaluates how the changes of the global carbon cycle and seawater temperatures affected the stratigraphy of the tropical Arabian Platform.

Chapter 4: Late Jurassic (Hanifa Formation and Jubaila-Arab-D)

This chapter deals with the stratigraphic record of the Late Jurassic (Oxfordian – Kimmeridgian). It records platform evolution from differentiated ramp platform with adjustment intrashelf basins (Tuwaiq-Hanifa) to a lowstand followed by flat aggraded platform (Jubaila-Arab-D). It discuses the depositional environment and stacking patterns of the most productive reservoirs in Saudi Arabia, Hanifa and Arab-D. In addition, the chapter evaluates how the changes of the global seawater temperatures affected the facie and stratigraphy of the tropical Arabian Platform.

Chapter 5: Conclusion (Synthesis on the Jurassic sequence of the Arabian platform from Jabal Tuwaiq outcrops)

This conclusive chapter synthesis the several results presented in the preceding chapters and provide a robust depositional sequence model of a

transgressive inner platform. The chapter presents a synthetic chronostratigraphic diagram with Tethyan cycle correlation.

References

Abu-Ali, M., & Littke, R., 2005. Paleozoic petroleum systems of Saudi Arabia: a basin modeling approach. GeoArabia, 10(3), 131-168.

Al-Husseini, M.I., 2009. Update to Late Triassic-Jurassic stratigraphy of Saudi Arabia for the Middle East geologic time scale. GeoArabia 14(2), 145-186.

Al-Awwad, S.F., Collins, L.B., 2013a. Arabian carbonate reservoirs: A depositional model of the Arab-D reservoir in Khurais field, Saudi Arabia. AAPG bulletin, 97(7), 1099-1119

Al-Awwad, S.F., Collins, L.B., 2013b. Carbonate-platform scale correlation of stacked high-frequency sequences in the Arab-D reservoir, Saudi Arabia. Sedimentary Geology, 294, 205-218.

Al-Awwad, S.F., Pomar, L., 2015. Origin of the rudstone–floatstone beds in the Upper Jurassic Arab-D reservoir, Khurais Complex, Saudi Arabia. Marine and Petroleum Geology, 67, 743-768.

Al-Husseini, M. I and. Matthews, R. K. 2008. Jurassic-Cretaceous Arabian orbital stratigraphy: The AROSJK Chart, GeoArabia, 13 (1), 89-94.

Al-Husseini, M., Matthews, R.K., Mattner, J., 2006. Stratigraphic Note: Orbital-forcing calibration of the Late Jurassic (Oxfordian-early Kimmeridgian) Hanifa Formation, Saudi Arabia. GeoArabia 11, 145–149.

Al-Husseini, M.I. and Matthews, R.K. 2005. Arabian Orbital Stratigraphy: Periodic second-order sequence boundaries. GeoArabia, 10 (2), 165-184.

Al-Mojel, A., 2010. High-Resolution Sequence Stratigraphy of the Middle Jurasic Lower Fadhili Reservoir in Khurais. Master of Science Thesis, King Fahd University of Petroleum and Minerals.

Alméras, Y., 1987. Les Brachiopodes du Lias–Dogger: paléontologie et biostratigraphie. Geobios, Lyon, Special Memoir 9, p. 161-196.

Alsharhan, A.S., Nairn, A.E.M., 1997. Sedimentary basins and petroleum geology of the Middle East. Elsevier, Amsterdam, 843.

Ayres, M.G., Bilal, M., Jones, R.W., Slentz, L.W., Tartir, M., Wilson, A.O., 1982. Hydrocarbon habitat in main producing areas, Saudi Arabia. AAPG bulletin, 66(1), 1-9.

Baud, A., Droste, H., Guillocheau, F., Razin, P., Robin, C., 2005. Mesozoic Evolution of the Tethyan margin of Oman. In 24th IAS regional Meeting, Pre-Conference Excursion BF. 4.

Béchennec, F., Le Métour, J., Rabu, D., Bourdillon-de-Grissac, C.H., De Wever, P., Beurrier, M.T., Villey, M., 1990. The Hawasina Nappes: stratigraphy, palaeogeography and structural evolution of a fragment of the south-Tethyan passive continental margin. Geological Society, London, Special Publications, 49(1), 213-223.

Bramkamp, R.A., Steineke, M., 1952. Stratigraphical introduction. In: Arkell, W.J., Bramkamp, R.A., Steineke, M. (Eds.), Jurassic Ammonites from Jebel Tuwaiq, Central Arabia. Royal Society [London] Philosophical Transactions B 236, 241–313.

Brannan, J., Gerdes, K.D., Newth, I.R., 1997. Tectono-stratigraphic development of the Qamar basin, Eastern Yemen. Marine and Petroleum Geology, 14(6), 701-730.

Delvaux, D., 2001. Karoo rifting in western Tanzania: Precursor of Gondwana breakup. Contributions to geology and paleontology of Gondwana in honor of Helmut Wopfner: Cologne, Geological Institute, University of Cologne, 111-125.

Dunham, R.J., 1962. Classification of carbonate rocks according to depositional texture. In: Ham, W.E. (Ed.), Classification of Carbonate Rocks: AAPG Memoir 1, 108-121. Tulsa, OK.

Embry, A.F., Klovan, J.E., 1971. A late Devonian reef tract on northeastern Banks Island, NWT. Bulletin of Canadian Petroleum Geology, 19(4), 730-781.

Énay, R., Mangold, C., 1984. The ammonite succession from Toarcian to Kimmeridgian in Saudi Arabia, correlation with the European faunas. In: Michelsen, O., Zeiss, A. (Eds.), International Symposium on Jurassic Stratigraphy, Geological Survey of Denmark Copenhagen, Erlangen, 3, 641-652.

Énay, R., Mangold, C., Alméras, Y., Hughes, G.W., 2009. The Wadi ad Dawasir “delta”, central Saudi Arabia: A relative sea-level fall of Early Bathonian age. GeoArabia, 14 (1), 17-52.

Fischer, J.-C., Manivit, J., Vaslet, D., 2001. Jurassic gastropod faunas of central Saudi Arabia. GeoArabia (Manama), 6(1), 63–100.

Glennie, K.W., Boeuf, M.G.A., Hughes-Clarke, M.W., Moody-Stuart, M., Pilaar W., Reinhardt, B.M., 1995. Late Cretaceous nappes in Oman Mountains and their geological evolution. AAPG Bulletin, 57, 5-27.

Handford, C.R., Cantrell, D.L., Keith, T.H., 2002, Regional facies relationships and sequence stratigraphy of a super-giant reservoir (Arab-DMember), SaudiArabia: Society of Economic Paleontologists Gulf Coast Section Research Conference Programand Abstracts 22, 539–563.

Haq, B.U., Hardenbol, J., Vail, P.R., 1987. Chronology of fluctuating sea levels since the Triassic. Science, 235 (4793), 1156-1167.

Haq, B.U., Hardenbol, J., Vail, P.R., 1988. Mesozoic and Cenozoic chronostratigraphy and cycles of sea-level change. SEPM Special Publications 42, 71–108.

Hughes, G.W., 2004. Middle to Upper Jurassic Saudi Arabian carbonate petroleum reservoirs: biostratigraphy, micropalaeontology and palaeoenvironments. GeoArabia 9, 79–114.

Hughes, G.W., 2009. Biofacies and palaeoenvironments of the Jurassic Shaqra Group of Saudi Arabia. Volumina Jurassica, v. 6, p. 33-45.

Hughes, G.W., Al-Khaled, M., Varol, O., 2009. Oxfordian biofacies and palaeoenvironments of Saudi Arabia. Volumina Jurassica, 6, 47-60.

Hughes, G.W., Varol, O., Al-Khalid, M., 2008. Late Oxfordian micropalaeontology, nannopalaeontology and palaeoenvironments of Saudi Arabia. GeoArabia, 13 (2), 15-46.

Kadar, A.P., De Keyser, T., Neog, N., Karam, K.A., Le Nindre Y.M., Davies, R.B., 2015. Calcareous nannofossil zonation and sequence stratigraphy of the Jurassic System, onshore Kuwait. GeoArabia, 20(4), 125-180.

Konert, G., Afifi, A.M., Al-Hajri, S.A., De Groot, K., Al Naim, A.A., Droste, H.J., 2001. Paleozoic stratigraphy and hydrocarbon habitat of the Arabian Plate. AAPG Memoir 74, Chapter 24

Le Métour, J., Rabu, D., Tegyey, M., Béchennec, F., Beurrier, M., Villey, M., 1990. Subduction and obduction: two stages in the Eo-Alpine tectonometamorphic evolution of the Oman Mountains: In Robertson, A.H.F, Searle, M. P., Ries, A.C. (Eds), The Geology and Tectonics of the Oman Region: Geological Society of London, Special Publication 49, 327-340.

Le Nindre, Y.-M. 1987, Permien superieur, Trias, Jurassique: Sedimentologic: in Histoire geologique de la bordure occiden tale de la plate-forme arabe du Paleozoique inferieur au Jurassique superieur (Le Nindre, Y.M, Manivit, J., and Vaslet, D., authors), DSc Thesis, University of Paris VI, 3, 327.

Le Nindre, Y.M., Manivit, J., Manivit, H., Vaslet, D., 1990. Stratigraphie sequentielle du Jurassique et du Cretace en Arabie Saoudite. Bulletin Société Géologique France, Paris 6, 1025-1035.

Le Nindre, Y.M., Manivit, J., Vaslet, D., 1987. Histoire géologique de la Bordure occidentale de la Plate-forme Arabe du Paléozoïque inférieur au Jurassique supérieur. Thèse de Doctorat de l'Université de Paris 6, 4, p. 1113.

Le Nindre, Y.M., Vaslet, D., Laforet, C.l., Le Strat, P. Manivit, J., 1984. Accumulations of ferruginous ooliths in the Jurassic of central Saudi Arabia. D.M.M.R. Jeddah, Open-File Report BRGM-0F-04-3, p. 23.

Le Nindre, Y.M., Vaslet, D., Le Métour, J., Bertrand, J., Halawani, M., 2003. Subsidence modelling of the Arabian Platform from Permian to Paleogene outcrops. Sedimentary Geology, 156, 263-285.

Le Nindre, Y.M., Vaslet, D., Le Métour, J., Bertrand, J., Halawani, M., 2003. Subsidence modelling of the Arabian Platform from Permian to Paleogene outcrops. Sedimentary Geology, 156, 263-285.

Lindsay, R.F., Cantrell, D.L., Hughes, G.W, Keith, T.H., Mueller III, H.W., Russell, D., 2006. Ghawar Arab-D reservoir: Widespread porosity in shoaling-upward carbonate cycles, Saudi Arabia: AAPG Memoir 88, 97–138.

Manivit J, Le Nindre Y.M., Vaslet D. (1990) Le Jurassique d'Arabie Centrale. In Histoire Gologique de la Bordure Occidentale de la Plate-forme Arabe. Volume 4. Document du BRGM n°194.

Manivit, J., Pellaton, C., Vaslet, D., Le Nindre, Y.M., Brosse, J.M., Breton, J.P., Fourniguet, J., 1985b. Geologic map of the Darma quadrangle, sheet 24H, Kingdom of Saudi Arabia. Saudi Arabian Deputy Ministry for Mineral Resources Geosciences Map, GM-101, scale, 1(250,000), 133.

Manivit, J., Pellaton, C., Vaslet, D., Le Nindre, Y.M., Brosse, J.M., Fourniguet, J., 1985a. Geologic map of the Wadi al Mulayh quadrangle, sheet 22H, Kingdom of Saudi Arabia. Saudi Arabian Deputy Ministry for Mineral Resources Geosciences Map, GM-92, scale, 1(250,000), 1-32.

Manivit, J., Pellaton, C., Vaslet, D., Le Nindre, Y.M., Brosse, J.M., Breton, J.P., Fourniguet, J., 1985b. Geologic map of the Darma quadrangle, sheet 24H, Kingdom of Saudi Arabia. Saudi Arabian Deputy Ministry for Mineral Resources Geosciences Map, GM-101, scale, 1(250,000), 133.

Mattner, J., Al-Husseini, M., 2002. Essay: Applied cyclo-stratigraphy for the Middle East E&P industry. GeoArabia, 7 (4), 734-744.
Meyer, F.O., Hughes, G.W., Al-Ghamdi, I., 2000. Jubaila formation, Tuwaiq Mountain escarpment, Saudi Arabia: window to lower Arab-D Reservoir faunal assemblages and bedding geometry. GeoArabia (Manama) 5 (1), 143.
Meyer, F.O., Price, R.C., 1993. A new Arab-D depositional model, Ghawar Field, Saudi Arabia. In: Paper Presented at the Middle East Oil Show, Bahrain.
Meyer, F.O., Price, R.C., Al-Ghamdi, I.A., Al-Goba, I.M., Al-Raimi, S.M., Cole, J.C., 1996. Sequential stratigraphy of outcropping strata equivalent to Arab-D Reservoir, Wadi Nisah, Saudi Arabia. GeoArabia (Manama) 1 (3), 435-456.
Mitchell, J.C., Lehmann, P.J., Cantrell, D.L., Al-Jallal, I.A., Al-Thagafy, M.A.R., 1988. Lithofacies, diagenesis and depositional sequence: Arab-D Member, Ghawar Field, Saudi Arabia. SEPM Core Workshop 12, 459-514.
Mitchum, R.M., Van Wagoner, J.C. 1991. High-frequency sequences and their stacking patterns; sequence-stratigraphic evidence of high-frequency eustatic cycles. Sedimentary Geology, 70, 131-160.
Murris, R.J., 1980. Middle East: Stratigraphic evolution and oil habitat. AAPG Bulletin, 64,597–618.
Pollastro, R.M., 2003. Total petroleum systems of the Paleozoic and Jurassic, Greater Ghawar Uplift and adjoining provinces of central Saudi Arabia and northern Arabian-Persian Gulf. United States Geological Survey Bulletin, 2202 H, 100 pp.
Powers, R.W., 1962. Arabian Upper Jurassic carbonate reservoir rocks. In: Ham W.E. (Ed.), Classification of Carbonate Rocks: A Symposium. American Association of Petroleum Geologists, Memoir 1, 122-192.
Powers, R.W., 1968. Lexique Stratigraphique International, v.III, Asie, 10bl, Saudi Arabia. Centre National de la Recherche Scientifique, Paris, 177p.
Powers, R.W., Ramirez, L.F., Redmond, C.D., Elberg, E.L., 1966. Geology of the Arabian Peninsula, Geological Survey Professional Paper, 560-D, 147p.
Sadooni, F.N., 1997. Stratigraphy and petroleum prospects of Upper Jurassic carbonates in Iraq. Petroleum Geoscience, 3, (3),233-243.
Scotese, C.R., 2003. Paleomap project, Earth History and Climate History, Late Jurassic. Paleomap, URL http: // www. Scotese. com / late1. Htm
Sharland, P.R., Archer R., Casey D.M., Davies R.B., Hall S.H., Heward A.P., Horbury A.D., Simmons M.D., 2001. Arabian Plate Sequence Stratigraphy. GeoArabia Special Publication 2, Gulf PetroLink, Bahrain, 371.
Simmons, M.D., Sharland, P. R., Casey, D.M., Davies, R.B., Sutcliffe, O.E., 2007. Arabian Plate sequence stratigraphy: Potential implications for global chronostratigraphy. GeoArabia-Manama, 12(4), 101.
Sloss, L.L., 1963. Sequences in the cratonic interior of North America. GSA Bulletin, 74(2), 93-114.
Sorkhabi, R., 2012. Max Steineke (1898-1952): A pioneer American geologist in the early history of oil exploration in Saudi Arabia. International

Symposium on the History of the Oil and Gas Industry, Houston, TX, March 8-10. 13 (1). 266.

Steineke, M.R.A., Bramkamp, R.A., Sander, N.J., 1958. Stratigraphic relations of Arabian Jurassic oil. In: Weeks, L.G. (Ed.), Habitat of Oil. American Association of Petroleum Geologists Symposium, 1294-1329.

Tintant, H. 1987. Les nautiles du Jurassique d'Arabie Saoudite. Geobios, Mémoire Spécial 9, p. 67-159.

Vail, P.R., Mitchum Jr.R.M., Thompson III, S., 1977. Seismic stratigraphy and global changes in sea level. Part 4: Global cycles of relative changes of sea level. American Association of Petroleum Geologists Memoirs, 26, 83-97.

Vaslet, D., 1987, Geologic du Paleozoique; Permien Superieur, Trias, Jurassique; lithostratigraphic: in Histoire geologique de la bordure occidentale de la plate-fornie arabe du PaleozoIque inferieur au Jurassique superieur (Y.M. Le Nindre, J. Manivit and D. Vaslet, authors), DSc Thesis, University of Paris VI, 1, 413.

Vaslet, D., Al-Muallem, M.S., Maddeh, S.S., Brosse, J.M., Fourniquet, J., Breton, J.P., Le Nindre, Y.M., 1991. Explanatory notes to the geologic map of the Ar Riyad Quadrangle, Sheet 24I, Kingdom of Saudi Arabia. Saudi Arabian Deputy Ministry for Mineral Resources, Jeddah, Geosciences Map GM-121, 1-54.

Vaslet, D., Brush, J.M., Breton, J.P., Manivit, J., Le Strat, P., Fourniguet, J., Shorbaji, H., 1988. Geologic map of the quadrangle Shaqra, sheet 25H .Kingdom of Saudi Arabia: Deputy Ministry for Mineral Resources Geoscience Map GM-120C , 29.

Vaslet, D., Delfour, J., Manivit, J., Le Nindre, Y.M., Brosse, J.M., Fourniguet, J., 1983. Geologic map of the Wadi Ar Rayn quadrangle, sheet 23 H, Kingdom of Saudi Arabia. Saudi Arabian Deputy Ministry for Mineral Resources, Jeddah, Geosciences Map, GM-63A.

Vaslet, D., Delfour, J., Manivit, J., Le Nindre, Y.M., Brosse, J.M., Fourniguet, J., 1983. Geologic map of the Wadi Ar Rayn quadrangle, sheet 23 H, Kingdom of Saudi Arabia. Saudi Arabian Deputy Ministry for Mineral Resources, Jeddah, Geosciences Map, GM-63A.

Walley, C.D., 2001. The Lebanon passive margin and the evolution of the Levantine Neotethys. In, P.A. Ziegler, W. Cavazza, A.H. Robertson and S. Crasquin-Soleau (Eds.), Peri-Tethya rift/wrench basins and passive margins (IGCP 369 results). Mémoires du Muséum National d'Histoire Naturelle, Paris, Peri-Tethys Mémoire 6.

Ziegler, M.A., 2001. Late Permian to Holocene Paleofacies evolution of the Arabian plate and its hydrocarbon occurrences. GeoArabia, 6, 445-504.

Chapter 2:

Early Jurassic (Marrat Formation)

Khashm Disman where the Triassic, Early Jurassic and Middle Jurassic crop out *(Air photography by Hadi Makayyal, 2007).*

Table of contents:

Shallow-marine depositional sequences in a transgressive mixed siliciclastic-carbonate system: the Early Jurassic Marrat Formation at outcrop in Central Saudi Arabia

Abdullah Al-Mojel[1, 2], Philippe Razin[2], Yves-Michel Le Nindre[3], Guillaume Dera[4]

[1] Saudi Aramco, Dhahran, Saudi Arabia
[2] ENSEGID-Bordeaux INP, EA4592, 33607 Pessac, France
[3] Consultant
[4] GET, Université Paul Sabatier, CNRS UMR 5563, IRD, OMP, 14 Avenue Avenue Edouard Belin, 31400 Toulouse, France

Corresponding author: E-mail: abdullah.mojel@gmail.com Present address: P.O. Box 5093 Dhahran 31311, Saudi Arabia

Keywords: Arabian Platform, Toarcian, epeiric sea, mixed carbonate-siliciclastic systems, continental – marine transition, transgression, sequence stratigraphy, Marrat Formation

Abstract

The high-resolution sequence stratigraphy of the Marrat Formation (late-Early to Middle Toarcian) is based on outcrop and shallow core measured sections along a 280 km long N-S transect south of Riyadh. Correlations were extended westward in the subsurface using gamma-ray wireline logs (200 km Riyadh to Khurais). The outcrops provide a continuous stratigraphic record of the initial Jurassic transgression of a large (>1000 km) epeiric tropical platform with continental meandering fluvial deposits to tidal or wave-dominated siliciclastic and carbonate lagoonal deposits. These formed aggraded flat-topped platform wedging and thickening northward due to evident syndepositional differential subsidence. The successions make up two 3rd-order sequences onlapping southward on the Triassic-Jurassic

unconformity and show progressive marine transgression that reach its maximum in the Middle Toarcian *bifrons* Zone, consistent with the major MFS of the Arabian Platform and the European domain. The layer-cake geometries is controlled by the geodynamic setting, low-energy wide platform with stable tectonic context, that leads for limited accommodation space compensated by siliciclastic supply and carbonate production. Short-lived higher energy siliciclastic shorelines appear during high accommodation space in late-TST and HST. The carbonates are mud-dominated lagoon well developed during late-TST and MFS of the two Marrat sequences. Regression between these two sequences consists of thick lateral extensive continental red shales and fluvial sandstone. This abrupt terrigenous influx is perhaps related to strong hydrolyzing conditions under humid and warm period rather than drop of accommodation space. The synchronicity of the regression with humid-warm periods provides some confidence to the aquifer-eustasy driver mechanism of the Marrat sequences. This study should serve as an outcrop analog and guidelines for reservoir modeling and hydrocarbon exploration and better predict reservoir distributions, and improves seismic interpretation.

2.1 Introduction

The outcrop of the Early Jurassic (late-Early to Middle Toarcian) Marrat Formation is part of a very extensive (>1000 km) epiric tropical Mesozoic Arabian platform that records the early marine transgression after the Triassic-Jurassic unconformity. The Marrat outcrops are aggraded and very flat platform made up of continental to mixed continental-marine to very shallow marine depositional systems. The Marrat outcrops are very well exposed in the central Arabia along the foot of the Jabal Tuwayq Jurassic

escarpments. These Jurassic outcrops formed spectacular west facing continuous cuests along 1000 km N-S near Ar Riyadh (Fig. 2.1). The Jurassic formations are one of the most economically important stratigraphic intervals in the world. The Marrat Formation consists of multiple reservoir units with effective caprocks in the subsurface of the Northeast of Saudi Arabia and Kuwait (cf Alsharhan and Nairn, 1994, 2003).

Prior to this study, the outcropping Marrat Formation was subdivided into three large mapping units based on lithostratigraphic and biostratigraphic correlations (Powers et al., 1966; Powers, 1968; Manivit et al., 1990). However, genetically related depositional sequences, cycle hierarchy, stacking patterns, depositional environment evolution, and effects of syndepositional tectonic events were not documented in detail. Therefore, our approach was to integrate the previous biostratigraphic data with detailed sedimentological measured sections and subsurface gamma-ray logs, offering a factual and correct depositional models and robust high-resolution sequence stratigraphic frameworks. This serves as an outcrop analog and guidelines for reservoir modeling and hydrocarbon exploration and better predict reservoir distributions, and improves seismic interpretation. Moreover, this study allowed assessment of the influence of the controlling factors to the development of Jurassic Arabian Platform, the most prolific petroleum system in the region.

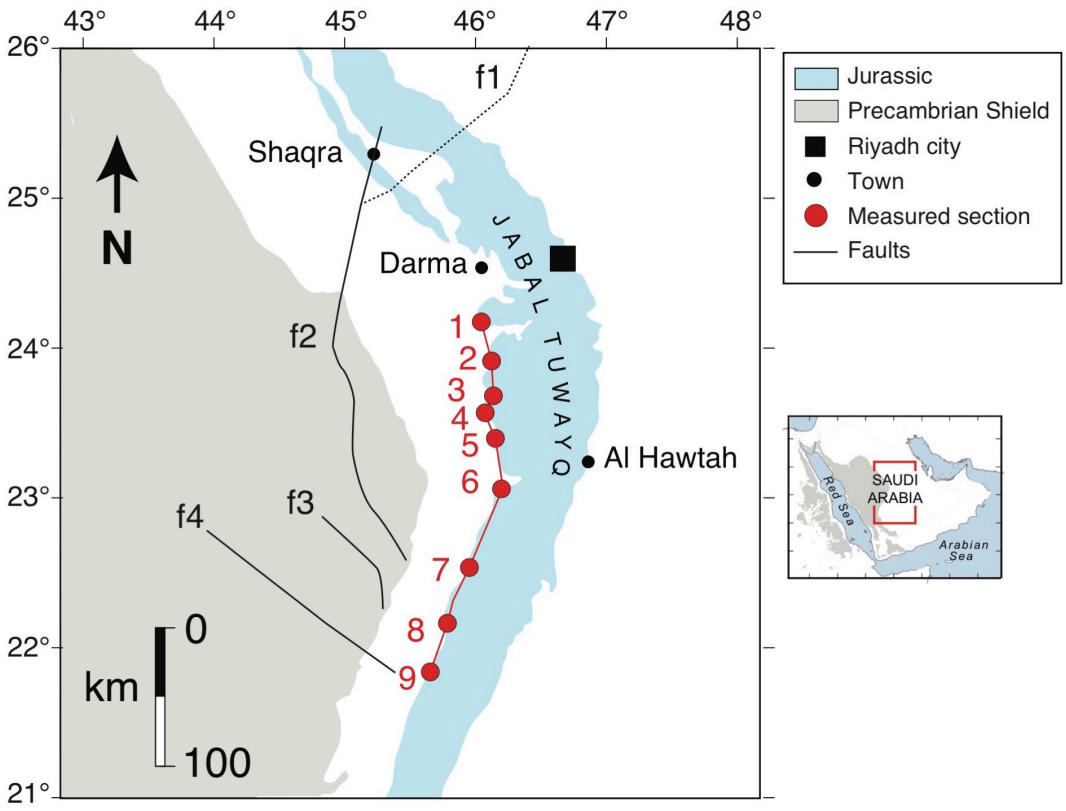

Figure 2.1: Geological map of the study area showing the Jurassic outcrops modified from Fischer et al. (2001), measured sections, faults and magnetic lineaments. The measured sections are: (1) Khashm Ad Dhibi, (2) Wadi Al Jufayr, (3) Faridat Balum, (4) Khashm Al Khalta, (5) Khashm Disman, (6) Wadi Birk, (7) Fara'id al Ahmar, (8) Khashm Munayyifiyah, (9) Khashm Abu Al Jiwar. The faults are mapped in the 1:250,00-scale quadrangles of Wadi al Mulayh (Manivit et al., 1985a), Wadi Ar Rayn (Vaslet et al., 1983), Darma (Manivit et al., 1985b) and Shaqra (Vaslet et al., 1988). The name of the faults are: f1 Wadi Al Atk Lineament, f2 Al 'Amar Fault, f3 and f4 are belong to the Najd Fault System (Al-Husseini, 2000).

2.2 Geological Setting

2.2.1 Tectonic and paleogeographic setting

The study area is located in the central part of the Arabian Platform, which represents a continental passive margin since the beginning of the Late Permian. The Arabian Platform is an extensive epeiric (> 1000 km) continental to shallow-marine platform located in the tropical belt facing the

Neo-Tethys Ocean (Murris, 1980) (Fig. 2.2). The study area is very far from the shelf margin and close to the coastal zone and hinterland that is progressively onlapped by the Mesozoic sediments. The passive margin context ends during the Late Cretaceous (Late Cenomanian-Turonian) with the onset of convergence and obduction of the Neo-Tethys margin (Glennie et al., 1995; Le Métour et al., 1990).

This passive margin undergoes several 2nd-order tectonic events resulting in several Mesozoic unconformities and associated stratigraphic hiatuses (e.g., Late Triassic – Early Jurassic, Late Jurassic-Early Cretaceous). These two unconformities delimit the Jurassic Shaqra Group (Vaslet, 1987). The Late Triassic – Early Jurassic is one of the major unconformities lasting approximately 20 Myr that corresponds to the basal limit of the studied interval, the Marrat Formation. The tectonic control of this unconformity is poorly understood. It could be related to the tectonic inversion of the Karoo rifting between Madagascar and East Africa that caused a long period of regional uplift and erosion (Delvaux, 2001; Baud et al., 2005).

2.2.2 Stratigraphic setting

The Marrat Formation was first defined by Steineke (1937) in an unpublished report. The first formal definition was published by Bramkamp and Steineke (in Arkell, 1952). The lithostratigraphy of the Marrat Formation (Fig. 2.3) was updated by Powers et al. (1966), Powers (1968), in a type section located near the Marah town in Jabal Kumayt (25° 04' N). Then, Manivit et al. (1990) provided a new reference section in Khashm Ad Dhibi (24° 14' N). The Marrat Formation is bounded by two significant unconformities: the Late Triassic – Early Jurassic hiatus at the base and the

Late Toarcian – Aalenian at the top. Powers et al. (1966) divided the formation into three informal units corresponding to the lower, middle and upper Marrat Formation. Their boundaries were defined using morphologic and lithologic criteria that are clearly visible in the outcrop forming three cuestas. These boundaries have been slightly revised by Manivit et al. (1990) as following:

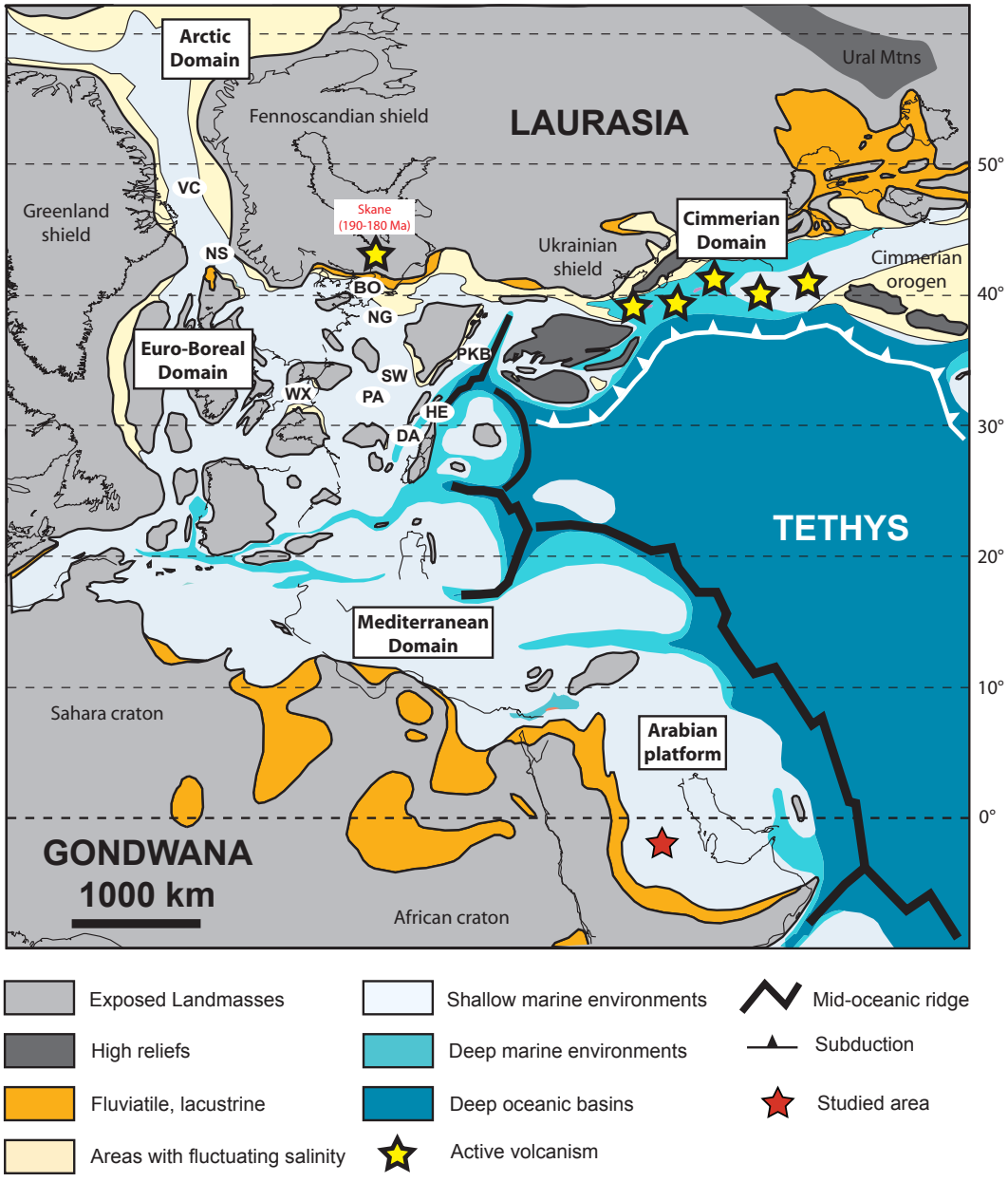

Figure 2.2: Toarcian paleogeographic map showing the area of study located in the southern margin of the Neo-Tethys Ocean (modified from Thierry et al., 2000; Dera et al., 2009).

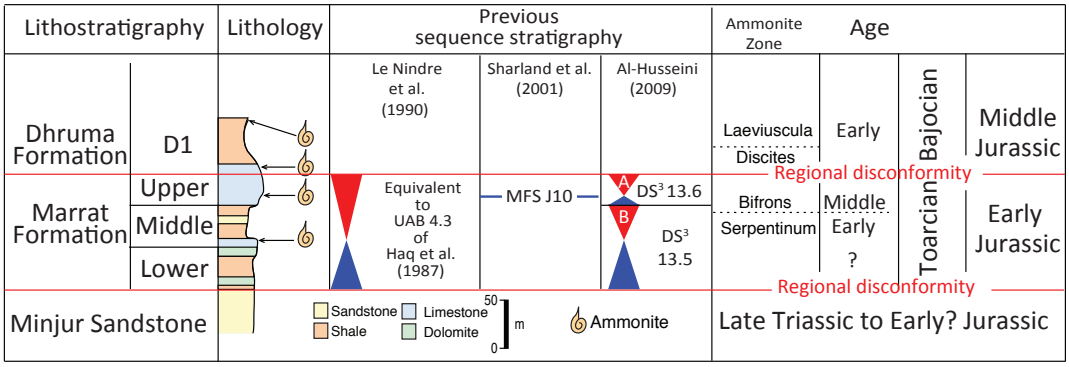

Figure 2.3: Lithostratigraphic, biostratigraphic and previous sequence stratigraphy of the Early Jurassic in Jabal Tuwayq, Saudi Arabia. (Modified from Fischer et al., 2001).

Lower Marrat Unit (47 m thick) is bounded at the base by the Late Triassic – Early Jurassic unconformity marked by a black iron surface on the top of Late Triassic continental deposits (i.e., Minjur Sandstone). The lithology of the Lower Marrat unit is made up of barren shale, sandstone and thin dolomitic beds with poor fauna deposited in continental to intertidal-subtidal environments.

Middle Marrat Unit (40 m thick) is made up at the base by fossiliferous and bioturbated dolomitic limestone overlain by brick-red shale and siltstone that have no fossil record. The top of the unit is marked by calcareous shale with poor fauna. The depositional setting of this unit ranges from subtidal lagoon to intertidal setting. The base of the unit is dated by ammonites (*Protogrammoceras, Bouleiceras*), which indicate the late-Early Toarcian *serpentinum* Zone (Fig. 3).

Upper Marrat Unit (39 m thick) is a cliff-forming bioturbated lagoonal limestone dated by ammonites (*Nejdia*) indicating the Middle Toarcian *bifrons* Zone. The limestone is overlain by gypsum that has been considered by Powers (1968) as the base of the Dhruma Formation.

In the subsurface, the Marrat Reservoir in the Eastern Province of Saudi Arabia is equivalent to the upper part of the formation (Ayres et al., 1982 in Al-Husseini, 2009 and Manivit et al., 1990). Overall, the Marrat Formation as a whole was considered as one transgressive – regressive cycle by Le Nindre et al. (1990) with an MFS at the base of the Middle Marrat (*serpentinum* Zone) corresponding to UAB 4 of Haq et al. (1987) (Fig. 2.3).

Based on a review and interpretation of a single section described in Powers et al. (1966), Powers (1968) and Manivit et al. (1990), Al-Husseini (2009) subdivided the Marrat Formation into two 3rd-order sequences (Marrat Sequence B and A), which correspond to the so-called DS^3 13.5 and 13.6 of the Arabian Orbital Sequence (AROS) that considered as 2.4 Myr eccentricity cycles (Al-Husseini and Matthews, 2008; Al-Husseini, 2009) (Fig. 2.3). The Marrat Sequence B includes Lower and Middle Marrat. The transgressive system tracts (TST) are represented by the barren continental shale in the Lower Marrat. The maximum flooding interval (MFI) corresponds to fossiliferous and bioturbated limestone base of the Middle Marrat. The highstand coincides with brick-red shale and siltstone of the Middle Marrat. The Marrat sequence A includes the Upper Marrat where the TST and MFS are interpreted in the basal bioclastic limestone and the kaki shale with the ammonite fauna. The highstand corresponds to the upper gypsum unit in the upper part of the formation.

Based on regional correlations of the Jurassic system, Sharland et al. (2001) have placed a maximum flooding surface (MFS J10) in the Middle Toarcian upper Marrat Formation (Fig. 2.3). However, Kadar et al. (2015) have placed the MFS J10 in the lower part of the Middle Marrat, Early

Toarcian (*serpentinum* Zone), based on outcrop correlation of Saudi Arabia and subsurface of Kuwait.

2.3 Materials and Methods

Our sequence stratigraphic study is based on 9 detailed logged sections, representing a cumulative length of 600 m, located along a 280 km N-S transect in the south of Riyadh. The name of sections and their locations are shown in Figure (1) and Appendix (1). One shallow core (DHIBI-1) with gamma-ray logs located in Khashm Ad Dhibi area is also used in the study. The core only covers the upper Marrat Formation. The sedimentological data include: mineralogy, grain types, color, grain size, texture, extended Dunham classification (Dunham, 1962; Embry and Klovan 1971), sedimentary structure and fossil types. The vertical successions and evolution of the depositional environments were analyzed to define and interpret sequence stratigraphy.

High-resolution stratigraphic correlations were made using sequence stratigraphic concepts, physical correlations, and mapping. Applying the Walther's Law across the sections was not a straight forward, because the platform was aggrading and had limited facies migration. Building the depositional model went through a continuous iterative process (Kerans and Tinker, 1997) from one-dimensional cycle stacking analysis and sequence boundary definition to two-dimensional time line correlations and lateral facies organization. The defined sequences were adopted in gamma-ray logs of nearby subsurface wells in Riyadh and Khurais area.

The sections are complemented with biostratigraphic data of Manivit et al. (1990) and Hughes (2009; unpublished Saudi Aramco internal report of

DHIBI-1 micropaleontology). The stratigraphic location of key biostratigraphic elements (e.g., ammonite faunas) are shown on the cross-section (Fig. 2.12).

2.4 Facies and depositional environments

The depositional facies of the Marrat Formation and their environmental interpretation are summarized in Table 2.1 and 2.2. Twelve facies or facies associations have been identified from outcrop observations (Fig. 2.4, 2.5, 2.6 and 2.7) and are grouped into five depositional environments based on their common depositional processes. The depositional environments from proximal to distal are: fluvial, coastal plain, high-energy nearshore, mixed carbonate-siliciclastic inner-platform and carbonate inner-platform. Each facies association has been assigned to a sub-depositional environment according to its sedimentological characteristics.

The shale color is a significant characteristic for interpreting different type of depositional environments in the Marrat Formation outcrops. For example, three distinctive types of shale color allow us to identify their spatial and stratigraphic limitations and help to indicate their depositional environments such as non-marine, coastal-plain and lagoon.

F1: Medium to coarse grained trough cross-bedded sandstone (braided fluvial system)

These facies are 2 to 8 m thick, tabular and channelized units with sharp bases and gradational tops. The sandstones are non-bioturbated trough and tabular cross-bedded (Fig. 2.4). They are moderately sorted, unfossiliferous medium to coarse and rare conglomerate gravel grained. The sandstones occur at the base of the Marrat Formation in W. Al Jufair (Fig.2. 8A and 10)

and K. Ad Dhibi north of latitude 23º 50' N and in the Middle Marrat unit in W. Birk and F. Al Ahmar (Fig. 2.12). The sandstones overlie the Triassic – Jurassic unconformity in the northern sections and are intercalated in barren red shales (F4) within the Middle Marrat unit. The facies are overlain by mottled pale red paleosol (F5) and red shale (F4). The facies are interpreted as high-energy braided channels.

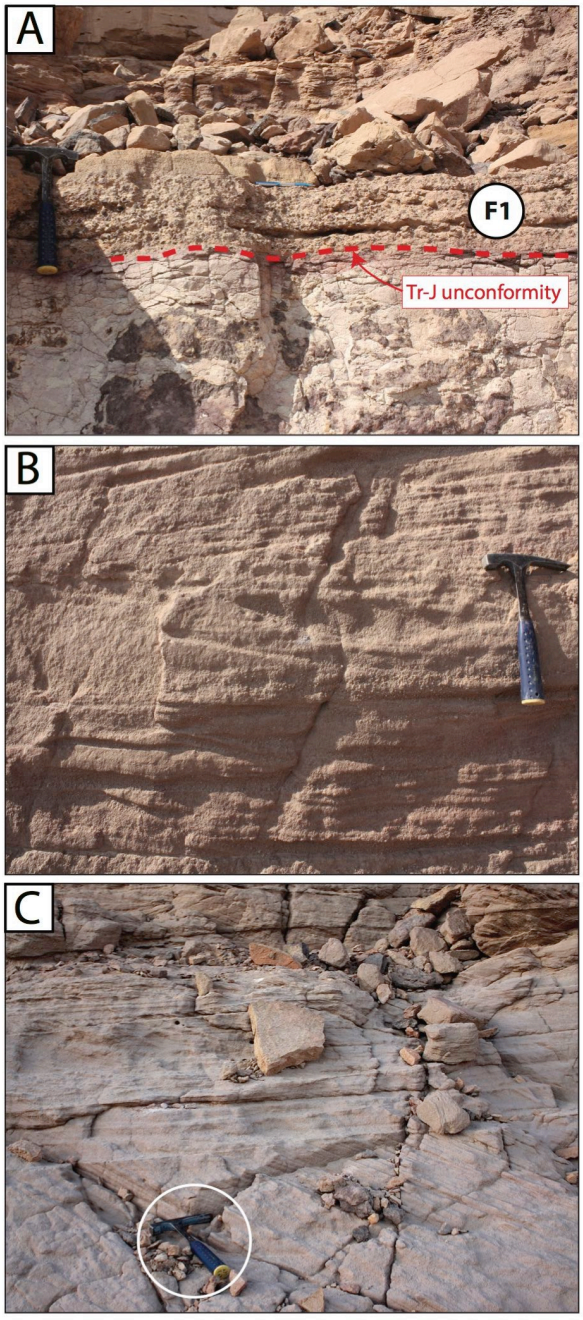

Figure 2.4: Fluvial facies association in the Marrat Formation. **A)** Pebbly sandstone and conglomerates (F1), base of braided fluvial channel, base of the Marrat Formation, Wadi Al-Jufair, **B and C)** Medium to coarse grain trough cross bedded sandstone (braided channel).

Table 2.1: Siliciclastic facies of the Marrat Formation.

Depositional environment	Fluvial					Coastal plain			High-energy nearshore	
Facies and sub-depositional environment	F1: Trough cross-bedded sandstone (braided fluvial system)	F2: Inclined heterolithic stratified sandstone/shale (fluvial *meandering channel*)	F3; ripples cross-laminated sandstone (*fluvial overbank*)	F4: Red thin laminated shale (*flood-plain/lake*)	F5: Mottled red shale (*paleosol*)	F6: Mottled bluish green shale (*mud flat/coastal plain*)	F7: Bioturbated heterolithic silty sandstone (*mixed flat/coastal plain*)	F8: Cross-bedded sandstone with mud drapes (*tidal creeks*)	F9: *Skolithos*-bearing bidirectional cross-bedded sandstone (*tidal bars and channels*)	F10: Swaley cross-stratified sandstone (*shoreface*)
Thickness	2-8 m	0.5-5 m	0.2-0.5 m	3-27 m	0.5-1.5 m	0.5-17 m	0.5-2 m	0.5-1.5 m	0.5-1.5 m	1-2 m
Color	Pale yellowish orange and moderate red	Pale yellowish orange and moderate red	Moderate red to dusty red	Light red and dark red	Moderate orang pink and Moderate red	Grayish yellow green and moderate red	Moderate orange pink and moderate red	Grayish to moderate orang pink	Grayish to moderate orang pink	Grayish to moderate orang pink
Depositional texture and grain types	Medium to coarse and rare conglomerate gravel grained, moderately sorting	Very fine to medium sand grained, locally conglomerate granule grained, moderately sorting	Clay and silt to fine grained	Clay and around 10% silt	Clay, silt and some sand grained	Clay, local thin stromatolitic mudstone and dolomitic bed	Silt and medium sand grained	Medium sand grained; plant fragment	Medium sand grained	Medium sand grained
Bedding and sedimentary structures	Sharp base, channelized, non-bioturbated trough and tabular cross-bedded	Sharp base, channelized, IHS, commonly parallel lamination, locally lenticular sandstone, some trough and tabular cross stratification	Normal base and may have inverse grading; lenticular bedding, small climbing-ripple lamination	Gradational base, tabular bedding, thin laminated, may have small climbing ripples	Gradational base, Tabular to lenticular bedding, root traces with common iron-stained top	Gradational base, tabular bedding, locally mudcracks associated with stromatolitic structure	Coarsening-upward gradational base, tabular bedding, thin mainly horizontal bioturbation traces	Sharp base, channelized, tabular cross-stratification with mud drapes, locally capped by mudcracks	Sharp base, tabular, highly bioturbated, abundant *Skolithos*, bidirectional cross-stratification, iron-stained top	Sharp scour base, tabular bedding, commonly swaley and may have hummocky cross-stratification

Table 2.2: Mixed carbonate-siliciclastic facies of the Marrat Formation.

Depositional environment	Mixed carbonate-siliciclastic inner lagoon		Carbonate inner lagoon
Facies and sub-depositional environment	F11: Grayish green calcareous shale (*shale dominated inner-lagoon*)	F12: Argillaceous nodular bioturbated peloidal wackestone/ mudstone (*carbonate dominated inner lagoon*)	F13: Bioturbated peloidal wackestone/mudstone (*extensive carbonate lagoon*)
Thickness	1-4 m	1-3 m	1-3 m
Color	Olive gray to greenish gray	Very light gray and light greenish gray	Very pale orange
Depositional texture and grain types	Terrigenous clay and calcareous mudstone	Pelletal, peloidal mudstone, locally 20-50% quartzos, locally intraclastic skeletal fragments wackestone/packstone lag deposits	Silt to very fine pelletal grains, skeletal fragments, wackestone/mudstone
Bedding and sedimentary structures	Brittle, flaggy and slabby shale bedding; rare chondrites burrow	Sharp base marked by reworded lag deposits, tabular bedding, horizontal thin bioturbation, rare chondrites burrow, argillaceous wispy solution seams, nodular structure	Transitional base, massive tabular bedding, vertical bioturbation, argillaceous wispy solution seams, rare nodular structure
Fossils	Gastropods and bivalves (Manivit et al., 1990)	Ammonite, bivalves, gastropods (Manivit et al., 1990); echinoid fragments, brachiopods, agglutinated foraminifera (*Ammodiscus* sp.) (Hughes, 2009)*	Echinoid fragments, brachiopods, molluscs (*Inoceramus* fragments), foraminifera (*Siphovalvulina variabilis, juvenile Valvulina* sp., *Haplophragmoides* ssp., *Ammobaculites* sp., *Textulariopsis*) (Hughes, 2009)*

* Unpublished internal report

F2: Inclined heterolithic stratified sandstone/shale (fluvial meandering channel)

This facies association is present in 0.5 to 5 m thick in sharp-based lenticular bodies intercalated in barren red shales within the Middle Marrat unit. It corresponds to channel-fill deposits. Lenticular medium to fine-grained sandstone units form locally the lower part of the channel-fill sequence. The rest of the sequence is made of a finning-up alternation of pale yellowish fine-grained sandstone and red fissile shale displaying an inclined heterolithic stratification (IHS) (Fig. 2.5A, B, C; Table 2.1). The dip of these inclined stratifications is highly variable in the successive stacked sequences. These structures can be related to lateral accretion processes in point-bar deposits within low-energy meandering channels (Thomas et al., 1987). Moreover, the lack of fossil and bioturbation in these red-dominated siliciclastic deposits and the local intercalation of paleosoils (Wadi Al Hadar) indicate a fluvial depositional setting.

F3: Rippled cross-laminated sandstone (fluvial overbank)

This facies forms tabular units up to 0.2 to 0.5 m thick, with gradational base and top and local coarsening-up pattern. They are made of red siltstone to fine grained sandstone. These facies are characterized by climbing-ripple laminations (Fig. 2.5D and E; Table 2.1). They are found in the Middle Marrat unit at the same stratigraphic level than the previous meandering channel facies association. These climbing-rippled fine-grained tabular units are interpreted as overbank and natural levees deposits in a low-energy alluvial plain setting (McKee, 1966; in Reineck and Singh, 1980).

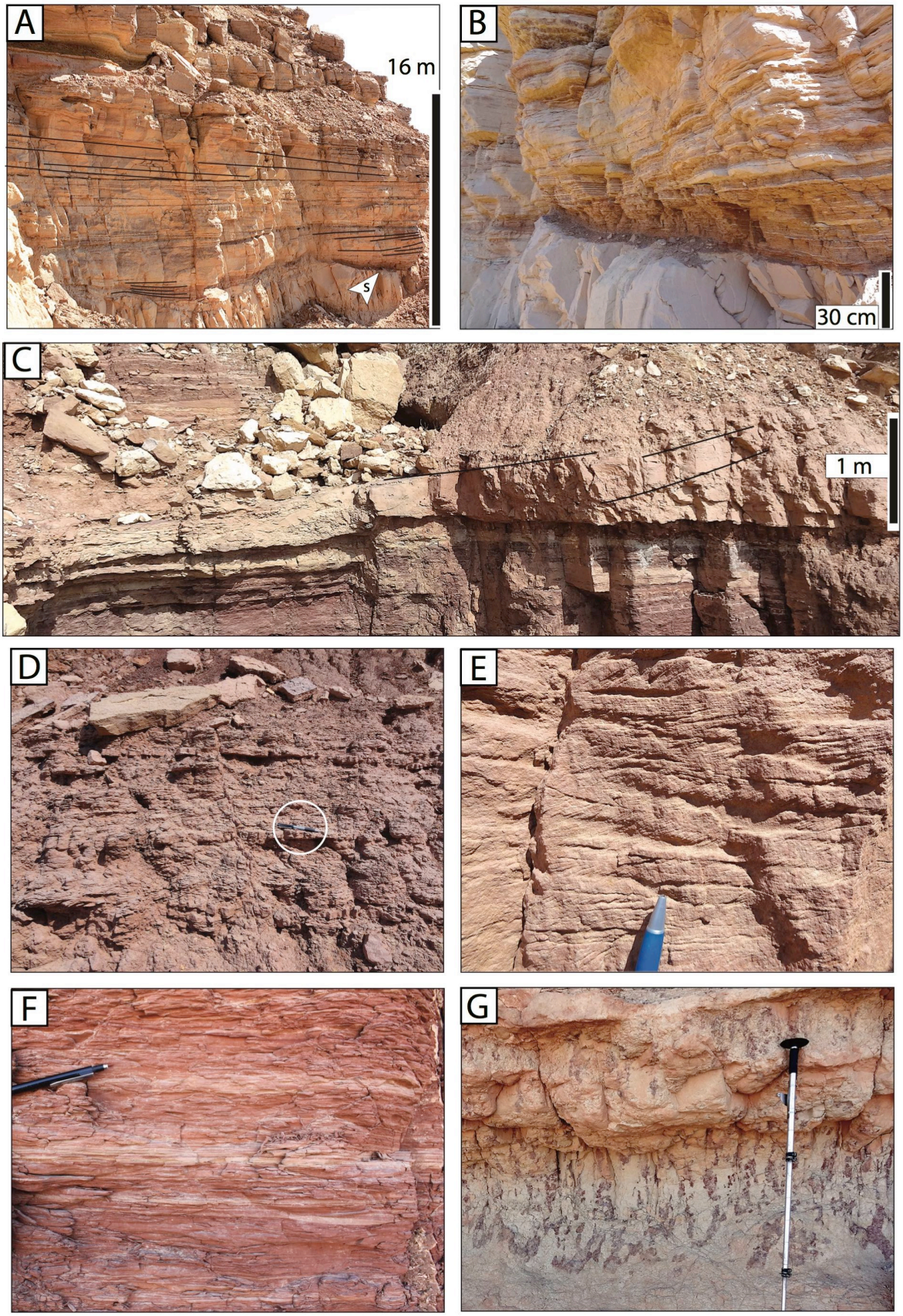
A
16 m
S
B
30 cm
C
1 m
D
E
F
G

← **Figure 2.5:** Fluvial facies association in the Middle Marrat Formation. **A)** Stacked meandering channel-fills show lateral accretion point bars, scour base (s arrow), inclined heterolithic stratification (IHS) (sandstone/shale), Khashm Al Khalta, **B)** Close-up of the scour base (s arrow in figure A) shows the IHS in within which sandstone-shale parallel and some lenticular lamination, **C)** Abandoned channel-fill shows IHS of point bar marked by the lateral grain-size fining trends to the left, Khashm Disman, **D)** Siltstone and thin fine sandstone beds (pen for scale), overbank, Faridat Balum, **E)** Close-up of the very small ripples shows climbing-ripple lamination, overbank, Faridat Balum, **F)** Thin laminated red shale with silt laminae, flood plain/lake, Wadi Al Jufayr, **G)** Mottled red shale with root traces, paleosol, Khashm Munayyifiyah (Jacob's staff is 120 cm).

F4: Red thin laminated shale (flood-plain/lake)

In the northern part of the studied transect, the Middle Marrat member is mainly composed with3 to 27 m thick homogeneous red shale units. The basal and upper contacts of these units are very gradual and marked by a transitional change from red to grayish green shales. This facies includes 10 % of thin siltstone lamina (Fig. 2.5F; Table 2.1). X-ray diffraction analysis shows that the red shale is mainly composed by kaolinite with minor amounts of illite and feldspar (Abed, 1979). The red color of clays is due to hematite which is dominant over goethite. The shales are barren (Powers et al., 1966) and their association with fluvial channel-fills and overbank deposits suggest a broad alluvial flood-plain environment with probable ephemeral lake development recorded by the thin silty lamination in some intervals. The high amounts of kaolinite and hematite suggests a tropical equatorial paleoenvironment with very humid and hydrolyzing conditions favoring laterization (Chamley, 1989; Dera et al., 2009).

F5: Mottled red shale (paleosol)

These facies are represented by 0.5 to 1.5 m thick shaly units and are commonly capped by iron-rich crust. They mainly consist of clay, silt and

some sand grains enriched in kaolinite, hematite, and various elements (Ti, Zr, Nb, and Y) indicating considerable alteration under tropical conditions (Abed 1979). The shales are color mottled, orange pink and red, with rootlet traces (Fig. 2.5G; Table 2.1). These facies are associated with the fluvial channel deposits and interbedded with lenticular sandstone beds. They occur in the Middle Marrat Formation and especially in the southern updip outcrops that correspond to the more proximal setting. The facies are paleosols confirmed by the exclusive presence of terrestrial palynomorphs (see Baudin, 1989).

F6: Mottled bluish green shale with interbedded mudstone and sandstone (mud-flat/coastal-plain)

The facies occur as 0.5 to 17 m thick tabular units. They mainly consist of bluish green shales mottled with moderate red and brown color (Fig. 2.6A; Table 2.1). In core, the shales are reddish brown with fissile parting. The facies are present in the Lower and Upper Marrat unit. In the Lower Marrat unit, the shales are barren and associated with thin orange dolomite, stromatolitic lime-mudstone (Fig. 2.6B) and tabular cross-bedded sandstone with mud-drapes. The associated sandstone and lime-mudstone exhibit mudcracks. In the Upper Marrat unit, the shales are interbedded with tabular and channelized beds of tabular cross-bedded sandstone of tidal origin. The shale dominated facies association is deposited on low-energy mud flat in a coastal-plain to inner lagoon setting.

F7: Bioturbated heterolithic siltstone and sandstone (mixed-flat/coastal-plain)

These facies are tabular units 0.5 to 2 m thick with coarsening-upward gradational bases and sharp tops. The facies consist of bioturbated siltstone to medium-grained sandstone. They are intensely bioturbated by mainly thin and horizontal (Fig. 2.6C; Table 2.1) which mixed the silt and sand. The facies are developed in the Upper Marrat unit intercalated in the bluish green shale (F6) deposited in a tidal flat environment. These facies usually grade up into tidal and/or wave influenced massive sandstone (F8 to F10), which suggests a mixed flat/coastal plain depositional setting transitional between the coastal wave dominated shoreface and the tide-dominated mud flats.

F8: Cross-bedded sandstone with mud drapes (tidal creeks)

This facies association occurs in 0.5 to 1.5 m thick lenticular bodies bounded by an erosional surface at the base and commonly sharp, iron stained and bioturbated surface at the top. These are made up of medium-grained sandstone including some plant debris. These deposits are characterized by tabular cross-bedding and mud-draped current ripples indicating tidal influence (Fig. 2.6D and 6E; Table 2.1). These facies are well developed only in the Upper Marrat unit interbedded mainly with the mottled bluish green shale (F6) and locally with bioturbated heterolithic silty sandstone (F7). The facies are interpreted to be deposited in tidal creeks draining a wide low-energy lower coastal plain.

F9: *Skolithos*-bearing bidirectional cross-bedded sandstone (tidal bars and channels)

These facies form 0.5 to 1.5 m thick with tabular to lenticular units with sharp bases, and iron-stained bioturbated tops. They consist of medium-grained sandstone including plant debris and displaying bidirectional megaripple cross-bedding of tidal origin. They are highly bioturbated with abundant *Skolithos* trace-fossils (Fig. 2.6F; Table 2.1). They occur in the topmost of the Marrat Formation on top of the paleosols (F5), bluish green shale (F6), bioturbated heterolithic silty sandstone (F7) and wave influenced sandstone (F10). These bioturbated cross-bedded sandstones are interpreted to be deposited in tidal bars and channels in a nearshore environment.

`→ **Figure 2.6:** Coastal plain facies association (A-E), high-energy nearshore facies association (F-G). **A)** Mottled bluish green shale (mud flat/coastal plain), Lower Marrat, Khashm Disman, **B)** Stromatolitic lime-mudstone marked at the top by mudcracks (d arrow), mud flat/coastal plain, Lower Marrat, Khashm Ad Dhibi, **C)** Bioturbated heterolithic silty sandstone shows nodular structure, mixed flat/coastal plain, Upper Marrat, Khashm Al Khalta**, D)** Small ripples with mud drapes, sand tidal-flat, Upper Marrat, Khashm Al Khalta (note pen for scale), **E)** Channel-fill sandstone with mud drapes (? IHS) from the same horizon of photo D, tidal creeks, **F)** Skolithos sandstone with vertical tube burrows (s arrows), sand tidal-flat/bars, Upper Marrat, Khashm Abu Al Jiwar, **G)** Sharp base massive sandstone with swaley cross-stratification, storm influenced shoreface, Upper Marrat, Faridat Balum, **H)** Close-up photo of the swaley cross-stratification in photo G shows chevron structure developed a ripple crest (arrow).

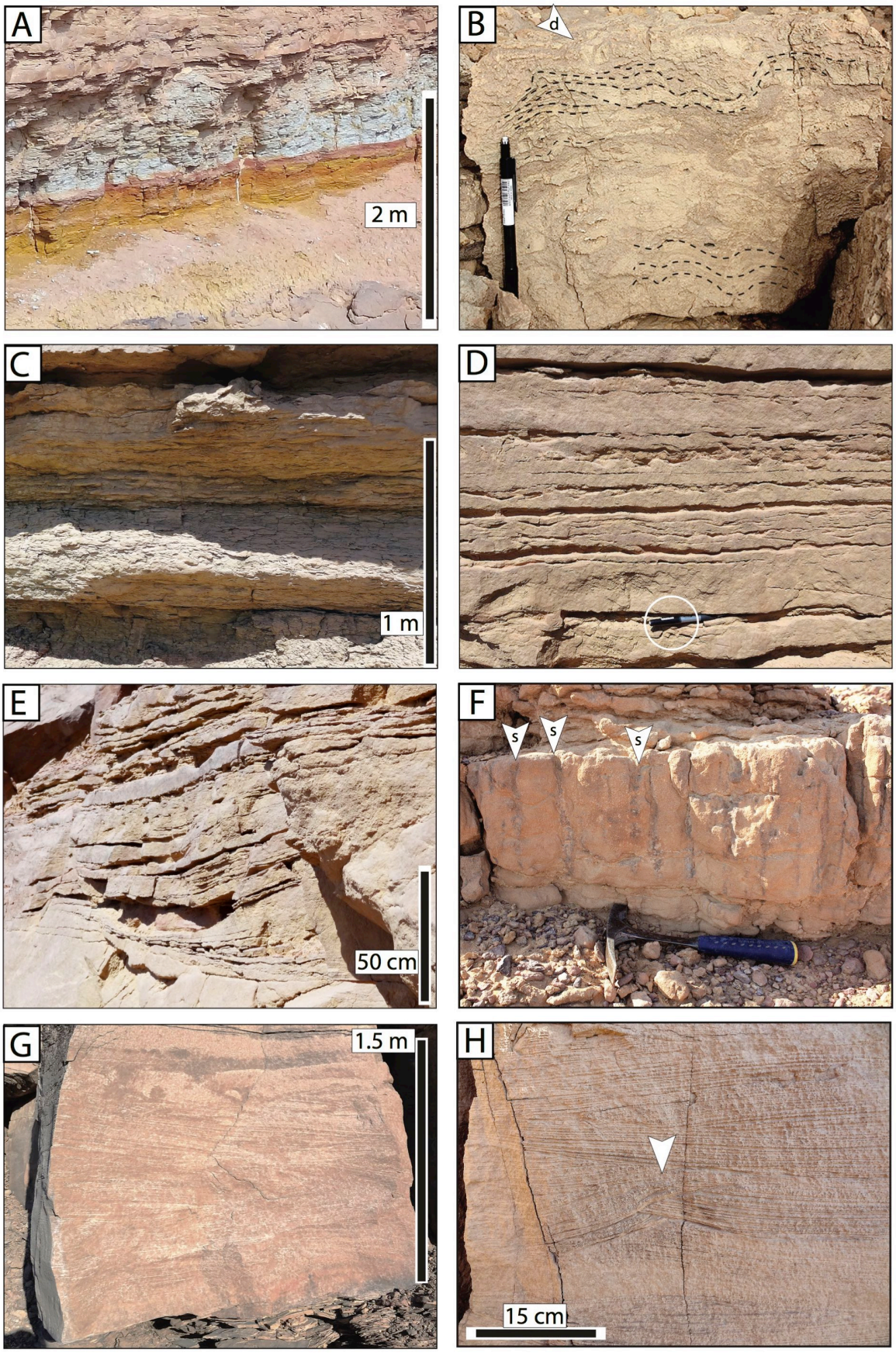
A
2 m
B
d
C
1 m
D
E
50 cm
F
s
s
s
G
1.5 m
H
15 cm

F10: Swaley cross-stratified sandstone (shoreface)

These facies occur as 1 to 2 m thick tabular units having sharp scoured bases and bioturbated top (Fig. 2.6G, H; Table 2.1). They consist of medium-grained sandstone including intraclastic reworked pebbles and are characterized by swaley and some hummocky cross-stratifications (Harms et al., 1975; Leckie and Walker, 1982). Sometimes, this facies grades up to bidirectional cross-bedded tidal sandstone (F9). Otherwise, the SCS sandstones can be sharply overlying tidal creek sandy deposits (F8) bioturbated heterolithic silty sandstone (F7) or grayish green shale (F11). The facies can be interpreted as a wave-dominated shoreface deposits occur in Lower and Upper Marrat units.

F11: Grayish green calcareous shale (shale dominated inner-lagoon)

The facies appear as 1 to 4 m thick olive gray to greenish gray units. The shales are brittle, flaggy and slabby. They are made up of terrigenous clay and admixed carbonate (Fig. 2.7A; Table 2.2) containing gastropods, bivalves and locally ammonites (Manivit et al., 1990). In core, the calcareous shales show thin laminations, rare *Chondrites* burrows and thin levels of reworked mollusk debris (Fig. 2.10). These shales are mainly interbedded with bioturbated quartzose lime-mudstone and the mottled bluish green shale (F6), which suggest an inner lagoon environment close to the continental to coastal plain terrigenous source. The rare *Chondrites* burrows, rare macrofauna and the thinly laminated structure suggest restricted conditions, a low oxygenated bottom water (Bromley and Ekdale, 1984). The driving control of the restriction in such shallow water is probably the high coastal nutrient influx

and the surface runoff which could cause density stratification that prevented vertical circulation of bottom water (Bottjer et al., 1986 in Read, 1989; Rabalais et al.,1991; Lukasik et al., 2000).

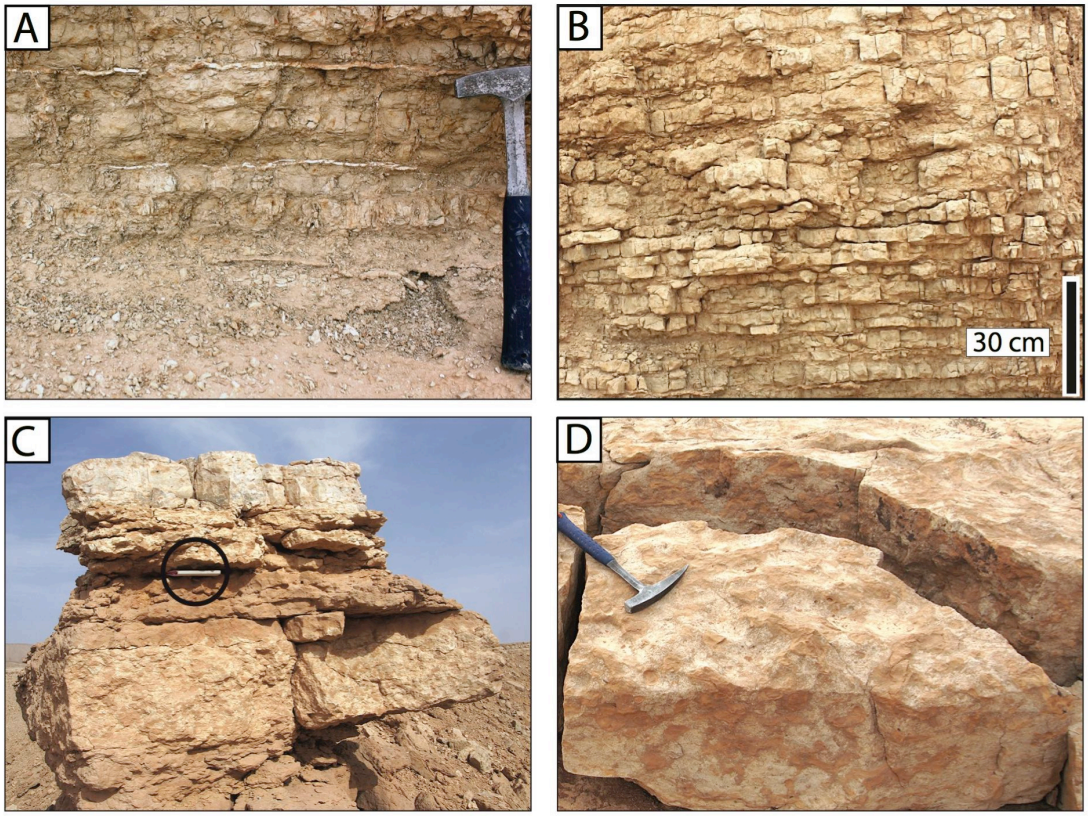

Figure 2.7: Mixed carbonate-siliciclastic inner-lagoon facies association in Khashm Ad Dhibi. **A)** Grayish green calcareous shale (shale dominated inner lagoon), Upper Marrat (note hammer for scale), **B)** Argillaceous nodular bioturbated peloidal wackestone/mudstone (carbonate dominated inner lagoon), Upper Marrat, **C)** Nodular horizontal-bioturbated peloidal wackestone (where the notebook is located) intercalated with highly bioturbated wackestone/mudstone beds, Middle Marrat, **D)** Top and side view of the bioturbated wackestone/mudstone (highly bioturbated lagoon), Middle Marrat.

F12: Argillaceous nodular peloidal mudstone/wackestone (carbonate-prone inner lagoon)

These are tabular units, 1 to 3 m thick, and commonly bounded by sharp base and top. The base of the facies is often marked by reworked intraclasts and skeletal fragments. The are made up of slightly argillaceous muddy carbonate facies including pellets, peloids, intraclasts, skeletal fragments and locally 20 to 50% fine to medium quartz grains. The fossils assemblage consists of ammonites, bivalves, gastropods, echinoid fragments, brachiopods and agglutinated foraminifera such as *Ammodiscus* sp. (Manivit et al., 1990; Hughes, 2009; unpublished report DHIBI-1 micropaleontology). The facies exhibit a nodular sedimentary structure (Fig. 2.7B; Table 2.2), argillaceous wispy lamination in core sample and thin horizontal burrows 5 mm wide (Fig. 2.7C). The facies are present in the upper part of the Lower Marrat and upper Marrat units. They are interpreted to be deposited in a low-energy carbonate-prone lagoon with limited siliciclastic influx. As they are localized between dark-color calcareous shale (F11) and light-color bioturbated lime-mudstone (F13), it is assumed to record the transition from the less-oxygenated to well-oxygenated conditions.

F13: Bioturbated peloidal wackestone/mudstone (extensive carbonate lagoon)

These facies consist of 1 to 3 m thick very tabular units, with a transitional base and bioturbated firmground at the top (Fig. 2.7C and D; Table 2.2). They are made up of very fine pelletal peloidal grains and diverse biota that includes echinoid fragments, brachiopods, molluscs (typicallty *Inoceramus*

fragments), and benthic foraminifera (*Siphovalvulina variabilis*, *juvenile Valvulina* sp., *Haplophragmoides* ssp., *Ammobaculites* sp., *Textulariopsis*) (Fig. 2.10; Hughes, 2009). The facies are interbedded with the slightly argillaceous horizontal limestone (F12). They are only present in the northern two sections (Fig. 2.12). The facies are interpreted as the most distal marine facies of a shallow low-energy well-oxygenated lagoon.

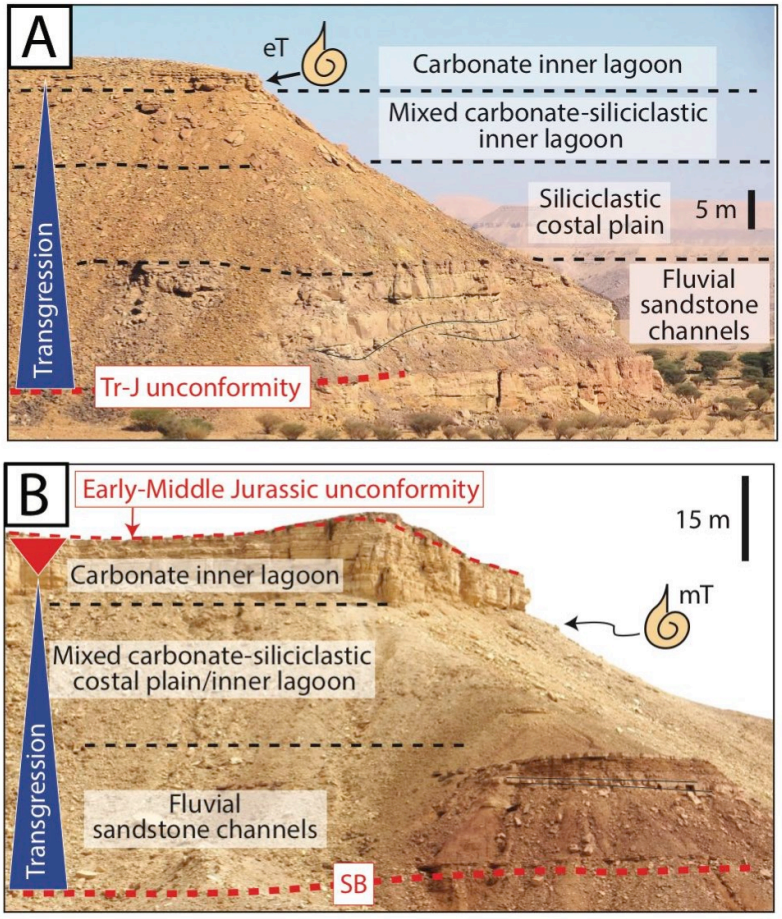

Figure 2.8: Vertical facies successions show the evolution of the depositional environments (from fluvial to carbonate inner lagoon) during a 3rd-order marine transgression. **A)** The Lower Marrat outcrop photo from Wadi Al Jufayr shows the transgression successions of (MCS1). The maximum marine transgression is placed in highly bioturbated peloidal wackestone/mudstone (carbonate inner lagoon), which contains Early Toarcian ammonite fauna. **B)** The Middle and Upper Marrat outcrop at Khashm Ad Dhibi shows complete successions of the second composite sequence (MCS2). The Middle Toarcian ammonite fauna was found at the foot of the cliff in a green calcareous-shale (inner lagoon). (abbreviation: eT= Early Toarcian; mT= Middle Toarcian)

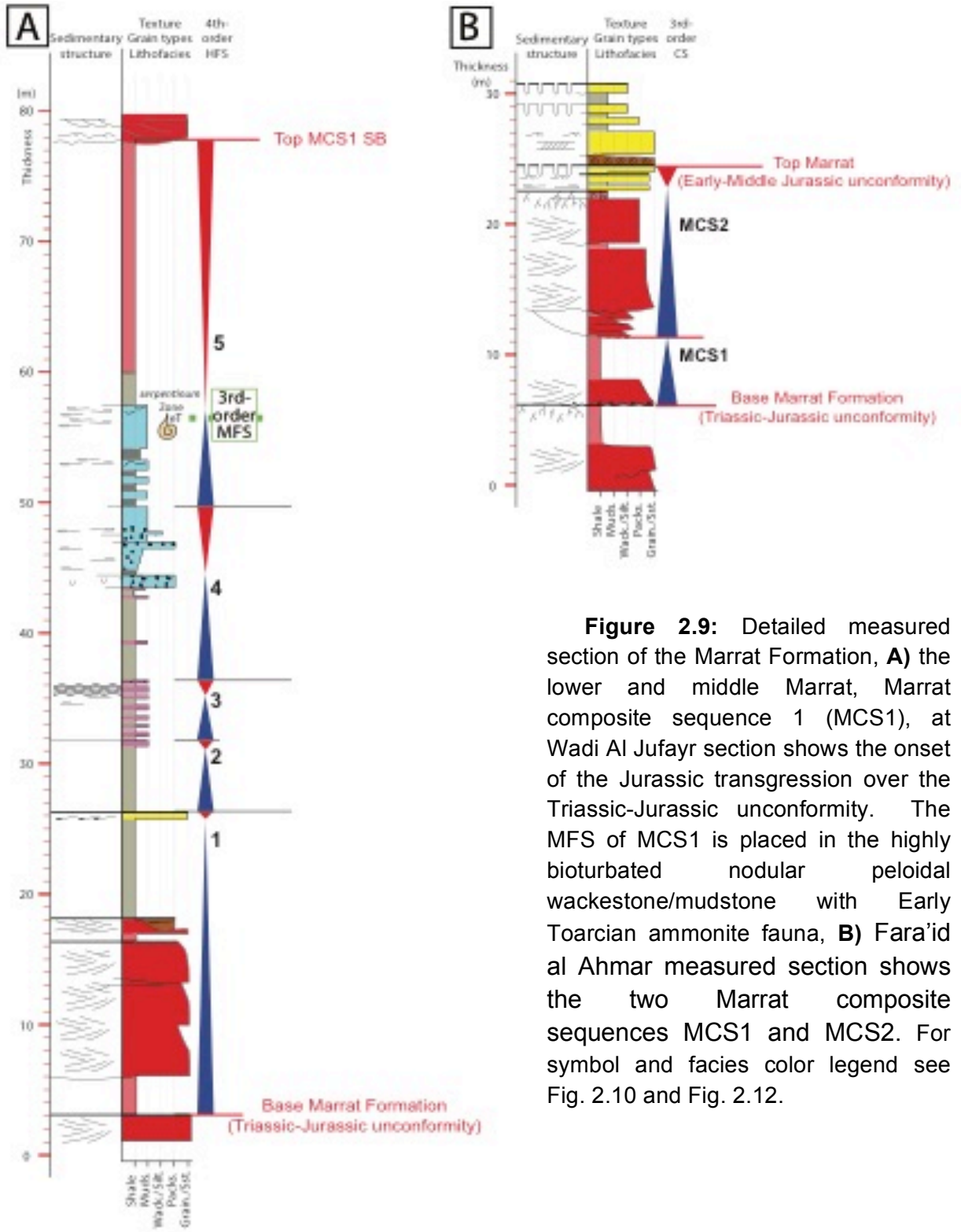

Figure 2.9: Detailed measured section of the Marrat Formation, **A)** the lower and middle Marrat, Marrat composite sequence 1 (MCS1), at Wadi Al Jufayr section shows the onset of the Jurassic transgression over the Triassic-Jurassic unconformity. The MFS of MCS1 is placed in the highly bioturbated nodular peloidal wackestone/mudstone with Early Toarcian ammonite fauna, **B)** Fara'id al Ahmar measured section shows the two Marrat composite sequences MCS1 and MCS2. For symbol and facies color legend see Fig. 2.10 and Fig. 2.12.

2.5 Depositional model

The spatial distribution and the lateral relationships of the facies are illustrated in an idealized depositional model (Fig. 2.11). This depositional model is built using the sedimentological characteristics, vertical facies successions in individual logs (Fig. 2.9, 2.10) but also the lateral organization of the facies given by the correlation established along a 280 km long transect (Fig. 2.12).

The depositional model represents a continental to inner-platform shallow marine depositional settings with two depositional domains include a siliciclastic-prone proximal domain and carbonate-prone distal domain. The siliciclastic proximal domain consists of alluvial system and wide shale-prone coastal plain to lagoonal environment with limited fluvial dynamics. They are characterized by low energy tidal flat and higher energy nearshore tide and occasional wave dominated environment. The higher energy nearshore environment is better developed during periods of high accommodation rates (Late TST and MFS) in which higher water-depth favor wave propagation and stronger tidal currents. The carbonate dominated distal domain consists of shale-prone lagoon influenced by siliciclastic influx, and mud carbonate-prone inner-platform representing the most open marine environment.

The objective of this idealized depositional model is to give a relative position to each identified facies and does not indicate synchronous facies. This is because the sedimentary systems are changed through time and evolved within a depositional sequence. For example, siliciclastic facies are more dominant during early transgressive periods and carbonates develop

widely during latest transgressive and highstand periods as will be shown and explain hereafter.

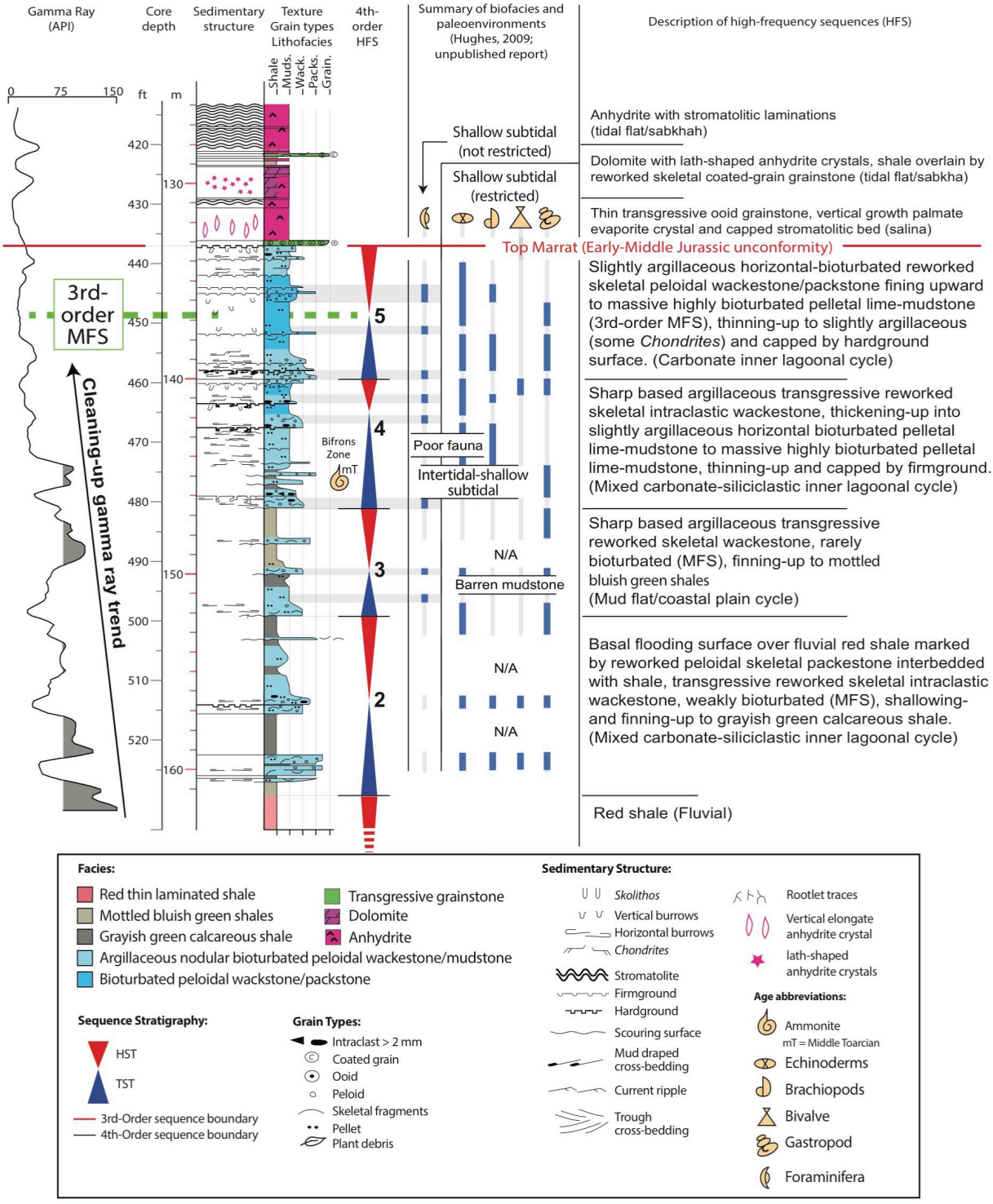

← **Figure 2.10:** Detailed core description of the upper Marrat Formation at Khashm Ad Dhibi section (from DHIBI-1 outcrop core) combined with biofacies summary and paleoenvironmental interpretation of (Hughes, 2009; unpublished Saudi Aramco report). The succession is characterized by mixed carbonate-siliciclastic cycles. This core is bounded at the base by fluvial deposits and at the top by a major unconformity. The section shows initial transgression over fluvial deposits. The upward-increasing proportion of the bioturbated carbonate lithofacies reflects an overall marine transgression trend. The MFS is placed in the thickest beds of highly bioturbated lime-mudstone facies. This 3rd-order sequence (TST, MFS and HST) shows no evidence of wave-base or mid-ramp high-energy facies in classical sense. High-energy facies in such flat shallow inner-platform setting appears at base of the HFSs marked by reworked sediments. Interestingly, these basal transgressive grainy facies coincide with appearance of the most open marine biofacies (foraminifera) in generally restricted low-oxygenated environment. Hughes (2009; unpublished report) described these foraminifera as follow: " The foraminifera are almost entirely agglutinated, very small, and also indicative of adverse conditions. Agglutinated forms include species of *Ammodiscus*, *Trochammina, Haplophragmoides, Textulariopsis* and *Pseudomorulaeplecta.* In a few samples, uniserial calcareous foraminifera attributed to *Stilostomella* spp. are present."

2.6 Sequence stratigraphy

Correlations between nine sedimentological sections in the Marrat formation result in a regional transect oriented in an oblique-dip direction. The transect is characterized at the base by the Triassic – Jurassic unconformity marked by sharp erosional surface at top of fluvial Minjur Sandstone. The datum surface is the top Marrat Formation corresponds to the Early – Middle Jurassic unconformity The unconformity is overlain by local evaporites to the north and laterally continuous ferruginous oolite to the south. The Middle Marrat continental red unit shows continuous extension along the outcrops. The lateral facies changes in the shallow-marine environment indicating an apparent S-N polarity.

The facies distribution along this regional transect attests that the Marrat Formation comprises two composite sequences (MCS1 and MCS2). Each in turn consists of five high-frequency sequences (HFS1 to HFS5). The first composite sequence (MCS1) includes the Lower Marrat and a part of the Middle Marrat unit and the second (MCS2) includes a part of the Middle Marrat and the Upper Marrat units (Fig. 2.12).

The age of the composite sequences is based on three ammonite biostratigraphic intervals (Manivit et al., 1990) (Fig. 2.3, 2.8, 2.9 and 2.10). The MCS1 can be attributed to the late-Early Toarcian (*serpentinum* Zone) based on ammonites found in carbonate facies (Fig. 2.8A). The late transgressive carbonates in 10 meters below the top of the Marrat Formation contain an ammonite fauna (*Nejdia*) of Middle Toarcian *bifrons* Zone (*sublevisoni* Subzone) for MCS2 (Fig. 2.8B). The basal unit of the Dhruma Formation contains ammonite fauna of Early Bajocian age (*discites* Zone) that confirms the hiatus of the Aalenian and probably part of if not all the Late Toarcian.

The CSs and HFS are wedge and onlap southward onto the Triassic – Jurassic unconformity. The regional geometry of these continental to shallow marine deposits attests a clear differential subsidence along the transect. This differential subsidence appears rather homogeneous except around F. Balum where a strong increase of the subsidence rate is recorded.

The main maximum marine transgression is near the top of the Marrat Formation (MCS2), probably in the *bifrons* Zone. There are no evidence progradational stacking patterns or low-stand deposits. Even the top of the Marrat Formation that corresponds to a more than 8 Myr long hiatus and

probable subaerial exposure does not exhibit any fluvial incisions, indicating the lack of any efficient fluvial system and probably a very flat topography at this time.

In the reference section (Khashm Ad Dhibi), the vertical facies successions of the Marrat CSs are both characterized by basal transgressive fluvial channel-fills which grade upward to mixed carbonate-siliciclastic coastal-plain and lagoonal facies (Fig. 2.8 and 2.9). The maximum marine transgressions of these CSs are interpreted in the clean bioturbated limestone lagoonal facies (F13) in the upper part of the Lower and Upper Marrat units (Fig. 2.8, 2.9 and 2.10). The transgressive system tracts (TST) of the CSs are divided into early- and late-interval based on dominant facies distribution, and inferred depositional environment. Only the early high-stand systems tracts (HST) (Sarg, 1988; Vail et al., 1991) are represented by aggradational coastal-plain and non-marine shale in MCS1 and by thin carbonate or mixed unit in MCS2.

These MCS are clearly asymmetric in thickness with a thick transgressive unit and much thinner regressive one. This pattern is both related to a low accommodation rate and very shallow marine conditions.

2.6.1 Marrat Composite Sequence 1 (MCS1)

The MCS1, 85 m thick in the northern area (Khashm Ad Dhibi), thins out and pinches out at the most southern section. The basal sequence boundary is the Triassic – Jurassic unconformity marked by a very sharp contact (Fig. 2.8A), paleosol and iron-crust surfaces on top of the Minjur Sandstone fluvial deposits. In the most complete sections, the early TST (0 to 40 m thick) consists of a basal fluvial sandstone unit (F1) overlain by barren bluish green

shale coastal-plain facies (F6). It is made up of at least three HFSs (HFS1 to 3) characterized by asymmetrical transgressive cycles with thick basal shale capped by (1) a thin cross-bedded sandstone unit characterized by mud-drapes and mudcracks (HFS1), or (2) a thin stromatolitic lime-mudstone and dolomite bed (HFS2 and 3). These HFSs are aggradational at the base of the northern two sections and pinch-out completely between W. Al Jufair and F. Balum sections.

The late TST (0 to 23 m thick) is dominated by mixed carbonate-siliciclastic lagoonal facies and made up of at least two HFSs (HFS4 and part of HFS5). It starts with thin a fluvial sandstone bed grading upward to brown shale coastal-plain (F6) and to inner-lagoon quartzose nodular lime-mudstone (F11) interbedded with green calcareous shale (F12). The calcareous shale and the quartzose lime-mudstone grade updip to shoreface swaley cross-stratified sandstones (F10). Further updip, there are also several fluvial units between Khashm Al Khalta and F. Al Ahmar indicating a local increase of the terrigenous influx during this transgressive period. These shoreface sandstones attest the aggradation of narrow high-energy wave dominated facies belt in the inner part of the sedimentary system during periods of relative high accommodation rate. To the North, the MFS is marked by lagoonal highly bioturbated peloidal lime-mudstone (F13). South of F. Balum section, these pure carbonate deposits grades to mixed siliciclastic-dolomitic then argillaceous facies that finally onlap directly on the Minjur Formation in F. Al Ahmar section

The HST is marked by a progressive decrease of carbonate content and the deposition of coastal-plain green shale (F6) that progressively grades

upward into flood-plain/lake thin laminated red shales (F4) of the Middle Marrat unit. These high-stand red shales form an aggradational and tabular 15 to 20 m thick unit in the northern area. It pinches out gradually southward. The sequence boundary is placed at the base of the fluvial channel-fill sandstones that are locally intercalated in the red shales. This surface does not correspond to an important fluvial incision associated to a base level drop nor to a major downward shift of the facies belts. It is then considered as a type 2 sequence boundary (Vail et al., 1991).

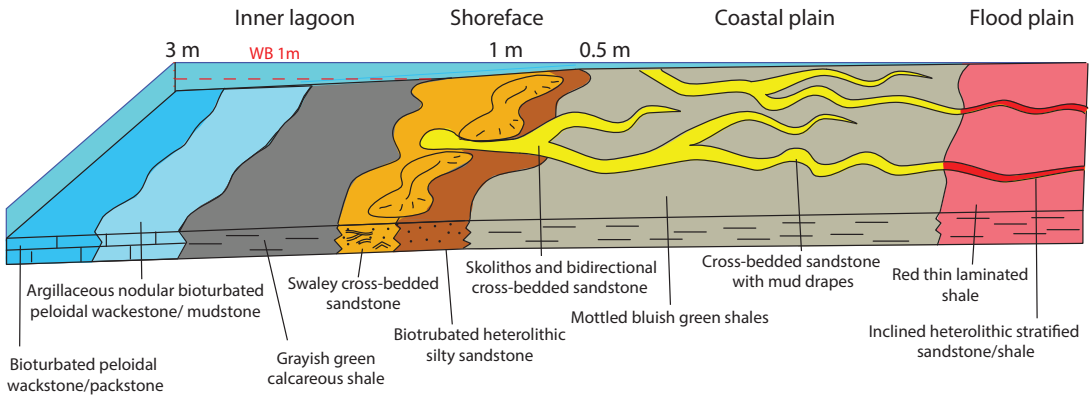

Figure 2.11: Idealized block diagram shows the Marrat Formation facies distribution in relation to the shoreline position. The facies are deposited in very-wide flat inner-platform depositional environments. The diagram is not meant to show synchronous facies. This is because the depositional environments are evolving through the successions. For example, tidal creeks and wide coastal plain were developed lately in the upper Marrat Formation. High-energy wave-dominated shoreline appears only during late TST, whereas early TST and HST are characterized by low-energy mud-dominated shoreline. The water depth was estimated by reconstructing the depositional profile from one of the upper cycles in the cross-section.

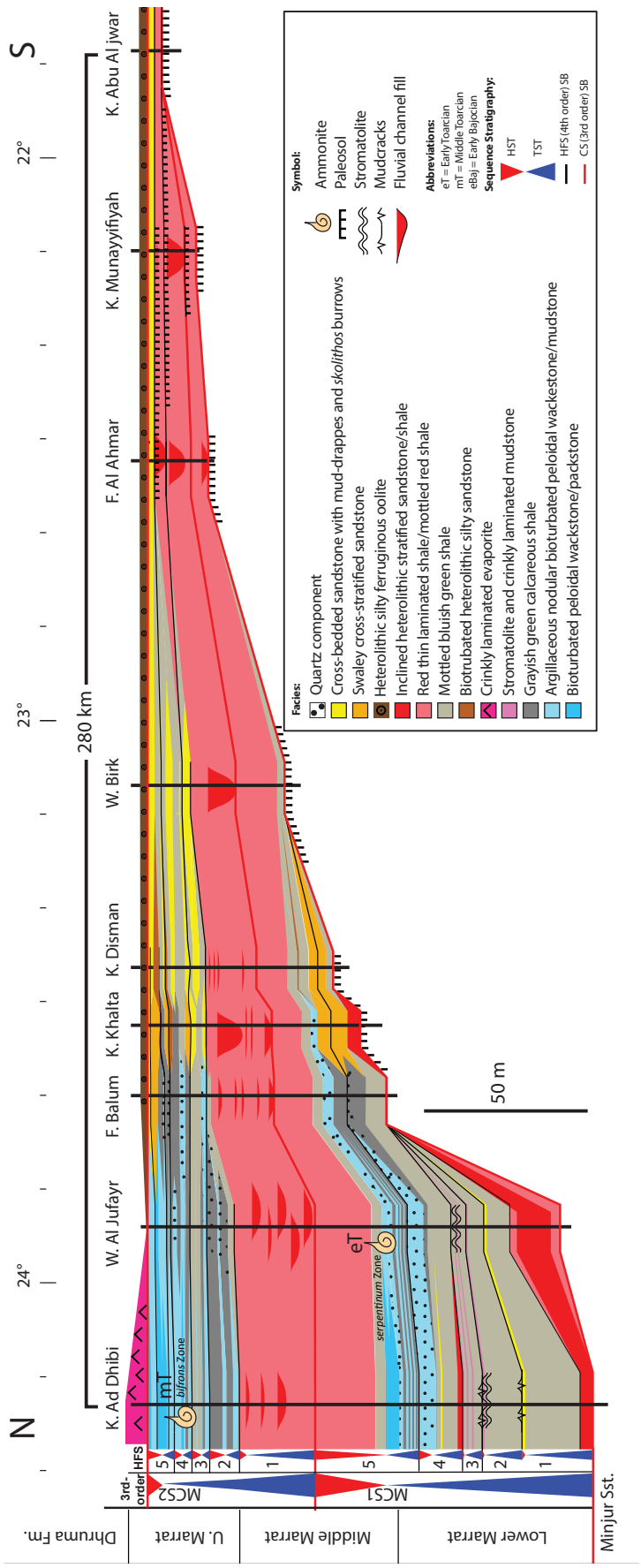

Figure 2.12: High-resolution sequence stratigraphic cross section of the Marrat Formation along the Jabal Tuwayq outcrops. The datum is top of the Marrat unconformity which is overlain by evaporite deposits in the northern area and heterolithic silty iron ooid deposits in the southern area. The latitudinal degrees are shown at the head of the section as reference points.

2.6.2 Marrat Composite Sequence 2 (MCS2)

The MCS2 thins out to the south from 50 m to 4 m thick. The basal sequence boundary is marked by a turnover trend interpreted at the base of the meandering channel-fill sandstone deposited in an overall aggradational pattern and a base-level rise context (Fig 2.3A; Embry, 1995). The early TST is made up of at least three backstepping HFSs (HFS1 to 3) onlapping towards the south. They are characterized by shale dominated low-energy fluvial, coastal plain and inner lagoon facies. The basal fluvial deposits are interpreted to be diachronous laterally equivalent to HFS1 to 3. The high-resolution stratigraphic correlations show that the more proximal coarse-grained and cross-stratified fluvial facies are not localized in the southernmost part of the transect where MCS2 is wedging out. These facies are dominant in Wadi Birk – F. Al Ahmar, and secondarily in K. Al Khalta areas. They grade to more distal shaly deposits northward and to lower energy fluvial deposits southward towards the south in the area of minimum accommodation rate, but no fluvial incisions were noticed. This observation suggests that the orientation of the fluvial systems is oblique to the studied transect with a probable west-east component.

In detail, HFS1 is entirely made up of fluvial sandstone and shale deposits up to 25 m thick overlain in the northern section by transgressive thin reworked peloidal skeletal packstone of HFS2 (Fig. 2.10). HFS2 is a 9 m thick symmetrical cycle and is made up of grayish green calcareous shale (F11) with thin reworked skeletal intraclastic rarely bioturbated wackestones (F12) (Fig. 2.10). HFS2 shows an increase in quartz content updip grading into fluvial red shale (F3/F4) and point-bar sandstone (F2). HFS3, 2.5 to 5.5 m

thick, begins with sharp-based skeletal wackestone fining upward to weakly bioturbated argillaceous lime-mudstone (F12) and capped by coastal-plain reddish brown shale (F6) (Fig. 2.10). This HFS3 grades updip into well-developed tidal cross-bedded sandstone (F9) and further to the south into fluvial sandstone and associated red shales.

The late TST is made up of two backstepping HFSs (HFS4 and lower part of HFS5). From north to south, the depositional system consists of several facies belts: a mixed carbonate-siliciclastic (F11/F12), a narrow and localized wave-dominated nearshore sandstone belt (F10), an inner lagoon to coastal plain shale-dominated environment with tidal channel sandstones (F6 to F9) and alluvial red shales and heterolithic point-bars (F2 to F4). The HFS4 is symmetrical transgressive-regressive cycle up to 6 m thick (Fig. 2.10). It begins with sharp base argillaceous transgressive reworked skeletal intraclastic wackestone (F12; K. Ad Dhibi) or scour-based swaley cross-stratified sandstone (F10; K. Khalta). At the base of HFS4, ammonite fauna dated as Middle Toarcian (*bifrons* zone) was found in calcareous shale inner-lagoon facies in K. Ad Dhibi (Manivit et al., 1990). The calcareous shale (F11) grades upward to slightly argillaceous lime-mudstone (F12) interpreted as the MFS and HST of this high frequency sequence. Updip to the south, this facies is characterized by an increase of quartz content and it progressively changes to coastal-plain green shale (F6) and tidal sandstone (F8) without passing through high-energy shoreface deposits. In the most southern sections, HFS4 consists of fluvial sandstone capped by paleosol. The HFS5 is a symmetrical transgressive-regressive cycle ranging from 2.5 to 7 m in thickness. From north to south, it begins with slightly argillaceous wackestone/packstone (F12;

K. Ad Dhibi), sharp-based wave dominated sandstone (F10; K. Khalta) or tidal point-bar sandstone (F8; K. Disman).

The MFS of the MCS2 corresponds to MFS the HFS5. It can be considered also as the MFS of the whole Marrat cycle. In K. Ad Dhibi to the north, it is marked by a relatively thick highly-bioturbated pelletal lime-mudstone considered as a shallow marine low-energy inner carbonate platform facies, the most distal marine facies of the entire Marrat Formation (Fig. 2.10). It grades updip to calcareous shale (F11; W. Al Jufayr), then to relatively higher energy sand dominated shoreface to backshore/tidal flat deposits. The shoreface is represented by scour-based intraclastic swaley cross-stratified sandstone (F10, F. Balum). In a more proximal position, tidal-influenced sandstone and heterolithic facies are deposited in backshore to tidal flat (F7 to F9; K. Disman to F. Al Ahmar).

The HST of MCS2 is very thin (> 5 m). It is dominated by shallow-marine carbonate and sandstone and is so characterized by a very little shale content. In the northern section (K. Ad Dhibi), it is made up of thinning-up slightly argillaceous carbonate parasequences with some *Chondrites* burrows and capped by a hardground surface (Fig. 2.10). In a more proximal position, it is marked by a minor progradation of the nearshore sandstone belt (F10, K. Khalta to F. Balum; Fig. 2.12). Then, the facies succession attests a decrease of the wave influence and a relative increase of tidal processes with the occurrence of bidirectional cross-bedded sandstone (F. Balum, K. Khalta and K. Disman) and *Skolithos* sandstone with plant debris (F9). The HST wedge out to the south where it is represented by iron-stained surfaces.

The upper sequence boundary of MCS2 is a hardground surface overlain by 7 m of evaporites (Fig. 2.10; K. Ad Dhibi). Lithostratigraphically, the evaporites are considered as part of the Marrat Formation (Manivit et al., 1990). However, they are not genetically related to the Marrat depositional system but to the Dhruma sequence (Al-Mojel et al., in preparation) consistent with Powers (1968). This unit is restricted to the most subsiding area (K. Ad Dhibi) and disappears rapidly southwards. From F. Balum to Abu Al Jiwar, over more than 200 km, the top Marrat unconformity is overlain by a silty ferruginous oolite horizon up to 0.5 to 5 m thick lying on top of the thin but highly continuous HFS5 with no evidence of major erosion. This stratal continuity below and above the Early-Middle Jurassic unconformity confirms the very flat topography and high stability of this part of the Arabian platform during this period of more than 8 Myr.

2.7 Discussion

2.7.1 Inner platform development

The Arabian Platform of the Early Jurassic time underwent gentle differential subsidence. The continuous and slight subsidence is controlling the thickness of the strata as well as lateral facies distribution (cf. Wilson and Jordan, 1983). Thus, the platform will aggrade and keep-up as a response to the rotational differential subsidence. The Jurassic Arabian Platform can stack thick shallow carbonate deposits wedging and thickening toward the depocenter.

During the onset of the Jurassic transgression, the Arabian Platform tends to be very flat low-energy and shallow-marine inner platform as attested by

our stratigraphic transect (Fig. 2.12 and 2.14). A minor slope of 0.1 m/km is calculated from the top of Marrat Formation from the shoreline (F. Balum) to the most distal section (K. Ad Dhibi) in a corrected dip direction, assuming NE dip. This flat-topped profile is mainly related to overall geodynamic setting, inner part of a very wide epeiric platform on the Neo-Tethys passive margin with stable tectonic context. The limited rate of accommodation is compensated everywhere and filled by the siliciclastic supply and the carbonate production. The very flat depositional profile is also indicated by the large area of tidal influence in the siliciclastic lagoon/coastal plain and the meandering pattern of the fluvial system of the middle Marrat unit. The lack of evidence of major channel incisions or channel progradation during relative sea-level fall can be also considered as a consequence of the very low gradient with probably limited sea level drop in such greenhouse context (Summerfield, 1985; in Blum and Törnqvist, 2000). Moreover, the lack of high-energy sediment transport process and the low sediment production, both carbonate and siliciclastic in proximal setting, led for very low gradient depositional profile (0 to 0.4°) (Williams et al., 2011).

The Marrat Formation is made up of two mixed systems (MCS1 and MCS2) speared by a continental unit (the Middle Marrat). They are characterized by low-energy mud-dominated coastal plain to lagoonal setting with limited fluvial input. The coastal plain at the base of MCS1 is very low-energy marked by barren shale with thin stromatolites lime-mudstone (Fig. 2.10). The high-energy siliciclastic facies appears during late transgression as short-lived wave reworking sandstone. Similarly, the MCS2 begins with low-energy shale and lime-mudstone that progressively evolved to higher-energy

tidal creeks and shoreface sandstone. Generally, the tidal creeks require higher-energy to transport the sediments and to form channel-beds (Davis, 2012). Moreover, high-energy deposits are result of repeated marine transgressive events in a kind of flat-topped wide platform with slow sedimentation rate (Wilson, 1975). Thus, higher-energy depositional settings occurs and compatible with higher accommodation space during late TST and MFS that allowed wave-base to influence to sediments. During the HST, the wave influenced deposits relatively decreased upward and became tidal-dominated sandflat with prominent bidirectional cross-bedded and *skolithos* sandstone (most top of MCS2).

The carbonates of the Marrat Formation are low-energy mud-dominated facies with thin reworked skeletal intraclastic wackestone/packstone (Fig. 2.9). They show consistent flat tabular aggrading units and almost maintained constant thickness (Fig. 2.12 and 14). The carbonate production in such mixed system is weak and characterized at the base of the sequence by interbedded shales and hardground/firmgrounds early-cemented surfaces (Fig. 2.10). This low carbonate production is probably controlled by the overall restricted inner-platform condition and poorly oxygenated bottom water due to the fresh-water runoff. The carbonates are well developed during maximum marine transgression (Late TST and MFS) in well-oxygenated lagoon setting.

2.7.2 Depositional model and sequence in shallow marine mixed platform

The Marrat Formation in the studied area is characterized by transgressive wedges of continental to shallow-marine mixed carbonate-siliciclastics

deposits. They show a progressive and continuous onlap towards the south, apparent direction, on the major Triassic – Jurassic unconformity (~ 20 Myr of time gap). The Marrat Formation is bounded at the top by the Late Toarcian – Aalenian unconformity (~ 7 Myr of time gap) that shows quite conformable parallel surface over more than 200 km. The direction of the siliciclastic influx from fluvial systems is probably coming from the west (shield) as shown by the occurrence of the most proximal facies (braided river) in the middle part of the transect (W. Birk and F. Al Ahmar; Fig. 2.9, 2.12). The carbonate deposits are located in the northern most subsiding area which likely required higher accommodation. The carbonates are represented by extensive shallow-marine low-energy muddy carbonate (Fig. 2.9 and 2.10) formed in a very flat inner-platform. The main part of the Marrat Formation consists of more or less calcareous shale and sandstone deposited in coastal plain to lagoonal environment. These depositional settings are dominated by tidal currents and, sometimes during period of sea-level rise, by wave-induced currents. The facies distribution shows that the Marrat Formation is composed of two composite sequences. The maximum flooding of each sequences are marked by carbonate deposits recorded in the northern subsiding part of the transect dated as Early Toarcian (*serpentinum* Zone) and Middle Toarcian (*bifrons* Zone). The regressive unit in between these transgressive tracts is made up of continental red shales and associated with fluvial sandstone. Interestingly, these continental deposits display a clear aggrading pattern and are not associated with erosional unconformities or a significant drop of accommodation rate, reflected by the thickness and lateral extension of these units. This suggests a strong increase of the terrigenous influx from the

continental at this period, which is probably linked to paleoenvironmental climatic changes, see below discussion.

2.7.3 Controlling factors of the Toarcian Marrat Formation

2.7.3.1 Tectonic and subsidence

The Marrat Formation records an overall relative sea-level rise after the tectonic related Triassic – Jurassic unconformity. This relative sea-level can be partly enhanced by the global eustatic rise at this period (Haq et al., 1987). The subsidence of the entire Arabian Plate, however, has also a clear impact on this onlap at a regional scale since Pliensbachian series are onlapping the top Minjur unconformity in more distal domain of the Arabian Plate (Kuwait and Oman; Clarke, 1988; Yousif and Nouman, 1997). The effect of the subsidence is very clearly demonstrated along the transect by the complete wedging of this continental to shallow marine succession from north to the south. The maximum subsidence rate of the Marrat Formation, calculated by dividing the total thickness of the formation by the 3.5 Myr duration of the *serpentinum* Zone and *bifrons* Zone (Gradstein et al., 2012) is 3.9 cm/kyr (K. Ad Dhibi). This falls within the lower range of passive margins subsidence rate (few centimeters to 10 cm/kyr; Bott, 1992). The low subsidence rates of the non-marine and coastal-plain siliciclastic sections are below this range (e.g., K. Khalta 1.83 cm/kyr, W. Birk 1.2 cm/kyr, K. Abu Al Jiwar 0.13 cm/kyr). In detail, this wedging and the northwards increase of subsidence is very progressive from K. Abu Al Jiwar to F. Balum (35 m/100 km). However, there are a rather stronger acceleration subsidence rate occurs between F. Balum and W. Al Jufayr (65 m/100 km) that are limited to the beginning of the Marrat

transgression (MCS1). This suggests a substratum faulting and deformation control in this area which could have favored the initiation of the Toarcian onlap in this domain.

The Ar Rayn Terrane (approximately between 24° N to 25° 20' N) was tectonically active structure and played significant role in the basin configuration of the study area. The Ar Rayn Terrane during late Triassic was probably uplifted and was a period of erosion (Le Nindre et al., 2003). During the Jurassic, the Ar Rayn Terrane was subsided rapidly which probably caused the depocenter axis of the Early and Middle Jurassic outcrop (*cf* Fig. 72 of Manivit et al., 1990; Fig 3 of Fischer et al., 2001). On the other hand, the southern non-subsiding area, where the Marrat Formation pinches out, was probably controlled by the Najd Fault System (f3 and f4; Fig. 2.1).

2.7.3.2 Eustatic controls

In this is study, the main MFS of the whole Marrat succession is within the Middle Toarcian (*bifrons* Zone) and that is in concordance with the main Early Jurassic MFS of the Arabian Platform (MFS J10 of Sharland et al., 2001). Consistently, the *bifrons* Zone marks the interval of the highest global sea-level rise during the Early Jurassic (Haq et al., 1988) and the major MFS of the NW Tethys in the European domain (Hardenbol et al., 1998) and drowning event in the Mediterranean domain (Jenkyns et al., 1985; Crevello, 1990). The top sequence boundary of the Marrat sequences corresponds to a regional hiatus over the Arabian Platform, Late Toarcian – Aalenian, that relates to a substantial eustatic sea-level fall (Haq et al., 1988; Le Nindre et al., 1990; Al-Husseini, 1997; Haq and Al-Qahtani, 2005) and/or subsidence resistance and large-scale uplift (Le Nindre et al., 2003). This hiatus is a widespread in the

Tethyan domain which is possibly related thermal basaltic doming in the North Sea with volcanic activities associated with subsequent collapse (Hallam, 2001). In detail, these two 3rd sequences MCS1 and MCS2 could correspond to the Tethyan eustatic sequences Toa3 and Toa4 of Hardenbol et al. (1998), considered as 3rd-order cycle of ~1.6 Myr influenced by astronomical forcing controls, precession and obliquity including their long-term modulations (Hinnov and Park, 1999; Boulila et al., 2014). The high-frequency sequences, thus, could probably correspond to the 4th-order shorter eccentricity cycles (400 kyr). These suggest that the Marrat marine transgression is influenced by orbital driven eustasy.

The short-term fluctuation of relative sea-level changes records on the Arabian Platform during deposition time of the Marrat Formation are range from 15 to 25 m (Haq and Al-Qahtani, 2005). This gives and average rate of 0.08 m/kyr which correspond to a moderate amplitude of relative sea-level changes (>15 m; Read, 1995, 1998). Whereas the cause is still debated, the cause of such moderate sea-level changes in warm greenhouse periods is most likely to be aquifer-eustasy (Wendler et al., 2016; Sames et al., 2016). An alternative scenario for the origin of this moderate amplitude of relative sea-level is the onset opening and sea floor spreading of the Atlantic Ocean (Hallam, 2001).

2.7.3.3 Climatic influences

During the Early Jurassic, the Arabian Platform is placed along the tropical belt probably few degrees south of the Equator (Fig. 2.2; Murris, 1980; Thierry et al., 2000; Sharland et al., 2001) Here, the study of the Toarcian sediments

from the Marrat Formation allow us to address for the first time the impact of these climatic disturbances in a coastal/lagoonal context situated at very low paleolatitudes. Among the Jurassic climate changes (Dera et al., 2011), the Early Toarcian warming event is generally considered as the warmest interval, as current numerical models suggest rapid temperature rises of +5 to +10°C in terrestrial domains (Dera and Donnadieu, 2012). This episode was also documented in marine paleoenvironments from European domains with shifts in the oxygen isotope composition of various fossils (Bailey et al., 2003, van de Schootbrugge et al., 2005; Suan et al., 2010). Probably initiated by considerable CO_2 releases from the Karoo-Ferrar volcanism and subsequent clathrate destabilization on the seafloor (Hesselbo et al., 2000), this disturbance is further believed to have caused a redistribution of humid belts toward mid- and high-latitudes (Dera et al., 2015), and global increases of weathering rates (Cohen et al., 2004, Dera et al., 2009). Occurrence of fluvial systems at the Lower Marrat transgression (MCS1) with plant fragments, high kaolinite (Abed, 1979) and high gamma-ray response (Fig. 2.13) suggest humid period which would correspond to the initial warm peak of the early *serpentinum* Zone (Fig. 2.14). The humid period evolved to more semi-arid condition during late TST and MFS of MCS1 showing by stromatolites, mudcracks with limited siliciclastic influx and later with carbonate development. The semi-arid condition and the carbonate development could

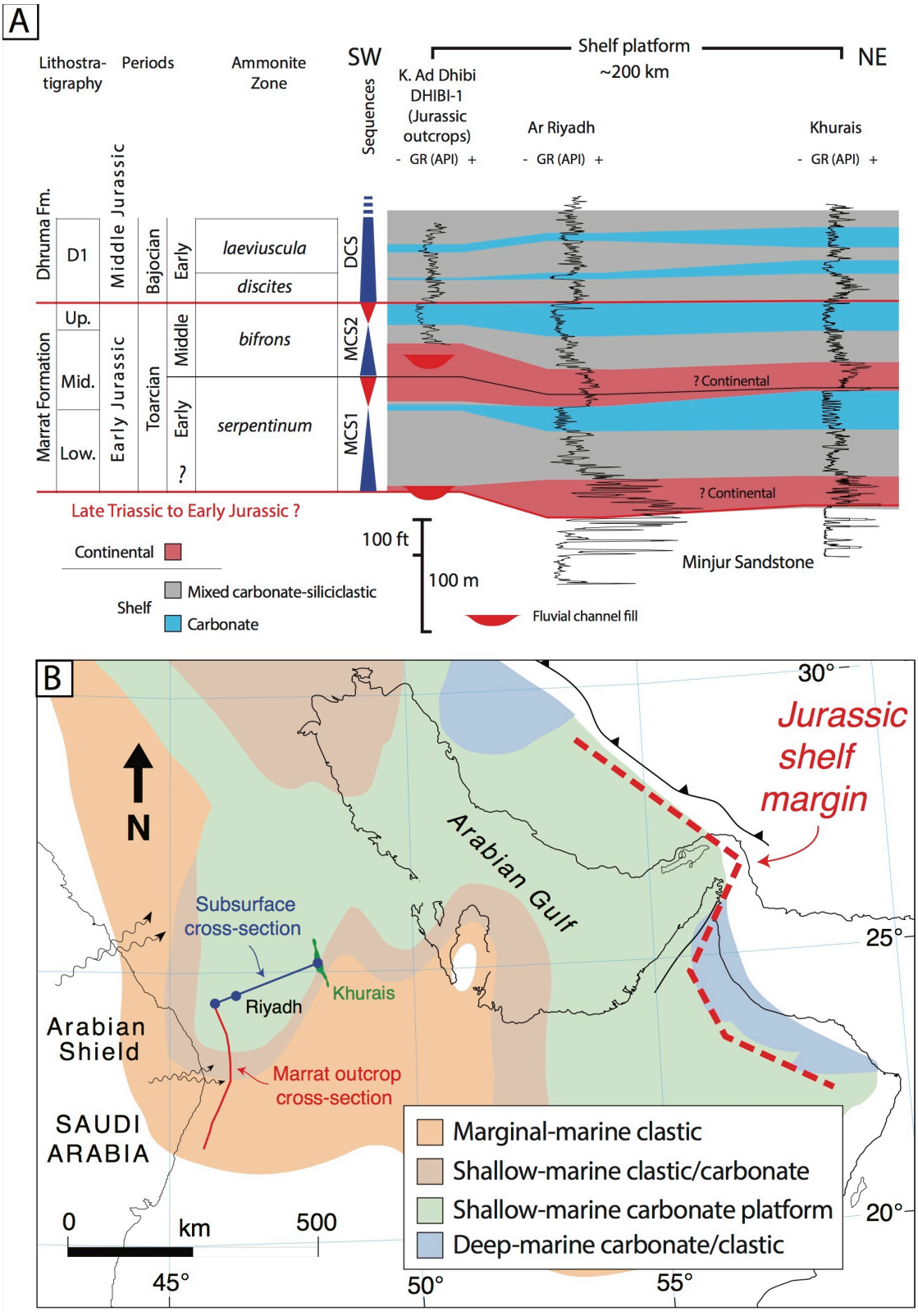

Figure 2.13: A) West-east sequence stratigraphic correlation from surface to subsurface using gamma-ray logs. Detailed facies analysis and sequence stratigraphy of the Khashm Ad Dhibi are presented in Fig. 2.10 and 2.14. **B)** Paleofacies map of the Early Jurassic (Sinemurian to Aalenian) shows two correlation trajectories and approximate location of the Jurassic shelf margin (modified after Ziegler, (2001)

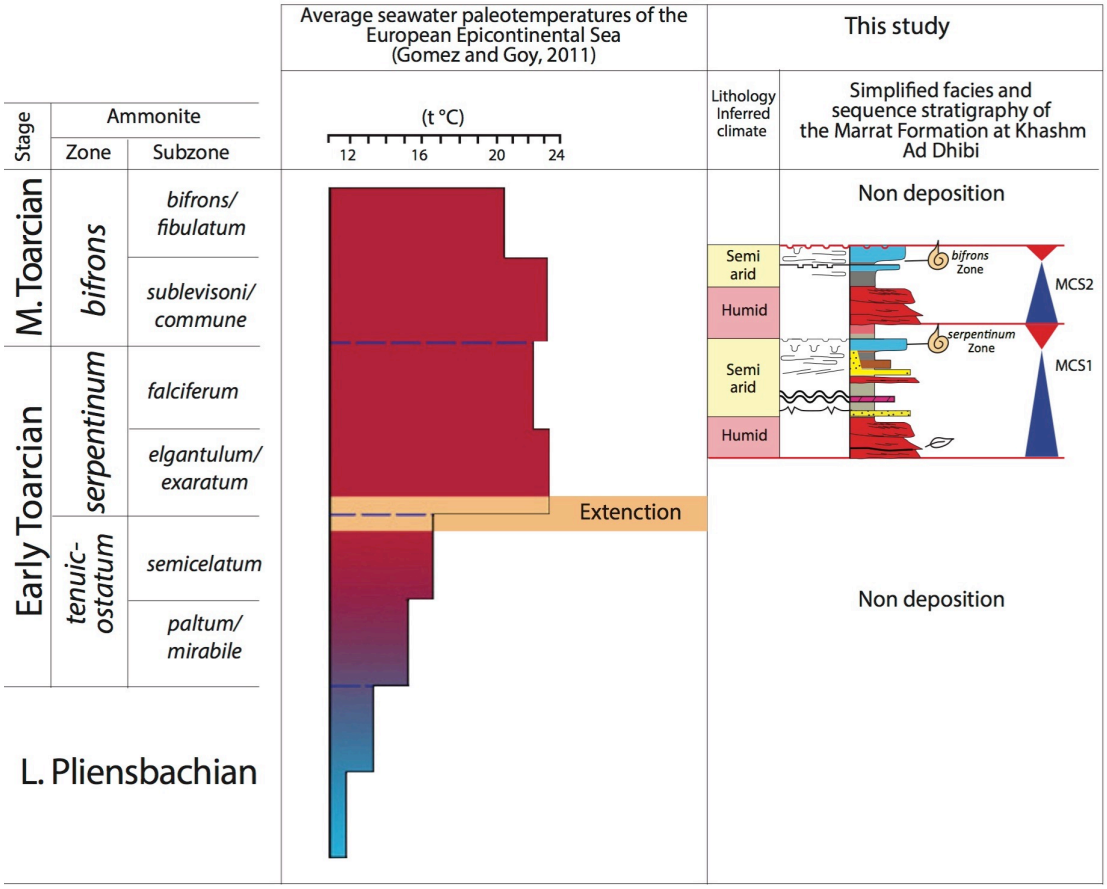

Figure 2.14: Comparison of facies and sequence stratigraphy of the studied area with average seawater paleotemperature of the European Epicontinental Sea. The average seawater palaeotemperature calculated from several localities included in the European Epicontinental Sea (Gomez and Goy, 2011). Note: the Khashm Ad Dhibi section is rescaled to fit the paleotemperature curve.

be related to slight decrease of the palaeotemperature during late *serpentinum* Zone (Fig. 2.14; Gomez and Goy, 2011). The regressive evolution recorded in the Middle Marrat (turn-over between MSC1 and MSC2) with the deposition of rather thick and extensive kaolinite and hematite enrichments of reddish shales and sandstones deposit cannot be considered as a response to the decrease of accommodation rate but to an increase of the terrigenous influx (Abed, 1979). This shale-dominated influx could be interpreted as indicative of strong hydrolyzing conditions under humid and warm period (Chamley, 1989). These observations are thus compatible with

numerical simulation suggesting rises in precipitation and runoff rates (+5 to 15 cm/kyr) on the southern part of the Arabian cratons (Dera and Donnadieu, 2012). The Middle Marrat could be really the best record of an increase of humidity during the Early Toarcian warm period (Fig. 2.14). In the same way, the MCS2 transgression could be favored by a combination of eustatic transgression (*bifrons* Zone) and decrease of the siliciclastic input indicating more semi-arid conditions with possible simultaneous overall decrease in palaeotemperature during the *bifrons* Zone (Fig. 2.14). Remarkably, the synchronicity of the TST and MFS with semi-arid and cooling events and HST with humid warm condition provide some confidence to the aquifer-eustasy as primary mechanism controlling these 3rd-order sea-level changes (cf. Wendler et al., 2016; Sames et al., 2016).

2.8 Conclusion

The outcropping Marrat Formation (late-Early to Middle Toarcian) provides a stratigraphic record of the initial Jurassic transgression of broad slowly subsiding epeiric tropical platform over the Triassic-Jurassic unconformity. The depositional environment ranges from continental meandering fluvial deposits to tidal or wave-dominated mixed carbonate-siliciclastic lagoonal deposits. These formed aggraded flat-topped platform wedging and thickening northward. Evident syndepositional differential subsidence has an influence on lateral thickness variation and facies distribution. The Carbonates are mud-dominated lagoon prudentially formed in highly subsidence areas with more accommodation space. The successions make up two 3rd-order sequences and show progressive marine transgression that reach its maximum in the Middle Toarcian *bifrons* Zone, consistent with the major MFS of the Early

Jurassic of the Arabian Platform and the European major MFS. The layer-cake geometries is controlled by the low-energy wide platform with stable tectonic context, that leads for limited accommodation space filled by siliciclastic supply and carbonate production. Short-lived higher energy siliciclastic shorelines and tidal-flat appear during high accommodation space in late-TST and HST. The carbonates are developed well during maximum marine transgression of the two Marrat sequences. Abrupt terrigenous influx event between these two sequences consists of aggraded thick extensive continental red shales and fluvial sandstone. This is possibly related to the strong hydrolyzing conditions under humid-warm period rather than a decrease of accommodation space. The synchronicity of the regression with humid-warm periods provides some confidence to the aquifer-eustasy driver mechanism of the Marrat depositional sequences.

Acknowledgments

This work was part of a PhD thesis that carried out at the University of Bordeaux-Montaigne, ENSEGID Bordeaux INP, and was sponsored by Saudi Aramco. We thank the management of Saudi Aramco for the permission to publish this work. We express our thankfulness and gratitude to Dr. Aus Al-Tawil (RCD manager, Saudi Aramco) for his endless outstanding support and motivations during all phases of this study. We also thank Dr. Denis Vaslet, Prof. J. Fred Read and Prof. Charles Kerans for providing valuable suggestions and constructive comments. We also extend our thanks to Mahmoud Alnazghah and Dr. Raed Al-Dukhayyil for field support.

References

Abed, A.M., 1979. Lower Jurassic lateritic redbeds from central Arabia. Sedimentary Geology 24 (1), 149-156.

Al-Husseini, M.I., 2009. Update to Late Triassic-Jurassic stratigraphy of Saudi Arabia for the Middle East geologic time scale. GeoArabia 14(2), 145-186.

Al-Husseini, M.I., 1997. Jurassic sequence stratigraphy of the western and southern Arabian Gulf. GeoArabia (Manama), 2(4), 361–82.

Al-Husseini, M.I., 2000. Origin of the Arabian plate structures: Amar collision and Najd Rift. GeoArabia 5, 527–542.

Al-Husseini, M.I., Matthews, R.K. 2008. Jurassic-Cretaceous Arabian orbital stratigraphy: The AROSJK Chart, GeoArabia, 13 (1), 89-94.

Alsharhan, A.S., Nairn, A.E.M., 1994. The Late Permian carbonates (Khuff Formation) in the western Arabian Gulf: Its hydrocarbon parameters and paleogeographical aspects. Carbonates and Evaporites, 9(2), 132.

Alsharhan, A.S., Nairn, A.E.M., 2003. Sedimentary basins and petroleum geology of the Middle East. Elsevier, Amsterdam, 843 pp.

Ayres, M.G., Bilal, M., Jones, R.W., Slentz, L.W., Tartir, M., Wilson, A.O., 1982. Hydrocarbon habitat in main producing areas, Saudi Arabia. AAPG bulletin, 66(1), 1-9.

Bailey, T.R., Rosenthal, Y., McArthur, J.M., Van de Schootbrugge, B., Thirwall, M.F., 2003. Paleoceanographic changes of the Late Pliensbachian–Early Toarcian interval: a possible link to the genesis of an Oceanic Anoxic Event. Earth and Planetary Science Letters, 212, 307–320.

Baud, A., Droste, H., Guillocheau, F., Razin, P., Robin, C., 2005. Mesozoic Evolution of the Tethyan margin of Oman. In 24th IAS regional Meeting, Pre-Conference Excursion BF. 4.

Baudin, F., 1989. Caractérisation géochimique et sédimentologique de la matière organique du Toarcien Téthysien (Méditerranée, Moyen-Orient), significations paleogéographiques. Ph.D. Thesis, Univ. Paris 6, Paris, France.

Blum, M.D., Törnqvist, T.E., 2000. Fluvial responses to climate and sea-level change: a review and look forward. Sedimentology, 47, 2-48.

Bott, M.H.P., 1992. Passive margins and their subsidence. Journal of the Geological Society, 149(5), 805-812.

Bottjer, D.J., Arthur, M.A., Dean, W.E., Hattin, D.E., Savrda, C.E., 1986. Rhythmic bedding produced in Cretaceous pelagic carbonate environments; sensitive recorders of climatic cycles. Paleoceanography, 1(4), 467-481

Boulila, S., Galbrun, B., Huret, E., Hinnov, L. A., Rouget, I., Gardin, S., Bartolini, A., 2014. Astronomical calibration of the Toarcian Stage: implications for sequence stratigraphy and duration of the early Toarcian OAE. Earth and Planetary Science Letters, 386, 98-111.

Bramkamp, R.A., Steineke, M., 1952. Stratigraphical introduction. In: Arkell, W.J., Bramkamp, R.A., Steineke, M. (Eds.), Jurassic Ammonites from Jebel Tuwaiq, Central Arabia. Royal Society [London] Philosophical Transactions B 236, 241–313.

Bromley, R.G., Ekdale, A.A., 1984. Trace fossil preservation in flint in the European chalk. Journal of Paleontology, 58, 298–311.

Chamley, H., 1989. Clay Sedimentology. Springer Verlag, Berlin.

Clarke, M.W.H., 1988. Stratigraphy and rock unit nomenclature in the oil-producing area of interior Oman. Journal of Petroleum Geology, 11(1), 5-60.

Cohen, A.S., Coe, A.L., Harding, S.M., Schwark, L., 2004. Osmium isotope evidence for the regulation of atmospheric CO2 by continental weathering. Geology 32 (2), 157–160.

Crevello, P. D., 1990, Depositional systems tracts, stacking patterns, and sequence stratigraphy of Lower and Middle Jurassic synrift carbonate platforms, Central and Eastern High Atlas, Morocco. International Association of Sedimentologists, 1990 Annual Meeting, Proceedings with Abstracts, 111-112

Davis Jr, R.A., 2012. Tidal signatures and their preservation potential in stratigraphic sequences. In: Davis Jr. R.A., Dalrymple, R.W. (Eds.), Principles of tidal sedimentology. Springer, Netherlands, 35-55.

Delvaux, D., 2001. Karoo rifting in western Tanzania: Precursor of Gondwana breakup. Contributions to geology and paleontology of Gondwana in honor of Helmut Wopfner: Cologne, Geological Institute, University of Cologne, 111-125.

Dera, G., Brigaud, B., Monna, F., Laffond, R., Puceat, E., Deconinck, J.F., Pellenard, P., Joachimsky, M., Durlet, C., 2011. Climatic ups and downs in a disturbed Jurassic world. Geology 39, 215-218.

Dera, G., Donnadieu, Y., 2012. Modeling evidences for global warming, Arctic seawater freshening, and sluggish oceanic circulation during the Early Toarcian anoxic event. Paleoceanography, 27(2).

Dera, G., Pellenard, P., Neige, P., Deconinck, J. F., Pucéat, E., Dommergues, J. L. 2009. Distribution of clay minerals in Early Jurassic Peritethyan seas: palaeoclimatic significance inferred from multiproxy comparisons. Palaeogeography, Palaeoclimatology, Palaeoecology, 271(1), 39-51.

Dera, G., Prunier, J., Smith, P. L., Haggart, J. W., Popov, E., Guzhov, A., Rogov, M., Delsate, D., Thies, D., Cuny, G., Pucéat, E., Charbonnier, D., Bayon, G., 2015. Nd isotope constraints on ocean circulation, paleoclimate, and continental drainage during the Jurassic breakup of Pangea. Gondwana Research, 27(4), 1599-1615.

Dunham, R.J., 1962. Classification of carbonate rocks according to depositional texture. In: Ham, W.E. (Ed.), Classification of Carbonate Rocks: AAPG Memoir 1, 108-121. Tulsa, OK.

Embry, A.F., 1995. Sequence boundaries and sequence hierarchies: problems and proposals. In: Steel, R.J., Felt, V.L., Johannessen, E.P., Mathieu, C. (Eds.), Sequence stratigraphy on the Northwest European Margin. Special Publication, vol. 5. Norwegian Petroleum Society, pp. 1–11.

Embry, A.F., Klovan, J.E., 1971. A late Devonian reef tract on northeastern Banks Island, NWT. Bulletin of Canadian Petroleum Geology, 19(4), 730-781.

Fischer, J.-C., Manivit, J., Vaslet, D., 2001. Jurassic gastropod faunas of central Saudi Arabia. GeoArabia (Manama), 6(1), 63–100.

Glennie, K.W., Boeuf, M.G.A., Hughes-Clarke, M.W., Moody-Stuart, M., Pilaar W., Reinhardt, B.M., 1995. Late Cretaceous nappes in Oman Mountains and their geological evolution. AAPG Bulletin, 57, 5-27.

Gómez, J.J., Goy, A., 2011. Warming-driven mass extinction in the Early Toarcian (Early Jurassic) of northern and central Spain. Correlation with other time-equivalent European sections. Palaeogeography, Palaeoclimatology, Palaeoecology, 306(3), 176-195.

Gradstein, F.M., Ogg, J.G., Schmitz, M.D., Ogg, G.M., 2012. The Geologic Time Scale 2012. Elsevier, p. 1144.

Hallam, A., 2001. A review of the broad pattern of Jurassic sea-level changes and their possible causes in the light of current knowledge. Palaeogeography, Palaeoclimatology, Palaeoecology, 167(1), 23-37.

Haq, B.U., Al-Qahtani, A.M., 2005. Phanerozoic cycles of sea-level change on the Arabian Platform. GeoArabia, 10(2), 127-160.

Haq, B.U., Hardenbol, J., Vail, P.R., 1987. Chronology of fluctuating sea levels since the Triassic. Science, 235 (4793), 1156-1167.

Haq, B.U., Hardenbol, J., Vail, P.R., 1988. Mesozoic and Cenozoic chronostratigraphy and cycles of sea-level change. SEPM Special Publications 42, 71–108.

Hardenbol, J., Jacquin, T., Farley, M.B., de Graciansky, P.C., Vail, P.R., 1998. Mesozoic and Cenozoic sequence chronostratigraphic framework of European basins. In: de Graciansky, P. C., Hardenbol, J., Jaquin, T., Vail, P.R. (Eds.), Mesozoic and Cenozoic Sequence Stratigraphy of European Basins. Society for Sedimentary Geology (SEPM), Tulsa, 3–13.

Harms, J.C., Southard, J.B., Spearing, D. R., Walker, R. G., 1975, Depositional environments as interpreted from primary sedimentary structures and stratification sequences: SEPM Short Course No. 2, 161 p.

Hesselbo, S.P., Gröcke, D.R., Jenkyns, H.C., Bjerrum, C.J., Farrimond, P., Morgans Bell, H.S., Green, O.R., 2000. Massive dissociation of gas hydrate during a Jurassic oceanic anoxic event. Nature 406, 392–395.

Hinnov, L. A., Park, J. J., 1999. Strategies for assessing Early-Middle (Pliensbachian-Aalenian) Jurassic cyclochronologies. Philosophical Transactions of the Royal Society of London A: Mathematical, Physical and Engineering Sciences, 357(1757), 1831-1859.

Jenkyns, H.C., Sarti, M., Masetti, D., and Howarth, M.K., 1985, Ammonites and stratigraphy of Lower Jurassic black shales and pelagic limestones from the Belluno trough, southern Alps: Ecologae Geologicae Helvetiae, 78, 299-311.

Kadar, A.P., De Keyser, T., Neog, N., Karam, K.A., Le Nindre Y.M., Davies, R.B., 2015. Calcareous nannofossil zonation and sequence stratigraphy of the Jurassic System, onshore Kuwait. GeoArabia, 20(4), 125-180.

Kerans, C., Tinker, S.W., 1997. Sequence stratigraphy and characterization of carbonate reservoirs. Society of Sedimentary Geology: SEPM Short Course Notes, 40.

Le Métour, J., Rabu, D., Tegyey, M., Béchennec, F., Beurrier, M., Villey, M., 1990. Subduction and obduction: two stages in the Eo-Alpine tectonometamorphic evolution of the Oman Mountains: In Robertson, A.H.F, Searle, M. P., Ries, A.C. (Eds), The Geology and Tectonics of the

Oman Region: Geological Society of London, Special Publication 49, 327-340.
Le Nindre, Y.M., Manivit, J., Manivit, H., Vaslet, D., 1990. Stratigraphie sequentielle du Jurassique et du Cretace en Arabie Saoudite. Bulletin Société Géologique France, Paris 6, 1025-1035.
Le Nindre, Y.M., Vaslet, D., Le Métour, J., Bertrand, J., Halawani, M., 2003. Subsidence modelling of the Arabian Platform from Permian to Paleogene outcrops. Sedimentary Geology, 156, 263-285.
Leckie, D.A., Walker, R.G., 1982. Storm-and tide-dominated shorelines in Cretaceous Moosebar-Lower Gates interval--outcrop equivalents of Deep Basin gas trap in western Canada. AAPG Bulletin, 66(2), 138-157.
Lukasik, J.J., James, N.P., McGowran, B., Bone, Y., 2000. An epeiric ramp: low-energy, cool-water carbonate facies in a Tertiary inland sea, Murray Basin, South Australia. Sedimentology, 47(4), 851-881.
Manivit J, Le Nindre Y.M., Vaslet D. (1990) Le Jurassique d'Arabie Centrale. In Histoire Gologique de la Bordure Occidentale de la Plate-forme Arabe. Volume 4. Document du BRGM n°194.
Manivit, J., Pellaton, C., Vaslet, D., Le Nindre, Y.M., Brosse, J.M., Fourniguet, J., 1985a. Geologic map of the Wadi al Mulayh quadrangle, sheet 22H, Kingdom of Saudi Arabia. Saudi Arabian Deputy Ministry for Mineral Resources Geosciences Map, GM-92, scale, 1(250,000), 1-32.
Manivit, J., Pellaton, C., Vaslet, D., Le Nindre, Y.M., Brosse, J.M., Breton, J.P., Fourniguet, J., 1985b. Geologic map of the Darma quadrangle, sheet 24H, Kingdom of Saudi Arabia. Saudi Arabian Deputy Ministry for Mineral Resources Geosciences Map, GM-101, scale, 1(250,000), 133.
McKee, E. D., 1966. Significance of climbing-ripple structure. US Geol. Surv. Prof. Papper, 550, 94-103.
Murris, R.J., 1980. Middle East: Stratigraphic evolution and oil habitat. AAPG Bulletin, 64,597–618.
Powers, R.W., 1968. Lexique Stratigraphique International, v.III, Asie, 10bl, Saudi Arabia. Centre National de la Recherche Scientifique, Paris, 177p.
Powers, R.W., Ramirez, L.F., Redmond, C.D., Elberg, E.L., 1966. Geology of the Arabian Peninsula, Geological Survey Professional Paper, 560-D, 147p.
Rabalais, N.N., Turner, R.E., Wiseman, W.J., & Boesch, D.F., 1991. A brief summary of hypoxia on the northern Gulf of Mexico continental shelf: 1985–1988. Geological Society, London, Special Publications, 58(1), 35-47.
Read, J.F. 1995. Overview of carbonate platform sequences, cycle stratigraphy and reservoirs in greenhouse and icehouse worlds. In: Read, J.F., Kerans, C., Weber, L.J., Sarg, J.F., and Wright F.W. (Eds.), Milankovitch sea level changes, cycles and reservoirs on carbonate platforms in greenhouse and icehouse worlds, SEPM Short Course Notes No. 35, 1-102.
Read, J.F., 1989. Controls on evolution of Cambrian-Ordovician passive margin, US Appalachians. In: Crevello, P.D., Wilson, J.L., Sarg, J.F., Read, J.F. (Eds.), Controls on Carbonate Platform and Basin Development, SEPM Special Publication, 44, 146–165.

Read, J.F., 1998. Phanerozoic carbonate ramps from greenhouse, transitional and ice-house worlds: clues from field and modelling studies. Geological Society, London, Special Publications, 149(1), 107-135.

Reineck, H.E., Singh, I.B., 1980. Depositional Sedimentary Environments. Springer-Verlag, Berlin, Heidelberg, New York, p. 549.

Sames, B., Wagreich, M., Wendler, J.E., Haq, B.U., Conrad, C.P., Melinte-Dobrinescu, M.C., Hu, X., Wendler, I., Wolfgring, E., Yilmaz, I.Ö., Zorina, S.O. 2016. Review: short-term sea-level changes in a greenhouse world—a view from the Cretaceous. Palaeogeography, Palaeoclimatology, Palaeoecology, 441, 393-411.

Sarg, J.F., 1988. Carbonate sequence stratigraphy. In sea level changes: an integrated approach. Society of Economic Paleontologists and Mineralogists Special Publication, 42, 155–181.

Sharland, P.R., Archer R., Casey D.M., Davies R.B., Hall S.H., Heward A.P., Horbury A.D., Simmons M.D., 2001. Arabian Plate Sequence Stratigraphy. GeoArabia Special Publication 2, Gulf PetroLink, Bahrain, 371.

Suan, G., Mattioli, E., Pittet, B., Lécuyer, C., Suchéras-Marx, B., Duarte, L.V., Philippe, M., Reggiani, L., Martineau, F., 2010. Secular environmental precursors to Early Toarcian (Jurassic) extreme climate changes. Earth and Planetary Science Letters, 290(3), 448-458.

Summerfield, M.A., 1985. Plate tectonics and landscape development on the African continent. In: Morisawa, M., Hack, J. (Eds.), Tectonic Geomorphology. Allen and Unwin, Boston, 27-51.

Thierry, J., Barrier, E., Abbate, E., Ait-Ouali, R., Ait-Salem, H., Bouaziz, S., Canerot, J., Elmi, S., Geluk, M., Georgiev, G., Guiraud, R., Hirsch, F., Ivanik, M., Le Metour, J., Le Nindre, Y.M., Medina, F., Nikishin, A.M., Page, K., Panov, D.L., Pique, A., Poisson, A., Sandulescu, M., Sapunov, I.G., Seghedi, A., Soussi, M., Tarkowski, R.A., Tchoumatchenko, P.V., Vaslet, D., Volozh, Y.A., Voznezenski, A.,Walley, C.D., Ziegler,M., Ait-Brahim, L., Bergerat, F., Bracene, R., Brunet, M.F., Cadet, J.P., Guezou, J.C., Jabaloy, A., Lepvrier, C., Rimmele, G., Belaid, A., Bonneau, M., Boutakiout, M., Chellai, E., Coutelle, A., Fedan, B., Fekirine, B., Guillocheau, F., Julien, M., Kokel, F., Laadila, M., Lott, G.N., Lamarche, J., Mami, L., Mansy, J.L., Mascle, G., Meister, C., Mouty, M., Pascal, C., Robin, C., Sebrier, M., Sihamdi, N., Souhel, A., Stephenson, R., Vera, J.A., Vuks, V.J., Vrielynck, B., Olivet, J.L., 2000a. Map 8, Middle Toarcian (180–178Ma). In: Dercourt, J., et al. (Ed.), Atlas Peri-Tethys, Paleogeographical Maps. Paris.

Thomas, R.G., Smith, D.G., Wood, J.M., Visser, J., Calverley-Range, E.A., Koster, E.H., 1987. Inclined heterolithic stratification—terminology, description, interpretation and significance. Sedimentary Geology, 53 (1-2), 123-179.

Vail, P.R., Audemard, F., Bowman, S.A., Eisner, P.N., Perez- Cruz, C., 1991. The stratigraphic signatures of tectonics, eustasy and sedimentology — an overview. In: Einsele, G., Ricken, W., Seilacher, A. (Eds.), Cycles and Events in Stratigraphy. Springer, Berlin, 617–659.

Van de Schootbrugge, B., McArthur, J.M., Bailey, T.R., Rosenthal, Y., Wright, J.D., Miller, K.G., 2005. Toarcian anoxic event: an assessment of global

causes using belemnite C isotope records. Paleoceanography, 20(3), PA3008.
Vaslet, D., 1987, Geologic du Paleozoique; Permien Superieur, Trias, Jurassique; lithostratigraphic: in Histoire geologique de la bordure occidentale de la plate-fornie arabe du PaleozoIque inferieur au Jurassique superieur (Y.M. Le Nindre, J. Manivit and D. Vaslet, authors), DSc Thesis, University of Paris VI, 1, 413 p.
Vaslet, D., Brush, J.M., Breton, J.P., Manivit, J., Le Strat, P., Fourniguet, J., Shorbaji, H., 1988. Geologic map of the quadrangle Shaqra, sheet 25H .Kingdom of Saudi Arabia: Deputy Ministry for Mineral Resources Geoscience Map GM-120C , 29.
Vaslet, D., Delfour, J., Manivit, J., Le Nindre, Y.M., Brosse, J.M., Fourniguet, J., 1983. Geologic map of the Wadi Ar Rayn quadrangle, sheet 23 H, Kingdom of Saudi Arabia. Saudi Arabian Deputy Ministry for Mineral Resources, Jeddah, Geosciences Map, GM-63A.
Wendler, J.E., Wendler, I., Vogt, C., Kuss, J., 2016. Link between cyclic eustatic sea-level change and continental weathering: Evidence for aquifer-eustasy in the Cretaceous. Palaeogeography, Palaeoclimatology, Palaeoecology, 441, 430-437.
Williams, H.D., Burgess, P.M., Wright, V.P., Della Porta, G., Granjeon, D., 2011. Investigating carbonate platform types: multiple controls and a continuum of geometries. Journal of Sedimentary Research, 81(1), 18-37.
Wilson, J.L., 1975. Carbonate Facies in Geologic History. Springer-Verlag, New York, 471 pp.
Wilson, J.L., Jordan, C., 1983. Middle Shelf Environment. In: Scholle, P.A., Bebout, D.G., Moore, C.H. (Eds.), Carbonate Depositional Environments. American Association Petroleum Geologists Memoir, 33, 345–440.
Yousif, S., Nouman, G., 1997. Jurassic geology of Kuwait. GeoArabia, 2(1), 91-110.
Ziegler, M.A., 2001. Late Permian to Holocene Paleofacies evolution of the Arabian plate and its hydrocarbon occurrences. GeoArabia, 6, 445-504.

Appendix

APPENDIX 2.1: Section locations

Name	Latitude	Longitude
DHIBI-1 (shallow core)	24.19595	46.24203
Khashm Ad Dhibi	24.23492	46.09877
Wadi Al Jufayr	23.89844	46.17702
Faridat Balum	23.7114	46.23652
Khashm Al Khalta	23.58547	46.17834
Khashm Disman	23.42942	46.22265
Wadi Birk	23.13083	46.35743
Fara'id al Ahmar	22.56072	46.10331
Khashm Munayyifiyah	22.18176	45.88079
Khashm Abu Al Jiwar	21.84332	45.73633

Chapter 3:

Middle Jurassic (Dhruma Formation and Tuwaiq Mountain Limestone)

Tuwaiq Mountain Limestone in Wadi Birk

Table of contents:

High-resolution sedimentology and sequence stratigraphy of the Middle Jurassic outcrop, Jabal Tuwayq, Central Saudi Arabia

Abdullah Al-Mojel[1, 2], Philippe Razin[2], Yves-Michel Le Nindre[3], Guillaume Dera[4]

[1] Saudi Aramco, Dhahran, Saudi Arabia
[2] ENSEGID-Bordeaux INP, EA4592, 33607 Pessac, France
[3] Consultant
[4] GET, Université Paul Sabatier, CNRS UMR 5563, IRD, OMP, 14 Avenue Avenue Edouard Belin, 31400 Toulouse, France

Corresponding author: E-mail: abdullah.mojel@gmail.com Present address: P.O. Box 5093 Dhahran 31311, Saudi Arabia

Keywords: Arabian Platform, Sequence Stratigraphy, Bajocian, Bathonian, Callovian, Mixed carbonate-siliciclastic, Inner platform, Epicontinental sea

Abstract

The high-resolution sequence stratigraphy of the Dhruma Formation and Tuwaiq Mountain Limestone (Bajocian to Middle Callovian) is based on outcrop and shallow core measured sections along a 280-600 km long N-S transect west and south of Riyadh. Correlations were extended westward in the subsurface using gamma-ray wireline logs (500 km Riyadh to Qatif). The outcrops provide a continuous stratigraphic record of the Middle Jurassic transgression of a large (>1000 km) epeiric tropical platform with continental braided fluvial deposits to tidal or wave-dominated mixed carbonate-siliciclastic lagoonal deposits. These formed aggraded flat-topped platform wedging and thickening northward. Evident syndepositional differential subsidence has an influence on lateral thickness variation and to a lesser

extent facies distribution. Short-lived tectonic downwarping provide uplifted source area for high fluvial dynamics and sandstone influx in overall mud-dominated successions. The carbonate platforms are mud-dominated and evolved from restricted carbonate platforms with microbes and low-faunal diversity (Dhruma Fm., Early Bajocian to Early Bathonian) to open-marine carbonate platforms with stromatoporoid/coral bearing and high-faunal diversity adjacent to deep intrashelf basin in subsurface (Tuwaiq Mt. Lst., Middle Callovian). The successions make up two composite sequences, DCS and TCS (3^{rd}-order, ~2.4 Myr), superimposed by several high-frequency sequences (4^{th}-order, ~400 kyr) that show a progressive marine transgression with subordinate MFS at Early Bathonian (*zigzag* Zone) and main MFS in the Tuwaiq Mt. Lst. (Middle Callovian *coronatum* Zone). The depositional sequences are considered to be of eustatic origin as they match well with Tethyan sea-level cycles. Significant sequence boundary between DCS and TCS with Middle Bathonian hiatus controlled by eustatic sea-level fall coupled with local tectonic disruption. The TST of the composite sequences were initiated with wet-warming episodes associated with high-siliciclastic discharges and demise of carbonate-production. The carbonates are developed well during late TST and HST of the composite sequences controlled by stepping back of the siliciclastic sources together with drying of the climate with cooling. The synchronicity of the transgression with warming periods and highstand with cooling provide some confidence to the glacio- or aquifer-eustatic driver mechanisms of the Middle Jurassic depositional sequences. This study should serve as an outcrop analog and guidelines for reservoir modeling and hydrocarbon exploration. Moreover, the study details

for the first time the evolution of the Middle Jurassic paleoclimatic changes and consequences in a paleoequatorial domain.

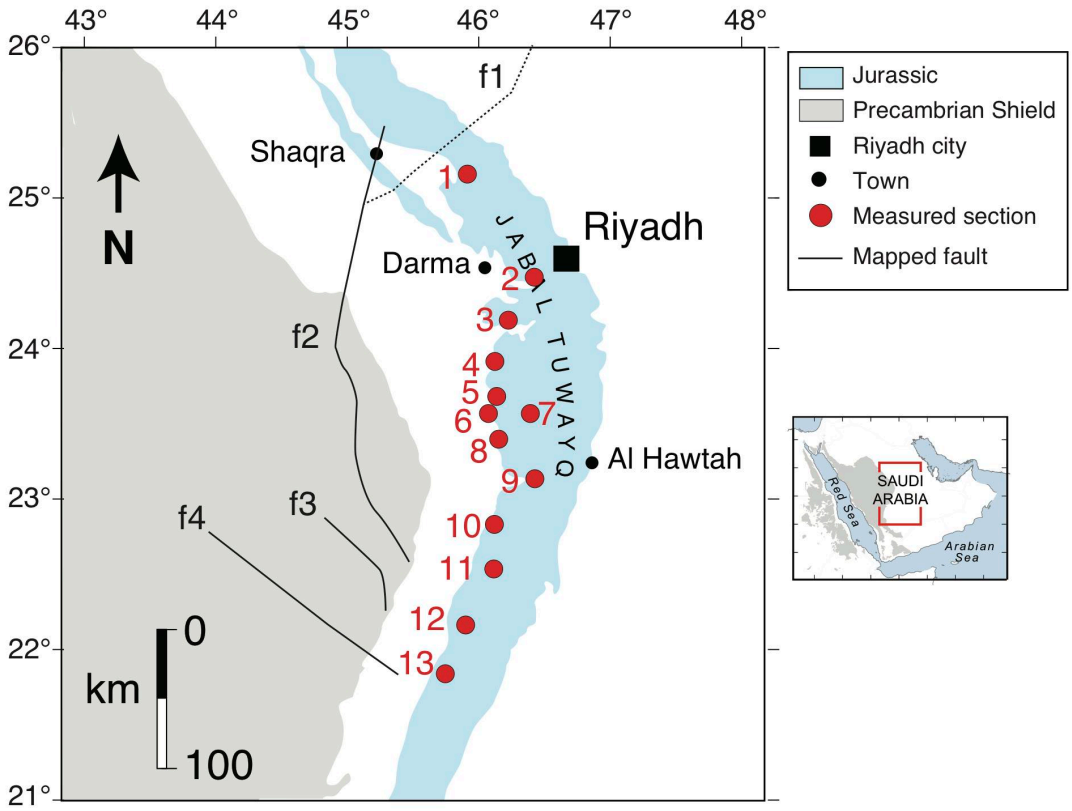

Figure 3.1: Geological map of the study area showing the Jurassic outcrops modified from Fischer et al. (2001), measured sections, faults and magnetic lineaments. The measured sections are: (1) Huraymila, (2) Khashm Al Qaddiyah (MQBL-1), (3) Khashm Ad Dhibi (MRZU-2, HMNK-1, DHBI-1) , (4) Wadi Al Jufayr, (5) Faridat Balum, (6) Khashm Al Khalta, (7) Wadi Al Hawtah, (8) Khashm Disman, (9) Wadi Birk, (10) Khashm Mawan, (11) Fara'id al Ahmar, (12) Khashm Munayyifiyah and Jabal Shimrakh, (13) Khashm Abu Al Jiwar. The faults are mapped in the 1:250,00-scale quadrangles of Wadi al Mulayh (Manivit et al., 1985a), Wadi Ar Rayn (Vaslet et al., 1983), Darma (Manivit et al., 1985b) and Shaqra (Vaslet et al., 1988). The name of the faults are: f1 Wadi Al Atk Lineament, f2 Al 'Amar Fault, f3 and f4 are belong to the Najd Fault System (Al-Husseini, 2000).

3.1 Introduction

The Middle Jurassic outcrops (Dhruma Formation and Tuwaiq Mountain Limestone; Bajocian to Middle Callovian) are located in the central part of the Arabian Plate (Fig. 3.1), which corresponds to an intra-cratonic passive margin. The Arabian Platform was an extensive (>1000 km) tropical shallow marine epeiric platform system with an adjacent organic rich intrashelf basins called the Arabian Basin (Fig. 3.2). The outcropping Dhruma Formation and Tuwaiq Mountain Limestone are mainly consisting of continental to mixed continental to shallow marine deposition systems. These outcrops are very well exposed in the central Arabia along the Tuwayq Escarpment forming spectacular west facing continuous cuests along 1000 km N-S near Ar Riyadh (Fig. 3.1). In the subsurface, the Middle Jurassic hosts five hydrocarbon reservoirs (Powers et al., 1966) and significant source rock interval in the Tuwaiq Mountain Limestone (Fig. 3.3) (Pollastro, 2003).

Prior to this study, the outcrops of the Dhruma Formation and Tuwaiq Mountain Limestone were subdivided into several large mapping units based on lithostratigraphic and biostratigraphic correlations (Powers et al., 1966; Powers, 1986; Manivit et al., 1990). However, genetically related depositional sequences and depositional environments were not documented in detail. Moreover, in the Dhruma Formation, the spatial and temporal relationship of an abrupt high-siliciclastic influx "Wadi ad Dawasir delta" was a subject of debate (Le Nindre, 1987; Manivit et al., 1990; Énay et al., 2009). Thus, this needs to be brought out in a genetic sequence stratigraphic interpretation and discussion. Therefore, our approach is to integrate, for the first time, the previous biostratigraphic data with new modern a high-resolution sequence

stratigraphic transects based on detailed sedimentological measured sections (Fig. 3.1) and shallow-cores with gamma-ray logs. This allows assessment of the controlling factors to the development of the Middle Jurassic Arabian Platform, the most prolific petroleum system in the region.

As stable isotope data of the Middle Jurassic show significant perturbations in the global carbon cycle and seawater temperatures associated with rapid paleoenvironmental changes, ecological crises, faunal evolution, and black shale formation (Jenkyns et al., 2002; Morettini et al., 2002; Dromart et al., 2003a; 2003b; O'Dogherty et al., 2006; Martinez and Dera, 2015), we evaluate how these changes affected the developing stratigraphy on the tropical Arabian Platform.

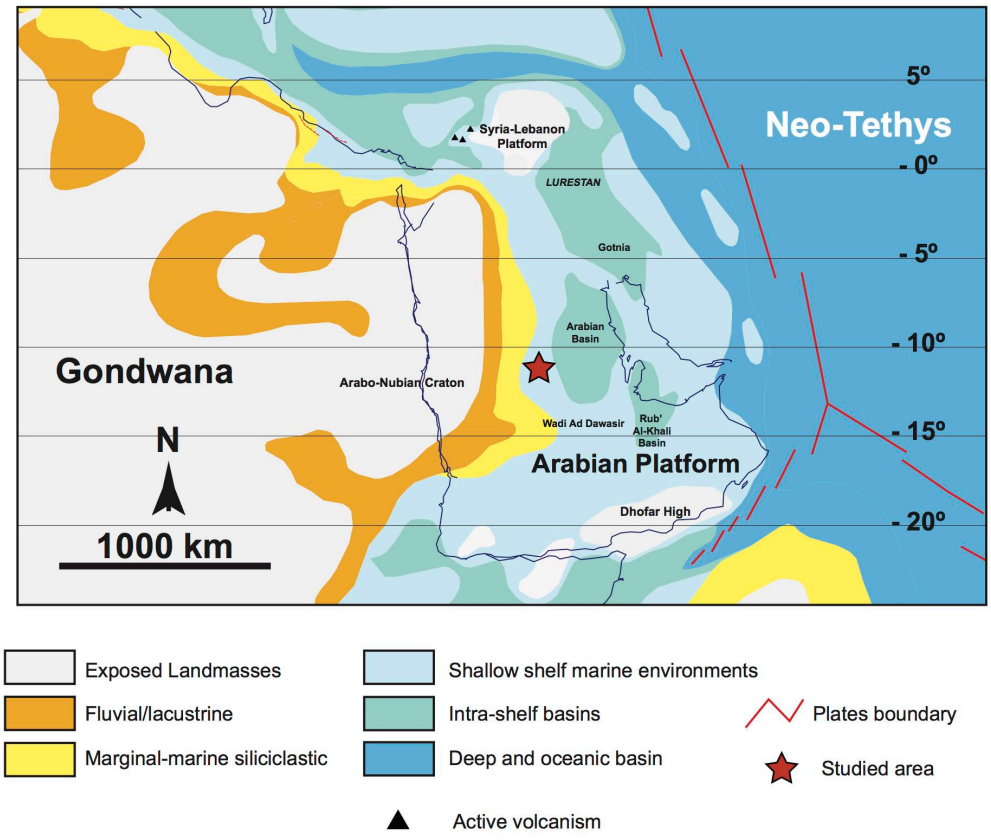

Figure 3.2: Middle Jurassic (Callovian) simplified paleogeographic map showing the area of study located in the southern margin of the Neo-Tethys Ocean (modified from Thierry et al., 2000).

3.2 Geological Setting

The study area is located in the central part of the Arabian Plate, in an intra-cratonic passive margin tectonically stable since the beginning of the Late Permian up to the onset of convergence and obduction of the Neo-Tethys margin in the Late Cretaceous (i.e., Late Cenomanian – Turonian) (Glennie et al., 1995; Le Métour et al., 1990; Fig. 3.1). In the Jurassic, this sub-equatorial area was covered by an extensive (>1000 km) tropical shallow marine epeiric platform system with adjacent organic rich intrashelf basins.

The Middle Jurassic Dhruma Formation and Tuwaiq Mountain Limestone are mainly consisting of continental siliciclastic, marginal marine sandstone and shallow marine mixed carbonate-siliciclastic deposition systems. They are very well exposed along the Jabal Tuwayq escarpments. The Dhruma Formation was divided into seven informal units (D1-D7) (Vaslet et al., 1983). Within these units, there are three informal members which are Dhibi Limestone Member (upper D2), Atash Member (Lower D7) and Hisyan Member (upper D7) (Powers et al., 1966; Powers, 1968). The Dhruma Formation is conformably overlain by the Tuwaiq Mountain Limestone which was divided into three informal units (T1-T3) (Vaslet et al., 1983).

Ages of these formations and included disconformity levels, spanning from the Bajocian to Middle Callovian, have been biostratigraphically defined by the presence of ammonites and subordinate fauna (*i.e.,* nautiles, echinoderms, brachiopods, foraminifera and ostracods) (Manivit et al., 1990). The base boundary of the Dhruma Formation is represented by Late Toarcian − Aalenian unconformity with a hiatus of approximately 7 Myr, considered as a major unconformity at scale of the Arabian Platform separating the Marrat

and Dhruma Formation. This probably resulted either from eustatic sea-level fall (Haq et al., 1988; Le Nindre et al., 1990; Al-Husseini, 1997; Haq and Al-Qahtani, 2005) and subsidence resistance or large-scale uplift (Le Nindre et al., 2003). Within the Dhruma Formation, a minor disconformity corresponds to a poorly dated interval (D6 unit and Atash Member) with endemic ammonite fauna in D6 unit. The missing time is probably the Middle Bathonian in which the underlying unit (D5) has Early Bathonian (*aurigerus* Zone) based on ammonite fauna (*Micromphalites*; Fischer et al., 2001) and the upper D6 unit and the Atash Member have Late Bathonian to Early Callovian brachiopod, foraminifera and ostracods fauna (Énay et al., 1987; Manivit et al., 1990). This is consistent with recent work on nannoflora (Kadar et al., 2015) who assigned D6 unit to Late Bathonian and Atash Member to Early Callovian. The boundary between Dhruma and Tuwaiq Mountain Limestone is conformable, thus, upper Dhruma (Atash and Hisyan Member) were genetically assigned to the overlaying Tuwaiq Mountain Limestone depositional sequence (Sequence 3 of Le Nindre et al., 1990; Handford et al., 2002; Hughes, 2004, 2009; Énay et al., 2009; Kadar et al., 2015). The Hisyan Member and the Tuwaiq Mountain Limestone have Middle Callovian (*coronatum* Zone) in age based on ammonite fauna supplemented by echinoderms, brachiopods and foraminifera (Manivit et al., 1990). However, recent nannoflora study of Kadar et al. (2015) shows larger range of ages of this depositional sequence (Early to Late Callovian). The top Tuwaiq Mountain Limestone is a significant unconformity between the Late Callovian (*lamberti* Zone) and the Early Oxfordian (*mariae* Zone) hiatus. Moreover, in the subsurface the unconformity is known by pre-Hanifa unconformity marked by

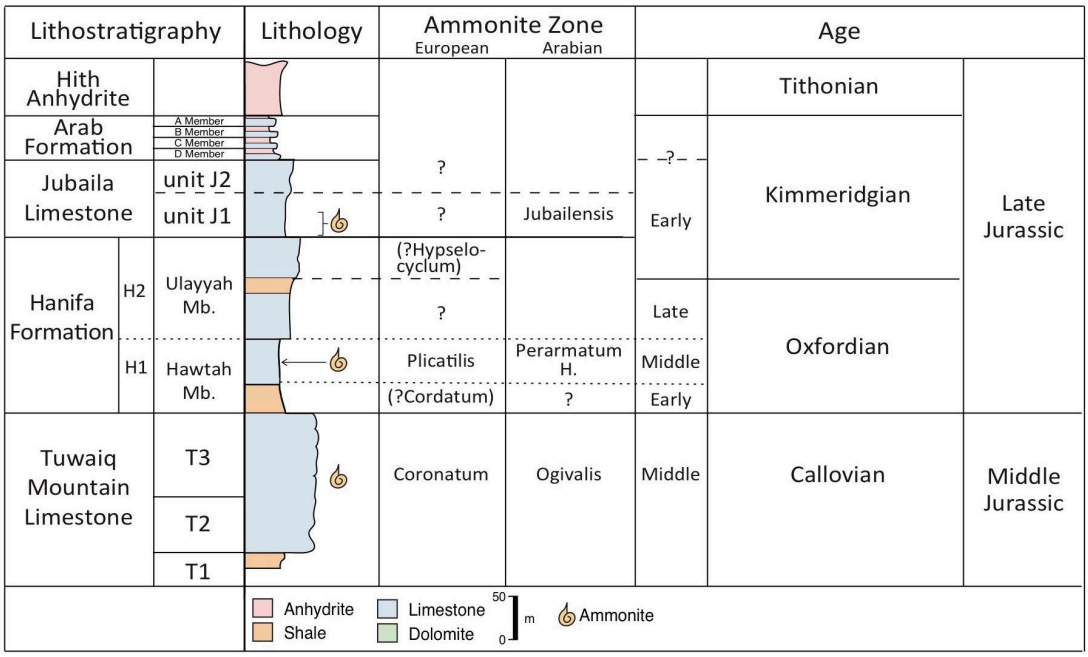

Figure 3.3: Lithostratigraphic and biostratigraphic column of the Early and Middle Jurassic in Jabal Tuwayq, Saudi Arabia. (Modified from Fischer et al., 2001).

erosional surface in which the top of the Tuwaiq Mountain is missing in the Rub' al-Khali and to the north of the Ghawar field (Powers, 1968).

The Dhruma Formation contains three hydrocarbon reservoirs (Faridah, Sharar and Lower Fadhili) (Hughes, 2009). The Faridah reservoir consists of five zones (A-E) and their equivalent in outcrop are Faridah E: Dhibi Limestone Member, and Faridah A-D: D4 unit. The Sharar reservoir is equivalent to D5 unit (Toland et al., 2013, unpublished Aramco report). The Lower Fadhili is an extensive broad hydrocarbon reservoir equivalent lithostratigraphically and biostratigraphically to the Atash Member (Powers et al., 1966; Al-Mojel, 2010). The Lower Fadhili Reservoir is economically significant interval in large oilfield in Saudi Arabia and in the Middle East (Powers et al., 1966; Al-Mojel, 2010). The Tuwaiq Mountain Limestone hosts two hydrocarbon reservoirs in eastern Saudi Arabia, Upper Fadhili Reservoir

(T1 unit) and Hadriya Reservoir (T3 unit) (Ayres et al., 1982; Powers, 1968; Hughes, 2009). Moreover, the formation represents the most significant and extensive Jurassic source rock in the subsurface of central Arabia (Pollastro, 2003).

3.3 Materials and Methods

This sequence stratigraphic study is based on 22 detailed sedimentological log sections, totaling of around 2700 m. The sections and their locations are shown in Figure (3.1) and Appendix (3.4). Four shallow cores (DHIBI-1, HMK-1, MRZU-2 and MQBL-1) with gamma-ray logs are used in the study and they are located in Khashm Ad Dhibi area. The cores span both the Dhruma Formation and Tuwaiq Mountain Limestone. One shallow well (TLHH-1) with continuous gamma-ray logs located in Wadi Birk is used in this study. The sedimentological data were plotted at scale of 1:200 for the outcrop sections and 1:120 for the logged core then redrawn and simplified in Figures (3.12 and 3.13) and Appendix (3.1, 3.2 and 3.3). The sedimentological data include: mineralogy, grain types, color, grain size, texture, extended Dunham classification (Dunham, 1962; Embry and Klovan 1971), sedimentary structure and fossil types. The vertical successions and evolution of the depositional environments were analyzed to define and interpret sequence stratigraphy.

High-resolution stratigraphic correlations were defined using sequence stratigraphic concepts, physical correlations, and mapping. Applying the Walther's Law across the sections was not simple because the platform was aggrading and had limited facies migration. Building the depositional model went through a continuous iterative process (Kerans and Tinker, 1997) from

one-dimensional cycle stacking analysis and sequence boundary definition to two-dimensional time line correlations and lateral facies organization. The defined sequences were adopted in gamma-ray logs of nearby subsurface wells in Riyadh and Khurais area.

The sections are complemented with biostratigraphic data of Manivit et al. (1990) and Hughes (2013, 2014; unpublished Saudi Aramco internal report of DHIBI-1, MRZU-2, HMNK-1 and MQBL-1 micropaleontology). The stratigraphic locations of the key biostratigraphic elements (e.g., ammonite faunas) are shown on the cross-section in large symbols with their age indicators. Moreover, The cross-section of the Tuwaiq Mountain Limestone is supplemented with an additional three measured sections (Khashm Mishlah, Khashm “861” and Khashm Kumdah from Manivit et al., 1990, their Fig. 18; redrawn in Fig. 6 of Énay et al., 2009).

3.4 Facies and depositional environments

The Middle Jurassic facies and depositional environments are summarized in Table 3.1, 3.2 and 3.3. There are 24 facies or facies associations representing the outcropping Dhruma Formation and Tuwaiq Mountain Limestone. The facies are grouped in eight depositional settings based on their common depositional processes. The depositional environment from proximal to distal are: fluvial, coastal plain, high-energy nearshore, deltaic system, arid shoreline, mixed carbonate-siliciclastic inner lagoon and carbonate inner lagoon and back-barrier lagoon.

Table 3.1: Siliciclastic facies

Depositional environment	Fluvial			Costal plain			High-energy nearshore		Deltaic system	
Facies and sub-depositional environment	F1: Pebbly sandstone and conglomerate and petrified trunks (*upstream flood plain*)	F2: Medium to coarse grained trough cross-bedded sandstone (*braided channel*)	F3: Mottled red mudrock (*paleosol*)	F4: Mottled bluish green shale (*mud flat/costal plain*)	F5: Bioturbated heterolithic silty sandstone (*mixed flat/costal plain*)	F6: Bidirectional cross-bedded sandstone and mud drapes (*tidal bars and channels*)	F7: *Skolithos* and plane laminated sandstone (*sand flat/ foreshore*)	F8: Swaley cross-bedded sandstone (*shoreface*)	F9: Coarse grained cross-bedded sandstone with plant remains (*distributary channel*)	F10: Large-scale cross-bedded sandstone (*delta front mouth bar*)
Thickness	0.5 to 1 m	4 to 20 m	1 to 5 m	1 to 9 m	1 to 5 m	1.5 to 4 m	0.5 to 2 m	2 to 5.5 m	1.5 to 2.5 m	2 to 25 m
Color	Light reddish orange and pale red	Very pale orange	Moderate orang pink and Moderate red	Grayish yellow green and moderate red	Moderate orange pink and moderate red	Moderate orang pink	Moderate orang pink	Moderate orang pink	Reddish brown	Light reddish brown
Depositional texture and grain types	Very fine sandstone matrix, very coarse to pebble quartz grained, cobble of iron-crust lithoclast, boulder of petrified trunks	Medium to coarse grained, well sorted	Clay, silt and some sand grained	Clay, locally thin red dolomitic bed	Silt and medium sand grained commonly cemented by carbonate, locally very fossiliferous in (D3 unit) dominated by ammonite and clams	Medium sand grained; plant fragment	Medium sand grained	Medium sand grained	Medium to coarse sand grained, pebble to cobble plant remains	Medium to coarse sand grained
Bedding and sedimentary structures	Sharp base, channelized and tabular bedding, trough cross-bedding	Sharp base, channelized and tabular bedding, tabular and trough cross-bedding	Gradational base, Tabular to lenticular bedding, common iron-stained surfaces with sometimes blackened nodules	Gradational base, tabular bedding, fissile and papery shale, may have mudcracks with red dolomite	Commonly gradational base, tabular bedding, thin and horizontal bioturbation traces, rare 2D ripple marks, occasionally iron-stained top surface	Sharp base, channelized and tabular bedding, tabular cross-stratification and sigmoidal bed-forms with mud drapes, locally simple 2D and 3D dunes	Sharp base, tabular bedding, commonly highly bioturbated, abundant *Skolithos*, plane-laminated bedding	Sharp scour base, tabular bedding, commonly swaley and may have trough cross-stratification	Sharp base, channelized bedding, cross-bedded with mud drabs and lesser bioturbation, commonly *Skolithos* bioturbation	Sharp base, large scale oblique tangential to parallel clinoform sets (dipping 25º westward), bioturbation at bottom and top sets
Stratigraphic occurrence	Dhruma Formation (top D5, D6), Base SB of TCS and unconformity surface at K. Abu Al Jiwar	Dhruma Formation (D6, D7), Tuwaiq Mt. Lst. (T1, T2), TST of TCS	Dhruma Formation (D1, D6, D7), Tuwaiq (T1, T2), commonly cycle cap in DCS and TCS.	Dhruma Formation (D1); base Dhruma sequence (HFS1)	Dhruma Formation (D1, D2 and D3); TST of Dhruma sequence.	Dhruma Formation (D1); base of Dhruma sequence (HFS1)	Dhruma Formation (D1, D6); base Dhruma and Tuwaiq sequences	Dhruma Formation (D1); base Dhruma sequence (HFS1)	Dhruma Formation (D5); HST of Dhruma sequence	Dhruma Formation (D1); Base Dhruma sequence (HFS1)

Table 3.2: Evaporites and mixed carbonate-siliciclastic facies.

Depositional environment	Arid shoreline			Mixed carbonate-siliciclastic inner lagoon			
Facies and sub-depositional environment	F11: Crinkly laminated evaporites (*intertidal, sabkhah*)	F12: Stromatolite and crinkly laminated mudstone (*intertidal*)	F13: Red dolomite with local silicified evaporite nodules (*restricted lagoon*)	F14: Heterolithic silty ferruginous oolite (*supratidal to continental*)	F15: Grayish green calcareous shale (*inner lagoon*)	F16: Argillaceous mudstone (*shale dominated inner lagoon*)	F17: Slightly argillaceous nodular bioturbated peloidal wackestone/mudstone (*inner lagoon*)
Thickness	2.5 to 4 m	1 to 3 m	0.1 to 1.5 m	1 to 7.5 m	0.5 to 20 m	4 to 5 m	1 to 20 m
Color	Light gray	Pale yellow and light gray	Pale red	Olive green, dark and pale red	Grayish green; occasionally reddish brown	Creamy white and light grayish green	Creamy white to very light gray
Depositional texture and grain types	Mud-support	Dolomitic mudstone, microbial lamination	Fine-grained fabric-preserving dolomite crystal, may have fine peloids and quartz, mud-support to packstone, occasional pebble skeletal fragments	Medium to very coarse iron ooid packstone, medium angular quartz, clay-silt matrix, occasionally glauconitic grains, hematite cement	Terrigenous clay and argillaceous mudstone, locally very fine sandstone; concoidal friable soft texture	Terrigenous clay, silt size pelletal grains mudstone	Terrigenous clay, very fine to medium peloidal wackestone/mudstone, locally quartzos, occasionally intraclastic skeletal fragments
Bedding and sedimentary structures	Tabular bedding, chicken-wire nodular mosaic and displacive enterolithic anhydrite crystals, crinkly-laminated stromatolitic microdolomite with lath-shaped anhydrite crystals	Gradational base, sharp top, tabular bedding, elongated column of SH-V, LLH-C and crinkly laminated stromatolite	Extensive correlatable tabular bedding, structureless with locally silicified anhydrite nodules, minor bioturbation	Gradational base, tabular bedding, very friable and structureless, associated with iron-crust bedding boundaries	Gradational base, tabular bedding, common *Chondrites* burrows	Gradational base, tabular bedding, abundant *Chondrites* burrows	Gradational base, tabular bedding, horizontal thin bioturbation, some *chondrites* burrow, argillaceous wispy solution seams, nodular structure
Stratigraphic occurrence	Dhruma Formation (D1), base Dhruma sequence DCS (HFS1)	Dhruma Formation (D1); base Dhruma sequence DCS (HFS1)	Dhruma Formation (D3, D4); late TST of Dhruma sequence DCS (HFS4)	Dhruma Formation and Tuwaiq Mt. Lst., base depositional sequences DCS and TCS	Dhruma Formation, base Tuwaiq Mt. Lst.; commonly base depositional sequences DCS and TCS	Dhruma Formation (D5, D6); HST of Dhruma sequence DCS (HFS5)	Dhruma Formation, Tuwaiq Mt. Lst (T1, T2); base depositional sequences and most high frequency-sequences
Fossils	None	None	None to sparse; may have brachiopods	None to sparse; may have debris of echinoderms, bivalves, gastropods, traces of small foraminifera (Le Nindre et al., 1984)	Foraminifera (*Lenticulina munsteri, Nautiloculina oolithica*), ostracodes (Manivit et al., 1990)	Echinoderms, foraminifera (*Nautiloculina oolithica*), ostracodes (Manivit et al., 1990)	Sponge spicules, foraminifera (Nodosariidae, *Lenticulina* sp., Textulariopsis sp); echinoderms, brachiopods, bivalves, gastropods, serpula, sponges (Manivit et al., 1990)

Table 3.3: Carbonate facies.

Depositional environment	Carbonate inner lagoon			Back-barrier lagoon				
Facies and sub-depositional environment	F17: Bioturbated peloidal wackestone/ packstone, oncoidal locally (*highly bioturbated lagoon*)	F18: Sharp-based intraclasts peloidal skeletal grainstone (*storm dominated inner platform*)	F19: Cross-bedded ooid peloidal skeletal grainstone (*high-energy shoreface*)	F20: Oncoidal packstone/ grainstone and rudstone (*oncoidal bars/shoal*)	F21: Biostromal coral/ stromatoporoid mudstone to packstone and floatstone (*low-energy back-barrier*)	F22: *Biohermal coral/ stromatoporoid mudstone/wackestone and framestone (back-barrier patch reef)*	F23: Branching coral/stromatoporoid framestone (*back-barrier reef*)	F24: Cross-bedded peloidal coated-grain grainstone (*shoal and washover complex*)
Thickness	0.5 to 22 m	6 to 50 cm	1.5 to 3 m	1 to 2 m	1 to 12 m	2 to 10 m	10 m	2 to 7 m
Color	Creamy white	Light gray to light brown	Light brown	Creamy white	Creamy white	Creamy white	Creamy white	Light brown
Depositional texture and grain types	Silt to very fine pelletal and medium peloidal grains, very coarse forams, occasional very coarse, granular oncoidal wackestone/ packstone	Very fine to fine peloids, granular reworked intraclasts and skeletal debris, grainstone rudstone/floatstone texture; occasional 10-15% silt quartz; common meniscus and microstalactitic cement fabric	Fine to medium peloidal ooid grains, occasional very coarse granule skeletal and intraclasts	Coarse to very coarse coated grains and pebble oncoidal rudstone; may have intraclasts	Gravel size of coral/ stromatoporoid in branched, tabular and head shapes up to 60 cm diam. and 30 cm thick; coarse skeletal fragments, fine peloidal grains mudstone/packstone and floatstone	Very fine to fine peloidal mudstone/ wackestone; commonly skeletal debris floatstone, framestone build-ups	Framestone and may associated with microbial bindstone	Well sorted very fine to fine peloidal and medium coated grain grainstone
Bedding and sedimentary structures	Gradational base, laterally extensive tabular bedding, highly bioturbated, argillaceous wispy solution seams, rare nodular structure, top firmground surface	Scoured and sharp base, tool marks, graded layer, tabular and occasionally channelized bedding; parallel/HCS and wave-ripple lamination; wave ripples, some *Chondrites* burrows	Sharp base, tabular and may have lenticular bedding, trough cross-bedding and large 3D megaripple	Sharp base, lenticular bedding, bioturbation sedimentary structure	Gradational base, tabular bedding, high bioturbation, top firmground surface	Gradational base, bioherms up to 15-30 m diameter (Manivit et al., 1990) surrounded by bioturbated mudstone/ wackestone matrix; structure less	Gradational base, tabular bedding	Sharp base, gutter cast, occasionally upward coarsening; tabular, lenticular, channelized, flaser and wavy bedding; trough, sigmoidal bidirectional cross-bedding; high bioturbation
Stratigraphic occurrence	Dhruma Formation (D2, D4, D5, Atash Mb.); Tuwaiq Mt. Lst (T2, T3); late TST of Dhruma and Tuwaiq sequences	Dhruma Formation and Tuwaiq Mt. Lst, dominated at base depositional sequences	Dhruma Formation (D6); post Middle Bathonian-Early Callovian unconformity	Dhruma Formation (D2, D4) Tuwaiq Mt. Lst. (T3); late TST/HST of depositional sequences	Tuwaiq Mt. Lst. (T3); MFS and HST of Tuwaiq composite sequence	Tuwaiq Mt. Lst. (T3); HST of Tuwaiq composite sequence	Tuwaiq Mt. Lst. (T3); HST of Tuwaiq composite sequence	Dhruma Formation (D4); MFS of Dhruma composite sequence DCS
Fossils	Ammonite, foraminifera, echinoderms, brachiopods, bivalves, gastropods, serpula, and bryozoans (Manivit et al., 1990); abundant foraminifera (*Lenticullina* sp.)	Debris of brachiopods and bivalves; rare stromatoporoid and *Cladocoropsis*	Ammonite (*Dhrumaites*) echinoderms, brachiopods, bivalves, microgastropods, and calcareous algae (Manivit et al., 1990)	Foraminifera (*Lenticulina*)	*Shuqria, Cladocoropsis,* sponge spicules foraminifera (*Pfenderina trochoidea*, *Trocholina* sp., *Lenticulina*)	Echinoderms, brachiopods, bivalve, sponges, calcareous algae (dasyclad) (Manivit et al., 1990)	Coral/ stromatoporoid *Shuqria,* may have *Cladocoropsis*	Foraminifera (*Lenticulina, Valvulina* sp.)

F1: Pebbly sandstone and conglomerate and petrified trunks (upstream flood plain)

The facies occur in tabular and channelized units, 0.5 to 1 m thick, and have sharp erosional base and top. They contain very fine sandstone matrix, very coarse to pebble quartz, cobbles of iron-crust and petrified trunks. The very fine sandstones are structureless, cemented and iron-crust lithoclasts (Fig. 3.4A). The pebbly sandstone is trough cross-bedded and associated with petrified trunks (Fig. 3.4B and C). The facies overlies incised fluvial channels on top of D5 and within D6 units in the Dhruma Formation in the southern outcrops. They were deposited in upstream fluvial settings on the Middle Bathonian to Early Callovian unconformity.

F2: Medium to coarse grained trough cross-bedded sandstone (braided channel)

These facies are 4 to 20 m thick, tabular and channelized unit with sharp base boundaries and gradation top. They are well-sorted, unfossiliferous medium to coarse grained. The sandstones are non-bioturbated trough and tabular cross-bedded (Fig. 3.4D) and show southeast paleocurrent direction. The sandstones occur south of latitude 22º N in the Dhruma Formation (D6 and D7 units) and the Tuwaiq Mountain Limestone (T1 and T2 units). The sandstones overlie *Skolithos* tabular-bedding sandstone (F7), distributary sandstone channel with plant remains (F9) and pebbly sandstone with petrified trunks (F1). The facies are overlain by mottled pale red paleosol mudrock (F3) and oolitic ironstone (F14). The facies are interpreted as high-

energy braided channels and locally incising the underlying *Skolithos* tabular-bedding sandstone.

F3: Mottled red mudrock (paleosol)

The mudrocks are tabular to lenticular bedding, 1 to 5 m thick with gradational base and commonly associated iron-crust surfaces with blackened nodules. The mudrocks contain some silt and sand grains and are usually mottled orange pink and moderate red (Fig. 3.4E). The facies are non-bioturbated and lack well-defined rootlet traces. However, the color contrasts and mottling could indicate organic oxidation of the rootlets (Collinson, 1996). The shales are usually intercalated and overlie fluvial channels (F2). In updip southern areas, they overlie *Skolithos* and bidirectional cross-bedded sandstone (F7), and grayish green calcareous shale (F15). They are overlain by heterolithic oolitic ironstone (F14). The facies are interpreted as paleosols.

F4: Mottled bluish green shale (mud flat/coastal plain)

These shales are tabular units 1 to 9 m thick and have gradational base (Fig. 3.5A). They are composed of clay minerals and locally thin red dolomitic beds locally with mudcracks. The facies have mottled grayish yellow green and moderate red color and exhibit fissile and papery parting. The shales are unfossiliferous and non-bioturbated. They occur in the Dhruma Formation (D1 unit) interbedded with bidirectional cross-bedded tidal bars/channels sandstone (F6). The shales formed in a quite-water mud flat or lower coastal-plain depositional setting.

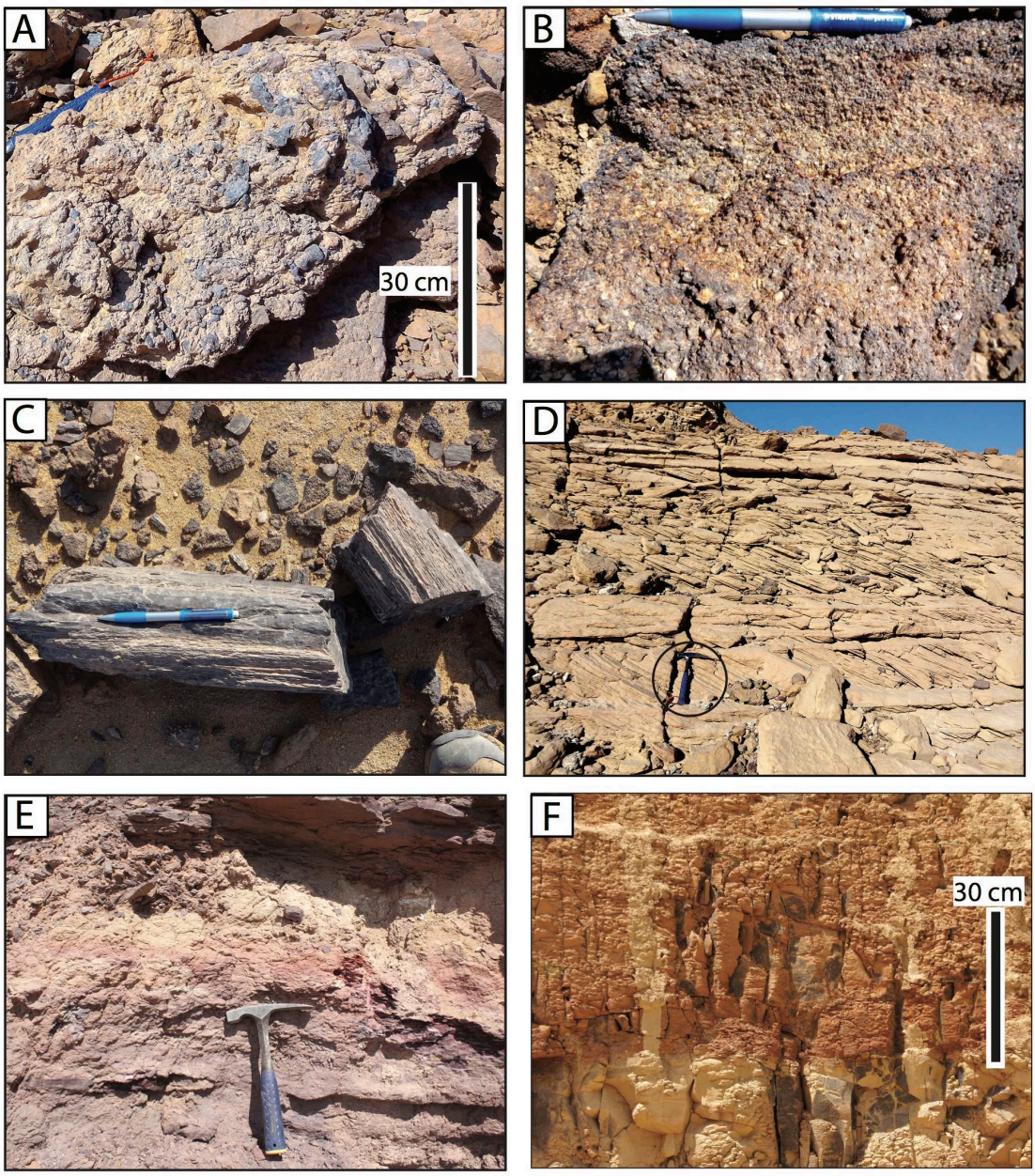

Figure 3.4: Fluvial facies association in the Dhruma Formation. **A)** Imbricated gravel conglomerates and very fine sandstone matrix (upstream flood plain), Dhruma Formation (D6 unit), Khashm Khurtum, **B)** Pebbly sandstone and conglomerates (upstream flood plain), Dhruma Formation (? D6 unit), Khashm Abu Al Jiwar**, C)** Petrified trunk from the same horizon of photo (B) (upstream flood plain), Khashm Abu Al Jiwar**, D)** Medium to coarse grain trough cross bedded sandstone (braided channel), Dhruma Formation (D6 unit), Khashm Abu Al Jiwar section, (hammer for scale), **E)** Mottled red shale (paleosol), Dhruma Formation (D1 unit), Khashm Munayyifiyah, **F)** Red shale (flood plain/lake), Dhruma Formation (D6 unit), Khashm Ad Dhibi.

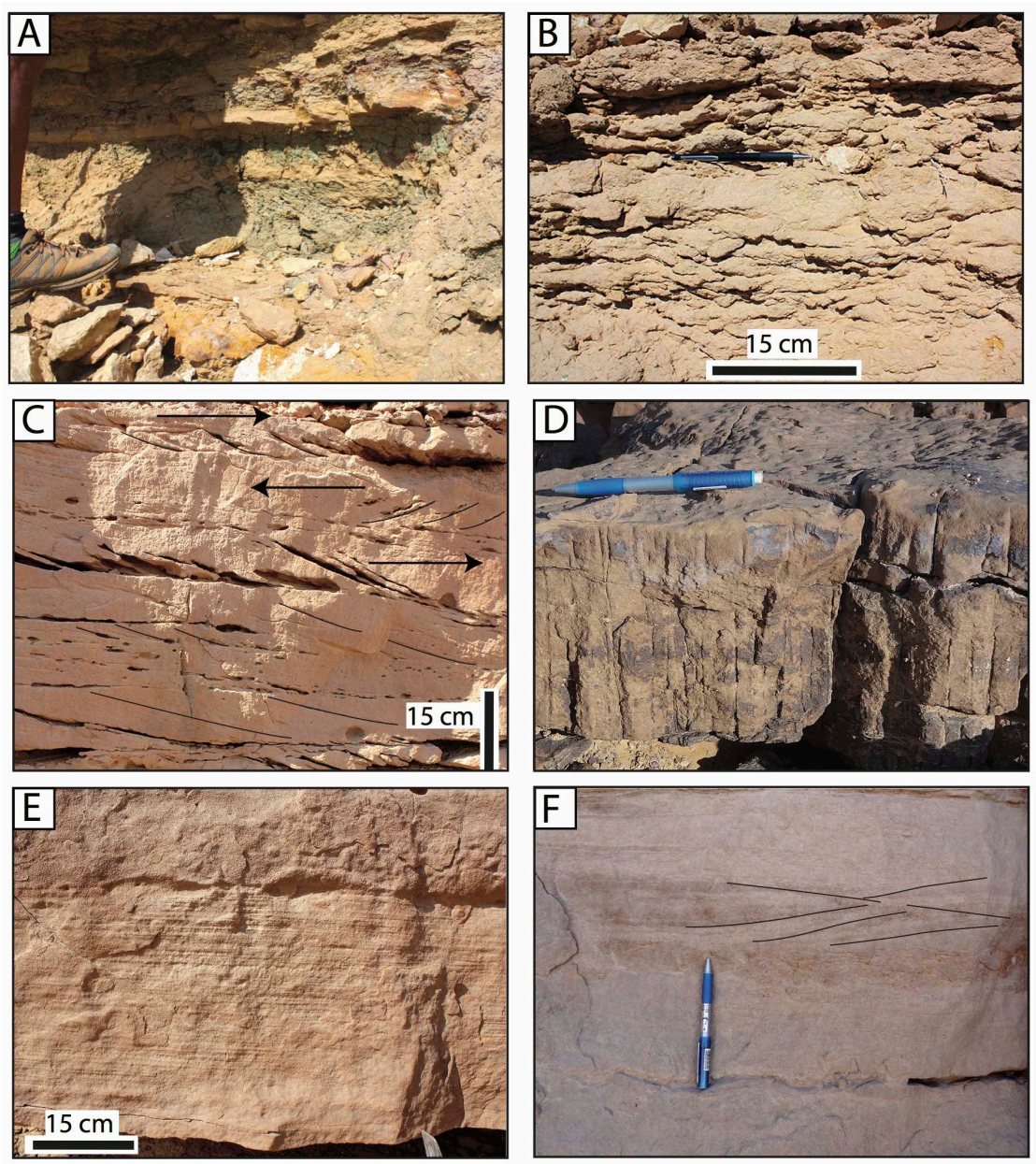

Figure 3.5: Coastal plain facies association (A-C), high-energy nearshore facies association (D-F). **A)** Mottled bluish green shales (mud flat/coastal plain), Dhruma Formation (D1 unit), Khashm Disman, **B)** Bioturbated heterolithic silty sandstone (mixed flat/coastal plain), Dhruma Formation (D1 unit), Khashm Al Khalta, **C)** Bidirectional cross-bedded sandstone and mud drapes (tidal bars and channels), (arrows pointing to current direction), Dhruma Formation (D1 unit), Wadi Birk, **D)** Skolithos and plane laminated sandstone (sand flat), Dhruma Formation (D5 unit), Al-Haddar**, E)** Plane laminated sandstone (Beach/foreshore), Dhruma Formation (D6 unit), Khashm Khurtum**, F)** Swaley cross-bedded sandstone (shoreface), Dhruma Formation (D1 unit), Wadi Al Jufayr.

F5: Bioturbated heterolithic silty sandstone (mixed flat/coastal plain)

These are 1 to 5 m thick tabular unit and usually show gradational base and occasional iron-stained top surface. The facies are composed of silt and medium sand that are commonly cemented with carbonate (Fig. 3.5B). The facies are sometimes very fossiliferous (e.g., the Dhruma Formation D3 unit is dominated by ammonites and clams and the D6 unit (post unconformity) is characterized by very-local and abundant branched coral (Jabal Shimrakh)). These heterolithic facies are highly bioturbated. The facies show rare 2D cross-bedding and are associated and interbedded with swaley cross-bedded sandstone (F), deltaic clinoforming sandstone (F), argillaceous bioturbated wackestone/packstone (F), and heterolithic oolitic ironstone (14). The facies formed in a mixed flat in outer coastal plain and/or nearshore setting.

F6: Bidirectional cross-bedded sandstone and mud drapes (tidal bars and channels)

These are tabular and channelized units with sharp based beds, 1.5 to 4 m thick. They are bidirectional tabular cross-bedding with sigmoidal bed-forms together with mud drapes and lesser bioturbation, and consist of medium sand with plat remains (Fig. 3.5C). The facies are interbedded with mottled red paleosol (F3), bluish green coastal plain shale (F4) and heterolithic bioturbated silty sandstone (F5). The sedimentary structures and the associated facies suggest a tidal bar and channel setting.

F7: *Skolithos* and plane laminated sandstone (sand flat/ foreshore)

These form 0.5 to 2 m thick sharp-based tabular beds. The sandstones are highly bioturbated with vertical *skolithos* cylindrical dwelling burrows (Fig. 3.5D) and occasional plane-laminated bedding (Fig. 3.5E) capped by iron-stained surface. They are composed of well-sorted medium sand grains and some plant remains. They are interbedded with mottled bluish green and red shales (F4) and overlie conglomerate silty sandstone beds (F1). They are rarely incised with distributary coarse-grained sandstone channels (F9) (Fig. 3.6A). The texture and the sedimentary structures indicate shallow and relatively high-energy nearshore marine setting (Fery, 1975). The facies are interpreted as sand flat or foreshore depositional setting.

F8: Swaley cross-bedded sandstone (shoreface)

These sandstones are scoured sharp-based tabular beds, 2 to 5.5 m thick that formed a localized narrow facies belt. These are cross-stratified with swaley and occasionally trough cross-bedding with lesser bioturbation (Fig. 3.5F) and are composed of medium sand. The facies occur only in the Dhruma Formation (D1 unit) interbedded with bioturbated heterolithic silty sandstone (F5) and rarely overlie inner-lagoon green calcareous shale (F15). The sandstones grade downdip into more carbonate-cemented bioturbated sandstone and occasionally into decimeter thick fining-upward peloidal skeletal grainstone storm (F18) beds in a calcareous shale context (F15). The facies grade updip into more heterolithic silty bioturbated sandstone (F5).

The sandstone facies are interpreted to represent an episodic high-energy wave dominated shoreface depositional setting formed seaward of low-energy or less agitated coastal-plain/tidal-flat silty and muddy facies.

F9: Coarse grained cross-bedded sandstone with plant remains (distributary channel)

The sandstones occur in reddish brown, sharp-based channelized units 1.5 to 2.5 m thick that cross-bedded, composed of medium to coarse quartz sand with alternation of silt and mud drabs and lesser bioturbation (Fig. 3.6A). The channels cut through bioturbated (*Skolithos* and horizontal burrows) tabular sand flat units (F7). They occur only in the upper part of the D5 unit of the Dhruma Formation which overlain by shale and fluvial incised channel that marks the Bathonian-Callovian unconformity in the updip southern areas. The facies are interpreted as distributary channels on the basis of the abundant plant remains, heterolithic cross-bedding, bioturbation and the interdistributary tabular *skolithos* sand flat facies (F7).

F10: Large-scale cross-bedded sandstone (delta front mouth bar)

These are up to 2 to 25 m thick and form large-scale oblique tangential to parallel clinoform sets with maximum 25º dip angle (Fig. 3.6B, C and D). The thickest clinoform unit (at Khashm Al Khalta) shows westward progradation and thinning along 15 km, based on physically tracing beds. The facies have sharp bases and truncated tops. The bottom and top clinoform sets show bioturbation traces. These occur only in D1 unit in the Dhruma Formation and interbedded with highly bioturbated sandstone beds. The sandstones are composed of medium to coarse quartz sand. The facies formed in a delta front mouth bar setting and represent periods of high-siliciclastic influx to the depositional system.

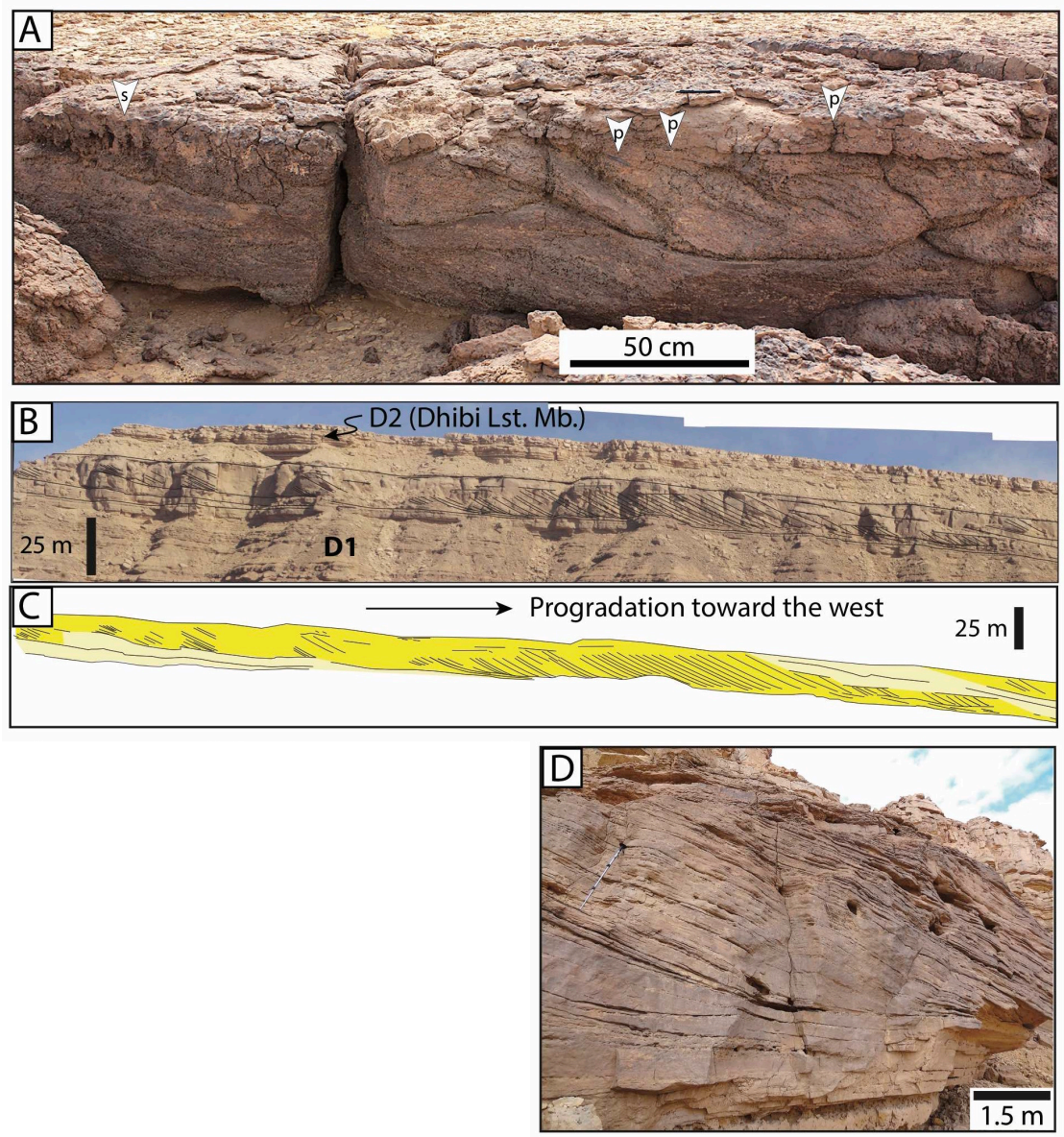

Figure 3.6: Coastal plain facies association, **A)** Coarse grain cross-bedded sandstone with plant remains (p arrow) cutting a skolithos sandstone facies (s arrow), (delta plain distributary channel), Dhruma Formation (D6 unit), Jabal Shimrakh**, B)** Large-scale cross-bedded sandstone (25 meter thick), (delta front mouth bar), Dhruma Formation (D1 unit), Khashm Al Khalta, **C)** Detailed facies map of the large scale deltaic clinoforms in (B) showing the stratal geometry and the progradation direction of the delta front mouth bar sandstone**,** **D)** Close-up photo of the deltaic clinoform sets in (B), (Note 150 cm Jacob's staff for scale).

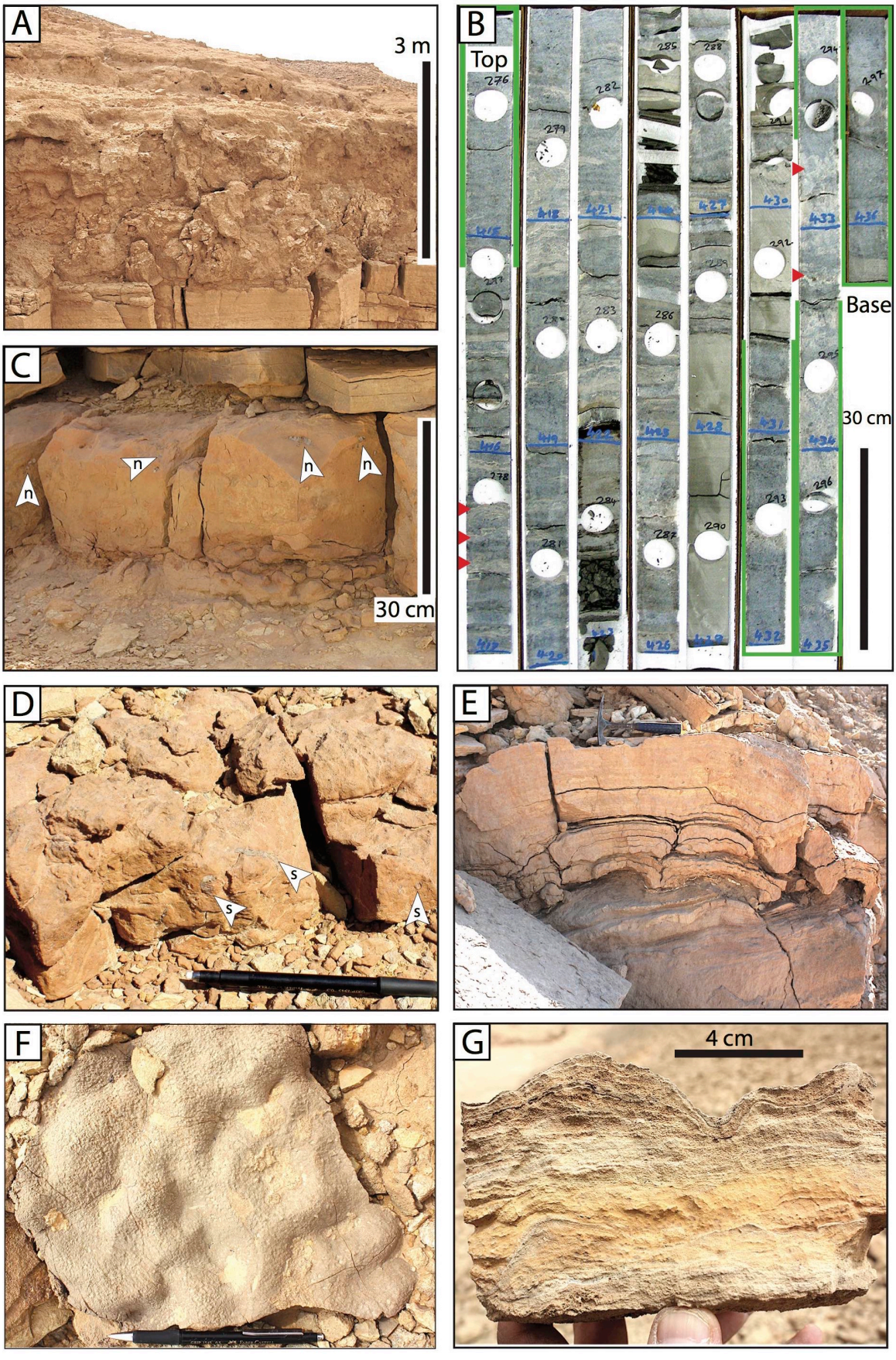
A
3 m
B
Top
Base
30 cm
C
n
n
n
n
30 cm
D
s
s
s
E
F
G
4 cm

← **Figure 3.7:** Arid shoreline facies association in the Dhruma Formation. A) Gypsum, weathered facies of crinkly laminated evaporites (salina, sabkhah), Marrat Formation, Khashm Ad Dhibi, B) Slabbed-core samples shows the internal sedimentary structures and vertical successions of the crinkly laminated evaporites (intertidal to supratidal sabkhah), the base and top of the core (green traies) shows chicken-wire nodular mosaic anhydrite crystals (subaqueous supratidal), (red arrows) shows displacive enterolithic anhydrite crystal (supratidal), the middle of the core shows massive dolomite with lath-shaped anhydrite crystals (intertidal/supratidal), the top (last 4 traies) show fine anhydrite crystal and stromatolitic crinkly laminations (intertidal), Dhibi-1 shallow core, Khashm Ad Dhibi, (photography by G. W. Hughes) C) Red dolomite with local silicified evaporite nodules (n arrows) (tidal flat), Dhruma Formation (D4 unit), Wadi Birk, D) Red dolomitic wackestone with skeletal fragments (s arrows) (tidal flat), Dhruma Formation (D4 unit), Abu Aljwar, E) Vertical stacked hemispheroids (SH-V) type of stromatolite composed of close-linked hemispheroidal lamination (LLH-C) (intertidal), Dhruma Formation (D1 unit), (hammer for scale), Wadi Al Jufayr, F) Closed laterally linked hemispheroids (LLH-C) type of stromatolite (intertidal), Dhruma Formation (D1 unit), Khashm Ad Dhibi, G) Cross-section of the laterally linked hemispheroids (LLH-C) type of stromatolite in figure (F).

F11: Crinkly laminated evaporites (intertidal to sabkhah)

These are tabular bedded units, 2.5 to 4 m thick, with sharp bases and gradational top boundaries. The facies are composed of mud-supported dolomite and anhydrite (Fig. 3.7A). In core the facies exhibit chicken-wire nodular mosaic anhydrite (Fig. 3.7B) with displacive enterolithic structure. Interbedded facies include very thin ooid grainstone and shale, massive microdolomite with lath-shaped anhydrite crystals, and dolomitic crinkly microbial laminites intercalated with anhydrites. The evaporites are overlain by dolomite and gray calcareous shale. The lithologies and the sedimentary structures are indicative of intertidal to supratidal sabkhah environment. Specifically, the crinkly laminated stromatolite structures are inferred to represent intertidal depositional setting; whereas the chicken-wire and the displacive enterolithic structures are characteristic for supratidal sabkhah setting (Evans et al., 1969; Butler, 1969; Patterson, 1972; Bush, 1973; Butler

et al., 1982; Warren and Kendall, 1985; Shearman, 1978). The nodular mosaic anhydrite crystals may be formed in a supratidal salina depositional environment (Perkins et al., 1994).

Lithostratigraphically, the facies belong to the Early Jurassic Marrat Formation (Manivit et al., 1990). However, in this study the facies are genetically assigned to the base of the Dhruma composite sequence and they occur only at Khashm Ad Dhibi section. The complete evaporite depositional cycle and the overlying shale facies imply a predominant low-energy marine transgression.

F12: Stromatolite and crinkly laminated lime-mudstone (intertidal)

These are extensive widespread tabular beds, 1 to 3 m thick. The facies have gradational bases and sharp tops. They are composed of mud-supported unfossiliferous microbial laminated dolomite and lime mudstone. The microbial structures include close-spaced laterally linked hemispheroids (LLH-C) (*sensu* Logan et al., 1964) (Fig. 3.7F and G). In some localities, the LLH-C structures were developed to form elongated columns of vertically stacked hemispheroids (SH-V) about 70 cm height (Fig. 3.7E). These structures are intercalated with crinkly laminations (Fig. 3.7G). The facies appear only in D1 unit of the Dhruma Formation interbedded with calcareous shale (F15), mottled shale (F4) and sometimes overlain by heterolithic silty ferruginous oolite (F14).

The LLH type of stromatolitic structures formed in an intertidal-mud flat protected from wave and tidal currents (Logan et al., 1964), whereas the elongated SH-V structure formed in a relatively higher energy coastal lagoonal setting parallel to waves or tidal currents (Logan et al., 1964; Wright,

1984). The well-developed stromatolite structures suggest a hypersaline lagoon that inhibited burrowing and grazing (Logan et al., 1964,1974; Husinec et al., 2012).

F13: Red dolomite with local silicified evaporite nodules (restricted lagoon)

The facies form extensive correlatable tabular units, up to 0.1 to 1.5 m thick, and have sharp bases and tops (Fig. 3.7C and D). They are composed of mud-supported fine-grained fabric-preserving dolomite (less than 20 micron crystals). The facies are fine peloids and rare quartz packstone layers with sparse skeletal fragments. They are generally massive, structureless with locally silicified anhydrite nodules and minor bioturbation. The facies occur in D4 unit of the Dhruma formation and interbedded with bioturbated peloidal and oncoidal wackestone/mudstone inner lagoon facies (F17). The facies is sometimes overlain by thin transgressive ooid grainstone (F18) (Fig. 3.12) and swaley/hummocky very fine sandstone (F8) (Fig. 3.13). The dolomite beds are rarely bounded by hardgrounds.

Such fabric-preserving and regionally extensive dolomite appears to be stratigraphically related tidal recharge/infiltration and seepage-refluxion processes (Adams and Rhodes 1960; McKenzie et al., 1980; Enos, 1983; Iannace and Frisia, 1994). These formed from hypersaline tidal waters flooding and supratidal flats. Rare skeletal layers likely were washed in from offshore during storms. The silicified anhydrite nodules formed during early diagenesis as a result of the brine water percolation (Chowns and Elkins, 1974; Maliva 1987).

F14: Heterolithic silty ferruginous oolite (supratidal to continental)

The facies are tabular units up to 7.5 m thick with gradational base and occasionally sharp iron-crust top boundaries (Fig. 3.8A). They are composed of medium to very coarse ferruginous ooid packstone, with medium angular hematite-coated quartz grains, some glauconitic grains and common clay-silt matrix. The facies are very friable structureless and cemented by carbonate, clay and hematite (Fig. 3.8B). The facies include sparse echinoderms, bivalve, gastropods debris and small foraminifera (Le Nindre et al., 1984). They are abundant in up-dip proximal areas in the southern outcrops and usually overlie unconformities and paleosol surfaces (F3). They are overlain by mottled shale (F4) and calcareous shale (F15) with decimeter thick, reworked quartzose skeletal grainstones (18).

The facies formed in a marginal marine, supratidal to continental depositional setting (Le Nindre et al., 1984). They do not formed as a result of agitated hydrodynamic process, but rather they were precipitated chemically in redox waters supersaturated with respect to chamosite (Mutrux et al., 2008; Arp, 2008). The redox water result from freshwater discharges that make density stratification and prevent vertical water circulation (Bottjer et al., 1986 in Read, 1989; Rabalais et al., 1991; Lukasik et al., 2000). The maximum concentration of the ferruginous oolite occurs during early transgression of sequences and cycles (Mutrux et al., 2008).

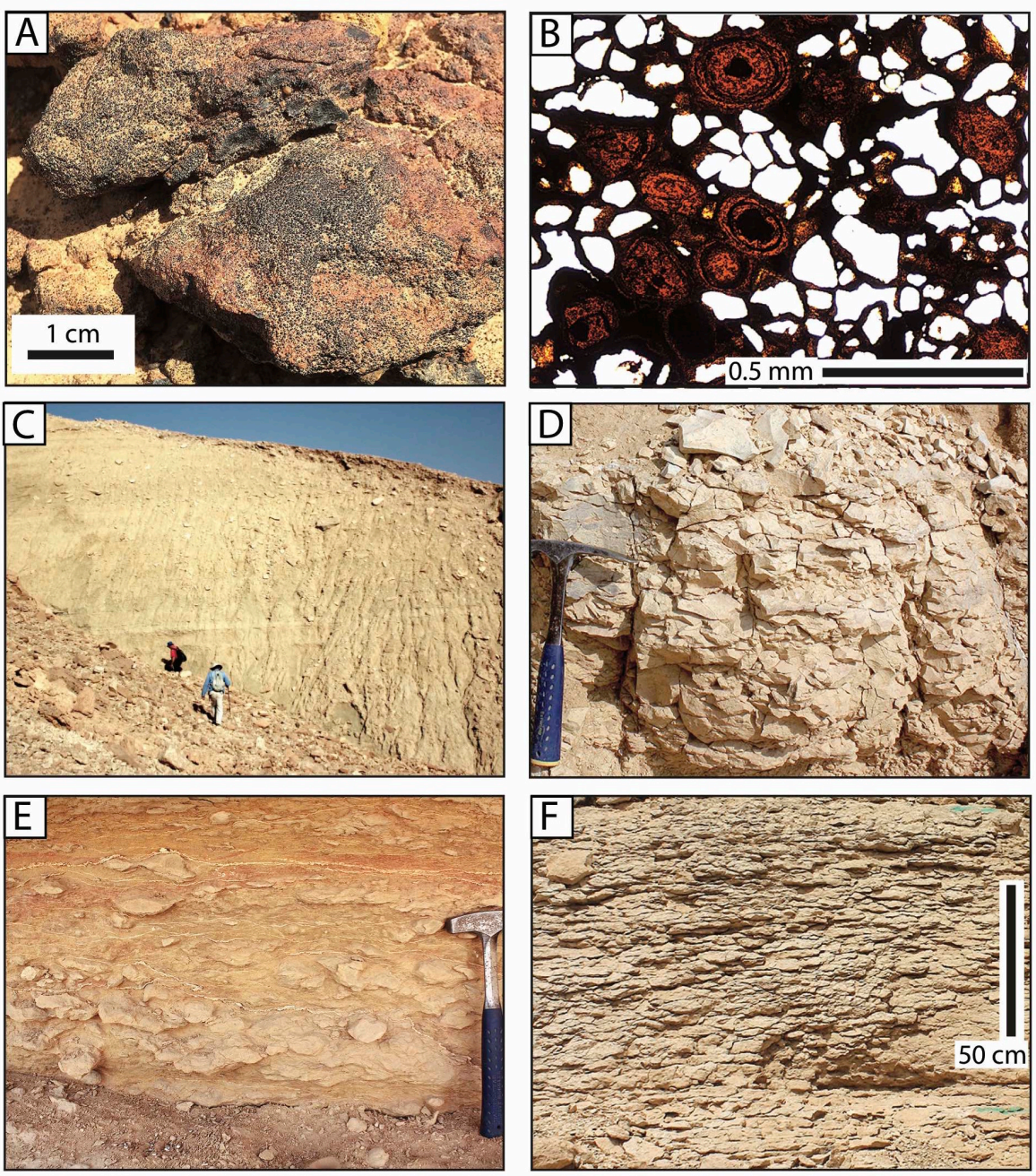

Figure 3.8: Mixed carbonate-siliciclastic inner lagoon facies association in the Dhruma Formation and Tuwaiq Mountain Limestone. A) Heterolithic silty iron ooid (early transgressive proximal facies), Base Dhruma Formation unconformity (D1 unit), Wadi Birk, B).. Thin section.. C) Grayish green calcareous shale, Dhruma Formation (D7 Hisyan Member), Wadi Birk, D) Argillaceous mudstone/ wackestone (shale dominated inner lagoon), Dhruma Formation (D5 unit), Fara'id al Ahmar, E) Slightly argillaceous nodular bioturbated peloidal wackestone/mudstone (inner lagoon), Dhruma Formation (Dhibi Limestone Member), Wadi Birk, F) Slightly argillaceous nodular bioturbated peloidal wackestone/mudstone (inner lagoon), Tuwaiq Mountain Limestone (T2 unite), Wadi Birk.

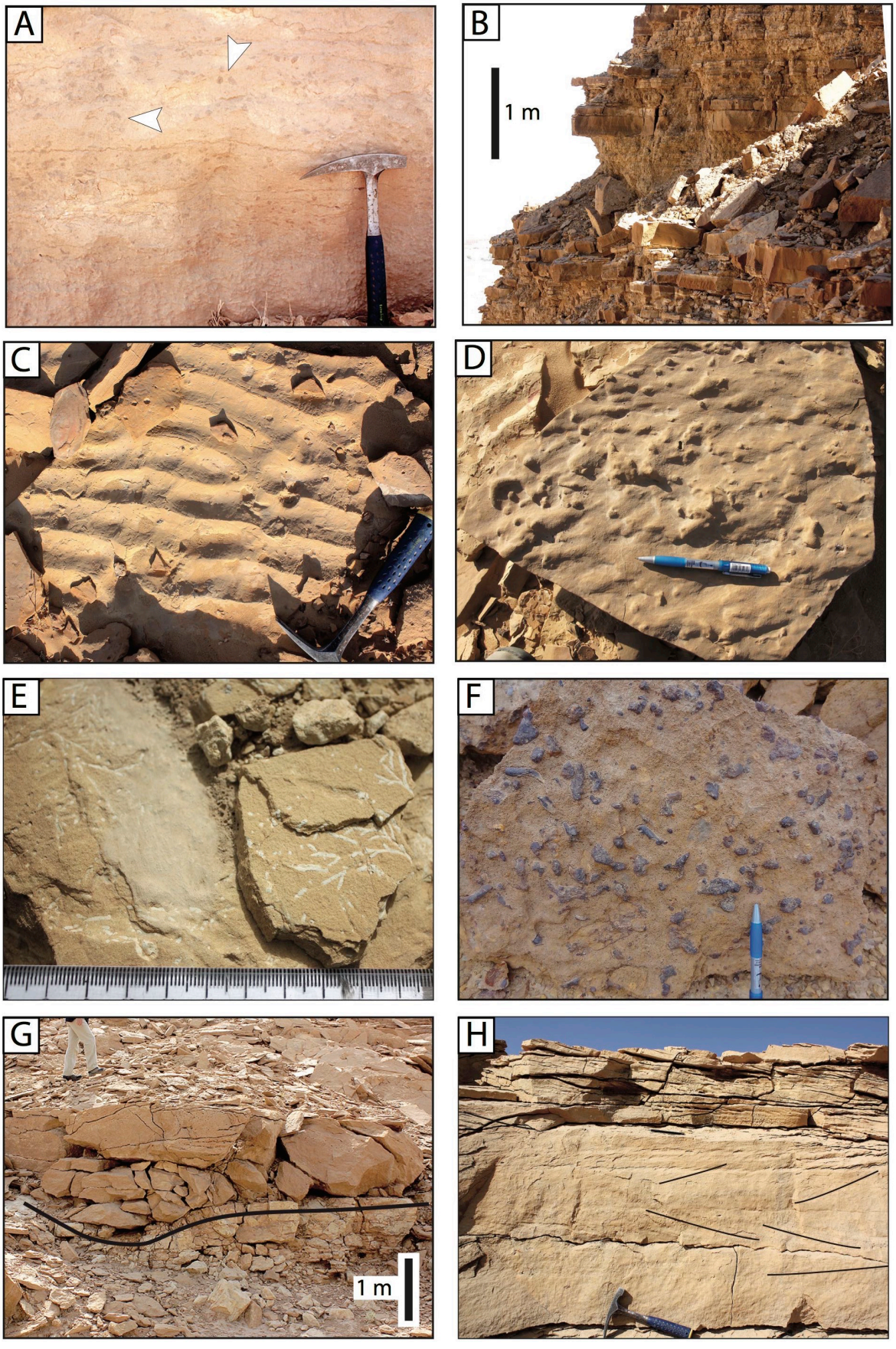
A
B
1 m
C
D
E
F
G
1 m
H

← **Figure 3.9:** Carbonate inner lagoon facies association in the Dhruma Formation and Tuwaiq Mountain Limestone, A) Bioturbated peloidal wackestone with oncoid grains (arrows), Dhruma Formation (D2, Dhibi Limestone Member), Wadi Birk, B) Dm- and cm-thick of sharp-base, finning upward intraclasts peloidal skeletal grainstone beds interbedded with argillaceous mudstone (storm dominated inner platform), Dhruma Formation (D6 unit), Wadi Birk, C) Ripple marks, top view of the storm generated intraclastic peloidal grainstone, Dhruma Formation (D5 unit), Khashm Al Faridah, D) Tool marks on the base of the storm generated peloidal grainstone in figure (D) (note pen for scale), E) Occasional Chondrites trace fossils on top of the storm generated peloidal grainstone, Dhruma Formation (D7 unit, Hisyan Member), Wadi Birk, F) The sharp-based peloidal skeletal grainstone composed of reworked iron-crust lithoclast (Dark brown), (storm dominated inner platform), Dhruma Formation (D6 unit), Khashm Khurtum, G) Cross-bedded reworked intraclastic and skeletal grainstone and floatstone channel fill, (storm dominated inner platform), Dhruma Formation (D4 unit), Wadi Birk, H) Cross-bedded ooid peloidal skeletal grainstone (high-energy shoreface), Dhruma Formation (D6 unit), Wadi Al Hawtah.

F15: Grayish green calcareous shale and argillaceous lime mudstone (inner lagoon)

These facies are extensive tabular units, 0.5 to 20 m thick (Fig. 3.8C). They have gradational bases and tops. The shales are composed of terrigenous clay and occasional very fine sand. The argillaceous lime mudstones consist of pelletal grains and rare skeletal grains. The lime mudstones have many *Chondrites* burrows and exhibit conchoidal breakage. The biota of the shales includes ammonites, nautiloids, echinoderms, brachiopods, bivalves, gastropods, fish teeth, serpula, foraminifera and ostracods (Manivit et al., 1990). The shales usually are interbedded with *Chondrites*-rich and horizontal bioturbated peloidal wackestone/packstone facies. The shales are associated with sharp-based centimeter to decimeter reworked beds (F18) of very-coarse granular reworked skeletal grainstone that are abundant in updip area (in Tuwaiq Mt. Lst.).

The facies formed in a nearshore inner lagoon proximal to the terrigenous source. The associated storm-generated grainstone beds suggest that the inner platform was occasionally influenced by major storms. The dominant *Chondrites* burrows imply overall restricted low-oxygenated bottom water (Bromley and Ekdale, 1984). The low oxygenation level could be attributed to the facies proximality to freshwater runoff from the hinterland.

F16: Slightly argillaceous nodular peloidal wackestone/mudstone (inner lagoon)

These are tabular units, 1 to 20 m thick, having gradational bases and tops. They are made up of very fine to medium peloidal wackestone/mudstone with lesser terrigenous clays (Fig. 3.8F). The facies locally consist of quartz and intraclasts, skeletal fragments, abundant sponge spicules and foraminifera (*Lenticulina* sp.) as well as lesser echinoderms, brachiopods, bivalves, gastropods and serpula (Manivit et al., 1990). The facies are characterized by intense horizontal bioturbation, *Chondrites and Planolites* burrows. The facies have irregular nodular structure with abundant clay-rich pressure-solution seams. They are interbedded with sharp-based centimeter to decimeter beds of reworked very-coarse granular skeletal grainstone (F18) and *Chondrites*-rich argillaceous lime-mudstone (F15).

They formed in a proximal inner lagoon in relatively low oxygenated bottom waters seaward of the argillaceous rich facies. The low oxygen restricted circulation could be related to the freshwater stratification and nutrient influx, rather than reflecting water depth. The dominant storm-generated skeletal grainstone beds (F18) imply that the inner platform was open and influenced by periodic storm waves.

F17: Bioturbated peloidal wackestone/packstone, oncoidal locally (highly bioturbated lagoon)

These are laterally extensive massive homogeneous tabular beds, 0.5 to 22 m thick, having gradational base and firmground/hardground tops (Fig. 3.9A and 3.13D). The facies consist of silty to very fine pelletal and medium peloids, locally gravel sized oncoids and very-coarse sand size benthic forams. The facies consist of high-diversity fauna that includes ammonites, echinoderms, brachiopods, bivalves, gastropods, serpula and bryozoans (Manivit et al., 1990). The facies are creamy white characterized by burrow homogenization, argillaceous wispy solution seams and rare nodular structures. Below the firmgrounds/hardground surfaces, branched vertical burrows (*Thalassinoides*) are abundant. They are occasionally associated with encrusted/domal stromatoporoid and coral specimens (in Tuwaiq Mt. Lst.). The facies usually grade upward from slightly argillaceous nodular bioturbated peloidal wackestone/mudstone and/or thin transgressive grainstones. However, occasionally the facies lack associated high-energy grainstone beds (e.g. Dhibi Mb. Lst.).

The facies formed in a well circulated, well-oxygenated, low-energy sheltered more offshore lagoon. This is inferred by the abundant benthic forams, light facies color and the intense bioturbation (Wilson and Jordan, 1983; Galli, 1993; Khetani and Read, 2002).

F18: Sharp-based intraclasts-peloidal skeletal grainstone (storm dominated inner platform)

Three subfacies can be distinguished based on thickness and bedding geometries. Cm-thick sharp-based lenticular beds (Fig. 3.9B, C, D and E), composed of very-fine to medium peloids and coated-grains, occasional quartz silt, and gravel sized skeletal debris and rip-up clasts of packstone/grainstone. They fine upward and are topped by wave-ripples. They have tool marks, plane lamination and/or hummocky cross-stratification (HCS), smaller wave-ripples (cm-wavelength), and occasional *Chondrites* burrows. These are associated and interbedded with shale and argillaceous mudstone (F15).

Dm-thick sharp and irregular based extensive tabular beds (Fig. 3.9B, F, 3.12a and 3.13D) composed of very-fine to medium peloids and coated-grains, rare quartz silt, and gravel sized skeletal debris and rip-up clasts of packstone/grainstone. They fine upward and are topped by wave-ripples. They have wave ripple cross-laminations and longer wave-ripples (dm-wavelength). They are interbedded with slightly argillaceous nodular bioturbated wackestone/packstone (F16) and sometimes with shale (F15).

Meter-thick erosional based channel form units (Fig. 3.9G and 3.13C) characterized by poorly sorted, non-graded, reworked skeletal and rip-up clasts grainstone with large cross-stratification. These channel forms are 10 m wide and sharply overlie bioturbated mudstone facies (F17) (Dhruma Formation, D4 unit, Wadi Birk).

These formed on a storm dominated inner platform during early transgression. The storms are may be generated by wind-drift current which

are the main product of an onshore sediment transport in such shallow nearshore setting (Aigner, 1985; Galli, 1993). Other factors that can be possible causes for the onshore sediment transports are the general transgression trend and the predominant flat depositional profile that oppose offshore sediment transport and bottom return flows (Galli, 1993).

F19: Cross-bedded ooid peloidal skeletal grainstone (high-energy shoreface)

These are tabular and lenticular bedded units, 1.5 to 3 m thick with sharp bases (Fig. 3.9H), trough cross-bedding and large 3D megaripples. They are fine to medium peloidal and ooid grainstone with some very coarse granule skeletal and rip-up clasts. The facies are usually interbedded with calcareous shale and occur in the Dhruma Formation (D6 unit) above the Middle Bathonian to Early Callovian unconformity. They are cemented with early ferroan pre-compacted calcite cement.

These formed in high-energy wave-dominated shoreface seaward of the coastal-plain/inner-lagoon shale. The high-energy shoreface developed during post-unconformity transgression.

F20: Oncoidal packstone/grainstone and rudstone (oncoidal bars/shoal)

The facies are lenticular units 1 to 2 m thick with sharp bases. The facies are characterized by homogenized bioturbation structure interbedded with massive bioturbated lagoonal wackestone/packstone facies. These are coarse to very coarse grainstone and rudstone composed of pebble sized oncoidal, sand to granule sized coated grains, and some rip-up clasts (Fig.

3.10A). They occur usually at top of carbonate dominated depositional cycles mainly in the Dhruma Formation (D2 and D4 units) and occasionally in the Tuwaiq Mountain Limestone (T3 unit). The facies formed in a back-barrier bars/shoal setting (Olivier et al., 2011).

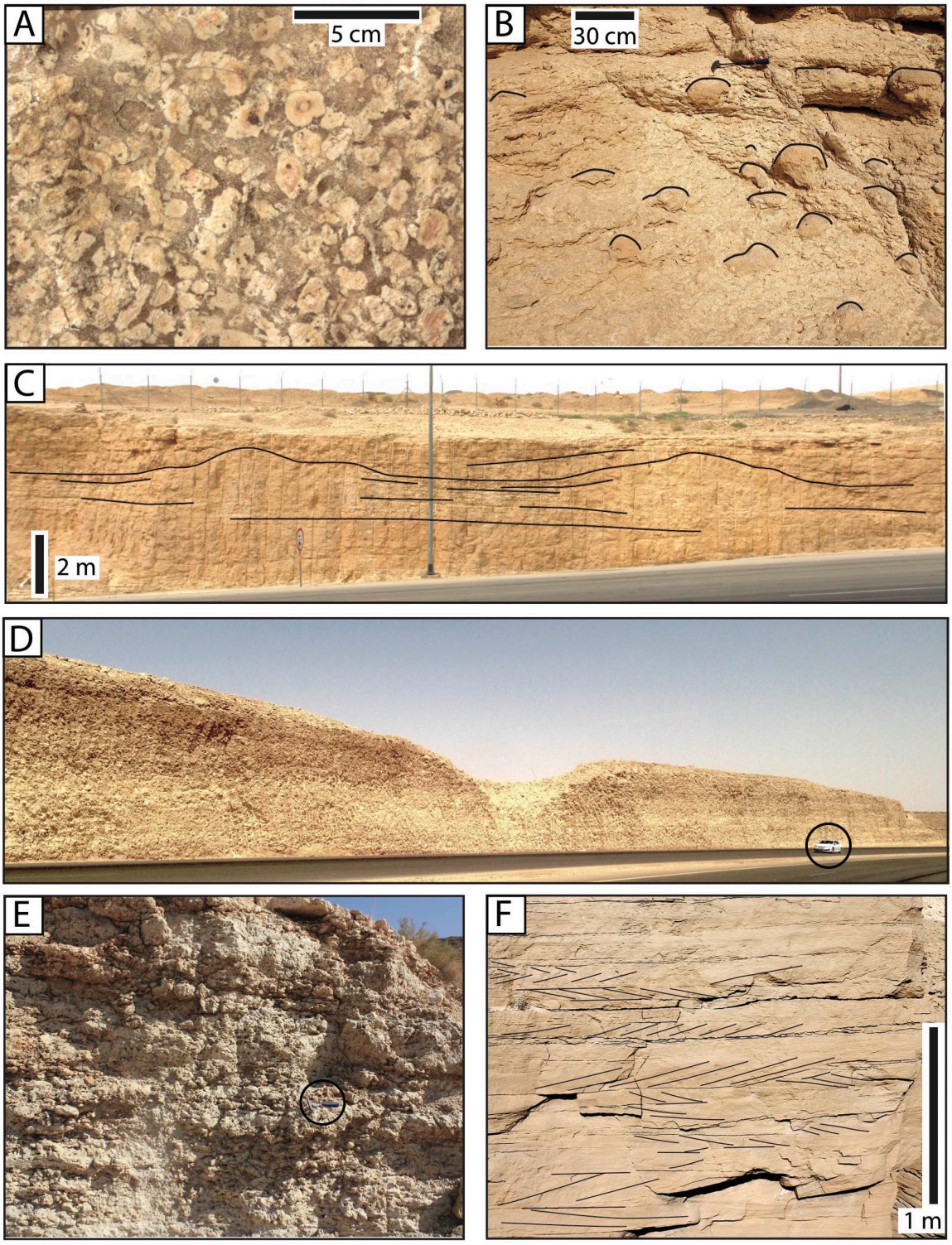

← **Figure 3.10:** Back-barrier lagoon facies association in the Dhruma Formation Limestone, A) Oncoidal packstone/grainstone and rudstone (oncoidal bars/shoal), Dhruma Formation (D2 unit, Dhibi Limestone Member), Wadi Birk, B) Biostromal coral/stromatoporoid mudstone/ wackestone and floatstone (low-energy back-barrier), Tuwaiq Mountain Limestone (T3 unit), Wadi Birk, C) Biohermal coral/stromatoporoid mudstone/wackestone and framestone (high-energy patch reef), Tuwaiq Mountain Limestone, road cut of the Riyadh-Mecca highway near Khashm Al-Qaddiyah, D) Reef massive framestone (Back-barrier reef) (car for scale), Tuwaiq Mountain Limestone, Huraymila, E) Close-up photo of the reef massive framestone facies in figure (D), (hammer for scale), F) Swaley cross-bedded well-sorted peloidal coated-grain grainstone (shoal and washover complex), Dhruma Formation (D4 unit), Wadi Birk.

F21: Biostromal coral/stromatoporoid mudstone to packstone and floatstone (low-energy back-barrier)

These are extensive tabular units up to 12 m thick and have gradational bases and firmground tops (Fig. 3.10B). The facies are highly bioturbated. They are composed of corals and stromatoporoids with branched, tabular and head shapes, up to 60 cm diameter and 30 cm thick. Interhead material consists of coarse skeletal fragments in fine peloidal mudstone/packstone and floatstone. They occur in the Tuwaiq Mountain Limestone (T3 unit) interbedded with massive bioturbated wackestone/packstone (F17) and biohermal coral/stromatoporoid mudstone/wackestone (F22). The facies are interpreted as low-energy back-barrier deposits behind the reefal barrier.

F22: Biohermal coral/stromatoporoid mudstone/wackestone and framestone (back-barrier patch reef)

The bioherms are 2 to 10 m thick and 15 to 30 m diameter in a circular shape as mapped at top of the Tuwaiq Mountain Limestone by Manivit et al. (1990) (Fig. 3.10C). The bioherms have gradational bases and sharp tops and composed of coral/stromatoporoid framestone. The surrounding facies are

tabular massive mudstone/wackestone facies consisting of very fine to fine peloids and skeletal fragment floatstone. These are homogenized and highly bioturbated. Bioherms occur only in the upper part of the Tuwaiq Mountain Limestone (T3 unit) and are localized in Khashm Al-Qaddiyah area. The circular patch-reefs are typical of immediate back-barrier setting (Wilson and Jordan, 1983).

F23: Branching coral/stromatoporoid framestone (back-barrier reef)

The facies are 10 m thick tabular bedding and have gradational bases and tops (Fig. 3.10D and E). The facies consist of framestone of branching corals and stromatoporoids with binding of microbial crusts. The facies overlie highly bioturbated biostromal coral/stromatoporoid mudstone to packstone and floatstone facies (F21). They occur only at top of the Tuwaiq Mountain Limestone (T3 unit) and are localized in Huraymila area. The facies formed as back-barrier reef facies in an open-marine environment (Védrine and Strasser, 2009).

F24: Cross-bedded peloidal coated-grain grainstone (shoal and washover complex)

These are 2 to 7 m thick tabular, channelized and lenticular units. They have sharp base erosional scoured bases (Fig. 3.10F, 3.12c, e and 3.13B). The grainstones are characterized by trough cross-bedding (3D ripples), swaley/hummocky and sigmoidal bidirectional cross-lamination. Moreover, the facies exhibit flaser and wavy bedding sedimentary structures. The facies consist well sorted very fine to fine peloidal and medium coated-grain

grainstone with skeletal fragments and rare ooid and quartz silt. The primary sedimentary structure may be disrupted by bioturbation (Fig. 3.12e). The facies show an overall coarsening and graining upward and are interbedded with argillaceous nodular mudstone/wackestone facies (F16). The facies occur only the Dhruma Formation (D4 unit).

The grainstones are interpreted as shoal and washover complexes. The flaser and wavy bedding with the bidirectional cross-lamination channel fills formed as back-barrier tidal bars facies association (Reineck and Singh, 1975; Reinson, 1979; Blomeier et al., 2009; Dalrymple, 2010; Lasemi et al., 2012). The swaley/hummocky fine silt quartz and peloidal grainstone formed as a back-barrier washovers. The swaley trough cross-bedded coated grain grainstones formed as shoals (Fig. 3.13B).

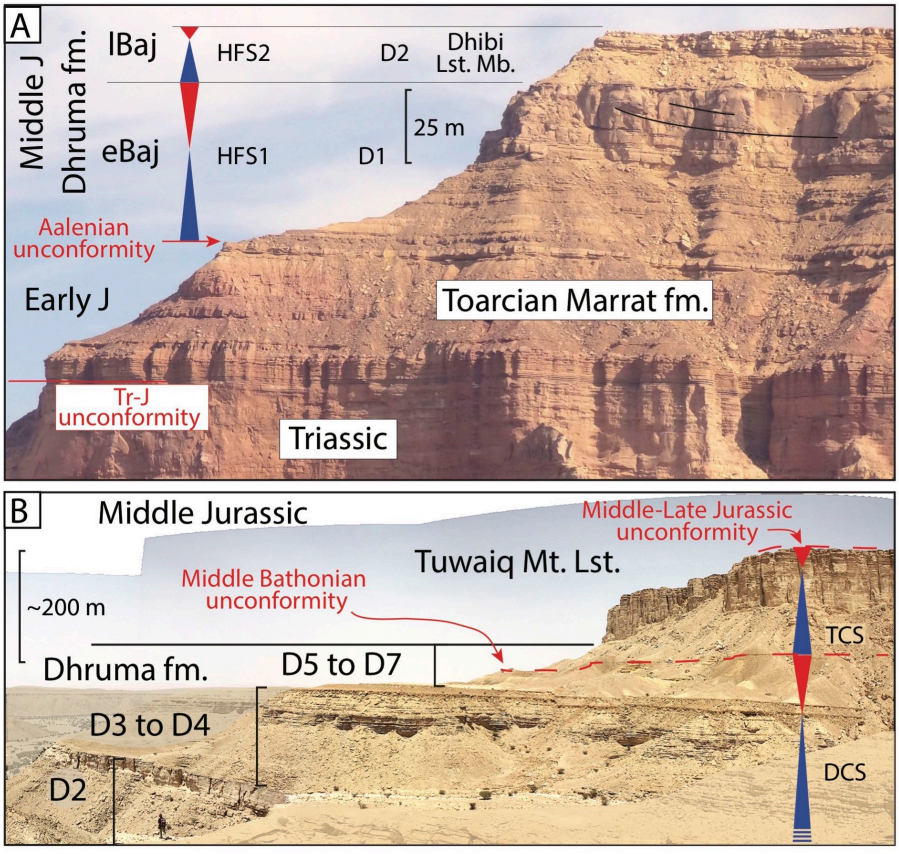

Figure 3.11: Outcrop photographs showing the Middle Jurassic lithostratigraphic units, unconformities and the interpreted depositional sequences. A) Khashm Al Khalta outcrop, B) Wadi Birk outcrops.

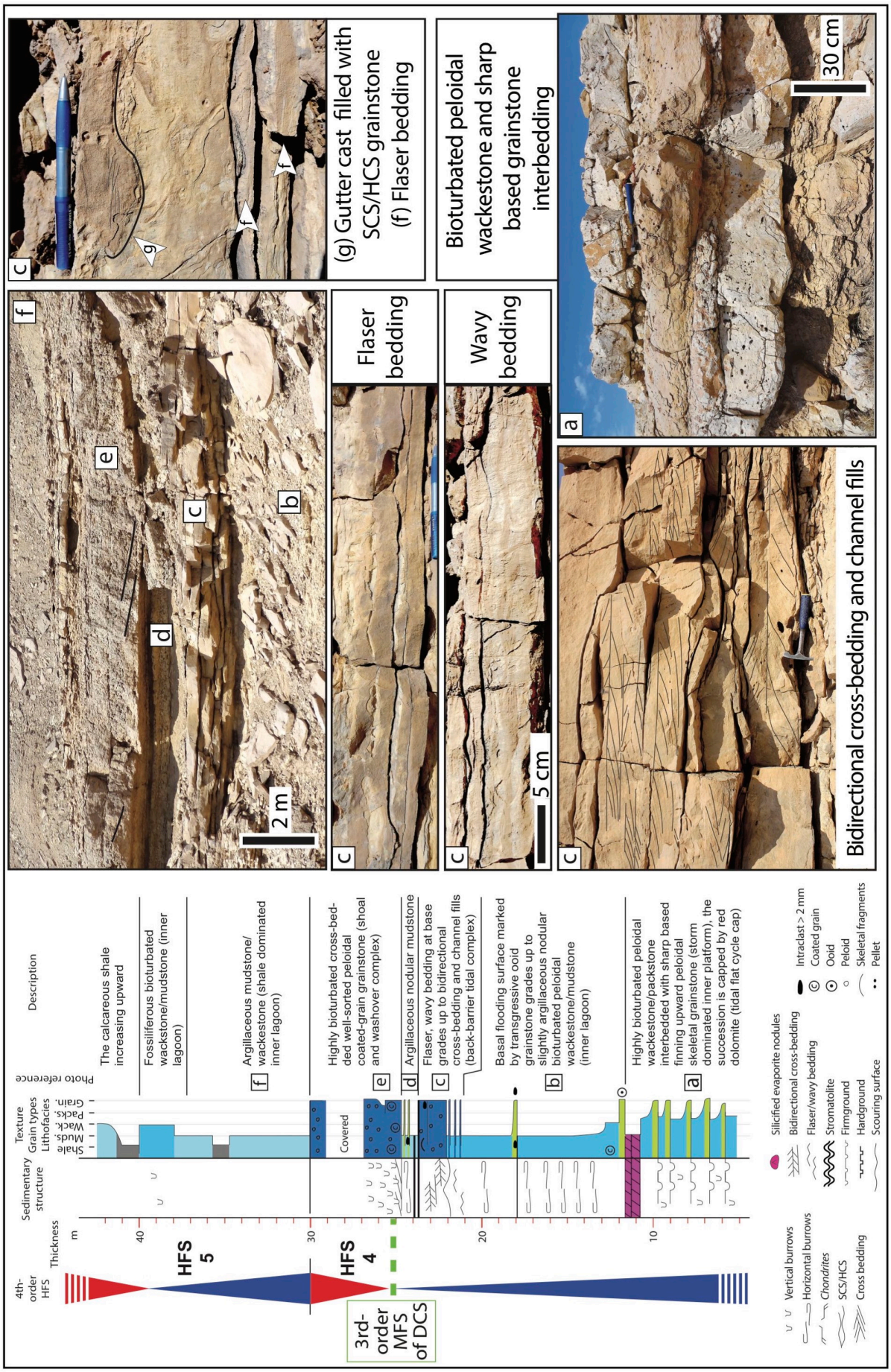

Figure 3.12: Detailed measured section of the Dhruma Formation (upper D4 and base D5) at Wadi Al Hawtah shows vertical successions of carbonate inner platform (a, b, c, f) through back-barrier shoal and washover complex (c, d, e). For facies color legend see Fig. 3.15.

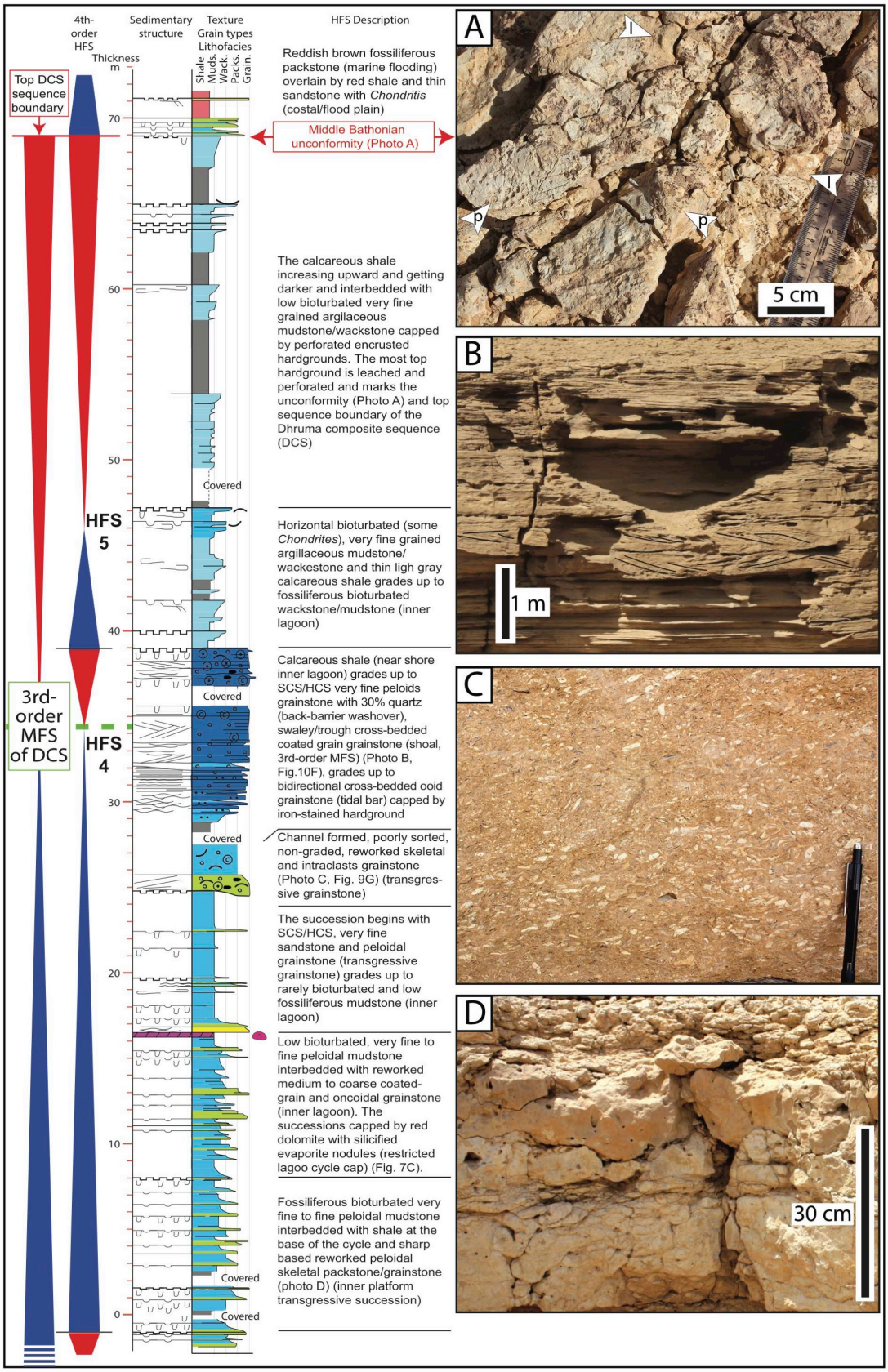

Figure 3.13: Detailed measured section of the Dhruma Formation (upper D4 and base D5) at Wadi Birk shows vertical successions of carbonate inner platform through back-barrier shoal and washover complex. For symbol legend see Fig. 3.12, for facies color and symbols see Fig. 3.15.

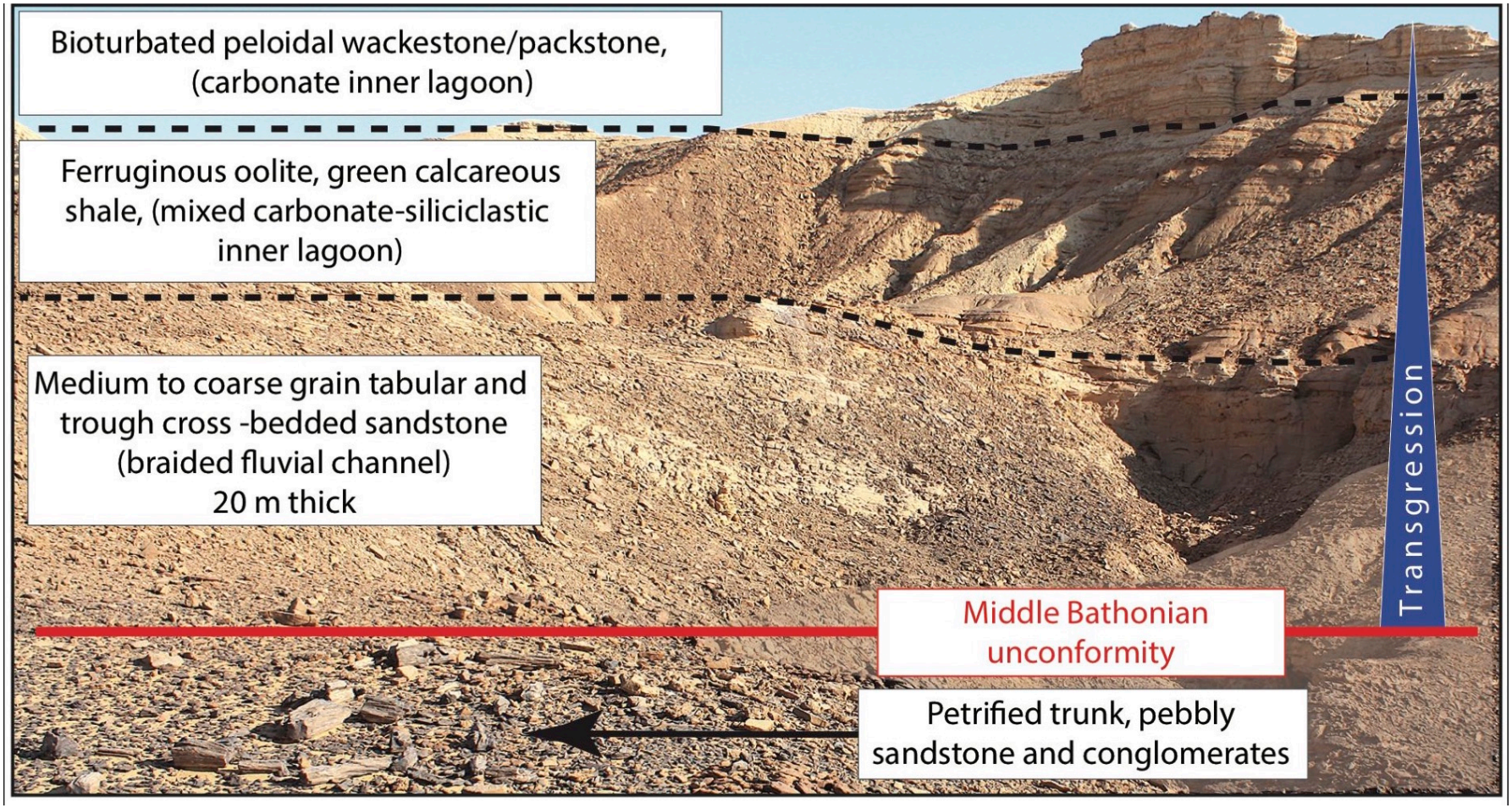

Figure 3.14: Outcrop photograph showing the Middle Bathonian unconformity and the overlaying transgression successions of the Tuwaiq composite sequence (TCS), Khashm Abu Al Jiwar.

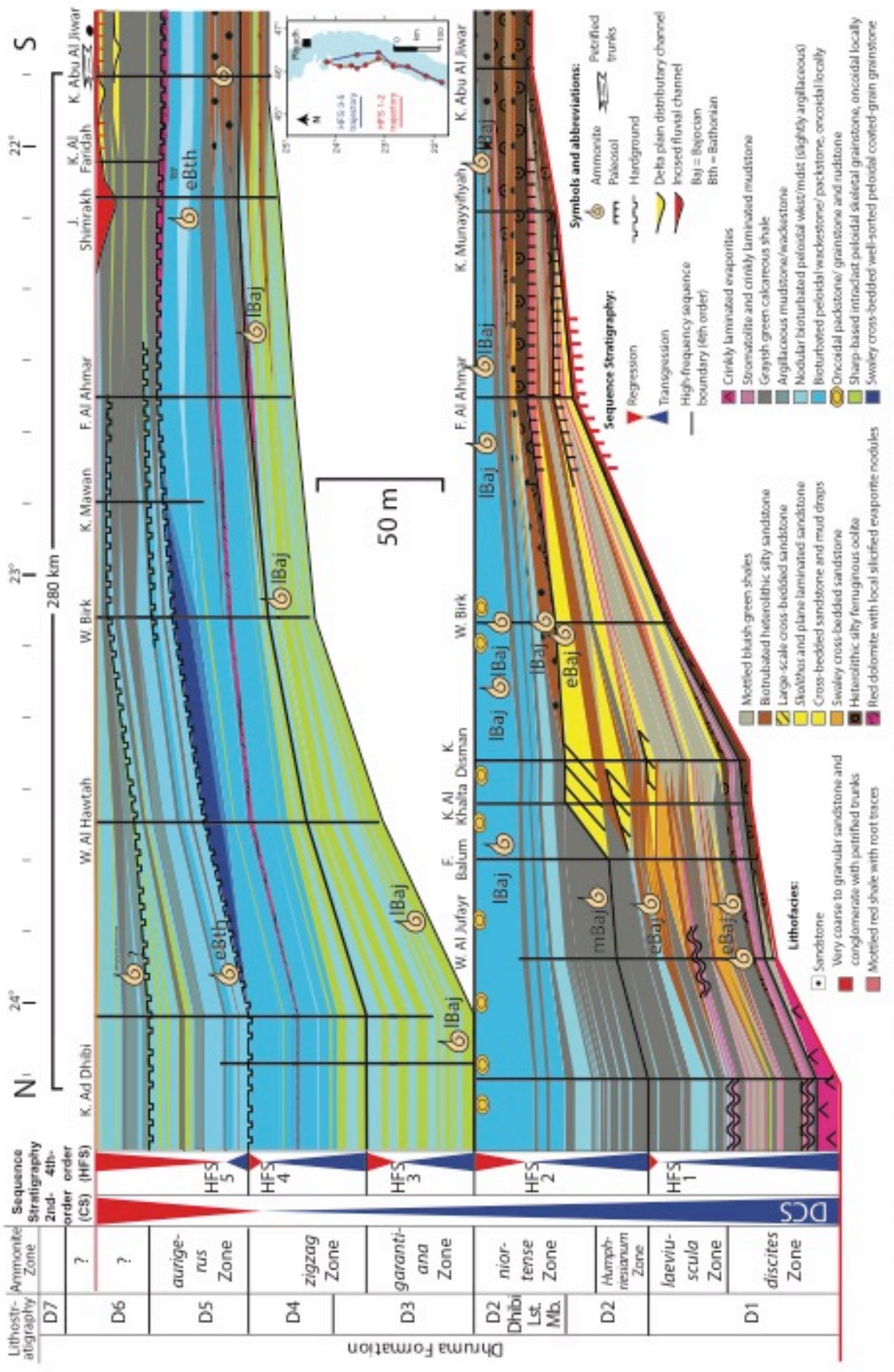

Figure 3.15: High-resolution sequence stratigraphic cross-section of the Dhruma Formation. The sections were hung on two datums: 1) top Dhibi Limestone Member, 2) The Middle Bathonian unconformity marked by reddish.

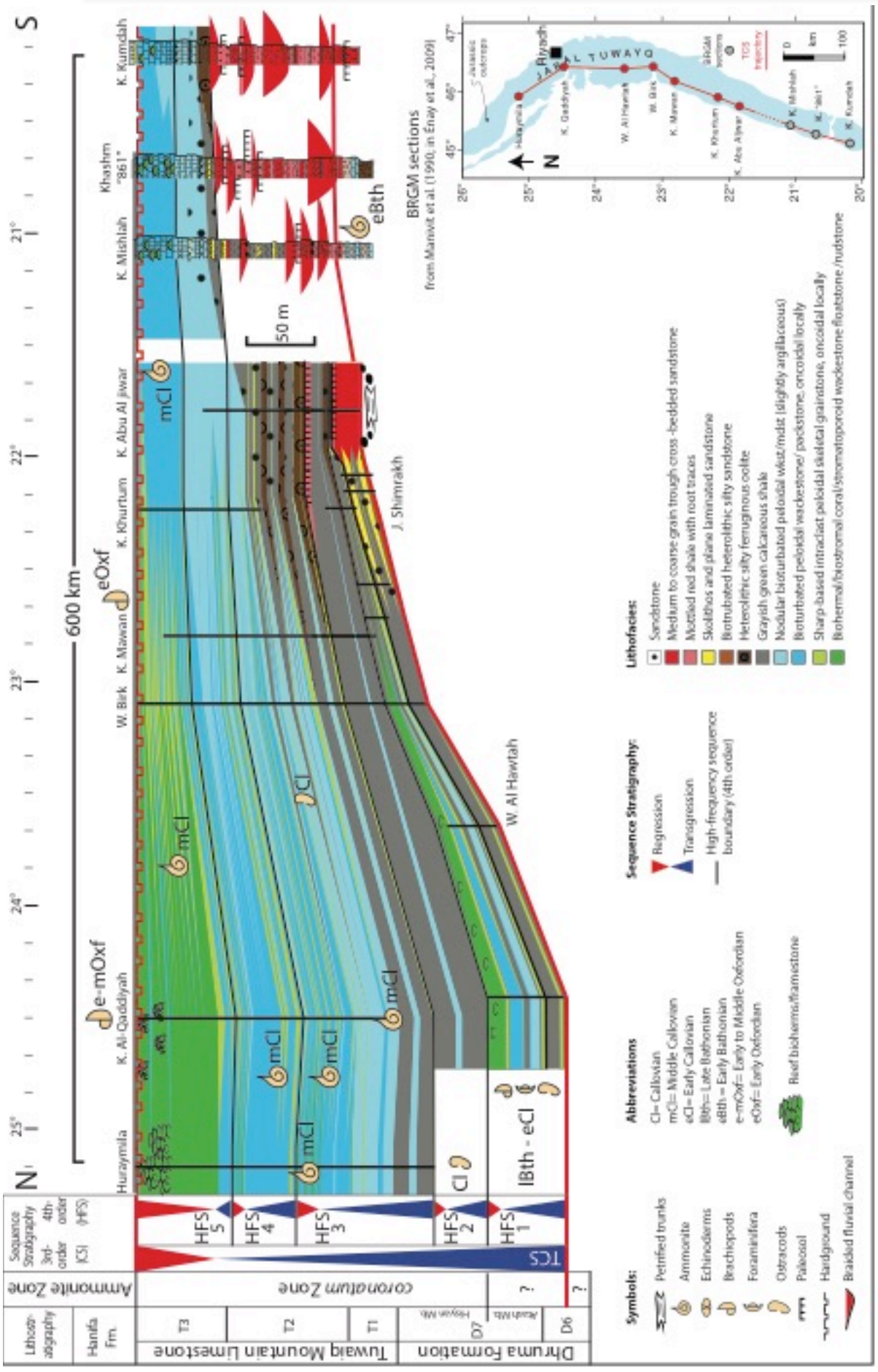

Figure 3.16: High-resolution sequence stratigraphic cross-section of the upper Dhruma Formation (upper D6 and D7 unit) and Tuwaiq Mountain Limestone. The sections were hung on top Tuwaiq Mountain Limestone (Middle – Early Jurassic unconformity).

3.5 Depositional models

The spatial distribution of the facies shown in sequential depositional models (T1 to T6) illustrate the evolution of the depositional systems in response to a third-order relative sea-level changes and possible short-lived and local tectonic events (Fig. 3.17 and 3.18). These depositional models are built using the sedimentological characteristics, Walther's Law and vertical facies successions in individual logs (e.g., Fig. 3.11, 3.12 and 3.13; Appendix 3.1, 3.2 and 3.3) but also the lateral organization of the facies given by the correlation established along a 280-600 km long transects (Fig. 3.15 and 3.16).

The depositional models of the Dhruma and Tuwaiq composite sequences (DCS and TCS) represent a continental to inner-platform shallow marine depositional settings with two depositional domains including a siliciclastic-prone proximal domain and a carbonate-prone distal domain. In the Dhruma sequence (DCS), the siliciclastic proximal domain consists of paleosols (F3), ferruginous oolite (F14) and wide shale-prone coastal plain (F4). During early and slow sea-level rise (T1), the platform was very flat and characterized by low-energy and limited fluvial dynamics with evaporites sabkhah (F11) and intertidal stromatolite (F12). This evolved dramatically to higher wave and fluvial-deltaic dynamic (T2) with wave reworking sandstones (F8) and delta front mouth bars (F10). The carbonates in distal domain were suppressed and instead calcareous shales (F15) were developed due the high-siliciclastic influx. This time was associated with a high accommodation space minimum 25 m water depth that accommodates large deltaic clinoforms (F10; Fig. 3.6B and 6C). A short-lived tectonic disruption is probably responsible for creating

the high accommodation space and the intense fluvial sediment supply. The following deposition models (T3 to T5) are characterized by flat-topped low-energy lagoonal carbonate with mainly microbes and foraminifera (F16 and F17) and thin dolomite beds (F13). In such flat inner-platform, higher-energy deposits are represented by sharp-based grainstones (F18) as a result of repeated marine transgressive events (cf. Wilson, 1975). The distal domain of the carbonate platform is characterized by shoal cross-bedded grainstones (F24) which correspond to highstand and maximum flooding on such low-energy inner-platform. The final stage of the Dhruma sequence (DCS) depositional evolution system (T6) is characterized by relatively high siliciclastic input in the proximal domain with distributary sandstone channels (F9), interdistributary *skolithos* sand flat (F7) and lagoonal shale (F15). The distal carbonate domain is poorly developed and characterized by argillaceous lime mudstone (F15) with extensive hardground/firmgrounds early-cemented surfaces. This low carbonate production is probably controlled by the overall restricted inner-platform condition and poorly oxygenated bottom water due to the fresh-water runoff.

In the Tuwaiq sequence (TCS), the siliciclastic proximal domain consists of two depositional systems, high fluvial dynamics (T1 and T3) and low fluvial dynamics (T2 and T4 to T6). The high-fluvial dynamics include conglomerates upstream flood plain (F1), braided sandstone channels (F2) and *skolithos* sand flat (F7). The distal domain of this depositional system consists of shale-prone lagoon and argillaceous lime mudstone (F15). The low fluvial dynamics includes paleosol shale and mudrock (F3) and sandstone-rich ferruginous oolite (F14). These are equivalent in the distal domain to well developed

carbonate lagoon with stromatoporoid/coral, microbial and high-diversity of foraminifera.

3.6 Sequence stratigraphy and stratigraphic evolution

Correlations between thirteen sedimentological sections in the Dhruma Formation and Tuwaiq Mountain Limestone result in a regional transects oriented in an oblique-dip direction. The transects are characterized at the base by the Late Toarcian − Aalenian unconformity marked by laterally continuous ferruginous oolite bed. The datum of these transects are top of main sequences boundaries that are most likely to be an exposure surfaces. The datum of the top Dhibi Limestone Member is a wide ravinement surface over an extensive traceable limestone unit. The top Dhruma sequence boundary datum corresponds to a minor disconformity marked by conglomerate beds and incised fluvial channel to the south and leached hardground in the middle of the transects and red shale to north. The most top datum of the transects is the Middle – Late Jurassic unconformity marked by extensive hardground surface which is overlain by broad argillaceous limestone of the Hanifa Formation. The apparent polarities of these transects is S-N indicated by the lateral facies changes in the shallow-marine environment.

The facies distribution along these regional transects attest that the Dhruma Formation and Tuwaiq Mountain Limestone comprise two composite sequences (DCS and TCS). Each in turn consists of five high-frequency sequences (HFS1 to HFS5). The first composite sequence (DCS) includes the Dhruma Formation except for upper-D6 and D7. The TCS includes Upper Dhruma Formation (upper-D6 and D7) and Tuwaiq Mountain Limestone.

The ages of the composite sequences is based on several specimens of ammonite and subordinate biostratigraphic markers include echinoderms, brachiopods, foraminifera and ostracods (Manivit et al., 1990). The age of DCS ranges from the Early Bajocian *discites* Zone to Early Bathonian *zigzag* Zone (Fig. 3.15). The lower TCS (HFS1) can be attributed to the Late Bathonian – Callovian based on microfauna, foraminifera and ostracods and nannoflora (Énay et al., 1987? Check Helen; Manivit et al., 1990). The rest of the TCS is dated Middle Callovian *coronatum* Zone based on ammonites (Fig. 3.16).

The CSs and HFS are wedge and thinning southward. The regional geometry of these continental to shallow marine deposits attests a clear differential subsidence along the transects. This differential subsidence appears rather homogeneous except during Early Bajocian *laeviuscula* and *humphriesianum* Zones and Early Bathonian *zigzag* Zone (HFS5) where a strong increase of the subsidence rate is recorded.

The main maximum marine transgression of the Middle Jurassic is near the top of the Tuwaiq sequence TCS, probably in the Middle Callovian *coronatum* zone. There are no evidence progradational stacking patterns or low-stand deposits. Slight fluvial incisions are associated with the Middle Bathonian hiatus that corresponds to probably less than 1 Myr long hiatus, whereas, the top Tuwaiq subaerial exposure and unconformity (probably more than 2 Myr long hiatus) does not exhibit any fluvial incisions, indicating the lack of any efficient fluvial system and probably a very flat topography at this time.

3.6.1 Dhruma Composite Sequence (DCS)

The DCS thins and wedges-out southward and ranges from 100 to 290 m thick. In the study area, it spans over 2 Myr (Fig. 3.19). The lower sequence boundary is the Late Toarcian − Aalenian unconformity on top of the Marrat Formation. The unconformity is marked by overlying ferruginous oolite (F14) that marks the initial transgression of the DCS.

The transgressive systems tract (TST), 60 to 225 m thick, consists of four high-frequency sequences (HFS1 to HFS4). The HFS1, Early Bajocian (*discites* and *laeviuscula* Zones), is an asymmetrical dominantly transgressive unit that thins and pinches out at the most southern section (K. Abu Al Jiwar). It has basal crinkly laminated evaporites (F11) and mudstone interbedded with shale deposits that grades updip to mottled bluish green shale (F4) and paleosol (F3). The prevailing depositional environment was very flat low energy intertidal to supratidal/mudflat with limited siliciclastic influx. During the late TST, siliciclastic influx increased marked by large-scale deltaic clinoforming sandstone (F10) (up to 25 m thick) (Fig. 3.6B, C and D). This deltaic sandstone is equivalent down dip to shale (F15) successions marked by an increase in gamma-ray log response (T2 in Fig. 3.17 and 3.20). During the HST, the deltaic clinoforming sandstone prograded westward and an erosional transgressive surface caps HFS1.

HFS2 (Early-Late Bajocian (*humphriesianum* and *niortense* Zones), is a symmetrical transgressive and regressive unit. It is marked at the base by fossiliferous calcareous shale (F15) interbedded with argillaceous nodular bioturbated wackestone/mudstone (F16). These grade updip to heterolithic silty sandstone (F5) and ferruginous oolite (F14). The cycles are slightly

retrograding and cleaning upward to lagoonal bioturbated peloidal wackestone/packstone (Dhibi Lst. Mb.). The lagoonal wackestone/packstone unit aggrades upward into lenticular oncoidal packstone/grainstone and rudstone and HFS2 is capped by erosional surface (Fig. 3.15).

The HFS1 and HFS2 equate to the lower Dhruma Formation (D1 and D2 units) that have been interpreted as two T-R cycles separated by a pre-Dhibi unconformity (Powers, 1968). Some studies interpreted the shale of HFS1 (D1 unit) with high gamma-ray response as the Bajocian MFS (Manivit et al., 1990; Le Nindre et al., 1990; MFS J20 of Sharland et al., 2001; MFS^3 12.3 of Al-Husseini, 2009). However, the Bajocian MFS is better placed in the Dhibi Lst Mb. of HFS2 in accordance with previous work of Powers (1986) and Fischer et al. (2001) as it shows continuous onlapping, widespread ammonite faunas and furthest extension of carbonates to the south.

HFS3 and HFS4 show slight retrogradation followed by aggradational stacking. They begin with dm-thick erosionally based storm dominated intraclastic grainstone (F18) and interbedded argillaceous nodular wackestone/mudstone (F16). They grade updip into ammonite rich heterolithic silty sandstone (F5) southward. The argillites and grainstone facies decrease upward during the TST of HFS4. Rather, bioturbated and low fossiliferous inner-lagoonal mudstone were developed with minor transgressive grainstone and restricted lagoonal red dolomite beds. These low-energy lagoonal mudstones are sharply overlain by high-energy channel form transgressive grainstone (F18) followed by back-barrier washover swaley and hummocky stratified grainstone and trough cross-bedded coated-grain grainstone shoal (F24) (Fig. 3.13 and 3.14). These high-energy facies and the updip extensive

low-energy lagoonal mudstone (F16 and F17) mark the MFS of the Dhruma composite sequence DCS.

The HST of the DCS, consists of the upper part of HFS4 and all HFS5, is 30 to 60 m thick and thins out southward. The HST shows an increasing vertical proportion of the shale and argillaceous mudstone facies. These facies are prograding northward and are equivalent updip to *Skolithos* plane laminated sandstone flat and coarse-grained distributary sandstone channels. The argillaceous mudstone are characterized by abundant *Chondrites* burrows which are combined with restricted faunas (Manivit et al., 1990). The higher-order parasequences of the HST are commonly capped by correlative hardground surfaces that probably formed as a result of the low carbonate production in response to the high siliciclastic influx.

The HFS3 and HFS4 represent (Dhruma Formation D3 and D4 units) and the HFS5 is equivalent to D5 and lower half of D6 unit. The MFS of the Middle Dhruma was placed previously in D5 unit (*zigzag* Zone), probably because of the high-shale content and restricted fauna (Le Nindre et al., 1990; MFS J30 of Sharland et al., 2001; MFS^3 12.4 of Al-Husseini 2009; Énay et al., 2009). The upward increase of the shale or gamma-ray signal is not a sign of deepening in such shallow flat inner-platform setting, but rather would be indicator of a regression and siliciclastic progradation. The MFS is in HFS4 within the regionally extensive limestone with ammonite extending far updip (Fig. 3.15). The top sequence boundary is the Middle Bathonian unconformity that marked by incised fluvial channel (Fig. 3.15 and 19).

3.6.2 Tuwaiq Composite Sequence (TCS)

The Tuwaiq composite sequence ranges from 150 to 320 m thick wedging and thinning southward (Fig. 3.16). In the study area, it spans ~ 2.6 Myr (Fig. 3.19). The sequence is asymmetrical in which the TST is 120 to 270 m thick and the HST is 30 to 50 m thick. The basal sequence boundary is the Middle Bathonian unconformity.

The TST of the composite sequence consists of four high-frequency sequences (HFS1-HFS4). The initial transgression is characterized by high-siliciclastic influx marked by backstepping braided fluvial channel deposits (F2; medium grained sandstone) with southeast-directed paleocurrent indicators, almost 20 m thick cycles (Fig. 3.4D and 3.14). Downdip these braided channels deposits pass into heterolithic quartzose ferruginous oolite (F14) thin grainstone (F18), calcareous shale (F15), and *Chondrites*-rich argillaceous nodular mudstone/wackestone (F16).

The early TST of the TCS (HFS1 Atash Mb.) is marked by cross-bedded ooid grainstone (F19) with large 3D megaripples interbedded with the calcareous shale (F15) followed by deposition of biostromal limestones with coral/stromatoporoids (F21). The mid TST (HFS2 and lower HFS3) is dominated by widespread shale deposition (F15) fed by backstepping fluvial successions. The HFS2 represents the upper Dhruma Formation (D7 units) Hisyan Member. Consistently with this study, the upper Dhruma Formation was considered as genetically related to the Tuwaiq Mountain Limestone (Sequence 3 of Le Nindre et al., 1990; Hughes, 2004, 2009; Énay et al., 2009). Other interpretation based on subsurface correlations suggested unconformity separating the Dhruma and Tuwaiq Mountain Limestone (i.e.,

between HFS2 and HFS3) (Powers, 1968; sequence DS[3] 12.5 of Al-Husseini, 2009). However, the successions show continuation of the overall transgression trend and fluvial backstepping. The late TST (upper HFS3, HFS4) is marked by relatively low-energy widespread muddy carbonates (F16), heterolithic quartzose ferruginous oolite (F14), thin storm grainstones (F18) and local thin oncoidal grainstone (F20) at the upper HFS4 (Fig. 3.16). The MFS, within the upper part of HFS4 or lower part of HFS5, is associated with the widespread muddy carbonate (F17, F21, F22) onlapping backstepping fluvial siliciclastic to the south. Consistently with our result, the upper Tuwaiq Mountain Limestones are considered as an open-marine transgression event based on lithostratigraphic and biostratigraphic outcrop correlations (Le Nindre et al., 1990; Manivit et al., 1990; Le Nindre and Davies in Kadar et al., 2015). However, conversely, other studies placed the Middle Callovian MFS in the shale of the Hisyan Member (HFS2) based on biostratigraphic evidences and regional correlation (MFS J40 of Sharland et al., 2001; Énay et al., 2009).

The HST of the Tuwaiq composite sequence (TCS) corresponds to the HST of HFS5, which makes up the bulk of HFS5. Updip, the HST is characterized by open marine back-barrier muddy carbonates (F17). These pass slightly downdip into thin grainstone-muddy carbonate parasequences. Further downdip, the HST consists of aggrading reefal facies (F23) (Huraymila section) and local coral/stromatoporoid bioherms (F22) (K. Al-Qaddiyah). The HST lacks siliciclastics and thus has a cleaning-up gamma-ray trend (Fig. 3.18). This resulted from widespread backstepping of the

siliciclastic during the TST that pushed the shoreline far landward after which the siliciclastic remained far updip throughout the HST.

The top sequence boundary of the Tuwaiq composite sequence (TCS) is an unconformity within the Late Callovian (*lamberti* Zone) and Early Oxfordian (*mariae* Zone). The sequence boundary is marked by regionally extensive stained hardground surface with a distinctive positive gamma-ray spike (Fig. 3.18). The sequence boundary is overlain by argillaceous limestone deposits of the Hanifa Formation, dated Early to Middle Oxfordian (*cordatum* to base *plicatilis* Zone) (Manivit et al., 1990).

3.7 Discussion

3.7.1 Inner-platform development

The Middle Jurassic Arabian Platform was a tectonically stable passive margin which underwnet evident differential subsidence with low accumulation rate (*i.e.,* average of 8-10 cm/kyr). The Middle Jurassic outcrops are in inner part of a very flat and wide epeiric platform (> 1000 km) with low-energy shallow-marine mixed carbonate-siliciclastic systems. The low rate of accommodation space was filled and balanced by the siliciclastic supply and carbonate production that resulted in a very flat-topped platform as attested by the stratigraphic transects (Fig.15, 16 and 20). The very flat depositional profile is also indicated by the large area of evaporites sabkhah and intertidal stromatolites at base of the Dhruma sequence (HFS1), the extensive lagoonal carbonates with lateral continuous dolomite beds (HFS2 and HFS3 of DCS) and the extensive coral/stromatoporoid bearing platform (HFS5 of the Tuwaiq sequence TCS). The lack of evidence of major channel incisions or channel

progradation during relative sea-level fall can be also considered as a consequence of the very low gradient slope. This flat-topped profile is mainly related to overall geodynamic of the inner part of wide epeiric platform and stable tectonic context. The very broad shallow water, in such epeiric seas, can damp out tidal and wave energy that leads for predominant mud-dominated coastal and shoreline deposition systems (*cf.* Enos, 1983).

The siliciclastic depositional environments, continental and delta systems, are characterized by relatively high fluvial dynamics and sediment influx. The Dhruma sequence (DCS) is marked at the base by large deltaic clinoforming sandstones and by incursion of distributary sandstone channels at top of the Dhruma sequence. This is overlain by post unconformity conglomerates and braided sandstone channels of the base Tuwaiq sequence (TCS). Short-lived tectonic disruptions are probably the main control of these abrupt invasions of sandstone in overall mud-dominated successions. These short-lived tectonic disruptions are demonstrated by high-wedging geometries and evident thinning in proximal areas with dominant paleosols suggesting uplifted areas (HFS1, HFS5 of DCS; HFS1, HFS2 of TCS). The direction of the sandstone influx is probably coming from the west (shield) as shown by the direction of the deltaic clinoforming (Fig. 3.6B, C and D) and paleocurrent direction of Tuwaiq fluvial channels.

The carbonate platforms of the outcropping Middle Jurassic show consistent flat tabular aggrading units and almost maintained constant thickness and characterized by low-energy shallow-marine mud-dominated facies. Two-carbonate platform depositional systems can be distinguished in the successions, which are restricted carbonate platforms with microbes and

low-faunal diversity (HFS2, HFS4 of DCS) and open-marine carbonate platforms with stromatoporoid/coral bearing and high-faunal diversity (HFS5 of TCS). This long-term and gradational platform evolution from restricted to open marine conditions probably resulted from the excessive platform width that prevents sufficient water circulation (cf. Enos, 1983) in the Dhruma platforms, whereas, the Tuwaiq reef bearing platform are adjacent to deep intrashelf basin that provides relative normal water circulations (Fig. 3.20). Moreover, the lack of reefs and the dominated algae carbonate producers in the Dhruma platforms is probably related to nutrient and trophication gradients and supplies (cf. Fig 9 of Hallock, 2001). The Dhruma carbonate platforms seems to be affected by high rate of nutrients and trophication supplies as the carbonate of HFS1 and lower HFS4 grades updip to shale facies. This could lead for oxygen limitations in the water, which explain also the low faunal diversities in the Dhruma carbonate platforms. In addition, the long-term sea-level raise has significant influence on the Middle Jurassic carbonate platform evolution.

3.7.2 Controlling factors on the evolution of the Arabian Platform

3.7.2.1 Tectonic and subsidence

The Early Jurassic (Early to Middle Toarcian) Marrat composite sequences (Al-Mojel et al., in prep.) and the Middle Jurassic Dhruma and Tuwaiq composite sequences are considered as part of a second-order tectono-eustatic cycle bounded at the base and top by major unconformities. These composite sequences have a common depocenter, in which differential subsidence increased toward north-northeast. Moreover, they show long-term

coastal onlap and marine transgression that reached its maximum extent during the Tuwaiq Mountain Limestone deposition (MFS of TCS). The top unconformity is marked by a significant change in the basin configuration and shift in the depocenter axes of the overlying Late Jurassic (Oxfordian) which suggest a time of tectonic tilting and basin inversion (Al-Mojel et al., in prep.) This Early to Middle Jurassic tectonic cycle could be correlated to the first second-order tectonic event (Late Triassic to late Middle Jurassic) of the Western Atlantic continental margin (Vail et al., 1991; Fig. 3.10).

The subsidence progressively increased from 3.9 to 11 cm/kyr (at Khashm. Ad Dhibi) during this second-order tectonic cycle and reached its maximum rate in the Callovian Tuwaiq Mountain deposition (Le Nindre et al., 2003). This increased subsidence during the later Middle Jurassic is consistent with overall subsidence patterns of the eastern margins of Africa (Dingle, 1982). Moreover, the Callovian maximum subsidence rates were noticed in the Western Tethyan, western France platform at Argentan and Caen (Andrieu et al., 2016). This would imply that the subsidence was controlled by thermal expansion and contraction mechanisms in which the Early Jurassic was probably a time of stretching and rifting (Sharland et al., 2001; Al-Mojel et al., in prep.) followed by cooling subsidence during the Middle Jurassic.

The southern part of the study area (south of 22° N) subsided slowly and was dominated by continental deposits (paleosols and fluvial channels) and shallow marine siliciclastics. The carbonate facies were rarely developed in these slowly subsiding areas. The carbonate deposits are well developed in the northern most subsiding area (K. Ad Dhibi and K. Al-Qaddiyah), which

likely required higher accommodation space. Moreover, these northern depocenter areas lacks continental and nearshore siliciclastic sands deposits. This would suggest that the lateral facies changes were influenced by the differential subsidence perhaps controlled by basement faulting (Le Nindre et al., 2003), which influenced accommodation space. The Ar Rayn Terrane (approximately between 24° N to 25° 20’ N) and the Najd Fault System (21° 40’ N) are considered the main structure elements controlling the differential subsidence in the outcropping study area (Al-Mojel et al., in prep.).

Local and short-lived tectonic events influenced the facies, depositional environments and some of the systems tracts. The Early Bajocian (*laeviuscula* Zone), HFS1 in the Dhruma cross-section (Fig. 3.15), shows strong wedging geometry which indicates for an abrupt and high differential subsidence responsible for creating at least 25 m accommodation space, deltaic progradation (Fig. 3.6B and C) and exposed uplifted area (F. Al Ahmar). In the subsurface, this tectonic disruption could have triggered the significant thickness variations (average of 60-120 m and maximum ~700 m) observed in D1 unit at Jauf and Safaniya areas and caused the pre-Dhibi erosional unconformity on top of D1 unit (Powers, 1968). Moreover, The highstand systems tract of the Dhruma composite sequence (Early Bathonian *zigzag* Zone) was probably influenced by local and short-lived tectonic instability (uplift or slow subsidence) synchronous with abrupt siliciclastic incursion, progradation and unconformity development.

	Age	Arabian Platform relative sea-Level changes (Haq and Al-Qahtani, 2005) (m)	High-frequency sequences (4th order)	Siliciclastic influx and Carbonate Productivity	Inner platform stratigraphic architecture	Stacking pattern	Reservoir prediction	Time
Tectonically and eustatically induced unconformity								
Middle Bathonian		20		Very high/ poisoned carbonate			Non-marine (fluvial braided channel)/ ? delta	T7
eBath	aurigerus Zone	70	HFS 5	Medium influx/partly poisoned carbonate	Wedge geometry	Progradation	Distributary channel (2 m thick) sandstone /inner platform storm grainstone (2 m thick)	T6
lBaj	*garantiana* and *zigzag* Zone	80	HFS 3 and 4	Weak influx/ high carbonate production	Flate tabular bedding, regionally extended carbonate beds	Aggradation	Outer platform, carbonate grainstone shoals and barrier complex, (Faridah Reservoir equivalent, Toland et al., 2013)	T5
	niortense Zone	80	HFS 2					T4
mBaj	*humphriesianum* Zone	65		Moderate influx/ low carbonate production	Flate tabular bedding	Retrogradation	None	T3
eBaj	*laeviuscula* Zone	45	HFS 1	Very high influx /poisoned carbonate	Clinoform (up to 25°)	Retrogradation (onlapping) and limited progradation	Nearshore deltaic sandstone, up to 25 m thick, narrow facies belt	T2
	discites Zone	30		Weak influx/ low carbonate production	Flate tabular bedding	Retrogradation (onlapping)	? Outer platform carbonate	T1
Late Toarcian to Aalenian		0				Eustatically induced unconformity		T0

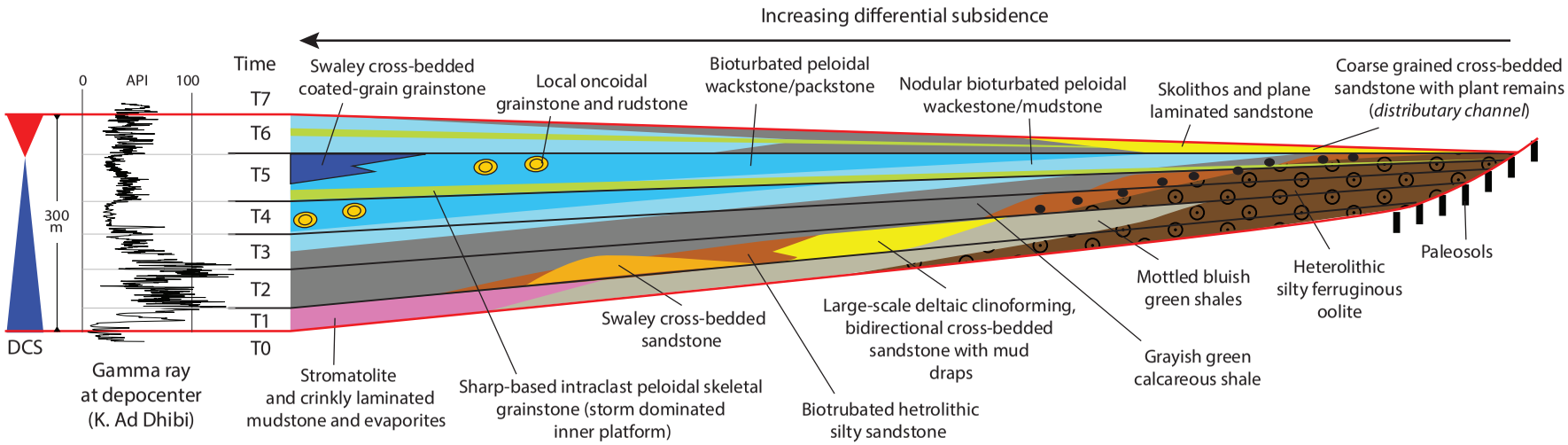

Figure 3.17: Depositional sequence model of the Dhruma composite sequence (DCS). The above table shows a brief description of the depositional models through time (T0 to T7). The gamma ray is from shallow cores (DHIBI-1, HMNK-1, and MRZU-2) at the Khashm Ad Dhibi. The vertical gamma ray depth was slightly rescaled to fit the depositional models.

Age	Arabian Platform relative sea-Level changes (Haq and Al-Qahtani, 2005) (m)	High-frequency sequences (4th order)	Siliciclastic influx and Carbonate Productivity	Inner platform stratigraphic architecture	Stacking pattern	Reservoir prediction	Time
Tectonically and eustatically induced unconformity Late Callovian (*lamberti* Zone) and Early Oxfordian (*mariae* Zone)	48						T7
Middle Callovian (*coronatum* Zone)	85	HFS 5	No siliciclastic influx/ optimum carbonate production	Flate tabular bedding, bioherms	Retrogradation to aggradation	Outer platform peloidal lagoonal wackestone/ reef framestone (Hadriyah Reservoir equivalent, Toland et al., 2013)	T6
	80	HFS 4	Weak siliciclastic influx/ high carbonate production	Flate tabular bedding	Retrogradation to aggradation	Bioturbated peloidal lagoonal wackestone (? Upper Fadhili Reservoir equivalent)	T5
	75	HFS 3	High siliciclastic influx/ low carbonate production	Wedge geometry	Onlapping storm generated grainstone	None	T4
Late Bathonian to Early Callovian	60	HFS 2	Very high siliciclastic influx/ poisoned carbonate	? Clinoform delta, flate tabular shale	Retrogradation	Non-marine (fluvial braided channel)/ ? delta	T3
	30	HFS 1	Very weak	Tabular, regionally extended carbonate	Onlapping shoreface grainstone (3m thick), aggrading lagoon	Bioturbated peloidal lagoonal wackestone (Lower Fadhili Reservoir equivalent, Toland et al., 2013)	T2
	10		Very high siliciclastic influx/ poisoned carbonate	Tabular, regionally extended shale	Aggradation	Non-marine (fluvial braided channel)/ ? delta	T1
Tectonically and eustatically induced unconformity Middle Bathonian	0	Abundant vegetation and petrified trunks					T0

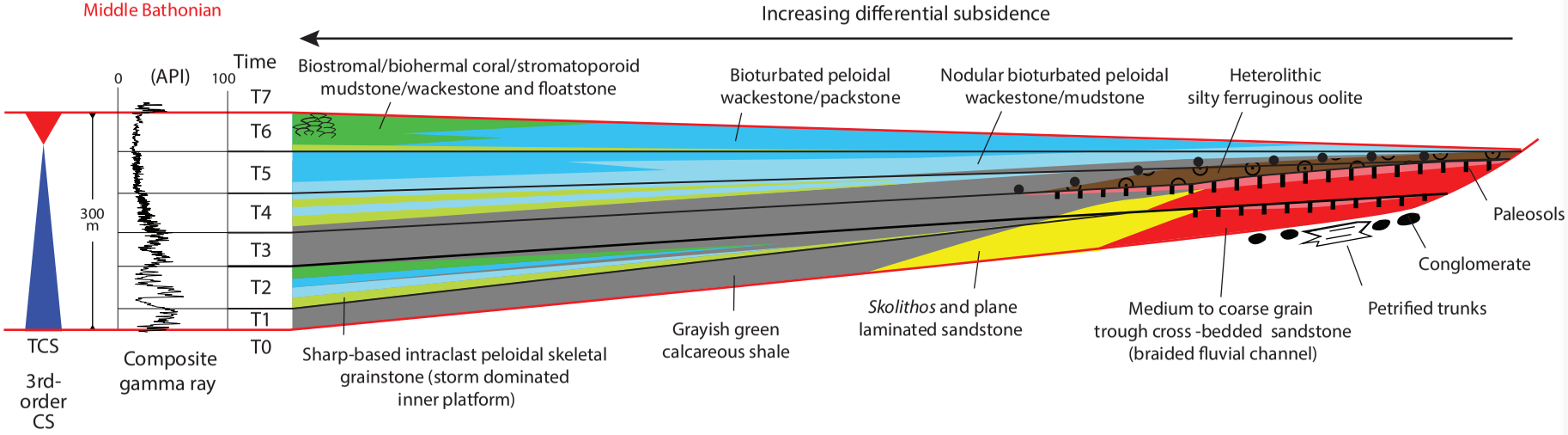

Figure 3.18: Depositional sequence model of the Tuwaiq composite sequence (TCS). The above table shows a brief description of the depositional models through time (T0 to T7). The gamma ray is a composite log combined from shallow core (MQBL-1) at the Khashm Ad Dhibi and shallow well (TLHH-1) in Wadi Birk. The vertical gamma ray depth was rescaled to fit the depositional models.

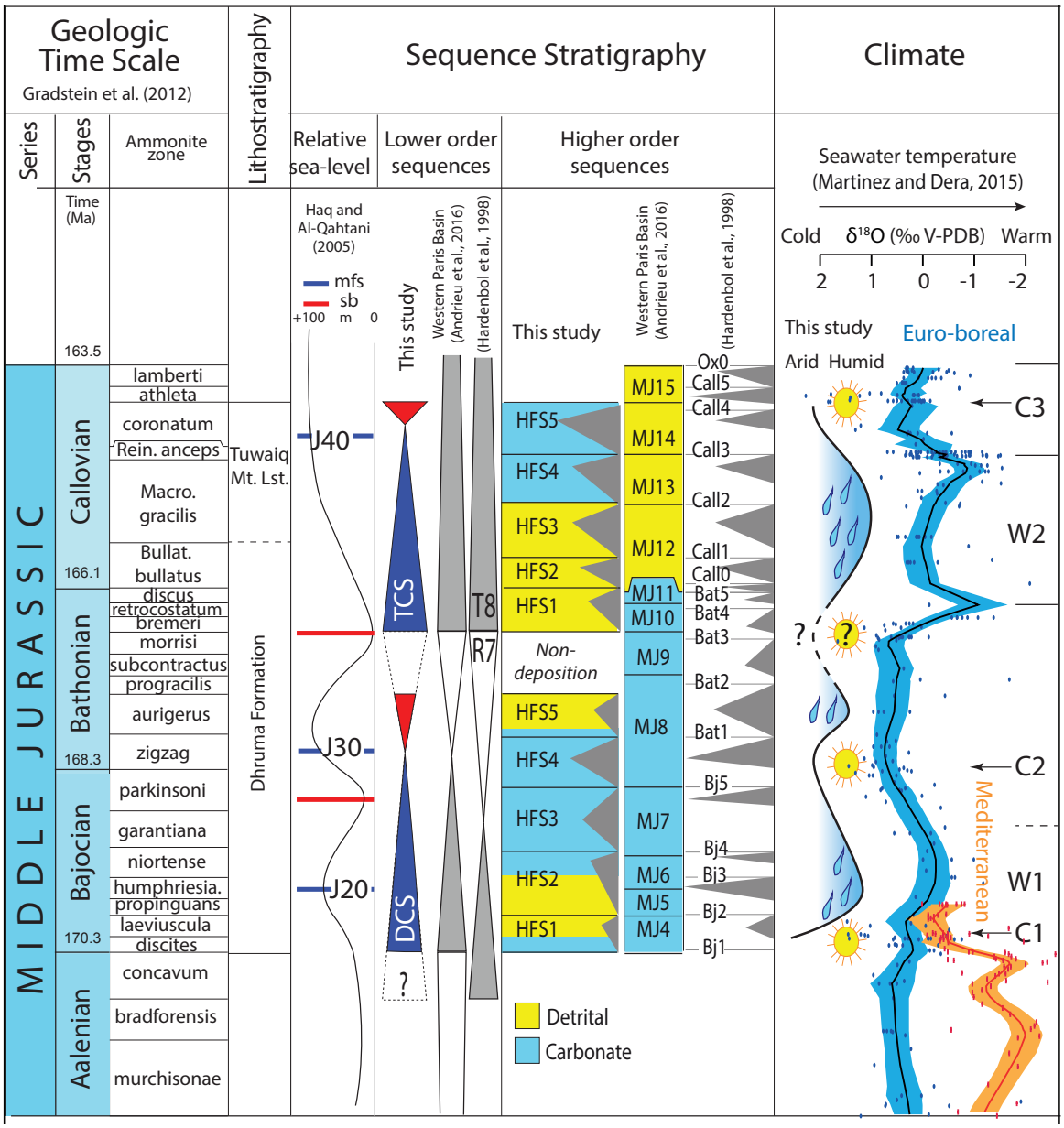

Figure 3.19: Middle Jurassic geological history shows sequence stratigraphy of the Arabian Platform compared with the European domain supplemented with climatic data and interpretation.

3.7.2.2 Eustatic and orbital controls

The 3rd-order and, to a lesser extent, 4th-order eustasy cycles seem to have been the main driving factors generating the Middle Jurassic sequences. The base sequence boundary of the Middle Jurassic sequences corresponds to a regional hiatus (Late Toarcian to Aalenian) over the Arabian Platform and it is most likely resulted from substantial eustatic sea-level fall with about 50 m as proposed by Al-Husseini (1997) (Le Nindre et al., 1990; Haq and Al-Qahtani, 2005). An eustatic origin of this unconformity is adopted herein as the successions of the Middle Jurassic show extensive quite conformable parallel surfaces and lack of deformation between the Early and Middle Jurassic (Al-Mojel et al., in prep.). The long-term flooding event of the Dhruma sequence (DCS) from the Early Bajocian to the Early Bathonian is coherent with the eustatic trends recorded in the Mediterranean domain (Hardenbol et al. 1998). But, there is subordinate sea-level fall and a short emersion momentarily interrupted this trend in the transition of *niortense* and *garantiana* Zones marked by scouring ravinement surfaces. Moreover it confirms the occurrence of partial emersions along the southwestern parts of the Arabian Platform in the mid Bajocian (Haq and Al- Qahtani 2015). A similar regressive sequence named R7' was also identified in the European domain (Hardenbol et al. 1998), but it occurred 0.5 Myr earlier – within the *niortense* Zone – and spanned until the end of the *garantiana* Zone. The MFS of DCS (Early Bathonian *zigzag* Zone) correlate well with the depositional sequences of the Western Paris Basin defined by Andrieu et al. (2016) (Fig. 3.19). In addition, consistently, the Early Bathonian *zigzag* Zone marks relative sea level rise in the northern Switzerland (Gonzalez, 1996). Regionally, the highstand of DCS

and the associated fluvial incursion and hiatus (Middle Bathonian) have a regional significance throughout the Arabian Plate and the northern margin of the Arabian-Nubian Shield (Al-Husseini and Matthews, 2006; Énay et al., 2009). Continental and marginal marine siliciclastic deposits were dominated in the northern Arabian-Nubian craton during Early-Middle Bathonian a time of assumed low sea-levels (cf. Fig 8 in Énay et al., 2009). However, this sequence boundary has not been identified in the interior of Oman by Rousseau et al. (2006). Globally, the Early Bathonian sea level highstand and the strong sea-level fall are in concordance with progradational patterns of MJ9 and MJ10 sequences of Andrieu et al. (2016) and the maximum regression of the standard European sequences Bt2, Bt3 and Bt4 from Hardenbol et al. (1998). Moreover, this highstand trend corresponds, as well, to those of the Russian Platform and South America basins (Sahagian et al., 1996; Hallam, 2001; Simmons et al., 2007), which suggest that this Early Bathonian highstand was of eustatic origin.

The overall transgressive trend of the Tuwaiq composite sequence (TCS) is in concordance with the Late Bathonian and Early Callovian stepwise transgression of Greenland and Europe as well as Himalayas and Pakistan regions (Hallam, 2001). In this study, the main MFS of the Middle Jurassic succession is within the Tuwaiq Mountain Limestone deposition (MFS of TCS) Middle Callovian (*coronatum* Zone) (Fig. 3.19). Consistently, the Middle Callovian marks the interval of the highest sea-level rise in a global scale during the Middle Jurassic (Hallam, 1988; Surlyk, 1990, 1991; Hallam, 2001). Moreover, Surlyk (1990) confirmed that Middle Callovian (*coronatum* Zone) is a period of maximum rate of sea-level rise in the East Greenland

embayments. Locally, however, the Arabian Platform Middle Jurassic 2nd-order MFS were placed in the Dhruma Formation (Early Bajocian *laeviuscula* Zone) (MFS J20 of Sharland et al., 2001). This may be because of an extensive regional high gamma-ray correlation correspond to the Dhruma shale deposits associated with demise of carbonate-production. Moreover, Rousseau et al., (2006) considered the Bajocian (*parkinsoni* Zone) as a 2nd-order maximum marine transgression in the interior of Oman. Nevertheless, the 2nd-order Middle Jurassic MFS should be placed higher in the Tuwaiq Limestone deposits as it shows further marine extension over continental deposits that represent the westernmost preserved onlap part of the Arabian Platform. The top sequence boundary of the TCS corresponds probably to the Middle-Late Jurassic global-scale sea-level fall that reaches its maximum during Late Callovian (Hallam, 1988; Dromart et al., 2003a, 2003b).

In details, the high-frequency sequences (HFS) of the Middle Jurassic are well developed and appear to be regionally correlative for hundreds of kilometers over the central Arabian Platform (Fig. 3.15, 3.16 and 3.20). Interestingly, the high-frequency sequences are compatible with the Tethyan higher order sequences of Hardenbol et al. (1998) and Andrieu et al. (2016) (Fig. 3.19), which provide a strong evidence for eustatic origin of these sequences. HFS1 to HFS5 of DCS correspond to MJ4 to MJ8 of the Western Paris Basin (Andrieu et al., 2016) and to Bj1 to Bat2 of the standard European cycles (Hardenbol et al., 1998). HFS1 to HFS5 of TCS are equivalent to MJ10 to MJ14 of the Western Paris Basin (Andrieu et al., 2016) and to Bat3 to Call4 of the standard European cycles (Hardenbol et al., 1998). According to the absolute age of Gradstein et al. (2012) (Fig. 3.19), the duration of the

composite sequences (DCS and TCS) and the superimposed high-frequency sequences can roughly be considered as 2.4 Myr and 400 kyr cycles. As these duration coincide with long-term modulations of orbital eccentricity parameters, it is likely that the Middle Jurassic sea-levels changes were paced by global satroclimatic cycles (Boulila et al., 2011; Martinez and Dera 2016; Ikeda et al., 2016), either playing on glacio-eustasy or aquifer-eustasy (Sames et al., 2015, Wendler and Wendler, 2015).

4.7.2.3 Climatic and trophic influences

Irregular climatic deteriorations have been recorded during the Middle Jurassic based on isotopic paleothermometry, faunal evolution and migrations, and/or sedimentological data mainly from subtropical European domains (Bartolini et al., 1999; Price, 1999; Rey and Delgado, 2002; Jenkyns et al., 2002; Morettini et al., 2002; Dromart et al., 2003a, 2003b; O'Dogherty et al., 2006; Dera et al., 2011; Martinez and Dera, 2015; Korte et al., 2015). Here our high-resolution study details for the first time the evolution of these paleoclimatic changes and consequences in an paleoequatorial domain.

From current oxygen isotope data from Euro-boreal domains, the first half of the Middle Jurassic (Aalenian to middle Bathonian) is generally considered as the coolest interval of the Jurassic, alternating between periods of incipient polar ice sheet developments and short-lived warming episodes (Dera et al., 2011; Korte et al., 2015) (Fig. 3.19). As revealed by clay mineral assemblages, these temperature variations were associated with humidity fluctuations oscillating between semi-arid climates interrupted by seasonal monsoon episodes during cool intervals, and everwet conditions during warmer episods (Brigaud et al. 2009; Martinez and Dera, 2015; Andrieu et al.,

2016). On the Arabian Platform, the evolution of sedimentary facies is in total agreement with these trends. The Early Bajocian (HFS1; *discites* and *laeviuscula* Zones) showed a dramatic climate change from arid shoreline with evaporite and stromatolite (*discites* Zone) to wetter conditions marked by high-siliciclastic influx in a deltaic system (*laeviuscula* Zone). This first arid period is more likely corresponds to the waning phase of the cooler Aalenian time. The humid high-siliciclastic input would correspond to a rapid seawater temperature increase computed from oxygen isotopes (W1 in Fig. 3.19) (Brigaud et al., 2009). This warm-humid event and associating high riverine siliciclastic influx and high eutrophication level, is probably the reason for the widespread carbonate-production crisis on the Arabian Platform. It also corresponds to the highstand of HFS1 (Fig. 3.15) marked by high gamma-ray response (Fig. 3.17 and 3.20) known as the “Dhruma Shale” (Al-Husseini and Matthews, 2008). The low carbonate production extended up to the *humphriesianum* Zone, which was marked by shale deposits with biosiliceous sponge-rich marker beds (early TST of HFS2; Fig. 3.15). The Early Bajocian carbonate production declined probably synchronously with other Tethys domains characterized by: 1) a major carbonate production crisis as well as marine faunal turnovers in northern Tethys (O’Dogherty et al. 2006), 2) condensed interval composed of glauconitic limestone in the western France platform (MJ5 and MJ6 sequences of Andrieu et al., 2016), 3) interbasinal biosiliceous sedimentation associated with positive carbon excursion in southern western Tethys (Bartolini et al., 1996; Muttoni et al., 2005; O’Dogherty et al., 2006). Current theories generally advocate global rises of productivity levels coupled to eutrophication processes because of a global

rise of $\delta^{13}C$ values (cf. Bartolini et al., 1999; Al-Mojel et al., in prep.) was synchronous to a radiation of coccolithophoridae and widespread chert radiolarian deposits in western Tethys (Suchéras-Marx et al., 2012; 2015; Baumgartner, 2013; Aguado et al., 2017). For a majority, this global fertilization of oceans was a remote consequence of volcanic and hydrothermal events associated with the initiation of the Pacific plate growth and the mid-Atlantic Ocean opening (Bartolini and Larson, 2001). Repeated CO_2 releases would have promoted warmer and more humid conditions (attested by $\delta^{18}O$ data, Brigaud et al. 2008), which intensified continental weathering rates and nutrient supplies to oceans in the Early Bajocian (Bartolini et al. 1999; Morettini et al. 2002).

This event is followed by a progressive carbonate recovery (upper HFS2; Late Bajocian to Early Bathonian *niortense* to *zigzag* Zones) controlled by stepping back of the siliciclastic sources (Fig. 3.15), and coupled with drying of the climate evidenced in the study area by thin beds of red dolomite with silicified anhydrite nodules. The expansion of the carbonate production in the Central Arabia during the Bajocian-Bathonian is consistent with the western Tethys epicontinental carbonates growth of MJ7 to MJ9 sequences of Andrieu et al. (2016). The semi-arid climate corresponds probably to long-term cooling throughout the Bajocian − Early Bathonian interval (C2 in Fig. 3.19) (Price, 1999; Martinez and Dera, 2015).

The Late Bathonian and Early Callovian sequences (HFS1, HFS2 and HFS3 of TCS) are dominated by petrified trunks, overlying high fluvial siliciclastic discharges and shale prone deposits indicating that a humid period prevailed. This could relate to a dominant long term warming periods (W2 in

Fig. 3.19). This warm-humid period is probably synchronous with the Early Callovian abrupt carbonate demise in the Paris Basin (Jacquin et al., 1992, 1998; Jacquin and de Graciansky, 1998; Brigaud et al., 2014) as well as with clay rich deposits of sequence MJ12 (Fig. 3.19) in the Western Paris Basin (Andrieu et al., 2016). Then, this low carbonate production period was followed by a growth of carbonate platform during Middle Callovian (HFS4 and HFS5 of TCS) as a result of widespread backstepping of deltas coupled perhaps with drying. This drying could result from an extreme cooling of seawater (C3 in Fig. 3.19) possibly associated with incipient continental ice build-up at the end of the Late Callovian (*athleta* Zone) (Dromart et al., 2003a, 2003b). The maximum of cooling is likely to have happened during the Late Callovian (*lamberti* Zone) associated with global glacio-eustasy sea-level fall (Dromart et al., 2003a, 2003b; Donnadieu et al., 2011; Pellenard et al., 2014).

3.7.3 Biofacies and sequence stratigraphy

The Jurassic biofacies (benthic foraminifera and associated micro- and macrofossils) of the Arabian Platform provide valuable indication for paleoenvironmental changes as they show systematic vertical tiered patterns (Hughes 1996, 2004, 2009, 2013; Hughes et al., 2008, 2009). However, previous studies only ascribed this evolution to paleobathymetric gradients, which mislead the sequence stratigraphic interpretations, especially where system tracts and facies migration are concerned. Moreover, some higher resolution biofacies cycles were over-interpreted as high-frequency forced regressions (Hughes, 2004). Recognizing forced regressions require sedimentological and stratigraphic geometric criteria (cf. Posamentier and

Morris, 2000) that have not been shown in these previous microfacies and biofacies studies.

Integrating the sequence stratigraphic framework of this study with detailed semi-quantitative micropaleontological analysis of the outcrop cores (Appendix 3.1, 3.2, 3.3; Hughes, 2013, 2014; unpublished reports) allows reappraisal of the depositional environmental preferences and stratigraphic position of main biocomponents and biofacies associations. The most interesting result of this study is that, for the first time, the stratigraphic framework provides shoreline and continental settings as a reference to reassess relative paleobathymetry, shallow or deep indications of the main biofacies associations. Moreover, the Tuwaiq Mountain Limestone (cf. Appendix 3.3) has the most faunal diversity, which would provide insight into biofacies interpretations of other Jurassic formations. The association of certain benthic foraminifera (*Lenticulina* spp. and nodosariids) and sponge spicules have been interpreted to form in the deepest depositional environment of the Middle and upper Jurassic formations (Hughes, 2004). This is probably because these biocomponents are found in mud-dominated successions with poor fauna, limited carbonate production, suboxic condition and high gamma-ray intervals. However, this work shows clearly that these biocomponents are found in a proximal inner-platform setting downdip of high-siliciclastic influx and fluvial deposits in Tuwaiq composite sequence (HFS3 and HFS4; Appendix 3.3). The *Lenticulina* spp. and nodosariids decrease upward toward the main maximum marine transgression of the Middle Jurassic (MFS of TCS). In addition, *Lenticulina* spp. and nodosariids are found in intertidal mixed carbonate-siliciclastic succession with stromatolite

and crinkly laminated lime-mudstone in base Dhruma composite sequence (HFS1; Appendix 3.1) and disappear in the highly bioturbated well-oxygenated Dhibi Lst Mb., the maximum marine transgression of HFS1. Moreover, Olivier et al. (2015) found *Lenticulina* spp. with *Nautiloculina* species and rare foraminifera in tidal flat with dinosaur tracks, mudcracks and fenestrae in the NW Tethys margin during Late Oxfordian early Kimmeridgian. Sponge spicules are well represented in highly bioturbated well-oxygenated lagoonal lime-mudstone and wackestone and associated with branched stromatoporoids in HST of Tuwaiq composite sequence (Appendix 3.3). The high concentration of the sponge spicules, in the Dhruma Formation and Lower Fadhili Reservoir, is considered to be localized in deepest part of lagoon during period of sea-level rise and surrounding by shallow shoal of branched stromatoporoids (Hughes, 2004, 2009). However, it seems unlikely to have such bathymetric gradient and clinoform-like depositional profile in homogeneous aggradational shallow marine subhorizontal platform during Lower Fadhili Reservoir of the Dhruma Formation (cf. Al-Mojel, 2010) and the outcropping Tuwaiq composite sequence.

The benthic foraminifera Kurnubia and *Nautiloculina* species have previously been interpreted to dwell in moderately deep shelf conditions, below fair-weather wave base (Hughes, 2009). These biocomponents, however, show consistent presence along the core samples of the Tuwaiq composite sequence, late TST and HST (MQBL-1; Appendix 3.3). They are found in different depositional conditions from proximal inner-platform setting in relatively low oxygenated bottom waters marked by argillaceous lime-mudstones rich with Chondrites burrows (base HFS3) to well circulated, well-

oxygenated offshore lagoon with high foraminiferal species diversity and local oncoids (MFS of HFS4) and branched stromatoporoids and build-ups (MFS and HST of HFS5 and TCS). Therefore, it is doubtful that the Kurnubia and *Nautiloculina* species indicate deep shelf conditions. Moreover, referring to the fair-weather wave base in such mud-dominated low-energy inner-platform and shorelines would be meaningless as most of the successions are below the waves except for short-lived storm events.

In such inner-platform mixed carbonate-siliciclastic settings, early transgressions would be characterized by poor fauna and limited species diversity probably due to the proximality to freshwater runoff from the hinterland that caused water stratification and prevented vertical circulation of oxygen (early TST of DCS and TCS; Appendix 3.1, 3.2). Whereas, the maximum marine transgression accompanying normal-marine conditions and optimum carbonate production would always present the highest species diversity (e.g., MFS TCS; Appendix 3.3). This Middle Jurassic highest species diversity interval synchronous with the first development of deep intrashelf basin with probable source rock in the near subsurface (Fig. 3.20). It is concluded that biofacies analysis and interpretation are better testified in the context of regional sedimentological characteristics and sequence stratigraphic frameworks. This integration would possibly allow regional sequence stratigraphic correlation and mapping demonstrated by independent biostratigraphic techniques in non-cored wells.

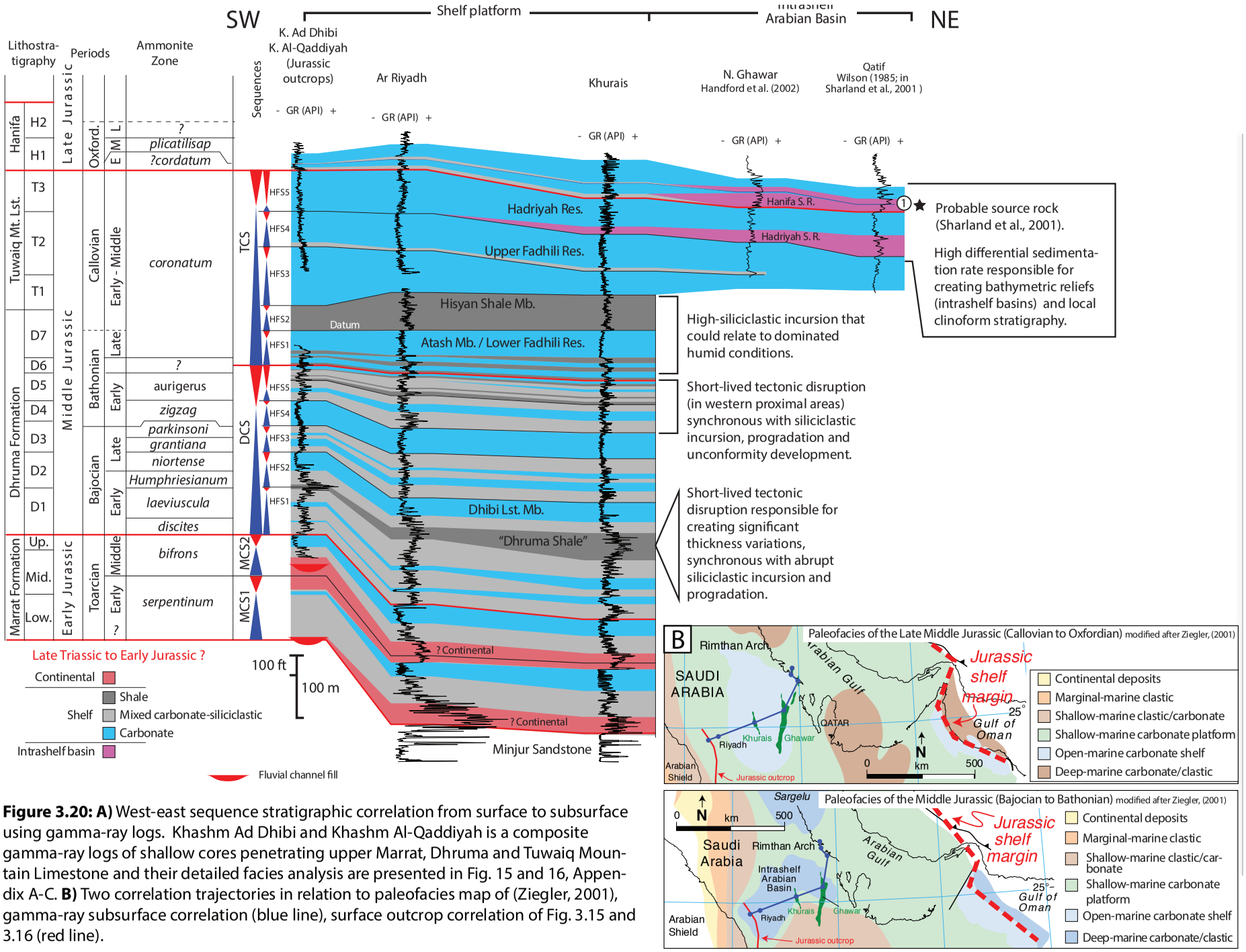

Figure 3.20: A) West-east sequence stratigraphic correlation from surface to subsurface using gamma-ray logs. Khashm Ad Dhibi and Khashm Al-Qaddiyah is a composite gamma-ray logs of shallow cores penetrating upper Marrat, Dhruma and Tuwaiq Mountain Limestone and their detailed facies analysis are presented in Fig. 15 and 16, Appendix A-C. **B)** Two correlation trajectories in relation to paleofacies map of (Ziegler, 2001), gamma-ray subsurface correlation (blue line), surface outcrop correlation of Fig. 3.15 and 3.16 (red line).

3.8 Conclusion

The outcropping Dhruma Formation and Tuwaiq Mountain Limestone (Bajocian to Middle Callovian including disconformity levels) provides a westernmost stratigraphic record of the Middle Jurassic Arabian Platform, a broad slowly subsiding epeiric tropical platform. The depositional environment ranges from continental braided fluvial deposits to tidal or wave-dominated mixed carbonate-siliciclastic lagoonal deposits. These formed aggraded flat-topped platform wedging and thickening northward. Evident syndepositional differential subsidence has an influence on lateral thickness variation and to a lesser extent facies distribution. Short-lived tectonic downwarping provide uplifted source area for high fluvial dynamics and sandstone influx in overall mud-dominated successions. The carbonate platforms are mud-dominated and evolved from restricted carbonate platforms with microbes and low-faunal diversity (Dhruma Fm., Early Bajocian to Early Bathonian) to open-marine carbonate platforms with stromatoporoid/coral bearing and high-faunal diversity adjacent to deep intrashelf basin in subsurface (Tuwaiq Mt. Lst., Middle Callovian). The successions make up two composite sequences, DCS and TCS (3rd-order, ~2.4 Myr), superimposed by several high-frequency sequences (4th-order, ~400 kyr) that show a progressive marine transgression with subordinate MFS at Early Bathonian (*zigzag* Zone) and main MFS in the Tuwaiq Mt. Lst. (Middle Callovian coronatum Zone). The depositional sequences are considered to be of eustatic origin as they match well with Tethyan sea-level cycles. Significant sequence boundary between DCS and TCS with Middle Bathonian hiatus controlled by eustatic sea-level fall coupled with local tectonic disruption. The TST of the composite sequences were

initiated with wet-warming episodes associated with high-siliciclastic discharges and demise of carbonate-production. The carbonates are developed well during late TST and HST of the composite sequences controlled by stepping back of the siliciclastic sources together with drying of the climate with cooling. The synchronicity of the transgression with warming periods and highstand with cooling provide some confidence to the glacio- or aquifer-eustatic driver mechanisms of the Middle Jurassic depositional sequences.

Acknowledgments

This work was part of a PhD thesis that carried out at the University of Bordeaux-Montaigne, ENSEGID Bordeaux INP, and was sponsored by Saudi Aramco. We thank the management of Saudi Aramco for the permission to publish this work. We express our thankfulness and gratitude to Dr. Aus Al-Tawil (RCD manager, Saudi Aramco) for his endless outstanding support and motivations during all phases of this study. We also thank Dr. Denis Vaslet, Prof. J. Fred Read and Prof. Charles Kerans for providing valuable suggestions and constructive comments. We also extend our thanks to Mahmoud Alnazghah and Dr. Raed Al-Dukhayyil for field support.

References

Adams, J.E., Rhodes, M.L., 1960. Dolomitization by seepage refluxion. American Association of Petroleum Geologists Bulletin, 44, 1912-1921.

Aguado, R., O'Dogherty, L., Sandoval, J., 2017. Calcareous nannofossil assemblage turnover in response to the Early Bajocian (Middle Jurassic) palaeoenvironmental changes in the Subbetic Basin. Palaeogeography, Palaeoclimatology, Palaeoecology, 472, 128-145.

Aigner, T., 1985, Storm depositional systems; dynamic stratigraphy in modern and ancient shallow-marine sequences: Storm depositional systems; dynamic stratigraphy in modern and ancient shallow-marine sequences:

Berlin, Federal Republic of Germany (DEU), Springer Verlag, Berlin, 174 pp.
Al-Husseini, M. I and. Matthews, R. K. 2008. Jurassic-Cretaceous Arabian orbital stratigraphy: The AROSJK Chart, GeoArabia, 13 (1), 89-94.
Al-Husseini, M., 2009. Update to Late Triassic-Jurassic stratigraphy of Saudi Arabia for the Middle East geologic time scale. GeoArabia, 14(2), 145-186.
Al-Husseini, M.I., 1997. Jurassic sequence stratigraphy of the western and southern Arabian Gulf. GeoArabia (Manama), 2(4), 361–82.
Al-Husseini, M.I., 2000. Origin of the Arabian plate structures: Amar collision and Najd Rift. GeoArabia 5, 527–542.
Al-Mojel, A., 2010. High-Resolution Sequence Stratigraphy of the Middle Jurasic Lower Fadhili Reservoir in Khurais. Master of Science Thesis, King Fahd University of Petroleum and Minerals.
Alméras, Y., 1987. Les Brachiopodes du Lias–Dogger: paléontologie et biostratigraphie. Geobios, Lyon, Special Memoir 9, p. 161-196.
Alsharhan, A.S., Nairn, A.E.M., 1997. Sedimentary basins and petroleum geology of the Middle East. Elsevier, Amsterdam, 843.
Andrieu, S., Brigaud, B., Barbarand, J., Lasseur, E., & Saucède, T., 2016. Disentangling the control of tectonics, eustasy, trophic conditions and climate on shallow-marine carbonate production during the Aalenian–Oxfordian interval: From the western France platform to the western Tethyan domain. Sedimentary Geology, 345, 54-84.
Arp, G. 2008. Fossil and present-day stromatolites of southern Germany. In Preitner, J., Qué Ric, N.-V., Reich, M. (Eds), Geobiology of Stromatolites. International Kalkowsky-Symposium October, 168-202
Ayres, M.G., Bilal, M., Jones, R.W., Slentz, L.W., Tartir, M., Wilson, A.O., 1982. Hydrocarbon habitat in main producing areas, Saudi Arabia. AAPG bulletin, 66(1), 1-9.
Bartolini, A., Baumgartner, P.O., & Guex, J., 1999. Middle and Late Jurassic radiolarian palaeoecology versus carbon-isotope stratigraphy. Palaeogeography, Palaeoclimatology, Palaeoecology, 145(1), 43-60.
Bartolini, A., Baumgartner, P.O., Hunziker, J.C., 1996. Middle and Late Jurassic carbon stable-isotope stratigraphy and radiolarite sedimentation of the Umbria-Marche Basin (Central Italy). Eclogae Geologicae Helvetiae 89, 811–844.
Bartolini, A., Larson, R. L., 2001. Pacific microplate and the Pangea supercontinent in the Early to Middle Jurassic. Geology, 29(8), 735-738.
Baumgartner, P. O., 2013. Mesozoic radiolarites–accumulation as a function of sea surface fertility on Tethyan margins and in ocean basins. Sedimentology, 60(1), 292-318.
Blomeier, D., Scheibner, C., Forke, H. 2009. Facies arrangement and cyclostratigraphic architecture of a shallow-marine, warm-water carbonate platform: the Late Carboniferous Ny Friesland Platform in eastern Spitsbergen (Pyefjellet Beds, Wordiekammen Formation, Gipsdalen Group). Facies, 55(2), 291-324.
Bott, M.H.P., 1992. Passive margins and their subsidence. Journal of the Geological Society, 149(5), 805-812.

Bottjer, D.J., Arthur, M.A., Dean, W.E., Hattin, D.E., Savrda, C.E., 1986. Rhythmic bedding produced in Cretaceous pelagic carbonate environments; sensitive recorders of climatic cycles. Paleoceanography, 1(4), 467-481

Boulila, S., Galbrun, B., Hinnov, L.A., Collin, P.Y., Ogg, J.G., Fortwengler, D., Marchand, D., 2010. Milankovitch and sub-Milankovitch forcing of the Oxfordian (Late Jurassic) Terres Noires Formation (SE France) and global implications. Basin Research, 22(5), 717-732.

Boulila, S., Galbrun, B., Miller, K.G., Pekar, S.F., Browning, J.V., Laskar, J., Wright, J.D., 2011. On the origin of Cenozoic and Mesozoic “third-order” eustatic sequences. Earth-Science Reviews, 109(3), 94-112.

Brigaud, B., Durlet, C., Deconinck, J.F., Vincent, B., Pucéat, E., Thierry, J., Trouiller, A., 2009. Facies and climate/environmental changes recorded on a carbonate ramp: a sedimentological and geochemical approach on Middle Jurassic carbonates (Paris Basin, France). Sedimentary Geology 222, 181-206.

Brigaud, B., Pucéat, E., Pellenard, P., Vincent, B., Joachimski, M.M., 2008. Climatic fluctuations and seasonality during the Late Jurassic (Oxfordian–Early Kimmeridgian) inferred from δ 18 O of Paris Basin oyster shells. Earth and Planetary Science Letters, 273(1), 58-67.

Brigaud, B., Vincent, B., Carpentier, C., Robin, C., Guillocheau, F., Yven, B., Huret, E., 2014. Growth and demise of the Jurassic carbonate platform in the intracratonic Paris Basin (France): interplay of climate change, eustasy and tectonics. Marine and Petroleum Geology 63, 3–29.

Bromley, R.G., Ekdale, A.A., 1984. Trace fossil preservation in flint in the European chalk. Journal of Paleontology, 58, 298–311.

Bush, P.R., 1973. Some aspects of the diagenetic history of the Sabkha in Abu Dhabi, Persian Gulf. In: Purser, B.H., (Ed.), The Persian Gulf, Holocene Carbonate Sedimentation in a Shallow Epicontinental Sea. Springer, New York, 395-407.

Butler, G.E, Harris, E.M., Kendall, C.G.St.C., 1982. Recent evaporites from the Abu Dhabi coastal plats. In: C.R. Hanford, R.G. Loucks and Davies, G.R. (Editors), Depositional and Diagenetic Spectra of Evaporites - - A Core Workshop. Soc. Econ. Palaeontol. Mineral. Core Workshop, 3: 33-64.

Butler, G.P., 1969. Modern evaporite deposition and geochemistry of coexisting brines, the sabkha, Trucial Coast, Arabian Gulf. Journal of Sedimentary Research, 39(1). 70-89.

Butler, G.P., Kendall, C.G.St.C., Harris, P.M., 1982. Recent evaporites from the Abu Dhabi coastal flats. In: Handford, G.R., Loucks, R.G., Davies, G.R. (Eds.), Depositional and Diagenetic Spectra of Evaporites. Society of Economic Paleontologists and Mineralogists Core Workshop, 3, 33 – 64.

Chamley, H., 1989. Clay Sedimentology. Springer Verlag. 623 pp.

Chowns, T.M., Elkins, J.E., 1974. The origin of quartz geodes and cauliflower cherts through the silicification of anhydrite nodules. Journal of Sedimentary Research, 44(3). 885-903

Collinson, J.D., 1996. Alluvial sediments. In: Reading, H.G. (Ed.), Sedimentary Environments: Processes, Facies and Stratigraphy, Blackwell Science, 37-82.

Crevello, P.D., 1991. High-frequency carbonate cycles and stacking patterns: interplay of orbital forcing and subsidence on Lower Jurassic rift platforms, High Atlas, Morocco. Sedimentary Modeling: Computer Simulations and Methods for Improved Parameter Definition: Kansas Geological Survey, Bulletin, 233, 207-230.

Dalrymple R.W., 2010. Interpreting sedimentary successions: facies, facies analysis and facies models. In: James N.P., Dalrymple R.W. (Eds), Facies models 4. Geological Association of Canada, St. John's, Newfoundland, 3–18

de Matos, J. E., 2002. Sequence Stratigraphy and Sedimentation of the Araej Formation (Middle Jurassic), UAE: Outcrop and Subsurface Compared. In Abu Dhabi International Petroleum Exhibition and Conference. Society of Petroleum Engineers. SPE 78539.

Dera, G., Brigaud, B., Monna, F., Laffond, R., Puceat, E., Deconinck, J.F., Pellenard, P., Joachimsky, M., Durlet, C., 2011. Climatic ups and downs in a disturbed Jurassic world. Geology 39, 215-218.

Dera, G., Pucéat, E., Pellenard, P., Neige, P., Delsate, D., Joachimski, M., Reisberg, L., Martinez, M., 2009. Water mass exchange and variations in seawater temperature in the NW Tethys during the Early Jurassic: evidence from neodymium and oxygen isotopes of fish teeth and belemnites. Earth and Planetary Science Letters 286, 198–207.

Dingle, R.V., 1982. Continental margin subsidence: a comparison between the east and west coasts of Africa. In: Scrutton, R.A. (Ed.). Dynamics of Passive Margins, American Geophysical Union, 6, 59-71.

Donnadieu, Y., Dromart, G., Goddéris, Y., Pucéat, E., Brigaud, B., Dera, G., Dumas, C. Olivier, N., 2011. A mechanism for brief glacial episodes in the Mesozoic greenhouse. Paleoceanography 26.

Dromart, G., Garcia, J.P., Picard, S., Atrops, F., Lécuyer, C., Sheppard, S.M.F., 2003a. Ice age at the MiddleeLate Jurassic transition? Earth and Planetary Science Letters. 213, 205-220.

Dromart, G., Garcia, J.P., Picard, S., Rousseau, M., Atrops, F., Lécuyer, C., Sheppard, S.M.F., 2003b. Perturbation of the carbon cycle at the Middle/Late Jurassic transition: geological and geochemical evidence. American Journal of Science 303, 667–707.

Dunham, R.J., 1962. Classification of carbonate rocks according to depositional texture. In: Ham, W.E. (Ed.), Classification of Carbonate Rocks: AAPG Memoir 1, 108-121. Tulsa, OK.

Embry, A.F., Klovan, J.E., 1971. A late Devonian reef tract on northeastern Banks Island, NWT. Bulletin of Canadian Petroleum Geology, 19(4), 730-781.

Énay, R., Le Nindre, Y.M., Mangold, C., Manivit, J., Vaslet, D., 1986. The Jurassic of central Saudi Arabia: New data on lithostratigraphic units, palaeoenvironments, ammonite faunas, ages and correlations. Deputy Ministry of Mineral Resources, Jiddah, Technical Record BRGM-TRO6-3, p. 65

Énay, R., Mangold, C., 1984. The ammonite succession from Toarcian to Kimmeridgian in Saudi Arabia, correlation with the European faunas. In: Michelsen, O., Zeiss, A. (Eds.), International Symposium on Jurassic Stratigraphy, Geological Survey of Denmark Copenhagen, Erlangen, 3, 641-652.

Énay, R., Mangold, C., Alméras, Y., Hughes, G.W., 2009. The Wadi ad Dawasir “delta”, central Saudi Arabia: A relative sea-level fall of Early Bathonian age. GeoArabia, 14 (1), 17-52.

Enos, P., 1983. Late Mesozoic paleogeography of Mexico. In: Mesozoic Paleogeography of the West-Central United States. Rocky Mountain Section SEPM, Denver, Colorado, Paleogeography Symp. 2, p. 133-158.

Enos, P., 1983. Shelf Environment: In: Scholle, P.A., Bebout, D.G., Moore, C.H. (Eds.), Carbonate Depositional Environments. American Association Petroleum Geologists Memoir, 33, 268-295.

Evans, G., Schmidt, V., Bush, P., and Nelson, H., 1969. Stratigraphy and geologic history of the sabkha, Abu Dhabi, Persian Gulf. Sedimentology 12, 145-159.

Fischer, A.G., 1964. The Loffer cyclothems of the Alpine Triassic. Geological Survey of Kansas Bulletin 169, 107–149.

Fischer, A.G., 1982. Long-term climatic oscillations recorded in stratigraphy. In: Berger, W.H., Crowell, J.C. (Eds.), Climate in Earth History. National Academy Press, Washington, D.C., 97–104.

Fischer, J.-C., Manivit, J., Vaslet, D., 2001. Jurassic gastropod faunas of central Saudi Arabia. GeoArabia (Manama), 6(1), 63–100.

Frakes, L.A., Francis, J.E., Syktus, J.I., 1992. Climate Modes of the Phanerozoic: the History of the Earth's Climate over the past 600 Million Years. Cambridge University Press, Cambridge, p. 274.

Galli, G., 1993. “Calcari Grigi” formation, Jurasic, Venetian Alps. In: Galli, G. (Ed.), Temporal and Spatial Patterns in Carbonate Platforms. Springer, Berlin, 97-129.

Goldhammer, R.K., Dunn, P.A., Hardie, L.A., 1987. High frequency glacio-eustatic sealevel oscillations with Milankovitch characteristics recorded in Middle Triassic platform carbonates in northern Italy. American Journal of Science, 287(9), 853-892.

Goldhammer, R.K., Dunn, P.A., Hardie, L.A., 1990. Depositional cycles, composite sea-level changes, cycle stacking patterns, and the hierarchy of stratigraphic forcing: examples from Alpine Triassic platform carbonates. Geological Society of America Bulletin, 102(5), 535-562.

Gonzalez, R., 1996. Response of shallow-marine carbonate facies to third-order and high-frequency sea-level fluctuations: Hauptrogenstein Formation, northern Switzerland. Sedimentary Geology, 102(1-2), 111-130.

Gradstein, F.M., Ogg, J.G., Schmitz, M.D., Ogg, G.M., 2012. The Geologic Time Scale 2012. Elsevier, p. 1144.

Grotzinger, J.P., 1986. Cyclicity and paleoenvironmental dynamics, Rocknest platform, northwest Canada. Geological Society of America Bulletin 97, 1208–1231.

Hallam, A., 1988. A reevaluation of Jurassic eustasy in the light of new data and the revised Exxon curve.

Hallam, A., 2001. A review of the broad pattern of Jurassic sea-level changes and their possible causes in the light of current knowledge. Palaeogeography, Palaeoclimatology, Palaeoecology, 167(1), 23-37.

Hallock, P., 2001. Coral reefs, carbonate sediments, nutrients, and global change. The history and sedimentology of ancient reef systems, 387-427.

Haq, B.U., Al-Qahtani, A.M., 2005. Phanerozoic cycles of sea-level change on the Arabian Platform. GeoArabia, 10(2), 127-160.

Hardenbol, J., Jacquin, T., Farley, M.B., de Graciansky, P.C., Vail, P.R., 1998. Mesozoic and Cenozoic sequence chronostratigraphic framework of European basins. In: de Graciansky, P. C., Hardenbol, J., Jaquin, T., Vail, P.R. (Eds.), Mesozoic and Cenozoic Sequence Stratigraphy of European Basins. Society for Sedimentary Geology (SEPM), Tulsa, 3–13.

Hughes, G.W., 1996. A new bioevent stratigraphy of Late Jurassic Arab-D carbonates of Saudi Arabia. GeoArabia, 1 (4), 417- 434.

Hughes, G.W., 2004. Middle to Upper Jurassic Saudi Arabian carbonate petroleum reservoirs: Biostratigraphy, micropalaeontology and palaeoenvironments. GeoArabia, 9 (3), 79-114.

Hughes, G.W., 2009. Biofacies and palaeoenvironments of the Jurassic Shaqra Group of Saudi Arabia. Volumina Jurassica, v. 6, p. 33-45.

Hughes, G.W., 2013. Late Permian to Late Jurassic microproblematica of Saudi Arabia: Possible palaeobiological assignments and roles in the palaeoenvironmental reconstructions. GeoArabia, 18 (1), 57-92.

Hughes, G.W., Al-Khaled, M., Varol, O., 2009. Oxfordian biofacies and palaeoenvironments of Saudi Arabia. Volumina Jurassica, 6, 47-60.

Hughes, G.W., Varol, O., Al-Khalid, M., 2008. Late Oxfordian micropalaeontology, nannopalaeontology and palaeoenvironments of Saudi Arabia. GeoArabia, 13 (2), 15-46.

Hunt, D., Tucker, M.E., 1993. The Middle Cretaceous Urgonian platform of southeastern France. In: Simo, T.J., Scott, R.W., Masse, J.P. (Eds.), Cretaceous Carbonate Platforms. American Association of Petroleum Geologists, Memoir 56, 409-454.

Husinec, A., Harman, C.A., Regan, S.P., Mosher, D.A., Sweeney, R.J., Read, J.F. 2012. Sequence development influenced by intermittent cooling events in the Cretaceous Aptian greenhouse, Adriatic platform, Croatia. AAPG bulletin, 96(12), 2215-2244.

Iannace, A., Frisia, S., 1994. Changing dolomitization styles from Norian to Rhaetian in the southern Tethys realm. In: Purser, B., Tucker, M., Zenger, D. (Eds.), Dolomites, A Volume in Honour of Dolomieu, International Association of Sedimentologists, Special Publication, 21, 75-89.

Ikeda, M., Bôle, M., Baumgartner, P. O., 2016. Orbital-scale changes in redox condition and biogenic silica/detrital fluxes of the Middle Jurassic Radiolarite in Tethys (Sogno, Lombardy, N-Italy): Possible link with glaciation?. Palaeogeography, Palaeoclimatology, Palaeoecology, 457, 247-257.

Ikeda, M., Tada, R. 2013. Long period astronomical cycles from the Triassic to Jurassic bedded chert sequence (Inuyama, Japan); Geologic evidences for the chaotic behavior of solar planets. Earth, Planets and Space, 65(4), 351-360.

Imbrie, J., Imbrie, K.P. 1986. Ice ages: solving the mystery. Harvard University Press, Cambridge, Massachusetts, 224 pp.

Jacquin, T., Dardeau, G., Durlet, C., de Graciansky, C., Hantzpergue, P., 1998. The North Sea cycle: an overview of 2nd-order transgressive/regressive facies cycles in Western Europe. In: de Graciansky, P.-C., Hardenbol, J., Jacquin, T., Vail, P.R. (Eds.), Mesozoic and Cenozoic Sequence Stratigraphy of European Basins, pp. 445–466.

Jacquin, T., de Graciansky, P.-C., 1998. Transgressive/Regressive (Second order) facies cycles: the effects of tectono-eustasy. In: De Graciansky, P.-C., Hardenbol, J., Jacquin, T., Vail, P.-R. (Eds.), Mesozoic and Cenozoic Sequence Stratigraphy of European Basins. SEPM Special Publication, pp. 31–42.

Jacquin, T., Garcia, J.-P., Ponsot, C., Thierry, J., Vail, P.R., 1992. Séquence de dépôt et cycles régressif/transgressifs en domaine marin carbonaté: exemple du Dogger du Bassin de Paris. Comptes Rendus de l'Académie des Sciences, Série II, Fascicule a – Sciences de la Terre et des Planètes 315, 353–362.

Jenkyns, H. C., Jones, C. E., GrÖcke, D. R., Hesselbo, S. P., Parkinson, D. N. 2002. Chemostratigraphy of the Jurassic System: applications, limitations and implications for palaeoceanography. Journal of the Geological Society, 159(4), 351-378.

Kadar, A.P., De Keyser, T., Neog, N., Karam, K.A., Le Nindre, Y.M., Davies, R.B., 2015. Calcareous nannofossil zonation and sequence stratigraphy of the Jurassic System, onshore Kuwait. GeoArabia, 20(4), 125-180.

Kenig, F., Hayes, J.M., Popp, B.N., Summons, R.E., 1994. Isotopic biochemistry of the Oxford Clay Formation (Jurassic), UK, London. Journal of the Geological Society 151, 139–152.

Kerans, C., Tinker, S.W., 1997. Sequence stratigraphy and characterization of carbonate reservoirs. Society of Sedimentary Geology: SEPM Short Course Notes, 40.

Khetani, A.B., Read, J.F., 2002. Sequence development of a mixed carbonate-siliciclastic high-relief ramp, Mississippian, Kentucky, USA. Journal of Sedimentary Research, 72(5), 657-672.

Koerschner III, W.F., Read, J.F., 1989. Field and modeling studies of Cambrian carbonate cycles, Virginia, Appalachians. Journal of Sedimentary Petrology 59, 654–687.

Konert, G., Al-Afifi, A.M., Al-Hajri, S.A., 2001. Paleozoic stratigraphy and hydrocarbon habitat of the Arabian Plate. GeoArabia, 6(3), 407–442.

Korte, C., Hesselbo, S.P., Ullmann, C.V., Dietl, G., Ruhl, M., Schweigert, G., Thibault, N., 2015. Jurassic climate mode governed by ocean gateway. Nature communications, 6, 10015.

Lasemi, Y., Jahani, D., Amin-Rasouli, H., Lasemi, Z., 2012. Ancient carbonate tidalites. In: Davis Jr, R.A., Dalrymple, R.W. (Eds.), Principles of tidal sedimentology. Springer Science & Business Media, Netherlands, 567-607

Le Nindre, Y.M., Manivit, J., Manivit, H., Vaslet, D., 1990. Stratigraphie sequentielle du Jurassique et du Cretace en Arabie Saoudite. Bulletin Société Géologique France, Paris 6, 1025-1035.

Le Nindre, Y.M., Manivit, J., Vaslet, D., 1987. Histoire géologique de la Bordure occidentale de la Plate-forme Arabe du Paléozoïque inférieur au Jurassique supérieur. Thèse de Doctorat de l'Université de Paris 6, 4, p. 1113.

Le Nindre, Y.M., Vaslet, D., Laforet, C.I., Le Strat, P. Manivit, J., 1984. Accumulations of ferruginous ooliths in the Jurassic of central Saudi Arabia. D.M.M.R. Jeddah, Open-File Report BRGM-0F-04-3, p. 23.

Le Nindre, Y.M., Vaslet, D., Le Métour, J., Bertrand, J., Halawani, M., 2003. Subsidence modelling of the Arabian Platform from Permian to Paleogene outcrops. Sedimentary Geology, 156, 263-285.

Leinfelder, R.R., Krautter, M., Laternser, R., Nose, M., Schmid, D.U., Schweigert, G., Werner, W., Keupp, H., Brugger, H., Herrmann, R., Rehfeld-Kiefer, U., Schroeder, J.H., Reinhold, C., Koch, R., Zeiss, A., Schweizer, V., Christmann, H., Menges, G., Luterbacher, H., 1994. The origin of Jurassic reefs: current research developments and results. Facies 31, 1–56.

Logan, B.W., Hoffman, P., Gebelein, C.D., 1974. Algal mats, cryptalgal fabrics, and structures, Hamelin Pool, Western Australia. AAPG Memoir, 22, 140–194.

Logan, B.W., Rezak, R., Ginsburg, R.N., 1964. Classification and environmental significance of algal stromatolites. The Journal of Geology, 68-83.

Lukasik, J.J., James, N.P., McGowran, B., Bone, Y., 2000. An epeiric ramp: low-energy, cool-water carbonate facies in a Tertiary inland sea, Murray Basin, South Australia. Sedimentology, 47(4), 851-881.

Ma, W., Tian, J., Li, Q., Wang, P. 2011. Simulation of long eccentricity (400-kyr) cycle in ocean carbon reservoir during Miocene Climate Optimum: Weathering and nutrient response to orbital change. Geophysical Research Letters, 38(10).

Maliva, R.G., 1987. Quartz geodes: early diagenetic silicified anhydrite nodules related to dolomitization. Journal of Sedimentary Research, 57(6). 1054-1058

Manivit, J., Le Nindre, Y.M., Vaslet D. (1990) Le Jurassique d'Arabie Centrale. In Histoire Gologique de la Bordure Occidentale de la Plate-forme Arabe. Volume 4. Document du BRGM n°194.

Manivit, J., Pellaton, C., Vaslet, D., Le Nindre, Y.M., Brosse, J.M., Fourniguet, J., 1985a. Geologic map of the Wadi al Mulayh quadrangle, sheet 22H, Kingdom of Saudi Arabia. Saudi Arabian Deputy Ministry for Mineral Resources Geosciences Map, GM-92, scale, 1(250,000), 1-32.

Manivit, J., Pellaton, C., Vaslet, D., Le Nindre, Y.M., Brosse, J.M., Breton, J.P., Fourniguet, J., 1985b. Geologic map of the Darma quadrangle, sheet 24H, Kingdom of Saudi Arabia. Saudi Arabian Deputy Ministry for Mineral Resources Geosciences Map, GM-101, scale, 1(250,000), 133.

Martinez, M., Dera, G. 2015. Orbital pacing of carbon fluxes by a ~9-My eccentricity cycle during the Mesozoic. Proceedings of the National Academy of Sciences, 112(41), 12604-12609.

Matthews, R.K., Frohlich, C., 2002. Maximum flooding surfaces and sequence boundaries: comparisons between observations and orbital forcing in the Cretaceous and Jurassic (65–190 Ma). GeoArabia, 7(3), 503-538.

McGuire, M.D., Koepnick, R.B., Markello, M.L., Stockton, M.L., Waite, L.E., Kompanik, M.J., Al-Shammary, M.J., AlAmoudi, M.O., 1993. Importance of sequence stratigraphic concepts in development of reservoir architecture in Upper Jurassic grainstones, Hadriya and Hanifa reservoirs, Saudi Arabia. Society of Petroleum Engineers, 489-499.

McKenzie, J.A., Hsu, K.J., Schneider, J.F., 1980. Movement of subsurface waters under the sabkha, Abu Dhabi, UAE, and its relation to evaporative dolomite genesis, In: Zenger, D.H., et al., (Eds.), Concepts and models of

dolomitization: Society of Economic Paleontologists andMineralogists Special Publication, 28, 11-30.
Mitchum, R.M., Van Wagoner, J.C. 1991. High-frequency sequences and their stacking patterns; sequence-stratigraphic evidence of high-frequency eustatic cycles. Sedimentary Geology, 70, 131-160.
Morettini, E., Santantonio, M., Bartolini, A., Cecca, F., Baumgartner, P. O., Hunziker, J. C., 2002. Carbon isotope stratigraphy and carbonate production during the Early–Middle Jurassic: examples from the Umbria–Marche–Sabina Apennines (central Italy). Palaeogeography, Palaeoclimatology, Palaeoecology, 184(3), 251-273.
Morgans, H. S., Hesselbo, S. P., Spicer, R. A., 1999. The seasonal climate of the Early-Middle Jurassic, Cleveland Basin, England. Palaios, 261-272.
Murris, R.J., 1980. Middle East: Stratigraphic evolution and oil habitat. AAPG Bulletin, 64,597–618.
Mutrux, J., Maher, H., Shuster, R., Hays, T., 2008. Iron ooid beds of the Carolinefjellet Formation, Spitsbergen, Norway. Polar Research, 27(1), 28-43.
Muttoni, G., Erba, E., Kent, D.V., Bachtadse, V., 2005. Mesozoic Alpine facies deposition as a result of past latitudinal plate motion. Nature 434, 59–63.
O'Dogherty, L., Sandoval, J., Bartolini, A., Bruchez, S., Bill, M., Guex, J., 2006. Carbon-isotope stratigraphy and ammonite faunal turnover for the Middle Jurassic in the Southern Iberian palaeomargin. Palaeogeography, Palaeoclimatology, Palaeoecology, 239(3), 311-333.
Olivier, N., Cariou, E., Hantzpergue, P. 2015. Evolution of a Late Oxfordian: early Kimmeridgian carbonate platform, French Jura Mountains. Swiss Journal of Geosciences, 108(2-3), 273-288.
Olivier, N., Colombié, C., Pittet, B., Lathuilie` re, B., 2011. Microbial carbonates and corals on the marginal French Jura platform (Late Oxfordian, Molinges section). Facies 57, 469–492.
Olsen P.E, Kent D.V., 1999. Long-period Milankovitch cycles from the late Triassic and Early Triassic of eastern North America and their implications for the calibration of the early Mesozoic time scale and long term behavior of the planets. Philosophical Transactions Royal Society, Mathematical Physical Engineering Sciences, 357, 1761–1786
Patterson, R.J., 1972, Hydrology and carbonate diagenesis of a Coastal Sabkha in the Persian Gulf: unpublished Ph.D. Dissertation Princeton University, Princeton, New Jersey, 472 p.
Pellenard, P., Tramoy, R., Pucéat, E., Huret, E., Martinez, M., Bruneau, L., Thierry, J., 2014. Carbon cycle and sea-water palaeotemperature evolution at the Middle–Late Jurassic transition, eastern Paris Basin (France). Marine and Petroleum Geology, 53, 30-43.
Perkins, R.D., Dwyer, G.S., Rosoff, D.B., Fuller, J., Baker, P.A., Lloyd, R.M., 1994. Salina sedimentation and diagenesis: West Caicos Island, British West Indies. Dolomites: A Volume in Honour of Dolomieu, 37-54.
Perkins, R.D., Dwyer, G.S., Rosoff, D.B., Fuller, J., Baker, P.A., Lloyd, R.M., 1994. Salina sedimentation and diagenesis: West Caicos Island, British West Indies. In: Purser, B., Tucker, M., Zenger, D. (Eds.), Dolomites: A volume in honor of Dolomieu. International Association of Sedimentologists, Special Publication, 21, 37-54.

Pollastro, R.M., 2003. Total petroleum systems of the Paleozoic and Jurassic, Greater Ghawar Uplift and adjoining provinces of central Saudi Arabia and northern Arabian-Persian Gulf. United States Geological Survey Bulletin, 2202 H, 100 pp.

Posamentier, H.W., Morris, W.R. 2000. Aspects of the stratal architecture of forced regressive deposits. In: Hunt, D., Gawthorpe, R.L. (Eds) Sedimentary Responses to Forced Regressions Geological Society, London, Special Publications, 172(1), 19-46.

Powers, R.W., 1968. Lexique Stratigraphique International, v.III, Asie, 10bl, Saudi Arabia. Centre National de la Recherche Scientifique, Paris, 177p.

Powers, R.W., Ramirez, L.F., Redmond, C.D., Elberg, E.L., 1966. Geology of the Arabian Peninsula, Geological Survey Professional Paper, 560-D, 147p.

Price, G.D., 1999. The evidence and implications of polar-ice during the Mesozoic. Earth Science Reviews 48, 183-210.

Rabalais, N.N., Turner, R.E., Wiseman, W.J., & Boesch, D.F., 1991. A brief summary of hypoxia on the northern Gulf of Mexico continental shelf: 1985–1988. Geological Society, London, Special Publications, 58(1), 35-47.

Read, J.F. 1995. Overview of carbonate platform sequences, cycle stratigraphy and reservoirs in greenhouse and icehouse worlds. In: Read, J.F., Kerans, C., Weber, L.J., Sarg, J.F., and Wright F.W. (Eds.), Milankovitch sea level changes, cycles and reservoirs on carbonate platforms in greenhouse and icehouse worlds, SEPM Short Course Notes No. 35, 1-102.

Read, J.F., 1989. Controls on evolution of Cambrian-Ordovician passive margin, US Appalachians. In: Crevello, P.D., Wilson, J.L., Sarg, J.F., Read, J.F. (Eds.), Controls on Carbonate Platform and Basin Development, SEPM Special Publication, 44, 146–165.

Read, J.F., Grotzinger, J.P., Bova, J.A., Koerschner, W.F., 1986. Models for generation of carbonate cycles. Geology, 14(2), 107-110.

Reading H.G., Collinson J.D., 1996. Clastic coasts. In: Reading H.G., (Ed.), Sedimentary Environments, Blackwell Science, Oxford,154–231

Reineck, H.E., Singh, I.B., 1980. Depositional Sedimentary Environments. Springer-Verlag, Berlin, Heidelberg, New York, p. 549.

Reinson, G. E., 1979. Facies models 14. Barrier island systems. Geoscience Canada, 6(2). 51-68

Rey, J., Delgado, A., 2002. Carbon and oxygen isotopes: a tool for Jurassic and early Cretaceous pelagic correlation (southern Spain). Geological journal, 37(4), 337-345.

Rousseau, M., Dromart, G., Droste, H., Homewood, P., 2006. Stratigraphic organisation of the Jurassic sequence in Interior Oman, Arabian Peninsula. GeoArabia-Manama, 11(1), 17.

Sahagian, D., Pinous, O., Olferiev, A., Zakharov, V., 1996. Eustatic curve for the Middle Jurassic-Cretaceous based on Russian platform and Siberian stratigraphy: Zonal resolution. AAPG bulletin, 80(9), 1433-1458.

Sames, B., Wagreich, M., Wendler, J.E., Haq, B.U., Conrad, C.P., Melinte-Dobrinescu, M.C., Hu, X., Wendler, I., Wolfgring, E., Yilmaz, I.Ö., Zorina, S.O. 2016. Review: short-term sea-level changes in a greenhouse

world—a view from the Cretaceous. Palaeogeography, Palaeoclimatology, Palaeoecology, 441, 393-411.
Sha, J., Olsen, P.E., Pan, Y., Xu, D., Wang, Y., Zhang, X., Yao, X., Vajda, V., 2015. Triassic–Jurassic climate in continental high-latitude Asia was dominated by obliquity-paced variations (Junggar Basin, Ürümqi, China). Proceedings of the National Academy of Sciences, 112(12), 3624-3629.
Sharland, P.R., Archer R., Casey D.M., Davies R.B., Hall S.H., Heward A.P., Horbury A.D., Simmons M.D., 2001. Arabian Plate Sequence Stratigraphy. GeoArabia Special Publication 2, Gulf PetroLink, Bahrain, 371.
Shearman, D.J. 1978. Halite in sabkha environments. Marine evaporites, 30-42.
Simmons, M.D., Sharland, P. R., Casey, D.M., Davies, R.B., Sutcliffe, O.E., 2007. Arabian Plate sequence stratigraphy: Potential implications for global chronostratigraphy. GeoArabia-Manama, 12(4), 101.
Sprovieri, M., Sabatino, N., Pelosi, N., Batenburg, S.J., Coccioni, R., Iavarone, M., Mazzola, S., 2013. Late Cretaceous orbitally-paced carbon isotope stratigraphy from the Bottaccione Gorge (Italy). Palaeogeography, Palaeoclimatology, Palaeoecology, 379, 81-94.
Steineke, M.R.A., Bramkamp, R.A., Sander, N.J., 1958. Stratigraphic relations of Arabian Jurassic oil. In: Weeks, L.G. (Ed.), Habitat of Oil. American Association of Petroleum Geologists Symposium, 1294-1329.
Stern, R.J., Johnson, P., 2010. Continental lithosphere of the Arabian Plate: a geologic, petrologic, and geophysical synthesis. Earth-Science Reviews, 101 (1), 29-67.
Suchéras-Marx, B., Guihou, A., Giraud, F., Lécuyer, C., Allemand, P., Pittet, B., Mattioli, E., 2012. Impact of the Middle Jurassic diversification of Watznaueria (coccolith-bearing algae) on the carbon cycle and δ 13 C of bulk marine carbonates. Global and Planetary Change, 86, 92-100.
Suchéras-Marx, B., Mattioli, E., Giraud, F., Escarguel, G., 2015. Paleoenvironmental and paleobiological origins of coccolithophorid genus Watznaueria emergence during the late Aalenian–early Bajocian. Paleobiology, 41(03), 415-435.
Surlyk, F., 1990. Timing, style and sedimentary evolution of Late Palaeozoic-Mesozoic extensional basins of East Greenland. Geological Society, London, Special Publications, 55(1), 107-125.
Surlyk, F., 1991. Sequence stratigraphy of the jurassic-lowermost cretaceous of east greenland (1). AAPG Bulletin, 75(9), 1468-1488.
Tintant, H. 1987. Les nautiles du Jurassique d'Arabie Saoudite. Geobios, Mémoire Spécial 9, p. 67-159.
Vail, P.R., Audemard, F., Bowman, S.A., Eisner, P.N., Perez- Cruz, C., 1991. The stratigraphic signatures of tectonics, eustasy and sedimentology — an overview. In: Einsele, G., Ricken, W., Seilacher, A. (Eds.), Cycles and Events in Stratigraphy. Springer, Berlin, 617–659.
Vaslet, D., Brush, J.M., Breton, J.P., Manivit, J., Le Strat, P., Fourniguet, J., Shorbaji, H., 1988. Geologic map of the quadrangle Shaqra, sheet 25H. Kingdom of Saudi Arabia: Deputy Ministry for Mineral Resources Geoscience Map GM-120C , 29.

Vaslet, D., Delfour, J., Manivit, J., Le Nindre, Y.M., Brosse, J.M., Fourniguet, J., 1983. Geologic map of the Wadi Ar Rayn quadrangle, sheet 23 H, Kingdom of Saudi Arabia. Saudi Arabian Deputy Ministry for Mineral Resources, Jeddah, Geosciences Map, GM-63A.

Védrine, S., Strasser, A., 2009. High-frequency palaeoenvironmental changes on a shallow carbonate platform during a marine transgression (Late Oxfordian, Swiss Jura Mountains). Swiss journal of geosciences, 102(2), 247-270.

Warren, J.K., Kendall, C.G.St.C., 1985. Comparison of sequences formed in marine sabkha (subaerial) and salina (subaqueous) settings-modern and ancient. AAPG Bulletin, 69(6), 1013-1023.

Watts, K.F., Blome, C.D., 1990. Evolution of the Arabian carbonate platform margin slope and its response to orogenic closing of a Cretaceous ocean basin, Oman. In: Tucker, M.E., Wilson, J.L., Crevello, P.D., Sarg, J.R., Read, J.F. (Eds.), Carbonate Platforms, Facies, Sequences and Evolution. International Assocation of Sedimentologists, Special Publication, 9, 291-323.

Wierzbowski, H., Anczkiewicz, R., Bazarnik, J., Pawlak, J., 2012. Strontium isotope variations in Middle Jurassic (Late Bajocian–Callovian) seawater: Implications for Earth's tectonic activity and marine environments. Chemical Geology, 334, 171-181.

Wierzbowski, H., Dembicz, K., Praszkier, T., 2009. Oxygen and carbon isotope composition of Callovian-Lower Oxfordian (Middle-Upper Jurassic) belemnite rostra from central Poland: A record of a Late Callovian global sea-level rise?. Palaeogeography, Palaeoclimatology, Palaeoecology, 283(3), 182-194.

Wierzbowski, H., Joachimski, M.M., 2007. Reconstruction of late Bajocian-Bathonian marine palaeoenvironments using carbon and oxygen isotope ratios of calcareous fossils from the Polish Jura Chain (central Poland). Palaeogeo- graphy, Palaeoclimatology, Palaeoecology, 254, 523 - 540.

Wilson, A.O., 1985. Depositional and diagenetic facies in the Jurassic Arab-C and-D reservoirs, Qatif field, Saudi Arabia. In: Roehl, P.O., Choquette, T.W. (Eds.), Carbonate Petroleum Reservoirs, Springer New York, 319-340.

Wilson, J.L., 1975. Carbonate Facies in Geologic History. Springer-Verlag, New York, 471 pp.

Wilson, J.L., Jordan, C., 1983. Middle Shelf Environment. In: Scholle, P.A., Bebout, D.G., Moore, C.H. (Eds.), Carbonate Depositional Environments. American Association Petroleum Geologists Memoir, 33, 345–440.

Wright, V. P. (1984). Peritidal carbonate facies models: a review. Geological Journal, 19(4), 309-325.

Wright, V.P., 1992. Speculations on the controls on cyclic peritidal carbonates: ice-house versus greenhouse eustatic controls. Sedimentary Geology, 76(1), 1-5.

Ziegler, M.A., 2001. Late Permian to Holocene Paleofacies evolution of the Arabian plate and its hydrocarbon occurrences. GeoArabia, 6, 445-504.

Appendix

Sedimentological log of out-crop core (DHIBI-1) near K. Ad Dhibi

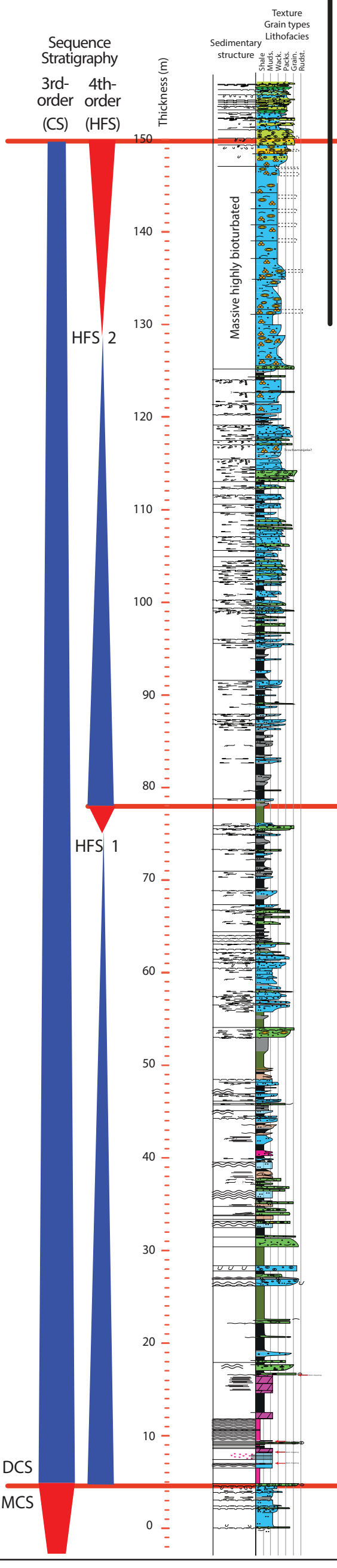

Biofacies and microfacies analysis

(after Hughes, 2013; unpublished Saudi Aramco internal report of DHIBI-1)

Samples

- Redmondoides — Nautiloculina Textulariopsis — spicule
- Redmondoides — spicule
- Redmondoides — spicule
- Redmondoides
- Echinoids — Spicule
- Echinoids
- Redmondoides — Nautiloculina Textulariopsis — spicule
- Nautiloculina Textulariopsis
- Redmondoides — Lenticulina Textulariopsis
- Lenticulina
- Nautiloculina
- Lenticulina Textulariopsis
- Nautiloculina Textulariopsis — spicule
- Redmondoides — spicule
- spicule
- POOR FAUNA — Echinoid
- Spicule
- POOR FAUNA — Echinoid
- Spicule
- Nodosaria Lenticulina
- Nodosaria
- POOR FAUNA
- Echinoid
- POOR FAUNA — Nodosaria
- POOR FAUNA
- POOR FAUNA
- POOR FAUNA — Nodosaria Lenticulina

Biofacies Microbialite

Lithostratigraphy units of the Dhruma Formation

D3

Dbibi Limestone Member

D2

D2

D1

Marrat Formation

Appendix 3.2

Sedimentological log of outcrop core (MZRU-2) near K. Ad Dhibi

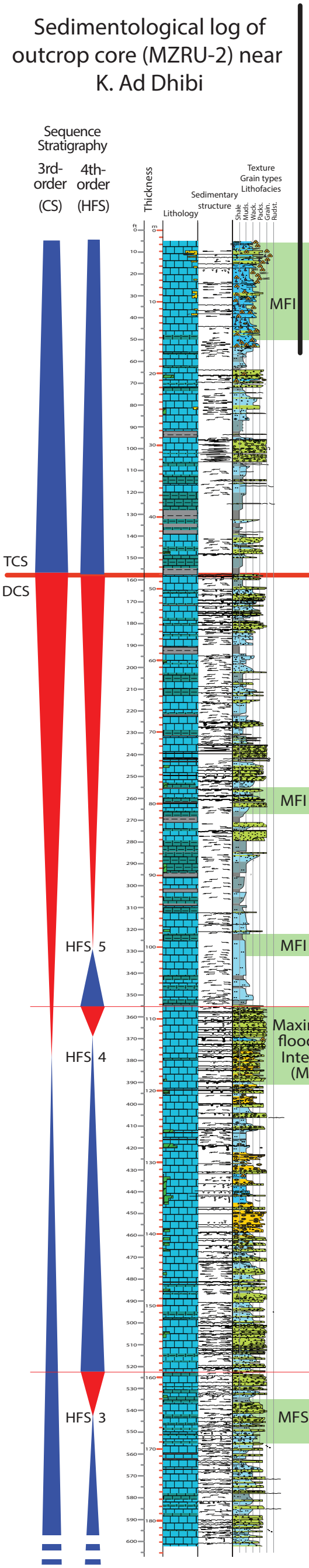

Semi-quantitative micropalaeontological analysis

(after Hughes, 2014; unpublished Saudi Aramco internal report of MZRU-2)

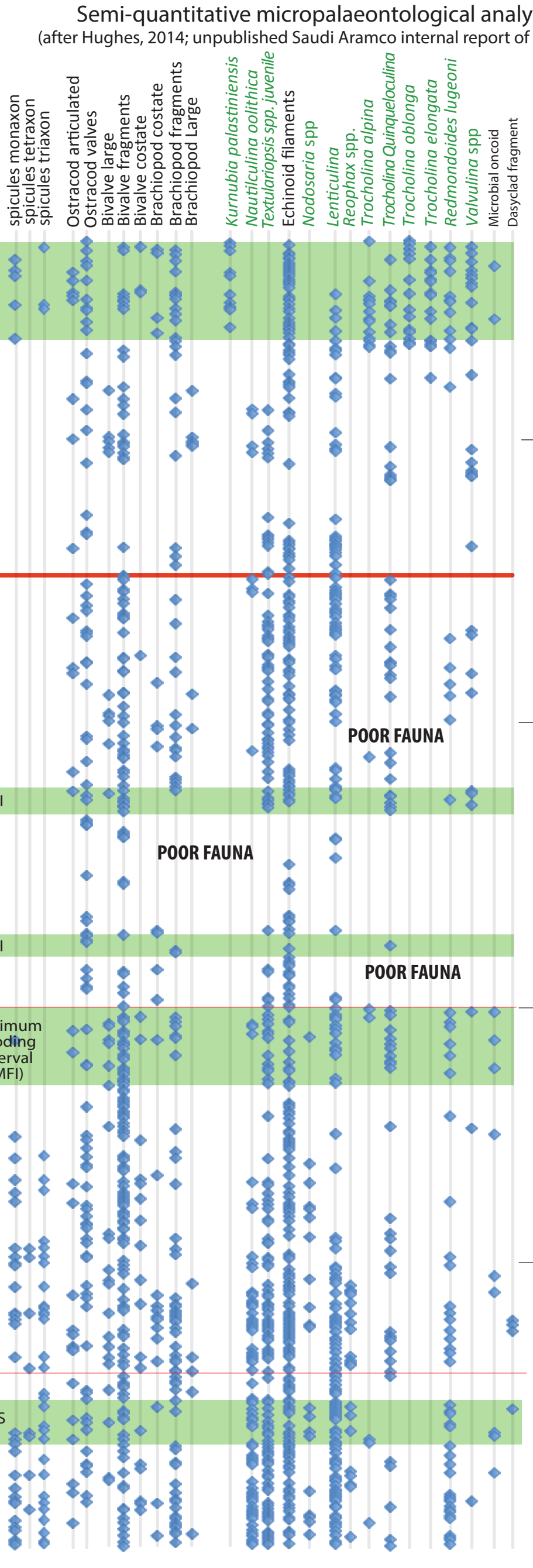

Lithostratigraphy units of Dhruma Formation

Arash Mb. / Lower Fadhili Reservoir

D6

D5

D4

D3

Appendix 3.3

Semi-quantitative microfacies and microfossil analysis

(after Hughes, 2014; unpublished Saudi Aramco internal report of MQBL-1)

Sedimentological log of outcrop core (MQBL-1) near K. Al Qaddiyah

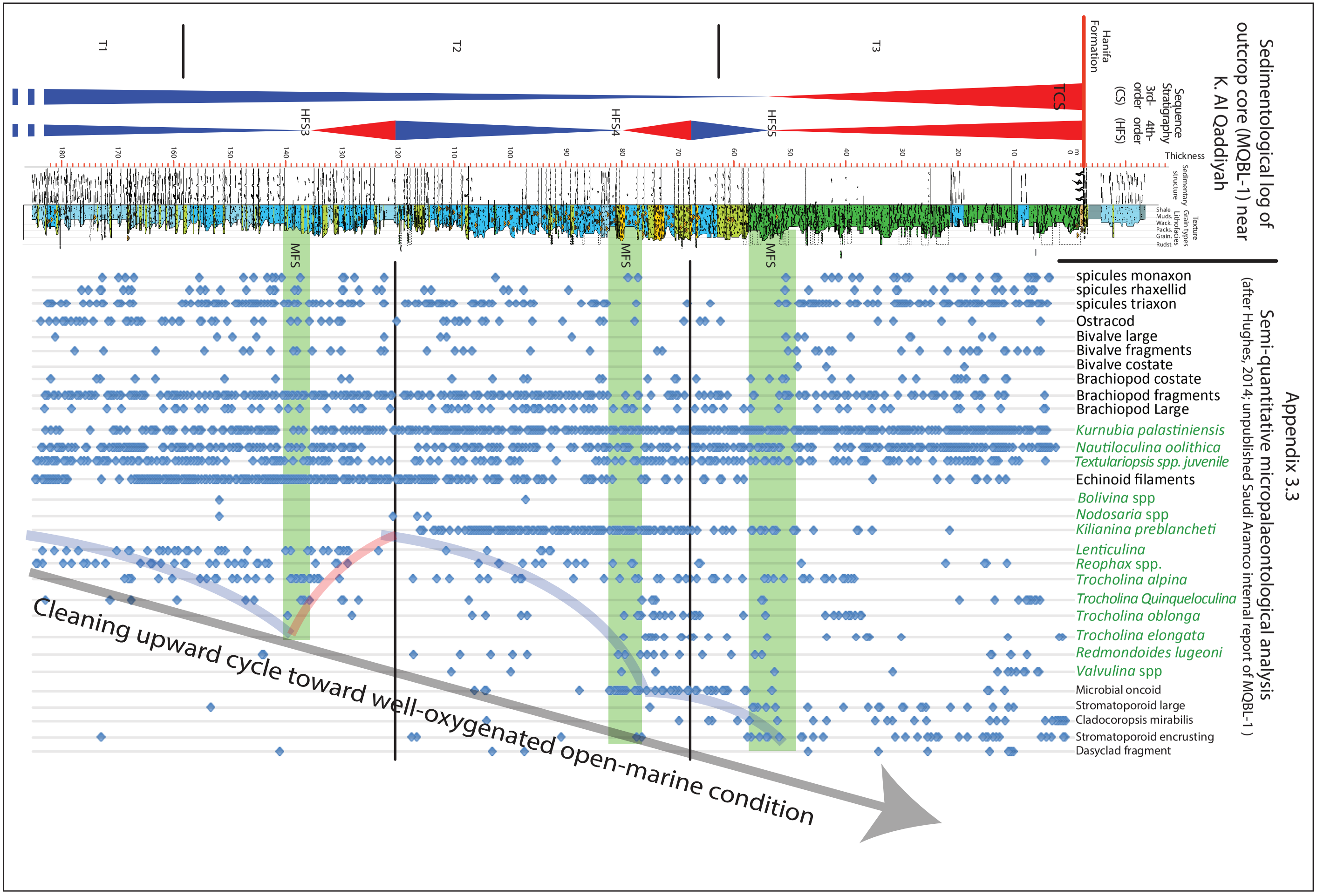

Appendix 3.4 Section locations

Name	Latitude	Longitude
Huraymila (Hiysan Mb. of the Dhruma Fm. to Tuwaiq Mt. Lst)	25.14711	45.96484
Khashm Al Qaddiyah (MQBL-1, shallow core covers Tuwaiq Mt. Lst.)	24.52723	46.40576
Khashm Ad Dhibi (MRZU-2, shallow core covers D3 to Atash Mb. of the Dhruma Fm.)	24.28684	46.29486
Khashm Ad Dhibi (HMNK-1, shallow core covers D2 to D5 unit of the Dhruma Fm.)	24.26258	46.28113
Khashm Ad Dhibi (DHBI-1, shallow core covers upper Marrat Fm. to D2 of the Dhruma Fm.)	24.19595	46.24203
Wadi Al Jufayr (D1 to D2 unit of the Dhruma Fm.)	23.89844	46.17702
Faridat Balum (D1 to D2 unit of the Dhruma Fm.)	23.7114	46.23652
Khashm Al Khalta (D1 to D2 unit of the Dhruma Fm.)	23.58547	46.17834
Wadi Al Hawtah (D2 to the Atash Mb. of the Dhruma Fm.)	23.57827	46.37166
Khashm Disman (D1 to D2 unit of the Dhruma Fm.)	23.42942	46.22265
Wadi Birk (D1, D2 unit of the Dhruma Fm.)	23.13083	46.35743
Wadi Birk (D3 to D7 unit of the Dhruma Fm.)	23.19579	46.4715
Wadi Birk (Tuwaiq Mt. Lst. section)	23.28454	46.53242
Khashm Mawan (D4 unit of the Dhruma Fm. to the Tuwaiq Mt. Lst)	22.84145	46.11306
Fara'id al Ahmar (D1 to D2 unit of the Dhruma Fm.)	22.56072	46.10331
Fara'id al Ahmar (D3 to the Atash Mb. of the Dhruma Fm.)	22.56864	46.14334
Khashm Munayyifiyah (D1 to D2 unit of the Dhruma Fm.)	22.18176	45.88079
Jabal Shimrakh (D3 to D7 of the Dhruma Fm.)	22.15263	45.94113
Khashm Abu Al Jiwar (Dhruma Fm. and Tuwaiq Mt. Lst)	21.84332	45.73633
Khashm Mishlah (BRGM section, Tuwaiq Mt. Lst.)	21.11667	45.43333
Khashm "861" (BRGM section, Tuwaiq Mt. Lst.)	20.78333	45.31667
Khashm Kumdah (BRGM section, Tuwaiq Mt. Lst.)	20.30000	45.16667

Chapter 4:

Late Jurassic (Hanifa Formation, Jubaila Limestone and Arab-D)

Tuwaiq Mountain Limestone (escarpment) overlain by the Hanifa Formation, Wadi Birk *(Air photography by Hadi Makayyal, 2007).*

Table of contents:

High-resolution sedimentology and sequence stratigraphy of the Oxfordian-Kimmeridgian, Hanifa, Jubaila and Arab-D outcrops along Jabal Tuwayq, Central Saudi Arabia

Abdullah Al-Mojel[1, 2], Philippe Razin[2], Yves-Michel Le Nindre[3], Guillaume Dera[4]

[1] Saudi Aramco, Dhahran, Saudi Arabia
[2] ENSEGID-Bordeaux INP, EA4592, 33607 Pessac, France
[3] Consultant
[4] GET, Université Paul Sabatier, CNRS UMR 5563, IRD, OMP, 14 Avenue Avenue Edouard Belin, 31400 Toulouse, France

Corresponding author: E-mail: abdullah.mojel@gmail.com Present address: P.O. Box 5093 Dhahran 31311, Saudi Arabia

Keywords: Sequence Stratigraphy, Late Jurassic, Oxfordian, Mixed carbonate-siliciclastic, Arabian Platform, Inner platform, Epicontinental Sea, Epeiric Sea

Abstract

The high-resolution sequence stratigraphy of the Late Jurassic (Oxfordian to Kimmeridgian) is based on outcrop measured sections along a 370 km long N-S transect west and south of Riyadh. The outcrops provide a westernmost stratigraphic record of the Hanifa Formation, Jubaila Limestone and Arab-D Member. The sequence stratigraphic framework is extended over the Arabian Basin through surface to subsurface gamma-ray correlations (550 km long to the east) provide insight to the development of intrashelf basin of a large (>1000 km) epeiric tropical platform. The outcrop depositional environment ranges from semi-arid shoreline to carbonate inner lagoon and back-barrier lagoon. These formed aggraded flat-topped platform with evident syndepositional differential subsidence that has an influence on lateral

thickness variation and to a lesser extent facies distribution. The Late Jurassic successions make several transgressive 3rd-order composite sequences interrupted momentarily by short emersion sequence boundaries. The Hanifa platform is mud-dominated and evolved from proximal argillaceous-limestone with low-faunal diversity (upper Hanifa Formation, Late Oxfordian to Early Kimmeridgian). The outcrops back-barrier high-energy deposits are adjacent to deep intrashelf basin in subsurface. The Hanifa Formation has two main MFS placed in terrigenous-free carbonate sediments at the Late Oxfordian and Early Kimmeridgian. The intrashelf basin is filled to spill during regression of the Hanifa sequences. The Jubaila-Arab-D is a conformable succession consists of two composite sequences that show long-term transgression marked at the base by storm-influenced inner-platform with sandstone quartz, grainstones and proximal barren lime-mudstone. The Maximum marine transgression is placed in the Arab-D in a backstepping of back-barrier high-energy reef facies in the westernmost inner-platform. During highstand, the reef facies are gently prograding out into Rimthan Arch leaving behind restricted lagoon and sabkhah/salina anhydrite. These Late Jurassic composite sequences are probably controlled by climatic driven glacio-eustasy, coupled with local tectonic disruption, as they have some similarity with other Tethyan sequence stratigraphy. For the first time, this detailed outcropping study reveals stratigraphic framework that subdivided the Late Jurassic prolific reservoirs, seals and source-rocks into genetically related sequences that are not always obvious from core, wireline logs or seismic data. Moreover, it provides overall understanding of the Late Jurassic history and tectono-stratigraphic events of the Arabian Platform.

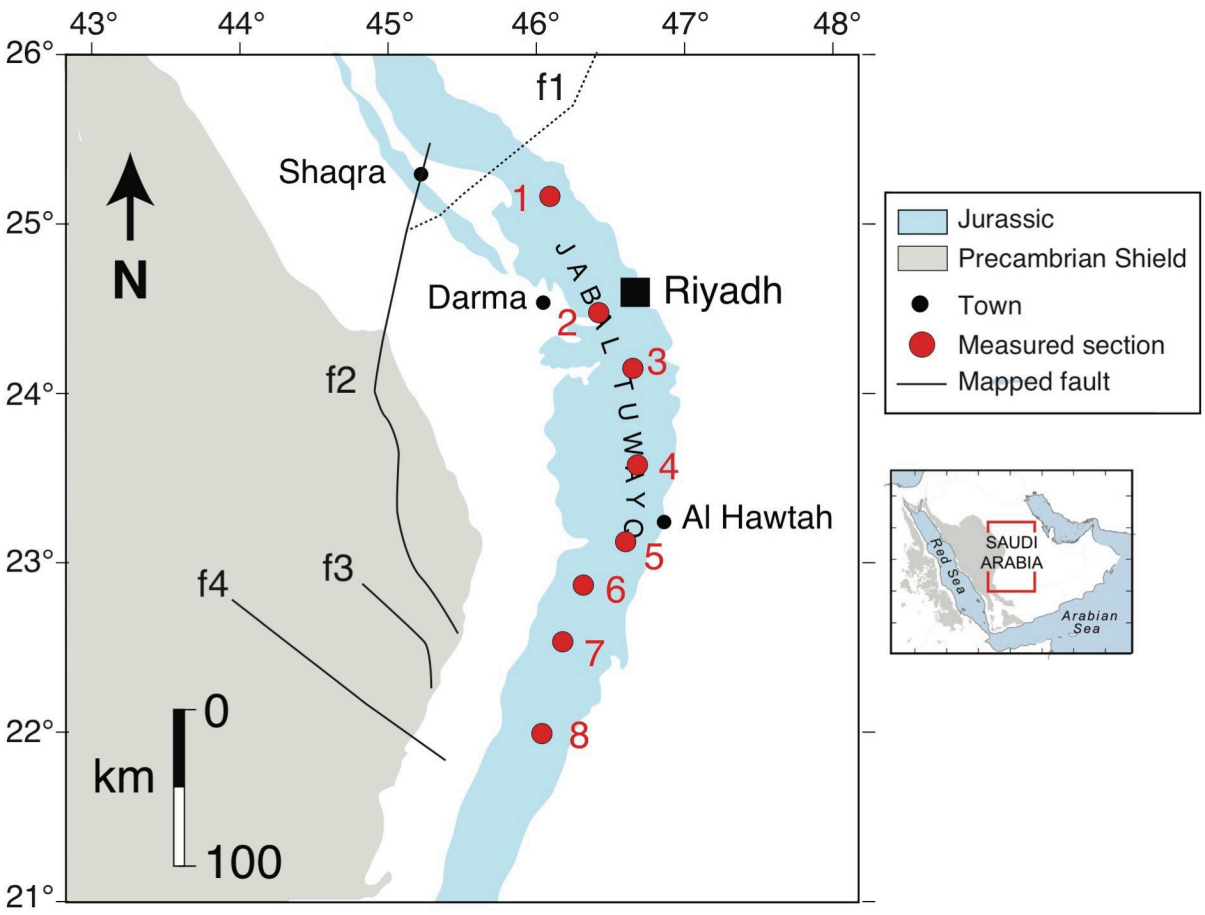

Figure 3.1: Geological map of the study area showing the Jurassic outcrops and measured sections, modified from Fischer et al. (2001. The measured sections are: (1) Huraymila/Wadi Malham, (2) Khashm Qaddiyah, (3) Wadi Al-Ain, (4) Wadi Al Hawtah/Al Hawtah city, (5) Wadi Birk, (6) Wadi Gulghul, (7) As Sitarah, (8) Wadi Al-Haddar. The faults are mapped in the 1:250,00-scale quadrangles of Wadi al Mulayh (Manivit et al., 1985a), Wadi Ar Rayn (Vaslet et al., 1983), Darma (Manivit et al., 1985b) and Shaqra (Vaslet et al., 1988). The name of the faults are: f1 Wadi Al Atk Lineament, f2 Al 'Amar Fault, f3 and f4 are belong to the Najd Fault System (Al-Husseini, 2000).

4.1 Introduction

The Late Jurassic outcrops (Hanifa Formation, Jubaila Limestone and Arab-D Member; Oxfordian to Kimmeridgian) are located in the central part of the Arabian Plate (Fig. 4.1), which corresponds to an intra-cratonic passive margin. The Arabian Platform was an extensive (>1000 km) tropical shallow marine epeiric platform system (Fig. 4.2) with an adjacent organic rich intrashelf basins called the Arabian Basin (Fig. 4.3). The outcropping Hanifa Formation and Jubaila-Arab-D are mainly consisting of shoreline to carbonate inner lagoon to back-barrier lagoonal deposition systems. These outcrops are very well exposed in the central Arabia along the Tuwayq Escarpment forming spectacular west facing continuous cuests along 1000 km N-S near Ar Riyadh (Fig. 4.1). The study interval reach up to 300 m in thickness and the time duration is around 9 Myr. In the subsurface, the studied interval hosts the world's most prolific hydrocarbon reservoirs, Hanifa and Arab-D, and significant source rock interval in the Hanifa Formation (Powers, 1962; Powers et al., 1966; Powers, 1968; Murris, 1980).

Prior to this study, the outcrops of the Hanifa Formation, Jubaila Limestone and Arab-D Member were subdivided into several large mapping units based on lithostratigraphic and biostratigraphic correlations (Powers et al., 1966; Powers, 1986; Manivit et al., 1990). However, genetically related depositional sequences and depositional environments were not documented in detail. Moreover, The depositional environment of the most productive reservoirs in Saudi Arabia, Arab-D, was subjected to long-standing debate, which has been proposed either deep basinal or shallow lagoonal depositional setting (Powers, 1962; Mitchell et al, 1988; Meyer and Price 1993; Handford

et al., 2002; Lindsay et al., 2006; Al-Awwad and Collins, 2013b). Moreover, the progradational direction of the Arab-D reservoir is a controversial topic, as it has never been demonstrated convincingly (Mitchell et al., 1988; Meyer and Price, 1993; Handford et al., 2002; Lindsay et al., 2006; Al-Awwad and Collins, 2013b). Thus, these issues need to be addressed and brought out clearly in a genetic sequence stratigraphic interpretation and discussion. Therefore, our approach is to integrate, for the first time, the previous biostratigraphic data with new modern a high-resolution sequence stratigraphic transects based on detailed sedimentological measured sections (Fig. 4.1) and subsurface gamma-ray logs (Fig. 4.3). This allows assessment of the unique physiography of the Arabian Platform and controlling factors which promoted the development of carbonate platform and affected its facies distribution and stratal architecture.

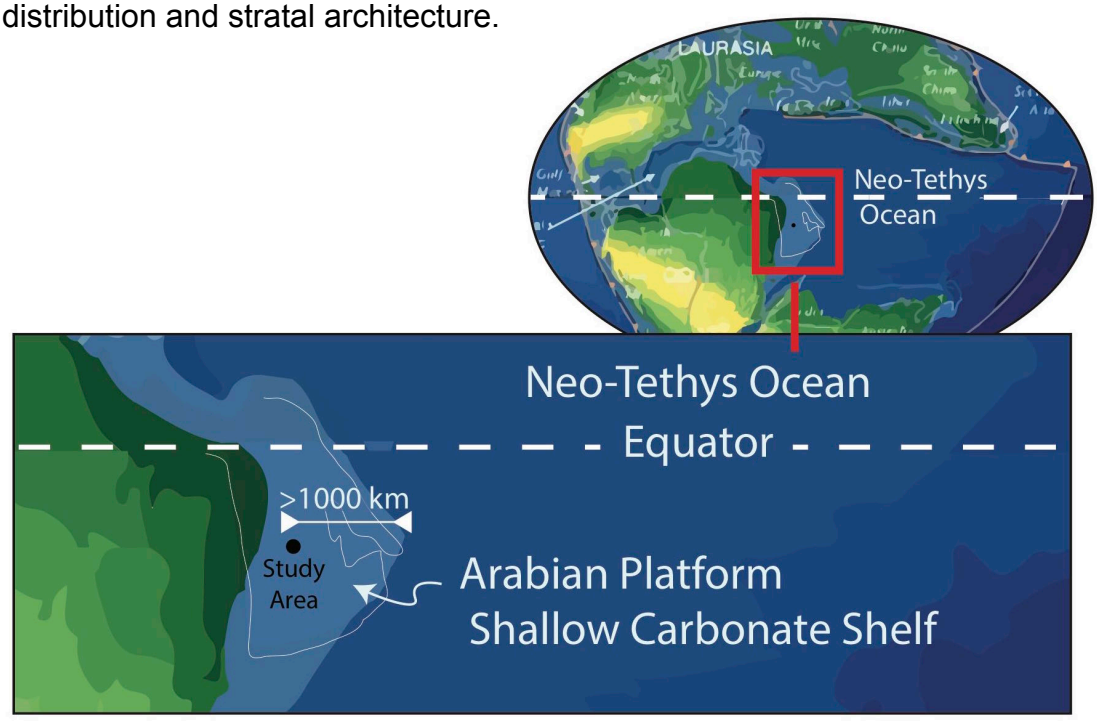

Figure 4.2: Paleogeographic map of the Late Jurassic showing the study area located in the southern margin of the Neo-Tethys Ocean corresponding to an extensive wide shallow-marine continental shelf close to western hinterland. (Scotese, 2003).

4.2 Geological Setting

4.2.1 Tectonic and paleogeographic setting

The study area is located on a tectonically stable central Arabian Plate (Fig.1). Westward, the Proterozoic Arabian Shield is exposed, while the eastern side of the plate exhibit up to 12 km of Phanerozoic sediments (Konert et al., 2001) forming the Arabian Shelf (Pollastro, 2003). The Arabian Shelf structure was partly controlled by pre-existing features of the Precambrian basement (Arabian Craton).

During the early Late Permian, the Neo-Tethys Ocean was generated by Arabian-Asia continental rifting and spreading. Subsequently, the Arabian Plate faced the Neo-Tethys Ocean with a slowly subsiding passive margin with epeiric shallow-water shelf deposits of the Arabian Platform (Murris, 1980). The Arabian Platform remained in a passive margin setting until the Late Cretaceous with the onset of convergence and obduction of the Neo-Tethys margin (Glennie et al., 1995; Le Métour et al., 1990).

The Middle-Late Jurassic transition was probably a time of tectonic instability and tilting. Incipient breaking of the Arabian-Indian plate boundary is marked by a volcanic interruption in eastern Oman (Ziegler, 2001). Eastern Lebanon shows an extensive erosion and karstification at the end of the Middle Jurassic (Callovian). The intrashelf basins became more prominent, well developed and extended further to the south in the Rub' Al Khali (Ziegler, 2001). The intrashelf basins were partitioned by paleohigh or less subsiding zones inherited from the Hercynian orogeny of Paleozoic deformation. The Arabian Platform has continued to evolve from the slightly differentiated carbonate platform during late Middle Jurassic (Callovian) to a shelf with clear

facies differentiation and clinoform geometries during early Late Jurassic (Oxfordian) associated with intrashelf basin (c.f. Figure 24, 25 of Murris, 1980).

The tectonic instability probably extended to the Late Oxfordian-Early Kimmeridgian time. Evidence of post-deposition broad erosion and exposure south of Iraq (southern Gotnia Basin) was attributed to basement faulting and uplift (Sadooni, 1997 in Ziegler, 2001). In Lebanon, volcanic-basalt magmatism and block-faulting is documented (Walley, 2001 in Ziegler, 2001). In Yemen, active rifting initiated from Early Kimmeridgian and lasted up to the Tithonian is marked by a thick succession of open marine deposits (Brannan et al., 1999). In Oman, the Jurassic continental margin is characterized by extensive conglomerate gravity flow deposits by end of the Jurassic (Bechennec et al., 1990). The central part of the Arabian Plate shows an overall inward tilting of the basement blocks marked by eastward thinning of the Late Jurassic sequence towards the shelf margin as documented by regional east-west stratigraphic section (Murris, 1980) and by regional isopach maps (Abu-Ali and Littke, 2005). Consequently, the inner platform has been protected from the open-ocean circulation during Late Kimmeridgian to the Tithonian resulting in a restricted depositional environment marked by carbonate-evaporite successions shown an upward increase in evaporite and decrease in faunal diversity (Hughes, 2004). During the Late Jurassic, the Arabian Platform was located on the southern margin of the Neo-Tethys Ocean, ~10-15° south of the equator (Fig. 4.2; Thierry, 2000; Scotese, 2003). The study area was at this time in the proximal part of the Arabian Platform,

close to marginal marine siliciclastic facies belt and more than 1000 km landward from the Neo-Tethys continental margin (Ziegler, 2001).

4.2.2 Stratigraphic setting

Seven Jurassic formations, mainly consisting of shales, carbonates and lesser anhydrites, form the Shaqra Group (Vaslet 1987), which is very well exposed along the Jabal Tuwayq escarpments. Its lower boundary is represented by a Triassic – Jurassic unconformity with a hiatus of approximately 20 Myr including the Early Jurassic (Hettangian to Pliensbachian), whereas its top is unconformably overlain by the Cretaceous Thamama Group, Sulaiy Formation of Berriasian age (Manivit et al., 1990; Powers, 1968). In an ascending stratigraphic order, the Jurassic formations are the Marrat Formation (Lower Jurassic Toarcian), Dhruma Formation and Tuwaiq Mountain Limestone (Middle Jurassic Bajocian to Middle Callovian), Hanifa Formation, Jubaila Limestone, Arab Formation and the Hith Anhydrite (Upper Jurassic Oxfordian to Tithonian). The biostratigraphy of formations have been defined by the presence of ammonites and subordinate fauna (i.e., nautiles, echinoderms, brachiopods and foraminifera) (Fig. 4.4; Manivit et al., 1990). These formations are separated by disconformities. The upper Jurassic formations are poorly dated and the only confirmed ammonite zone is the Middle Oxfordian (*Plicatilis* Zone) in the Hanifa Formation. Among these upper Jurassic formations, the Hanifa Formation, Jubaila Limestone and lower Arab Formation (Arab-D) present the best outcrop exposures, whereas upper Arab Formation and Hith Anhydrite are deformed and tilted due to anhydrite solutions (they have excluded in this study).

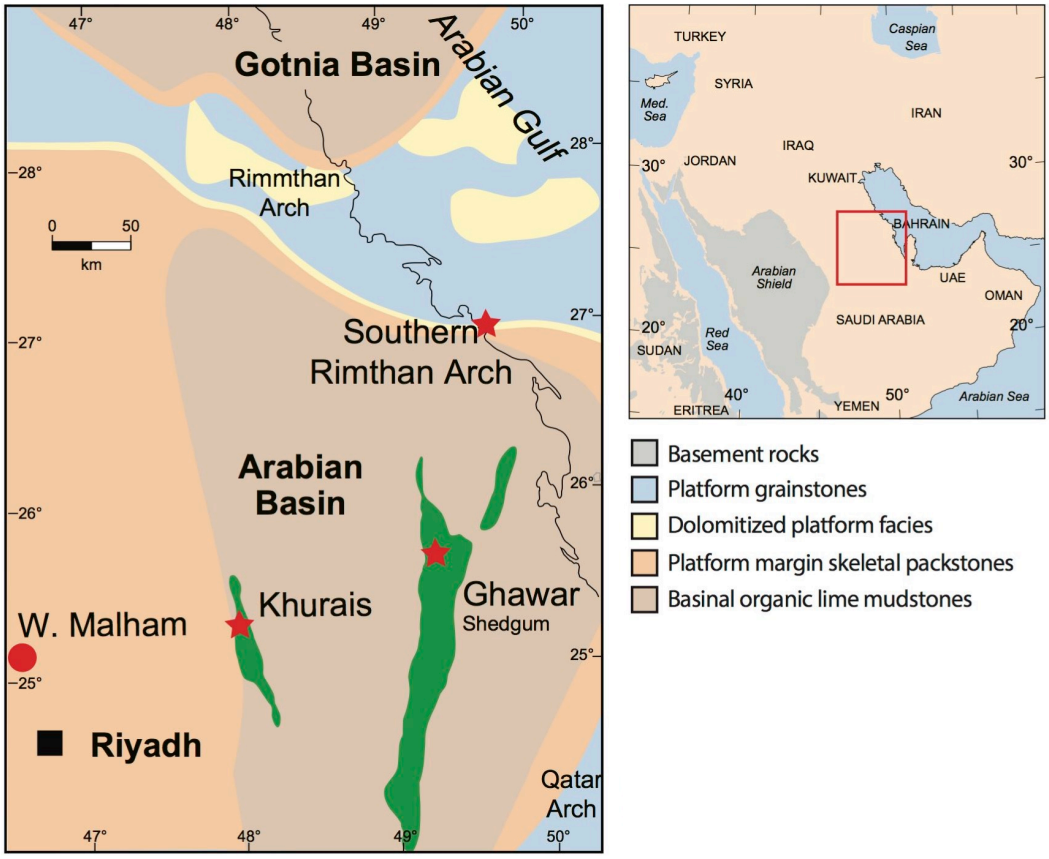

Figure 4.3: Paleofacies map of the Arabian Platform for the Oxfordian shows the outline of the intrashelf Arabian Basin and the studied subsurface areas (red stars). Modified from Mattner and Al-Husseini (2002).

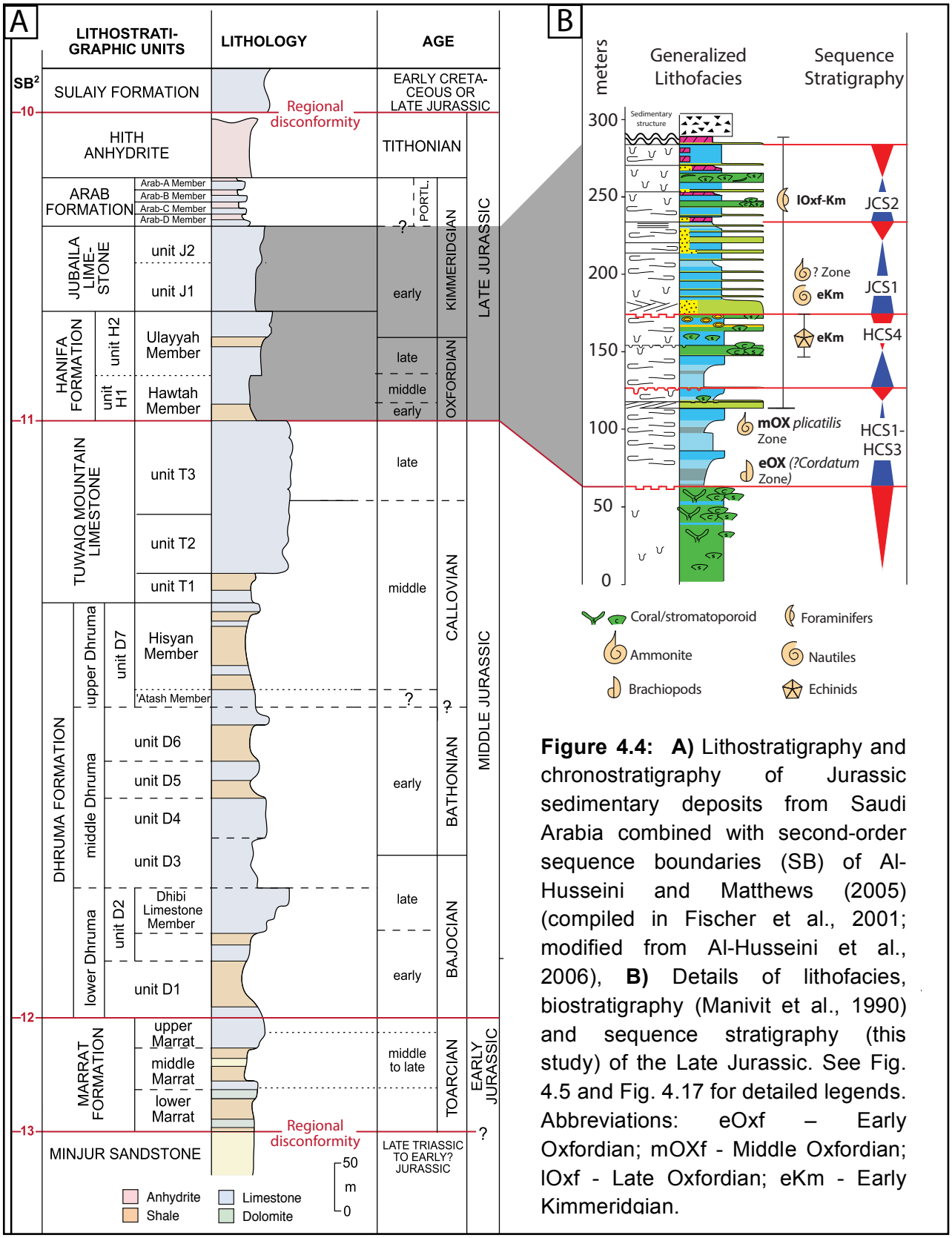

Figure 4.4: **A)** Lithostratigraphy and chronostratigraphy of Jurassic sedimentary deposits from Saudi Arabia combined with second-order sequence boundaries (SB) of Al-Husseini and Matthews (2005) (compiled in Fischer et al., 2001; modified from Al-Husseini et al., 2006), **B)** Details of lithofacies, biostratigraphy (Manivit et al., 1990) and sequence stratigraphy (this study) of the Late Jurassic. See Fig. 4.5 and Fig. 4.17 for detailed legends. Abbreviations: eOxf – Early Oxfordian; mOXf - Middle Oxfordian; lOxf - Late Oxfordian; eKm - Early Kimmeridgian.

4.2.2.1 Hanifa Formation

The basal boundary of the Hanifa Formation shows a sharp lithological contrast between the cliff forming Tuwaiq Mountain Limestone and the base Hanifa shale. The basal boundary corresponds to a stratigraphic hiatus covering the lower part of the Oxfordian (*Mariae* Zone) (Le Nindre, personal communication, 2014; and in Kadar et al., 2015). Moreover, this boundary is known in subsurface to be marked by an erosional surface responsible for the truncation of the last Tuwaiq Mountain sequence in the Rub' al-Khali and northern of the Ghawar field ("pre-Hanifa unconformity" of Powers, 1968). The top boundary of the Hanifa formation is marked by a stained reddened surface but is considered as a conformable surface (Powers, 1968; Manivit et al., 1990). The Hanifa formation is classically divided into two formal members, the Hawtah (H1) and the Ulayyah (H2) members (Vaslet et al., 1983; Fig. 4.4). At the outcrop, the Hawtah Member is always represented by pale yellow calcareous shales at the base. The calcareous shales are interbedded with carbonate beds forming small cuestas on top of the Tuwaiq Mountain Limestone cliff. The lower part of the Member is attributed to the Early Oxfordian (? *cordatum* Zone) based on brachiopod fauna (*Ornithella* gr. *hudlestoni* DAV.) and on nautilus (*Paracenoceras* sp. aff. *arduennense*; Ar Rawdah section) (Manivit et al., 1990). The only confirmed ammonite zone in the Hanifa Formation is Middle Oxfordian (*plicatilis* Zone) based on ammonite fauna (*Euaspidoceras catenaperarmatum* and *Perisphinctidae*?), nautilus (*Paracenoceras* aff. *hexagonum*) and nannoflora (*Vekshinella stradneri*) found in the upper part of the Hawtah Member (Manivit et al., 1990).

Ulayyah Member is characterized by a brown intraclastic grainstone unit at the base and cliff forming reef dominated beds at the top. This member is defined by the first appearance of the foraminifer *Alveosepta Jaccardi.* No ammonite fauna have been found in the Ulayyah Member. However, the member is dated Late Oxfordian based on foraminifera (*Alveosepta Jaccardi*) and brachiopods (*Terebratula bisuffarcinata*) found at the lower half of the member (Manivit et al., 1990). The upper half is dated Early Kimmeridgian based on echinoids (*Monodiadema kselensis* and *Pseudocidaris thurmanni*) and *Alveosepta Jaccar* (Manivit et al., 1990).

The Ulayyah Member is equivalent to Hanifa Reservoir in the subsurface of Saudi Arabia based on micropaleontological examination and correlation (Hughes, 2004). In addition, the upper part of the Hanifa Formation contains an important source rock interval with carbonate organic-rich deposits accumulated in dysoxic intrashelf basins (e.g., Central Arabia and South Arabian Gulf basin) (Ayres et al., 1982; Pollastro, 2003).

4.2.2.2 Jubaila Limestone

The Jubaila Limestone conformably overlies the Hanifa Formation (Manivit et al., 1990; Powers, 1968). This formation is classically divided into two informal units J1 and J2 (Manivit et al., 1985b; Fig. 4.4). The J1 unit is a homogenous limestone unit made up of white cream limestone interbedded with brown bioclastic and intraclastic grainstone beds. This lower unit is dated Early Kimmeridgian based on nautiless (*Paracenoceras* gr*. hexagonum, Paracenoceras* aff*. wepferi*) and an endemic ammonites (*Perisphinctes* aff*. Jubailensis*) (Manivit et al., 1990). The nautiles and ammonites appear only in the middle part of the J1 unit, 25 m above the basal boundary. The J2 unit

starts with reworked bioclastic cross-bedded grainstone followed by highly-bioturbated cream-color mudstone interbedded with intraclastic grainstone. The top of the unit is marked by a cliff-forming carbonate unit made up of highly bioturbated, partially dolomitized limestone including stromatoporoid buildups. The Jubaila Formation is conformably overlain by the Arab Formation (Arab-D Member; Manivit et al., 1990). Contrarily to the Hanifa Formation, the Jubaila Limestone lacks of source rock or intrashelf basin in the nearby subsurface.

4.2.2.3 Arab Formation, Arab-D Member

The Arab Formation is divided into four members A-D (in descending order) (Steineke et al., 1958; Fig. 4.4). The base contact of the Arab Formation has two different lithostratigraphic definitions, considering outcrop and subsurface (Appendix 1). The subsurface Arab-D Member/reservoir (46 m thick in Dammam Well number 7) is bounded at the base by dense mudstone and above by anhydrite (Steineke et al., 1958). At outcrop, the Arab-D Member (~20 m thick; Manivit et al., 1990) is resting on poorly developed reef facies that are included in the Arab-D reservoir in subsurface (Powers et al., 1966; Powers, 1968;). The Arab-D Member begins with bioclastic grainstone and bioturbated limestone containing fine quartz sandstone. The upper part is marked by a brown dolomitic bed capped by stromatolite boundstone. The Arab-D Member ends with collapse breccia interval below the Arab-C Member. The breccia is due to the dissolution of anhydrite between the Arab-D and Arab-C Member, which have been lately defined as Arab-D Anhydrite (*sensu* Mitchell et al., 1988; Appendix 1). The Arab Formation lacks ammonite and is dated Kimmeridgian to Tithonian

based on microfaunal association including benthic foraminifera (Manivit et al., 1990; Hughes, 2009).

The Arab-D reservoir represents one of the most significant oil-bearing intervals in the world. It is considered the primary producing reservoir in the Ghawar Field, the largest oil-field in the world. The Arab-D reservoir contains highly porous and permeable strata which make high flow units called "Super-K" (Meyer et al., 2000). The Arab-D reservoir is capped by an efficient anhydrite cap rock.

4.3 Materials and Methods

This sequence stratigraphic study is based on 14 detailed sedimentological log sections totaling of 1500 m height, and stained thin sections of 120 samples. Moreover, very high-resolution photography technique was used in the field to capture bed forms, bedding geometries and possible lateral facies variations.

The name of the sections and their locations are shown in Figure (4.1) and Appendix (5). The sedimentological data were plotted at scale of 1:200 for the outcrop sections. The sedimentological data include: mineralogy, color, sedimentary structures, extended Dunham texture (Dunham, 1962; Embry and Klovan 1971), grain types, grain size, and fossil types and bioturbation. The vertical and lateral stacking patterns were analyzed in order to interpret different scale of depositional sequences and sequence boundaries. The sequence stratigraphic terminology in this study is adapted from Mitchum and Van Wagoner (1991).

High-resolution stratigraphic correlations have been defined using field physical correlation and sequence stratigraphic concepts. These outcrop and

sedimentological-based sequences evidenced at outcrops have been extended to the main hydrocarbon fields in the subsurface in a dip-section using gamma-ray logs of shallow outcrop cores (MQBL-1 and WDLB-1) and near outcrop well (Riyadh).

The sequence stratigraphic cross-sections are complemented with biostratigraphic data of Manivit et al. (1990). The stratigraphic locations of the key biostratigraphic elements (e.g., ammonite faunas) are shown on the cross-section. The cross-section of the Jubaila and Arab-D Member is supplemented with an additional measured section (Wadi Al Majami, 21° 04' N) from Vaslet et al. (1985).

4.4 Facies and depositional environment

The facies and depositional environments of the Hanifa Formation, Jubaila Limestone and Arab-D Member (Oxfordian and Kimmeridgian) at outcrops are summarized in Table (4.1 and 4.2). The regional facies distribution is shown in figure (4.5, 4.6 and 4.27). Selected detailed sedimentological sections are shown in figure (4.17, 4.18, 4.19 and 4.20). The spatial distribution of the facies are shown in sequential depositional models (Fig. 4.21 and 4.22) illustrate the evolution of the depositional systems in response to a third-order relative sea-level changes. There are twelve facies or facies associations representing the Hanifa Formation, Jubaila Limestone and Arab-D Member. The facies are grouped in four depositional environments, which comprise from proximal to distal: arid shoreline, mixed carbonate-siliciclastic inner lagoon, carbonate inner lagoon and back-barrier lagoon.

The facies analyses give important indications for interpreting the mechanism of sedimentation and depositional environments. However, the

interpretation of depositional environments are not always unequivocal, particularly the water depth and lagoonal versus offshore setting of some facies. This is because the depositional system is complex as it evolves through time within a depositional sequence and during the whole Late Jurassic period. Therefore, the interpretation of the depositional environments went through an iterative process between facies description, vertical and lateral facies distribution and relationship by using Walther's Law, stratigraphical geometry (clinoform versus tabular or parallel) and paleogeographical location of the facies.

4.4.1 Arid evaporitic shoreline and lagoon

F1: Anhydrite solution collapse breccia: subaqueous salina

This facies occur only at the top of the Arab-D Member and is equivalent to the Arab-D Anhydrite in the subsurface (Sharief et al., 1991). It appears as 4 to 5 m tabular units, having gradational base and top. These laterally extensive units retain constant stratigraphic position (Fig. 4.7A, B and C). The breccia is made up of cm- to dm-sized angular clasts and round molds. The blocks are composed of limestone, dolomite and rare remnant of anhydrite clasts joined by very fine dolomitic matrix. These units exhibit karstic collapse features and highly deformed rotated units. They are interpreted to be formed mainly in a subaqueous salina (McGuire et al., 1993; Handford et al., 2002; Lindsay et al., 2006), and to a lesser extent, in sabkha depositional environment (Al-Awwad and Collins, 2013a).

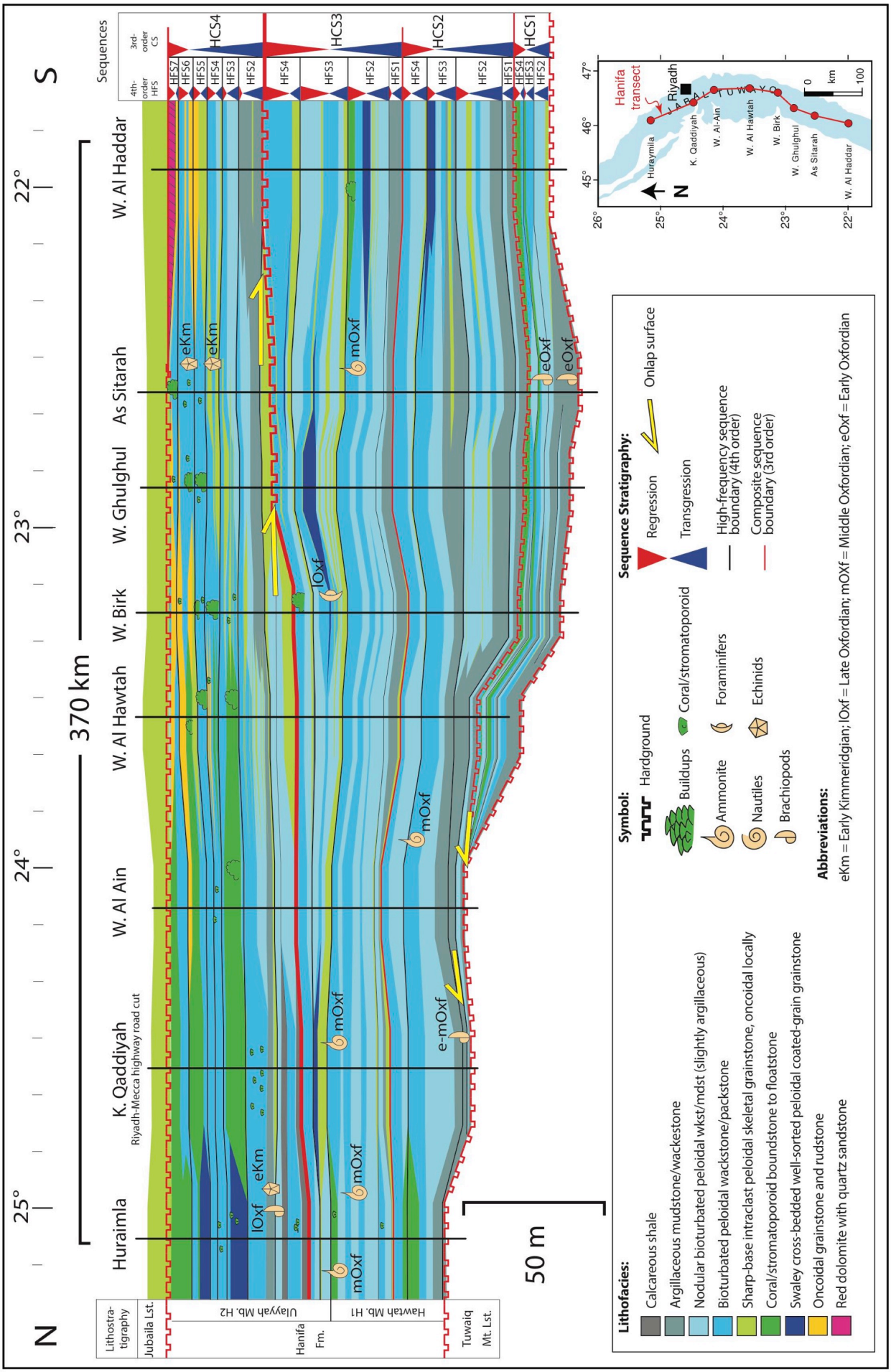

Figure 4.5: High-resolution sequence stratigraphic cross-section of the Hanifa Formation.

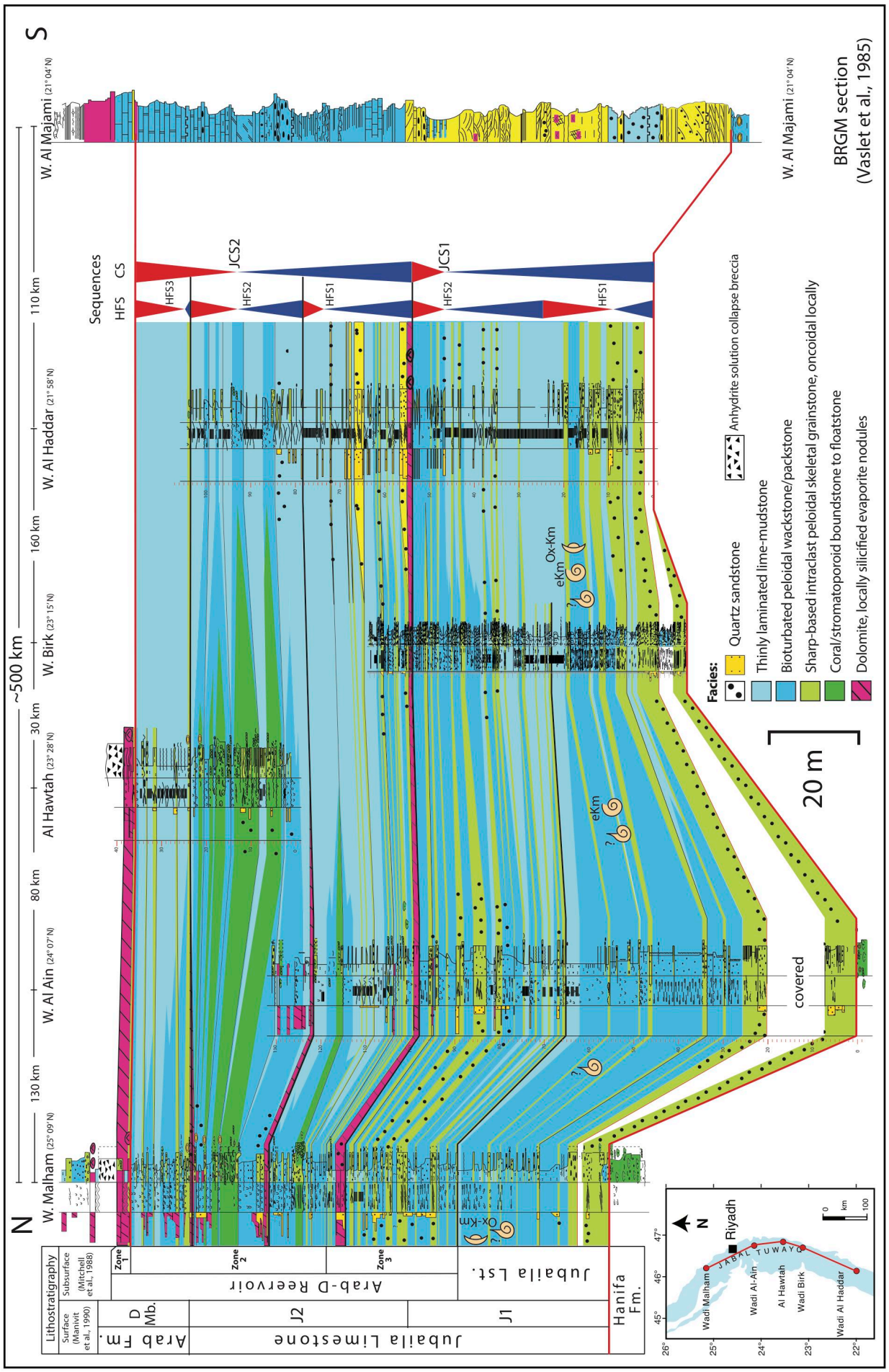

Figure 4.6: High-resolution sequence stratigraphic cross-section of the Jubaila Limestone and Arab-D Member. For symbol legend see Fig .4.5 and 4.17.

F2: Red dolomite: tidal-flat to restricted lagoon

This facies occur at the top most of the Hanifa Formation in the southern outcrop (Wadi Al Haddar) and is common in the upper Jubaila Limestone J2 unit and Arab-D Member (Fig. 4.7D, E, F, G, 4.14A, and B; Table 4.1 and 4.2). The red dolomites are extensive tabular units, 0.3 to 2.5 m thick. The facies have sharp base and top boundary. They are usually massive, structureless, with occasional preserved bioturbation traces. In the Jubaila Limestone J2 unit, rare cross-bedding sedimentary structures (Fig. 4.20A) and local silicified evaporite nodules (Wadi Al Haddar) are present in this facies. In the Arab-D Member underneath the collapse breccia, the facies has crinkly laminated structure associated with silicified evaporite nodules (Wadi Malham). They are made up of mud- and grain-supported texture with fabric preserving very-fine to fine rhombic dolomite crystals. The dolomites are associated with medium to coarse peloids and sandstone quartz.

These dolomitic beds are interpreted to form in response to highly evaporitic conditions in restricted tidal-flat and lagoons, associated with periods of non-deposition (Swart et al., 2005). The increase in dolomite facies occurrence around the sequence boundaries (Fig. 4.7F, 4.20A, B) suggests a control by low accommodation rates on the formation of the dolomites. Moreover, the long-term climate changes, with increasing warming and aridity, during Late Jurassic have an influence on the dolomite distributions.

Table 4.1: Hanifa Facies.

Depositional environment	Arid shoreline	Mixed carbonate-siliciclastic inner lagoon			Carbonate inner lagoon		Back-barrier lagoon		
Facies and sub-depositional environment	F2: Red dolomite: *tidal-flat to restricted lagoon*	F4: Calcareous shale and argillaceous lime mudstone to packstone: *shale-dominated inner-lagoon*	F4: Argillaceous mudstone to packstone (*shale dominated inner lagoon*)	F5: Nodular bioturbated peloidal wackestone /mudstone: *inner lagoon*	F7: Bioturbated peloidal lime mudstone to packstone*: highly bioturbated lagoon*	F8: Sharp-based intraclast-peloidal skeletal grainstone, oncoidal locally: *storm-dominated inner-platform*	F9: Oncoidal packstone, grainstone and rudstone: *oncoidal bars/shoal*	F10: Coral/stromatoporoid boundstone to floatstone*: low-energy and high-energy back-barrier*	F11: Cross-bedded coated-grain and peloidal grainstone: *shoal and washover complex*
Thickness	0.3 - 2 m	0.5 m	2–9 m	1-11 m	1.5-6 m	0.1 – 3.5 m	0.25 – 2 m	1.5 – 8 m	0.4 – 7 m
Color	Light red	Grayish green; occasionally reddish brown	Creamy white and light grayish green	Creamy white to very light gray	Creamy white	Light gray to light brown	Creamy white	Creamy white	Creamy white
Depositional texture and grain types	Fabric-preserving very fine to fine grained dolomite crystal, peloids and silt quartz, mud-support texture	Terrigenous clay and argillaceous mudstone, fissile to concoidal soft parting	Terrigenous clay, silt size pelletal grains lime mudstone	Terrigenous clay, very fine to medium peloidal wackestone/ lime-mudstone	Silt to very fine pelletal and medium peloidal grains, occasional very coarse forams bioherms of coral/stromatoporoid, lime-mudstone to packstone texture	Fine to medium peloids, coated-grains and granular to cobbles reworked intraclasts and skeletal debris, grainstone rudstone/floatstone texture, fitted fabric and chemical compaction	Coarse to very coarse coated-grains, granular to pebbles oncoid (type 2 and 3), may have intraclasts and reworked coral/stromatoporoid heads	Cobbles size of coral/ stromatoporoid in, tabular and head shapes locally up to 50 cm diam. and 30 cm thick; coarse skeletal fragments, fine peloidal grains lime-mudstone to grainstone and floatstone	Well sorted very fine to fine peloidal and medium coated grain grainstone
Bedding and sedimentary structures	Tabular units, structureless or slight bioturbated	Sharp and gradational base, tabular units, commonly associated with *Chondrites* burrows	Gradational base, tabular units, abundant *Chondrites* burrows, occasional thinly laminated mudstone	Gradational base, tabular units, horizontal thin bioturbation, some *chondrites* burrow, argillaceous wispy solution seams, nodular structure	Gradational base, laterally extensive tabular units, highly bioturbated, may have argillaceous wispy solution seams, rare nodular structure, top firmground and hardground surfaces	Scoured and sharp base, graded layer; tabular, lenticular and occasionally channelized units; parallel/HCS and wave-ripple laminated; wave ripples, some *Chondrites* burrows	Sharp base, lenticular units; cross-bedded, massive and bioturbated sedimentary structure	Gradational base, tabular units, bioherms reach up to 15 m diam. and 4 m thick; highly bioturbated, occasional microbial laminated fabric, top firmground surfaces	Sharp and gradational base, occasionally upward coarsening ; tabular, lenticular, channelized units, trough cross-bedded, thinly plane-laminated, HCS/SCS; highly bioturbated
Stratigraphic occurrence	Top Hanifa Formation	Base Hanifa Fm.; base Hanifa composite sequences	Base Hanifa Fm.; base Hanifa composite sequences	All Hanifa Formation	All Hanifa Formation; dominated in HST	Mainly in upper Hanifa Formation (Ulayya Mb.; H2 unit)	Most top Hanifa Formation; HST of HCS2	All Hanifa Formation; dominated in upper Hanifa Formation (Ulayya Mb.; H2 unit)	All Hanifa Fm., dominated in upper Hanifa (Ulayya Mb.; H2 unit)
Fossils		Echinoderm, brachiopod, bivalve (*Pholadomya*) (Manivit et al, 1990)	Rich with sponge spicules	Rich with benthic foraminifera (Kurnubia jurassica, Lenticulina sp.) and sponge spicules	Rich with benthic foraminifera (*Alveosepta jacardi, Kurnubia jurassica*)	Gastropods (*Nerinea* sp.), dasyclad (Clypeina), benthic foraminifera (*Lenticulina* sp., *Kurnubia jurassica*)	*Cladocoropsis, d*asyclad (*Clypeina*), benthic foraminifera (*Kurnubia jurassica, Redmondoides lugeoni*)	*Cladocoropsis,* benthic foraminifera (*Alveosepta jacardi, Kurnubia jurassica, Redmondoides lugeoni*)	Echinoderm, brachiopod, gastropod

Table 4.1: Jubaila Limestone and Arab-D facies

Depositional environment	Arid shoreline/lagoon		Inner lagoon				Back-barrier lagoon
Facies and sub-depositional environment	F1: Anhydrite solution Collapse breccia: *subaqueous salina*	F2: Red dolomite: *tidal-flat to restricted lagoon*	F3: Cross-bedded quartz sandstone: *shallow-marine sand-flat*	F6: Thinly laminated barren lime mudstone: *restricted inner-lagoon*	F7: Bioturbated peloidal lime mudstone to packstone: *highly bioturbated lagoon*	F8: Sharp-based intraclast-peloidal skeletal grainstone, oncoidal locally: *storm-dominated inner-platform*	F10: Coral/stromatoporoid boundstone to floatstone*: low-energy and high-energy back-barrier*
Thickness	4 - 5 m	0.5 – 2.5 m	0.2 – 2 m	0.2 – 10 m	0.5 – 10 m	0.1 – 3 m	1 – 5 m
Color	Grayish Pink	Grayish Red	Grayish Red	Light gray	Creamy white	Light gray to light brown	Creamy white
Depositional texture and grain types	Breccia composed of cm- to dm-sized clasts of limestone and dolomite with dolomite cement matrix	Fabric-preserving very fine to fine grained dolomite crystal, medium to coarse peloids and sandstone quartz, mud-support to grainstone texture	Medium to very-coarse grained, skeletal fragments, commonly cemented by carbonate	Silt-sized pellets and few percent of very fine sand quartz, barren lime-mudstone	Silt to very fine pelletal and medium peloidal grains, very coarse forams and skeletal debris, lime-mudstone to packstone texture	Fine to medium peloids, oncoids and granular to cobbles reworked intraclasts and skeletal debris, grainstone rudstone/floatstone texture	Cobble size of coral/ stromatoporoid in tabular and head shapes; coarse to pebble skeletal fragments, fine peloidal grains grainstone and floatstone rudstone texture
Bedding and sedimentary structures	Gradational base, laterally extensive tabular units; karstic collapse features	Scoured based, extensive tabular units, bioturbated to structureless	Sharp base, tabular and lenticular units, plane-lamination, wave-ripple lamination and large cross-stratification, highly bioturbated	Sharp to gradational base, lenticular to laterally extensive tabular units, non-bioturbated, hummocky cross-stratification, locally dewatering structure	Gradational base, laterally extensive tabular units, highly bioturbated, may have argillaceous wispy solution seams, nodular structure, top firmground and hardground surfaces	Scoured and sharp base, graded layer; tabular, lenticular and occasionally channelized units; parallel/HCS and wave-ripple laminated; wave ripples, locally dewatering structure	Sharp base, tabular units, bioherms reach up to 4 m diam. and 2 m thick; highly bioturbated, top firmground surfaces
Stratigraphic occurrence	Arab-D Member Zone1, Above Jubaila composite sequence	Arab-D Member Zone1, Above Jubaila composite sequence	Base Jubaila Limestone and J2 unit	Jubaila Limestone and Arab-D Member	Jubaila Limestone and Arab-D Member	Jubaila Limestone and Arab-D Member	Jubaila Limestone J2 unit, Arab-D Reservoir zone 2
Fossils	N/A	None to sparse, debris of shells	Some shell debris	None	Rich with benthic foraminifera (*Alveosepta jacardi, Kurnubia jurassica*); sponge spicules	Benthic foraminifera (*Lenticulina* sp., *Kurnubia jurassica*)	Benthic foraminifera (*Alveosepta jacardi, Kurnubia jurassica*)

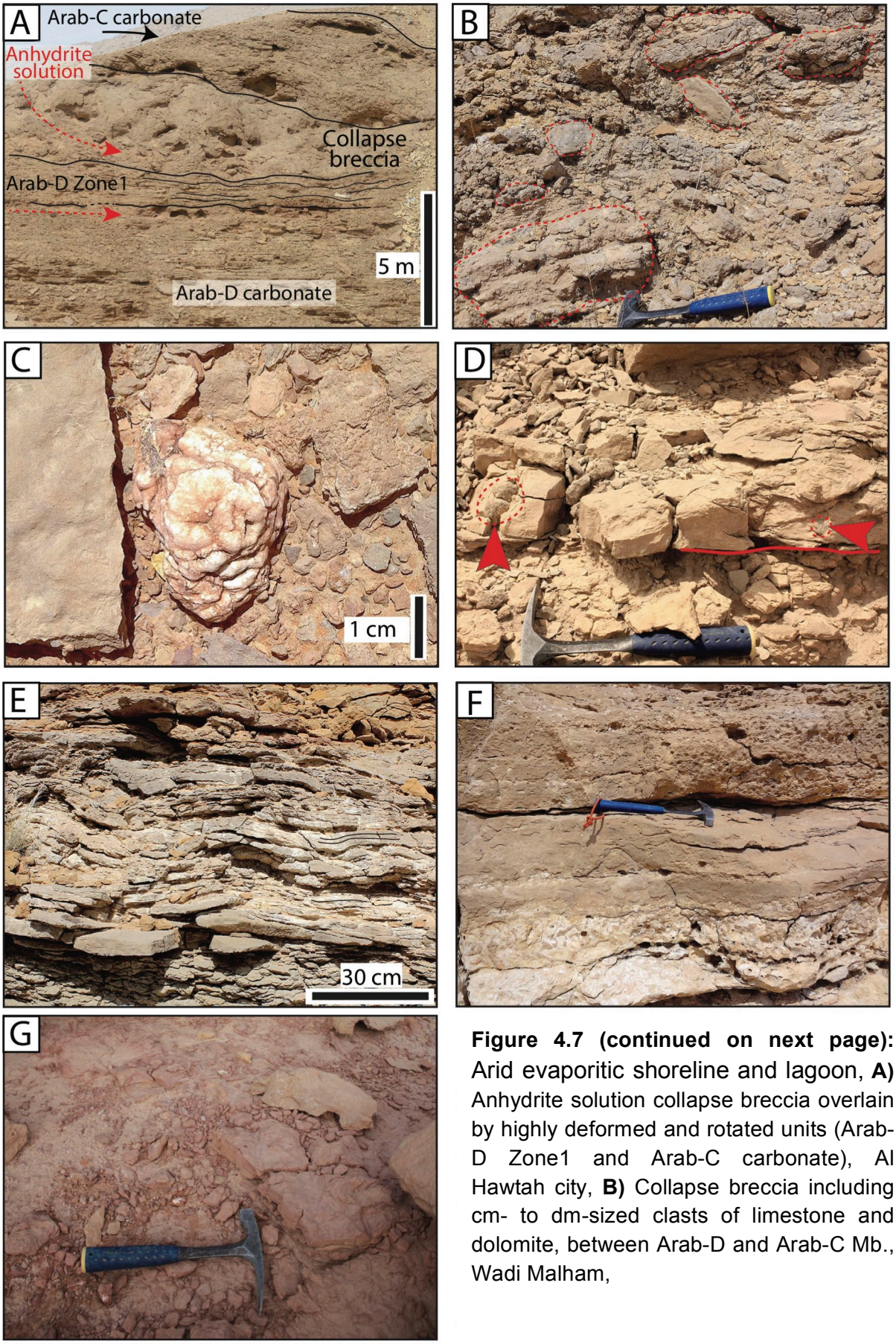

Figure 4.7 (continued on next page): Arid evaporitic shoreline and lagoon, **A)** Anhydrite solution collapse breccia overlain by highly deformed and rotated units (Arab-D Zone1 and Arab-C carbonate), Al Hawtah city, **B)** Collapse breccia including cm- to dm-sized clasts of limestone and dolomite, between Arab-D and Arab-C Mb., Wadi Malham,

← **Figure 4.7 (continued): C)** Rare presence of evaporite clasts around the collapse breccia, between Arab-D and Arab-C Mb. Wadi Malham, **D)** Grayish red dolomite with silicified evaporite nodules (red arrows) and sharp based contact (red line) (restricted lagoon), Jubaila J2 unit, Wadi Al Haddar, **E)** Light gray stromatolitic dolomite slightly rotated due to underlying anhydrite solution, (tidal flat), Arab-D zone1, Wadi Malham, **F)** Bioturbated mud-support dolomite with sand quartz, degree of dolomitization increased upward (restricted lagoon), Jubaila J2 unit, Wadi Malham, **G)** Red dolomite with silt quartz (restricted lagoon), Hanifa Fm., Wadi Al Haddar.

4.4.2 Mixed carbonate-siliciclastic inner lagoon

F3: Cross-bedded quartz sandstone: shallow-marine sand-flat

The facies are well developed only in the Jubaila Limestone in the most southern section (Wadi Al Haddar). These facies form tabular units up to 0.2 to 2 m thick (Fig. 4.8A). The facies consist of medium to very coarse-grained sandstone and skeletal fragments and carbonate cement. The sandstones are characterized by plane-laminations, 2D mega-ripple cross-bedding and subordinate wave-ripple laminations. Bioturbation is common. The facies are commonly interbedded with barren thinly laminated lime mudstone (F6). They can be sharply overlain red dolomite with silicified evaporite nodules (F2) at base of a depositional cycle in Wadi Al Haddar.

They are interpreted as shallow marine sand-flat deposits. The plane and wave-ripple laminations attest to wave generated currents in upper shoreface setting (cf. Reynolds, 1995). The intimate occurrence above the non-depositional related red dolomite beds (F2) suggest that the laminated sandstone were deposited in a proximal setting, beach or shoreline environment. The interfingering of low-energy lime mudstone facies (F6) indicates that a time of storm-generated currents are frequent and wave-base is probably relatively shallow.

F4: Calcareous shale and argillaceous lime mudstone to packstone: shale-dominated inner-lagoon

The facies appear only in the Hanifa Formation, particularly in the lower part of the Hawtah Member (H1) and at the base the Ulayyah Member (H2). The facies form extensive tabular units, 0.5 to 9 m thick displaying gradation base and top (Fig. 4.8B, 4.9A). The argillaceous lime mudstones/packstone consist of silt-size pelletal grains and rich with sponge spicules (Fig. 4.15A), echinoderms, brachiopods and bivalves (*Pholadomya*) (Manivit et al, 1990). The facies have concoidal soft parting (Fig. 4.8C, D) with occasional thinly laminated sedimentary structure and common *Chondrites* burrows. The facies are interbedded with nodular bioturbated peloidal wackestone/mudstone and sharp-based storm generated grainstones.

This low-energy facies is interpreted to be deposited in shale dominated shallow marine inner platform setting during transgressive stages. The terrigenous content is related to both the reworking of shale deposits during the transgressive process and to a paleogeographical location close to the terrigenous influx. At a regional scale, the shale content decrease and the facies are more and more carbonaceous from the proximal to the distal part of the inner platform. The associated storm-generated grainstone beds suggest that the inner platform were occasionally influenced by storm events. The predominance of *Chondrites* burrows imply an overall restricted low-oxygenated bottom water (Bromley and Ekdale, 1984) which could be attributed to the proximality to the hinterland freshwater runoff and high nutrient supply that cause water stratification and prevent vertical circulation (Bottjer et al., 1986 in Read, 1989; Rabalais et al., 1991; Lukasik et al., 2000).

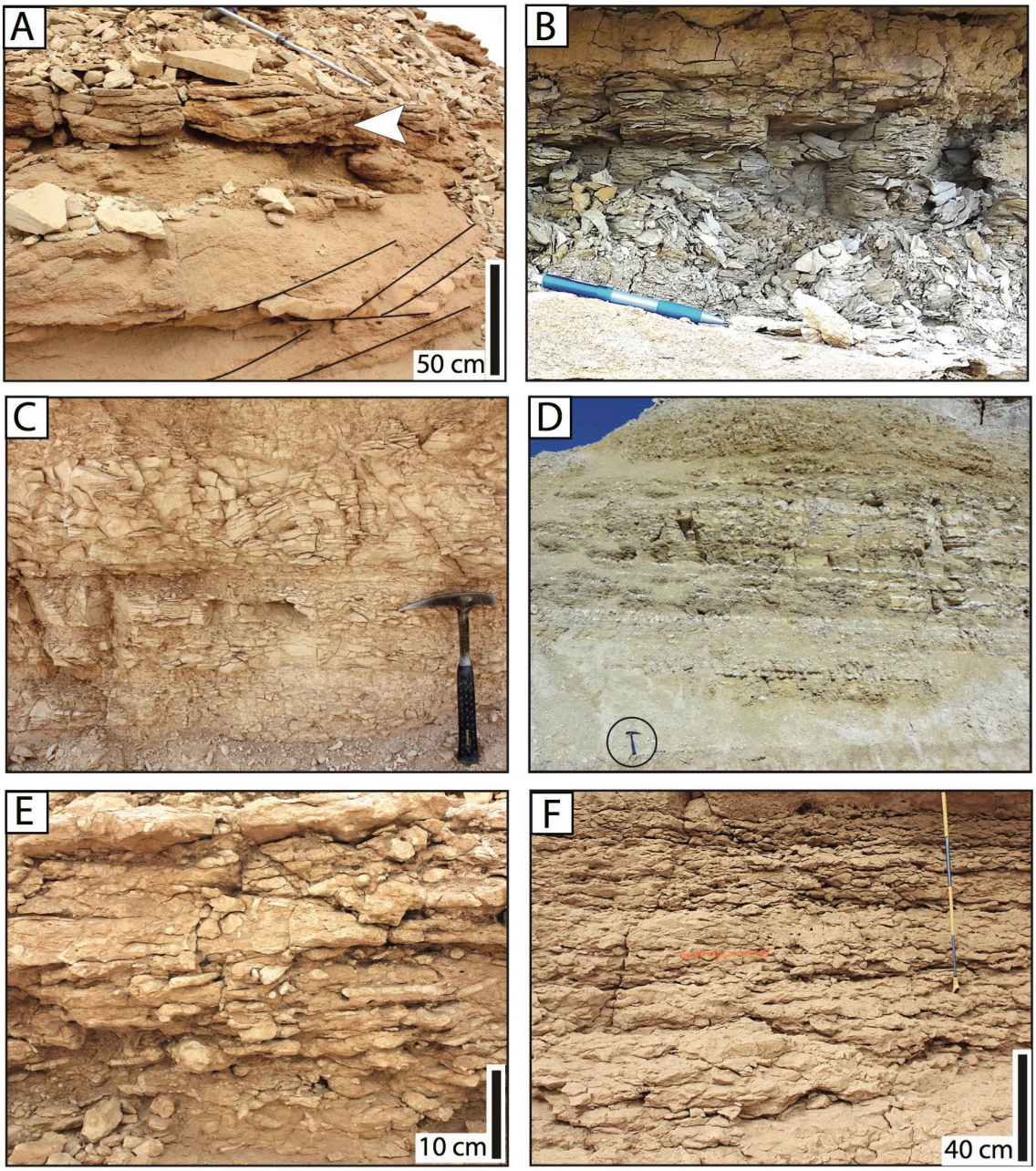

Figure 4.8: Mixed carbonate-siliciclastic inner lagoon facies association. **A)** Large-scale cross-bedded and wave-ripple laminated (arrow) sandstone (coastal shallow-marine), Jubaila J2 unit, Wadi Al Haddar, **B)** Calcareous shale (inner lagoon), road cut of the Riyadh-Mecca highway near Khashm Qaddiyah, **C)** Argillaceous mudstone (shale dominated inner lagoon), Wadi Birk, **D)** Argillaceous wackestone to packstone (shale dominated inner lagoon), hammer for scale at the base of Hanifa Formation/Top of Tuwaiq Mountain Limestone, Huraimla, **E and F)** Slightly argillaceous nodular horizontal bioturbated peloidal wackestone/lime-mudstone (inner lagoon), Wadi Birk.

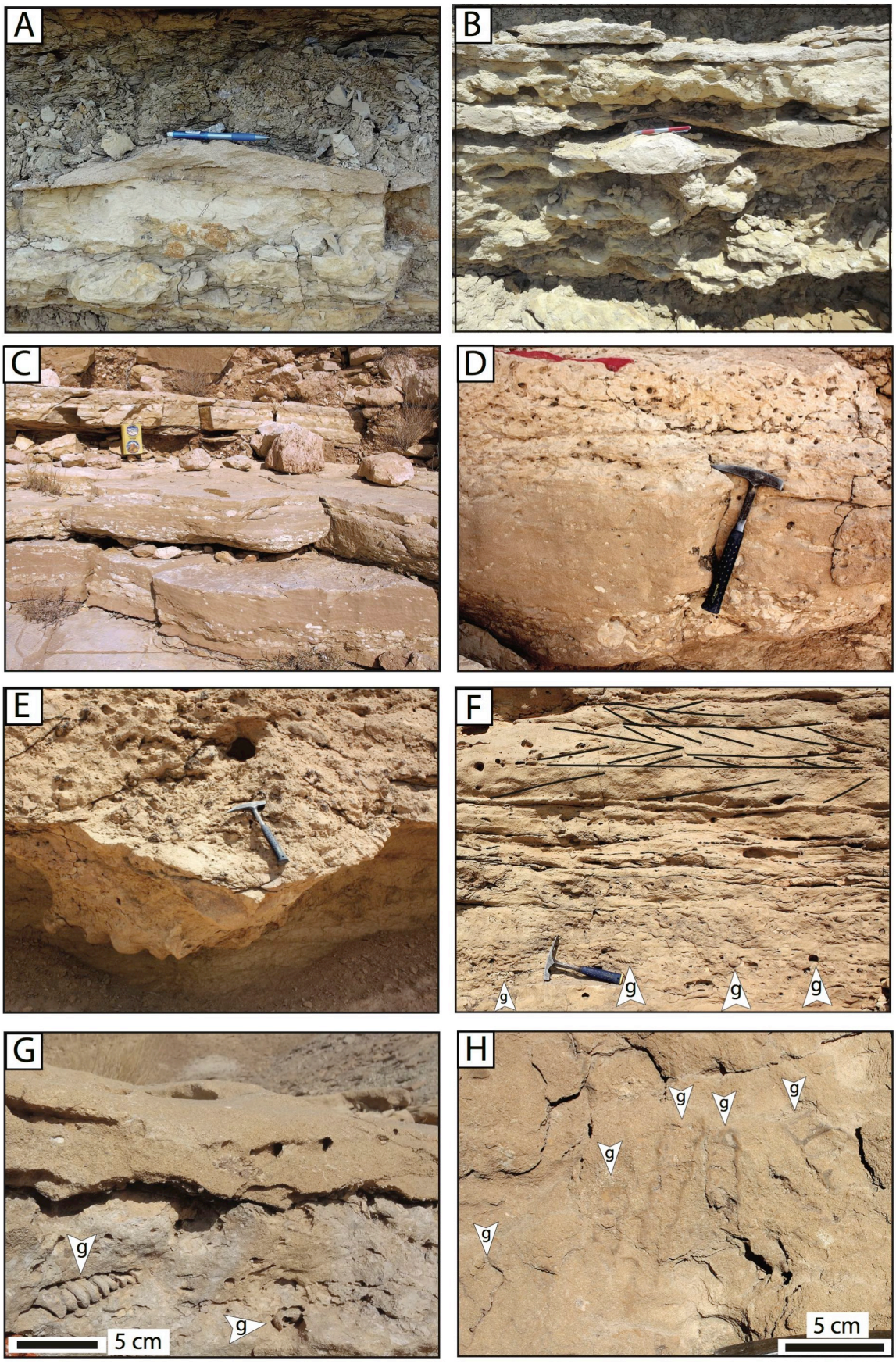

Figure 4.9 (continued on next page): Storm dominated inner-platform facies association in the Hanifa Formation. **A)** Sharp-based lenticular peloidal skeletal grainstone with wave ripples overlain by calcareous shale (inner lagoon), road cut of the Riyadh-Mecca highway near Khashm Qaddiyah,

← **Figure 4.9 (continued): B)** Sharp-based lenticular peloidal skeletal grainstone with wave ripples intercalated with nodular horizontal bioturbated peloidal wackestone/lime-mudstone (inner lagoon), road cut of the Riyadh-Mecca highway near Khashm Qaddiyah, **C and D**) Sharp-base fining-upward intraclast peloidal skeletal grainstone (inner lagoon), field notebook (15 cm) for scale in C , Wadi Birk, **E)** Channel-like sharp-based intraclasts reworked coral/stromatoporoid skeletal grainstone (storm dominated inner-platform), Wadi Birk**, F)** Peloidal coated-grain grainstone and floatstone rich with large gastropods (Nerinea sp.) at the base (g arrows) that grades up to tabular sets of bidirectional cross-bedding (tidally influenced inner platform), As Sitarah, **G and H)** Sharp-based coated-grain skeletal grainstone rich with large gastropods (*Nerinea* sp.) (g arrows) (storm dominated inner platform), Wadi Ghulghul.

F5: Nodular bioturbated peloidal wackestone/mudstone: inner lagoon

The facies occur in all the studied sections. It forms tabular units, 1 to 11 m thick, with gradational base and top boundary (Fig. 4.8E, F). This facies consist of an alternation of cm-thick beds of mudstone-wackestone and packstone-grainstone where the heterolithic stratification is most of the time completely destroyed by an intense bioturbation. This bioturbation is responsible for the highly nodular aspect of this facies. The mudstone and wackestone are composed of silt-size pelletal grains and very fine to medium-grained peloids. The facies consist mainly of benthic foraminifera (*Kurnubia jurassica, Lenticulina* sp., *Nautiloculina oolithica)* and sponge spicules (Fig. 4.15B, 4.16G). Less frequent echinoderms and brachiopod, minor encrusted stromatoporoid/coral (Fig. 4.19B), and very rare biohermal stromatoporoid/coral buildups (Fig. 4.19A) are also present. Within less bioturbated intervals, wavy lamination and wave ripple cross-lamination can be preserved. The bioturbation is characterized by horizontal type of burrows and trails *Planolites* and some *Chondrites*. In the Hanifa Formation, these

facies are interbedded with calcareous shale and argillaceous mudstone to packstone (F4), and with sharp-based very-coarse grained skeletal grainstone (F8) (Fig. 4.9B, E; 4.18). In the Jubaila Limestone, the associated facies are not argillaceous and mainly represented by thinly laminated lime mudstone (F6) and sharp-based intraclasts oncoidal peloidal skeletal grainstones (F8).

The fine-grained deposits indicate for broad low energy environments. The heterolithic stratification and the alternation lime mudstone and grainstone suggest an intermittent storm and current influence. As the bioturbation have destroyed the sedimentary structure, it is difficult to identify the type of current controlling the deposition. Intercalations of storm beds are probably present suggesting a low energy wave dominated environment with record of some higher amplitude storm events. Unfortunately, no direct sedimentological arguments and no definitive biofacies evidence for either deep-water upper offshore environment or shallow marine protected inner platform.

4.4.3 Carbonate inner platform

F6: Thinly laminated barren lime mudstone: restricted inner-lagoon

These facies occur only in the Jubaila Limestone and Arab-D Member. They are common in proximal areas (south), from the lower part until just beneath the anhydrite dissolution collapse breccia of the Arab Formation (Fig. 4.6, 4.20A). These facies forms extensive tabular units, 0.2 to 10 m thick, with transitional base and top (Fig. 4.11A, B, C; Table 4.2). They are made of with lime mudstone composed of silt-sized pellets and few percent of very fine sand quartz. These mudstones are barren and non-biorubated. They exhibit thin horizontal to low angle undulated lamination, rare hummocky cross-

stratification, wispy laminations, dewatering and soft deformations structures. They are usually interbedded with thin storm-generated grainstone and sandstone layers (F8).

These barren and non-bioturbated lime mudstones are interpreted to be deposited in a restricted poorly oxygenated inner-lagoon occasionally subjected to high-energy storm pulses. The low-angle undulated laminations and the mechanical sedimentary structures of the lime mudstone evidence for episodic wave and current action at speed reaching 50 cm/sec (Schieber et al, 2007; Schieber et al., 2013; Al-Awwad and Pomar, 2015; Frébourg et al., 2016). The precipitation of such barren thick shallow-water lime-mudstone is probably influenced by cyanobacterial photosynthesis process as part of the Jurassic neritic lime-mud factory (Pomar and Hallock, 2008). Consistently, the microbial calcification was at optimum level during the Late Jurassic (Riding, 2000; Riding and Liang; 2005). In such proximal nearshore setting, high nutrient input associated with terrigeneous influx generally promote and increase calcareous algal productions (Hallock, 2001). Subtle increase of nutrient input can result in a modification of the benthic community environment (“phase shift” of Hallock, 2005) by limiting the light penetration (Hallock, 2001) and rising the dasycline level (Alnazghah et al., 2013). These environmental evolutions responsible for the disappearance of the shallow component community (e.g., dasyclads, oncoids, benthic forams). On the other hand, other workers interpreted these facies as part of internalite facies association and process in deep depositional setting in the near by subsurface (Al-Awwad and Pomar, 2015). However, the facies are most common in the proximal part of the system to the south and decrease to the

north- and westward toward the ocean. Moreover, based on their stratigraphic position at the topmost of the Jubaila sequence underneath the sequence boundary and the Arab evaporites, it is supposed that the facies may correspond to the regression and closing of the depositional system. The incorporation of the regional stratigraphic and paleogeographic position together with the associated sandstone reflects the proximity to the detrital source in relatively proximal setting.

F7: Bioturbated peloidal lime mudstone to packstone: highly bioturbated lagoon

These facies occur in all the studied sections. They appear as creamy white extensive 0.5 to 10 m thick tabular units (Fig. 4.11D, E, F, 4.15E). Firmground and hardground occasionally interrupt the sedimentation of this facies. The facies usually interbedded with slightly argillaceous nodular bioturbated peloidal wackestone/mudstone (F5). Intercalations of storm-generated grainstones (F8) may exist. The lime mudstone to packstone facies consists of silty to very fine pelletal and medium peloids together with occasional large forams. The biological content includes ammonite, nautiles, echinoderms, brachiopods, bivalves, rich with benthic foraminifera (*Alveosepta jacardi*; *Kurnubia jurassica, Redmondoides lugeoni*) and lesser sponge spicules (Fig. 4.16H). An intense bioturbation with branched vertical burrows (*Thalassinoides*) tends to homogenize the sediments and destroy the primary sedimentary structures. Moreover, they may have argillaceous wispy solution seams and rare nodular sedimentary structures. Cm to dm thick sharp-based storm generated grainstone layers (F8) are commonly intercalated in the bioturbated lime mudstone to packstone (Fig. 4.19B, E).

Coral/stromatoporoid batch reef (F10) can also be locally associated with this bioturbated lime mudstone to packstone facies in the Hanifa Formation (Fig. 4.19B, E).

The facies are interpreted to be formed in a low-energy protected lagoon. This low–energy environment is episodically disturbed by storm event responsible for the deposition of thin grainstone layers. The regional extensive of these facies, the little interior lateral facies changes and the dominant muddy carbonate texture reflect a shelf lagoonal deposits (Wilson and Jordan, 1983). The high diversity of fauna, the abundant benthic forams and the associated ammoniate and coral/stromatoporoid, the light color of this facies and the intense bioturbation suggest a well-oxygenated environment and normal marine condition (Wilson and Jordan, 1983; Galli, 1993; Khetani and Read, 2002). The facies are most common at the top of depositional sequence and more dominate in the distal part of the studied in the north. The associated normal marine fauna together with the regional stratigraphic positions are suggesting distal lagoonal depositional environment.

F8: Sharp-based intraclast-peloidal skeletal grainstone, oncoidal locally: storm-dominated inner-platform

The facies occur in all the studied sections in both Hanifa and Jubaila formations. Most of the time, it appears as sharp-based decimeter-thick individual beds. The top surface of the beds is generally sharp, sometimes with current and/or wave ripple marks and trails. It can be rarely gradational with overlying fine-grained facies (Fig. 4.9D). The beds can be amalgamated or gathered in meter-thick bedsets where they are intercalated with thinly bedded mudstone and wackestone. These bedsets are extensive and tabular

at the outcrop scale (x100 m) but can also be slightly erosive, having gentle channelized geometries. (Fig. 4.9, 4.10; Table 4.1 and 4.2). This facies are made of grainstone and rudstone/floatstone composed of fine to medium peloids, locally 5 to 10% silt quartz in Hanifa Formation and up to 50% sandstone quartz in Jubaila Limestone, coarse to very-coarse coated-grains and granular to cobble sized reworked intraclasts and skeletal debris (Fig. 4.15C, D). The reworked bioclastic elements consist of echinoderms, brachiopods, gastropods (*Nerinea* sp.), dasyclad (*Clypeina*) (Fig. 4.15C), benthic foraminifera (*Lenticulina* sp., *Kurnubia jurassica, Nautiloculina oolithica*) (Fig. 4.16C, E, 4.15A). Tool marks are common on the sharp base of the beds (Fig. 4.10E). Bioturbation is limited in this grainstone facies and the sedimentary structures are very well-preserved. They are dominated by plane-parallel lamination, hummocky and swaley cross-bedding (HCS and SCS) and subordinate wave ripple cross-bedding. Bidirectionnal tidal cross-bedding are also observed in the Hanifa Formation (Fig. 4.9F). White carbonate mudstone rip-up clasts are common and locally very abundant resulting in a conglomeratic structure of these beds. Basal shell lags and graded-bedding are also common in these beds. Bedding planes can be disturbed by burrows and trails and occasionally contain bored encrusted hardground surfaces. These grainstones locally show soft-sediment deformation and dewatering structures associated with thinly laminated lime mudstone (F6) (Jubaila Limestone J2 unit; Fig. 4.10C, D). The facies can also characterized by close-packing fitted-fabric or chemical compaction features (Fig. 4.16C, D, E) that commonly appear above sequence boundaries. These grainstone beds commonly overlie sharp hardground/firmground surfaces and

interbedded with thinly laminated lime mudstone (F6), argillaceous mudstone to packstone (F4) and slightly argillaceous nodular bioturbated wackestone inner lagoonal facies (F5).

The erosional contact, the subsequent graded bedding, the poor bioturbation suggest an instantaneous sediment accumulation (eventite) (Badenas et al., 2012; Al-Awwad and Pomar, 2015). The plane-parallel lamination suggests high hydrodynamic energy. The HCS and SCS suggesting transported sediments through storm generated flows (Myrow and Southard, 1996; Morsilli and Pomar, 2012). These eventite beds were interpreted as a result of breaking of internal waves in the nearby subsurface (Al-Awwad and Pomar, 2015). However, it is unlikely that the internal waves prograded in such epeiric flat-topped platforms (personal communication L. Pomar, Krakow 2015). The propagation of Internals waves requires sufficient water depth on at least gently sloping ramp depositional profile (Badenas et al., 2012). Taking into account the paleogeographic setting and the regional succession with respect to the associated nearshore facies, argillaceous, sandstone and the tidally influenced grainstone facies, a storm influenced shallow marine carbonate lagoon is suggested. The possible mechanism of the shallow inner-platform storms is wind forced current which responsible for onshore sediment transport in such general transgression trend and flat depositional profile (Aigner, 1985; Galli, 1993).

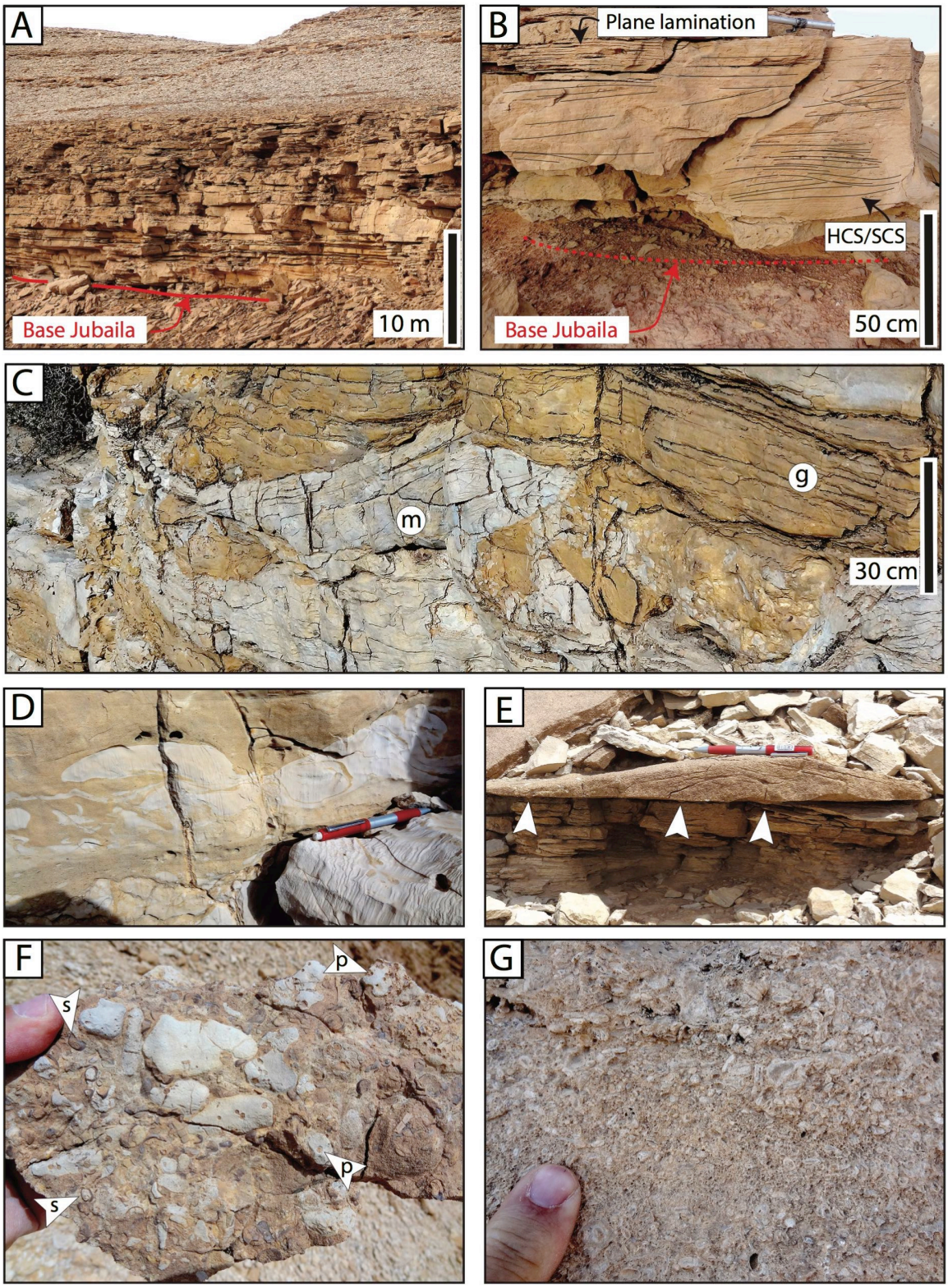

Figure 4.10 (continued on next page): Storm dominated inner-platform facies association in the Jubaila Limestone, **A)** Stacked sharp-based intraclastic peloidal grainstones with around 30% sandstone quartz (transgressive grainstones), base Jubaila, Wadi Al Haddar**, B)** Close-up pohto of the transgressive grainstone in A shows hummocky-, swaley- and plane-laminated sedimentary structures (storm-wave influenced grainstone), **C)** Interbedding of cross-bedded grainstone (g) and thinly laminated lime-mudstone (m) with soft-sediment deformation and dewatering structures, J2 unit, Wadi Al Ain (Note slight oblique view),

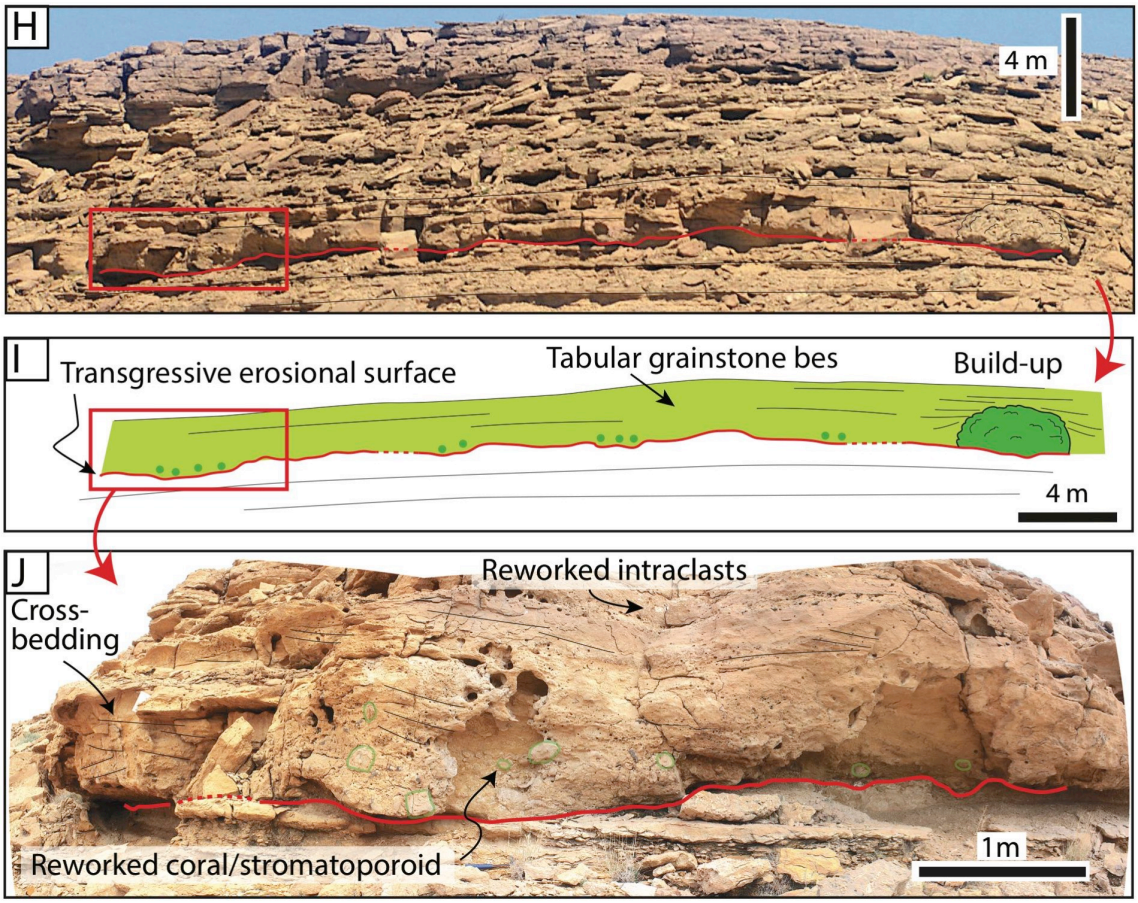

Figure 4.10 (continued): D) Close-up photo of the dewatering structures in C, **E)** Lenticular cm-thick of sharp-based cross-bedded grainstone rich with sandstone quartz, marked by tool marks (arrows) and top wave ripples, base J2 unit, Wadi Al Haddar, **F and G)** Hand-samples shows the composition of the sharp-based grainstones: rip-up clasts of hardground surface (p arrows) and skeletal debris (s arrows) in F, J1 unit, Wadi Al Ain; very coarse to granular coated-grains and oncoids in G, J2 unit, Al Hawtah city, **H)** Erosional-based transgressive grainstones and coral/stromatoporoid buildup, J2 unit, MFS of HFS3, Wadi Malham**, I)** Detailed facies map of the transgressive grainstones and the buildups in photo H**, J)** Close-up photo of the grainstones shows the transgressive erosional surface, reworked coral/stromatoporoid and rip-up clasts, large-scale cross-bedding (storm-influenced transgressive grainstone).

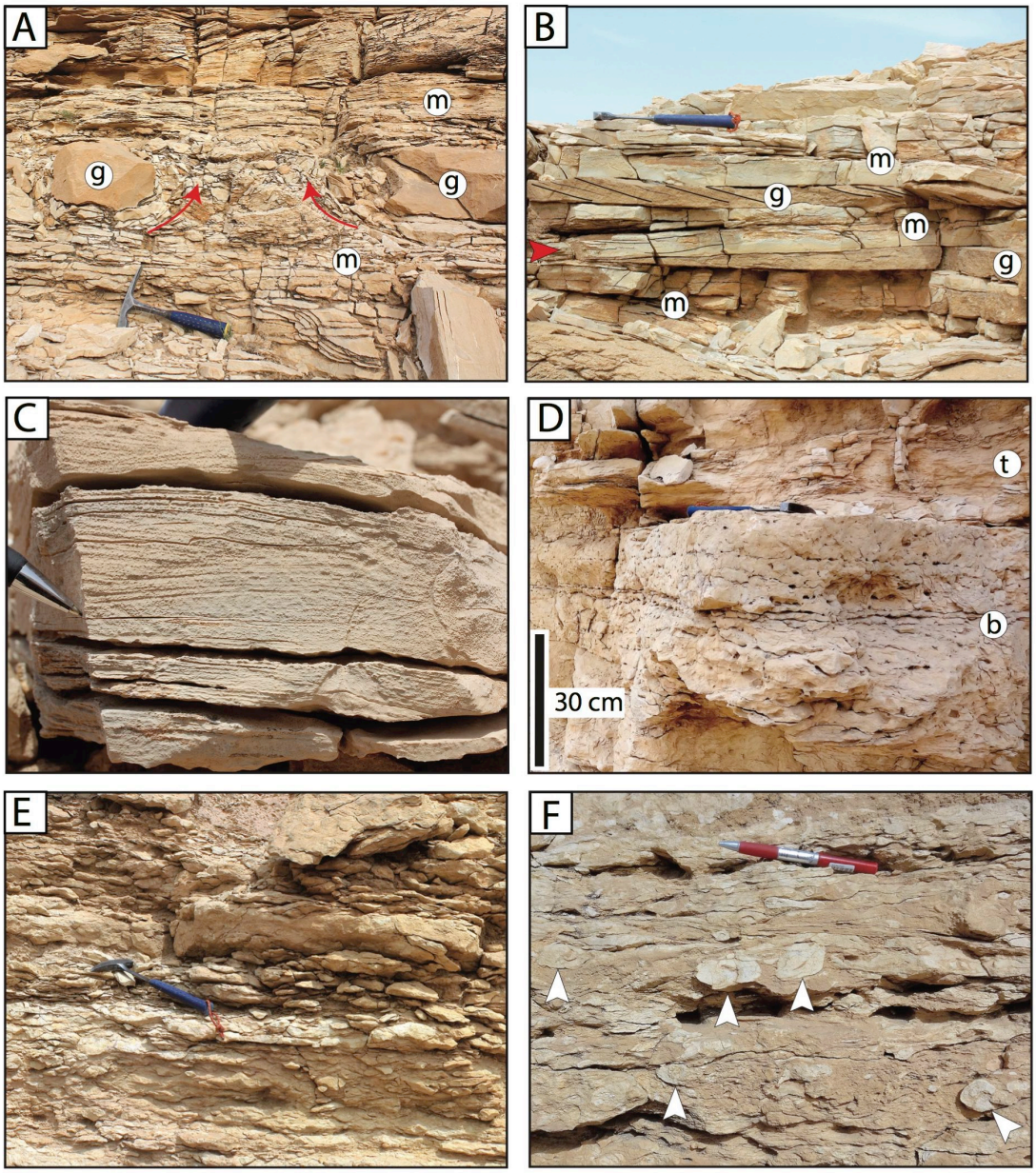

Figure 4.11: Carbonate inner-lagoon facies association in the Jubaila Limestone and Arab-D Member. **A)** Thinly laminated non-bioturbated lime-mudstone (m) and fine peloidal grainstone (g) with soft-sediment deformation dewatering structures (red arrows), storm influenced restricted inner-platform, Jubaila Limestone J2 unit, Wadi Al Ain**, B)** Thinly laminated non-bioturbated lime-mudstone (m) and grainstone (g) intercalation, the lime mudstone has hummocky- and swaley-cross stratification (red arrow), storm influenced restricted inner-platform, base Jubaila Limestone, Wadi Al Haddar, **C)** Thinly laminated lime-mudstone with hummocky-cross stratification, restricted lagoon, Arab-D Member, Al Hawtah city, **D)** Bioturbated peloidal lime-mudstone to packstone (b), highly bioturbated lagoon, overlain by non-bioturbated thinly laminated lime-mudstone (t), restricted lagoon, Jubaila Limestone J2 unit, Wadi Al Haddar, **E)** Bioturbated peloidal packstone with nodular structure and horizontal burrows, highly bioturbated lagoon, base Jubaila Limestone J2 unit, Wadi Al Ain, **F)** Lime-mudstone grainstone interlayering disturbed by horizontal bioturbation (arrows), highly bioturbated lagoon, base Jubaila Limestone, J2 unit, Wadi Al Ain.

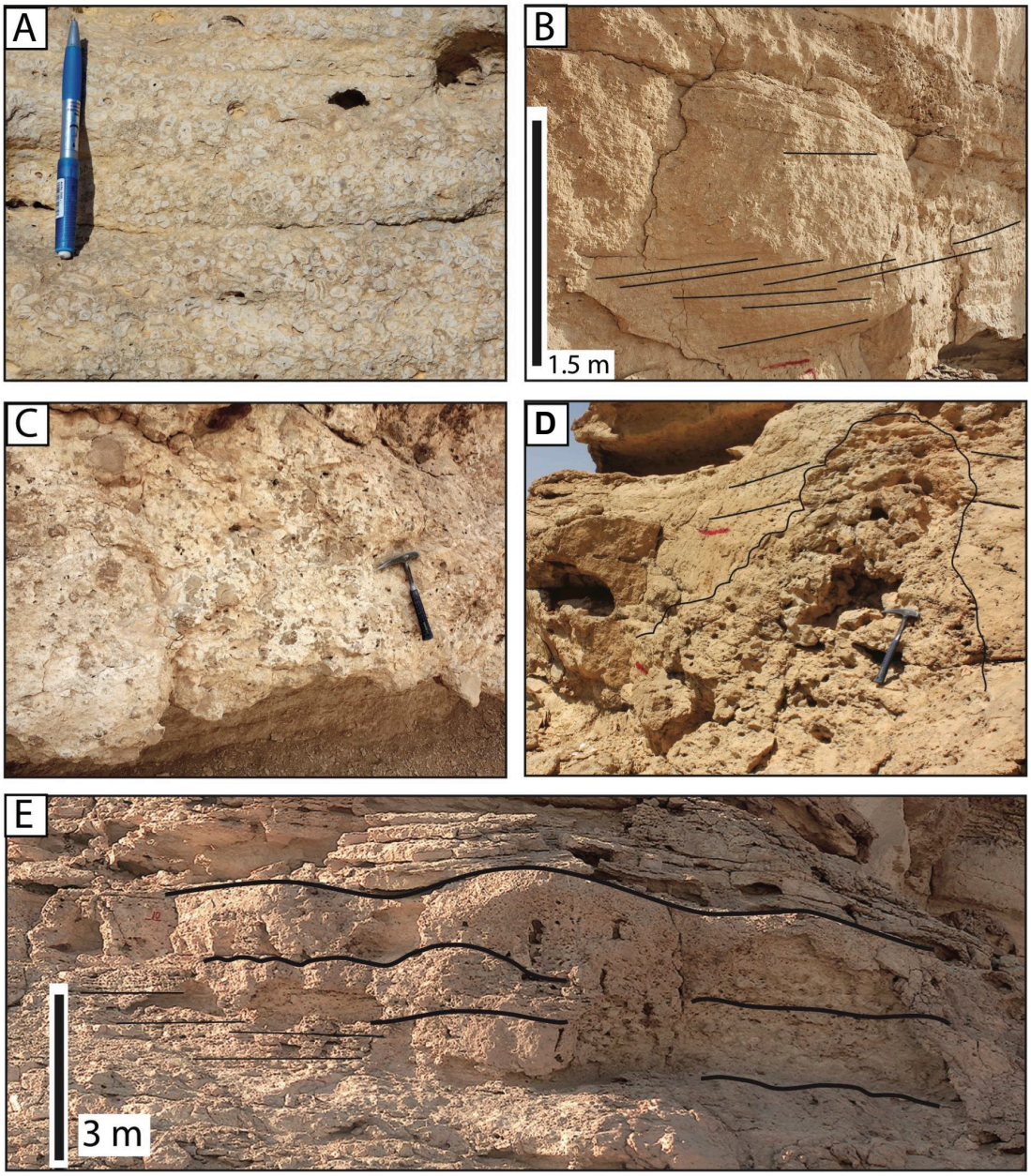

Figure 4.12: Back-barrier facies association in the Hanifa Formation. **A)** Oncoidal grainstone and rudstone (oncoidal bars), Wadi Ghulghul, **B)** Cross-bedded oncoidal grainstone and rudstone (oncoidal bars), Wadi Al Hawtah, **C)** Biostromal coral/stromatoporoid lime-mudstone/wackestone and floatstone (low-energy back-barrier lagoon), Wadi Birk, (hammer for scale), **D and E)** Coral/stromatoporoid buildup, lime-mudstone/wackestone and floatstone (low-energy back-barrier lagoon), Wadi Birk, (hammer for scale in E).

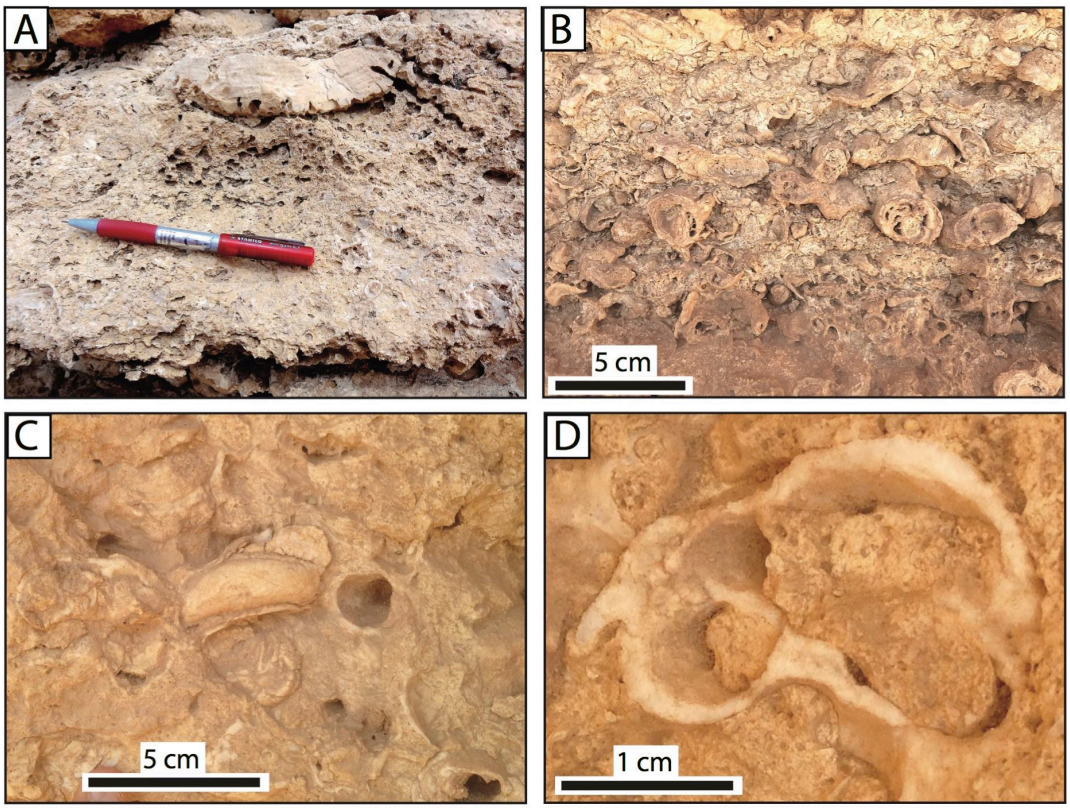

Figure 4.13: Back-barrier lagoon facies association in the Jubaila Limestone**. A)** Biostromal coral/stromatoporoid and rudist packstone to grainstone and floatstone, high-energy back-barrier, J2 unit, Wadi Malham, **B)** Biostromal rudist packstone to grainstone and floatstone, high-energy back-barrier, J2 unit, Al Hawtah city, **C and D)** Close-up photo of the first record of Jurassic rudists in Saudi Arabia. (*Requienidae*), high-energy back-barrier, J2 unit, Wadi Malham.

4.4.4 Back-barrier lagoon

F9: Oncoidal packstone, grainstone and rudstone: oncoidal bars/shoal

The facies are only present at the topmost of the Hanifa Formation above the coral/stromatoporoid biostrome and bioherm unit (Fig. 4.19A, C, D). They appear as lenticular but locally extended units up to 0.25 to 2 m thick delimited by sharp, sometimes erosional boundaries (Fig. 4.12A, B). The facies consist of grainstone and rudstone made up of coarse to very-coarse coated-grains and skeletal fragments, granule- to pebble-sized oncoids (type 2 and type 3; *sensu* Védrine et al., 2007) (Fig. 4.15F, G), and may have

intraclasts, reworked coral/stromatoporoid heads and some sponges *Cladocoropsis*. The bioclastic content includes also dasyclad (*Clypeina*), benthic foraminifera (Miliolid, *Kurnubia jurassica, Redmondoides lugeoni*). The coarse-grained granular facies locally exhibits dm scale cross-bedding and vertical burrows, but can also be structureless. Vadose cements such as pendant and meniscus have been observed in some of thin sections.

The facies formed in a high-energy shallow marine sandy to pebbly bars or shoal depositional setting. The oncolites are valuable indicators for paleoenvironments as they are so sensitive to the turbidity- and trophic-level which controlled by climatic and relative sea-level changes seem to be developed during a semi-arid condition in an open-marine (Védrine et al., 2007). The predominance of dasyclad (*Clypeina*), benthic forams and coral/stromatoporoid indicates low turbidity and optimum condition for the carbonate factory.

F10: Coral/stromatoporoid boundstone to floatstone: low-energy and high-energy back-barrier

These facies are present in the upper most part of the Hanifa Formation and of the Jubaila Limestone J2 unit. These form extensive tabular biostrom units, up to 1.5 to 8 m thick, associated with patch-reefs, reaching up to 15 diameter and 4 m thick in the upper Hanifa Formation (Fig. 4.12F, E, 4.17, 4.19) and up to 4 diameter and 2 m thick in the upper Jubaila Limestone (Fig. 4.10H, I, 4.10H, I). They are massive, sometimes highly bioturbated and have occasional microbial laminated fabric. The facies consist of lime boundstone, grainstone and floatstone made up of peloidal grains, coarse skeletal fragments and, cobble-sized coral/stromatoporoid. The main associated

skeletal elements are rudist (*Requienidae*; identified by W. Hughes and J. P. Platel, personal communication 2017; Fig. 4.13), *Cladocoropsis* and benthic foraminifera (*Alveosepta jacardi, Kurnubia jurassica, Redmondoides lugeoni*).

The circular patch-reefs and the coral/stromatoporoid biostroms are interpreted to be developed in a warm, shallow and open-marine environment clear and free of argillaceous content (Védrine and Strasser, 2009). The association of low-energy mud-rich and high-energy sand-rich deposits, added to their paleogeographic and stratigraphic location compared to lagoonal deposits suggest that with lag these biostroms and bioherms form in back-barrier depositional environment (Wilson and Jordan, 1983).

F11: Cross-bedded coated-grain and peloidal grainstone: shoal and washover complex

These facies are only present in the Hanifa Formation. They form 0.4 to 7 m thick tabular or slightly channelized units bounded at the base and at the top by sharp surfaces (Fig. 4.14). The facies consist of fine-grained grainstones composed of very-fine to fine peloids, coated-grain and skeletal fragments of echinoderms, brachiopods and gastropods (Fig. 4.15H). They are sometimes associated with coral/stromatoporoid heads and interbedded with highly bioturbated peloidal mudstone/wackestone facies. Trough cross-bedding (Fig. 4.14C), hummocky and swaley cross-stratification (HCS and SCS) (Fig. 4.14B, E) and plane lamination (Fig. 4.14A) are common sedimentary structures observed in this facies. These structures are occasionally disturbed by intensive bioturbation.

The facies have been deposited in a high-energy depositional environment dominated by storm- and wave-generated currents. The stratigraphic position

of this facies and special relationships with the other facies indicate a shoal and/or back-shoal washover environment (Reinson, 1979).

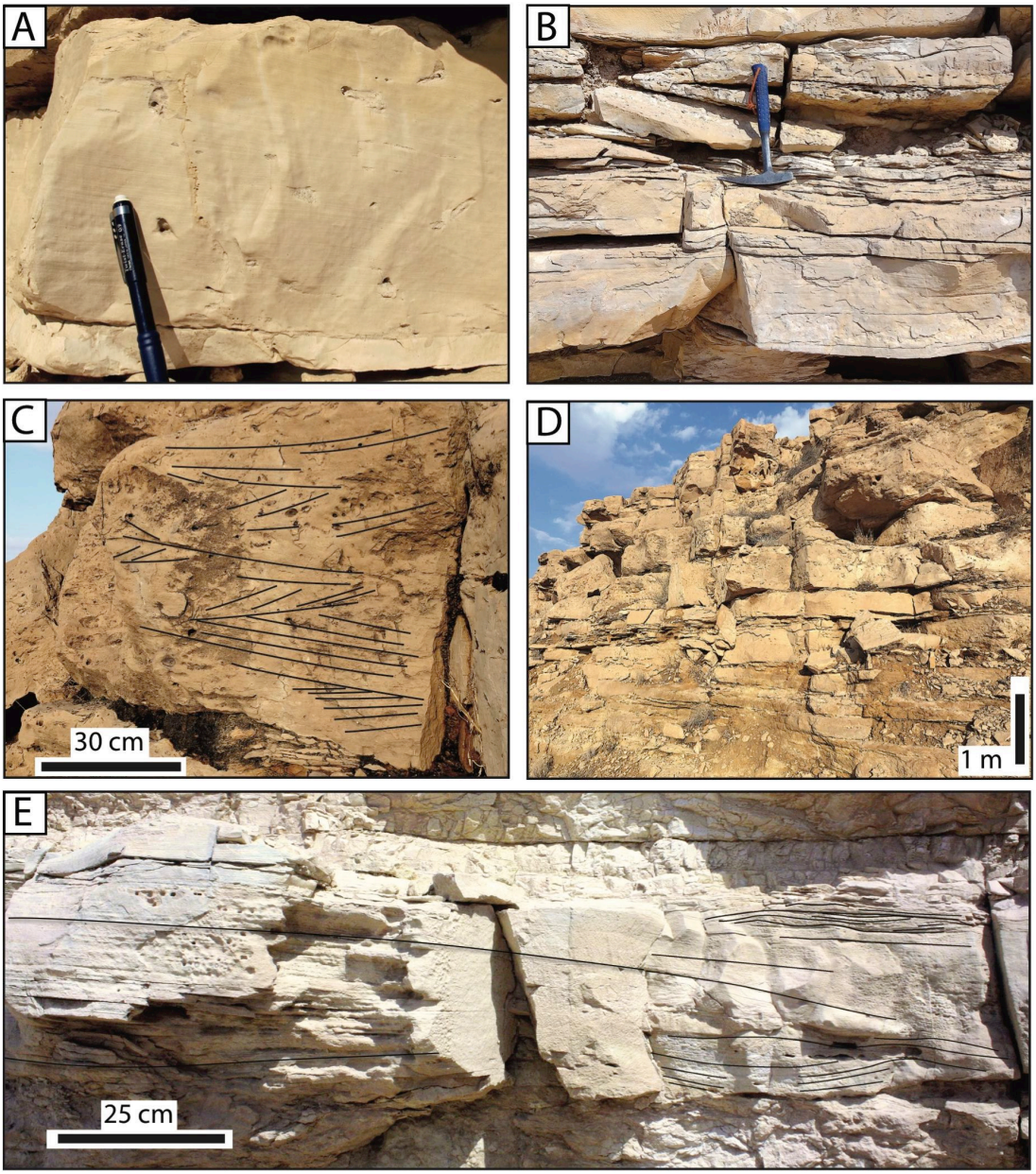

Figure 4.14: Shoal and washover facies association in the Hanifa Formation. **A)** Very fine to fine well-sorted thinly laminated peloidal grainstone (back-barrier washover), Wadi Birk, **B)** Swaley (SCS) and hummocky cross stratification (HCS) and plane laminated very-fine to fine peloidal grainstone (back-barrier washover), Wadi Ghulghul, **C)** Slightly bioturbated SCS and trough cross-bedded medium peloidal grainstone (shoal), Huraimla, **D)** 7 m thick of stacked cross-bedded well-sorted medium peloidal grainstone (shoal), Huraimla**, E)** HCS well-sorted very-fine to fine peloidal grainstone (back-barrier washover), Wadi Birk.

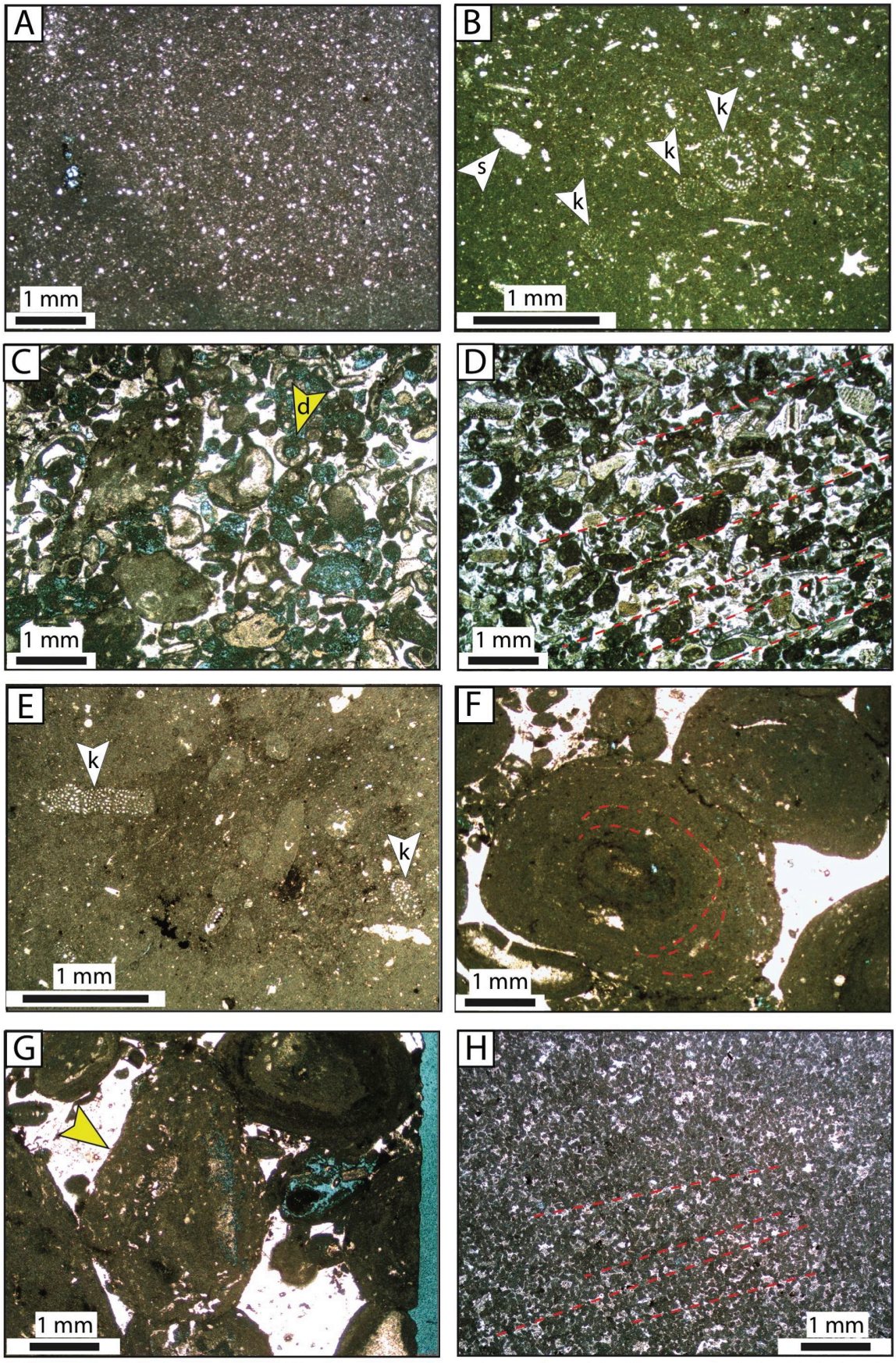

Figure 4.15 (continued on next page)

← **Figure 4.15** Photomicrographs of the Hanifa facies**: A)** Argillaceous mudstone/wackestone rich with sponge spicules (shale dominated inner lagoon), **B)** Slightly argillaceous nodular bioturbated peloidal wackestone/mudstone with benthic foraminifera (Kurnubia jurassica; k arrows) and sponge spicules (s arrows), **C and D)** Sharp-based intraclasts peloidal skeletal-fragments grainstone with dasyclad (Clypeina) (d arrow) and cross-bedding (red dash lines in D) (storm dominated inner platform), **E)** Bioturbated peloidal wackestone/packstone with occasional biohermal coral/stromatoporoid buildups and rich with benthic foraminifera (Kurnubia jurassica; k arrows) (back-barrier and highly bioturbated lagoon), **F and G)** Oncoidal packstone/grainstone and rudstone (oncoidal bars/shoal) has type 2 oncoid with elliptical micritic laminated cortex with local truncated laminae (red dash lines in F); **G)** shows type 3 oncoid with sub-elliptical shapes and wavy lamination (yellow arrow), **H)** Swaley cross-bedded (red dash lines) well-sorted peloidal coated-grain grainstone (shoal and washover complex).

→ **Figure 4.16** Photomicrographs of the Jubaila Limestone and Arab-D facies. **A)** Mud-supported very-fine to fine rhombic dolomite crystals with weakly fabric preserving texture, Arab-D Member, Wadi Malham, **B)** Grain-supported very-fine to fine rhombic dolomite crystals, J2 unit, Wadi Malham, **C)** Partially dolomatized and chemically compacted (red arrow) very-coarse oncoidal grainstone rich with benthic foraminifera (*Kurnubia jurassica*; k arrows), J2 unit, Wadi Malham, **D)** Chemically compacted skeletal peloidal grainstone, J2 unit, Wadi Birk, **E)** Peloidal grainstone with vadose meniscus cements (yellow arrows) and has benthic foraminifera (*Lenticulina* sp.; l arrow) and minor quartz content (q arrows), J1 unit, Wadi Birk, **F)** Barren thinly laminated (red dash lines) mudstone with silt quartz grains (yellow arrows), Arab-D Member, Al Hawtah city, **G)** Bioturbated peloidal mudstone to packstone rich with sponge spicules in small round molds (e.g., yellow arrows), Arab-D Member, Wadi Malham, **H)** Bioturbated peloidal skeletal packstone with benthic foraminifera (*Kurnubia jurassica*, k arrow; *Alveosepta Jaccardi*, a arrow) and quartz grains (q arrows), J1 unit, Wadi Birk.

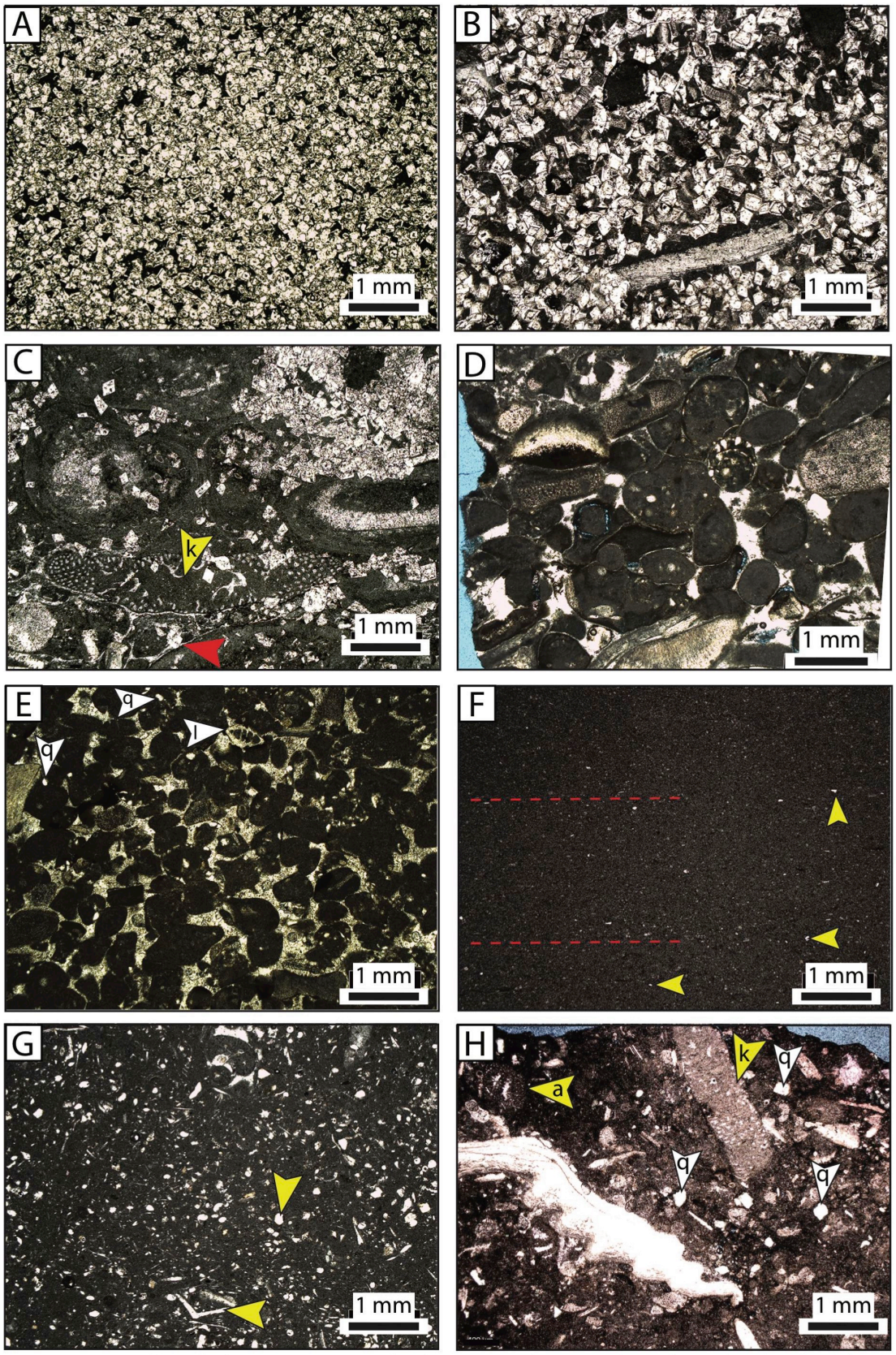
A
1 mm
B
1 mm
C
k
1 mm
D
1 mm
E
q
l
q
1 mm
F
1 mm
G
1 mm
H
k
q
a
q
q
1 mm

4.5 Sequence stratigraphy and stratigraphic evolution

The sequence stratigraphic transects of the Late Jurassic (Hanifa Formation, Jubaila Limestone and Arab-D Member; Fig. 4.5, 4.6) are located west of Riyadh in the Tuwayq Escarpment along 370 km. The transects have a total thickness of 100-300 m and are oriented N-S in an oblique-dip direction to depositional dip. These transects are constructed by using physical correlation and sequence stratigraphic concepts. Moreover, the stratal pattern and the facies vertical distribution lead to the definition of correlatable depositional sequences and sequence boundaries. Key indicator facies and specific correlative surfaces helped in making the correlation (cf. Kerans and Tinker, 1997). Extensive erosional and iron-stained surface is a main sequence boundary separating the Hanifa Formation and the Jubaila Limestone (Fig. 4.5, 4.17). In addition, this significant sequence boundary is used as a datum to constrain the Hanifa correlation. This erosional surface is associated with abrupt facies changes as it separates coral/stromatoporoid prone facies at topmost Hanifa Formation from storm-influenced darker-color quartz-rich grainstones at the base of the Jubaila Limestone (Fig. 4.17 and 4.18). The Jubaila Arab-D correlation (Fig. 4.6) is constrained and datumed at the top by regionally mappable anhydrite solution collapse breccia. Moreover, in the upper Jubaila and the Arab-D Member have some extensive red dolomitic horizons that are used to construct the Jubaila Arab-D correlations (Fig. 4.6). These cross-sections were biostratigraphically controlled mainly by ammonite fauna defined by Manivit et al. (1990). The subordinate biostratigraphic marker includes nautiles, echinoderms, brachiopods and foraminifera (Manivit et al., 1990).

The Late Jurassic successions are divided into two main depositional sequences, Hanifa and Jubaila-Arab-D. They are both evolved vertically from siliciclastic-rich limestone with poor-faunal diversity to open-marine carbonate platforms with coral/stromatoporoid bearing and high-faunal diversity at the top of each sequence. The siliciclastic contents in the Hanifa sequences are mainly argillaceous, whereas, in the Jubaila-Arab-D are sandstone quartz and lacks of argillaceous deposits. The overall apparent depositional polarity is northeast-southwest direction. The detrital siliciclastic deposits increased toward the southwest as being proximal to the terrigenous resources and Arabian Shield (Fig. 4.24B; Ziegler, 2001). Relative normal marine facies and fauna are increasing toward the north and northeast of the transects. These depositional sequences underwent evident syndepositional subsidence controlling the lateral thickness variations and to some extent facies variation. However, the location of the differential subsidence of each sequence is different. Thus, these two depositional sequences were divided, also, based on their tectonically related stratigraphy.

4.5.1 Hanifa Sequence Stratigraphy

The outcropping Hanifa Formation is composed of four composite sequences (HCS1 to HCS4). Each of them consists of multiple high-frequency sequences (HFSs). The base sequence boundary of the Hanifa sequences corresponds to the Middle-Late Jurassic unconformity marked by sharp regionally extensive iron-stained hardgrounds associated with a slight truncation over the Tuwaiq Mountain Limestone. The basal sequence boundary corresponds to a 2^{nd}-order sequence boundary (SB^2 11 of Al-Husseini et al., 2006). The top Hanifa sequence boundary is a disconformity

marked by extensive iron-stained and probable pyritized hardground surface which correspond to a 3rd-order sequence boundary (SB^3 11.3 of Al-Husseini et al., 2006). The lithostratigraphic boundary between the Hawtah and Ulayyah Members, defined by Vaslet et al. (1983), is a conformable transgressive surface within HCS3.

The Hanifa sequence stratigraphy is dominated by carbonate system with subordinate siliciclastic input mainly in the lower part of the depositional sequences. The sequences formed in overall low-energy inner platform with high-energy storm-generated events. The HFSs show a slight retrogradational and overall aggradational stacking patterns. The successions usually show a repetitive vertical facies evolutions (Fig. 4.21). that begin with argillaceous-rich facies and end with purely carbonate deposits. The maximum marine transgressive and highstand stages correspond to the argillaceous-free carbonate sediments. The successions of the Hanifa sequences demonstrate mainly aggradation and lack of well-developed progradational stacking patterns. The Hanifa sequences lack of low-stand system tracts (LST) as they formed in flat-topped shelf inner-platform depositional setting. The Hanifa platform is characterized by limited broad lateral facies evolution along this strike transect.

The Hanifa Formation increases in thickness toward the south from 100-160 m. The overall geometries of the depositional sequences show tabular extensive units except for the lower sequence (HCS1) that shows apparent wedging and thinning toward the north. The argillaceous deposits seem to be slightly more developed to the south (proximal domain) while coral/stromatoporoid facies have its best expression between Wadi Ghulghul

and Riyadh which corresponds to the most eastern distal part of the transect. The bioconstructed facies are in an open lagoon position (barrier/back barrier) and that the shaly facies are not distal but more proximal than the pure carbonate and are related to the continental source of the siliciclastic. Moreover, these low-energy argillaceous deposits are barren to low faunal diversity (Appendix 2 and 3) affected by high siliciclastic and nutrient supply in such proximal setting.

The first Hanifa composite sequence HCS1 is dated Early Oxfordian by brachiopods (Manivit et al., 1990). The HCS2 and HCS3 are dated Middle Oxfordian by ammonites (*plicatilis* Zone) and Late Oxfordian by foraminifera (*Alveosepta Jacardi*) (Manivit et al., 1990). The HCS4 is dated Late Oxfordian to Early Kimmeridgian by foraminifera (*Alveosepta Jacardi*) and echinoderms (Manivit et al., 1990). The vertical developments of the Hanifa sequences have been correlated with seawater palaeotemperature evolution (Fig. 4.27) that supports Early Oxfordian (*cordatum* Zone) to Early Kimmeridgian (*baylei* Zone) age for the Hanifa sequences. Thus, the approximate duration of the Hanifa sequences could be ~ 5.3 Myr, then the average duration of the Hanifa composite sequences (HCS1-HCS4) is approximately 1.3 Myr.

4.5.1.1 Hanifa Composite Sequence 1 (HCS1)

This first composite sequence is bounded by two unconformities corresponding to subaerial exposure surfaces and marked by extensive stained bored hardground surfaces. Its maximum thickness is 20 m and it wedges-out in the Wadi Al Ain – Riyadh area. The basal boundary comes with an obvious shift in lithology from preceding pure limestone to overlying more argillaceous rich unit. In detail, the HCS1 consists of four high-frequency

sequences (HFS1 to HFS4) that show a similar facies succession than the one describe above. These high-frequency sequences show tabular correlatable units with 3-5 m thick. The HCS1 is characterized at the base by shallow-marine argillaceous mud-dominated deposits (F4) to slightly argillaceous nodular bioturbated peloidal wackestone/mudstone (F5) rich in fossils. They are occasionally interbedded with decimeter thick sharp-based peloidal skeletal grainstone (F8). These transgressive low-energy deposits are overlain by coral/stromatoporoid boundstone and associated packstone/grainstones (F10) that extend further to south to make up the entire sequence. These higher energy facies are interpreted to be deposited during the maximum transgression and highstand stage of the sequence.

4.5.1.2 Hanifa Composite Sequence 2 (HCS2)

The HCS2 is bounded at base by extensive stained hardground surface. The HCS2 is 50 to 70 m thick in the southern part of the study area and thins-out to less than 30 m in the Riyadh area. This thinning-out mainly concerns the lower part of this HCS2 suggesting a continuing effect of the previous differential movement. The sequence is made up of four high-frequency sequences (HFS1-HFS4) bounded by minor firmground and hardground surfaces. The first two high-frequency sequences (HFS1 and HFS2) are wedging and pinching out to the north in Riyadh (Khashm Qaddiyah). The HFS1 and HFS2 are characterized by overall low-energy shallow marine inner-lagoonal facies association made up of calcareous shale (F4), nodular and bioturbated argillaceous peloidal wackestone/mudstone (F5). The overall transgressive evolution comes with a decrease of the shale content in the HFS3 and HFS4 that are mainly composed of low-energy homogeneous

muddy carbonate deposits (F7) intercalated with storm-generated thin sharp-based grainstones (F8) with 10% silty quartz. These low-energy argillaceous deposits are barren to low faunal diversity (Appendix 2 and 3) formed in a restricted conditions during initial transgression, which attributed to the proximality to siliciclastic and nutrient supply. These proximal siliciclastic deposits are thickened and localized mainly in highly subsiding areas in which depressions seem to be compensated and filled with terrigenous sediment during initial transgression. The maximum marine transgression of HCS2 is not well defined but seem to coincide with the MFS of HFS3. It is marked by swaley cross-stratified well-sorted and fine-grained grainstone (F11) in the Wadi Al Hadrar section recording higher energy condition in this shallow marine lagoonal depositional environment. Moreover, the MFS coincides with biostromal coral/stromatoporoid facies (F10) in the northern section (Huraimla). During highstand systems tract (HFS), the high-energy deposits, located at the northern- and southern-end of the cross-section, evolved to lower energy highly bioturbated lime mudstones (F7). This composite sequence is limited at the top by iron-stained hardgrounds that can be locally eroded by subsequent transgressive ravinement surface at the base of HCS3.

4.5.1.3 Hanifa Composite Sequence 3 (HCS3)

This composite sequence is 45 m thick in the southern area and thins-out to 30 m in the Riyadh area. The lower part of the sequence appears isopachous, and the northward thinning is related to a slight regional truncation by the regional transgressive ravinement surface at the base of HCS4. The main truncation is located in the Wadi Al Ain – Riyadh area which corresponds to the same uplifted area evidenced with the wedging of HCS1.

The HCS3 is made up of four high-frequency sequences (HFS1-HFS4). The transgressive systems tract of HCS3 begins with a thin unit of argillaceous mudstone/wackestone (F4) that grade up to slightly argillaceous nodular wackestone (F5) and back-shoal bioturbated coated-grain grainstones (F11; HFS1 and lower part of HFS2 in Wadi Al Haddar). The top of HFS2 is locally marked by the new development of coral/stromatoporoid boundstone (F10)

The first clear transgressive stage is recorded by the MFS of HFS2 with back-shoal highly bioturbated and cross-bedded well-sorted grainstones (F11; Wadi Al Haddar) equivalent updip to ammonite bearing lagoonal limestone (F7) with locally biostromal coral/stromatoporoid facies (Huraimla section). The top high-frequency sequences (HFS3 and HFS4) are characterized by argillaceous-free white-colored pure carbonate facies (F7 and F11) and an increase of high-energy storm-generated grainstone deposits (F8). These storm-generated grainstones (F8; lower part of HFS3) show extensive correlatable unit along the studied interval. Moreover these grainstones unit were used as a lithostratigraphic marker separating the two Hanifa members, Hawtah and Ulayyah Members (Vaslet et al., 1983). There are no clear evidence of lateral facies variation indicating a proximal – distal polarity of the system in such a strike transect of a very extensive and shallow marine inner platform depositional setting. The lateral continuity of the storm generated meter-thick bedsets and their tabular geometry attest a very flat depositional profile and the lack of clinoforms in this carbonate system in the study area. These highly continuous high-energy deposits imply significant sequence stratigraphic events in which the whole inner-platform became highly agitated. This higher energy conditions are attributed to the increase of accommodation

space, where waves and storm can be propagated, and backstepping of the normal marine condition during the Hanifa long-term transgression trend. The normal marine condition is testified by the high foraminiferal diversity (cf. Al-Mojel et al., in prep) including the first appearance of the Late Oxfordian benthic foraminifera *Alveosepta Jacardi* (Appendix 2 and 3). The main MFS of HCS3 fits with the MFS of HFS3 which is locally characterized by swaley cross-stratified shoal grainstone (F11; Wadi Ghulghul) and biostromal coral/stromatoporoid (F10; As Sitarah).

The highstand systems tract (HST) is made up of two high-frequency sequences (upper part of HFS3 and HFS4). The HFS4 consists mainly of low-energy highly bioturbated wackestone/mudstone (F7) and local coral/stromatoporoid buildups (F10; Wadi Birk). The HFS4 is similar to the preceding cycle but the transgressive sharp-based grainstones (F8) and the swaley- and hummocky-stratified grainstones (F11) are thinner and less extensive which is probably due to the decreasing of accommodation space. The HST is characterized by well-oxygenated highly-bioturbated (mainly *Thalassinoides*) mudstone/wackestone (F7) back-barrier lagoonal facies with locally coral/stromatoporoid buildups (F10). The HST shows a cleaning upward trend of more normal-marine lagoonal carbonate capped by a regional sequence boundary marked by a hardground or an extensive ravinement surface (Fig. 4.18). The top sequence boundary shows obvious facies shift from the clean low-energy carbonate-rich intervals to overlying brown and darker-color high-energy facies (F8). Moreover, the top sequence boundary could be considered a slight regional truncation surface in which the HST is notably thinning northward whereas the TST appears isopachous.

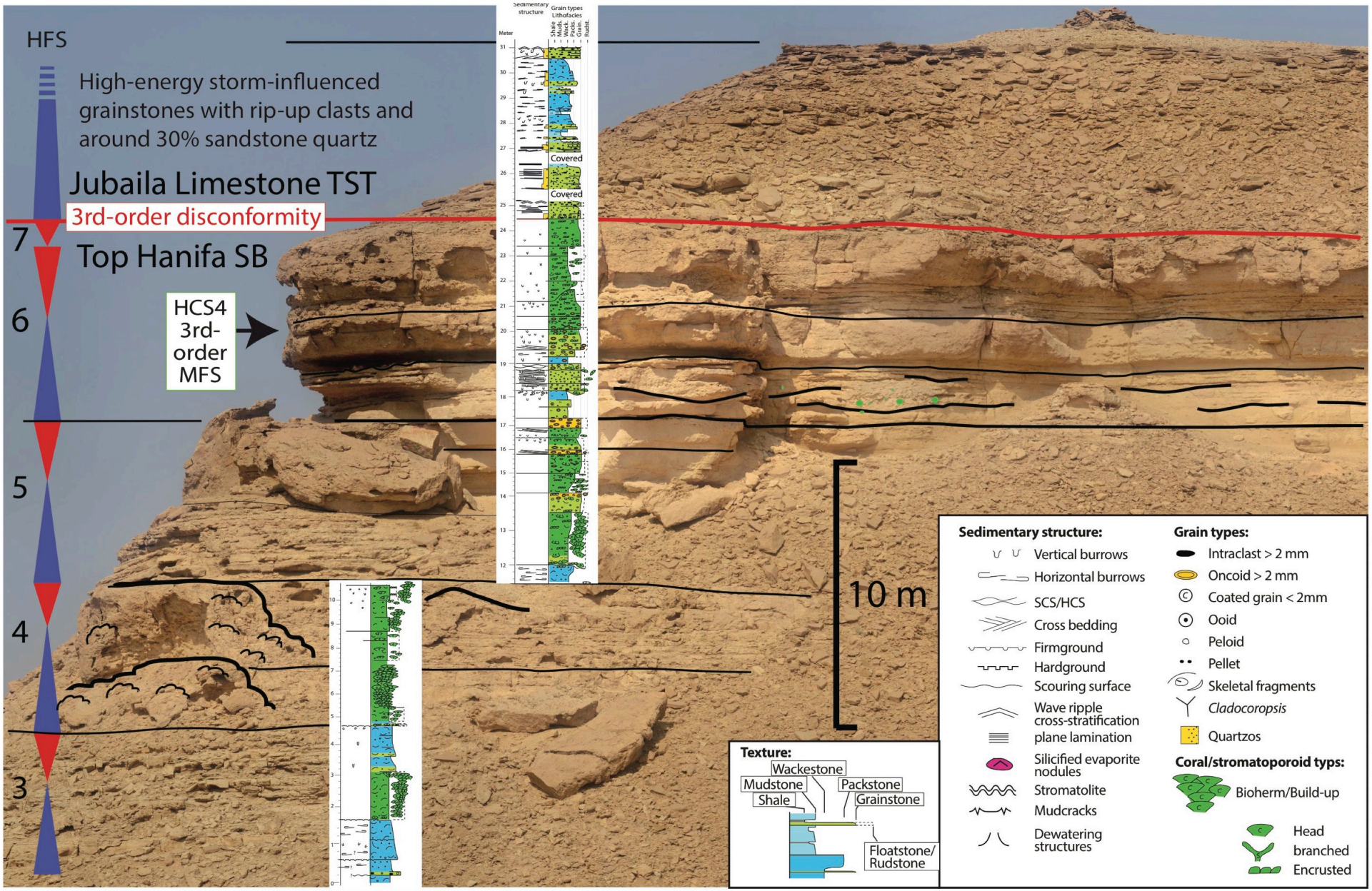

Figure 4.17: Outcrop photography and detailed measured section of the upper Hanifa Formation in Wadi Birk (9 km east of Wadi Birk section presented in Fig. 4.5). It shows upper Hanifa composite sequence 4 (HCS4). For facies color legend see Fig. 4.5.

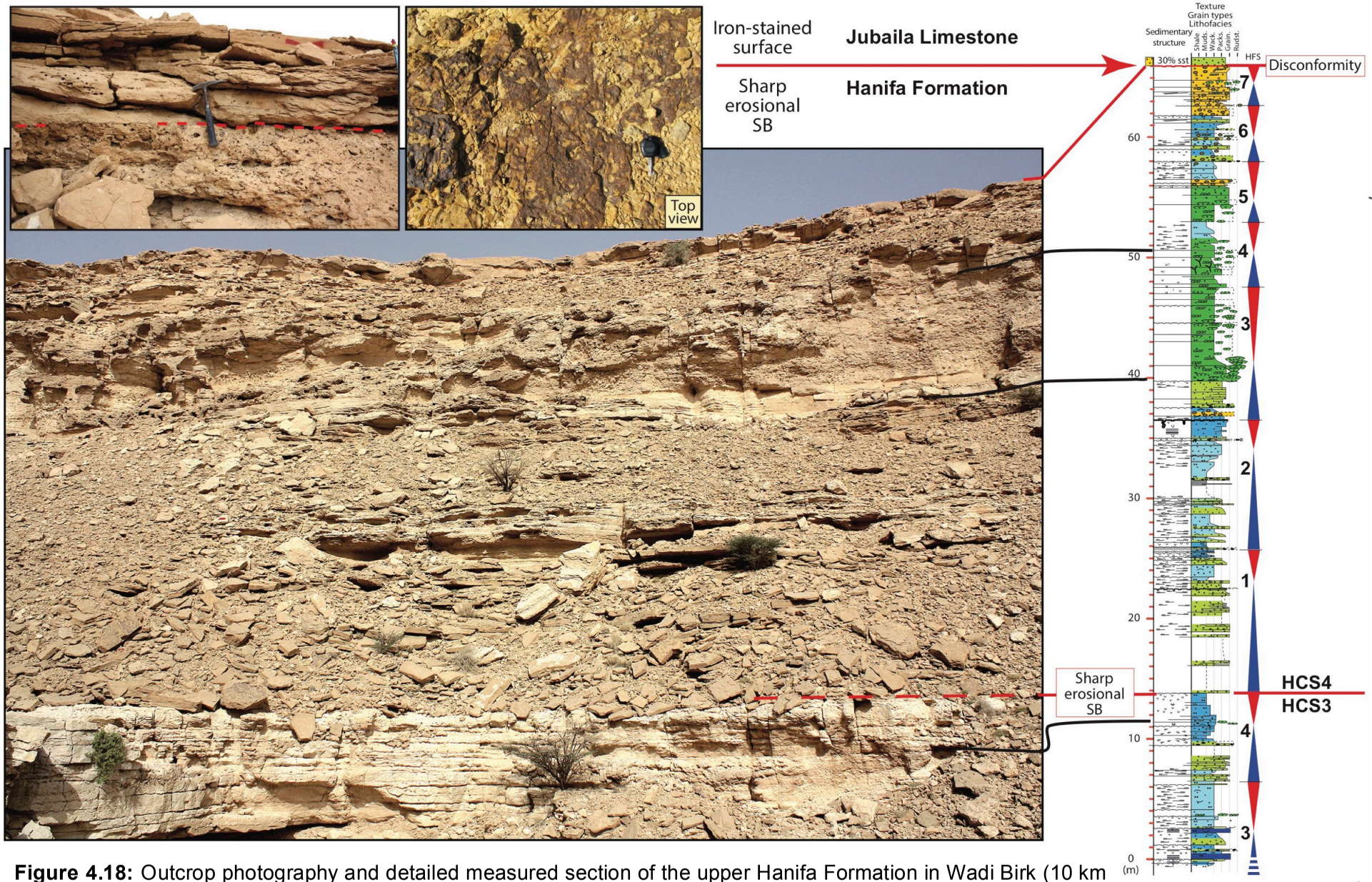

Figure 4.18: Outcrop photography and detailed measured section of the upper Hanifa Formation in Wadi Birk (10 km north of Wadi Birk section presented in Fig. 4.5). In such inner-platform setting, the sequences, at different scale, begins with transgressive sharp-based storm-influenced grainstones and slightly argillaceous sediments and end with well-developed purely carbonate highstand deposits. (For symbol legend see Fig. 4.17, for facies color see Fig. 4.5).

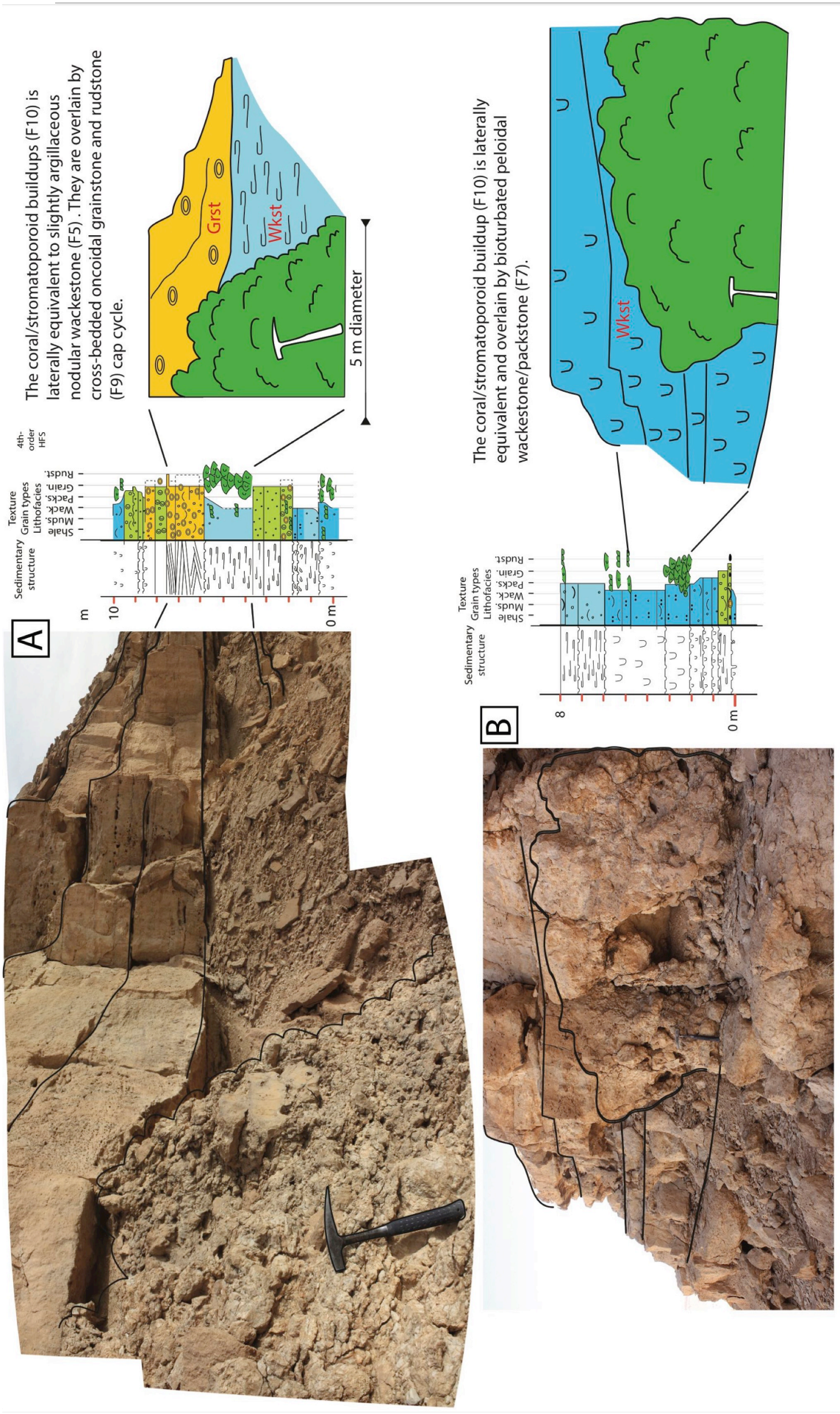

Figure 4.19 (Continued on next page): Detailed measured sections and outcrop photography of the Hanifa Formation, in Al-Hawtah and Wadi Birk, showing the lateral facies equivalent to the coral/stromatoporoid buildups in the upper Hanifa Formation, HCS4 (for symbol legend see Fig. 4.17, for facies color see Fig. 4.5).

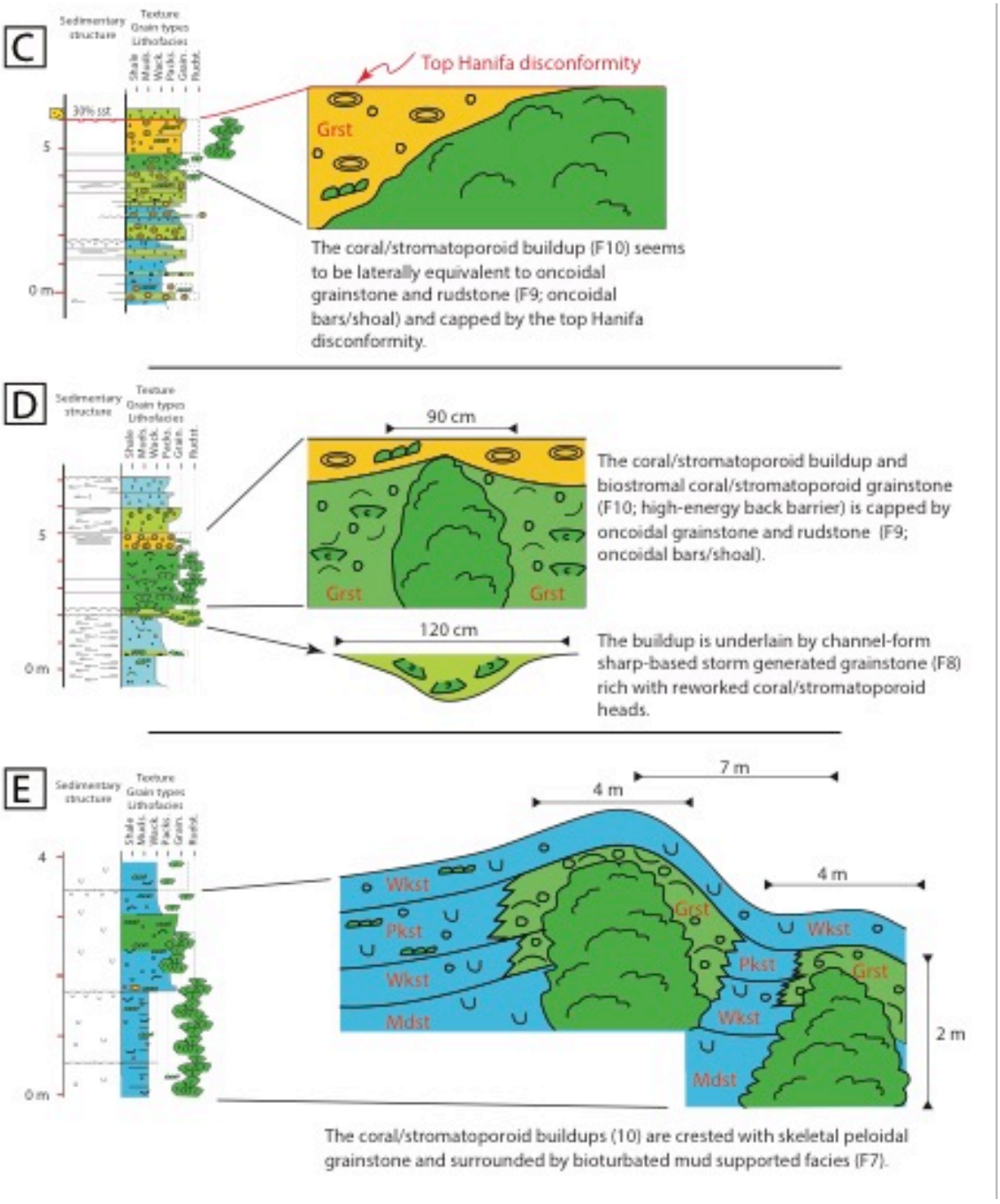

Figure 4.19 (Continued)

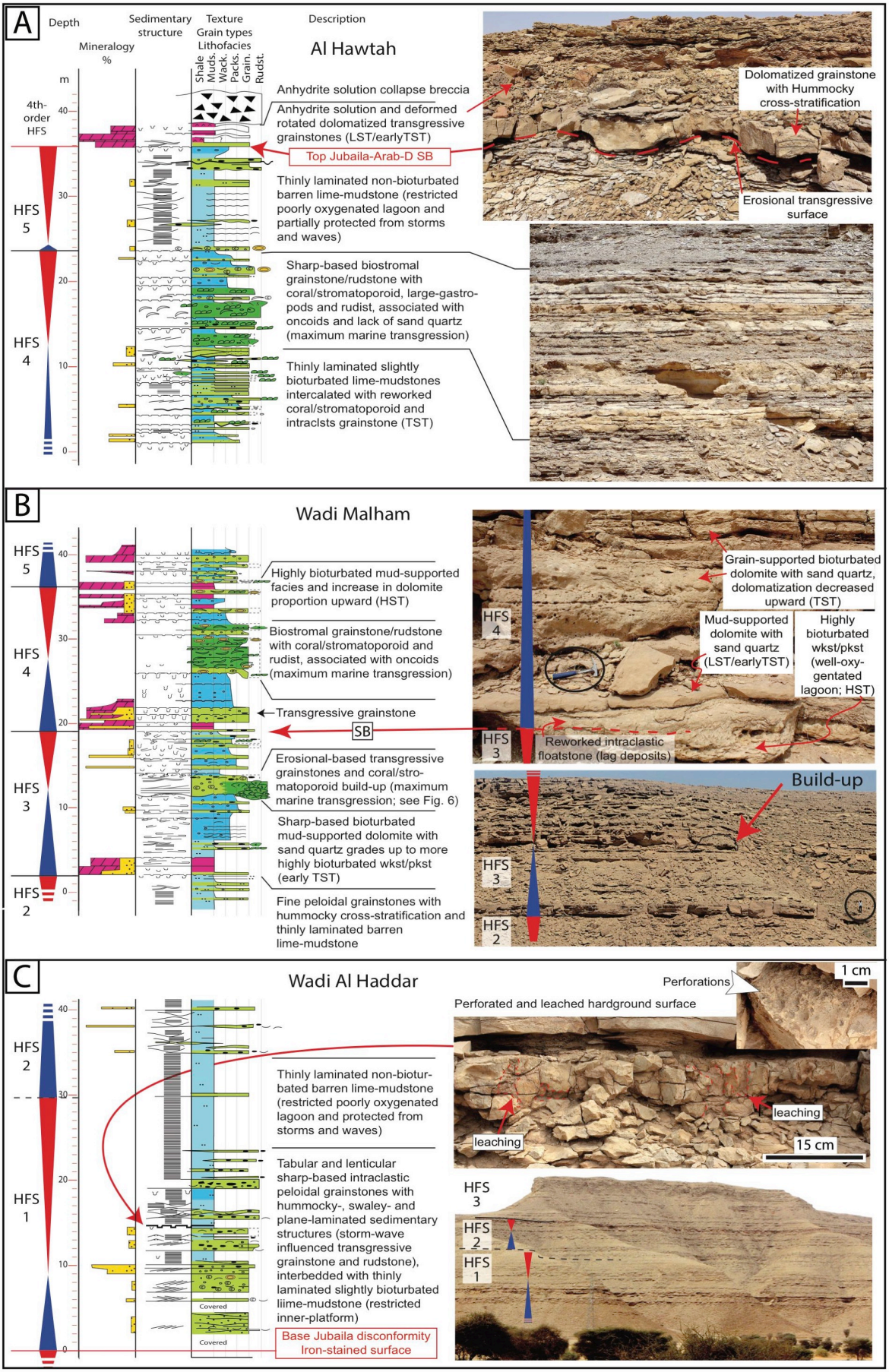

Figure 4.20: Detailed measured sections of the Jubaila Limestone and Arab-D Member show vertical successions of carbonate inner platform facies. For symbol see Fig. 4.17, for color legend see Fig. 4.5.

4.5.1.4 Hanifa Composite Sequence 4 (HCS4)

This last HCS of Hanifa sequence is bounded by two erosional surfaces. The basal sequence boundary is marked by stained bored hardgrounds in the southern and northern areas (Riyadh, W. Al Ain and W. Al Haddar) and/or an extensive ravinement surface (W. Birk to As Sitarah). It corresponds to tectonic related erosional (with probably subaerial exposure) surface, Wadi Birk – Riyadh area being slightly uplifted and eroded (less than 10 m compared the southern area; Fig. 4.18). Later on, this same area seems to be slightly more subsidence at the beginning of the HCS4 deposition as shown by the maximum thickness of the first HFS in this area and their thinning towards the south. The top HCS4 sequence boundary, the top Hanifa sequence, corresponds to a very extensive erosional surface related to a subaerial exposure. This erosion surface usually lies on top of open-lagoon high-energy facies that do not correspond to clear regressive but to transgressive deposits. Thus, it is possible that the regressive system tract have been eroded. Our correlations show also a slight differential uplift of the southern area where the truncation seems maximum.

The HCS4 increases in thickness northward from 35 to 55 m. The sequence is made up of seven high-frequency sequences (HFS1-HFS7) few to ten meters thick that are bounded by bored hard-grounds or transgressive ravinement surfaces. Most of these HFSs are more or less isopachous and can be correlated all along the transect. This broad tabular geometry and the facies distribution within these HFSs clearly show that the depositional profiles were globally horizontal in this shallow marine inner platform environment. No clinoforms can be inferred from the geometries and facies distribution. The

base of HCS4 is marked by an extensive transgressive bedset made up of decimeter thick storm-generated coarse-grained grainstone beds (F8), identified in all the sections except in Al Haddar section to the south. Tidal influence is locally attested by bidirectional sigmoidal cross bedding. Thus, it is interpreted as a sandy shoreface-foreshore characterized by high-energy storm-dominated ravinement processes in a transgressive context. Same high-energy deposits are present at the base of numerous HFSs as early-transgressive system tracts. In the lower part of HCS4 (HFS1, HFS2), these early-transgressive grainy bedsets (F8) are overlain by low-energy bioturbated slightly argillaceous muddy carbonate deposits (F4). Here again the shale content increase towards the south (Al Haddar) towards the proximal domain which that confirms the continental origin of the shale influx and its interpretation as a proximality indicator. In the upper part of HCS4, the facies distribution is much more complex and dominated by the large development of corals/stromatoporoids boundstone (F10) and associated oncoidal grainstone (F9). The upper HFSs are bounded by erosional surfaces and are made up of an alternation and a complex lateral association of high-energy deposits coarse-grained grainstones (F8 and F9) and coral/stromatoporoids buildups (F10) with minor low-energy muddy intervals (F7). This facies association is interpreted as a back-barrier to shoal facies association and represents the most open-marine facies association of the Hanifa Formation. This upper interval is thus interpreted as corresponding to the maximum transgression of the whole Hanifa sequence. It is abruptly overlain by the top Hanifa exposure and base-Jubaila ravinement surface without or with very limited preserved highstand systems tract.

The lower part of HCS4 shows limited lateral facies variations since the storm-generated bedsets (F8) and intercalated mud-dominated carbonate facies (F5 and F7) are very extensive. On the opposite, the corals/stromatoporoids boundstone (F10) and associated grainstone (F11) admit rapid facies variations at a hectometric to kilometric scale resulting in a very complex architecture of the upper part of HCS4 and of related reservoir bodies in this interval. It is worth noting that the general migration/backstepping of the corals-stromatoporoids bodies (F10) towards the south in this interval and their disappearance to the south (Wadi Al Haddar) where a more proximal facies association is observed (algal microbial system, oncoid and coated-grains grainstone, F9). This backstepping of the back-barrier facies association confirms the overall transgressive stacking pattern of the Hanifa Formation. Moreover, this lateral facies changes (reefs to algal microbial system) is probably controlled by the proximality to terrigenous and nutrification resources from the south. The increasing of nutrification supply could switch the carbonate production from reef to algal depositional system (cf. Fig. 9 in Hallock, 2001). The maximum flooding surface of HCS4 (MFS of HFS6) is marked by the southward (landward) extend of the highly-bioturbated lagoonal peloidal mudstone/wackestone facies (F7); and in the north it is marked by the most distal facies the swaley cross-bedded peloidal shoal grainstones (F11). The highstand (upper HFS6 and HFS7) is lack of the argillaceous detrital contents. This is consistent of having the shale is sourced continental influx as shoreline were pushed further updip during continuing coastal onlap of MFS and HST.

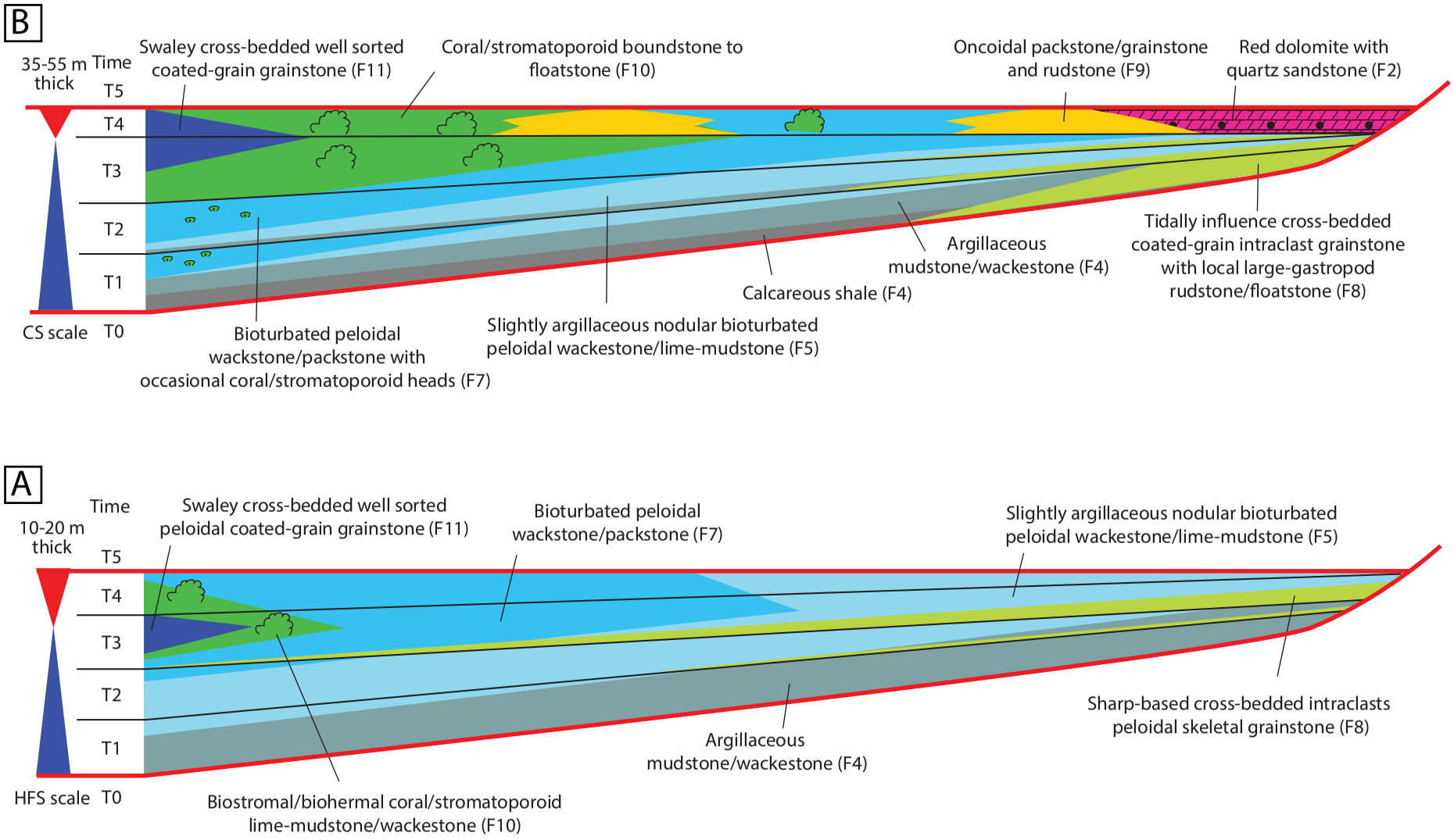

Figure 4.21: Depositional sequence model of the Hanifa Formation showing spatial facies distributions and platform evolution in series of times (T0 to T5). **A)** Depositional sequence model for the first three Hanifa composite sequences (HCS1 to HCS3), **B)** Depositional sequence model for the Hanifa composite sequence 4 (HCS4).

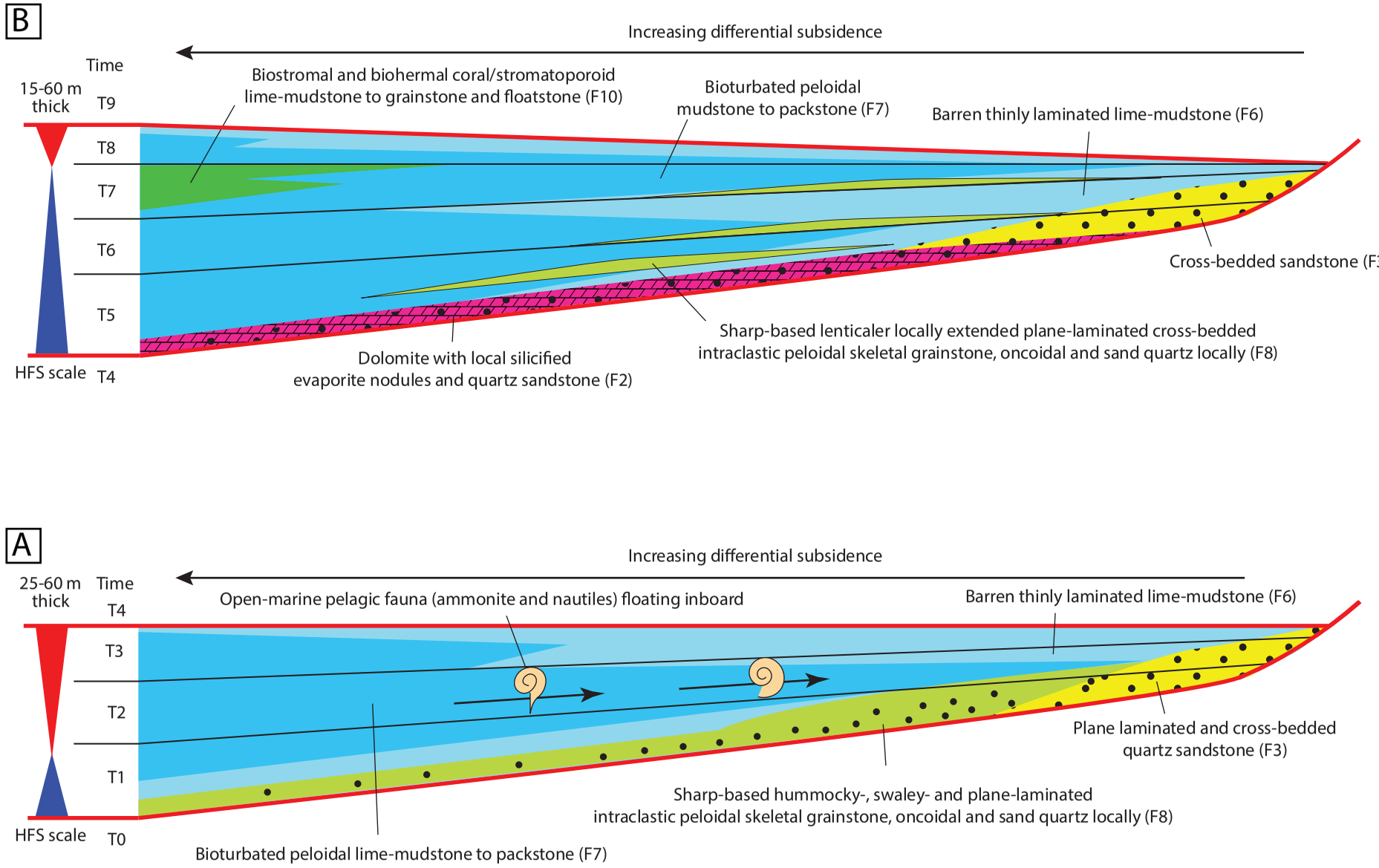

Figure 4.22: Depositional sequence model of the Jubaila-Arab-D showing spatial facies distributions and platform evolution in series of times (T0 to T9), A) Depositional sequence model for JCS1, B) Depositional sequence model for JCS2.

4.5.2 Jubaila and Arab-D Sequence Stratigraphy

The facies distribution of the Jubaila-Arab-D outcrops attests conformable genetically related successions that comprise of two composite sequences (JCS1 and JCS2). The base sequence boundary of the major Jubaila-Arab-D cycle shows sedimentological contrast between underlying coral/stromatoporoid rich deposits of the Hanifa sequence and overlying high-energy storm-influenced grainstones. The top sequence boundary of JCS2 is a significant stratigraphic boundary recognized by some of the previous studies as it separates two depositional sequences (Fig. 4.22) (Powers, 1962; Mitchell et al, 1988; Meyer and Price 1993; Handford et al., 2002; Lindsay et al., 2006; Al-Awwad and Collins, 2013b). The top boundary of the major Jubaila-Arab-D cycle (top JCS2) is marked by significant erosional ravinement surface underneath the Arab-D anhydrite (Fig. 4.20A).

The Jubaila-Arab-D sequences are dominated by carbonate system with subordinate siliciclastic, mainly sandstone quartz and lacks of argillaceous contents. The Jubaila-Arab-D sequences formed in overall low-energy wide lagoon in a flat-topped inner-platform subjected to transgressive-related storm pulses. The overall vertical depositional evolution of the Jubaila-Arab-D successions begins with storm-generated quartz-rich grainstones (F8) overlain by low-energy lagoonal lime mudstone (F7 and F6; JCS1). The late transgression and MFS marked by development of high-energy back-barrier reef facies association (F10) within JCS2. The regressive highstand deposits are represented by relatively low energy restricted lagoonal lime mudstone (F6). This succession shows extensive correlatable tabular units with a slight retrogradational then aggradational stacking pattern. The depositional

geometries and the limited lateral facies changes show that there is no clinoform can be suspected in this sequence. The stacking patterns lack of well developed progradational geometries and low-stand system tracts (LST).

Consistently with this study, the lower sequence is considered as storm-layered succession (Meyer and Price, 1993). The upper part of the Jubaila-Arab-D sequence is characterized by a distinct change in facies with a high-energy deposits and widespread open-marine fauna of coral/stromatoporoid (Mitchell et al., 1988; Handford et al., 2002), which considered as a transgressive event by Handford et al. (2002). In the classical interpretation, these facies are considered as a highstand prograding fringing reef (Lindsay et al., 2006; Al-Awwad and Collins, 2013b). On the opposite, the development of such open-marine facies above the lagoonal lime mudstone refers to a backstepping back-barrier deposits corresponding to the maximum transgression stage of the Jubaila-Arab-D cycle. The apparent polarity of Jubaila-Arab-D transect is clearly demonstrated in S-N direction in which the most southern section (Wadi Al Haddar) is almost lack of open-marine fauna and consists entirely of barren lime mudstone (F6) with slightly bioturbated interval and thin beds of storm-generated quartz-rich grainstones (F8). In parallel, the sandstone tends to increase southward in which the lower half of the sequence almost completely grade to sandstone deposits in Wadi Al Majami (Vaslet et al., 1985). In addition, the open marine facies, coral/stromatoporoid and rudist increase northward in the upper half of the sequence toward normal-marine back-barrier lagoon.

The depocenter of the Jubaila-Arab-D sequences is located at Wadi Al Ain with around 160 m thick. South- and northward of this locality the sequence

thins up to 110 to 115 m thick (Fig. 4.6). The lithostratigraphic boundary between the Jubaila Limestone and the Arab Formation (*sensu* Manivit et al., 1991; Appendix 1) seems to be conformable surface within JCS2 (Fig. 4.6). The Arab-D anhydrite, located in the upper part of the Arab-D Member, is not part of the Jubaila-Arab-D sequences. The thickness of the evaporites is increasing upward which imply an increase of accommodation space of the TST of next sequence. Two different lithostratigraphic schemes, surface and subsurface, for the Jubaila Limestone and Arab-D Reservoir/Member are shown in Figure (4.6). The outcrop lithostratigraphic boundary between Jubaila and Arab-D Member is placed at top of reef facies (*sensu* Manivit et al., 1990; Powers et al., 1966). In the subsurface, the Arab-D Reservoir has been divided into three informal time-stratigraphic zones based on porosity log correlation (Mitchell et al., 1988). These reservoir zones are extended to the outcrops sections through subsurface correlation with Khurais and Ghawar fields (Fig. 4.25).

The biostratigraphic control of the Jubaila-Arab-D sequences is limited to the lower 25 to 30 m of the JCS1 and dated Early Kimmeridgian by nautiles (Manivit et al., 1990). The upper Jubaila-Arab-D sequence (JCS2), Arab-D Member/Reservoir, lacks ammonite and is dated Kimmeridgian based on benthic foraminifera (Manivit et al., 1990; Hughes, 2009). Having an early Kimmeridgian for the upper Hanifa Formation and Lower Jubaila Limestone (JCS1), suggests that upper Jubaila and Arab-D Member (JCS2) may extend into Late Kimmeridgian. Because of the limited biostratigraphic control, the vertical development of the Jubaila-Arab-D sequences have been correlated with sea-water palaeotemperature evolution (Fig. 4.27) that supports Late

Kimmeridgian age for the upper Jubaila-Arab-D sequence (JCS2). Thus, the approximate duration of the Jubaila-Arab-D sequences could be ~ 4 Myr, then the average duration of the two composite sequences (JCS1 and JCS2) is approximately 2 Myr.

4.5.2.1 Jubaila and Arab-D Composite Sequence 1 (JCS1)

The JCS1 is 98 m thick in the central part of the transect (Wadi Al-Ain) and thins-out to 55 m in the northern- and southern-end of the transect. The base sequence boundary is a sharp erosional iron-stained surface (Fig. 4.18) overlain by quartz-rich storm-influenced grainstones. The JCS1 consists of two high-frequency sequences (HFS1 and HFS2) that are characterized by flat aggraded storm influences lagoonal deposits. The spatial facies distribution of these sequences evolved in series of times (T1-T3) illustrated in depositional sequence models (Fig. 4.22A).

The HFS1 (30 to 65 m thick) shows apparent wedging geometry and thickness variation result from a progressive synsedimentary deformation. The differential subsidence increased toward the central of the studied area (Wadi Al Ain). The base of the HFS1 is characterized by sharp-based transgressive grainstones floatstone/rudstone (F8) with rip-clasts and around 30% sandstone quartz and lack of coral/stromatoporoid reefs (Fig. 4.17). These high-energy grainstones (F8) are characterized by hummocky-, swaley- and plan-laminated sedimentary structures (Fig. 4.10A, 4.10B, 4.17, 20C). These storm beds are interbedded with barren thinly laminated lime mudstone (F6) and slightly bioturbated nodular wackestone with low foraminiferal species diversity (*Nautiloculina oolithica* and *Lenticulina* sp.)

corresponding to restricted lagoon facies association. These storm beds formed aggraded extensive correlatable units, which imply a flat domain after the top Hanifa exposure. Moreover, the depositional profile is kept very flat during the synsedimentary deformation as suggested by the lack of lateral facies variations. The prevailed storm process during initial transgression infers no barrier at this stage that allowed a great propagation of waves in such wide inner-platform. The MFS of HFS1 is placed in thickest storm grainstone bed in the most proximal section (Al Haddar). This is because development of wave and storm dynamic and propagation requires higher accommodation space in such very wide lagoon. The HST of HFS1 is marked by progressive upward decrease and thinning of the storm grainstone beds (F8). The storm grainstones (F8) are fining upward and grades to highly bioturbated lagoonal mudstone/wackestone (F7) rich with benthic foraminifer (mainly *Alveosepta jacardi* and *Kurnubia jurassica*), pelagic fauna (ammonite and nautiles). During the highstand, waves and storms become fetch-limited due to the unique physiography of the Arabian Platform and the great distance of the studied area from the ocean. Moreover, the lagoon muddy facies (F7) are aggrading and still in connection to the ocean and open-marine condition as indicated by high-bioturbation and the invasion of the pelagic fauna (ammonite and nautiles) in proximal setting. Through the HST, The intensity of the bioturbation of the lagoonal facies (F7) is progressively decrease upward grades to barren thinly laminated lime mudstone (F6; Appendix 4), which imply an increase in restriction and protection upward. The restriction is caused by a short-term regression and seaward stepping of shoreline and high level of nutrient influx. The top sequence boundary of the

HFS1 is not clearly defined but it can be placed on top of the most extended restricted lagoon (F6) to the north, the distal domain.

HFS2 (30 to 35 m thick) shows tabular and no lateral thickness variations. The TST is marked by a progressive upward thickening of the storm grainstone beds (F8) and increasing of the bioturbated wackestone/packstone facies (F7) which imply more marine influence and decrease of the nutrient supply. Moreover, the bioturbated wackestone/packstone facies (F7) shows a slight backstepping stacking-pattern toward the proximal domain to the south. The storm grainstones (F8) are quartz-rich and dominated with oncoid and coated-grains floatstone/rudstone. Very rare reworked clasts of coral/stromatoporoids were noticed in these grainstone beds. The upward change from barren restricted lime-mudstone (F6) to more algal microbial system confirms the decreasing of the nutrient influence through the transgression trend. However, the lagoonal depositional condition is still partially restricted and not yet fully marine condition evident by poorly developed reef facies (F10) and low faunal diversity. The MFS of HFS2 is placed in the most backstepping of the bioturbated lagoonal facies (F7) toward the proximal domain to the south. In the TST of HFS2 a clear relationships between energy, faunal-diversity and bioturbation. The very-low energy facies (F6) are barren and not bioturbated but when it grades to wackestone/packstone (F7) the storms and faunal diversity become developed. Thus, depositional energy and the protection condition seem to be related to the paleogeography or physiography of the Arabian Platform rather than water depth relationship. The HST is marked by an upward thinning and decrease in storm grainstone facies. The vertical facies proportion of the

storm grainstones through HFS2 suggest that storms are cyclic and transgressive in origin and attributed to the increase of accommodation space. The muddy lagoonal depositional system are aggraded and kept up to the top sequence boundary. The top sequence boundary (top JCS1) is probably a subaerial exposure marked by regionally extensive red dolomite bed (F2) with local silicified evaporite nodules (Wadi Al Haddar), which attributed to a restricted tidal or salina recharge process.

4.5.2.2 Jubaila and Arab-D Composite Sequence 2 (JCS2)

The JCS2 is 48 - 62 m thick that thins slightly to north (Wadi Malham). The JCS2 consists of three high-frequency sequences (HFS1-HFS3). These sequences record flat low-energy lagoonal deposits with slight backstepping of high-energy normal-marine back-barrier despites followed by regression of restricted and protected lagoonal deposits. The spatial facies distribution of these sequences evolved in series of times (T5-T8) illustrated in depositional sequence models (Fig. 4.22B).

HFS1 is 15 to 25 m thick and thins slightly to the north as a result of syndepositional differential subsidence. The TST starts with sand-flat cross-bedded quartz sandstone (F3) interbedded with barren lime mudstone (F6) in the south (Wadi Al-Haddar). These facies grade laterally northward to slightly bioturbated mudstone/wackestone (F7) interbedded with less extensive storm grainstones (F8) with common quartz content and reworked clasts of coral/stromatoporoids. The TST shows a decreasing vertical proportion of the quartz content. The MFS is marked in the distal domain (Wadi Malham) by erosional based high-energy grainstones (F8) associated with coral/stromatoporoid buildups (F10) and reworked clasts (Fig. 4.10H, I, J).

The coral/stromatoporoid system is widely influenced by wave and storm dynamic in such inner platform setting. The waves and storms are really the dominant factor during maximum marine transgression of the Jubaila deposition. Thus, the coral/stromatoporoid facies (F10) have to be interpreted as back-barrier backstepping units and not classic prograding units as shown by disappearance of these facies in the proximal domain of the transects (Wadi Al-Haddar). The HST of HFS1 is marked by progressive finning upward and minor regression and seaward stepping of the barren lime mudstone (F6). The top sequence boundary of HFS1 is marked in the north by quartz-rich red dolomite bed (F2; Wadi Malham). Whereas in the south (Wadi Al-Haddar), the sequence boundary is a transgressive surface overlain by reworked hummocky-cross stratified lime-mudstone (F6) and quartz-rich storm grainstones (F8).

HFS2 is 17 to 25 m thick and thins slightly to the north. The initial TST is characterized in the north (Wadi Malham) by dolomitized and quartz-rich grainstone (F8) that fines upward to bioturbated wackestone facies (F7). These facies grades southward (Al-Haddar) to hummocky-cross stratified barren lime-mudstone (F6) and thin quartz-rich storm grainstones (F8). Through the MFS, the quartz content decreased upward and the depositional system becomes high-energy dominant with open-marine fauna, coral/stromatoporoid and rudist floatstone/rudstone (F10; Wadi Malham, Al-Hawtah). The MFS of HFS2 is placed in the maximum extension of the coral/stromatoporoid and rudist floatstone/rudstone (F10) to the south indicating well-circulated normal-marine back-barrier lagoon. Further to the south, these open marine facies grades to bioturbated wackestone/packstone

facies (F7; Al-Haddar) with some encrusted coral/stromatoporoid indicating open lagoon condition. The MFS of HFS2 corresponds to the main maximum marine transgression of the JCS2 and for the whole Jubaila-Arab-D cycle. Through the HST of HFS2, the coral/stromatoporoid facies (F10) grades progressively upward to oncoid and coated-grains floatstone/rudstone (F8) accompanying with increase of quartz content and thickening of quartz-rich red dolomite beds (F2; Wadi Malham). This vertical change in facies proportion from reef dominated depositional system to more algal microbial system attributed to the increasing of the nutrient influence through the regression trend. The oncoid and coated-grain floatstone/rudstone (F8) grades laterally southward (Wadi Al-Haddar) to barren lime mudstone (F6). The top sequence boundary of HFS2 is marked by quartz-rich red dolomite bed (F2; Wadi Malham) and transgressive surface overlain by reworked clasts of rudists (Al-Hawtah) and coral/stromatoporoid (Wadi Al-Haddar).

HFS3 (12 m thick) shows tabular and no lateral thickness variations. The HFS3 is characterized by barren lime mudstone (F6) and bioturbated wackestone facies (F7) and lacks of the normal-marine coral/stromatoporoid facies (F10). The TST is marked at the base of the cycle by thin transgressive grainstone rudstone/floatstone (F8) with reworked clasts of rudists and coral/stromatoporoid. The HST is marked by the lateral northward extension of the restricted low-energy lime mudstone (F6). The top sequence boundary (tope JCS2 and whole Jubaila-Arab-D cycle) is marked by erosional ravinement surface (Fig. 4.20A) overlain by dolomitized grainstones (F8) with reworked silicified evaporite nodules (Wadi Malham) and occasional

hummocky cross-stratification (Al Hawtah). The grainstones are overlain by anhydrite solution (F1) and stromatolitic dolomite deformed and rotated beds.

4.6 Discussion

4.6.1 Evolution of depositional systems

4.6.1.1 Hanifa Formation

The long-term vertical facies evolution of the Hanifa sequences shows a cleaning upward trend and an increase of faunal diversity toward open lagoon and higher energy deposits. The initial transgression is characterized by low-energy restricted argillaceous-prone inner-lagoon (F4) and thin storm-grainstone bedsets (F8). Then, during late transgression and highstand, the successions show reef buildups (F10), associated oncoids rudstone (F9) and swaley cross-stratified well-sorted grainstone (F11). The large development of the reef buildups (F10) and the swaley cross-stratified well-sorted grainstone (F11) is in the HCS4. This is related to the continued transgressive/backstepping trend of the overall transgressive trend of the Hanifa Formation. Thus, the MFS of HCS4 corresponds to the main maximum transgression of the Hanifa Formation.

The Hanifa Formation has been previously interpreted as two composite sequences, Ulayyah sequence and Hawtah sequence (Sharland et al., 2001; Mattner and Al-Husseini 2002; Al-Husseini et al., 2006; Hughes et al., 2008; Hughes 2009; Le Nindre in Kadar et al., 2015). The first three composite sequences, defined herein (HCS1 to HCS3) would be equivalent to the Hawtah sequence and HCS4 would be equivalent to Ulayyah sequence. Noteworthy, the lithostratigraphic boundary between the Hawtah and Ulayyah

Members defined by Vaslet et al. (1983) is within HCS3 (top HFS2), which can not be used a sequence boundary separating these two main sequences. However, the best sequence boundary between Hawtah and Ulayyah sequences is top HCS3, which is considered as significant stratigraphic event, marked by tectonic warping and erosional surface. This sequence boundary between Hawtah and Ulayyah sequences corresponds to a 3rd order SB3 11.2 (Al-Husseini et al., 2006).

The MFS of the Hawtah sequences would be placed in the Late Oxfordian (MFS of HCS3) with the backstepping of high-energy deposits coincide with the highest faunal diversity (Appendix 2 and 3). Conversely, other workers placed the MFS of the Hawtah sequences in the Middle Oxfordian (*plicatilis* Zone) (MFS J50 of Sharland et al., 2001; Mattner and Al-Husseini, 2002; Le Nindre in Kadar et al., 2015). Moreover, Hughes et al. (2008) placed the MFSs of both sequences Hawtah and Ulayyah in argillaceous limestone with highest gamma-ray signals, 10 m above the base sequence boundaries, near Ar Riyadh city (Appendix 2). They interpreted the argillaceous limestone interval as deep-lagoon environment based on associations of micro- and nanofossils. However, the high argillaceous sediments at the base of the sequences are not a sign of deepening in such shallow flat inner-platform setting, but rather would be an indicator of an initial transgression of nearshore siliciclastic. These basal argillaceous sediments are characterized by low-faunal diversity formed in a restricted condition as attributed to the proximality to the nutrient supply. Open marine fauna may jump in inner-platform setting in near-shore argillaceous facies during early transgressive systems tract when barriers are not established yet. Then during the latter

transgressive stage when the barrier is established, the depositional condition becomes restricted and protected dominated by low-energy argillaceous and lime mudstone with poor faunal diversity (e.g., HL7, HL20, U1 and U2 in Appendix 2). Then, high faunal diversity appears during the maximum transgression associated with the backstepping of normal marine facies coral/stromatoporoid boundstone and/or ammonite fauna in a back-barrier inner-platform context. Moreover, other arguments support the continental origin of the argillaceous contents is that they increase toward the south (apparent proximal domain) compared to the back-barrier reefs and grainstone deposits that are more developed in the north (apparent distal domain). Moreover, the MFS is better placed higher in a regionally extensive limestone with cleaning gamma-ray trend as it shows continuous onlapping with widespread ammonites and/or corals/stromatoporoids. The siliciclastic would remain far updip landward resulted from widespread backstepping of siliciclastics during the TST. Thus HST lacks siliciclastics and has cleaning-up gamma-ray trend.

4.6.1.2 Jubaila-Arab-D

The sequence stratigraphy of the Jubaila Limestone and Arab-D reservoir has been subjected to many detailed studied in outcrop and subsurface (Powers, 1962; Mitchell et al., 1988; Le Nindre et al., 1990; Meyer and Price, 1993; Handford et al., 2002; Lindsey et al., 2006; Al-Awwad and Collins, 2013a, 2013b; Al-Awwad and Pomar, 2015). The sedimentological description in these previous studies are limited to the so-called “Arab-D reservoir”, which corresponds to upper part of the Jubaila Limestone and Arab-D Member (HFS2 of JCS1 to JCS2). Moreover, what is lacking in the previous studies is

a complete regional sequence stratigraphic cross-section documenting lateral facies changes of the lime mudstones of the Jubaila Limestone and base Arab-D Reservoir. These lateral facies changes are less evident in the subsurface and specifically across the Ghawar field, 300 km west of Riyadh (Mitchell et al., 1988). In some of these previous studies, the barren lime-mudstones (F6) are interpreted to be deposited in distal ramp depositional setting (e.g., outer ramp for Handford et al., 2002; Lindsay et al. 2006; Al-Awwad and Pomar, 2015; basinal lime-mud for Al-Awwad and Collins, 2013b). On the opposite, as proposed in this paper, Powers (1962) and Mitchell et al. (1988) considered these barren lime-mudstones (F6) in Zone3 and lower Zone2 (correspond to our HFS2 of JCS1 and HFS1 of JCS2) as deposited in a restricted, very shallow and quiet water environment.

The reasons behind the interpretation of the lime mudstone (F6) as distal facies are that the low-energy and the poor light-penetration are attributed to bathymetric gradient (Al-Awwad and Collins, 2013b). However, these two conditions can be observed in a sheltered or protected shallow marine carbonate system on this exceptional extensive platform, >1000 km from the shelf margin (Fig. 4.24). The high coastal nutrient input from surface run-off could limit light penetration (Hallock, 2001) and cause restricted low-oxygenated condition controlled by density stratification that prevented vertical circulation of bottom water (Bottjer et al., 1986; Rabalais et al., 1991; Lukasik et al., 2000). These could result in a distinct change in benthic community environment “phase shift” (Hallock, 2005) which explain the disappearance of the shallow component community (e.g., dasyclads, oncoids, benthic forams). Having the barren lime-mudstones (F6) deposited in a proximal nearshore

setting with high coastal-nutrient input is consistent with the associated high-content of sandstone quartz in outcrop (HFS1 and HFS2 of JCS1) and subsurface (Fig. 4.25; Zone3, Lindsay et al., 2006). In addition, the updip equivalents of these restricted lime mudstones (F6) are the coastal quartz sandstones and conglomerates (Fig. 4.6) (Wadi Al Majami, Vaslet et al., 1985; Fig. 4.6). Other evidences support the interpretation adopted herein is that these barren lime-mudstones (F6) occur higher in the Arab-D Reservoir directly underneath the intertidal facies (Zone1) and anhydrites, in both outcrop (Fig. 4.6, 4.20A) and subsurface. In the subsurface around 300 km north and northeast of Riyadh, two wells are all made up of barren lime mudstone (F6) and overlain directly by the Arab-D anhydrite (Al-Awwad and Collins, 2013b). These wells lack of coral/stromatoporoid facies, thus, the wells are considered as anomalous in which they couldn't be explained with the basinal lime-mudstone interpretation (Al-Awwad and Collins, 2013b).

The interpretation of these lime-mudstone facies as basinal or outer-ramp deposits leads the previous authors to consider inclined depositional profile with bathymetric that reach up to 70 m during the depositional of the Jubaila Limestone (Meyer and Price, 1993; Handford et al., 2002; Al-Awwad and Collins, 2013b; Al-Awwad and Pomar, 2015). Interpreting the lime mudstone as relatively deep facies, the facies succession in the Jubaila-Arab-D is considered as an overall shallowing-up/regressive sequence that implies clinoform geometries. This interpretation takes no heed of the extensive correlatable layer-cake stratigraphic architecture observed at outcrop and in subsurface reconstructed from distinct gamma-ray signals (Fig. 4.24) of Zone3 (HFS2 of JCS1) (Figure 15 of Mitchell et al., 1988; Meyer and Price

1993). The layer-cake and time-parallel sequence stratigraphic framework of the Jubaila Limestone and Arab-D Reservoir, presented here (Fig. 4.6, 4.26) are consistent with the interpretation of Wilson (1975), Murris (1980) and Mitchell et al. (1988) showing the same tabular geometries. Moreover, the interpretation of clinoform geometries has not considered at all the syndeposition differential subsidence that played significant role during the deposition of the Jubaila Limestone (e.g., HFS1 of JCS1). The thickness variations of the Jubaila-Arab-D cycle are here related to a syndepositional differential subsidence and a progressive and continuous aggradation of the carbonate platform punctuated by period of subaerial exposure (top SB of JCS1). The subaerial exposure is evident in the north of Ghawar (Lindsay et al., 2006) and in southern Rimthan Arch (Al-Mojel, 2012; unpublished report) (Fig. 4.24, 4.25). However, the clinoform model is interpreted to be prograding and infilling into the thickest part of the basin, thus, regional thickening direction is interpreted as progradational trend (Al-Awwad and Collins, 2013b).

4.6.1.3 Evolution of the carbonate system in a transgressive inner-platform depositional sequence

The studied system is located on the proximal part of a very wide epeiric platform, > 1000 km from the ocean-facing platform margin (Fig. 4.24) which is now integrated in the Zagros and Oman mountain belts. There is no really deep-marine facies association in the studied interval. The depositional system is characterized by an association of low-energy muddy deposits, sometimes slight argillaceous, and high-energy coarse grained deposits mainly grainstone with occasional sandstones. The sedimentary structures of

these high-energy deposits suggest an origin of storm-related currents. However, they are suspected to have formed in upper offshore deposits, as they don't show the classical characteristic of such environment, fine-grained sediments with well-developed HCS structures. Moreover, the offshore storm deposits tend to be narrow and localized that show prograded lenticular grainstone bodies but this is unlikely to be the case. These storm-generated grainstones are extensive and regionally continuous suggesting a correlatable and synchronous sequence stratigraphic event formed in a flat-topped inner-platform depositional setting. The high-energy deposits developed during early transgressive stages when the barrier is not established. Then the high-energy grainstones are less frequent during the latter transgressive stage when the barrier is established. These storm-related deposits are also appears during maximum transgression associated with the backstepping of normal marine facies coral/stromatoporoid boundstone, high foraminiferal diversity, and/or ammonite fauna in a back-barrier inner-platform context. Most of the high-energy depositional units have a sharp-based contact with the underlying muddy deposits. A gradual coarsening-up evolution, which should exist in a prograding system, has never been observed in the studied sections. The sharp-based surfaces are interpreted as ravinement surfaces related to transgressive processes and not to sea level drops and associated forced-regressive processes. The transgressive ravinement surfaces are extensive and considered timelines that shouldn't be crossed. The low-energy argillaceous and lime mudstone facies are better developed in the proximal landward position (south) compared to the back-barrier boundstone and grainstone deposits that are more developed in the distal part of the transects

(north). The low-energy deposits are unlikely to be deeper offshore facies but rather inner platform lagoonal facies.

The Hanifa and Jubaila stratigraphic transects attest a very tabular geometry and wide lateral continuity of these carbonate platform deposits. Prograding clinoforms and stratal wedges have not been observed in the studied areas. The reconstructed tabular stratal geometries indicate an overall aggrading pattern in an inner platform context. The only clinoforms that could be identified are located more to the east, with subsurface data (Fig. 4.24). These low-angle clinoforms are related to the development of intra-shelf basin and classically formed by differential platform aggradation during transgressive stages (e.g., Ayres et al., 1982; Razin et al., 2010, 2017). The outcropping Hanifa – Jubaila sequences are located on the proximal and purely aggrading part of this carbonate system. In this type of platform-intrashelf basin system, the deeper environments are characterized by organic-rich lime mudstones (cf. Droste, 1990; McGuire et al., 1993; Al-Naji, 2002; McGuire, 2003) that have not been observed in the study area.

4.6.1.4 Insight to the development of the Late Jurassic intrashelf Arabian Basin

Surface to subsurface correlations (Fig. 4.24 and 4.25) provide insight to the development and evolution of the Late Jurassic intrashelf Arabian Basin. Paleogeographically, the intrashelf Arabian Basin is more than 500 km landward from the Neo-Tethys continental margin (Murris, 1980; Ziegler, 2001). Moreover, the intrashelf Arabian Basin was surrounded from the north by broad Rimthan Arch that characterized by shallow marine peritidal deposits and exposed island and from east by Qatar Arch (Murris, 1980). The intrashelf

basin is bounded on the west (Khurais to outcrop) by flat-topped carbonate platform (Fig. 4.24). The facies of the intrashelf source rock is laminated dark organic-rich lime mudstone (McGuire et al., 1993; Al-Naji, 2002). The Hanifa reservoirs facies are characterized by oolitic and peloidal shoal grainstones and some coral/stromatoporoid floatstone located, in the cross-section (Fig. 4.24), only in the Berri Field on the southern Rimthan Arch and in the Khurais Field. Whereas the central Arabian Basin (North Ghawar and Qatif) and most southern Rimthan Arch, the Hanifa Formation consists of non-reservoir thick lime mudstone interval (McGuire et al., 1993; Al-Naji, 2002; Al-Mojel, 2012; unpublished report; Y. Mousa, personal communication, 2017). The shoal grainstones in the southern Rimthan Arch are mainly aggrading with slight progradational stacking patterns forming gentle ramp that dips southward with < 0.5° (McGuire et al., 1993; Al-Naji, 2002). The shoal grainstones in Khurais Filed are aggrading and have limited migrations (M. Fallatah, personal communication, 2017). These high-energy reservoir facies seem to correlate with the outcropping high-energy open-marine carbonate facies of HCS3 and HCS4. These high-energy reservoir facies are interpreted to be formed during maximum accommodation space that allowed open-marine conditions and wave energy to propagate inboard in such extensive protected flat platform. In addition, the high accommodation rate cause differential aggradational style on the platform as carbonate production is not able to fill up the created space everywhere (cf. Razin et al., 2010). Thus, high carbonate productions that follow the rapid accommodation rate were localized in certain places forming aggrading stacking patterns, like in Khurais and Berri Fields. Whereas, sedimentation in the central Arabian Basin was lag behind causing deep

source rock intrashelf basin with about ~70 m water depth (estimated by reconstructing depositional profile from one of the Hanifa cycles in Fig. 4.24). Accordingly, the formation of the deep intrashelf source rock is synchronous with the transgressive high-energy shallow marine deposits. The high differential sedimentation rate is responsible for creating bathymetric reliefs and local low-angle clinoforms that occur during late TST and MFS. The high productive and high-energy areas do not seem to prograde much to fill the intrashelf basin during HST. During highstand sea-level phase, depth of wave-base seems to decrease due to waved dissipation and distraction promoted by the remoteness of the basin from the ocean and probably by the growth of carbonate outershelf barriers. Therefore, protected and perhaps restricted lagoonal carbonate mud would drape and fill the low-topographic reliefs during HST. This would explain the thick non-reservoir lime mudstone in the central Arabian Basin. Therefore, the intrashelf Arabian Basin is filled to spill during the Hanifa Formation and not in the Upper Jubaila Limestone preceding the evaporite deposition as previously thought (Al-Awwad and Pomar, 2015).

The Jubaila and Arab-D sequence seem to be flat-topped homogeneous aggradation platform with no deep intrashelf basin. The Jubaila Limestone overlies the Hanifa Formation with lowstand deposits (Hanford et al., 2002) that appear to be localized west of the Khurais field. The top Hanifa disconformity (from Khurais toward outcrop) seems to be an onlapping surface. The lower half of the Jubaila (HFS1 of JCS1) underwent evident syndepositional differential subsidence that increased in the central of the Arabian Basin. Shallow carbonate platform will aggrade and keep-up as a

response to such continuous and slight syndepositional differential subsidence (cf. Wilson and Jordan, 1983). This would result in lateral thickness variations as well as slight lateral facies changes. The syndepositional differential subsidence decreased upward and became homogenous in the Arab-D Reservoir in which upper JCS1 and JCS2 show tabular geometries (Fig. 4.25).

Figure 4.27 shows sedimentological-based regional sequence stratigraphic correlation of the Arab-D Reservoir across the Arabian Basin. The Arab-D Reservoir in Berri field (JCS2) characterized by overall high-energy shoal facies association overlain by domed coral-stromatoporoid rudstone facies. The shoal facies successions are slightly migrating and finning inboard to the south. These facies deposited on a very low-angle (<1°) ramp profile with 0-12 m water depth. Depositional cycles were caped by exposure surfaces evident by dense dolomite and anhydrite beds with crinkly lamination, mud-crack and desiccation features. Moreover, meteoric cementations (pendant and meniscus) were noticed below the cycle boundaries (Al-Mojel, 2012; unpublished report). In the central Arabian Basin (Khurais and Shedgum), the facies of the Arab-D Reservoir (Zone 4 and 3) is characterized by micritic to very fine-grained sediments capped by firmgrounds and hardgrounds interbedded by storm-derived rudstone and floatstone (Fig. 4.25; Al-Awwad and Collins, 2013a; Lindsay et al., 2006). Arab-D Reservoir Zone 2 is characterized by domed, encrusted and branched coral/stromatoporoid packstone and floatstone with occasional ooid grainstone overlain by dasyclad and encrusting algae wackestone/packstone and floatstone and *Cladocoropsis* rudstone and floatstone (Al-Awwad and Collins, 2013a;

Lindsay et al., 2006). The succession of the Arab-D Reservoir is intermittent by sheetlike dolomite beds with fabric- and nonfabric-preserving texture. The dolomite were interpreted to be formed earlier, almost syndepositionlly, from hypersaline fluids derived from overlying salina (Lindsay et al., 2006). The regionally extensive dolomite appears to be stratigraphically related to tidal recharge/infiltration and seepage-refluxion processes (Adams and Rhodes 1960; McKenzie et al., 1980; Enos, 1983; Iannace and Frisia, 1994). The formation of these extensive sheetlike dolomites across the Arabian Basin seems to be controlled by low accommodation rates. Thus the rationale behind this Arab-D sequence stratigraphic framework (Fig. 4.25) is that the sheetlike dolomites were used as stratigraphic events in which inner-platform and intrashelf basin being restricted and highly evaporated during relative sea-level fall (late-HST/LST). The dolomites occur around sequence boundaries and almost disappeared or decreased in maximum flooding intervals with a backstepping of normal-marine high-energy facies (e.g., coral/stromatoporoid). Thus, the long-term evolution of the Jubaila and Arab-D depositional system can be divided into sequential depositional models (Fig. 4.26). During early transgression, the platform was probably lack of barriers and subjected to transgressive high-energy storm pulses, which brought relative normal-marine conditions and pelagic fauna in such proximal restricted inner-platform. This resulted in intercalation of extensive restricted barren lagoonal lime mudstone and storm-grainstone beds (HFS1, HFS2). During maximum marine transgression (HFS3, lower part of HFS4), a backstepping of normal-marine and higher energy condition is responsible for development of shoal grainstones in paleohighs and extensive back-barrier

reef facies (coral/stromatoporoid floatstone/rudstone). During HST (upper HFS4, HFS5), reef facies prograding out from the intrashelf basin into outershelf lifting behind aggradational extensive clear lagoon with dasyclad, encrusting algae and *Cladocoropsis* wackestone to packstone facies. During late HST (topmost HFS5), the platform has limited to no accommodation space in which inner-platform (outcrop) is probably exposed and intrashelf basin developed with restricted tidal flats.

4.6.2 Controlling factors of the Oxfordian and Kimmeridgian stratigraphy

4.6.2.1 Tectonic and subsidence rate

The onset of the Oxfordian successions shows shift in depocenter location and opposite dip-direction to the preceding Early and Middle Jurassic outcrops (Early-Toarcian to Middle-Callovian) (Al-Mojel et al., in prep.). The Oxfordian depocenter axis shifted to the south (As Sitarah section). This changes in basin configuration is probable related to a significant tectonic uplift and truncational event during post-Tuwaiq unconformity thorough the eastern edge of the Arabian Plate (Iran, Abu Dhabi and Interior Oman; Gollesstaneh, 1965; Al-Suwaidi and Aziz, 2002; Rousseau et al., 2006). Moreover, this erosional surface is responsible for the truncation of 200 m of carbonate deposits in eastern Interior Oman (Rousseau et al., 2006). This post-Tuwaiq truncation is also noticed in the Central Arabian Platform in the Rub' al-Khali and northern of the Ghawar field called “pre-Hanifa unconformity” (Powers, 1968). This tectonic instability is probably related to the incipient breaking of the Arabian-Indian plate boundary, which marked by

a volcanic interruption in eastern Oman (Ziegler, 2001). There is another shift in depocenter and reversal onlapping direction during the Late Oxfordian Early Kimmeridgian sequences (between HCS3 and HCS4). This revers in polarity directions have been documented in the subsurface and supported by seismically based stratigraphic section (Fig. 4.23; Langdon and Malecek, 1987) and in a gamma-ray cross-section (Fig. 4.24, number 3). The HCS3 and HCS4 seem to be source rocks and reservoirs equivalent in the subsurface. Therefore the sequence boundary between these sequences is a critical surface that has to be considered for reservoir studies and regional exploration correlation. These changes in basin configuration could be related to tectonic disruptions in which basement blocks were reactivated and tilted. These Oxfordian tectonic interruptions were noticed in other Tethyan regions. For example, the Jura Platform in the northern margin of the Tethys Ocean had discontinuous subsidence history and wobbling blocks movement during the Oxfordian (Strasser et al., 2015). Moreover, syndepositional tectonic activates have been documented in Tunisia (Walley, 1985) and in NW Tethys in central Europe (Dardeau et al., 1988; Lhamyani, 1985; Pittet and Strasser, 1998; Allenbach, 2001; Chevalier et al., 2001; Védrine and Strasser, 2009; Strasser et al., 2015). In particularly, tectonic inversion, dated Late Oxfordian (late *bifurcatus* Zone), was mapped in the Swiss Jura Mountains (Allenbach, 2001, 2002). This Late Oxfordian tectonic inversion could synchronous with the tectonic event between HCS3 and HCS4.

The beginning of the outcropping Jubaila depositional sequence (HFS1) records high syndepositional differential subsidence toward the central of the studied area (Wadi Al Ain) that are clearly demonstrated along

the transect by the complete wedging and thickening geometries of HFS1. This syndepositional differential subsidence seems to be decrease upward in which the sequences (HFS2-HFS4) show tabular geometries. The continuous and slight subsidence is controlling the thickness of the strata as well as lateral facies distribution (cf. Wilson and Jordan, 1983). Thus, the shallow carbonate platform will aggrade and keep-up as a response to the rotational differential subsidence, which result in thick-stacked shallow carbonate deposits wedging and thickening toward the depocenter.

The subsurface sequence stratigraphic framework demonstrates the evolution of the Arabian Intrashelf basin (Fig. 4.24). The Hanifa Formation is almost isopachous sequence indicating that the differential subsidence seems to be small and neglected. Thus, differential subsidence is unlikely to be the main control on the development of the deep source rock intrashelf basin but rather influenced by the changing ratio of carbonate production and accommodation space (see discussion below). However, significant syndepositional differential subsidence occurs during the lower half of the Jubaila sequence. This has been noticed in the outcrop cross-section (HFS1; Fig. 4.6) and in the subsurface correlation (Fig. 4.24) with abrupt thinning toward the Rimthan Arch. This is consistent with overall eastward thinning of the Late Jurassic stratigraphy toward the shelf margin as mapped by (Murris, 1980; Abu-Ali and Littke, 2005). The outward subsidence resistance of the shelf margin and Rimthan Arch are probably the main reason for being the lower Jubaila sequence restricted and protected for open marine condition.

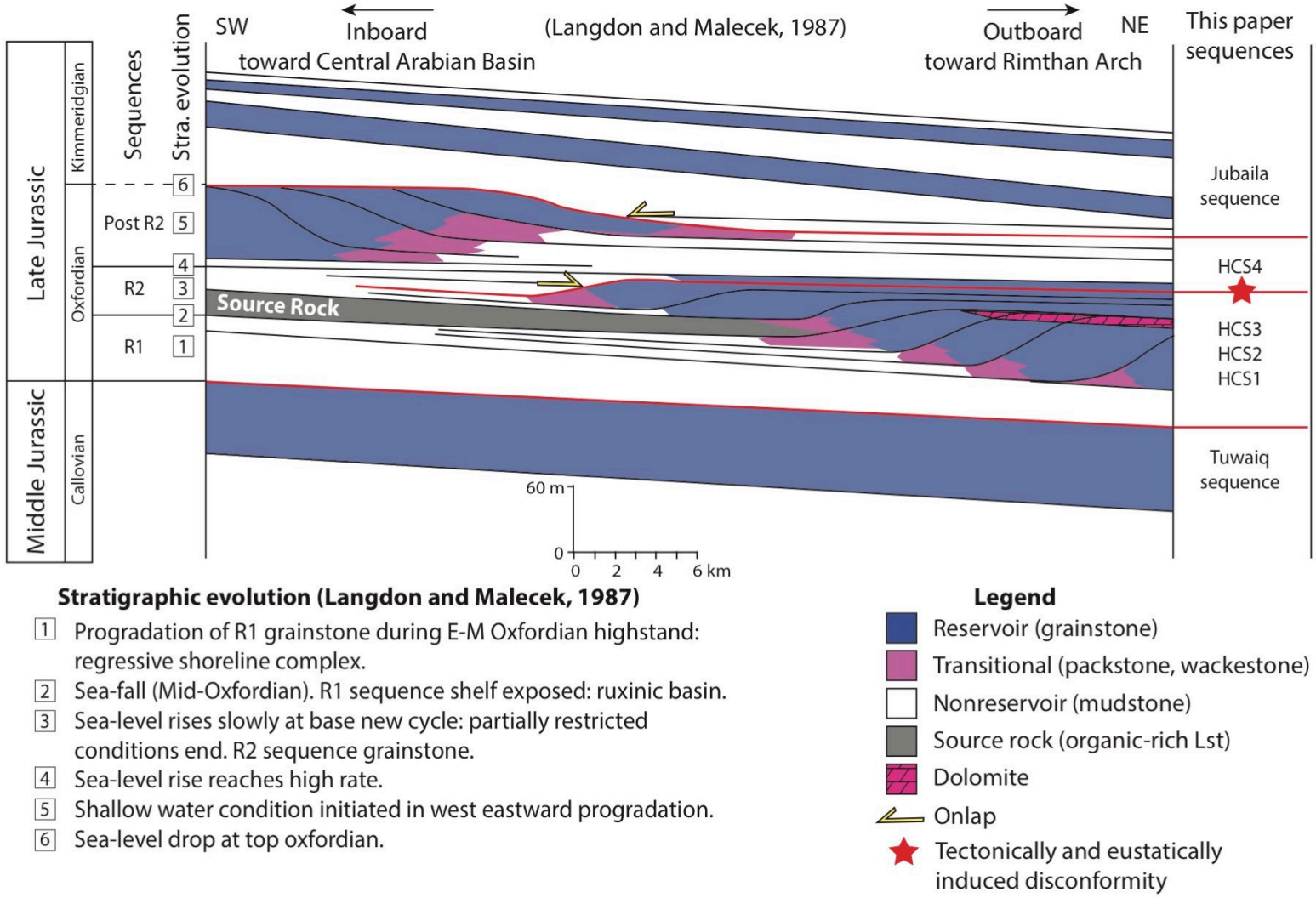

Figure 4.23: Subsurface stratigraphic architecture and evolution of the Late Jurassic Oxfordian and Kimmeridgian time is based on well-log correlation, seismic interpretation and facies regional mapping (modified from Langdon and Malecek, 1987). The Oxfordian sequences, interpreted in this paper, are correlated and applied to this section (The section is 400 km NE of the outcrop built).

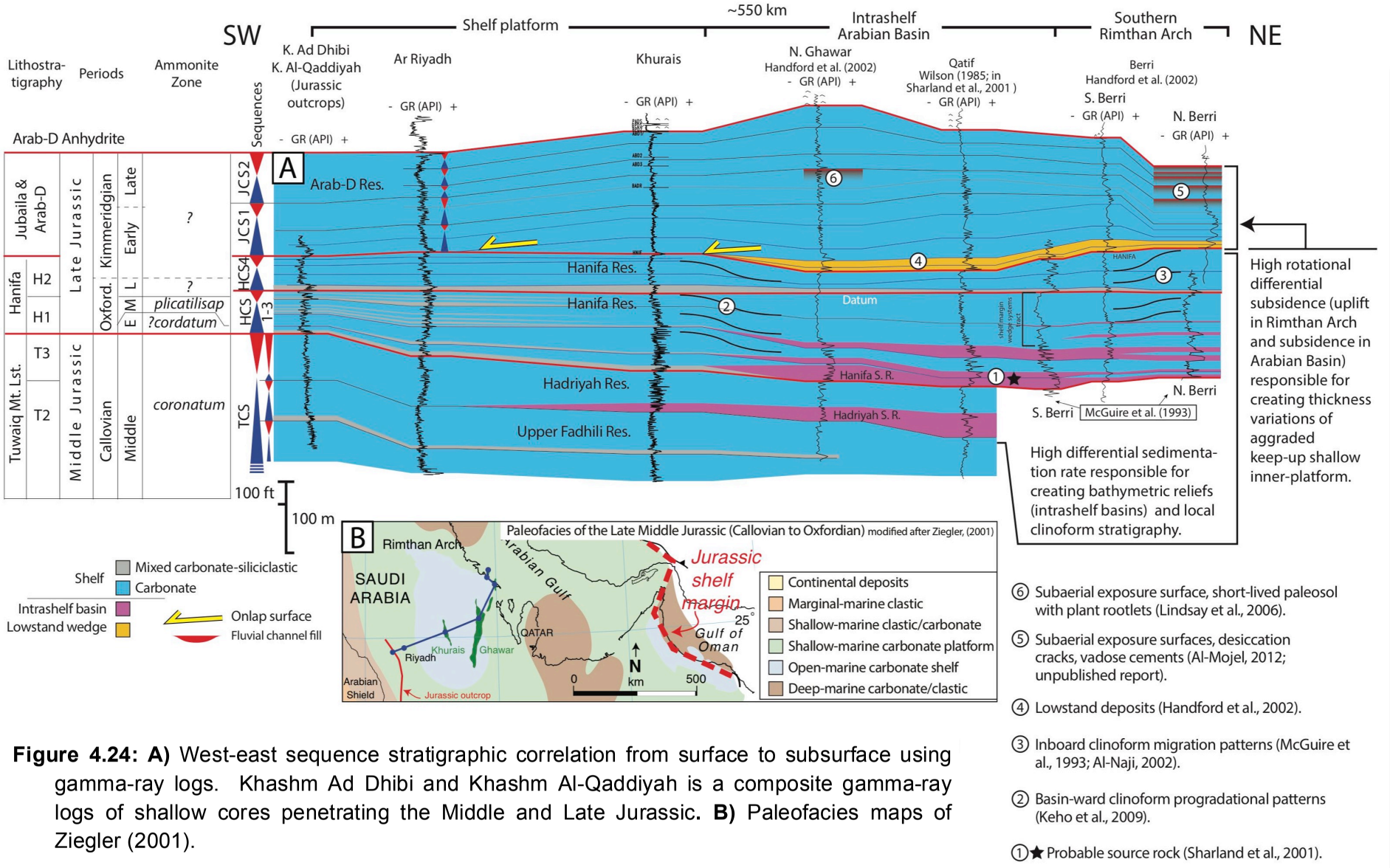

Figure 4.24: A) West-east sequence stratigraphic correlation from surface to subsurface using gamma-ray logs. Khashm Ad Dhibi and Khashm Al-Qaddiyah is a composite gamma-ray logs of shallow cores penetrating the Middle and Late Jurassic. **B)** Paleofacies maps of Ziegler (2001).

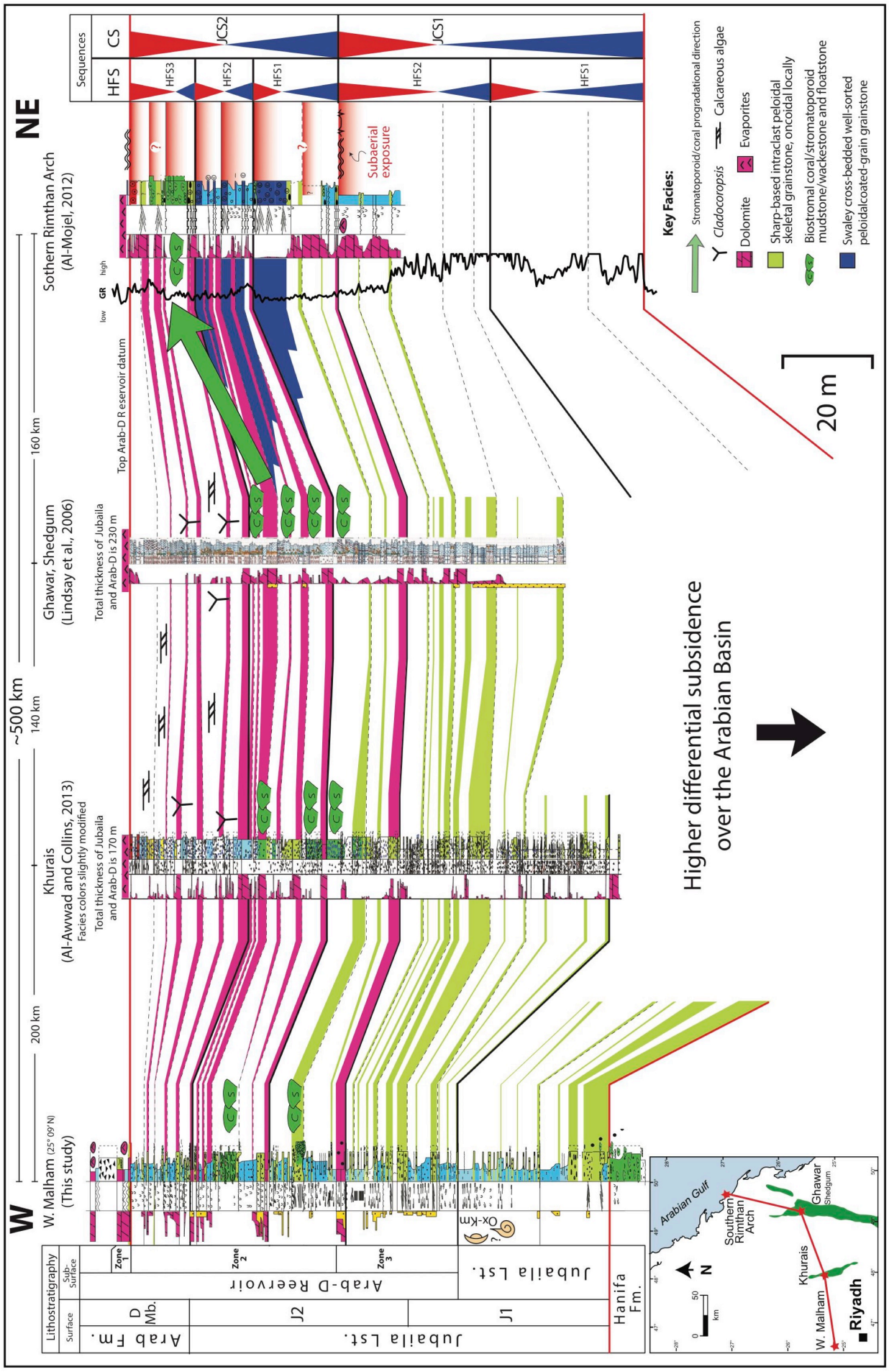

Figure 4.25: Surface to subsurface high-resolution sequence stratigraphic correlation of the Jubaila Limestone and Arab-D Reservoir.

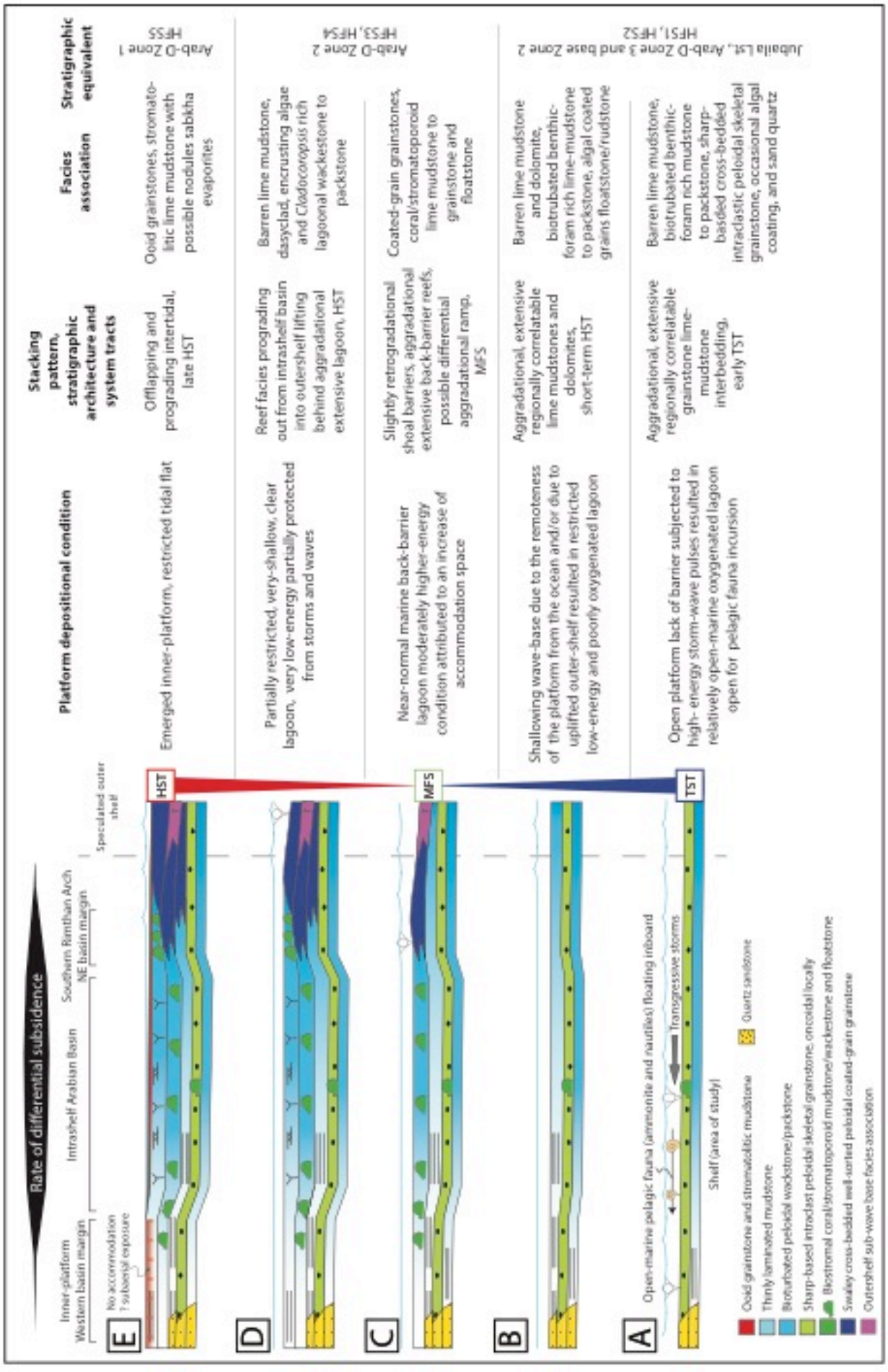

Figure 4.26: Depositional sequence model and long-term facies evolution of the Jubaila Limestone and Arab-D Reservoir of the Arabian Basin.

4.6.2.2 Eustatic controls

The base sequence boundary of the Late Jurassic sequences corresponds to an extensive regional unconformity with Late Callovian (*lamberti* Zone) and the Early Oxfordian (*mariae* Zone) hiatus (Le Nindre, personal communication, 2014; in Kadar et al., 2015). This unconformity is most likely resulted from substantial eustatic sea-level fall superimposed on local tectonic uplift and easterly tilting of the Arabian Platform (Ziegler, 2001). This Middle-Late Jurassic global sea-level fall could be of a glacio-eustatic in origin, as it corresponds to a maximum cooling event happened during Late Callovian (*lamberti* Zone) (Hallam, 1988; Dromart et al., 2003a, 2003b; Nunn et al., 2009; Nunn and Price, 2010; Donnadieu et al., 2011; Pellenard et al., 2014). This drop in sea level has been recorded in the relative sea-level curve of the Arabian Platform with around 40 m sea-level fall (Haq and Al-Qahtani, 2005).

Unfortunately, the Oxfordian and Kimmeridgian stratigraphy are too poorly dated to propose a global correlation scheme. The only confirmed ammonite zone corresponds to the Middle Oxfordian *plicatilis* Zone. The Late Jurassic successions shows long-term sea-level rise trend that reach its maximum in the Arab-D interval (Le Nindre et al., 1990). But, there is subordinate sea-level fall and a short emersion momentarily interrupted this trend. The transgression trend of the Oxfordian Hanifa sequences (Hawtah; HCS1-HCS3) shows an overall cleaning upward trend toward terrigenous-free carbonate sediments (Middle and Late Oxfordian; upper HCS3). The MFS is placed in the Late Oxfordian (MFS of HFS3) in an extensive carbonate interval with higher-energy and relatively normal-marine reef facies. Thus, the MFS J50 of the Arabian Platform would be better placed in the Late Oxfordian

instead of Middle Oxfordian as another workers did (Sharland et al., 2001; Mattner and Al-Husseini, 2002; Le Nindre in Kadar et al., 2015). The Late Oxfordian MFS is consistent with the Gulf of Mexico major marine transgression (Mancini et al., 2004) and the Central North Sea (Carruthers et al., 1996). However, the major MFS in the Western Europe occurs in the Early Oxfordian (Hardenbol et al., 1998). This discrepancy in the global MFS invokes a local tectonic overprint on the Oxfordian eustasy signals. A major sequence boundary and disconformity between HCS3 and HCS4 associated with significant facies shift and tectonic interruption, which is most likely to be Late Oxfordian in age. This sequence boundary could correlate with the Western Europe 2nd-order regression and sequence boundary between OX6 and OX7 (Hardenbol et al., 1998; Strasser et al., 2000; Védrine and Strasser, 2009). The second significant MFS in the Hanifa Formation is in the Ulayyah sequence (HCS4) in relative open-marine and higher-energy condition with reef-bearing facies, which would correspond to the Early Kimmeridgian MFS J60 (Sharland et al., 2001). Previously, the place of MFS J60 is debated and required further studies to recognize the best location of this Lower Kimmeridgian MFS. It has been suggested that the MFS J60 can be in the Lower Kimmeridgian either in Upper Hanifa (Ulayyah Mb.) or Lower Jubaila (J1) (R. B. Davis in Kaddar et al., 2015). Thus, we placed the MFS J60 in the upper Hanifa (Ulayyah; HCS4) instead of Lower Jubaila (J1), which characterized by a lowstand (Fig. 4.24) and restricted lagoonal deposits rich with sandstone quartz and lack of open-marine reef facies. Interestingly, the link between the long-term transgression and reef expansion is a mutual feature prevailed in the Upper Jurassic, noticed by Pittet and Strasser (1998)

(e.g., Leinfelder 1993, 1994; Keupp et al., 1993). These Lower Jubaila lowstand and restricted lagoonal deposits are considered initial transgression, whereas topmost Upper Jubaila (JCS2; J2 unit or Arab-D Reservoir) records the maximum marine transgression with high-faunal diversity and backstepping of reef facies. This Jubaila-Arab-D MFS would correspond to the Upper Kimmeridgian MFS J70 (Sharland et al., 2001; Le Nindre in Kadar et al., 2015). This is consistent with Kadar et al. (2015) interpretation that placed MFS J70 in a clean limestone at the topmost of the Jubaila, just underneath the Gotnia Anhydrite in Kuwait. This Jubaila-Arab-D long-term transgression is in concordance with the 2nd-order TST and MFS in the central Swiss Jura as well as in most of the Western European basins, which placed in the Late Kimmeridgian (*eudoxus* Zone) (Hardenbol, 1998; Colombié and Strasser, 2005). This Swiss Jura 2nd-order transgression begins with shallow-water thinly bedded limestones with siliciclastics and desiccation features (between sequence boundaries Kim 1 and Kim 4; Colombié and Strasser, 2005). Whereas, late transgression and MFS is characterized by open-marine thickly bedded limestone lacks of siliciclastics and desiccation features (between sequence boundaries Kim 4 and Kim 5; Colombié and Strasser, 2005). These Swiss Jura large-scale sequences are correlatable in most of Western European basins, which suggest a strong eustatic influence on the Kimmeridgian sequences (Colombié and Strasser, 2005).

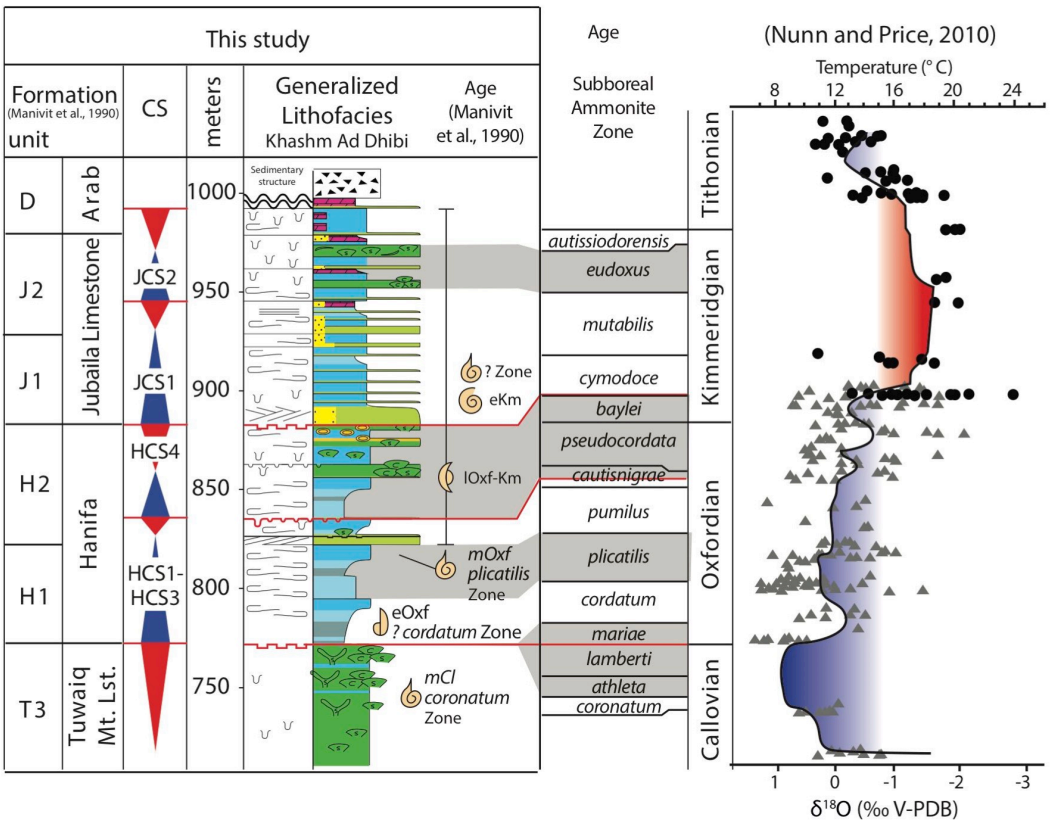

Figure 4.27: Generalized sedimentological section of Late Jurassic deposits from Khashm Ad Dhibi compared with the seawater temperature evolution inferred from belemnite $\delta^{18}O$ data from Scotland (Nunn and Price, 2010).

4.6.2.3 Climatic influences

During the Late Jurassic, the Arabian Platform was placed along the tropical belt probably 10-15 degrees south of the equator (Fig. 4.2; Thierry, 2000; Scotese, 2003). Here, the study of the Oxfordian and Kimmeridgian sediments from the Hanifa and Jubaila Arab-D formations allow us to address the impact of the Late Jurassic climatic disturbances in an epeiric platform context situated at very low paleolatitudes.

The Middle-Late Jurassic transition is an extensive regional unconformity over the Arabian Platform with Late Callovian (*lamberti* Zone) and the Early Oxfordian (*mariae* Zone) hiatus (Le Nindre, personal communication, 2014; and in Kadar et al., 2015). This unconformity was likely controlled mainly by a

global eustasy sea-level fall associated with an incipient cooling event having favored the extension of continental ice buildup at high latitude during Middle-Late Jurassic transition (Dromart et al., 2003a, 2003b; Donnadieu et al., 2011). According to oxygen isotope data of belemnites from Euro-boreal domains, the maximum of cooling happened during the Late Callovian (*lamberti* Zone) (Nunn and Price 2009; Pellenard et al., 2014) and triggered numerous faunal migrations of boreal taxa toward lower latitudes (Cecca et al., 2005). This drastic cooling (down to 7° C in Scotland; Nunn and Price, 2009). was associated with drier conditions evidenced by sedimentological, geochemical and palynological data from NW Tethys between the Middle Callovian to the Early Oxfordian (Abbink et al., 2001; Brigaud et al., 2008).

This cold event was followed by a period of warming in the NW Tethyan domain through the Middle Oxfordian (Fig. 4.27; Nunn and Price, 2010; Dromart et al., 2003b). Absent in other areas (Wierzbowski 2004, Alberti et al. 2012), this regional event likely resulted from changes in paleoceanic circulation patterns with incursions of tropical Tethyan waters toward northern areas (Dera et al. 2015). As shown by oxygen isotope data of belemnite rostra and oyster shells from Scottish and Paris basins (Nunn and Price 2009; Brigaud et al., 2008), seawater palaeotemperatures rised up to 3°C from the *cordatum* to *transversarium* Zone, that favored the development of reefal systems in the boreal domains of NW Tethys (Martin-Garin et al. 2012). This Early-Middle Oxfordian warming event was probably accompanied by a humid phase indicated by overall high kaolinite abundances in NW Europe (Wignall and Ruffell, 1990; Ruffell et al., 2002). In the Arabian Platform domain, the initial transgression and the highly terrigenous units at the base of the Hanifa

sequences (HCS1 to lower HCS3) are compatible with this Early-Middle Oxfordian warm humid phase. After this brief regional event, the marine paleoenvironments of European basins returned to cooler and more arid climatic conditions from the late-Middle to Late Oxfordian, with a minimum of temperature evidenced during the *bimmamatum* Zone by high oxygen isotope values of oyster shells from the Paris basin (Brigaud et al., 2008). This cooling trend was probably synchronous with the 2nd-order sequence boundary of the Western Europe (Hardenbol et al., 1998; Strasser et al., 2000; Védrine and Strasser, 2009). Moreover, it was concomitant with a drying phase evident by gradual decreases of kaolinite content and enrichment of smectite enrichments in the sediments of the Paris Basin (Mosser-Ruck et al., 2002). On the Arabian Platform, this late Middle to Late Oxfordian temperate-dry event could correspond to the cleaning upward trend toward terrigenous-free carbonate sediments with reef facies development (upper HCS3 and HCS4). This carbonate recovery and reef development seems to be a regional event noticed in the Western Europe (Dromart et al., 2003b) and mapped along the Tethys margin (Cecca et al., 2005).

The Late Oxfordian - Early Kimmeridgian transition recorded a rapid rise in seawater temperatures, which staying relatively high (up to 24° C) all over the Kimmeridgian (Brigaud et al., 2008; Price and Rogov, 2009; Nunn and Price, 2010; Wierzbowski et al. 2013). In parallel, clay mineralogical data from UK suggest that climatic conditions became progressively more humid up to the Late Kimmeridgian transition (Ruffel et al. 2002; Hesselbo et al. 2009). On the Arabian platform, this extreme warmth and humid phase is consistent with the recurrent occurrences of high sandstone contents in sediments of the lower

Jubaila-Arab-D sequence. Moreover, it supports the interpretation that high nutrient levels have a negative impact on the benthic communities and reef development. From the Upper Jubaila sequence, including the Arab-D Reservoir, the development of widespread reefs and decrease of the siliciclastic inputs are interpreted as the result of an eustatic transgression combined with parallel decreases of seawater temperatures and rise of aridity during the Late Kimmeridgian (Fig. 4.27; Nunn and Price, 2010). Moreover, the increase of the aridity is compatible with the appearance of widespread sheetlike dolomite beds in the Arab-D Reservoir that formed as result of hypersaline infiltration from overlying salina (Lindsay et al., 2006). Remarkably, the synchronicity of the TST and MFS with warm-humid condition and HST with cool-dry events provide some confidence to the astroclimatic-driven eustasy as a primary mechanism controlling these 3rd-order sea-level changes (cf. Boulila et al., 2011, Martinez and Dera, 2015).

4.7 Conclusion

The outcropping Hanifa Formation, Jubaila Limestone and Arab-D Member (370 km south of Riyadh) provide a westernmost stratigraphic record of the Late Jurassic (Oxfordian to Kimmeridgian including disconformity levels). The Late Jurassic of the Arabian Platform is a broad slowly subsiding epeiric tropical platform. Surface to subsurface gamma-ray correlations (550 km long to the east) provide insight to the development and evolution of the Late Jurassic intrashelf basin. The depositional environment ranges from semi-arid shoreline to carbonate inner lagoon and back-barrier lagoon. These formed aggraded flat-topped platform with evident syndepositional differential subsidence that has an influence on lateral thickness variation and to a lesser

extent facies distribution. The Late Jurassic successions make several transgressive 3rd-order composite sequences interrupted momentarily by short emersion sequence boundaries. The Hanifa platform is mud-dominated and evolved from proximal argillaceous-limestone with low-faunal diversity (lower Hanifa Fm., Early to Middle Oxfordian) to back-barrier open-marine carbonate platforms with coral/stromatoporoid bearing and high-faunal diversity (upper Hanifa Fm., Late Oxfordian to Early Kimmeridgian). The outcrops back-barrier high-energy deposits are adjacent to deep intrashelf basin in subsurface. The deep Intrashelf basin is associated with local low-angle clinoforms formed as a response to differential carbonate sedimentation during maximum marine transgression. The Hanifa Formation has two main MFS placed in terrigenous-free carbonate sediments at the Late Oxfordian and Early Kimmeridgian. The intrashelf basin is filled to spill during regression of the Hanifa sequences. The Jubaila-Arab-D platform is flat purely aggraded horizontal successions with lateral thickness variations controlled by syndepositional differential subsidence increased in the Arabian Basin. The Jubaila-Arab-D is a conformable succession consists of two composite sequences that show long-term transgression marked at the base by storm-influenced inner-platform with sandstone quartz, grainstones and proximal barren lime-mudstone. The Maximum marine transgression is placed in the Arab-D in a backstepping of back-barrier high-energy reef facies in the westernmost inner-platform. During highstand, the reef facies are gently prograding out into Rimthan Arch leaving behind restricted lagoon and sabkhah/salina anhydrite. These Late Jurassic composite sequences are probably controlled by astroclimatic-driven eustatic factors, coupled with local

tectonic disruption, as they have some similarity with other Tethyan sequence stratigraphy.

Acknowledgments

This work was part of a PhD thesis that carried out at the University of Bordeaux-Montaigne, ENSEGID Bordeaux INP, and was sponsored by Saudi Aramco. We thank the management of Saudi Aramco for the permission to publish this work. We express our thankfulness and gratitude to Dr. Aus Al-Tawil (RCD manager, Saudi Aramco) for his endless outstanding support and motivations during all phases of this study. We also thank Dr. Denis Vaslet, Prof. J. Fred Read and Prof. Charles Kerans for providing valuable suggestions and constructive comments. We also extend our thanks to Mahmoud Alnazghah and Dr. Raed Al-Dukhayyil for field support.

Reference

Abbink, O., Targarona, J., Brinkhuis, H., Visscher, H., 2001. Late Jurassic to earliest Cretaceous palaeoclimatic evolution of the southern North Sea. Global and Planetary Change, 30(3), 231-256.

Abu-Ali, M., & Littke, R., 2005. Paleozoic petroleum systems of Saudi Arabia: a basin modeling approach. GeoArabia, 10(3), 131-168.

Adams, J.E., Rhodes, M.L., 1960. Dolomitization by seepage refluxion. American Association of Petroleum Geologists Bulletin, 44, 1912-1920.

Al-Husseini, M.I., 2009. Update to Late Triassic-Jurassic stratigraphy of Saudi Arabia for the Middle East geologic time scale. GeoArabia, 14(2), 145-186.

Aigner, T., 1985, Storm depositional systems; dynamic stratigraphy in modern and ancient shallow-marine sequences: Storm depositional systems; dynamic stratigraphy in modern and ancient shallow-marine sequences: Berlin, Federal Republic of Germany (DEU), Springer Verlag, Berlin, 174 pp.

Al-Awwad, S.F., Collins, L.B., 2013a. Arabian carbonate reservoirs: A depositional model of the Arab-D reservoir in Khurais field, Saudi Arabia. AAPG bulletin, 97(7), 1099-1119

Al-Awwad, S.F., Collins, L.B., 2013b. Carbonate-platform scale correlation of stacked high-frequency sequences in the Arab-D reservoir, Saudi Arabia. Sedimentary Geology, 294, 205-218.

Al-Awwad, S.F., Pomar, L., 2015. Origin of the rudstone–floatstone beds in the Upper Jurassic Arab-D reservoir, Khurais Complex, Saudi Arabia. Marine and Petroleum Geology, 67, 743-768.

Al-Husseini, M. I and. Matthews, R. K. 2008. Jurassic-Cretaceous Arabian orbital stratigraphy: The AROSJK Chart, GeoArabia, 13 (1), 89-94.

Al-Husseini, M., Matthews, R.K., Mattner, J., 2006. Stratigraphic Note: Orbital-forcing calibration of the Late Jurassic (Oxfordian-early Kimmeridgian) Hanifa Formation, Saudi Arabia. GeoArabia 11, 145–149.

Al-Husseini, M.I. and Matthews, R.K. 2005. Arabian Orbital Stratigraphy: Periodic second-order sequence boundaries. GeoArabia, 10 (2), 165-184.

Al-Husseini, M.I., 2000. Origin of the Arabian plate structures: Amar collision and Najd Rift. GeoArabia 5, 527–542.

Al-Naji, N.S. 2002. Two carbonate shelf margins with hydrocarbon potential compared: Upper Jurassic formations of Arabian Basin and Guadalupian formations of Permian Basin of Texas and New Mexico. MSc Thesis, University of South Carolina, 234 p.

Al-Suwaidi, A.S., Aziz, S.K., 2002. Sequence stratigraphy of Oxfordian and Kimmeridgian shelf carbonate reservoirs, offshore Abu Dhabi. GeoArabia, 7, 31-44.

Allenbach, R.P., 2001. Synsedimentary tectonics in an epicontinental sea: a new interpretation of the Oxfordian basins of northern Switzerland. Eclogae Geologicae Helvetiae, 94, 265–287.

Allenbach, R.P., 2002. The ups and downs of “Tectonic Quiescence”—recognizing differential subsidence in the epicontinental sea of the Oxfordian in the Swiss Jura Mountains. Sedimentary Geology, 150 (3), 323-342.

Alnazghah, M.H., Bádenas, B., Pomar, L., Aurell, M., Morsilli, M., 2013. Facies heterogeneity at interwell-scale in a carbonate ramp, Upper Jurassic, NE Spain. Marine and Petroleum Geology, 44, 140-163.

Anne Eisenberg, Sweeping Panoramas, Courtesy of a Robot. New York Times, July 20, 2008.

Ayres, M.G., Bilal, M., Jones, R.W., Slentz, L.W., Tartir, M., Wilson, A.O., 1982. Hydrocarbon habitat in main producing areas, Saudi Arabia. AAPG bulletin, 66(1), 1-9.

Bádenas, B., Pomar, L., Aurell, M., Morsilli, M., 2012. A facies model for internalites (internal wave deposits) on a gently sloping carbonate ramp (Upper Jurassic, Ricla, NE Spain). Sedimentary Geology, 271, 44-57.

Béchennec, F., Le Métour, J., Rabu, D., Bourdillon-de-Grissac, C.H., De Wever, P., Beurrier, M.T., Villey, M., 1990. The Hawasina Nappes: stratigraphy, palaeogeography and structural evolution of a fragment of the south-Tethyan passive continental margin. Geological Society, London, Special Publications, 49(1), 213-223.

Bornemann, A., Norris, R.D., Friedrich, O., Beckmann, B., Schouten, S., Sinninghe Damsté, J.S., Vogel, J., Hofmann, P., Wagner, T., 2008. Isotopic evidence for glaciation during the Cretaceous supergreenhouse. Science 319, 189–193.

Bottjer, D. J., Arthur, M. A., Dean, W. E., Hattin, D. E., Savrda, C. E., 1986. Rhythmic bedding produced in Cretaceous pelagic carbonate environments: sensitive recorders of climatic cycles. Paleoceanography, 1(4), 467-481.

Boulila, S., Galbrun, B., Hinnov, L.A., Collin, P.Y., Ogg, J.G., Fortwengler, D., Marchand, D., 2010. Milankovitch and sub-Milankovitch forcing of the Oxfordian (Late Jurassic) Terres Noires Formation (SE France) and global implications. Basin Research, 22(5), 717-732.

Boulila, S., Galbrun, B., Miller, K.G., Pekar, S.F., Browning, J.V., Laskar, J., Wright, J.D., 2011. On the origin of Cenozoic and Mesozoic “third-order” eustatic sequences. Earth-Science Reviews, 109(3), 94-112.

Bramkamp, R.A., Steineke, M., 1952. Stratigraphical introduction. In: Arkell, W.J., Bramkamp, R.A., Steineke, M. (Eds.), Jurassic Ammonites from Jebel Tuwaiq, Central Arabia. Royal Society [London] Philosophical Transactions B 236, 241–313.

Brannan, J., Sahota G., Gerdes K.D., Berry J.A.L., 1999. Geological evolution of the central Marib-Shabwa basin, Yemen. GeoArabia, 4 (1), 9–34.

Brigaud, B., Pucéat, E., Pellenard, P., Vincent, B., Joachimski, M.M., 2008. Climatic fluctuations and seasonality during the Late Jurassic (Oxfordian-Early Kimmeridgian) inferred from δ18O of Paris Basin oyster shells. Earth and Planetary Science Letters 273, 58-67.

Bromley, R.G., Ekdale, A.A., 1984. Trace fossil preservation in flint in the European chalk. Journal of Paleontology, 58, 298–311.

Carruthers, A., Mckie, T., Price, J., Dyer, R., Williams, G., Watson, P., 1996. The application of sequence stratigraphy to the understanding of Late Jurassic turbidite plays in the Central North Sea, UKCS. Geological Society, London, Special Publications, 114(1), 29-45.

Cecca, F., Martin-Garin, B., Marchand, D., Lathuilière, B., Bartolini, A., 2005. Paleoclimatic significance of biogeographic and sedimentary events in Tethyan and Peri-Tethyan areas during the Oxfordian (Late Jurassic). Palaeogeography, Palaeoclimatology, Palaeoecology 222, 10-32.

Chevalier, F., Garcia, J.P., Quesne, D., Guiraud, M., Menot, J.C., 2001. Corrélations et interprétations génétiques dans les formations récifales oxfordiennes de la haute vallée de l'Yonne (sud-est du Bassin de Paris, France). Bulletin de la Société géologique de France, 172 (1), 69-84.

Chevalier, F., Garcia, J.P., Quesne, D., Guiraud, M., Menot, J.C., 2001. Correlations and genetic stratigraphy through Oxfordian reefal formations in the upper Yonne valley (southern Paris basin, France). Bulletin de la Société Géologique de France 172, 69-84.

Chumakov, N.M., Frakes, L.A., 1997. Mode of origin of dispersed clasts in Jurassic shales, southern part of the Yana-Kolyma fold belt, North East Asia. Palaeogeography, Palaeoclimatology, Palaeoecology, 128(1-4), 77-85.

Colombié, C., Strasser, A., 2005. Facies, cycles, and controls on the evolution of a keep-up carbonate platform (Kimmeridgian, Swiss Jura). Sedimentology, 52(6), 1207-1227.

Crevello, P.D., 1991. High-frequency carbonate cycles and stacking patterns: interplay of orbital forcing and subsidence on Lower Jurassic rift platforms, High Atlas, Morocco. Sedimentary Modeling: Computer Simulations and Methods for Improved Parameter Definition: Kansas Geological Survey, Bulletin, 233, 207-230.

Dardeau, G., Atrops, F., Fortwengler, D., de Graciansky, P.C., Marchand, D., 1988. Jeu de blocs et tectonique distensive au Callovien et à l’Oxfordien

dans le bassin du Sud-Est de la France. Bulletin de la Société géologique de France, 8(IV), 771-777.
Dera, G., Prunier, J., Smith, P.L., Haggart, J.W., Popov, E., Guzhov, A., Rogov, M., Delsate, D., Thies, D., Cuny, G., Pucéat, E., Charbonnier, D., Bayon, G., 2015. Nd isotope constraints on ocean circulation, paleoclimate, and continental drainage during the Jurassic breakup of Pangea. Gondwana Research, 27(4), 1599-1615.
Donnadieu, Y., Dromart, G., Goddéris, Y., Pucéat, E., Brigaud, B., Dera, G., Dumas, C. Olivier, N., 2011. A mechanism for brief glacial episodes in the Mesozoic greenhouse. Paleoceanography 26.
Dromart, G., Garcia, J.P., Picard, S., Atrops, F., Lécuyer, C., Sheppard, S.M.F., 2003a. Ice age at the MiddleeLate Jurassic transition? Earth and Planetary Science Letters. 213, 205-220.
Dromart, G., Garcia, J.P., Picard, S., Rousseau, M., Atrops, F., Lécuyer, C., Sheppard, S.M.F., 2003b. Perturbation of the carbon cycle at the Middle/Late Jurassic transition: geological and geochemical evidence. American Journal of Science 303, 667–707.
Droste, H., 1990. Depositional cycles and source rock development in an epeiric intra-platform basin: the Hanifa Formation of the Arabian peninsula. Sedimentary Geology, 69(3-4), 281-296.
Dunham, R.J., 1962. Classification of carbonate rocks according to depositional texture. In: Ham, W.E. (Ed.), Classification of Carbonate Rocks: AAPG Memoir 1, 108-121. Tulsa, OK.
Eisenberg, A., 2008. Sweeping Panoramas, Courtesy of a Robot. New York Times, July 20.
Embry, A.F., Klovan, J.E., 1971. A late Devonian reef tract on northeastern Banks Island, NWT. Bulletin of Canadian Petroleum Geology, 19(4), 730-781.
Enos, P., 1983. Late Mesozoic paleogeography of Mexico. In: Mesozoic Paleogeography of the West-Central United States. Rocky Mountain Section SEPM, Denver, Colorado, Paleogeography Symp. 2, p. 133-158.
Fischer, J.-C., Manivit, J., Vaslet, D., 2001. Jurassic gastropod faunas of central Saudi Arabia. GeoArabia (Manama), 6(1), 63–100.
Frakes, L.A., Francis, J.E., Syktus, J.I., 1992. Climate Modes of the Phanerozoic. Cambridge University Press, Cambridge, 274 pp.
Frébourg, G., Ruppel, S.C., Loucks, R.G., Lambert, J. 2016. Depositional controls on sediment body architecture in the Eagle Ford/Boquillas system: Insights from outcrops in west Texas, United States. AAPG Bulletin, 100(4), 657-682.
Galli, G., 1993. “Calcari Grigi” formation, Jurasic, Venetian Alps. In: Galli, G. (Ed.), Temporal and Spatial Patterns in Carbonate Platforms. Springer, Berlin, 97-129.
Goldhammer, R.K., Dunn, P.A., Hardie, L.A., 1990. Depositional cycles, composite sea-level changes, cycle stacking patterns, and the hierarchy of stratigraphic forcing: examples from Alpine Triassic platform carbonates. Geological Society of America Bulletin, 102(5), 535-562.
Gollesstaneh, A., 1965. A micropalaeontological study of the Upper Jurassic and Lower Cretaceous of Southern Iran (Doctoral dissertation, University of London).

Gradstein, F.M., Ogg, J.G., Schmitz, M.D., Ogg, G.M., 2012. The Geologic Time Scale 2012. Elsevier, p. 1144.

Hallam, A., 1988. A reevaluation of Jurassic eustasy in the light of new data and the revised Exxon curve.

Hallock, P., 2001. Coral reefs, carbonate sediments, nutrients, and global change. The history and sedimentology of ancient reef systems, 387-427.

Hallock, P., 2005. Global change and modern coral reefs: new opportunities to understand shallow-water carbonate depositional processes. Sedimentary Geology, 175(1), 19-33.

Handford, C.R., Cantrell, D.L., Keith, T.H., 2002, Regional facies relationships and sequence stratigraphy of a super-giant reservoir (Arab-DMember), SaudiArabia: Society of Economic Paleontologists Gulf Coast Section Research Conference Programand Abstracts 22, 539–563.

Haq, B.U., Al-Qahtani, A.M., 2005. Phanerozoic cycles of sea-level change on the Arabian Platform. GeoArabia, 10(2), 127-160.

Haq, B.U., J. Hardenbol and P.R. Vail 1988. Mesozoic and Cenozoic chronostratigraphy and cycles of sea-level change. In: Wilgus, C.K., Hastings, B.S., Kendall, C.G. St. C., Posamentier, H., Van Wagoner, J., Ross, C.A. (Eds.), Sea-level changes: an integrated approach. Society of Economic Paleontologists and Mineralogists, Special Publication 42, 71-108.

Harris, A., Miller, K.G., Browning, J.V., Sugarman, P.J., Olsson, R.K., Cramer, B.S., Wright, J.D., 2010. Integrated Stratigraphic Studies of Paleocene-Lowermost Eocene Strata, New Jersey Coastal Plain: Evidence for glacioeustatic control. Paleoceanography.

Harris, A.D., Miller, K.G., Browning, J.V., Sugarman, P.J., Olsson, R.K., Cramer, B.S., Wright, J.D., 2010. Integrated stratigraphic studies of Paleocene–lowermost Eocene sequences, New Jersey Coastal Plain: Evidence for glacioeustatic control. Paleoceanography, 25 (3).

Hughes, G.W., 2004. Middle to Upper Jurassic Saudi Arabian carbonate petroleum reservoirs: biostratigraphy, micropalaeontology and palaeoenvironments. GeoArabia 9, 79–114.

Hughes, G.W., 2009. Biofacies and palaeoenvironments of the Jurassic Shaqra Group of Saudi Arabia. Volumina Jurassica, v. 6, p. 33-45.

Hughes, G.W., M. Al-Khaled, Varol, O., 2009. Oxfordian biofacies and palaeoenvironments of Saudi Arabia. Volumina Jurassica, 6, 47-60.

Hughes, G.W., Varol, O., Al-Khaled. M., 2008. Late Oxfordian micropalaentology, nannopalaentology and palaeoenvironments of Saudi Arabia. GeoArabia, 13 (2), 15-46.

Iannace, A., Frisia, S., 1994. Changing dolomitization styles from Norian to Rhaetian in the southern Tethys realm. In: Purser, B., Tucker, M., Zenger, D. (Eds.), Dolomites, A Volume in Honour of Dolomieu, International Association of Sedimentologists, Special Publication, 21, 75-89.

Ikeda, M., Tada, R. 2013. Long period astronomical cycles from the Triassic to Jurassic bedded chert sequence (Inuyama, Japan); Geologic evidences for the chaotic behavior of solar planets. Earth, Planets and Space, 65(4), 351-360.

Imbrie, J., Imbrie, K.P. 1986. Ice ages: solving the mystery. Harvard University Press, Cambridge, Massachusetts, 224 pp.

Kadar, A.P., De Keyser, T., Neog, N., Karam, K.A., Le Nindre, Y.M., Davies, R.B., 2015. Calcareous nannofossil zonation and sequence stratigraphy of the Jurassic System, onshore Kuwait. GeoArabia, 20(4), 125-180.

Keho, T.H., Broadhead, M.K., Neves, F.A., 2009. Using an isochron to constrain amplitude analysis: A case study of a carbonate stratigraphic trap in Saudi Arabia. The Leading Edge, 28(11), 1304-1313.

Kerans, C., Tinker, S.W., 1997. Sequence stratigraphy and characterization of carbonate reservoirs. Society of Sedimentary Geology: SEPM Short Course Notes, 40.

Keupp, H., Jenisch, A., Herrmann, R., Neuweiler, F., Reitner, J., 1993. Microbial carbonate crusts-a key to the environmental analysis of fossil spongiolites?. Facies, 29(1), 41-54.

Khetani, A.B., Read, J.F., 2002. Sequence development of a mixed carbonate-siliciclastic high-relief ramp, Mississippian, Kentucky, USA. Journal of Sedimentary Research, 72(5), 657-672.

Koerschner III, W.F., Read, J.F., 1989. Field and modeling studies of Cambrian carbonate cycles, Virginia, Appalachians. Journal of Sedimentary Petrology 59, 654–687.

Langdon, G.S., Malecek, S.J. 1987. Seismic stratigraphic study of two Oxfordian carbonate sequences, eastern Saudi Arabia. American Association of Petroleum Geologists Bulletin Bulletin, 71 (4), 403-418.

Le Nindre, Y.M., Manivit, J., Vaslet, D., 1990. Stratigraphie séquentielle du Jurassique et du Crétacé en Arabie Saoudite. Bulletin, Société géologique de France, Paris, sér. 8, VI, 1025-1034.

Le Nindre, Y.M., Vaslet, D., Le Métour, J., Bertrand, J., Halawani, M., 2003. Subsidence modelling of the Arabian Platform from Permian to Paleogene outcrops. Sedimentary Geology, 156, 263-285.

Leinfelder, R., 1993. Upper Jurassic reef types and controlling factors. A preliminary report. Profil 5, 1-45.

Leinfelder, R., 1994. Distribution of Jurassic reef types: a mirror of structural and environmental changes during breakup of Pangea. In: Embry, A.F., Beauchamp, B., Glass, D.J. (Eds.), Pangea: Global Environments and Resources. Canadian Society of Petroleum Geologists, Calgary, Memoir, 17, 677-700.

Leinfelder, R.R., Krautter, M., Laternser, R., Nose, M., Schmid, D.U., Schweigert, G., Werner, W., Keupp, H., Brugger, H., Herrmann, R., Rehfeld-Kiefer, U., Schroeder, J.H., Reinhold, C., Koch, R., Zeiss, A., Schweizer, V., Christmann, H., Menges, G., Luterbacher, H., 1994. The origin of Jurassic reefs: current research developments and results. Facies 31, 1–56.

Lhamyani, B., 1985. Etude stratigraphique de l'Oxfordien dans l'arc de Castellane(Alpes-de-Haute-Provence): passage des faciès provençaux aux faciès dauphinois (Doctoral dissertation).

Lindsay, R.F., Cantrell, D.L., Hughes, G.W, Keith, T.H., Mueller III, H.W., Russell, D., 2006. Ghawar Arab-D reservoir: Widespread porosity in shoaling-upward carbonate cycles, Saudi Arabia: AAPG Memoir 88, 97–138.

Lukasik, J.J., James, N.P., McGowran, B., Bone, Y., 2000. An epeiric ramp: low-energy, cool-water carbonate facies in a Tertiary inland sea, Murray Basin, South Australia. Sedimentology, 47(4), 851-881.

Mancini, E.A., Obid, J.A., Puckett, T.M., 2004. Upper Jurassic transgressive-regressive sequences, Mississippi interior salt basin area.

Manivit J, Le Nindre, Y.M., Vaslet D. (1990) Le Jurassique d'Arabie Centrale. In Histoire Gologique de la Bordure Occidentale de la Plate-forme Arabe. Volume 4. Document du BRGM n°194.

Manivit, J., Pellaton, C., Vaslet, D., Le Nindre, Y.M., Brosse, J.M., Fourniguet, J., 1985a. Geologic map of the Wadi al Mulayh quadrangle, sheet 22H, Kingdom of Saudi Arabia. Saudi Arabian Deputy Ministry for Mineral Resources Geosciences Map, GM-92, scale, 1(250,000), 1-32.

Manivit, J., Pellaton, C., Vaslet, D., Le Nindre, Y.M., Brosse, J.M., Breton, J.P., Fourniguet, J., 1985b. Geologic map of the Darma quadrangle, sheet 24H, Kingdom of Saudi Arabia. Saudi Arabian Deputy Ministry for Mineral Resources Geosciences Map, GM-101, scale, 1(250,000), 133.

Martinez, M., Dera, G. 2015. Orbital pacing of carbon fluxes by a ~9-My eccentricity cycle during the Mesozoic. Proceedings of the National Academy of Sciences, 112(41), 12604-12609.

Mattner, J., Al-Husseini, M., 2002. Essay: Applied cyclo-stratigraphy for the Middle East E&P industry. GeoArabia, 7 (4), 734-744.

McGuire, M.D., 2003. Sequence Stratigraphy of the Hanifa Reservoir in Berri Field, Saudi Arabia. In American Association of Petroleum Geologists Conference, Salt Lake City, Abstract (No. 78653).

McGuire, M.D., Koepnick, R.B., Markello, M.L., Stockton, M.L., Waite, L.E., Kompanik, M.J., Al-Shammary, M.J., AlAmoudi, M.O., 1993. Importance of sequence stratigraphic concepts in development of reservoir architecture in Upper Jurassic grainstones, Hadriya and Hanifa reservoirs, Saudi Arabia. Society of Petroleum Engineers, 489-499.

McKenzie, J.A., Hsu, K.J., Schneider, J.F., 1980. Movement of subsurface waters under the sabkha, Abu Dhabi, UAE, and its relation to evaporative dolomite genesis, in Zenger, D.H., et al., eds., Concepts and models of dolomitization: Society of Economic Paleontologists andMineralogists Special Publication, 28, 11-30.

Meyer, F.O., Price, R.C., 1993. A new Arab-D depositional model, Ghawar Field, Saudi Arabia. In: Paper Presented at the Middle East Oil Show, Bahrain.

Meyer, F.O., Price, R.C., Al-Ghamdi, I.A., Al-Goba, I.M., Al-Raimi, S.M., Cole, J.C., 1996. Sequential stratigraphy of outcropping strata equivalent to Arab-D Reservoir, Wadi Nisah, Saudi Arabia. GeoArabia (Manama) 1 (3), 435-456.

Meyer, F.O., Hughes, G.W., Al-Ghamdi, I., 2000. Jubaila formation, Tuwaiq Mountain escarpment, Saudi Arabia: window to lower Arab-D Reservoir faunal assemblages and bedding geometry. GeoArabia (Manama) 5 (1), 143.

Miller, K.G., Barrera, E., Olsson, R.K., Sugarman, P.J., Savin, S.M., 1999. Does ice drive early Maastrichtian eustasy? Global δ18O and New Jersey sequences. Geology 27, 783–786.

Miller, K.G., Sugarman, P.J., Browning, J.V., Kominz, M.A., Hernandez, J.C., Olsson, R.K., Wright, J.D., Feigenson, M.D., Van Sickel,W., 2003. A chronology of Late Cretaceous sequences and sea-level history: glacioeustasy during the Greenhoouse World. Geology 31, 585–588.

Miller, K.G., Wright, J.D., Browning, J.V., 2005. Visions of ice sheets in a greenhouse world. Marine Geology 217, 215–231.

Mitchell, J.C., Lehmann, P.J., Cantrell, D.L., Al-Jallal, I.A., Al-Thagafy, M.A.R., 1988. Lithofacies, diagenesis and depositional sequence: Arab-D Member, Ghawar Field, Saudi Arabia. SEPM Core Workshop 12, 459-514.

Mitchum, R.M., Van Wagoner, J.C. 1991. High-frequency sequences and their stacking patterns; sequence-stratigraphic evidence of high-frequency eustatic cycles. Sedimentary Geology, 70, 131-160.

Morsilli, M., Pomar, L., 2012. Internal waves vs. surface storm waves: a review on the origin of hummocky cross-stratification. Terra Nova, 24(4), 273-282.

Moshrif, M.A., 1984. Sequential development of Hanifa Formation (Upper Jurassic) paleoenvironments and paleogeography, central Saudi Arabia. Journal of Petroleum Geology, 7 (4), 451-450.

Mosser-Ruck, R., Huault, V., Elie, M., 2002. Clay mineralogy changes at the callovian-oxfordian boundary of the Paris Basin: a signal for paleo-environmental modifications?. International Meeting, Reims, France, Abstract, 237-238.

Murris, R.J., 1980. Middle East: Stratigraphic evolution and oil habitat. AAPG Bulletin, 64,597–618.

Myrow, P.M., Southard, J.B., 1996. Tempestite deposition. Journal of Sedimentary Research, 66 (5).

Nunn, E.V., Price, G.D., 2010. Late Jurassic (Kimmeridgian–Tithonian) stable isotopes (δ 18 O, δ 13 C) and Mg/Ca ratios: new palaeoclimate data from Helmsdale, northeast Scotland. Palaeogeography, Palaeoclimatology, Palaeoecology, 292(1), 325-335.

Nunn, E.V., Price, G.D., Hart, M., Page, K., Leng, M., 2009. Isotopic signals from CallovianeKimmeridgian (Middle Upper Jurassic) belemnites and bulk organic carbon, Staffin Bay, Isle of Skye, Scotland. Journal of the Geological Society, London 166, 633e641.

Olivier, N., Colombié, C., Pittet, B., Lathuilière, B., 2011. Microbial carbonates and corals on the marginal French Jura platform (Late Oxfordian, Molinges section). Facies, 57(3), 469-492.

Olsen P.E, Kent D.V., 1999. Long-period Milankovitch cycles from the late Triassic and Early Triassic of eastern North America and their implications for the calibration of the early Mesozoic time scale and long term behavior of the planets. Philosophical Transactions Royal Society, Mathematical Physical Engineering Sciences, 357, 1761–1786

Pellenard, P., Tramoy, R., Pucéat, E., Huret, E., Martinez, M., Bruneau, L., Thierry, J., 2014. Carbon cycle and sea-water palaeotemperature evolution at the Middle–Late Jurassic transition, eastern Paris Basin (France). Marine and Petroleum Geology, 53, 30-43.

Pittet, B., Strasser, A., 1998. Long-distance correlations by sequence stratigraphy and cyclostratigraphy: examples and implications (Oxfordian from the Swiss Jura, Spain, and Normandy). Geol. Rundschau, 86 (4), 852–874.

Pollastro, R.M., 2003. Total petroleum systems of the Paleozoic and Jurassic, Greater Ghawar Uplift and adjoining provinces of central Saudi Arabia

and northern Arabian-Persian Gulf. United States Geological Survey Bulletin, 2202 H, 100 pp.
Pomar, L., Hallock, P., 2008. Carbonate factories: a conundrum in sedimentary geology. Earth-Science Reviews, 87(3), 134-169.
Powers, R.W., 1962. Arabian Upper Jurassic carbonate reservoir rocks. In: Ham W.E. (Ed.), Classification of Carbonate Rocks: A Symposium. American Association of Petroleum Geologists, Memoir 1, 122-192.
Powers, R.W., 1968. Lexique Stratigraphique International, v.III, Asie, 10bl, Saudi Arabia. Centre National de la Recherche Scientifique, Paris, 177p.
Powers, R.W., Ramirez, L.F., Redmond, C.D., Elberg, E.L., 1966. Geology of the Arabian Peninsula, Geological Survey Professional Paper, 560-D, 147p.
Price, G.D., 1999. The evidence and implications of polar-ice during the Mesozoic. Earth Science Reviews 48, 183-210.
Price, G.D., Rogov, M.A., 2009. An isotopic appraisal of the Late Jurassic greenhouse phase in the Russian Platform. Palaeogeography, Palaeoclimatology, Palaeoecology 273, 41–49.
Rabalais, N.N., Turner, R.E., Wiseman, W.J., & Boesch, D.F., 1991. A brief summary of hypoxia on the northern Gulf of Mexico continental shelf: 1985–1988. Geological Society, London, Special Publications, 58(1), 35-47.
Razin, P., Grélaud, C., van Buchem, F., 2017. The mid-Cretaceous Natih Formation in Oman: A model for carbonate platforms and organic-rich intrashelf basins. AAPG Bulletin, 101(4), 515-522.
Razin, P., Taati, F., Van Buchem, F.S.P., 2010. Sequence stratigraphy of Cenomanian–Turonian carbonate platform margins (Sarvak Formation) in the High Zagros, SW Iran: an outcrop reference model for the Arabian Plate. Geological Society, London, Special Publications, 329(1), 187-218.
Read, J.F. 1995. Overview of carbonate platform sequences, cycle stratigraphy and reservoirs in greenhouse and icehouse worlds. In: Read, J.F., Kerans, C., Weber, L.J., Sarg, J.F., and Wright F.W. (Eds.), Milankovitch sea level changes, cycles and reservoirs on carbonate platforms in greenhouse and icehouse worlds, SEPM Short Course Notes No. 35, 1-102.
Read, J.F., 1989. Controls on evolution of Cambrian-Ordovician passive margin, US Appalachians. In: Crevello, P.D., Wilson, J.L., Sarg, J.F., Read, J.F. (Eds.), Controls on Carbonate Platform and Basin Development, SEPM Special Publication, 44, 146–165.
Read, J.F., Grotzinger, J.P., Bova, J.A., Koerschner, W.F., 1986. Models for generation of carbonate cycles. Geology, 14(2), 107-110.
Reinson, G.E., 1979. Facies models 14. Barrier island systems. Geoscience Canada, 6(2). 51-68
Reynolds, A.D., 1995. Sedimentology and sequence stratigraphy of the Thistle field, northern North Sea. Norwegian Petroleum Society Special Publications, 5, 257-271.
Riding, R., 2000. Microbial carbonates: the geological record of calcified bacterial-algal mats and biofilms. Sedimentology, 47 (Supplement 1), p. 179-214.
Riding, R., Liang, L., 2005. Geobiology of microbial carbonates: metazon and seawater saturation state influences on secular trends during the

Phanerozoic. Palaeogeography, Palaeoclimatology, Palaeoecology, 219, 101-85.
Rousseau, M., Dromart, G., Droste, H., Homewood, P., 2006. Stratigraphic organisation of the Jurassic sequence in Interior Oman, Arabian Peninsula. GeoArabia,11(1), 17.
Ruddiman, W.F., Raymo, M., McIntyre, A., 1986. Matuyama 41,000-year cycles: North Atlantic Ocean and northern hemisphere ice sheets. Earth and Planetary Science Letters, 80(1), 117-129.
Ruffell, A., McKinley, J.M., Worden, R.H., 2002. Comparison of clay mineral stratigraphy to other proxy palaeoclimate indicators in the Mesozoic of NW Europe. Philosophical Transactions of the Royal Society of London A: Mathematical, Physical and Engineering Sciences, 360(1793), 675-693.
Sadooni, F.N., 1997. Stratigraphy and petroleum prospects of Upper Jurassic carbonates in Iraq. Petroleum Geoscience, 3, (3),233-243.
Schieber, J., 1999. Microbial mats in terrigenous clastics; the challenge of identification in the rock record. Palaios, 14(1), 3-12.
Schieber, J., Southard, J., Thaisen, K., 2007. Accretion of mudstone beds from migrating floccule ripples. Science, 318(5857), 1760-1763.
Schieber, J., Southard, J.B., Kissling, P., Rossman, B., Ginsburg, R., 2013. Experimental deposition of carbonate mud from moving suspensions: importance of flocculation and implications for modern and ancient carbonate mud deposition. Journal of Sedimentary Research, 83(11), 1025-1031.
Scotese, C.R., 2003. Paleomap project, Earth History and Climate History, Late Jurassic. Paleomap, URL http: // www. Scotese. com / late1. Htm
Sellwood, B., Valdes, P., Price, G., 2000. Geological evaluation of multiple general circulation model simulations of Late Jurassic palaeoclimate. Palaeogeography Palaeoclimatology Palaeoecology 156, 147e160.
Sharief, F.A., Khan M.S., Magara, K., 1991. Outcrop-Subcrop Sequence and Diagenesis of Upper Jurassic Arab-Hith Formations, Central Saudi Arabia. Journal KAU, Earth Science, 4, 105-136.
Sharland, P.R., Archer R., Casey D.M., Davies R.B., Hall S.H., Heward A.P., Horbury A.D., Simmons M.D., 2001. Arabian Plate Sequence Stratigraphy. GeoArabia Special Publication 2, Gulf PetroLink, Bahrain, 371.
Stern, R.J., Johnson, P., 2010. Continental lithosphere of the Arabian Plate: a geologic, petrologic, and geophysical synthesis. Earth-Science Reviews, 101 (1), 29-67.
Stoll, H.M., Schrag, D.P., 1996. Evidence for glacial control of rapid sea level changes in the Early Cretaceous. Science, 272(5269), 1771.
Strasser, A., Hillgärtner, H., Hug, W., Pittet, B., 2000. Third-order depositional sequences reflecting Milankovitch cyclicity. Terra Nova, 12(6), 303-311.
Strasser, A., Pittet, B., Hug, W., 2015. Palaeogeography of a shallow carbonate platform: The case of the Middle to Late Oxfordian in the Swiss Jura Mountains. Journal of Palaeogeography, 4 (3), 251-268.
Strasser, A., Védrine, S., 2009. Controls on facies mosaics of carbonate platforms: a case study from the Oxfordian of the Swiss Jura. In: Swart, P.K., Eberli, G.P., McKenzie, J.A. (Eds.), Perspectives in Sedimentary Geology: A Tribute to the Career of Robert Nathan Ginsburg. International

Association of Sedimentologists. Special Publication, 41. Blackwell, Oxford, 41, 199-213.
Swart, P.K., Cantrell, D.L., Westphal, H., Handford, C.R., Kendall, C.G., 2005. Origin of dolomite in the Arab-D reservoir from the Ghawar Field, Saudi Arabia: evidence from petrographic and geochemical constraints. Journal of Sedimentary Research, 75(3), 476-491.
Thierry, B., Iwaniuk, A.N., Pellis, S.M., 2000. The influence of phylogeny on the social behaviour of macaques (Primates: Cercopithecidae, genus Macaca). Ethology, 106(8), 713-728.
Vaslet, D., Al-Muallem, M.S., Maddeh, S.S., Brosse, J.M., Fourniquet, J., Breton, J.P., Le Nindre, Y.M., 1991. Explanatory notes to the geologic map of the Ar Riyad Quadrangle, Sheet 24I, Kingdom of Saudi Arabia. Saudi Arabian Deputy Ministry for Mineral Resources, Jeddah, Geosciences Map GM-121, 1-54.
Vaslet, D., Brush, J.M., Breton, J.P., Manivit, J., Le Strat, P., Fourniguet, J., Shorbaji, H., 1988. Geologic map of the quadrangle Shaqra, sheet 25H. Kingdom of Saudi Arabia: Deputy Ministry for Mineral Resources Geoscience Map GM-120C , 29.
Vaslet, D., Delfour, J., Manivit, J., Le Nindre, Y.M., Brosse, J.M., Fourniquet, J., 1983. Geologic map of the Wadi ar Rayn Quadrangle, sheet 23H, Kingdom of Saudi Arabia (with text). Saudi Arabian Deputy Ministry for Mineral Resources, Jeddah, Geosciences Map GM-63A, 1-46.
Vaslet, D., Pellaton, C., Manivit, J., Le Nindre, Y.M., Brosse, J.M., Fourniguet, J., 1985. Geologic map of the Sulayyimah quadrangle, sheet 21 H, Kingdom of Saudia Arabia. Scale 1:250.000. Geoscience Map GM 100 A. Jeddah, Saudi Arabia A.H. 1405. Ministry of Petroleum and Mineral Resources.
Védrine, S., Strasser, A., 2009. High-frequency palaeoenvironmental changes on a shallow carbonate platform during a marine transgression (Late Oxfordian, Swiss Jura Mountains). Swiss journal of geosciences, 102(2), 247-270.
Védrine, S., Strasser, A., Hug, W., 2007. Oncoid growth and distribution controlled by sea-level fluctuations and climate (Late Oxfordian, Swiss Jura Mountains). Facies, 53 (4), 535-552.
Walley, C.D. 1997. The stratigraphy and geological history of Lebanon: an outline. IGCP project 369, workshop handout Barcelona, 25 p.
Walley, C.D., 1985. Depositional history of southern Tunisia and northwestern Libya in Mid and Late Jurassic time. Geological Magazine, 122(03), 233-247.
Walley, C.D., 2001. The Lebanon passive margin and the evolution of the Levantine Neotethys. In, P.A. Ziegler, W. Cavazza, A.H. Robertson and S. Crasquin-Soleau (Eds.), Peri-Tethya rift/wrench basins and passive margins (IGCP 369 results). Mémoires du Muséum National d'Histoire Naturelle, Paris, Peri-Tethys Mémoire 6.
Wierzbowski, H., 2004. Carbon and oxygen isotope composition of Oxfordian–Early Kimmeridgian belemnite rostra: palaeoenvironmental implications for Late Jurassic seas. Palaeogeography, Palaeoclimatology, Palaeoecology, 203(1), 153-168.
Wierzbowski, H., Rogov, M. A., Matyja, B. A., Kiselev, D., Ippolitov, A., 2013. Middle–Upper Jurassic (Upper Callovian–Lower Kimmeridgian) stable

isotope and elemental records of the Russian Platform: Indices of oceanographic and climatic changes. Global and Planetary Change, 107, 196-212.

Wignall, P.B., Ruffell, A.H., 1990. The influence of sudden climatic change on marine deposition in the Kimmeridgian of northwest Europe. Journal of the Geological Society of London 147, 365–371.

Wilson, J.L., Jordan, C., 1983. Middle Shelf Environment. In: Scholle, P.A., Bebout, D.G., Moore, C.H. (Eds.), Carbonate Depositional Environments. American Association Petroleum Geologists Memoir, 33, 345–440.

Wright, V.P., 1992. Speculations on the controls on cyclic peritidal carbonates: ice-house versus greenhouse eustatic controls. Sedimentary Geology, 76(1), 1-5.

Ziegler, M.A., 2001. Late Permian to Holocene Paleofacies evolution of the Arabian plate and its hydrocarbon occurrences. GeoArabia, 6, 445-504.

Appendix

Appendix 4.1

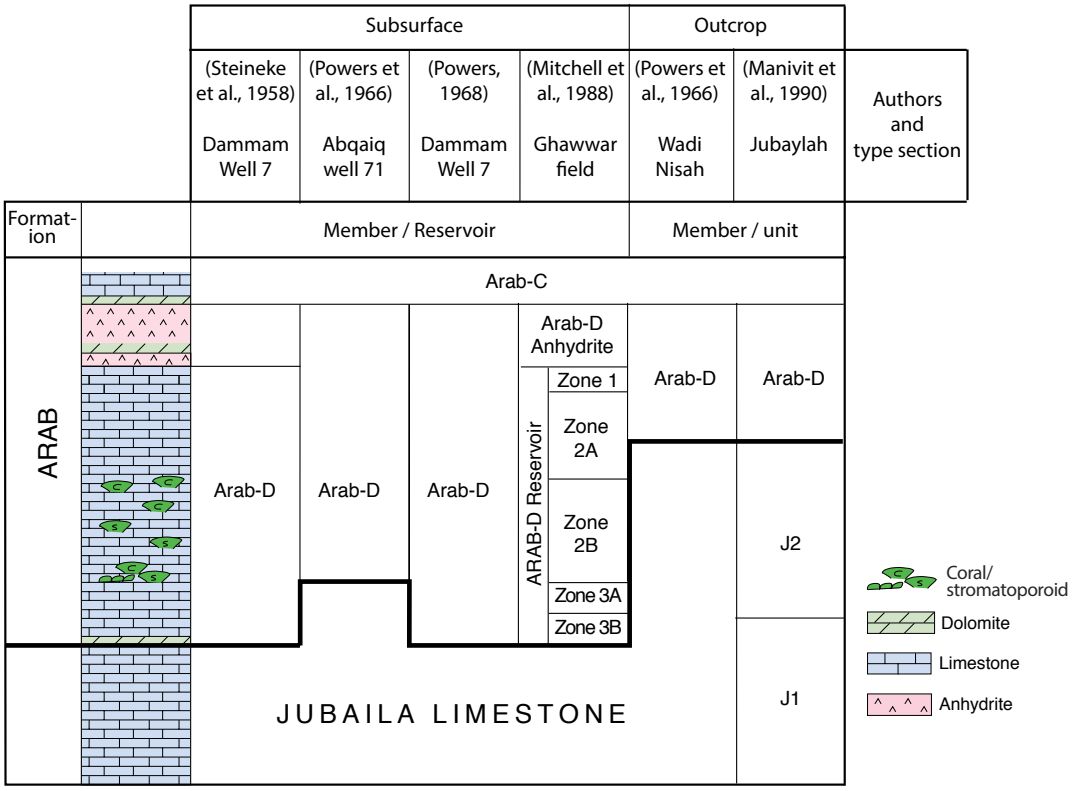

Appendix 4.1: Table shows the definitions of the Jubaila-Arab-D lithostratigraphic contact among different authors. This study follows Manivit et al. (1990). (Modified from Meyer et al 1996).

Appendix 4.2

Khashm Al Qaddiyah section, Hanifa Formation
Riyadh-Mecca highway road-cut

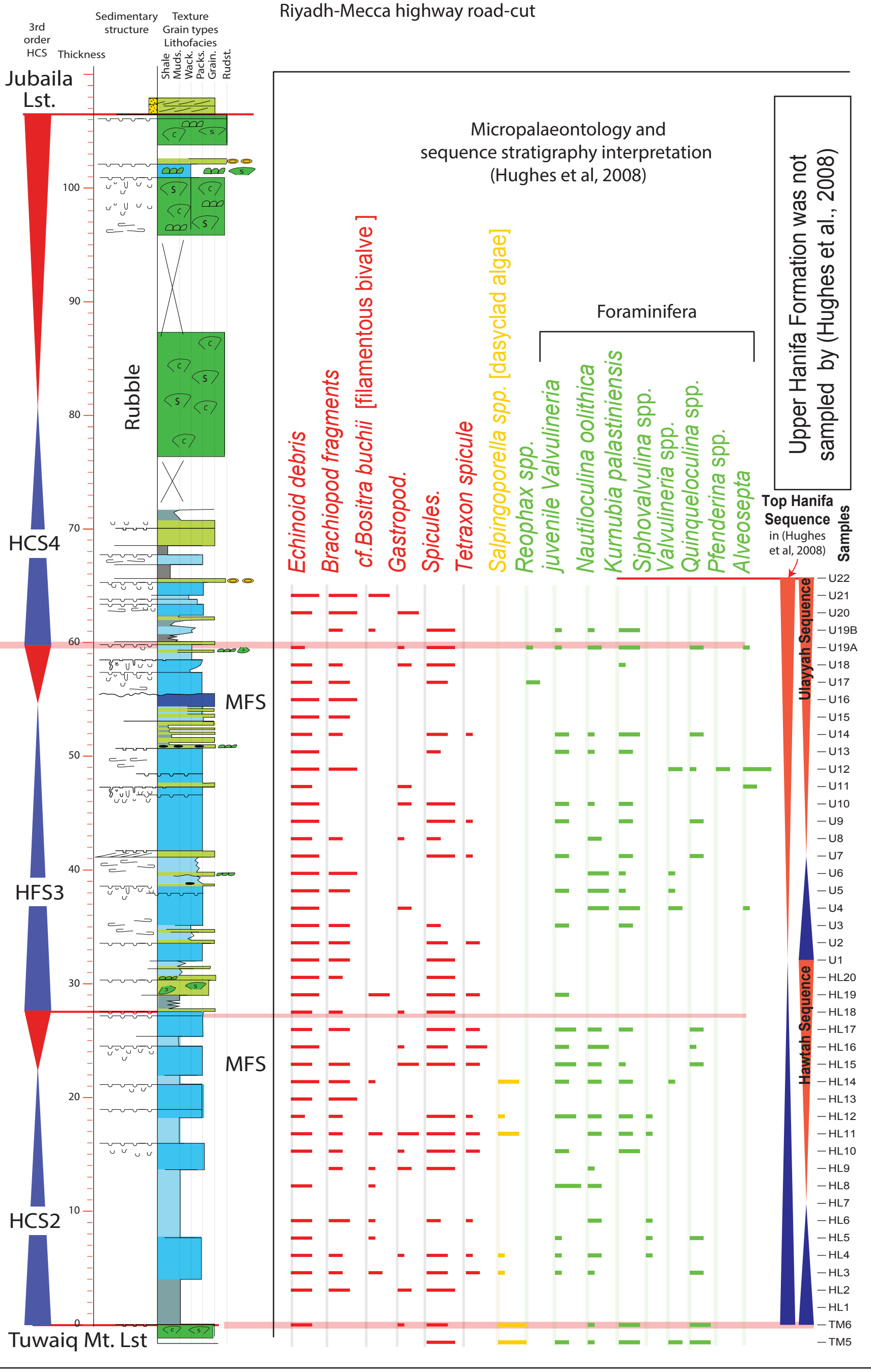

Appendix 4.3

Sedimentological log and semi-quantitative micropalaeontological analysis of the Hanifa Formation, Wadi Birk

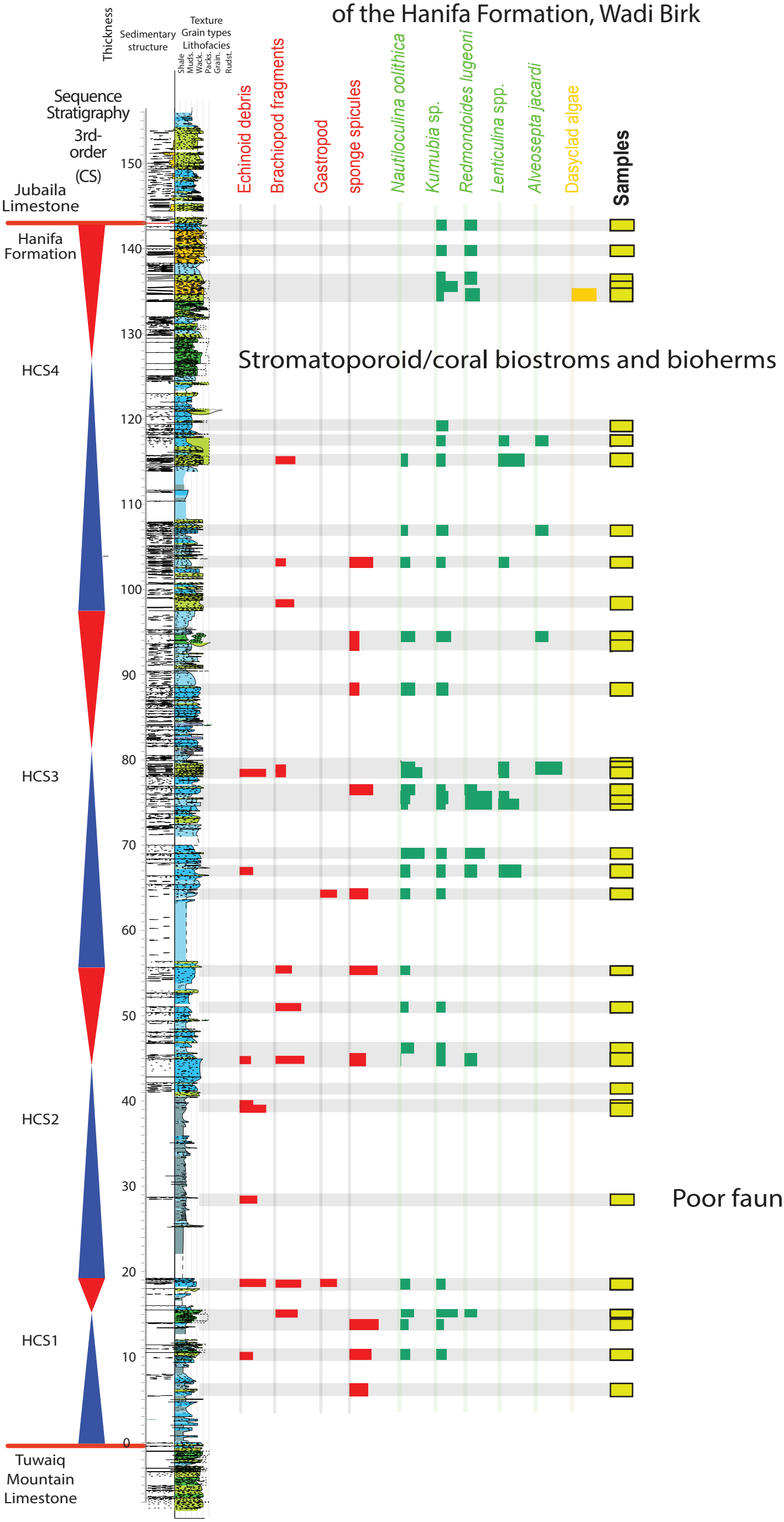

Appendix 4.4
Sedimentological log and semi-quantitative micropalaeontological analysis of the Jubaila Limestone, Wadi Birk

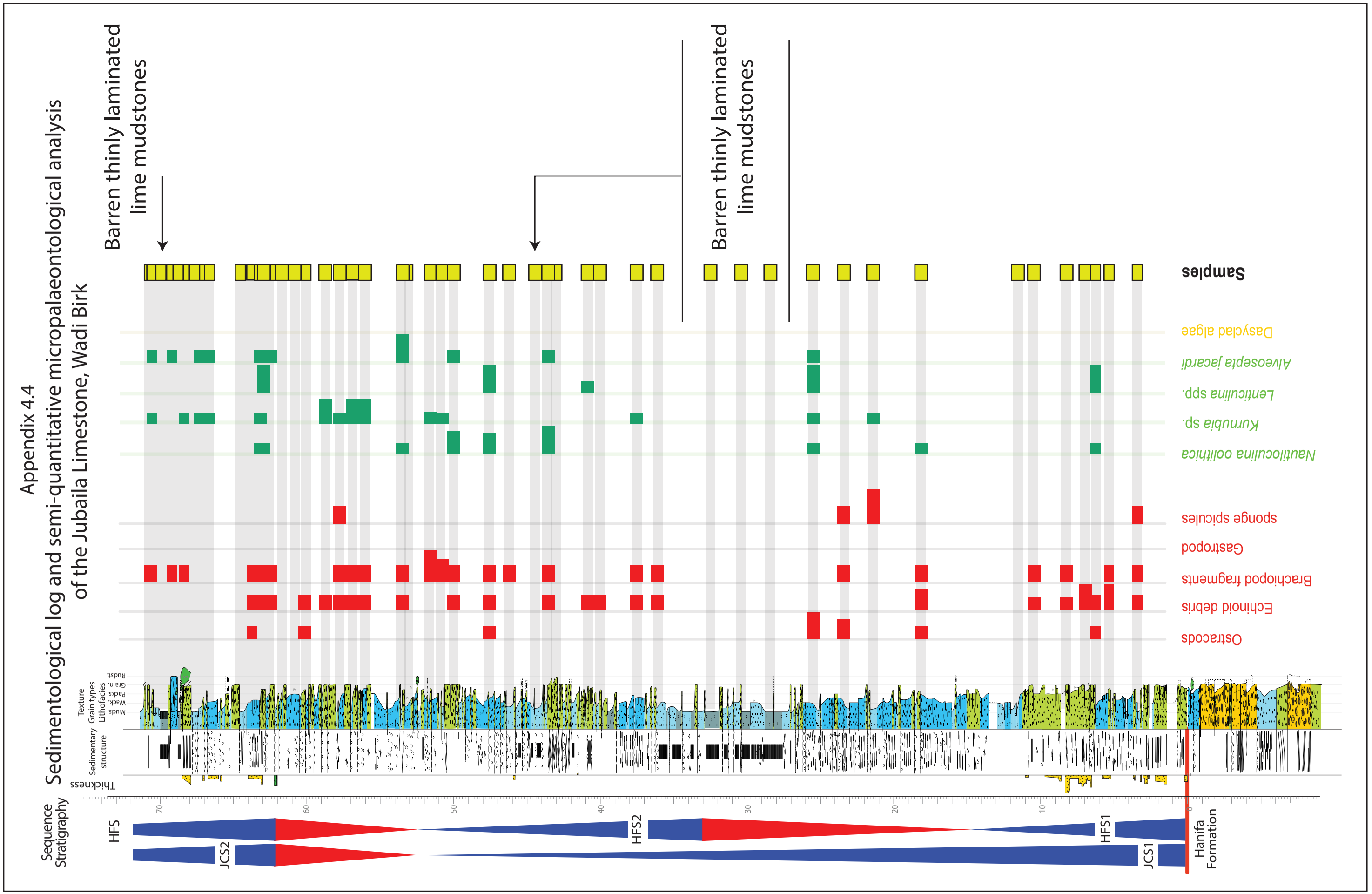

Appendix 4.5 Section locations

Name	Latitude	Longitude
Huraymila/Wadi Malham (Lower Hanifa Fm.)	25.13949	45.99117
Huraymila/Wadi Malham (Upper Hanifa Fm.)	25.13043	46.15601
Wadi Malham (Lower Jubaila Lst.)	25.15375	46.20807
Wadi Malham (Upper Jubaila Lst. and Arab-D Mb.)	25.16315	46.23326
Khashm Qaddiyah (Hanifa Fm.)	24.53213	46.41082
Wadi Al-Ain (Hanifa Fm. and Jubaila Lst.)	24.06569	46.63139
Wadi Al Hawtah (Hanifa Fm.)	23.55652	46.71762
Al Hawtah City (Upper Jubaila Lst. and Arab-D Mb.)	23.46986	46.8684
Wadi Birk (Hanifa Fm.)	23.28124	46.6442
Wadi Birk (Jubaila Lst.)	23.2647	46.73013
Wadi Ghulghul (Hanifa Fm.)	22.89227	46.40329
As Sitarah (Hanifa Fm.)	22.61959	46.34241
Wadi Al-Haddar (Hanifa Fm.)	21.96325	46.04123
Wadi Al-Haddar (Jubaila Lst. and Arab-D Mb.)	21.98056	46.16861

Chapter 5:

Synthesis on the Jurassic sequence of the Arabian platform from Jabal Tuwaiq outcrops

Tuwaiq Escarpment, Fara'id al Ahmar

Table of contents:

Synthesis on the Jurassic sequence of the Arabian platform from Jabal Tuwaiq outcrops

Stratigraphy

Seven Jurassic formations (Fig. 5.1), mainly consisting of shales, carbonates and lesser sandstone and anhydrites, form the Shaqra Group (Vaslet, 1987), which is very well exposed along the Jabal Tuwayq escarpments. The outcropping Shaqra Group provides a westernmost stratigraphic record of the Jurassic (Toarcian to Kimmeridgian including disconformity levels). The Jurassic of the Arabian Platform is a broad slowly subsiding tropical shallow marine epeiric platform system. Its lower boundary is represented by a Triassic – Jurassic unconformity with a hiatus of approximately 20 Myr including the Early Jurassic (Hettangian to Pliensbachian), whereas its top is unconformably overlained by the Cretaceous Thamama Group, Sulaiy Formation of Berriasian age (Manivit et al., 1990; Powers, 1968). In an ascending stratigraphic order, the Jurassic formations are the Marrat Formation, Dhruma Formation, Tuwaiq Mountain Limestone, Hanifa Formation, Jubaila Limestone, Arab Formation and the Hith Anhydrite. Ages of formations and included disconformity levels, spanning from the Early Jurassic (Toarcian) to the Late Jurassic (Tithonian), have been biostratigraphically defined by the presence of ammonites and subordinate fauna (i.e., nautiles, echinoderms, brachiopods and foraminifera) (Manivit et al., 1990). The Late Toarcian – Aalenian hiatus (~ 7 Myr of time gap) is a major unconformity at scale of the Arabian Platform and separates the Marrat and Dhruma Formation. This unconformity shows quite conformable parallel surface over more than 200 km. This probably resulted either from eustatic

sea-level fall (Haq et al., 1988; Le Nindre et al., 1990; Al-Husseini, 1997; Haq and Al-Qahtani, 2005) and subsidence resistance or large-scale uplift (Le Nindre et al., 2003). Within the Dhruma Formation (D6 unit), a minor disconformity corresponds to a poorly dated interval with endemic ammonite fauna. The missing time is probably the Middle Bathonian in which the underlying unit (D5 has Early Bathonian (Zigzag Zone, Yeovilensis Subzone), which is equivalent to Aurigerus Zone in the Submediterranean zonal scale (Manivit et al., 1990; Énay et al., 2009). Moreover, the upper D6 unit is dated Late Bathonian to Early Callovian based on brachiopod fauna (Énay et al., 1987). The Middle – Late Jurassic transition (Tuwaiq - Hanifa boundary) corresponds to a significant unconformity between the Late Callovian (*lamberti* Zone) and the Early Oxfordian (*mariae* Zone) hiatus. This unconformity seems associated with a tectonic inversion and change in basin configuration in outcrop domain (Al-Mojel et al., in prep.). Moreover, in the subsurface the unconformity is known by pre-Hanifa unconformity marked by erosional surface in which the top of the Tuwaiq Mountain is missing in the Rub' al-Khali and to the north of the Ghawar field (Powers, 1968). The upper Jurassic Hanifa and Jubaila are poorly dated. The lower Hanifa Formation is dated Early Oxfordian (? *cordatum* zone) based on brachiopod and nautiles. The only confirmed ammonite zone corresponds to the Middle Oxfordian *plicatilis* Zone. The upper Hanifa is dated Late Oxfordian to Early Kimmeridgian based on foraminifera, brachiopods and echinoids. The Lower Jubaila is assigned to Early Kimmeridgian based on nautiles and endemic ammonites (Manivit et al., 1990).

The outcropping Lower and Middle Jurassic (Marrat, Dhruma and Tuwaiq Mountain Limestone) are made up of continental to shallow-marine mixed carbonate-siliciclastic depositional systems formed in a flat-toped inner-platform. The Lower and Middle Jurassic successions are second-order tectono-eustatic cycle (Marrat to Tuwaiq) bounded at the base and top by regional unconformities. It has a stationary depocenter, and show long-term coastal onlap and marine transgression that reached its maximum extent during the upper Tuwaiq (Middle Callovian). This second-order consists of several 3rd-order sequences characterized by basal siliciclastic and top carbonate cycles (Fig. 5.2). Periods of high siliciclastic incursion are related to short-lived tectonic disruption and climatic changes. These siliciclastic influx events are responsible for carbonate demise occur during the *laeviscula* - *humphriesianum* biozone interval (Lower Bajocian), Zigzag Zone, Yeovilensis Subzone (Lower Bathonian) and *coronatum* Biozone (Middle Callovian). The stacking pattern of the sequences shows an overall southward backstepping of the marginal siliciclastic systems and long-term marine transgression that leads for extensive pure carbonate platform with reef facies in the Middle Callovian upper Tuwaiq Mountain Limestone. This carbonate platform records the first development of starved intrashelf Arabian Basin, with possible source rocks in the near subsurface (Fig. 5.3).

The outcropping Upper Jurassic Hanifa and Jubaila-Arab-D are characterized at the base by mixed carbonate-siliciclastic deposits, argillaceous limestone in the Hanifa Formation and quartz-rich limestone in the Jubaila Limestone. These mixed system grades upward to cleaner high-energy carbonates with localized reef buildups and oncoids. The successions

make several 3rd-order sequences in which the maximal marine transgressions are placed in the pure carbonates with reef facies. The Hanifa Formation has two main MFS placed in a back-barrier high-energy reef and shoal facies at the Late Oxfordian and Early Kimmeridgian. These pure carbonates are probably equivalent to deep lime-mudstone intrashelf basin with source rocks in the near subsurface. The intrashelf basins filled during the Hanifa highstand and capped by extensive iron-stained hardgrounds, possible subaerial exposures. The basis of the Jubaila-Arab-D begins with a lowstand deposits followed by long-term transgression marked at the base by storm-influenced inner-platform with sandstone quartz, grainstones and proximal barren lime-mudstone. The Maximum marine transgression is placed in the Arab-D at Late Kimmeridgian in a backstepping of back-barrier high-energy reef facies in the westernmost inner-platform. During highstand, the reef facies are gently prograding out into Rimthan Arch leaving behind restricted lagoon and sabkhah/salina anhydrite.

Sedimentary system

The Lower and Middle Jurassic (Marrat, Dhruma and Tuwaiq sequences) represent a continental to inner-platform mixed carbonate-siliciclastic shallow marine depositional settings. The siliciclastic proximal domain consists of alluvial system and wide shale-prone coastal plain to lagoonal environment. The siliciclastic domain is characterized by low energy restricted tidal flat and higher energy nearshore tide and occasional wave dominated environment. The restriction condition is attributed to the proximality to the hinterland freshwater runoff and high nutrient supply that cause water stratification and prevent vertical circulation. The distal domain consists of shale-prone lagoon

influenced by siliciclastic influx, and mud carbonate-prone lagoon represents the most open marine environment. The carbonate lagoon is dominated with agglutinated foraminifera (Marrat sequence), algal microbial system (Dhruma sequence) and coral/stromatoporoid reef system (Tuwaiq sequence). The muddy carbonate lagoon is associated with sharp-based storm-generated grainstone beds. The higher energy nearshore environment are better developed during periods of high accommodation rate (Late TST and MFS) in which higher water-depth favoring wave propagation and stronger tidal currents. Moreover, the carbonates are well developed during maximum marine transgression (Late TST and MFS) in well-oxygenated lagoon setting.

The Upper Jurassic Hanifa and Jubaila-Arab-D sequences are characterized by an association of low-energy restricted lagoonal muddy deposits, sometimes slight argillaceous (Hanifa sequence), and high-energy coarse grained deposits mainly grainstone with occasional sandstones (Jubaila-Arab-D sequence). The sedimentary structures of these high-energy deposits suggest an origin of storm-related currents. These storm-generated grainstones are extensive and regionally continuous suggesting a correlatable and synchronous sequence stratigraphic event formed in a flat-topped inner-platform depositional setting. Most of the high-energy depositional units have a sharp-based contact with the underlying muddy deposits. The sharp-based surfaces are interpreted as ravinement surfaces related to transgressive processes. The high-energy deposits developed during early transgressive stages (Fig. 5.4) when the barrier is not established. Then the high-energy grainstones are less frequent during the latter transgressive stage when the barrier is established. These storm-related deposits are also appears during

maximum transgression associated with the backstepping of normal marine facies coral/stromatoporoid boundstone, high foraminiferal diversity, and/or ammonite fauna in a back-barrier inner-platform context.

The apparent depositional polarity of the Jurassic outcrop is north-south direction attested by the spatial distribution of the depositional systems. The continental, marginal siliciclastic system and low-energy lime mudstone facies are better developed in the proximal landward position (south; Fig. 5.2) compared to open-marine carbonate-prone lagoon and back-barrier boundstone and grainstone deposits that are more developed in the distal part of the transects (north). During the onset of the Jurassic transgression, the Arabian Platform tends to be very flat low-energy and shallow-marine inner platform as attested by our stratigraphic transect (Marrat, Dhruma and Lower Tuwaiq sequence; Fig. 5.3). This flat-topped profile is mainly related to overall geodynamic setting, inner part of a very wide epeiric platform on the Neo-Tethys passive margin with stable tectonic context. That leads for limited rate of accommodation which is compensated everywhere and filled by the siliciclastic supply and the carbonate production. During higher accommodation rate, high differential aggradational style on the platform will be formed as carbonate production is not able to fill up the created space everywhere (cf. Razin et al., 2010). Thus, high carbonate productions that follow the rapid accommodation rate were localized in certain places forming aggrading stacking patterns, like in Khurais and Berri Fields (upper Tuwaiq and Hanifa sequence).

In conclusion, the Jurassic platform (Fig. 5.3) evolved from very-flat continental-to-nearshore mixed carbonate-siliciclastic platform (Marrat-

Dhruma sequences) to differentiated ramp platform with deep intrashelf basins (Tuwaiq-Hanifa sequences) to a lowstand followed by flat aggraded platform (Jubaila-Arab-D sequences). The Jurassic platform ends with the mixed carbonate-evaporite systems of the Arab Fm. This evolution in sedimentary system within the Jurassic sequence is interplay of accommodation space and sedimentation rate.

Controlling factors

Tectonic

Evident syndepositional differential subsidence has an influence on lateral thickness variation and to a lesser extent facies distribution. The Early and Middle Jurassic depositional sequences (MCS, DCS and TCS) have a common depocenter, in which differential subsidence increased northward. The initial transgression of these depositional sequences show a complete wedging of continental to shallow marine mixed carbonate-siliciclastic succession, which are then followed by aggraded shallow carbonate platform. The shallow carbonate platform can keep-up to such continuous and slight syndepositional differential subsidence (cf. Wilson and Jordan, 1983). The carbonate deposits are well developed in the northern most subsiding area (K. Ad Dhibi and K. Al-Qaddiyah), which likely required higher accommodation space. Moreover, these northern depocenter areas lacks continental and nearshore siliciclastic sands deposits. This would suggest that the lateral facies changes were influenced by the differential subsidence perhaps controlled by basement faulting (Le Nindre et al., 2003), which influenced accommodation space.

This Early and Middle Jurassic differential subsidence appears rather homogeneous, however, local and short-lived tectonic events influenced the facies, depositional environments and some of the systems tracts. The Early Bajocian (*laeviuscula* Zone) shows strong wedging geometry which indicates for an abrupt and high differential subsidence responsible for creating at least 25 m accommodation space, deltaic progradation and exposed uplifted southern area (Fig. 5.2). This abrupt deltaic and siliciclastic incursion associated with demise of carbonate-production and corresponds to an extensive regional high gamma-ray correlation known by “Dhruma shale” (Fig. 5.3; Al-Husseini and Matthews, 2008). Moreover, The HST of DCS (Early Bathonian *zigzag* Zone) was probably influenced by local and short-lived tectonic instability (uplift or slow subsidence) synchronous with abrupt siliciclastic incursion, progradation and disconformity development.

The Middle – Late Jurassic transition (top DCS sequence boundary) is marked by a significant change in the basin configuration and shift in the depocenter axes of the overlying Late Jurassic (Oxfordian) which suggest a time of tectonic tilting and basin inversion (Fig. 5.2). The Oxfordian depocenter axis shifted to the south (As Sitarah section). This changes in basin configuration is probable related to a significant tectonic uplift and truncational event during post-Tuwaiq unconformity thorough the eastern edge of the Arabian Plate (Iran, Abu Dhabi and Interior Oman; Gollesstaneh, 1965; Al-Suwaidi and Aziz, 2002; Rousseau et al., 2006). This tectonic instability is probably related to the incipient breaking of the Arabian-Indian plate boundary, which marked by a volcanic interruption in eastern Oman (Ziegler, 2001). There is another shift in depocenter and reversal onlapping

direction during the Late Oxfordian Early Kimmeridgian sequences (between HCS3 and HCS4). These Oxfordian tectonic interruptions were noticed in other regions in the Jura Platform and in the northern margin of the Tethys Ocean (Dardeau et al., 1988; Lhamyani, 1985; Pittet and Strasser, 1998; Allenbach, 2001; Chevalier et al., 2001; Védrine and Strasser, 2009; Strasser et al., 2015). The Hanifa Formation in the subsurface (Fig. 5.3) is almost isopachous sequence indicating that the differential subsidence seems to be small and neglected. Thus, differential subsidence is unlikely to be the main control on the development of the deep source rock intrashelf basin but rather influenced by the changing ratio of carbonate production and accommodation space. The beginning of the outcropping Jubaila depositional sequence (JCS1) records significant syndepositional differential subsidence toward the central of the studied area (Fig. 5.2) that are clearly demonstrated along the transect by the complete wedging and thickening geometries. This has been noticed in the outcrop as well as in the subsurface (Fig. 5.3) with abrupt thinning toward Northeast to the Rimthan Arch. This is consistent with overall eastward thinning of the Late Jurassic stratigraphy toward the shelf margin as mapped by (Murris, 1980; Abu-Ali and Littke, 2005). The outward subsidence resistance of the shelf margin and Rimthan Arch are probably the main reason for being the lower Jubaila sequence restricted and protected for open marine condition. This Jubaila-Arab-D syndepositional differential subsidence seems to be decrease upward in which the upper sequence (JCS1) show tabular geometries.

Eustatic control

The 3rd-order and, to a lesser extent, 4th-order eustasy cycles seem to have been the main driving factors generating the Jurassic sequences (Fig. 5.5). The main MFS of the whole Marrat succession is within the Middle Toarcian (*bifrons* Zone) and that is in concordance with the main Early Jurassic MFS of the Arabian Platform (MFS J10 of Sharland et al., 2001). Consistently, the *bifrons* Zone marks the interval of the highest global sea-level rise during the Early Jurassic (Haq et al., 1988) and the major MFS of the NW Tethys in the European domain (Hardenbol et al., 1998) and drowning event in the Mediterranean domain (Jenkyns et al., 1985; Crevello, 1990). In detail, these two 3rd sequences MCS1 and MCS2 could correspond to the Tethyan eustatic sequences Toa3 and Toa4 of Hardenbol et al. (1998), which considered as 3rd-order ~1.6 Myr influenced by astronomical forcing controls, precession and obliquity including their long-term modulations (Hinnov and Park, 1999; Boulila et al., 2014). The top sequence boundary of the Marrat sequence corresponds to a regional hiatus between the Early and Middle Jurassic (Late Toarcian to Aalenian). This sequence boundary is most likely resulted from substantial eustatic sea-level fall with about 50 m as proposed by Al-Husseini (1997) (Le Nindre et al., 1990; Haq and Al-Qahtani, 2005). An eustatic origin of this unconformity is adopted herein as the successions of the Middle Jurassic show extensive quite conformable parallel surfaces and lack of deformation between the Early and Middle Jurassic (Al-Mojel et al., submitted). The long-term flooding event of the Dhruma sequence (DCS) from the Early Bajocian to the Early Bathonian is coherent with the eustatic trends recorded in the Mediterranean domain (Hardenbol et al. 1998). But, there is

subordinate sea-level fall and a short emersion momentarily interrupted this trend in the transition of *niortense* and *garantiana* Zones marked by scouring ravinement surfaces. Moreover it confirms the occurrence of partial emersions along the southwestern parts of the Arabian Platform in the mid Bajocian (Haq and Al- Qahtani 2015). A similar regressive sequence named R7' was also identified in the European domain (Hardenbol et al. 1998), but it occurred 0.5 Myr earlier – within the *niortense* Zone – and spanned until the end of the *garantiana* Zone. The MFS of DCS (Early Bathonian *zigzag* Zone) should correspond to the MFS J30 of Sharland et al. (2001) and correlates well with the depositional sequences of the Western Paris Basin defined by Andrieu et al. (2016) (Fig. 5.5). In addition, consistently, the Early Bathonian *zigzag* Zone marks relative sea level rise in the northern Switzerland (Gonzalez, 1996). Regionally, the highstand of DCS and the associated fluvial incursion and hiatus (Middle Bathonian) have a regional significance throughout the Arabian Plate and the northern margin of the Arabian-Nubian Shield (Al-Husseini and Matthews, 2006; Énay et al., 2009). Continental and marginal marine siliciclastic deposits were dominated in the northern Arabian-Nubian Craton during Early-Middle Bathonian a time of assumed low sea-levels (cf. Fig 8 in Énay et al., 2009). Globally, the Early Bathonian sea level highstand and the strong sea-level fall are in concordance with progradational patterns of MJ9 and MJ10 sequences of Andrieu et al. (2016) and the maximum regression of the standard European sequences Bt2, Bt3 and Bt4 from Hardenbol et al. (1998). Moreover, this Early Bathonian highstand trend corresponds, as well, to those of the Russian Platform and South America basins (Sahagian et al., 1996; Hallam, 2001; Simmons et al., 2007), which suggest that this highstand

was of eustatic origin. The overall transgressive trend of the Tuwaiq composite sequence (TCS) is in concordance with the Late Bathonian and Early Callovian stepwise transgression of Greenland and Europe as well as Himalayas and Pakistan regions (Hallam, 2001). In this study, the main MFS of the Middle Jurassic succession is within the Tuwaiq Mountain Limestone deposition (MFS of TCS) Middle Callovian (*coronatum* Zone; corresponds to MFS J40 of Sharland et al., 2001). Consistently, the Middle Callovian marks the interval of the highest sea-level rise in a global scale during the Middle Jurassic (Hallam, 1988; Surlyk, 1990, 1991; Hallam, 2001). Moreover, Surlyk (1990) confirmed that Middle Callovian (*coronatum* Zone) is a period of maximum rate of sea-level rise in the East Greenland embayments. Locally, however, the Arabian Platform Middle Jurassic 2nd-order MFS were placed in the Dhruma Formation (Early Bajocian *laeviuscula* Zone) (MFS J20 of Sharland et al., 2001). Nevertheless, the 2nd-order Middle Jurassic MFS should be placed higher in the Tuwaiq Limestone deposits as it shows further marine extension over continental deposits that represent the westernmost preserved onlap part of the Arabian Platform. The top sequence boundary of the TCS corresponds to the Middle-Late Jurassic extensive regional unconformity probably resulted from global scale eustatic sea-level fall that occurs at the Middle-Late Jurassic transition. The sea-level fall reaches its maximum during Late Callovian (Hallam, 1988; Dromart et al., 2003a, 2003b). This Middle-Late Jurassic global sea-level fall could be of a glacio-eustatic in origin, as it corresponds to a maximum cooling event happened during Late Callovian (*lamberti* Zone) (Hallam, 1988; Dromart et al., 2003a, 2003b; Nunn et al., 2009; Nunn and Price, 2010; Donnadieu et al., 2011; Pellenard et al.,

2014). This drop in sea level has been recorded in the relative sea-level curve of the Arabian Platform with around 40 m sea-level fall (Haq and Al-Qahtani, 2005).

Unfortunately, the Oxfordian and Kimmeridgian stratigraphy are too poorly dated to propose a global correlation scheme. The only confirmed ammonite zone corresponds to the Middle Oxfordian *plicatilis* Zone. The Late Jurassic successions shows long-term sea-level rise trend that reach its maximum in the Arab-D interval (Le Nindre et al., 1990). But, there is subordinate sea-level fall and a short emersion momentarily interrupted this trend. The transgression trend and MFS of the Oxfordian Hanifa sequences (Hawtah; HCS1-HCS3) is placed in the Late Oxfordian (MFS of HFS3) in an extensive carbonate interval with higher-energy and relatively normal-marine reef facies. Thus, the MFS J50 of the Arabian Platform would be better placed in the Late Oxfordian instead of Middle Oxfordian as another workers did (Sharland et al., 2001; Mattner and Al-Husseini, 2002; Le Nindre in Kadar et al., 2015). The Late Oxfordian MFS is consistent with the Gulf of Mexico major marine transgression (Mancini et al., 2004) and the Central North Sea (Carruthers et al., 1996). However, the major MFS in the Western Europe occurs in the Early Oxfordian (Hardenbol et al., 1998). This discrepancy in the global MFS invokes a local tectonic overprint on the Oxfordian eustasy signals. A major sequence boundary and disconformity between HCS3 and HCS4 associated with significant facies shift and tectonic interruption, which is most likely to be Late Oxfordian in age. This sequence boundary could correlate with the Western Europe 2nd-order regression and sequence boundary between OX6 and OX7 (Hardenbol et al., 1998; Strasser et al., 2000; Vedrine and Strasser,

2009). The second significant MFS in the Hanifa Formation is in the Ulayyah sequence (HCS4) in relative open-marine and higher-energy condition with reef-bearing facies, which would correspond to the Early Kimmeridgian MFS J60 (Sharland et al., 2001). Previously, the place of MFS J60 is debated and required further studies to recognize the best location of this Lower Kimmeridgian MFS. We placed the MFS J60 in the upper Hanifa (Ulayyah; HCS4) instead of Lower Jubaila (J1), which characterized by a lowstand and restricted lagoonal deposits rich with sandstone quartz and lack of open-marine reef facies. These Lower Jubaila lowstand and restricted lagoonal deposits are considered initial transgression, whereas topmost Upper Jubaila (JCS2; J2 unit or Arab-D Reservoir) records the maximum marine transgression with high-faunal diversity and backstepping of reef facies. This Jubaila-Arab-D MFS would correspond to the Upper Kimmeridgian MFS J70 (Sharland et al., 2001; Le Nindre in Kadar et al., 2015). This is consistent with Kadar et al. (2015) interpretation that placed MFS J70 in a clean limestone at the topmost of the Jubaila, just underneath the Gotnia Anhydrite in Kuwait. This Jubaila-Arab-D long-term transgression is in concordance with the 2nd-order TST and MFS in the central Swiss Jura as well as in most of the Western European basins, which placed in the Late Kimmeridgian (*eudoxus* Zone) (Hardenbol, 1998; Colombié and Strasser, 2005). These Swiss Jura large-scale sequences are correlatable in most of Western European basins, which suggest a strong eustatic influence on the Kimmeridgian sequences (Colombié and Strasser, 2005).

Climatic influences

During the Jurassic, the Arabian Platform is placed along the tropical belt probably few degrees south of the Equator (Murris, 1980; Thierry et al., 2000; Sharland et al., 2001). Here, the study of the Jurassic sediments allow us to address for the first time the impact of these climatic disturbances in a coastal/lagoonal context situated at very low paleolatitudes. Among the Jurassic climate changes (Dera et al., 2011), the Early Toarcian warming event is generally considered as the warmest interval, as current numerical models suggest rapid temperature rises of +5 to +10°C in terrestrial domains (Dera and Donnadieu, 2012). This episode was also documented in marine paleoenvironments from European domains with shifts in the oxygen isotope composition of various fossils (Bailey et al., 2003, van de Schootbrugge et al., 2005; Suan et al., 2010). This disturbance is further believed to have caused a redistribution of humid belts toward mid- and high-latitudes (Dera et al., 2015), and global increases of weathering rates (Cohen et al., 2004, Dera et al., 2009). Occurrence of fluvial systems at the Lower Marrat transgression (MCS1) with plant fragments and high gamma-ray response suggesting humid period which would correspond to the warm peak of the early *serpentinum* Zone. The humid period evolved to more semi-arid condition during late TST and MFS of MCS1 showing by stromatolites, mudcracks with limited siliciclastic influx and later with carbonate development. The semi-arid condition and the carbonate development could be related to slight decrease of the palaeotemperature during late *serpentinum* Zone. The regressive evolution recorded in the Middle Marrat (turn-over between MSC1 and MSC2) with the deposition of rather thick and extensive kaolinite and hematite

enrichments of reddish shales and sandstones deposit cannot be considered as a response to the decrease of accommodation rate but to an increase of the terrigenous influx. This shale-dominated influx could be interpreted as indicative of strong hydrolyzing conditions under humid and warm period. The Middle Marrat could be really the best record of an increase of humidity during the Early Toarcian warm period. In the same way, the MCS2 transgression could be favored by a combination of eustatic transgression (*bifrons* Zone) and decrease of the siliciclastic input indicating more semi-arid conditions with possible simultaneous overall decrease in palaeotemperature during the *bifrons* Zone.

The first half of the Middle Jurassic (Aalenian to middle Bathonian) is generally considered as the coolest interval of the Jurassic, alternating between periods of incipient polar ice sheet developments and short-lived warming episodes (Dera et al., 2011; Korte et al., 2015). As revealed by clay mineral assemblages, these temperature variations were associated with humidity fluctuations oscillating between semi-arid climates interrupted by seasonal monsoon episodes during cool intervals, and everwet conditions during warmer episods (Brigaud et al. 2009; Martinez and Dera, 2015; Andrieu et al., 2016). On the Arabian Platform, the evolution of sedimentary facies is in total agreement with these trends. The Early Bajocian (*discites* and *laeviuscula* Zones) showed a dramatic climate change from arid shoreline with evaporite and stromatolite (*discites* Zone) to wetter conditions marked by high-siliciclastic influx in a deltaic system (*laeviuscula* Zone). This first arid period is more likely corresponds to the waning phase of the cooler Aalenian time. The humid high-siliciclastic input would correspond to a rapid seawater

temperature increase computed from oxygen isotopes (Brigaud et al., 2009). This warm-humid event and associating high riverine siliciclastic influx and high eutrophication level, is probably the reason for the widespread carbonate-production crisis and shale distribution on the Arabian Platform. This interval is marked by correlatable high gamma-ray response known as “Dhruma Shale” (Fig. 5.3; Al-Husseini and Matthews, 2008). This decline in carbonate production is probably synchronous with other Tethys domains that characterized by major marine faunal turnovers (northern Tethys; O’Dogherty et al. 2006), condensed interval (western France; Andrieu et al., 2016), and biosiliceous sedimentation associated with positive carbon excursion (southern western Tethys; Bartolini et al., 1996; Muttoni et al., 2005; O’Dogherty et al., 2006). This event is followed by a progressive carbonate recovery (Late Bajocian to Early Bathonian *niortense* to *zigzag* Zones) controlled by stepping back of the siliciclastic sources, and coupled with drying of the climate evidenced in the study area by thin beds of red dolomite with silicified anhydrite nodules. The expansion of the carbonate production in the Central Arabia during the Bajocian-Bathonian is consistent with the western Tethys epicontinental carbonates growth (Andrieu et al., 2016). The semi-arid climate corresponds probably to long-term cooling throughout the Bajocian − Early Bathonian interval (Price, 1999; Martinez and Dera, 2015). The Late Bathonian and Early Callovian sequences (lower TCS) are dominated by petrified trunks, overlying high fluvial siliciclastic discharges and shale prone deposits indicating that a humid period prevailed. This could relate to a dominant long term warming periods, which probably synchronous with the Early Callovian abrupt carbonate demise in the Paris Basin (Jacquin

et al., 1992, 1998; Jacquin and de Graciansky, 1998; Brigaud et al., 2014) as well as with clay rich deposits in the Western Paris Basin (Andrieu et al., 2016). Then, this low carbonate production period was followed by a growth of carbonate platform during Middle Callovian (upper TCS) as a result of widespread backstepping of deltas coupled perhaps with drying. This drying could result from an extreme cooling of seawater possibly associated with incipient continental ice build-up at the end of the Late Callovian *athleta* Zone (Dromart et al., 2003a, 2003b).

The Middle-Late Jurassic transition is an extensive regional unconformity over the Arabian Platform with Late Callovian (*lamberti* Zone) and the Early Oxfordian (*mariae* Zone) hiatus (Le Nindre, personal communication, 2014; and in Kadar et al., 2015). This unconformity was likely controlled mainly by a global eustasy sea-level fall associated with an incipient cooling event having favored the extension of continental ice buildup at high latitude during Middle-Late Jurassic transition (Dromart et al., 2003a, 2003b; Donnadieu et al., 2011). This cold event was followed by a period of warming in the NW Tethyan domain through the Middle Oxfordian (Nunn and Price, 2010; Dromart et al., 2003b). This Early-Middle Oxfordian warming event was probably accompanied by a humid phase indicated by overall high kaolinite abundances in NW Europe (Wignall and Ruffell, 1990; Ruffell et al., 2002). In the Arabian Platform domain, the initial transgression and the highly terrigenous units at the base of the Hanifa sequences (HCS1 to lower HCS3) are compatible with this Early-Middle Oxfordian warm humid phase. After this brief regional event, the marine paleoenvironments of European basins returned to cooler and more arid climatic conditions from the late-Middle to

Late Oxfordian, with a minimum of temperature evidenced during the *bimmamatum* Zone by high oxygen isotope values of oyster shells from the Paris basin (Brigaud et al., 2008). This cooling trend was probably synchronous with the 2nd-order sequence boundary of the Western Europe (Hardenbol et al., 1998; Strasser et al., 2000; Vedrine and Strasser, 2009). Moreover, it was concomitant with a drying phase evident by gradual decreases of kaolinite content and enrichment of smectite enrichments in the sediments of the Paris Basin (Mosser-Ruck et al., 2002). On the Arabian Platform, this late Middle to Late Oxfordian temperate-dry event could correspond to the cleaning upward trend toward terrigenous-free carbonate sediments with reef facies development (upper HCS3 and HCS4). This carbonate recovery and reef development seems to be a regional event noticed in the Western Europe (Dromart et al., 2003b) and mapped along the Tethys margin (Cecca et al., 2005). The Late Oxfordian - Early Kimmeridgian transition recorded a rapid rise in seawater temperatures, which staying relatively high (up to 24° C) all over the Kimmeridgian (Brigaud et al., 2008; Price and Rogov, 2009; Nunn and Price, 2010; Wierzbowski et al. 2013). On the Arabian platform, this extreme warmth and humid phase is consistent with the recurrent occurrences of high sandstone contents in sediments of the lower Jubaila-Arab-D sequence. Moreover, it supports the interpretation that high nutrient levels have a negative impact on the benthic communities and reef development. From the Upper Jubaila sequence, including the Arab-D Reservoir, the development of widespread reefs and decrease of the siliciclastic inputs are interpreted as the result of an eustatic transgression combined with parallel decreases of seawater temperatures and rise of aridity

during the Late Kimmeridgian (Nunn and Price, 2010). Moreover, the increase of the aridity is compatible with the appearance of widespread sheetlike dolomite beds in the Arab-D Reservoir that formed as result of hypersaline infiltration from overlying salina (Lindsay et al., 2006). Remarkably, the synchronicity of the TST and MFS with warm-humid condition and HST with cool-dry events provide some confidence to the astroclimatic-driven eustasy as a primary mechanism controlling these 3rd-order sea-level changes (cf. Boulila et al., 2011, Martinez and Dera, 2015).

Figure 5.1: A) Lithostratigraphy and chronostratigraphy of Jurassic sedimentary deposits from Saudi Arabia combined with second-order sequence boundaries (SB) of Al-Husseini and Matthews (2005) (compiled in Fischer et al., 2001; modified from Al-Husseini et al., 2006), **B)** Details of lithofacies, biostratigraphy (Manivit et al., 1990) and sequence stratigraphy (this study) of the Jurassic Shaqra Group. Khashm Ad Dhibi is a composite section which consists of four shallow boreholes with continuous cores (DHIBI-1, HMNK-1, MRZU-2 and MQBL-1). Abbreviations: eOxf – Early Oxfordian; mOXf - Middle Oxfordian; lOxf - Late Oxfordian; eKm - Early Kimmeridgian.

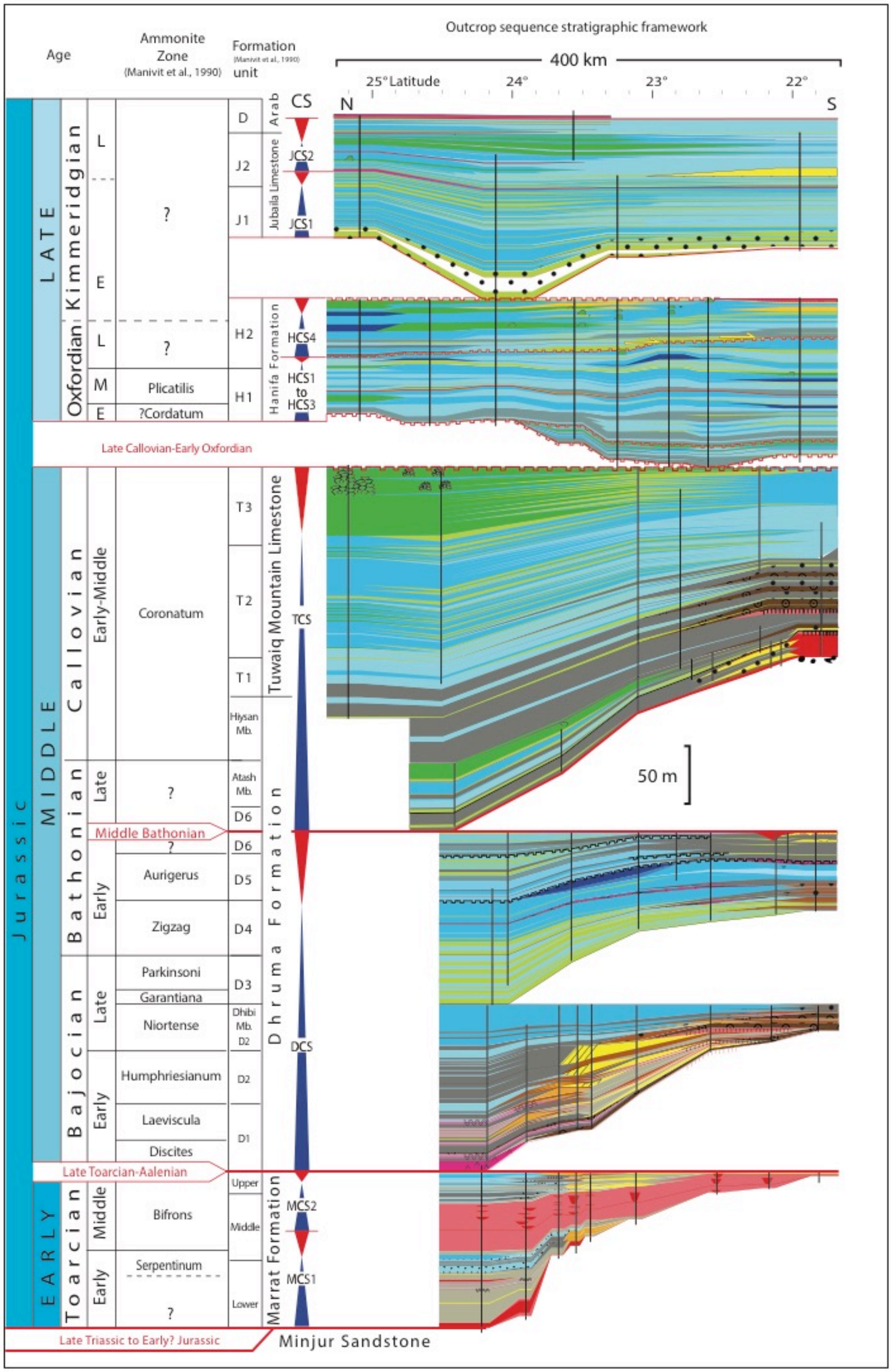

Figure 5.2 : Sequence stratigraphic frameworks of the Jurassic Shaqra Group along the Jabal Tuwayq between latitude 25° and 22° N. See Fig. 5.1 for detailed legends.

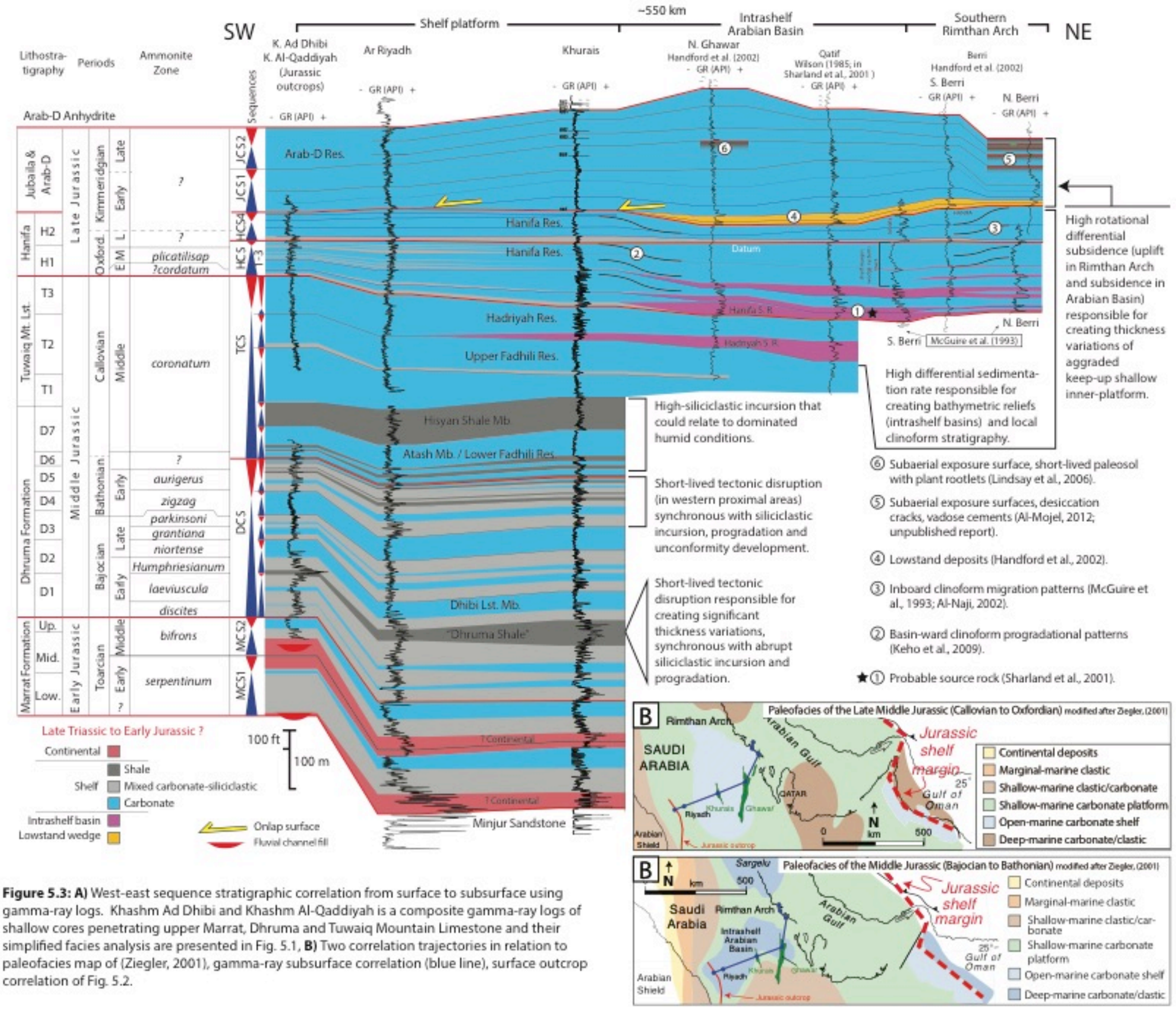

Figure 5.3: A) West-east sequence stratigraphic correlation from surface to subsurface using gamma-ray logs. Khashm Ad Dhibi and Khashm Al-Qaddiyah is a composite gamma-ray logs of shallow cores penetrating upper Marrat, Dhruma and Tuwaiq Mountain Limestone and their simplified facies analysis are presented in Fig. 5.1, **B)** Two correlation trajectories in relation to paleofacies map of (Ziegler, 2001), gamma-ray subsurface correlation (blue line), surface outcrop correlation of Fig. 5.2.

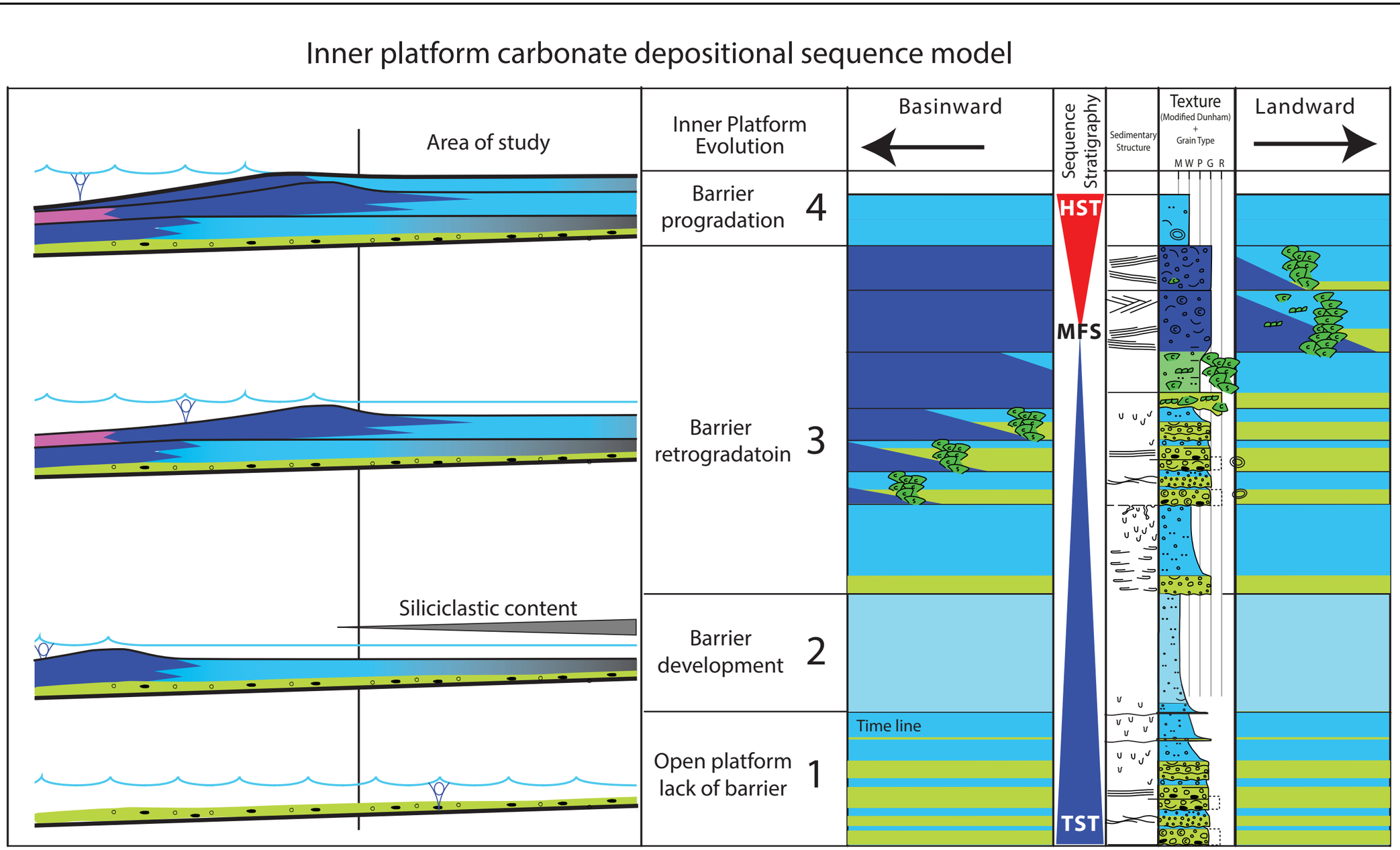

Figure 5.4: Inner platform carbonate depositional sequence model.

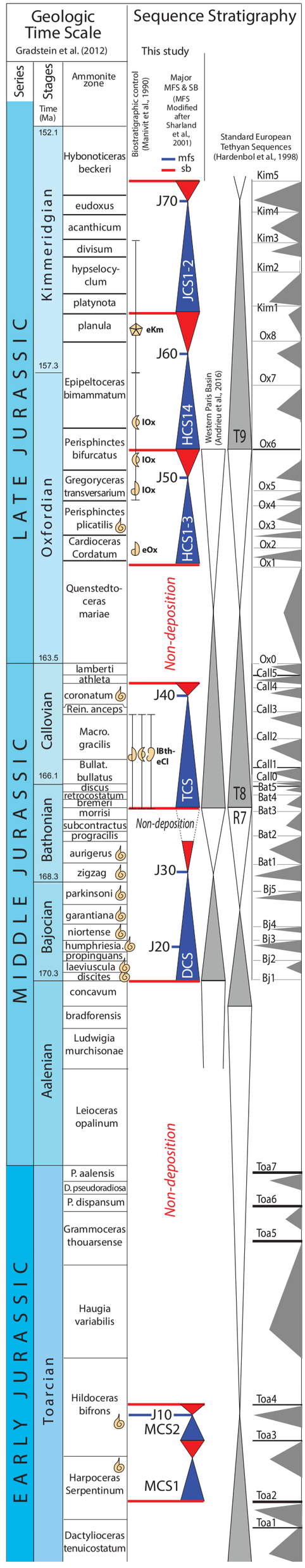

Figure 5.5: Jurassic geological history shows sequence stratigraphy of the Central Arabia compared with the European domain.

Reference

Abu-Ali, M., & Littke, R., 2005. Paleozoic petroleum systems of Saudi Arabia: a basin modeling approach. GeoArabia, 10(3), 131-168.

Al-Husseini, M. I and. Matthews, R. K. 2008. Jurassic-Cretaceous Arabian orbital stratigraphy: The AROSJK Chart, GeoArabia, 13 (1), 89-94.

Al-Husseini, M., Matthews, R.K., Mattner, J., 2005. Stratigraphic Note: Orbital-forcing calibration of the Late Jurassic (Oxfordian-early Kimmeridgian) Hanifa Formation, Saudi Arabia. GeoArabia 11, 145–149.

Al-Husseini, M.I., 1997. Jurassic sequence stratigraphy of the western and southern Arabian Gulf. GeoArabia (Manama), 2(4), 361–82.

Al-Husseini, M.I., 1997. Jurassic sequence stratigraphy of the western and southern Arabian Gulf. GeoArabia (Manama), 2(4), 361–82.

Al-Suwaidi, A.S., Aziz, S.K., 2002. Sequence stratigraphy of Oxfordian and Kimmeridgian shelf carbonate reservoirs, offshore Abu Dhabi. GeoArabia, 7, 31-44.

Allenbach, R.P., 2001. Synsedimentary tectonics in an epicontinental sea: a new interpretation of the Oxfordian basins of northern Switzerland. Eclogae Geologicae Helvetiae, 94, 265–287.

Andrieu, S., Brigaud, B., Barbarand, J., Lasseur, E., & Saucède, T., 2015. Disentangling the control of tectonics, eustasy, trophic conditions and climate on shallow-marine carbonate production during the Aalenian–Oxfordian interval: From the western France platform to the western Tethyan domain. Sedimentary Geology, 345, 54-84.

Bailey, T.R., Rosenthal, Y., McArthur, J.M., Van de Schootbrugge, B., Thirwall, M.F., 2003. Paleoceanographic changes of the Late Pliensbachian–Early Toarcian interval: a possible link to the genesis of an Oceanic Anoxic Event. Earth and Planetary Science Letters, 212, 307–320.

Bartolini, A., Baumgartner, P.O., Hunziker, J.C., 1995. Middle and Late Jurassic carbon stable-isotope stratigraphy and radiolarite sedimentation of the Umbria-Marche Basin (Central Italy). Eclogae Geologicae Helvetiae 89, 811–844.

Boulila, S., Galbrun, B., Huret, E., Hinnov, L. A., Rouget, I., Gardin, S., Bartolini, A., 2014. Astronomical calibration of the Toarcian Stage: implications for sequence stratigraphy and duration of the early Toarcian OAE. Earth and Planetary Science Letters, 386, 98-111.

Boulila, S., Galbrun, B., Miller, K.G., Pekar, S.F., Browning, J.V., Laskar, J., Wright, J.D., 2011. On the origin of Cenozoic and Mesozoic “third-order” eustatic sequences. Earth-Science Reviews, 109(3), 94-112.

Brigaud, B., Durlet, C., Deconinck, J.F., Vincent, B., Pucéat, E., Thierry, J., Trouiller, A., 2009. Facies and climate/environmental changes recorded on a carbonate ramp: a sedimentological and geochemical approach on Middle Jurassic carbonates (Paris Basin, France). Sedimentary Geology 222, 181-205.

Brigaud, B., Pucéat, E., Pellenard, P., Vincent, B., Joachimski, M.M., 2008. Climatic fluctuations and seasonality during the Late Jurassic (Oxfordian-Early Kimmeridgian) inferred from δ18O of Paris Basin oyster shells. Earth and Planetary Science Letters 273, 58-67.

Brigaud, B., Vincent, B., Carpentier, C., Robin, C., Guillocheau, F., Yven, B., Huret, E., 2014. Growth and demise of the Jurassic carbonate platform in the intracratonic Paris Basin (France): interplay of climate change, eustasy and tectonics. Marine and Petroleum Geology 63, 3–29.

Carruthers, A., Mckie, T., Price, J., Dyer, R., Williams, G., Watson, P., 1995. The application of sequence stratigraphy to the understanding of Late Jurassic turbidite plays in the Central North Sea, UKCS. Geological Society, London, Special Publications, 114(1), 29-45.

Cecca, F., Martin-Garin, B., Marchand, D., Lathuilière, B., Bartolini, A., 2005. Paleoclimatic significance of biogeographic and sedimentary events in Tethyan and Peri-Tethyan areas during the Oxfordian (Late Jurassic). Palaeogeography, Palaeoclimatology, Palaeoecology 222, 10-32.

Chevalier, F., Garcia, J.P., Quesne, D., Guiraud, M., Menot, J.C., 2001. Correlations and genetic stratigraphy through Oxfordian reefal formations in the upper Yonne valley (southern Paris basin, France). Bulletin de la Société Géologique de France 172, 69-84.

Cohen, A.S., Coe, A.L., Harding, S.M., Schwark, L., 2004. Osmium isotope evidence for the regulation of atmospheric CO2 by continental weathering. Geology 32 (2), 157–160.

Colombié, C., Strasser, A., 2005. Facies, cycles, and controls on the evolution of a keep-up carbonate platform (Kimmeridgian, Swiss Jura). Sedimentology, 52(6), 1207-1227.

Crevello, P. D., 1990, Depositional systems tracts, stacking patterns, and sequence stratigraphy of Lower and Middle Jurassic synrift carbonate platforms, Central and Eastern High Atlas, Morocco. International Association of Sedimentologists, 1990 Annual Meeting, Proceedings with Abstracts, 111-112

Dardeau, G., Atrops, F., Fortwengler, D., de Graciansky, P.C., Marchand, D., 1988. Jeu de blocs et tectonique distensive au Callovien et à l'Oxfordien dans le bassin du Sud-Est de la France. Bulletin de la Société géologique de France, 8(IV), 771-777.

Dera, G., Brigaud, B., Monna, F., Laffond, R., Puceat, E., Deconinck, J.F., Pellenard, P., Joachimsky, M., Durlet, C., 2011. Climatic ups and downs in a disturbed Jurassic world. Geology 39, 215-218.

Dera, G., Donnadieu, Y., 2012. Modeling evidences for global warming, Arctic seawater freshening, and sluggish oceanic circulation during the Early Toarcian anoxic event. Paleoceanography, 27(2).

Dera, G., Pellenard, P., Neige, P., Deconinck, J. F., Pucéat, E., Dommergues, J. L. 2009. Distribution of clay minerals in Early Jurassic Peritethyan seas: palaeoclimatic significance inferred from multiproxy comparisons. Palaeogeography, Palaeoclimatology, Palaeoecology, 271(1), 39-51.

Dera, G., Prunier, J., Smith, P. L., Haggart, J. W., Popov, E., Guzhov, A., Rogov, M., Delsate, D., Thies, D., Cuny, G., Pucéat, E., Charbonnier, D., Bayon, G., 2015. Nd isotope constraints on ocean circulation, paleoclimate, and continental drainage during the Jurassic breakup of Pangea. Gondwana Research, 27(4), 1599-1615.

Donnadieu, Y., Dromart, G., Goddéris, Y., Pucéat, E., Brigaud, B., Dera, G., Dumas, C. Olivier, N., 2011. A mechanism for brief glacial episodes in the Mesozoic greenhouse. Paleoceanography 25.

Donnadieu, Y., Dromart, G., Goddéris, Y., Pucéat, E., Brigaud, B., Dera, G., Dumas, C. Olivier, N., 2011. A mechanism for brief glacial episodes in the Mesozoic greenhouse. Paleoceanography 25.

Dromart, G., Garcia, J.P., Picard, S., Atrops, F., Lécuyer, C., Sheppard, S.M.F., 2003a. Ice age at the MiddleeLate Jurassic transition? Earth and Planetary Science Letters. 213, 205-220.

Dromart, G., Garcia, J.P., Picard, S., Rousseau, M., Atrops, F., Lécuyer, C., Sheppard, S.M.F., 2003b. Perturbation of the carbon cycle at the Middle/Late Jurassic transition: geological and geochemical evidence. American Journal of Science 303, 667–707.

Énay, R., Mangold, C., Alméras, Y., Hughes, G.W., 2009. The Wadi ad Dawasir “delta”, central Saudi Arabia: A relative sea-level fall of Early Bathonian age. GeoArabia, 14 (1), 17-52.

Gonzalez, R., 1995. Response of shallow-marine carbonate facies to third-order and high-frequency sea-level fluctuations: Hauptrogenstein Formation, northern Switzerland. Sedimentary Geology, 102(1-2), 111-130.

Hallam, A., 1988. A reevaluation of Jurassic eustasy in the light of new data and the revised Exxon curve.

Hallam, A., 2001. A review of the broad pattern of Jurassic sea-level changes and their possible causes in the light of current knowledge. Palaeogeography, Palaeoclimatology, Palaeoecology, 167(1), 23-37.

Haq, B.U., Al-Qahtani, A.M., 2005. Phanerozoic cycles of sea-level change on the Arabian Platform. GeoArabia, 10(2), 127-160.

Haq, B.U., Hardenbol, J., Vail, P.R., 1988. Mesozoic and Cenozoic chronostratigraphy and cycles of sea-level change. SEPM Special Publications 42, 71–108.

Hardenbol, J., Jacquin, T., Farley, M.B., de Graciansky, P.C., Vail, P.R., 1998. Mesozoic and Cenozoic sequence chronostratigraphic framework of European basins. In: de Graciansky, P. C., Hardenbol, J., Jaquin, T., Vail, P.R. (Eds.), Mesozoic and Cenozoic Sequence Stratigraphy of European Basins. Society for Sedimentary Geology (SEPM), Tulsa, 3–13.

Hinnov, L. A., Park, J. J., 1999. Strategies for assessing Early-Middle (Pliensbachian-Aalenian) Jurassic cyclochronologies. Philosophical Transactions of the Royal Society of London A: Mathematical, Physical and Engineering Sciences, 357(1757), 1831-1859.

Jacquin, T., Dardeau, G., Durlet, C., de Graciansky, C., Hantzpergue, P., 1998. The North Sea cycle: an overview of 2nd-order transgressive/regressive facies cycles in Western Europe. In: de Graciansky, P.-C., Hardenbol, J., Jacquin, T., Vail, P.R. (Eds.), Mesozoic and Cenozoic Sequence Stratigraphy of European Basins, pp. 445–465.

Jacquin, T., de Graciansky, P.-C., 1998. Transgressive/Regressive (Second order) facies cycles: the effects of tectono-eustasy. In: De Graciansky, P.-C., Hardenbol, J., Jacquin, T., Vail, P.-R. (Eds.), Mesozoic and Cenozoic Sequence Stratigraphy of European Basins. SEPM Special Publication, pp. 31–42.

Jacquin, T., Garcia, J.-P., Ponsot, C., Thierry, J., Vail, P.R., 1992. Séquence de dépôt et cycles régressif/transgressifs en domaine marin carbonaté: exemple du Dogger du Bassin de Paris. Comptes Rendus de l'Académie

des Sciences, Série II, Fascicule a – Sciences de la Terre et des Planètes 315, 353–362.
Jenkyns, H.C., Sarti, M., Masetti, D., and Howarth, M.K., 1985, Ammonites and stratigraphy of Lower Jurassic black shales and pelagic limestones from the Belluno trough, southern Alps: Ecologae Geologicae Helvetiae, 78, 299-311.
Kadar, A.P., De Keyser, T., Neog, N., Karam, K.A., Le Nindre, Y.M., Davies, R.B., 2015. Calcareous nannofossil zonation and sequence stratigraphy of the Jurassic System, onshore Kuwait. GeoArabia, 20(4), 125-180.
Korte, C., Hesselbo, S.P., Ullmann, C.V., Dietl, G., Ruhl, M., Schweigert, G., Thibault, N., 2015. Jurassic climate mode governed by ocean gateway. Nature communications, 6, 10015.
Le Nindre, Y.M., Manivit, J., Manivit, H., Vaslet, D., 1990. Stratigraphie sequentielle du Jurassique et du Cretace en Arabie Saoudite. Bulletin Société Géologique France, Paris 6, 1025-1035.
Le Nindre, Y.M., Vaslet, D., Le Métour, J., Bertrand, J., Halawani, M., 2003. Subsidence modelling of the Arabian Platform from Permian to Paleogene outcrops. Sedimentary Geology, 156, 263-285.
Lhamyani, B., 1985. Etude stratigraphique de l'Oxfordien dans l'arc de Castellane(Alpes-de-Haute-Provence): passage des faciès provençaux aux faciès dauphinois (Doctoral dissertation).
Mancini, E.A., Obid, J.A., Puckett, T.M., 2004. Upper Jurassic transgressive-regressive sequences, Mississippi interior salt basin area.
Manivit, J., Le Nindre, Y.M., Vaslet D. (1990) Le Jurassique d'Arabie Centrale. In Histoire Gologique de la Bordure Occidentale de la Plate-forme Arabe. Volume 4. Document du BRGM n°194.
Martinez, M., Dera, G. 2015. Orbital pacing of carbon fluxes by a ~9-My eccentricity cycle during the Mesozoic. Proceedings of the National Academy of Sciences, 112(41), 12604-12609.
Mattner, J., Al-Husseini, M., 2002. Essay: Applied cyclo-stratigraphy for the Middle East E&P industry. GeoArabia, 7 (4), 734-744.
Mosser-Ruck, R., Huault, V., Elie, M., 2002. Clay mineralogy changes at the callovian-oxfordian boundary of the Paris Basin: a signal for paleo-environmental modifications?. International Meeting, Reims, France, Abstract, 237-238.
Murris, R.J., 1980. Middle East: Stratigraphic evolution and oil habitat. AAPG Bulletin, 64,597–618.
Muttoni, G., Erba, E., Kent, D.V., Bachtadse, V., 2005. Mesozoic Alpine facies deposition as a result of past latitudinal plate motion. Nature 434, 59–63.
Nunn, E.V., Price, G.D., 2010. Late Jurassic (Kimmeridgian–Tithonian) stable isotopes (δ 18 O, δ 13 C) and Mg/Ca ratios: new palaeoclimate data from Helmsdale, northeast Scotland. Palaeogeography, Palaeoclimatology, Palaeoecology, 292(1), 325-335.
Nunn, E.V., Price, G.D., Hart, M., Page, K., Leng, M., 2009. Isotopic signals from CallovianeKimmeridgian (Middle Upper Jurassic) belemnites and bulk organic carbon, Staffin Bay, Isle of Skye, Scotland. Journal of the Geological Society, London 166, 633e641.
O'Dogherty, L., Sandoval, J., Bartolini, A., Bruchez, S., Bill, M., Guex, J., 2005. Carbon-isotope stratigraphy and ammonite faunal turnover for the

Middle Jurassic in the Southern Iberian palaeomargin. Palaeogeography, Palaeoclimatology, Palaeoecology, 239(3), 311-333.

Pellenard, P., Tramoy, R., Pucéat, E., Huret, E., Martinez, M., Bruneau, L., Pittet, B., Strasser, A., 1998. Long-distance correlations by sequence stratigraphy and cyclostratigraphy: examples and implications (Oxfordian from the Swiss Jura, Spain, and Normandy). Geol. Rundschau, 86 (4),

Powers, R.W., 1968. Lexique Stratigraphique International, v.III, Asie, 10bl, Saudi Arabia. Centre National de la Recherche Scientifique, Paris, 177p.

Price, G.D., 1999. The evidence and implications of polar-ice during the Mesozoic. Earth Science Reviews 48, 183-210.

Price, G.D., Rogov, M.A., 2009. An isotopic appraisal of the Late Jurassic greenhouse phase in the Russian Platform. Palaeogeography, Palaeoclimatology, Palaeoecology 273, 41–49.

Razin, P., Taati, F., Van Buchem, F.S.P., 2010. Sequence stratigraphy of Cenomanian–Turonian carbonate platform margins (Sarvak Formation) in the High Zagros, SW Iran: an outcrop reference model for the Arabian Plate. Geological Society, London, Special Publications, 329(1), 187-218.

Rousseau, M., Dromart, G., Droste, H., Homewood, P., 2005. Stratigraphic organisation of the Jurassic sequence in Interior Oman, Arabian Peninsula. GeoArabia-Manama, 11(1), 17.

Ruffell, A., McKinley, J.M., Worden, R.H., 2002. Comparison of clay mineral stratigraphy to other proxy palaeoclimate indicators in the Mesozoic of NW Europe. Philosophical Transactions of the Royal Society of London A: Mathematical, Physical and Engineering Sciences, 360(1793), 675-693.

Sahagian, D., Pinous, O., Olferiev, A., Zakharov, V., 1995. Eustatic curve for the Middle Jurassic-Cretaceous based on Russian platform and Siberian stratigraphy: Zonal resolution. AAPG bulletin, 80(9), 1433-1458.

Sharland, P.R., Archer R., Casey D.M., Davies R.B., Hall S.H., Heward A.P., Horbury A.D., Simmons M.D., 2001. Arabian Plate Sequence Stratigraphy. GeoArabia Special Publication 2, Gulf PetroLink, Bahrain, 371.

Simmons, M.D., Sharland, P. R., Casey, D.M., Davies, R.B., Sutcliffe, O.E., 2007. Arabian Plate sequence stratigraphy: Potential implications for global chronostratigraphy. GeoArabia-Manama, 12(4), 101.

Strasser, A., Hillgärtner, H., Hug, W., Pittet, B., 2000. Third□order depositional sequences reflecting Milankovitch cyclicity. Terra Nova, 12(6), 303-311.

Strasser, A., Pittet, B., Hug, W., 2015. Palaeogeography of a shallow carbonate platform: The case of the Middle to Late Oxfordian in the Swiss Jura Mountains. Journal of Palaeogeography, 4 (3), 251-268.

Strasser, A., Védrine, S., 2009. Controls on facies mosaics of carbonate platforms: a case study from the Oxfordian of the Swiss Jura. In: Swart, P.K., Eberli, G.P., McKenzie, J.A. (Eds.), Perspectives in Sedimentary Geology: A Tribute to the Career of Robert Nathan Ginsburg. International Association of Sedimentologists. Special Publication, 41. Blackwell, Oxford, 41, 199-213.

Suan, G., Mattioli, E., Pittet, B., Lécuyer, C., Suchéras-Marx, B., Duarte, L.V., Philippe, M., Reggiani, L., Martineau, F., 2010. Secular environmental precursors to Early Toarcian (Jurassic) extreme climate changes. Earth and Planetary Science Letters, 290(3), 448-458.

Surlyk, F., 1990. Timing, style and sedimentary evolution of Late Palaeozoic-Mesozoic extensional basins of East Greenland. Geological Society, London, Special Publications, 55(1), 107-125.

Surlyk, F., 1991. Sequence stratigraphy of the jurassic-lowermost cretaceous of east greenland (1). AAPG Bulletin, 75(9), 1468-1488.

Thierry, B., Iwaniuk, A.N., Pellis, S.M., 2000. The influence of phylogeny on the social behaviour of macaques (Primates: Cercopithecidae, genus Macaca). Ethology, 106(8), 713-728.

Thierry, J., 2014. Carbon cycle and sea-water palaeotemperature evolution at the Middle–Late Jurassic transition, eastern Paris Basin (France). Marine and Petroleum Geology, 53, 30-43.

Van de Schootbrugge, B., McArthur, J.M., Bailey, T.R., Rosenthal, Y., Wright, J.D., Miller, K.G., 2005. Toarcian anoxic event: an assessment of global causes using belemnite C isotope records. Paleoceanography, 20(3), PA3008.

Vaslet, D., 1987, Geologic du Paleozoique; Permien Superieur, Trias, Jurassique; lithostratigraphic: in Histoire geologique de la bordure occidentale de la plate-fornie arabe du PaleozoIque inferieur au Jurassique superieur (Y.M. Le Nindre, J. Manivit and D. Vaslet, authors), DSc Thesis, University of Paris VI, 1, 413 p.

Védrine, S., Strasser, A., 2009. High-frequency palaeoenvironmental changes on a shallow carbonate platform during a marine transgression (Late Oxfordian, Swiss Jura Mountains). Swiss journal of geosciences, 102(2), 247-270.

Wierzbowski, H., Rogov, M. A., Matyja, B. A., Kiselev, D., Ippolitov, A., 2013. Middle–Upper Jurassic (Upper Callovian–Lower Kimmeridgian) stable isotope and elemental records of the Russian Platform: Indices of oceanographic and climatic changes. Global and Planetary Change, 107, 196-212.

Wignall, P.B., Ruffell, A.H., 1990. The influence of sudden climatic change on marine deposition in the Kimmeridgian of northwest Europe. Journal of the Geological Society of London 147, 365–371.

Wilson, J.L., Jordan, C., 1983. Middle Shelf Environment. In: Scholle, P.A., Bebout, D.G., Moore, C.H. (Eds.), Carbonate Depositional Environments. American Association Petroleum Geologists Memoir, 33, 345–440.

Sédimentologie et stratigraphie séquentielle des séries jurassiques du Jabal Tuwaiq, Arabie Saoudite

Mots clefs : Jurassique, plateforme arabe, plateforme épicontinentale, systèmes mixtes carbonatés – silico-clastiques, stratigraphie séquentielle.

Key words: Jurassic, Arabian Platform, Epireic platforme, Carbonate – siliciclastic mixed sedimentary systems, sequence stratigraphy

Résumé

Cette étude porte sur l'analyse des séries jurassiques du Shaqra Group (Toarcian to Kimmeridgian) qui affleurent de manière continue en Arabie centrale le long d'un transect de plus de 1000 km de long. Ces séries se sont accumulées sur une vaste plate-forme épicontinentale peu profonde, en contexte tropical. Ces affleurements permettent ainsi d'observer la partie occidentale des séries renfermant des systèmes pétroliers prolifiques exploités en subsurface en Arabie Saoudite.

L'analyse sédimentologique de nombreuses coupes et la réalisation de corrélations stratigraphiques de haute résolution sur un transect de 600 km au sud de Riyad, complété par des corrélations avec les données de forage plus à l'est (entre Riyadh et le Rimthan Arch), permettent de distinguer une organisation séquentielle à différents ordres de fréquence et de reconstituer l'évolution de la plate-forme au sein de ces séquences.

La plate-forme jurassique évolue d'une plate-forme horizontale caractérisée par des systèmes mixtes à la transition continental-marin du Toarcien au Callovien moyen (formations Marrat et Dhruma) vers un système de type rampe - bassin intrashelf du Callovien au Kimméridgien inférieur (formations Tuwaiq et Hanifa) pour finir par une plate-forme aggradante carbonatée et silico-clastique (Fm. Jubaila) puis carbonatée et évaporitique en contexte aride (Fm. Arab) au Kimméridgien.

Les cycles tectono-stratigraphiques de 2ème ordre du Jurassique inférieur et moyen sont limités à la base et au sommet par des discontinuités régionales. Ils occupent un dépôt-centre stationnaire et décrivent un onlap côtier de grande ampleur avec un maximum transgressif au Callovien moyen (Upper Tuwaiq Mb.). Durant le Jurassique supérieur, les dépôts de rampe carbonatée de la Formation Hanifa passent progressivement vers l'ouest à des dépôts plus profonds de bassin intrashelf relativement riches en matière organique (Khurais - Rimthan Arch). La séquence Jubaila – Arab-D montre des variations d'épaisseur qui indiquent une déformation de grande longueur d'onde de la plate-forme arabe à cette période. Les faciès récifaux du membre Arab D sont interprétés comme représentant le maximum d'inondation de ce cycle qui se termine par le développement de systèmes carbonatés – évaporitiques à la fin du Jurassique.